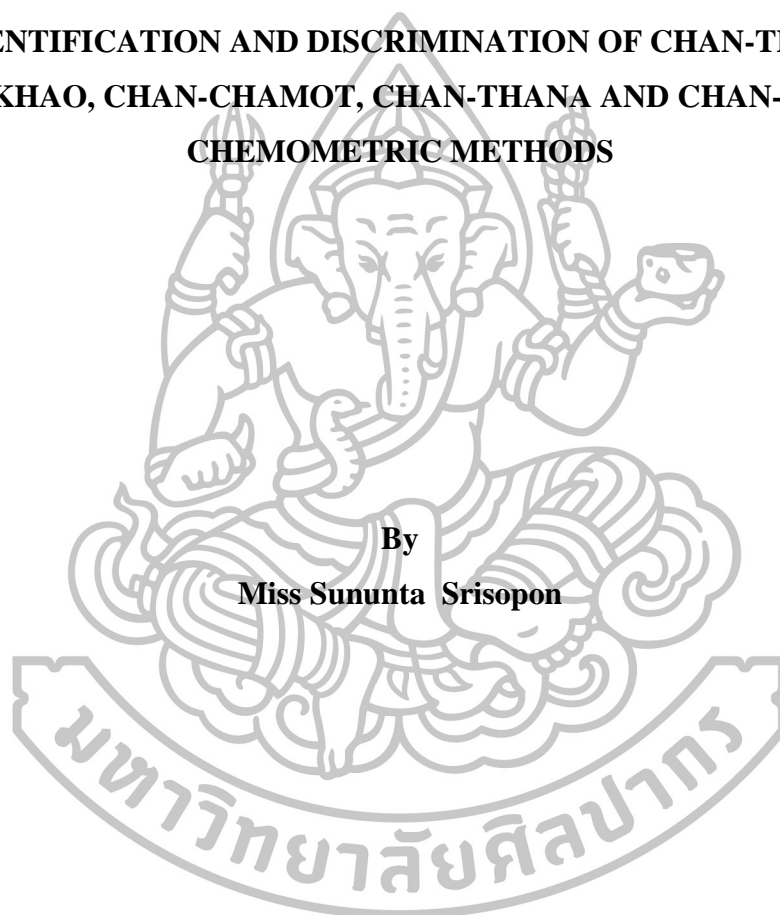




**IDENTIFICATION AND DISCRIMINATION OF CHAN-THET,
CHAN-KHAO, CHAN-CHAMOT, CHAN-THANA AND CHAN-HOM BY
CHEMOMETRIC METHODS**



By
Miss Sununta Srisopon

A Thesis Submitted in Partial Fulfillment of the Requirements for the Degree

Doctor of Philosophy

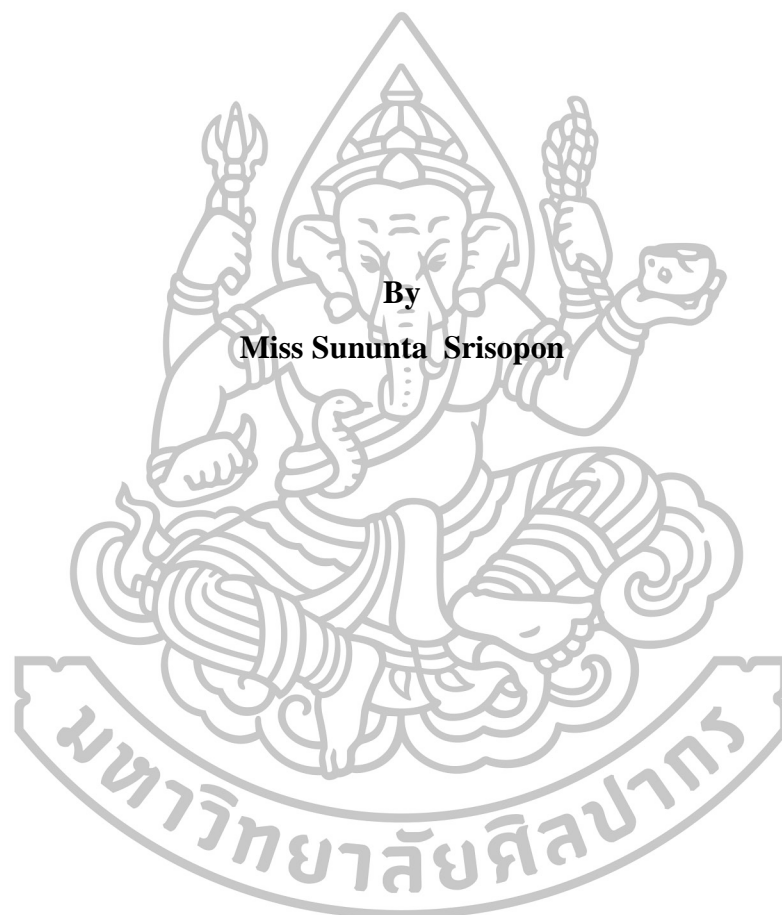
Program in Pharmaceutical Chemistry and Natural Products

Graduate School, Silpakorn University

Academic Year 2015

Copyright of Graduate School, Silpakorn University

**IDENTIFICATION AND DISCRIMINATION OF CHAN-THET,
CHAN-KHAO, CHAN-CHAMOT, CHAN-THANA AND CHAN-HOM BY
CHEMOMETRIC METHODS**



**A Thesis Submitted in Partial Fulfillment of the Requirements for the Degree
Doctor of Philosophy
Program in Pharmaceutical Chemistry and Natural Products
Graduate School, Silpakorn University
Academic Year 2015
Copyright of Graduate School, Silpakorn University**

การพิสูจน์เอกลักษณ์และการจำแนกชนิดของจันทน์เทศ จันทน์ขาว จันทน์ชะมด จันทนา และ
จันทน์หอม ด้วยวิธีเคมีเมตริก



วิทยานิพนธ์นี้เป็นส่วนหนึ่งของการศึกษาตามหลักสูตรปริญญาเภสัชศาสตรดุษฎีบัณฑิต
สาขาวิชาเภสัชเคมีและผลิตภัณฑ์ธรรมชาติ
บัณฑิตวิทยาลัย มหาวิทยาลัยศิลปากร
ปีการศึกษา 2558
ลิขสิทธิ์ของบัณฑิตวิทยาลัย มหาวิทยาลัยศิลปากร

The Graduate School, Silpakorn University has approved and accredited the Thesis title of “Identification and Discrimination of Chan-thet, Chan-khao, Chan-chamot, Chan-thana and Chan-hom by Chemometric methods” submitted by Sununta Srisopon as a partial fulfillment of the requirements for the degree of Doctor of Philosophy in Pharmaceutical Chemistry and Natural Products.

.....
(Assoc. Prof. Panjai Tantatsanawong, Ph.D.)
Dean of Graduate School
...../...../.....

The Thesis Advisor

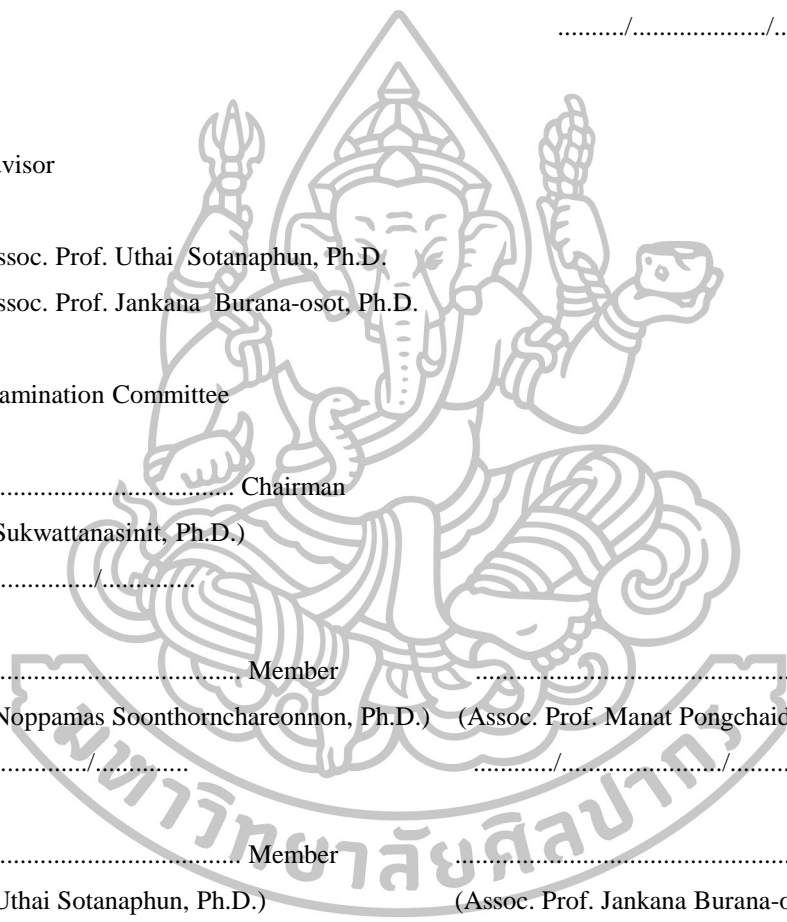
1. Assoc. Prof. Uthai Sotanaphun, Ph.D.
2. Assoc. Prof. Jankana Burana-osot, Ph.D.

The Thesis Examination Committee

..... Chairman
(Tasamaporn Sukwattanasinit, Ph.D.)
...../...../.....

..... Member Member
(Assoc. Prof. Noppamas Soonthornchareonnon, Ph.D.) (Assoc. Prof. Manat Pongchaidecha, Ph.D.)
...../...../.....

..... Member Member
(Assoc. Prof. Uthai Sotanaphun, Ph.D.) (Assoc. Prof. Jankana Burana-osot, Ph.D.)
...../...../.....



53356801 : MAJOR : PHARMACEUTICAL CHEMISTRY AND NATURAL PRODUCTS
KEY WORD : CHEMOMETRICS/IDENTIFICATION/CHAN-THET/CHAN-KHAO/
CHAN-CHAMOT/CHAN-THANA/CHAN-HOM
SUNUNTA SRISOPON : IDENTIFICATION AND DISCRIMINATION OF
CHAN-THET, CHAN-KHAO, CHAN-CHAMOT, CHAN-THANA AND CHAN-HOM BY
CHEMOMETRIC METHODS. THESIS ADVISORS : ASSOC. PROF. UTHAI SOTANAPHUN,
Ph.D., ASSOC. PROF. JANKANA BURANA-OSOT, Ph.D. 295 pp.

The objective of this study was to identify botanical species of crude drugs named Chan-thet, Chan-khao, Chan chamot, Chan-thana and Chan-hom currently available in Thai traditional drugstores. The discrimination models of these crude drugs were also developed. Fifteen samples of Chan-thet, eighteen samples of Chan-khao, seventeen samples of Chan-chamot, ten samples of Chan-thana and eleven samples of Chan-hom were randomly purchased. Three pure compounds isolated from laboratory, i.e. α -santalol, mansonone G and geniposidic acid, were used as chemical markers. TLC chromatograms of the crude drugs were compared with the authentic samples. Infrared (IR) spectra and gas chromatography (GC) chromatograms of crude drug samples were compared with authentic samples by using chemometric methods, i.e. similarity analysis (SA), hierarchical cluster analysis (HCA) and principal component analysis (PCA). Moreover gas chromatography/mass spectroscopy (GC/MS) was applied for the identification of chemical constituents. Afterward the models for botanical discrimination of these crude drugs were developed on the basis of IR spectral data. Two prediction methods, i.e. soft independent modeling of class analogy (SIMCA) and partial least squares-discriminant analysis (PLS-DA), were compared.

The results indicated that Chan-thet samples were identified as three species, i.e. *Santalum album*, *S. spicatum* and *S. lanceolatum*; as *S. spicatum* was mostly found. Most Chan-khao samples were *Tarenna hoensis*. One of them was *S. spicatum*, and the others were an unidentified species. All Chan-chamot samples were *Mansonia gagei*. Most Chan-thana samples were *T. hoensis* and some were other three unidentified species. Most Chan-hom samples were *S. spicatum* and some were *M. gagei*. Comparing among chemometric methods, PCA gave the better identification results than HCA and SA. The best discrimination method of these crude drugs using SIMCA was obtained from the PCA models using IR data in the range of $1498-501\text{ cm}^{-1}$. Its accuracy, sensitivity and specificity were 80, 70 and 100%, respectively. For PLS-DA, the best discrimination method was obtained from PLS models using second derivative IR in the range of $1801-501\text{ cm}^{-1}$. Its accuracy, sensitivity and specificity were 87, 80 and 100%, respectively.

Program of Pharmaceutical Chemistry and Natural Products

Graduate School, Silpakorn University

Student's signature.....

Academic Year 2015

Thesis Advisors' signature 1. 2.

53356801 : สาขาวิชาเภสัชเคมีและผลิตภัณฑ์ธรรมชาติ

คำสำคัญ : คีโมเมตริกซ์/การพิสูจน์เอกลักษณ์ทางเคมี/จันทน์เทศ/จันทน์ขาว/จันทน์ชะมด/จันทนา/จันทน์หอม

สุนันทา ศรีโสภณ : การพิสูจน์เอกลักษณ์และการจำแนกชนิดของจันทน์เทศ จันทน์ขาว จันทน์ชะมด จันทนา และ

จันทน์หอมด้วยวิธีคีโมเมตริก. อาจารย์ที่ปรึกษาวิทยานิพนธ์ : ภก.รศ.ดร.อุทัย โสธนะพันธุ์ และ ภญ.รศ.ดร.จันทนา บุรณะโอสถ. 295 หน้า.

งานวิจัยนี้มีวัตถุประสงค์เพื่อพิสูจน์ชนิดทางพฤกษศาสตร์ของเครื่องยาที่ชื่อ จันทน์เทศ จันทน์ขาว จันทน์ชะมด จันทนา และจันทน์หอม ที่มีจำหน่ายในร้านยาสมุนไพรในปัจจุบัน พร้อมทั้งสร้างแบบจำลองสำหรับจำแนกชนิดทางพฤกษศาสตร์ของเครื่องยาเหล่านี้ การศึกษาทำโดยสุ่มซื้อตัวอย่างเครื่องยาจันทน์เทศ 15 ตัวอย่าง จันทน์ขาว 18 ตัวอย่าง จันทน์ชะมด 17 ตัวอย่าง จันทนา 10 ตัวอย่าง และจันทน์หอม 11 ตัวอย่าง นำมาพิสูจน์เอกลักษณ์ด้วยวิธีโครมาโทกราฟีชนิดแผ่นบาง โดยใช้สารเทียบ 3 ชนิดที่สกัดแยกในห้องปฏิบัติการ คือ สาร α -santalol, mansonone G และ geniposidic acid และเปรียบเทียบที่แอลซีโครมาโทแกรมของตัวอย่างเครื่องยากับตัวอย่างพืชอ้างอิง และใช้วิธีทางคีโมเมตริกซ์ ได้แก่ similarity analysis (SA), hierarchical cluster analysis (HCA) และ principal component analysis (PCA) เพื่อวิเคราะห์ข้อมูลอินฟราเรดสเปกตรัมและแก๊สโครมาโทแกรมของตัวอย่างเครื่องยาเปรียบเทียบกับตัวอย่างพืชอ้างอิง นอกจากนี้ยังใช้วิธีแก๊สโครมาโทกราฟีที่ตรวจสอบด้วยแมสสเปกโตรสโกปีเพื่อวิเคราะห์ชนิดขององค์ประกอบทางเคมี จากนั้นสร้างแบบจำลองสำหรับจำแนกชนิดทางพฤกษศาสตร์ของตัวอย่างเครื่องยาจากข้อมูลอินฟราเรดสเปกตรัม เปรียบเทียบวิธีทำนาย 2 วิธี ได้แก่ soft independent modeling of class analogy (SIMCA) และ partial least squares-discriminant analysis (PLS-DA)

ผลการศึกษาพบว่า เครื่องยาจันทน์เทศจำแนกได้เป็น 3 ชนิด คือ *Santalum album*, *S. spicatum* และ *S. lanceolatum* โดยที่ส่วนใหญ่คือ *S. spicatum* เครื่องยาจันทน์ขาวส่วนใหญ่คือ *Tarenna hoagensis* พบชนิดที่เป็น *S. spicatum* จำนวน 1 ตัวอย่าง และไม่สามารถจำแนกชนิดได้อีก 1 ชนิด เครื่องยาจันทน์ชะมดทั้งหมดคือ *Mansonia gagei* เครื่องยาจันทนาส่วนใหญ่คือ *T. hoagensis* และไม่สามารถระบุชนิดได้อีก 3 ชนิด เครื่องยาจันทน์หอมส่วนใหญ่คือ *S. spicatum* และบางตัวอย่างคือ *M. gagei* การเปรียบเทียบการวิเคราะห์ข้อมูลด้วยวิธีทางคีโมเมตริกซ์พบว่า วิธี PCA ให้ผลดีกว่า HCA และ SA การสร้างแบบจำลองสำหรับจำแนกชนิดทางพฤกษศาสตร์ของเครื่องยาเหล่านี้พบว่า วิธี SIMCA ที่ใช้แบบจำลองที่สร้างจากข้อมูลในช่วง $1498-501\text{ cm}^{-1}$ ให้ผลดีที่สุด คือให้ความถูกต้องร้อยละ 80 ความไวร้อยละ 70 และความจำเพาะร้อยละ 100 ส่วนวิธี PLS-DA ที่ใช้แบบจำลองที่สร้างจากข้อมูลในช่วง $1801-501\text{ cm}^{-1}$ ของสเปกตรัมที่ผ่านการประมวลผลให้เป็นอนุพันธ์ลำดับที่สอง จะให้ผลดีที่สุด คือให้ความถูกต้องร้อยละ 87 ความไวร้อยละ 80 และความจำเพาะร้อยละ 100

สาขาวิชาเภสัชเคมีและผลิตภัณฑ์ธรรมชาติ

บัณฑิตวิทยาลัย มหาวิทยาลัยศิลปากร

ลายมือชื่อนักศึกษา.....

ปีการศึกษา 2558

ลายมือชื่ออาจารย์ที่ปรึกษาวิทยานิพนธ์ 1. 2.

Acknowledgements

I would like to express my grateful and sincere thanks to my advisor, Assoc. Prof. Uthai Sotanaphun, Ph.D. for his knowledge, guidance, support, valuable time, patience and kindness throughout this program. I would also like to thank my co-advisor, Assoc. Prof. Jankana Burana-osot, Ph.D. for her knowledge, advice and kindness. I really appreciate their kindness.

I would like to express sincere thanks to the members of thesis examination committee, Tasamaporn Sukwattanasinit, Ph.D., Assoc. Prof. Noppamas Soonthornchareonnon, Ph.D. and Assoc. Prof. Manat Pongchaidecha, Ph.D. for their comments.

I am also thankful to Medicinal Plant Research Institute, Department of Medicinal Sciences, Ministry of public Health, Mr. Kongsak Meekaew, Ph.D., Prachuap-Khiri-Khan Silvicultural Research Station, and Prof. Dhanushka S. Hettiarachchi, Wescrop group, Australia; for providing authentic samples used in this study.

I thank the staffs of Faculty of Pharmacy, Silpakorn University for facilities.

I would like to thank many experiences and point of views that had happened in a period of 5 years. I also thank everyone who has assisted and encouraged me.

Finally, I specially thank my parents for their love, care and everything. Thank you from bottom of my heart.

Table of Contents

	Page
English Abstract.....	iv
Thai Abstract.....	v
Acknowledgements.....	vi
List of Tables	vii
List of Figures.....	xv
List of Schemes.....	xxxiv
Chapter	
I Introduction.....	1
Goals and objectives	4
II Literature review.....	5
Thai traditional use of Chan(s)	5
Chan-thet.....	5
Chan-khao.....	5
Chan-chamot.....	6
Chan-thana	6
Chan-hom.....	6
Chan(s) in Thai traditional medicine formulae.....	6
<i>Santalum album</i> L.....	9
<i>Santalum spicatum</i> (R. Br.) A. DC.....	14
<i>Santalum lanceolatum</i> R.Br.....	15
<i>Myristica fragrans</i> Houtt.....	17
<i>Diospyros decandra</i> Lour.....	21
<i>Tarenna hoaensis</i> Pit.....	24
<i>Mansonia gagei</i> J.R.Drumm. ex Prain.....	25
<i>Aglaia silvestris</i> (M. Roem.) Merr.....	28
Chemical approach for identification and authentication of herbal medicines	30
Thin layer chromatography (TLC).....	30
Gas chromatography/Mass spectroscopy (GC/MS).....	31

Chapter	Page
Infrared spectroscopy (IR)	31
Preprocessing technique of chemical fingerprint.....	33
Smoothing	33
Normalization	34
Derivative.....	34
Alignment	35
Chemometric methods for quality control of herbal medicines.....	35
Introduction of chemometrics	35
Unsupervised pattern recognition	35
Supervised pattern recognition	39
Application of chemometrics on herbal identification.....	44
III Material and methods.....	46
Plant materials and authentic samples	46
Chemical markers	47
Isolation of chemical markers.....	47
Structure elucidation of chemical markers	53
Identification of Chan-thet, Chan-khao, Chan-chamot, Chan-thana and Chan-hom.....	53
Thin layer chromatography (TLC) fingerprint	53
Infrared spectroscopy (IR) fingerprint.....	55
Gas chromatography (GC) fingerprint.....	56
Development of authentication models	60
Sample preparation	60
Soft independent modeling of class analogy (SIMCA)	61
Partial least squares-discriminant analysis (PLS-DA).....	63
IV Results and discussions.....	65
Plant materials.....	65
Structure elucidation of chemical markers	70
α -Santalol	70
Mansonone G	72

Chapter	Page
Geniposidic acid.....	74
Identification of Chan-thet, Chan-khao, Chan-chamot, Chan-thana and Chan- hom.....	78
TLC fingerprint.....	78
IR fingerprint	93
Gas chromatography (GC) fingerprint.....	114
Conclusion of the identification.....	132
Development of authentication models	137
Sample preparation	137
Soft independent modeling of class analogy (SIMCA)	144
Partial least squares-discriminant analysis (PLS-DA).....	151
V Conclusions.....	158
References	161
Appendices	
Appendix A Crude drug of Chan-thet, Chan-khao, Chan-chamot, Chan-thana and Chan-hom samples.....	180
Appendix B Mass, IR and NMR spectra of chemical markers.....	187
Appendix C IR spectra of Chan-thet, Chan-khao, Chan-chamot, Chan-thana, Chan-hom and authentic samples.....	199
Appendix D Similarity index of Chan-thet, Chan-khao, Chan-chamot, Chan-thana, Chan-hom and authentic samples.....	210
Appendix E HCA dendrogram of Chan-thet, Chan-khao, Chan-chamot, Chan-thana, Chan-hom and authentic samples.....	227
Appendix F PCA result of IR spectra of Chan-thet, Chan-khao, Chan-chamot, Chan-thana, Chan-hom and authentic samples	261
Appendix G GC chromatogram of Chan-thet, Chan-khao, Chan-chamot, Chan-thana, Chan-hom and authentic samples	277
Appendix H Regression coefficient of PLS model.....	281
Appendix I Predicted response of test samples using PLS-DA method..	288
Biography	295

List of Tables

Tables	Page
1	Examples of some Thai traditional formulae containing Chan(s) as ingredient(s) 7
2	Pharmacological activity of <i>Santalum album</i> 11
3	Chemical constituents of <i>Santalum album</i> 12
4	Pharmacological activity of <i>Santalum spicatum</i> 14
5	Chemical constituents of <i>Santalum spicatum</i> 15
6	Pharmacological activity of <i>Santalum lanceolatum</i> 16
7	Chemical constituents of <i>Santalum lanceolatum</i> 16
8	Pharmacological activity of <i>Myristica fragrans</i> 18
9	Chemical constituents of <i>Myristica fragrans</i> 19
10	Pharmacological activity of <i>Diospyros decandra</i> 22
11	Chemical constituents of <i>Diospyros decandra</i> 23
12	Pharmacological activity of <i>Tarenna hoensis</i> 25
13	Chemical constituents of <i>Tarenna hoensis</i> 25
14	Pharmacological activity of <i>Mansonia gagei</i> 26
15	Chemical constituents of <i>Mansonia gagei</i> 27
16	Pharmacological activity of <i>Aglaia silvestris</i> 29
17	Chemical constituents of <i>Aglaia silvestris</i> 29
18	Interpretation of some important regions of infrared spectrum 32
19	Application of chemometrics on herbal identification..... 45
20	Sources and characters of crude drug samples 65
21	Sources and characters of authentic samples 69
22	NMR assignment of α -santalol 71
23	NMR assignment of mansonone G 73
24	NMR assignment of geniposidic acid 76
25	HMBC correlation of geniposidic acid 77
26	The similarity index of samples and authentic samples..... 115
27	Composition of the <i>n</i> -hexane extracts of Chan-thet, Chan-hom, Chan-khao and authentic samples..... 122

Tables	Page
28	Composition of the essential oils of Chan-thet samples and various authentic <i>Santalum</i> 130
29	Identification results of Chan(s) using TLC, IR and GC 133
30	Conclusion of species identification of Chan(s) in Thai traditional drugstores 136
31	The group of different species of Chan(s) 138
32	Training set and test set of the normalized IR spectra of <i>Santalum</i> group, MG group and TH group 142
33	Training set and test set of the second derivative IR spectra of <i>Santalum</i> group, MG group and TH group 143
34	Identification of blind samples 144
35	PCA models for the authentication of <i>Santalum</i> , TH and MG groups . 145
36	Classification of test samples and blind samples using SIMCA 146
37	Percentage of accuracy, sensitivity and specificity of test set and blind samples classification using SIMCA 148
38	Linearity, root mean square error of cross validation and optimum factors of PLS model 152
39	Cutoff values and cutoff ranges of PLS-DA methods of <i>Santalum</i> group, MG group and TH group 153
40	Classification of test samples and blind samples using PLS-DA 154
41	Percentage of accuracy, sensitivity and specificity of test set and blind samples classification using PLS-DA 156
42	Similarity index between the IR spectra of the <i>n</i> -hexane of Chan-thet and authentic samples 211
43	Similarity index between the IR spectra of the dichloromethane extracts of Chan-thet and authentic samples 211
44	Similarity index between the IR spectra of the ethyl acetate extracts of Chan-thet and authentic samples 212
45	Similarity index between the IR spectra of the acetone extracts of Chan-thet and authentic samples 212

Tables	Page
46	Similarity index between the IR spectra of the methanol extracts of Chan- thet and authentic samples 213
47	Similarity index between the IR spectra of the water extracts of Chan-thet and authentic samples 213
48	Similarity index between the IR spectra of the fine powders of Chan-thet and authentic samples 214
49	Similarity index between the IR spectra of the <i>n</i> -hexane extracts of Chan- khao and authentic samples..... 214
50	Similarity index between the IR spectra of the dichloromethane extracts of Chan-khao and authentic samples..... 215
51	Similarity index between the IR spectra of the ethyl acetate extracts of Chan-khao and authentic samples 215
52	Similarity index between the IR spectra of the acetone extracts of Chan- khao and authentic samples..... 216
53	Similarity index between the IR spectra of the methanol extracts of Chan- khao and authentic samples..... 216
54	Similarity index between the IR spectra of the water extracts of Chan-khao and authentic samples..... 217
55	Similarity index between the IR spectra of the fine powders of Chan-khao and authentic samples..... 217
56	Similarity index between the IR spectra of the <i>n</i> -hexane extracts of Chan- chamot and authentic samples..... 218
57	Similarity index between the IR spectra of the dichloromethane extracts of Chan-chamot and authentic samples..... 218
58	Similarity index between the IR spectra of the ethyl acetate extracts of Chan-chamot and authentic samples..... 219
59	Similarity index between the IR spectra of the acetone extracts of Chan- chamot and authentic samples..... 219
60	Similarity index between the IR spectra of the methanol extracts of Chan-chamot and authentic samples..... 220

Tables	Page
61	Similarity index between the IR spectra of the water extracts of Chan-chamot and authentic samples..... 220
62	Similarity index between the IR spectra of the fine powders of Chan- chamot and authentic samples..... 221
63	Similarity index between the IR spectra of the <i>n</i> -hexane extracts of Chan-thana and authentic samples..... 221
64	Similarity index between the IR spectra of the dichloromethane extracts of Chan-thana and authentic samples 222
65	Similarity index between the IR spectra of the ethyl acetate extracts of Chan-thana and authentic samples..... 222
66	Similarity index between the IR spectra of the acetone extracts of Chan-thana and authentic samples..... 222
67	Similarity index between the IR spectra of the methanol extracts of Chan-thana and authentic samples..... 223
68	Similarity index between the IR spectra of the water extracts of Chan-thana and authentic samples..... 223
69	Similarity index between the IR spectra of the fine powders of Chan-thana and authentic samples..... 223
70	Similarity index between the IR spectra of the <i>n</i> -hexane extracts of Chan-hom and authentic samples 224
71	Similarity index between the IR spectra of the dichloromethane extracts of Chan-hom and authentic samples 224
72	Similarity index between the IR spectra of the ethyl acetate extracts of Chan-hom and authentic samples 224
73	Similarity index between the IR spectra of the acetone extracts of Chan-hom and authentic samples 225
74	Similarity index between the IR spectra of the methanol extracts of Chan-hom and authentic samples 225
75	Similarity index between the IR spectra of the water extracts of Chan-hom and authentic samples 225

Tables		Page
76	Similarity index between the IR spectra of the fine powders of Chan-hom and authentic samples	226



List of Figures

Figures	Page
1 <i>Santalum album</i> L.	9
2 <i>Myristica fragrans</i> Houtt.	17
3 <i>Diospyros decandra</i> Lour.	21
4 <i>Tarenna hoaensis</i> Pit.....	24
5 <i>Mansonina gagei</i> J.R.Drumm. ex Prain.....	25
6 <i>Aglaia silvestris</i> (M. Roem.) Merr.....	28
7 Savitsky-Golay smoothing.....	33
8 The example of single linkage clustering method	37
9 Establishment of new variable to principle component.....	39
10 Relationship between data set, score, loading and noise for PCA.....	39
11 Illustration SIMCA steps using PCA: a) step 1 of one-dimension (1 PC) b) step 1 of two-dimension (2 PCs) c) step 2 of one-dimension (1 PC) and d) step 2 of two-dimensions (2 PCs)....	41
13 Structure of α -santalol.....	70
14 Structure of mansonone G	72
15 Structure of geniposidic acid	74
16 HMBC correlations of geniposidic acid	77
17 TLC chromatogram of Chan-thet methanol extracts using <i>n</i> -hexane : ethyl acetate : methanol (60:30:0.2) as mobile phase: (a) detection under UV 254 nm, (b) detection under UV 366 nm and (c) detection under visible light after spraying with anisaldehyde-sulfuric acid TS.....	80
18 TLC chromatogram of Chan-thet methanol extracts using <i>n</i> -hexane : ethyl acetate : methanol : acetic acid (60:10:0.2:0.01) as mobile phase: (a) detection under UV 254 nm, (b) detection under UV 366 nm and (c) detection under visible light after spraying with anisaldehyde-sulfuric acid TS and heat at 105 °C for 5 min.....	81

Figures	Page
19	TLC chromatogram of Chan-khao methanol extracts using <i>n</i> -hexane : ethyl acetate : methanol (60:30:0.2) as mobile phase: (a) detection under UV 254 nm, (b) detection under UV 366 nm and (c) detection under visible light after spraying with anisaldehyde-sulfuric acid TS and heat at 105 °C for 5 min 83
20	TLC chromatogram of Chan-khao methanol extracts using dichloromethane : methanol : formic acid (60:10:1) as mobile phase: (a) detection under UV 254 nm, (b) detection under UV 366 nm and (c) detection under visible light after spraying with anisaldehyde-sulfuric acid TS and heat at 105 °C for 5 min 84
21	TLC chromatogram of Chan-chamot methanol extract using <i>n</i> -hexane : ethyl acetate : methanol (60:30:0.2) as mobile phase : (a) detection under visible light, (b) detection under UV 254 nm, (c) detection under UV 366 nm and (d) detection under visible light after spraying with anisaldehyde-sulfuric acid TS and heat at 105 °C for 5 min 86
22	TLC Chromatogram of Chan-thana methanol extract using <i>n</i> -hexane : ethyl acetate : methanol (60:30:0.2) as mobile phase: (a) detection under UV 254 nm, (b) detection under UV 366 nm and (c) detection under visible light after spraying with anisaldehyde-sulfuric acid TS and heat at 105 °C for 5 min 88
23	TLC Chromatogram of Chan-thana methanol extract using dichloromethane : methanol : formic acid (60:10:1) as mobile phase: (a) detection under UV 254 nm, (b) detection under UV 366 nm and (c) detection under visible light after spraying with anisaldehyde-sulfuric acid TS and heat at 105 °C for 5 min 89

Figures	Page	
24	TLC Chromatogram of Chan-hom methanol extract using <i>n</i> -hexane : ethyl acetate : methanol (60:30:0.2) as mobile phase: (a) detection under visible light, (b) detection under UV 254 nm, (c) detection under UV 366 nm and (d) detection under visible light after spraying with anisaldehyde-sulfuric acid TS and heat at 105 °C for 5 min 91	91
25	TLC Chromatogram of Chan-hom methanol extracts using <i>n</i> -hexane : ethyl acetate : methanol : acetic acid (60:10:0.2:0.01) as mobile phase: (a) detection under UV 254 nm, (b) detection under UV 366 nm and (c) detection under visible light after spraying with anisaldehyde-sulfuric acid TS and heat at 105 °C for 5 min 92	92
26	HCA dendrogram the second derivative IR spectra of the <i>n</i> -hexane extracts of Chan-thet samples, <i>S. album</i> , <i>S. spicatum</i> , <i>S. lanceolatum</i> , <i>M. fragrans</i> , <i>T. hoaensis</i> , <i>D. decandra</i> , <i>M. gagei</i> and <i>A. silvestris</i> 95	95
27	HCA dendrogram the second derivative IR spectra of the methanol extracts of Chan-thet samples, <i>S. album</i> , <i>S. spicatum</i> , <i>S. lanceolatum</i> , <i>M. fragrans</i> , <i>T. hoaensis</i> , <i>D. decandra</i> , <i>M. gagei</i> and <i>A. silvestris</i> 95	95
28	HCA dendrogram the second derivative IR spectra of the fine powders of Chan-thet samples, <i>S. album</i> , <i>S. spicatum</i> , <i>S. lanceolatum</i> , <i>M. fragrans</i> , <i>T. hoaensis</i> , <i>D. decandra</i> , <i>M. gagei</i> and <i>A. silvestris</i> 96	96
29	PC1 and PC2 score plots of the second derivative IR spectra of the (a) <i>n</i> -hexane, (b) acetone and (c) methanol extracts of Chan-thet samples, <i>S. album</i> , <i>S. spicatum</i> , <i>S. lanceolatum</i> , <i>M. fragrans</i> , <i>T. hoaensis</i> , <i>D. decandra</i> , <i>M. gagei</i> and <i>A. silvestris</i> 97	97

Figures	Page
30	HCA dendrogram the second derivative IR spectra of the <i>n</i> -hexane extracts of Chan-khao samples, <i>S. album</i> , <i>S. spicatum</i> , <i>S. lanceolatum</i> , <i>M. fragrans</i> , <i>T. hoaensis</i> , <i>D. decandra</i> , <i>M. gagei</i> and <i>A. silvestris</i> 99
31	HCA dendrogram the second derivative IR spectra of the dichloromethane extracts of Chan-khao samples, <i>S. album</i> , <i>S. spicatum</i> , <i>S. lanceolatum</i> , <i>M. fragrans</i> , <i>T. hoaensis</i> , <i>D. decandra</i> , <i>M. gagei</i> and <i>A. silvestris</i> 99
32	HCA dendrogram the second derivative IR spectra of the acetone extracts of Chan-khao samples, <i>S. album</i> , <i>S. spicatum</i> , <i>S. lanceolatum</i> , <i>M. fragrans</i> , <i>T. hoaensis</i> , <i>D. decandra</i> , <i>M. gagei</i> and <i>A. silvestris</i> 100
33	HCA dendrogram the second derivative IR spectra of the methanol extracts of Chan-khao samples, <i>S. album</i> , <i>S. spicatum</i> , <i>S. lanceolatum</i> , <i>M. fragrans</i> , <i>T. hoaensis</i> , <i>D. decandra</i> , <i>M. gagei</i> and <i>A. silvestris</i> 100
34	HCA dendrogram the second derivative IR spectra of the fine powders of Chan-khao samples, <i>S. album</i> , <i>S. spicatum</i> , <i>S. lanceolatum</i> , <i>M. fragrans</i> , <i>T. hoaensis</i> , <i>D. decandra</i> , <i>M. gagei</i> and <i>A. silvestris</i> 101
35	PC1 and PC2 score plots of the second derivative IR spectra of the <i>n</i> -hexane of Chan-khao samples, <i>S. album</i> , <i>S. spicatum</i> , <i>S. lanceolatum</i> , <i>M. fragrans</i> , <i>T. hoaensis</i> , <i>D. decandra</i> , <i>M. gagei</i> and <i>A. silvestris</i> 102
36	PC1, PC2 and PC3 three dimension score plots of the second derivative IR spectra of the acetone extract of Chan khao, <i>S. album</i> , <i>S. spicatum</i> , <i>S. lanceolatum</i> , <i>M. fragrans</i> , <i>T. hoaensis</i> , <i>D. decandra</i> , <i>M. gagei</i> and <i>A. silvestris</i> 103

Figures	Page
37	HCA dendrogram the second derivative IR spectra of the ethyl acetate extracts of Chan-chamot samples, <i>S. album</i> , <i>S. spicatum</i> , <i>S. lanceolatum</i> , <i>M. fragrans</i> , <i>T. hoensis</i> , <i>D. decandra</i> , <i>M. gagei</i> and <i>A. silvestris</i> 104
38	HCA dendrogram the second derivative IR spectra of the acetone extracts of Chan-chamot samples, <i>S. album</i> , <i>S. spicatum</i> , <i>S. lanceolatum</i> , <i>M. fragrans</i> , <i>T. hoensis</i> , <i>D. decandra</i> , <i>M. gagei</i> and <i>A. silvestris</i> 105
39	HCA dendrogram the second derivative IR spectra of the methanol extracts of Chan-chamot samples, <i>S. album</i> , <i>S. spicatum</i> , <i>S. lanceolatum</i> , <i>M. fragrans</i> , <i>T. hoensis</i> , <i>D. decandra</i> , <i>M. gagei</i> and <i>A. silvestris</i> 105
40	PC1 and PC2 score plots of the normalized and second derivative IR spectra of the ethyl acetate of Chan-chamot samples, <i>S. album</i> , <i>S. spicatum</i> , <i>S. lanceolatum</i> , <i>M. fragrans</i> , <i>T. hoensis</i> , <i>D. decandra</i> , <i>M. gagei</i> and <i>A. silvestris</i> 106
41	PC1, PC2 and PC3 three dimension score plots of the second derivative IR spectra of the acetone extracts of Chan-chamot, <i>S. album</i> , <i>S. spicatum</i> , <i>S. lanceolatum</i> , <i>M. fragrans</i> , <i>T. hoensis</i> , <i>D. decandra</i> , <i>M. gagei</i> and <i>A. silvestris</i> 107
42	HCA dendrogram the second derivative IR spectra of the dichloromethane extracts of Chan-thana samples, <i>S. album</i> , <i>S. spicatum</i> , <i>S. lanceolatum</i> , <i>M. fragrans</i> , <i>T. hoensis</i> , <i>D. decandra</i> , <i>M. gagei</i> and <i>A. silvestris</i> 108
43	HCA dendrogram the second derivative IR spectra of the acetone extracts of Chan-thana samples, <i>S. album</i> , <i>S. spicatum</i> , <i>S. lanceolatum</i> , <i>M. fragrans</i> , <i>T. hoensis</i> , <i>D. decandra</i> , <i>M. gagei</i> and <i>A. silvestris</i> 109

Figures	Page
44	PC1, PC2 and PC3 three dimension score plots of (a) normalized IR spectra and (b) second derivative IR spectra of the acetone extract of Chan-thana, <i>S. album</i> , <i>S. spicatum</i> , <i>S. lanceolatum</i> , <i>M. fragrans</i> , <i>T. hoaensis</i> , <i>D. decandra</i> , <i>M. gagei</i> and <i>A. silvestris</i> 110
45	HCA dendrogram the second derivative IR spectra of the ethyl acetate extracts of Chan-hom samples, <i>S. album</i> , <i>S. spicatum</i> , <i>S. lanceolatum</i> , <i>M. fragrans</i> , <i>T. hoaensis</i> , <i>D. decandra</i> , <i>M. gagei</i> and <i>A. silvestris</i> 111
46	HCA dendrogram the second derivative IR spectra of the acetone extracts of Chan-hom samples, <i>S. album</i> , <i>S. spicatum</i> , <i>S. lanceolatum</i> , <i>M. fragrans</i> , <i>T. hoaensis</i> , <i>D. decandra</i> , <i>M. gagei</i> and <i>A. silvestris</i> 112
47	HCA dendrogram the second derivative IR spectra of the methanol extracts of Chan-hom samples, <i>S. album</i> , <i>S. spicatum</i> , <i>S. lanceolatum</i> , <i>M. fragrans</i> , <i>T. hoaensis</i> , <i>D. decandra</i> , <i>M. gagei</i> and <i>A. silvestris</i> 112
48	PC1 and PC2 score plots of the normalized and second derivative IR spectra of the methanol extracts of Chan-hom samples, <i>S. album</i> , <i>S. spicatum</i> , <i>S. lanceolatum</i> , <i>M. fragrans</i> , <i>T. hoaensis</i> , <i>D. decandra</i> , <i>M. gagei</i> and <i>A. silvestris</i> 113
49	HCA dendrogram of GC chromatograms of the <i>n</i> -hexane extracts of Chan thet, Chan-khao, Chan-hom, <i>S. album</i> , <i>S. spicatum</i> and <i>S. lanceolatum</i> in the range of 15 to 23 min 116
50	Score plots of (a) PC1 and PC2, and (b) PC1 and PC3 of the GC chromatograms of the <i>n</i> -hexane extracts of Chan-thet (T1-T15), Chan-hom (H1-H9), Chan-khao (K18), <i>S. spicatum</i> , <i>S. album</i> and <i>S. lanceolatum</i> 117

Figures	Page
51	Loading plots of (a) PC1, (b) PC2 and (c) PC3 of the GC chromatograms of the <i>n</i> -hexane extracts of Chan-thet (T1-T15), Chan-hom (H1-H9), Chan-khao (K18), <i>S. spicatum</i> , <i>S. album</i> and <i>S. lanceolatum</i> 118
52	Mean GC chromatograms of the <i>n</i> -hexane extracts of samples group 1 (T4, T6, T7 and T14), group 2 (T5 and H1), and group 3 (T1-T3, T8-T13 and H2-H9) and GC chromatograms of the <i>n</i> -hexane extracts of <i>S. album</i> , <i>S. spicatum</i> and <i>S. lanceolatum</i> 119
53	GC fingerprint of the <i>n</i> -hexane extracts of Chan-thet (T1-T15), Chan-hom (H1-H9), Chan-khao (K18), <i>S. album</i> , <i>S. spicatum</i> and <i>S. lanceolatum</i> 121
54	GC fingerprints of (a) authentic <i>S. album</i> , (b) distilled <i>S. album</i> , (c) authentic <i>S. spicatum</i> , (d) distilled <i>S. spicatum</i> , (e) distilled <i>S. lanceolatum</i> , (f) authentic <i>S. austrocaledonicum</i> , (g) authentic <i>S. paniculatum</i> , (h) distilled sample T1, (i) distilled sample T4 and (j) distilled sample T9..... 126
55	PC1 and PC2 score plots of the (a) normalized and (b) second derivative IR spectra of the acetone extract of Chan-thet samples, Chan-khao samples, Chan-chamot samples, Chan-thana samples, Chan-hom samples, <i>S. album</i> , <i>S. spicatum</i> , <i>S. lanceolatum</i> , <i>M. fragrans</i> , <i>T. hoaensis</i> , <i>D. decandra</i> , <i>M. gagei</i> and <i>A. silvestris</i> 139
56	PC1 and PC2 loading plots of the normalized IR spectra of the acetone extracts of Chan-thet, Chan-khao, Chan-chamot, Chan-thana, and Chan-hom samples, <i>S. album</i> , <i>S. spicatum</i> , <i>S. lanceolatum</i> , <i>M. fragrans</i> , <i>T. hoaensis</i> , <i>D. decandra</i> , <i>M. gagei</i> and <i>A. silvestris</i> 139

Figures	Page
57	PC1 and PC2 score plot with hotelling T^2 limit at 1% of confidence of normalized IR spectra and second derivative IR spectra of acetone extract of (a) <i>Santalum</i> group, (b) MG group and (c) TH group 141
58	Authentication of the blind samples using SIMCA 3; (a) sample distance between <i>Santalum</i> group and MG group, (b) sample distance between <i>Santalum</i> group and TH group, and (c) sample distance between MG group and TH group 150
59	Characters of fifteen Chan-thet crude drug samples..... 181
60	Characters of eighteen Chan-khao crude drug samples..... 182
61	Characters of seventeen Chan-chamot crude drug samples..... 183
62	Characters of ten Chan-thana crude drug samples..... 184
63	Characters of eleven Chan-hom crude drug samples..... 185
64	Characters of authentic samples: <i>S. spicatum</i> , <i>S. album</i> , <i>S. lanceolatum</i> , <i>M. fragrans</i> , <i>T. hoaensis</i> , <i>D. decandra</i> , <i>M. gagei</i> and <i>A. silvestris</i> 186
65	EI-MS mass spectrum of α -santalol..... 188
66	IR spectrum of α -santalol (dry film)..... 188
67	$^1\text{H-NMR}$ spectrum (300 MHz) of α -santalol (in CDCl_3)..... 189
68	$^{13}\text{C-NMR}$ spectrum (75 MHz) of α -santalol (in CDCl_3)..... 190
69	(+)-ESI-MS mass spectrum of mansonone G..... 191
70	IR spectrum of mansonone G (KBr)..... 191
71	$^{13}\text{C-NMR}$ spectrum (75 MHz) of mansonone G (in CDCl_3) 192
72	$^1\text{H-NMR}$ spectrum (300 MHz) of mansonone G (in CDCl_3) 193
73	(+)-ESI-MS mass spectrum of geniposidic acid 194
74	IR spectrum of geniposidic acid (dry film)..... 194
75	$^{13}\text{C-NMR}$, DEPT 90° and DEPT 135° spectrum (75 MHz) of geniposidic acid (in CD_3OD) 195
76	$^1\text{H-NMR}$ spectrum (300 MHz) of geniposidic acid (in CD_3OD) 196
77	HMBC spectrum of geniposidic acid (in CD_3OD) 197

Figures	Page
78	NOSEY spectrum of geniposidic acid (in CD ₃ OD)..... 198
79	IR spectra of the <i>n</i> -hexane extracts of Chan-thet, Chan-khao, Chan-chamot, Chan-thana and Chan-hom samples after normalization preprocessing..... 200
80	IR spectra of the dichloromethane extracts of Chan-thet, Chan-khao, Chan-chamot, Chan-thana and Chan-hom samples after normalization preprocessing..... 200
81	IR spectra of the ethyl acetate extracts of Chan-thet, Chan-khao, Chan-chamot, Chan-thana and Chan-hom samples after normalization preprocessing..... 200
82	IR spectra of the acetone extracts of Chan-thet, Chan-khao, Chan-chamot, Chan-thana and Chan-hom samples after normalization preprocessing 201
83	IR spectra of the methanol extracts of Chan-thet, Chan-khao, Chan-chamot, Chan-thana and Chan-hom samples after normalization preprocessing..... 201
84	IR spectra of the water extracts of Chan-thet, Chan-khao, Chan-chamot, Chan-thana and Chan-hom samples after normalization preprocessing..... 201
85	IR spectra of the fine powders of Chan-thet, Chan-khao, Chan-chamot, Chan-thana and Chan-hom samples after normalization preprocessing..... 202
86	IR spectra of the <i>n</i> -hexane extracts of Chan-thet, Chan-khao, Chan-chamot, Chan-thana and Chan-hom samples after normalization and second derivative preprocessing 202
87	IR spectra of the dichloromethane extracts of Chan-thet, Chan-khao, Chan-chamot, Chan-thana and Chan-hom samples after normalization and second derivative preprocessing..... 202

Figures	Page
88	IR spectra of the ethyl acetate extracts of Chan-thet, Chan-khao, Chan-chamot, Chan-thana and Chan-hom samples after normalization and second derivative preprocessing 203
89	IR spectra of the acetone extracts of Chan-thet, Chan-khao, Chan-chamot, Chan-thana and Chan-hom samples after normalization and second derivative preprocessing 203
90	IR spectra of the methanol extracts of Chan-thet, Chan-khao, Chan-chamot, Chan-thana and Chan-hom samples after normalization and second derivative preprocessing 203
91	IR spectra of the water extracts of Chan-thet, Chan-khao, Chan-chamot, Chan-thana and Chan-hom samples after normalization and second derivative preprocessing 204
92	IR spectra of the fine powders of Chan-thet, Chan-khao, Chan-chamot, Chan-thana and Chan-hom samples after normalization and second derivative preprocessing 204
93	IR spectra of the <i>n</i> -hexane extracts of <i>S. album</i> , <i>S. spicatum</i> , <i>S. lanceolatum</i> , <i>M. fragrans</i> , <i>T. hoaensis</i> , <i>D. decandra</i> , <i>M. gagei</i> and <i>A. silvestris</i> after normalization preprocessing 205
94	IR spectra of the dichloromethane extracts of <i>S. album</i> , <i>S. spicatum</i> , <i>S. lanceolatum</i> , <i>M. fragrans</i> , <i>T. hoaensis</i> , <i>D. decandra</i> , <i>M. gagei</i> and <i>A. silvestris</i> after normalization preprocessing 205
95	IR spectra of the ethyl acetate extracts of <i>S. album</i> , <i>S. spicatum</i> , <i>S. lanceolatum</i> , <i>M. fragrans</i> , <i>T. hoaensis</i> , <i>D. decandra</i> , <i>M. gagei</i> and <i>A. silvestris</i> after normalization preprocessing 205
96	IR spectra of the acetone extracts of <i>S. album</i> , <i>S. spicatum</i> , <i>S. lanceolatum</i> , <i>M. fragrans</i> , <i>T. hoaensis</i> , <i>D. decandra</i> , <i>M. gagei</i> and <i>A. silvestris</i> after normalization preprocessing 206
97	IR spectra of the methanol extracts of <i>S. album</i> , <i>S. spicatum</i> , <i>S. lanceolatum</i> , <i>M. fragrans</i> , <i>T. hoaensis</i> , <i>D. decandra</i> , <i>M. gagei</i> and <i>A. silvestris</i> after normalization preprocessing 206

Figures	Page
98	IR spectra of the water extracts of <i>S. album</i> , <i>S. spicatum</i> , <i>S. lanceolatum</i> , <i>M. fragrans</i> , <i>T. hoaensis</i> , <i>D. decandra</i> , <i>M. gagei</i> and <i>A. silvestris</i> after normalization preprocessing 206
99	IR spectra of the fine powders of <i>S. album</i> , <i>S. spicatum</i> , <i>S. lanceolatum</i> , <i>M. fragrans</i> , <i>T. hoaensis</i> , <i>D. decandra</i> , <i>M. gagei</i> and <i>A. silvestris</i> after normalization preprocessing 207
100	IR spectra of the <i>n</i> -hexane extracts of <i>S. album</i> , <i>S. spicatum</i> , <i>S. lanceolatum</i> , <i>M. fragrans</i> , <i>T. hoaensis</i> , <i>D. decandra</i> , <i>M. gagei</i> and <i>A. silvestris</i> after normalization and second derivative preprocessing 207
101	IR spectra of the dichloromethane extracts of <i>S. album</i> , <i>S. spicatum</i> , <i>S. lanceolatum</i> , <i>M. fragrans</i> , <i>T. hoaensis</i> , <i>D. decandra</i> , <i>M. gagei</i> and <i>A. silvestris</i> after normalization and second derivative preprocessing 207
102	IR spectra of the ethyl acetate extracts of <i>S. album</i> , <i>S. spicatum</i> , <i>S. lanceolatum</i> , <i>M. fragrans</i> , <i>T. hoaensis</i> , <i>D. decandra</i> , <i>M. gagei</i> and <i>A. silvestris</i> after normalization and second derivative preprocessing 208
103	IR spectra of the acetone extracts of <i>S. album</i> , <i>S. spicatum</i> , <i>S. lanceolatum</i> , <i>M. fragrans</i> , <i>T. hoaensis</i> , <i>D. decandra</i> , <i>M. gagei</i> and <i>A. silvestris</i> after normalization and second derivative preprocessing 208
104	IR spectra of the methanol extracts of <i>S. album</i> , <i>S. spicatum</i> , <i>S. lanceolatum</i> , <i>M. fragrans</i> , <i>T. hoaensis</i> , <i>D. decandra</i> , <i>M. gagei</i> and <i>A. silvestris</i> after normalization and second derivative preprocessing 208
105	IR spectra of the water extracts of <i>S. album</i> , <i>S. spicatum</i> , <i>S. lanceolatum</i> , <i>M. fragrans</i> , <i>T. hoaensis</i> , <i>D. decandra</i> , <i>M. gagei</i> and <i>A. silvestris</i> after normalization and second derivative preprocessing 209

Figures	Page	
106	IR spectra of the fine powders of <i>S. album</i> , <i>S. spicatum</i> , <i>S. lanceolatum</i> , <i>M. fragrans</i> , <i>T. hoaensis</i> , <i>D. decandra</i> , <i>M. gagei</i> and <i>A. silvestris</i> after normalization and second derivative preprocessing.....	206
107	HCA dendrogram the IR spectra of the <i>n</i> -hexane extracts of Chan-thet samples, <i>S. album</i> , <i>S. spicatum</i> , <i>S. lanceolatum</i> , <i>M. fragrans</i> , <i>T. hoaensis</i> , <i>D. decandra</i> , <i>M. gagei</i> and <i>A. silvestris</i> after normalization preprocessing.....	228
108	HCA dendrogram the IR spectra of the methanol extracts of Chan-thet samples, <i>S. album</i> , <i>S. spicatum</i> , <i>S. lanceolatum</i> , <i>M. fragrans</i> , <i>T. hoaensis</i> , <i>D. decandra</i> , <i>M. gagei</i> and <i>A. silvestris</i> after normalization preprocessing.....	228
109	HCA dendrogram the IR spectra of the dichloromethane extracts of Chan-thet samples, <i>S. album</i> , <i>S. spicatum</i> , <i>S. lanceolatum</i> , <i>M. fragrans</i> , <i>T. hoaensis</i> , <i>D. decandra</i> , <i>M. gagei</i> and <i>A. silvestris</i> after (a) normalization and (b) second derivative preprocessing....	229
110	HCA dendrogram the IR spectra of the ethyl acetate extracts of Chan-thet samples, <i>S. album</i> , <i>S. spicatum</i> , <i>S. lanceolatum</i> , <i>M. fragrans</i> , <i>T. hoaensis</i> , <i>D. decandra</i> , <i>M. gagei</i> and <i>A. silvestris</i> after (a) normalization and (b) second derivative preprocessing....	230
111	HCA dendrogram the IR spectra of the acetone extracts of Chan-thet samples, <i>S. album</i> , <i>S. spicatum</i> , <i>S. lanceolatum</i> , <i>M. fragrans</i> , <i>T. hoaensis</i> , <i>D. decandra</i> , <i>M. gagei</i> and <i>A. silvestris</i> after (a) normalization and (b) second derivative preprocessing....	231
112	HCA dendrogram the IR spectra of the water extracts of Chan-thet samples, <i>S. album</i> , <i>S. spicatum</i> , <i>S. lanceolatum</i> , <i>M. fragrans</i> , <i>T. hoaensis</i> , <i>D. decandra</i> , <i>M. gagei</i> and <i>A. silvestris</i> after (a) normalization and (b) second derivative preprocessing....	232

Figures	Page
113 HCA dendrogram the IR spectra of the fine powders of Chan-thet samples, <i>S. album</i> , <i>S. spicatum</i> , <i>S. lanceolatum</i> , <i>M. fragrans</i> , <i>T. hoaensis</i> , <i>D. decandra</i> , <i>M. gagei</i> and <i>A. silvestris</i> after normalization preprocessing.....	233
114 HCA dendrogram the IR spectra of the <i>n</i> -hexane extracts of Chan-khao samples, <i>S. album</i> , <i>S. spicatum</i> , <i>S. lanceolatum</i> , <i>M. fragrans</i> , <i>T. hoaensis</i> , <i>D. decandra</i> , <i>M. gagei</i> and <i>A. silvestris</i> after normalization and preprocessing	233
115 HCA dendrogram the IR spectra of the dichloromethane extracts of Chan-khao samples, <i>S. album</i> , <i>S. spicatum</i> , <i>S. lanceolatum</i> , <i>M. fragrans</i> , <i>T. hoaensis</i> , <i>D. decandra</i> , <i>M. gagei</i> and <i>A. silvestris</i> after (a) normalization and (b) second derivative preprocessing	234
116 HCA dendrogram the IR spectra of the ethyl acetate extracts of Chan-khao samples, <i>S. album</i> , <i>S. spicatum</i> , <i>S. lanceolatum</i> , <i>M. fragrans</i> , <i>T. hoaensis</i> , <i>D. decandra</i> , <i>M. gagei</i> and <i>A. silvestris</i> after (a) normalization and (b) second derivative preprocessing	235
117 HCA dendrogram the IR spectra of the acetone extracts of Chan-khao samples, <i>S. album</i> , <i>S. spicatum</i> , <i>S. lanceolatum</i> , <i>M. fragrans</i> , <i>T. hoaensis</i> , <i>D. decandra</i> , <i>M. gagei</i> and <i>A. silvestris</i> after (a) normalization and (b) second derivative preprocessing	236
118 HCA dendrogram the IR spectra of the methanol extracts of Chan-khao samples, <i>S. album</i> , <i>S. spicatum</i> , <i>S. lanceolatum</i> , <i>M. fragrans</i> , <i>T. hoaensis</i> , <i>D. decandra</i> , <i>M. gagei</i> and <i>A. silvestris</i> after (a) normalization and (b) second derivative preprocessing	237
119 HCA dendrogram the IR spectra of the water extracts of Chan-khao samples, <i>S. album</i> , <i>S. spicatum</i> , <i>S. lanceolatum</i> , <i>M. fragrans</i> , <i>T. hoaensis</i> , <i>D. decandra</i> , <i>M. gagei</i> and <i>A. silvestris</i> after (a) normalization and (b) second derivative preprocessing	238

Figures	Page
120	HCA dendrogram the IR spectra of the fine powders of Chan-khao samples, <i>S. album</i> , <i>S. spicatum</i> , <i>S. lanceolatum</i> , <i>M. fragrans</i> , <i>T. hoaensis</i> , <i>D. decandra</i> , <i>M. gagei</i> and <i>A. silvestris</i> after normalization preprocessing..... 239
121	HCA dendrogram the IR spectra of the <i>n</i> -hexane extracts of Chan-chamot samples, <i>S. album</i> , <i>S. spicatum</i> , <i>S. lanceolatum</i> , <i>M. fragrans</i> , <i>T. hoaensis</i> , <i>D. decandra</i> , <i>M. gagei</i> and <i>A. silvestris</i> after (a) normalization and (b) second derivative preprocessing.... 240
122	HCA dendrogram the IR spectra of the dichloromethane extracts of Chan-chamot samples, <i>S. album</i> , <i>S. spicatum</i> , <i>S. lanceolatum</i> , <i>M. fragrans</i> , <i>T. hoaensis</i> , <i>D. decandra</i> , <i>M. gagei</i> and <i>A. silvestris</i> after (a) normalization and (b) second derivative preprocessing.... 241
123	HCA dendrogram the IR spectra of the ethyl acetate extracts of Chan-chamot samples, <i>S. album</i> , <i>S. spicatum</i> , <i>S. lanceolatum</i> , <i>M. fragrans</i> , <i>T. hoaensis</i> , <i>D. decandra</i> , <i>M. gagei</i> and <i>A. silvestris</i> after (a) normalization and (b) second derivative preprocessing.... 242
124	HCA dendrogram the IR spectra of the acetone extracts of Chan-chamot samples, <i>S. album</i> , <i>S. spicatum</i> , <i>S. lanceolatum</i> , <i>M. fragrans</i> , <i>T. hoaensis</i> , <i>D. decandra</i> , <i>M. gagei</i> and <i>A. silvestris</i> after (a) normalization and (b) second derivative preprocessing.... 243
125	HCA dendrogram the IR spectra of the methanol extracts of Chan-chamot samples, <i>S. album</i> , <i>S. spicatum</i> , <i>S. lanceolatum</i> , <i>M. fragrans</i> , <i>T. hoaensis</i> , <i>D. decandra</i> , <i>M. gagei</i> and <i>A. silvestris</i> after (a) normalization and (b) second derivative preprocessing.... 244
126	HCA dendrogram the IR spectra of the water extracts of Chan-chamot samples, <i>S. album</i> , <i>S. spicatum</i> , <i>S. lanceolatum</i> , <i>M. fragrans</i> , <i>T. hoaensis</i> , <i>D. decandra</i> , <i>M. gagei</i> and <i>A. silvestris</i> after (a) normalization and (b) second derivative preprocessing.... 245

Figures	Page
127	HCA dendrogram the IR spectra of the fine powders of Chan-chamot samples, <i>S. album</i> , <i>S. spicatum</i> , <i>S. lanceolatum</i> , <i>M. fragrans</i> , <i>T. hoaensis</i> , <i>D. decandra</i> , <i>M. gagei</i> and <i>A. silvestris</i> after (a) normalization and (b) second derivative preprocessing.... 246
128	HCA dendrogram the IR spectra of the <i>n</i> -hexane extracts of Chan-thana samples, <i>S. album</i> , <i>S. spicatum</i> , <i>S. lanceolatum</i> , <i>M. fragrans</i> , <i>T. hoaensis</i> , <i>D. decandra</i> , <i>M. gagei</i> and <i>A. silvestris</i> after (a) normalization and (b) second derivative preprocessing.... 247
129	HCA dendrogram the IR spectra of the dichloromethane extracts of Chan-thana samples, <i>S. album</i> , <i>S. spicatum</i> , <i>S. lanceolatum</i> , <i>M. fragrans</i> , <i>T. hoaensis</i> , <i>D. decandra</i> , <i>M. gagei</i> and <i>A. silvestris</i> after (a) normalization and (b) second derivative preprocessing.... 248
130	HCA dendrogram the IR spectra of the ethyl acetate extracts of Chan-thana samples, <i>S. album</i> , <i>S. spicatum</i> , <i>S. lanceolatum</i> , <i>M. fragrans</i> , <i>T. hoaensis</i> , <i>D. decandra</i> , <i>M. gagei</i> and <i>A. silvestris</i> after (a) normalization and (b) second derivative preprocessing.... 249
131	HCA dendrogram the IR spectra of the acetone extracts of Chan-thana samples, <i>S. album</i> , <i>S. spicatum</i> , <i>S. lanceolatum</i> , <i>M. fragrans</i> , <i>T. hoaensis</i> , <i>D. decandra</i> , <i>M. gagei</i> and <i>A. silvestris</i> after (a) normalization and (b) second derivative preprocessing.... 250
132	HCA dendrogram the IR spectra of the methanol extracts of Chan-thana samples, <i>S. album</i> , <i>S. spicatum</i> , <i>S. lanceolatum</i> , <i>M. fragrans</i> , <i>T. hoaensis</i> , <i>D. decandra</i> , <i>M. gagei</i> and <i>A. silvestris</i> after (a) normalization and (b) second derivative preprocessing.... 251
133	HCA dendrogram the IR spectra of the water extracts of Chan-thana samples, <i>S. album</i> , <i>S. spicatum</i> , <i>S. lanceolatum</i> , <i>M. fragrans</i> , <i>T. hoaensis</i> , <i>D. decandra</i> , <i>M. gagei</i> and <i>A. silvestris</i> after (a) normalization and (b) second derivative preprocessing.... 252

Figures	Page
134	HCA dendrogram the IR spectra of the fine powders of Chan-thana samples, <i>S. album</i> , <i>S. spicatum</i> , <i>S. lanceolatum</i> , <i>M. fragrans</i> , <i>T. hoaensis</i> , <i>D. decandra</i> , <i>M. gagei</i> and <i>A. silvestris</i> after (a) normalization and (b) second derivative preprocessing.... 253
135	HCA dendrogram the IR spectra of the <i>n</i> -hexane extracts of Chan-hom samples, <i>S. album</i> , <i>S. spicatum</i> , <i>S. lanceolatum</i> , <i>M. fragrans</i> , <i>T. hoaensis</i> , <i>D. decandra</i> , <i>M. gagei</i> and <i>A. silvestris</i> after (a) normalization and (b) second derivative preprocessing.... 254
136	HCA dendrogram the IR spectra of the dichloromethane extracts of Chan-hom samples, <i>S. album</i> , <i>S. spicatum</i> , <i>S. lanceolatum</i> , <i>M. fragrans</i> , <i>T. hoaensis</i> , <i>D. decandra</i> , <i>M. gagei</i> and <i>A. silvestris</i> after (a) normalization and (b) second derivative preprocessing.... 255
137	HCA dendrogram the IR spectra of the ethyl acetate extracts of Chan-hom samples, <i>S. album</i> , <i>S. spicatum</i> , <i>S. lanceolatum</i> , <i>M. fragrans</i> , <i>T. hoaensis</i> , <i>D. decandra</i> , <i>M. gagei</i> and <i>A. silvestris</i> after (a) normalization and (b) second derivative preprocessing.... 256
138	HCA dendrogram the IR spectra of the acetone extracts of Chan-hom samples, <i>S. album</i> , <i>S. spicatum</i> , <i>S. lanceolatum</i> , <i>M. fragrans</i> , <i>T. hoaensis</i> , <i>D. decandra</i> , <i>M. gagei</i> and <i>A. silvestris</i> after (a) normalization and (b) second derivative preprocessing.... 257
139	HCA dendrogram the IR spectra of the methanol extracts of Chan-hom samples, <i>S. album</i> , <i>S. spicatum</i> , <i>S. lanceolatum</i> , <i>M. fragrans</i> , <i>T. hoaensis</i> , <i>D. decandra</i> , <i>M. gagei</i> and <i>A. silvestris</i> after (a) normalization and (b) second derivative preprocessing.... 158
140	HCA dendrogram the IR spectra of the water extracts of Chan-hom samples, <i>S. album</i> , <i>S. spicatum</i> , <i>S. lanceolatum</i> , <i>M. fragrans</i> , <i>T. hoaensis</i> , <i>D. decandra</i> , <i>M. gagei</i> and <i>A. silvestris</i> after (a) normalization and (b) second derivative preprocessing.... 259

Figures	Page	
141	HCA dendrogram the IR spectra of the fine powders of Chan-hom samples, <i>S. album</i> , <i>S. spicatum</i> , <i>S. lanceolatum</i> , <i>M. fragrans</i> , <i>T. hoaensis</i> , <i>D. decandra</i> , <i>M. gagei</i> and <i>A. silvestris</i> after (a) normalization and (b) second derivative preprocessing....	260
142	PC1 and PC2 score plots of the normalized and second derivative IR spectra of the (a) dichloromethane, (b) ethyl acetate, and (c) water extracts, and (d) the fine powders of Chan-thet samples, <i>S. album</i> , <i>S. spicatum</i> , <i>S. lanceolatum</i> , <i>M. fragrans</i> , <i>T. hoaensis</i> , <i>D. decandra</i> , <i>M. gagei</i> and <i>A. silvestris</i>	262
143	PC1 and PC2 score plots of the normalized and second derivative IR spectra of the (a) <i>n</i> -hexane, (b) dichloromethane, (c) ethyl acetate, (d) acetone, (e) methanol and (f) water extracts; and (g) the fine powders of Chan-khao samples, <i>S. album</i> , <i>S. spicatum</i> , <i>S. lanceolatum</i> , <i>M. fragrans</i> , <i>T. hoaensis</i> , <i>D. decandra</i> , <i>M. gagei</i> and <i>A. silvestris</i>	264
144	PC1 and PC2 score plots of the normalized and second derivative IR spectra of the (a) <i>n</i> -hexane, (b) dichloromethane, (c) ethyl acetate, (d) acetone, (e) methanol and (f) water extracts; and (g) the fine powders of Chan-chamot samples, <i>S. album</i> , <i>S. spicatum</i> , <i>S. lanceolatum</i> , <i>M. fragrans</i> , <i>T. hoaensis</i> , <i>D. decandra</i> , <i>M. gagei</i> and <i>A. silvestris</i>	267
145	PC1, PC2 and PC3 three dimension score plots of (a) normalized IR spectra and (b) second derivative IR spectra of the dichloromethane extracts of Chan-chamot, <i>S. album</i> , <i>S. spicatum</i> , <i>S. lanceolatum</i> , <i>M. fragrans</i> , <i>T. hoaensis</i> , <i>D. decandra</i> , <i>M. gagei</i> and <i>A. silvestris</i>	270

Figures	Page	
146	PC1 and PC2 score plots of the normalized and second derivative IR spectra of the (a) <i>n</i> -hexane, (b) dichloromethane, (c) ethyl acetate, (d) acetone, (e) methanol and (f) water extracts; and (g) the fine powders of Chan-thana samples, <i>S. album</i> , <i>S. spicatum</i> , <i>S. lanceolatum</i> , <i>M. fragrans</i> , <i>T. hoaensis</i> , <i>D. decandra</i> , <i>M. gagei</i> and <i>A. silvestris</i>	271
147	PC1 and PC2 score plots of the normalized and second derivative IR spectra of the (a) <i>n</i> -hexane, (b) dichloromethane, (c) ethyl acetate, (d) acetone, (e) methanol and (f) water extracts; and (g) the fine powders of Chan-hom samples, <i>S. album</i> , <i>S. spicatum</i> , <i>S. lanceolatum</i> , <i>M. fragrans</i> , <i>T. hoaensis</i> , <i>D. decandra</i> , <i>M. gagei</i> and <i>A. silvestris</i>	274
148	GC fingerprints of the <i>n</i> -hexane extracts of <i>S. spicatum</i> , <i>S. album</i> , <i>S. lanceolatum</i> , <i>M. fragrans</i> , <i>T. hoaensis</i> , <i>D. decandra</i> and <i>M. gagei</i>	278
149	GC fingerprints of the <i>n</i> -hexane extracts of Chan-thet samples	278
150	GC fingerprints of the <i>n</i> -hexane extracts of Chan-khao samples	279
151	GC fingerprints of the <i>n</i> -hexane extracts of Chan-chamot samples	279
152	GC fingerprints of the <i>n</i> -hexane extracts of Chan-thana samples	280
153	GC fingerprints of the <i>n</i> -hexane extract of Chan-hom samples	280
154	Regression coefficients of PLS models 1 (normalized IR spectra at 1801-501 cm ⁻¹) of (a) <i>Santalum</i> group, (b) MG group and (c) TH group	282
155	Regression coefficient of PLS model 2 (normalized IR spectra at 1801-1500 cm ⁻¹) of (a) <i>Santalum</i> group, (b) MG group and (c) TH group	283

Figures	Page
156	Regression coefficient of PLS model 3 (normalized IR spectra at 1498-501 cm ⁻¹) of (a) <i>Santalum</i> group, (b) MG group and (c) TH group 284
157	Regression coefficient of PLS model 4 (normalized and second derivative IR spectra at 1801-501 cm ⁻¹) of (a) <i>Santalum</i> group, (b) MG group and (c) TH group 285
158	Regression coefficient of PLS model 5 (normalized and second derivative IR spectra at 1801-1500 cm ⁻¹) of (a) <i>Santalum</i> group, (b) MG group and (c) TH group 286
159	Regression coefficient of PLS model 6 (normalized and second derivative IR spectra at 1498-501 cm ⁻¹) of (a) <i>Santalum</i> group, (b) MG group and (c) TH group 287
160	Prediction of test set samples using PLS-DA method 1 of (a) <i>Santalum</i> group, (b) MG group and (c) TH group 289
161	Prediction of test set samples using PLS-DA method 2 of (a) <i>Santalum</i> group, (b) MG group and (c) TH group 290
162	Prediction of test set samples using PLS-DA method 3 of (a) <i>Santalum</i> group, (b) MG group and (c) TH group 291
163	Prediction of test set samples of using PLS-DA method 4 of (a) <i>Santalum</i> group, (b) MG group and (c) TH group 292
164	Prediction of test set samples using PLS-DA method 5 of (a) <i>Santalum</i> group, (b) MG group and (c) TH group 293
165	Prediction of test set samples using PLS-DA method 6 of (a) <i>Santalum</i> group, (b) MG group and (c) TH group 294

List of Schemes

Schemes	Page
1 Isolation of α -santalol from heartwood of <i>S. album</i>	48
2 Isolation of mansonone G from Chan-chamot sample	50
3 Isolation of geniposidic acid from the heartwood of Chan-khao sample	52



CHAPTER I

INTRODUCTION

“Chan(s)” is name of many herbs or crude drugs of Thailand, e.g. Chan-thet, Chan-khao, Chan-chamot, Chan-thana, Chan-hom, etc. These crude drugs are popularly used in Thai traditional medicine. In advancement of the herb in health system supported by the National Pharmaceutical System Development Commission, the topic of herbal medicines was continuously introduced into the National List of Essential Medicines (NLEM) to allow application of the herb from Thai ancient wisdom. Many Thai traditional prescriptions in this List have “Chan(s)” as an important ingredient. For example, Ya-hom Thepjit (ยาหอมเทพจิตร) has Chan-khao or Chan-chamot. It is used for the symptoms concerning blood circular system. Ya-Apaisalee (ยาอภิบาลี) has Chan-thet. It is used for the symptoms concerning gastrointestinal system. Ya-Chanthaleela (ยาจันทลีลา) has Chan-khao or Chan-chamot. It is used to treat fever [1].

The problem of using herbs named Chan(s) is uncertainty and confusing in their species identification. Their scientific or botanical names are possibly both same and different. For example, Chan-thet in “Thai crude drug 1” and “The explanation of Narayana’s medicines textbook” is referred to a tree which has red aril. It is known as nutmeg or *Myristica fragrans* Houtt. (family Myristicaceae) [2-4]. But Chan-thet mentioned in “Quality of Thai crude drug from research to sustainable development” and “Handbook of Thai traditional pharmacy volume 2: crude drug from herbal plants” is a semi-parasitic small tree which the color of freshly bloom flower similar to rice straw then the color will change to magenta. Its wood has unique fragrance. It is *Santalum album* Linn. (family Santalaceae), sandalwood [5, 6], Mai-hom-gan-chan [7], Mai-hom-India, Indian sandalwood or white sandalwood [8, 9]. *S. album* is also described as a botanical name of Chan-khao [10, 11]. The other herb that was identified as Chan khao is *Diospyros decandra* Lour. (family Ebenaceae) of which fruit has strongly flavoring smell. It is known as “Luk-

in”, Chan-luk-hom, Chan-in, Chan-o and In [3, 8]. Moreover some references identified Chan-khao as the same species as Chan-thana which was identified as *Tarenna hoaensis* Pit. (family Rubiaceae) [4]. Chan-thana is also known as Chan-hom in Rayong province, Chan-bai-lek in Prachuap Khiri Khan and Chan-ta-nia in Khmer-Eastern [2, 4, 8]. Furthermore, Chan-khao is the synonym of Chan-chamot, Chan-phama and Chan-hom which was identified as *Mansonia gagei* J.R.Drumm. Ex Prain (family Sterculiaceae). This plant is a shed leaves tree. It is 10-20 m height with smooth white grey bark, dark brown heartwood, oblong margin ovate simple leaf, white flower, spindle fruit with one triangle wing and its died wood has like musk-like smell [2-4, 8]. The other identified species of Chan-chamot by some references is *Aglaia silvestris* (M.Roem) Merr. (family Meliaceae). It is a tree, 15-30 m height with white grey bark, dark-brown heartwood, pinnately compound leaves, lanceolate shape, entire margin, small yellow flower and circular fruit [2, 4, 8].

The crude drug named “Chan” originated from the plant genus *Santalum*, is the other concerning issue. More than 15 species of *Santalum* spp. are found in Timor Indonesia, India, Nepal, Sri Lanka, Java, Bali, Tonga, Fiji, Vanuatu, France and Australia. All of them have economical valuable essential oil [12-15]. However *S. album* (Indian sandalwood), *S. spicatum* (Western Australian sandalwood) and *S. lanceolatum* (Northern Australian sandalwood) are three important commercial species that were imported and exported to Australia, China, Taiwan, Sri Lanka, Indonesia and South East Asia [16-19]. Therefore *S. album* available in the market of Thailand may be substituted with the other *Santalum* species.

Substitution of herbal medicines may occur intentionally or unintentionally. Cause of unintentional adulteration or substitution may be come from the lack of proper evaluation methods of herbal medicines available in market. The issues that can initiate the substitution of herbal medicines are such as faulty collection, imperfect preparation, incorrect storage, some parts of plant material substitution, and substitution with exhausted drugs [20]. In the past, medicinal plants and crude drugs were identified by folk professional herbalists who can identify skillfully with their experience regarding aspect of medicinal plants such as size,

color, surface characteristics, texture, fracture characteristics, odor and taste. Currently, a number of folk professional herbalists have been decreased. Therefore the knowledge of proficient identification has been going lost. However herbal medicine authentication still has been concerned to ensure the accuracy of genuine material. Thus scientific analysis becomes an important method which contributes to correctly clarify herbal medicines, for example authentication and identification using chromatographic evaluation [21]. An analysis of general modern synthetic medicines may not be complex on account of knowing major active ingredients that can be directly compared with chemical standards and the analysis. Results generally relate to efficacy of the medicines. In contrast, herbal medicines analysis using only the major chemical constituents may not appropriate because biological or pharmacological activity and efficacy of herbal medicines are obtained from their overall chemical constituents [22]. Therefore chemical fingerprint analysis which will provide the overview of herbal medicine of chemical information is interesting.

Chemical fingerprint analysis is a technique which use for identification and authentication of herbs [22-24]. Due to health concerning, the World Health Organization (WHO) decided quality and efficacy assessment of single and formulae herbal medicines. Fingerprint analysis is an interesting technique since it is utilized to identify herbal medicines [25, 26]. Chemical fingerprints are the data that obtain from various analysis techniques such as thin-layer chromatography, gas chromatography, high performance liquid chromatography, ultraviolet/visible spectroscopy and infrared spectroscopy that are well-known techniques for analyst. Moreover the instrument can connect with many detectors such as mass spectroscopy detector, diode array detector and refractive index detector. The analysis data are difference depending on each technique and detector.

Owing to the complication of chemical fingerprint, chemometrics is applied to demonstrate the chemical fingerprint analysis. Chemometrics is science of extraction and integration chemical data by mathematics and/or statistics thus it handles complex or multivariate data, such as chemical fingerprint [27-29]. The pattern recognition part of chemometrics has been useful for herbal identification. It is separated to unsupervised learning and supervised learning. The examples of

unsupervised learning technique are similarity analysis (SA), hierarchical cluster analysis (HCA), principal component analysis (PCA), etc. As well, supervised learning techniques are soft independent modeling of class analogy (SIMCA), k-nearest neighbor (k-NN), linear discriminant analysis (LDA), partial least squares-discriminant analysis (PLS-DA), etc [28, 30]. Many previous studies have applied these chemometric methods to identify and authenticate herbs. Haidy *et al.* [31] reported the authentication and quality assessment of *Thymus* species which applied unsupervised learning techniques as hierarchical cluster analysis (HCA) and principal component analysis (PCA) to identify and classify the eight species of *Thymus* and Thyme tea. Furthermore soft independent modeling of class analogy (SIMCA), supervised learning technique, was used to distinguish *T. vulgaris* from other *Thymus* species. Wong *et al.* [32] used PLS-DA to differentiate two close species between *Pueraria lobata* and *P. thomsonii*. The PLS-DA was performed by unsupervised learning technique and it was a technique for the quality control of *P. lobata* and other herbal materials in the manufacture.

As mention above, the crude drugs named Chan(s), i.e. Chan-thet, Chan-khao, Chan-chamot, Chan-thana and Chan-hom possibly have a problem regarding substitution in the market. The application of chemical fingerprint analysis and chemometrics are interesting to resolve this problem. Therefore the aim of this study was to identify the botanical origins of these crude drugs by chemical fingerprint coupled with chemometric methods. The reliable models to discriminate and authenticate these crude drugs were also developed. Since botanical identification and authentication are the important issues of herbal quality control in pharmacopoeias and recommended by WHO [21], this study will gain more ideas for the quality control method of Thai medicinal plants.

Goals and objectives

1. To identify the botanical names of Chan-thet, Chan-khao, Chan-chamot, Chan-thana and Chan-hom.
2. To establish the methods for the discrimination of Chan-thet, Chan-khao, Chan-chamot, Chan-thana and Chan-hom.

CHAPTER II

LITERATURE REVIEW

1 Thai traditional use of Chan(s)

Chan-thet, Chan-khao and Chan-chamot have been recorded in Thai medical textbooks, whereas the names of Chan-thana and Chan-hom were found in some herbal textbooks. Their usage and character are explained as follows.

1.1 Chan-thet

Its heartwood has, aromatic and hot or mild tastes (รสหอมร้อนหรือหอมสุขุม) [33]. It is used to relieve fever, biliary diseases (ดีกำริบ), jactation (กระสับกระส่าย) and dizziness. Its fruit possesses aromatic smell and sour, astringent and hot tastes. It is used for dyspepsia, colic, catarrhal symptom (แก้อาเจา), diarrhea, aphthous ulcer, thirsty, uteralgia, and blood tonic (บำรุงเลือด). Its flower has aromatic smell and hot and spicy tastes (รสเผ็ดร้อน). It is used for blood tonic, carminative, pulmonohepatotonic (บำรุงตับปอด), cardiotoxic and choleric (บำรุงน้ำดี) [6]. Its aril (mace) has hot and spicy tastes (รสเผ็ดร้อน). It is used for blood tonic, element tonic (บำรุงธาตุ) and carminative. Its seed used for element tonic, disorder of four elements (แก้ธาตุพิการ), carminative, uterodinia (แก้ปวดมดลูก) and blood tonic [33]. This crude drug has ever been identified as *Santalum album* L. [34] or *Myristica fragrans* Houtt. [2, 4, 6, 34, 35].

1.2 Chan-khao

Its wood possesses bitter and sweet tastes. It is used for febrifugal, aphthous ulcer, thirsty, neurotonic, skin tonic and anthelmintic. Moreover it used for liver, pulmonary and bile diseases (ตับปอดน้ำดีพิการ). Its heartwood possesses aromatic and cool tastes (รสหอมเย็น). It is used for febrifugal, dizziness (แก้ลม) and choleric (บำรุงน้ำดี) [33]. This crude drug has ever been identified as *Diospyros decandra* Lour. [4, 34, 36, 37] or *Tarenna hoaensis* Pit. [2].

1.3 Chan-chamot

Its wood has mild taste (รสหอมสุขุม). It is used to relieve fever, nausea and vomiting and dizziness (แก้ลมวิงเวียน). Moreover it is utilized for cardiogenic, refreshment and analeptic (ทำให้ใจคอชื่นบานสดใสรุ่ก่าล้ง). Its heartwood has aromatic and cool taste (รสหอมเย็น). It is used for cardiogenic, debility and choleric [33]. This crude drug has ever been identified as *Mansonia gagei* J.R. Drumm. Ex Prain [4, 34] or *Aglaia silvestris* (M. Roem.) Merr. [4].

1.4 Chan-thana

Chan-thana was not recorded in Thai medical textbook. It has been identified as the heartwood of *T. hoensis* [8] which is used for pulmohepatogenic, cardiogenic, febrifugal, aphthous ulcer, thirsty, and plentifully sweating. Moreover it is used for stomatorrhagia gingivarum [8].

1.5 Chan-hom

Chan-hom was not recorded in Thai medical textbook. It has been identified as the stem of *M. gagei* [8] which is used as intestinal carminative and cardiogenic. It also relieves colic, abdominal discomfort, stomachache and dyspepsia. Its wood and heartwood are used for nausea, vomiting and dizziness. It is also used as cardiogenic, analeptic and febrifugal. Moreover it is used for disorder of four elements. Its leaf is utilized as skin tonic. Moreover it relieves aphthous ulcer, thirsty and abdominal discomfort [4].

2 Chan(s) in Thai traditional medicine formulae

Over thousands of Thai traditional medicinal formulae were applied for various somatic systems. Each herbal ingredient in formulae possesses its particular function. Chan-thet, Chan-khao, Chan-chamot, Chan-thana and Chan-hom were used as ingredients in approximate hundred of Thai traditional formulae [33, 39-40]. Fifteen examples which consist of one or more Chan(s) are listed in Table 1.

Table 1 Examples of some Thai traditional formulae containing Chan(s) as ingredient(s).

Chan(s) in formula	Name of formula	Traditional use	Reference
Chan-thet or Chan-chamot	Ya kaewhom (ยาเขียวหอม)	Fever, aphthous ulcer, thirsty, measles and chickenpox (แก้พิษหัว พิษอีสุกอีใส)	[1, 33]
Chan-khao or Chan-chamot or Chan-thet	Ya Chanthaleela (ยาจันทร์ลีลา)	Pyrexia (แก้ไข้ตัวร้อน), seasonal fever, various fever and fever cause of poisonous food	[1, 33, 39, 40]
Chan-thet	Ya Mahaniltangtong (ยามหานิลแทงทอง)	Exanthematous fever (แก้ไข้กาฬ), measles, chickenpox, aphthous ulcer and thirsty	[1, 33]
Chan-thana	Ya Bintan (ยาบินตัน)	Dysentery (แก้ตกมูกเลือด) and hot and cold fever (แก้ไข้ชนิดร้อนชนิดหนาว)	[39]
Chan-khao and Chan-thana	Ya Kaekai Narayanatonjak (ยาแก้ไข้ขึ้นราชฉัตรอนจักร)	Fever, delirium (ร้อนเพ้อคลั่ง) and withdraw febrile	[39]
Three types of Chan (จันทร์ทั้งสาม)	Ya Kaekai Chanharuethai (ยาแก้ไข้จันทร์ทั้งสาม)	Exanthematous fever, fever due to abnormality of combination of three of the following origin; (<i>Semha, Pitta, Wata, Kamdao,</i> <i>Lohita</i>) (ไฟสันนิบาต), hot and cold fever, and various fevers	[39]
Chan-thet, Chan-thana and Chan-chamot	Ya-uthai (ยาอุทัย)	Aphthous ulcer and thirsty	[40]
Chan-khao	Ya Mahakan (ยามหากาฬ)	Exanthematous fever, splenomegaly (แก้จุกกระพวมม้ามชื้อช), abscess, abdominal pain and hiccough	[39]
Chan-khao and Chan-thet	Yahom Thiposot (ยาหอมทิพโอสถ)	Dizziness	[1, 33]
Chan-khao and Chan-chamot	Yahom Thepjit (ยาหอมเทพจิตร)	Dizziness, nausea, blurred vision, palpitation and cardiac stimulant	[1, 33]

Table 1 Examples of some Thai traditional formulae containing Chan(s) as ingredient(s) (continued).

Chan(s) in formula	Name of formula	Traditional use	Reference
Chan-thet	Ya-hom-navakot (ยาหอมนาวโกฐ)	Dizziness in elder, nausea, dizziness, anorexia, flatulence and <i>Wata</i> arising convalescent period (แก้ลมปลงไข้)	[1, 33]
Chan-thet	Ya Apaisalee (ยาอภัยสาลี)	Abdominal discomfort	[1]
Chan-thet	Yahom Inthajak (ยาหอมอินทจักร์)	Angina, nausea, vomiting and flatulence	[1, 33]
Chan-hom	Ya Mahasan (ยามหาสาร)	Treatment various poisons	[40]
Chan-thet	Ya Munthatat (ยามันทรธาตุ)	Flatulence and hypoactivity of the four elements (แก้ธาตุ 4 ห่อน)	[1, 33, 39]
Chan-khao	Ya Thepmongkol (ยาเทพมงคล)	Infectious diseases in early childhood (ชาง) and membranous stomatitis (ละอองภายใน)	[39]



3 *Santalum album* L.



Figure 1 *Santalum album* L.

3.1 Introduction

S. album is a plant that commonly known as Indian sandalwood or white sandalwood. It was originated from Timor Indonesia for thousand years [41] and was taken to India by fragrance wood traders [42]. Thus currently most of them are mainly produced in India [43]. Moreover they have been extended throughout Nepal, Sri Lanka, Timor, Java, Bali and Australia [15]. *S. album* has been utilized as perfumes, cosmetics, scent, fragrance and aromatherapy in worldwide [43-48]. It is one of the mostly important economic and medical species [49, 50]. The quality of essential oil from *S. album* or sandalwood oil is varied based on age, color and cutting height of heartwood [50]. Sandalwood has been applied in ancient practice for thousand years ago. The smell of incenses which were formed by powdered sandalwood could alter mood quality e.g. removing depression, anxiety, nervousness, stress and insomnia [43, 51]. In ethnobotanical therapeutic usage in India, extracted oil from root and wood has been used for aphrodisiac [51, 52], diuretic and urinary antiseptic [51]. Moreover leaf and stem have been used for gastric irritability, dysentery, gonorrhoeal, urethral disorder, bronchial disorder and skin disorder [53, 54]. Furthermore essential oil has been used for the treatment of lymphatic, nervous system, respiratory system, genitourinary and integumentary disorders [43]. Wood has been used for anti-septic, anti-pyretic, anti-scabietic, diuretic, expectorant,

stimulant and treatments of bronchitis, dysuria, urinary infection and gonorrhoeal recovery [50]. For industrial, the heartwood should be harvested from the mature tree over 30 years for yielding fragrance oil [43, 55, 56].

3.2 Morphology

S. album is belonging to the family Santalaceae. It is a mid-sized tropical evergreen and semi-parasitic tree. Its height is approximately 6-20 m. It has terete trunk. Lower branches sometimes droop and branchlets slightly angular-striate. Bark is grey-brown or reddish-dark grey to almost black color. Leaves are simple and opposite or decussate and exstipule. Petiole is yellowish with approximately 5-15 mm length. The blade is ovate, lanceolate-elliptical or oblong. Base is obtuse, cuneate or acute. Margin is undulate, flat or slightly recurved. Apex is acuminate. It is slightly discolorous. It is pale green above and glaucous beneath. Venation is distinctly reticulate. Flowers are inflorescence which is a terminal or axillary panicle or raceme with 2-5 cm length. Floret is small, gamopetalous ancient bowl-shape and splitting into 4 lobes at the end. Fresh bloom is straw then changes to red-purple color. Perianth is campanulate tube and about 2 mm length. It has 4 lobed as triangular-ovate, initially yellowish turning brownish-red with a hair tuft behind the stamens. Four stamens cast over hair tufts. Disk is prominently 4-lobes and erect-recurved. They have orange-brown then turn to blackish-red. Pistil is superior to half inferior ovary with short style and small, slightly 3-lobed stigma. Fruit is an ellipsoidal consisting of 1-seeded drupe, approximately 1 cm length, with small apical collar. The mature fruit is round. It is blackish color and has 1 seed. Exocarp is blue to blackish-red. Mesocarp is succulent or firm. Endocarp is smooth. Seed has testa and epigeal germination [2, 6, 44, 46, 55-57].

3.3 Pharmacological activity

The pharmacological activities of *S. album* are listed in Table 2.

Table 2 Pharmacological activity of *Santalum album*.

Activity	Part	Reference
Analgesic	Wood	[58]
Aphrodisiac	Heartwood	[59]
Anthelmintic	Plant material*	[60]
Anti-bacteria	Leaves and stem	[53, 54]
	Leaves oil	[50]
	Heartwood and leaves	[61]
Anti-cancer	Essential oil	[62]
Anti-hyperlipidemic	Powder*	[63]
Anti-hyperglycemic	Powder*	[63]
	Sandalwood oil	[64]
	Essential oil	[65]
Anti-inflammation	Ripen fruits	[66]
Anti-oxidation	Essential oil	[65]
Anti-pyretic	Wood	[58]
	Stem	[67]
Anti-ulcer	Essential oil	[64, 68]
Anti-virus	Essential oil	[69, 70]
Chemoprevention	Heartwood	[46]
	Ripen fruits	[66]
Cytotoxicity	Essential oil	[65]
Insecticide	Essential oil	[71]
Larvicide	Essential oil	[71]

* Part was not specified.

3.4 Chemical constituents

Chemical constituents of *S.album* are listed in Table 3.

Table 3 Chemical constituents of *Santalum album*.

Compound	Part	Reference
Sesquiterpenes		
α -Acoradiene	Essential oil	[48]
β -Acoradiene	Essential oil	[48]
10- <i>epi</i> - β -Acoradiene	Essential oil	[48]
α - <i>trans</i> -Bergamotene	Essential oil	[48]
α - <i>trans</i> -Bergamotol	Essential oil	[48]
β -Bisabolene	Essential oil	[48]
(<i>E</i>)- α -Bisabolene	Essential oil	[48]
α -Bisabolol	Essential oil	[48]
Bulnesol	Essential oil	[48]
α -Cedrene	Essential oil	[48]
γ -Curcumene	Essential oil	[48]
<i>Ar</i> -Curcumene	Essential oil	[48]
(9 <i>E</i>)-11,13-Dihydroxy- α -santalol	Heartwood	[46]
(10 <i>R</i> ,11 <i>S</i>)-10,11-Dihydroxy- α -santalol	Heartwood	[46]
α -Funebrene	Essential oil	[48]
Helifolen-12-al	Essential oil	[48]
β -Himachalol	Essential oil	[48]
(9 <i>S</i> ,10 <i>E</i>)-9-Hydroxy- α -santalal	Heartwood	[46]
(10 <i>E</i>)-12-Hydroxy- α -santalal acid	Heartwood	[46]
12-Isoitalicenol	Essential oil	[48]
(<i>E</i>)-Nuciferol	Essential oil	[48]
α -Santalene	Essential oil	[48]
β -Santalene	Essential oil	[48]
<i>epi</i> - β -Santalene	Essential oil	[48]
β -Santalol	Essential oil	[48]
<i>epi</i> - β -Santalol	Essential oil	[48]
(<i>Z</i>)- α -Santalol	Heartwood	[46, 48]
α -Santalol acetate	Essential oil	[48]
Sesquisabinene	Essential oil	[48]

Table 3 Chemical constituents of *Santalum album* (continued).

Compound	Part	Reference
Monoterpenes		
7- <i>epi</i> -Sesquithujene	Essential oil	[48]
Lignans		
Dihydrodehydrodiconiferyl alcohol	Heartwood	[44]
2,3- <i>bis</i> [(4-Hydroxy-3,5-dimethoxyphenyl)-methyl]-1,4-butanediol	Heartwood	[44]
ω -Hydroxypropioiguaiacone	Heartwood	[44]
(-)- <i>seco</i> -Isolariciresinol	Heartwood	[44]
(7 <i>S</i> ,8 <i>R</i> ,8' <i>R</i>)-Lyoniresinol	Heartwood	[44]
(7 <i>S</i> ,8 <i>S</i>)-3-Methoxy-3',7-epoxy-8,4'-oxyneoligna-4,9,9'-triol	Heartwood	[44]
Neolignans		
(7 <i>S</i> ,8 <i>R</i>)-Dihydro-3'-hydroxy-8-hydroxy-methyl-7-(4-hydroxy-3-methoxyphenyl)-1'-benzofuranpropanol	Heartwood	[44]
7 <i>S</i> ,8 <i>S</i> -Nitidanin	Heartwood	[44]
7,8- <i>erythro</i> -4,9,9'-Trihydroxy-3,3'-dimethoxy-8.0.4'-neolignans	Heartwood	[44]
7,8- <i>threo</i> -4,9,9'-Trihydroxy-3,3'-dimethoxy-8.0.4'-neolignans	Heartwood	[44]
Aromatic ester		
Diethylene glycol monobenzoate	Heartwood	[44]
Phenylpropanoids		
<i>C</i> -Veratrolyglycol	Heartwood	[44]
3-Hydroxy-1-(4-hydroxy-3,5-dimethoxyphenyl)-1-propanone	Heartwood	[44]
Phenolic acids		
Isovanillic acid	Heartwood	[44]
Syringic acid	Heartwood	[44]
Vanillic acid	Heartwood	[44]
Vanillic acid 4- <i>O</i> -neohesperidoside	Heartwood	[44]

4 *Santalum spicatum* (R. Br.) A. DC.

4.1 Introduction

S. spicatum is known as western Australian sandalwood. It is an important commercial tree in Australia since 1845 A.D. which has been firstly exported to China [57, 72-74]. It has been widely distributed throughout semi-arid and arid area of Western Australia [75]. The quality of essential oil of *S. spicatum* is similar to the quality of essential oil of Indian sandalwood [75]. Bark has been used in ethnobotanical therapeutics to relieve cough [76].

4.2 Morphology

S. spicatum is belonging to the family Santalaceae. It is semi-root-parasitic shrub. It is 4 m height with tough grey bark and stiff spreading branches. Leaves are opposite with 3-5 mm petiole. Blade is lanceolate to narrowly elliptical with grey-green. Flowers are inflorescence with 3-5 mm peduncle and 1 mm pedicel. The receptacle is 1-1.5 mm length with 1.5-2 mm triangular-ovate of 4 tepals. It is red-green with small tufts of hairs at base inside. Hairs are persistent in fruit. Disk is short lobe. Style is 0.5 mm length. It has 2 lobes of stigma. A globose drupe fruit is 1.5-2 cm diameter with green or brown. Mesocarp is adheres to endocarp [57].

4.3 Pharmacological activity

The pharmacological activities of *S. spicatum* are listed in Table 4.

Table 4 Pharmacological activity of *Santalum spicatum*.

Activity	Part	Reference
Anthelmintic	Not specified	[77]
Anti-diabetes	Not specified	[78]
Anti-oxidation	Not specified	[78]
Anti-virus	Bark	[79]
Insecticide	Not specified	[80]

4.4 Chemical constituents

Chemical constituents of *S. spicatum* are listed in Table 5.

Table 5 Chemical constituents of *Santalum spicatum*.

Compound	Part	Reference
Sesquiterpenes		
(Z)- α -Santalol	Essential oil	[12, 48]
<i>epi</i> - α -Bisabolol	Essential oil	[48]
(Z)- β -Santalol	Essential oil	[12, 48]
<i>epi</i> - β -Santalol	Essential oil	[48]
(Z)- α - <i>trans</i> -Bergamotol	Essential oil	[48]
(<i>E,E</i>)-Farnesol	Essential oil	[12, 48]
(Z)-Nuciferol	Essential oil	[48]
(Z)-Lanceol	Essential oil	[48]
Triglycerides		
Triximenynoyl-glycerol (triximenynin)	Seed oil (fix oil)	[72]
Oleoyl-diximenynoyl-glycerol (oleic acid)	Seed oil (fix oil)	[72]
Dioleoylximenynoyl-glycerol (ximenynic acid)	Seed oil (fix oil)	[72]

5 *Santalum lanceolatum* R.Br

5.1 Introduction

S. lanceolatum is Northern Australian sandalwood. It has been widely distributed in Victoria and New South Wales which are not arid or semi-arid area [81]. In Australia, bark, stem and leaves have been traditionally used for cold, malaise, sore throat, venereal diseases and painful urination [76].

5.2 Morphology

S. lanceolatum is belonging to the family Santalaceae. It is a shrub with 3-7 m height. Leaves are ovate to narrow elliptic with 2-9 cm length and 5-25 mm width. Apex is acute to mucronate. Surface is concolorous or slightly discolorous and often slightly glaucous. Petiole is 2-10 mm length. Flowers are terminal or axillary panicles or racemes in upper axils. Its flowers rarely exceed the leaves. Peduncle is 5-30 mm length. Pedicle is 1 mm length. The greenish triangular

tepals are 3-5 mm length. The character of disc with knob likes lobes. Ovary is half-inferior with 4 lobed of stigma. Fruit is drupe ovoid, 7-15 mm length with dark blue or purple. It is often gall. It has circular subapical scar and smooth endocarp. Flowering is throughout year but mainly in August to December [82].

5.3 Pharmacological activity

The pharmacological activities of *S. lanceolatum* are listed in Table 6

Table 6 Pharmacological activity of *Santalum lanceolatum*.

Activity	Part	Reference
Anti-bacteria	Leaves	[76]
Anti-diabetes	Not specified	[78]
Anti-oxidation	Not specified	[78]
Anti-virus	Bark, stem and leaves	[79]

5.4 Chemical constituents

Similar to the other *Santalum* sp., santalol is one of the major compositions but its content is low. Chemical constituents of *S. lanceolatum* are listed in Table 7.

Table 7 Chemical constituents of *Santalum lanceolatum*.

Compound	Part	Reference
Curcumenol	Heartwood	[83]
Nuciferol	Heartwood	[83]
Santalol	Heartwood	[83]

6 *Myristica fragrans* Houtt.



Figure 2 *Myristica fragrans* Houtt.

6.1 Introduction

M. fragrans is a traditional plant of Maluku islands and nearby islands. Its common name is nutmeg tree [6] of which Thai name is Chan-thet or Chan-ban (Shan-Northern). It is shrub or tree that has been imported to Thailand for many years ago [8]. It is an aromatic plant which used as spices. Seed (nutmeg) and aril (mace) are major parts that are used as spices and traditional medicines [84]. The first fruit is produced when the plant is 8-9 years old until it is 30 years old [2, 6]. It has been used as aphrodisiac in Indian traditional medicine [52]. In China, nutmeg has been used as medicine for digestive disorder [84]. Moreover nutmeg has been used for the treatments of digestive, liver and skin disorder [84] and mace has been used as aromatic stomachic and analgesic [85].

6.2 Morphology

M. fragrans is belonging to the family Myristaceae. It is a shrub or tree with 8-18 m height. Bark is smooth with grey-black color. Leaves are leathery, simple, alternate and ovate shape. Margin is oblong with 4-5 cm width, 10-15 cm length. Apex is acuminate. Base is attenuate. Dorsal and ventral sides are entire and shiny. Flower is yellow. It does not have petal. Fruit is round or flat-round shape. It is creamy-yellow or red color, fleshy and consisting 2-valved capsule. Ripe fruit has 2 pieces when fissures. Thick seed is brown and called nutmeg. Aril is red and called mace [2, 4, 6, 35, 84].

6.3 Pharmacological activity

The pharmacological activities of *M. fragrans* are listed in Table 8.

Table 8 Pharmacological activity of *Myristica fragrans*.

Activity	Part	Reference
Analgesic	Seed	[86]
Anti-bacteria	Essential oil	[87]
	Aril	[88]
Anti-inflammation	Aril	[85]
	Seed	[86]
Anti-biofilm of bacteria cause of dental dysfunction activity	Seed	[89]
Anti-convulsant	Seed oil	[90]
Anti-fungus	Aril	[88]
	Seed	[91]
Anti-microbial	Fruits	[92]
Anti-oxidation	Aril	[88]
	Fresh fruit oil	[93]
	Seed oil	[94]
Anti-platelet	Seed	[95]
Anti-rotavirus	Seed	[96]
Anti-thrombotic	Seed	[86]
Anti-tyrosine phosphatase 1B (PTP1B)	Dried seed	[97]
Anxiogenic	Seed	[98]
Cytotoxicity	Fresh fruit oil	[93]
Anti-microbial cause of gastrointestinal disorders susceptibility	Seed	[99]

6.4 Chemical constituents

Chemical constituents of *M. fragrans* are mainly reported from essential oil of seed and aril. The details are listed in Table 9.

Table 9 Chemical constituents of *Myristica fragrans*.

Compound	Part	Reference
Monoterpenes		
Camphene	Seed oil (essential oil)	[100]
<i>d</i> -Citronellol	Fresh fruit	[93]
2,6-Dimethyl 2,6-octadiene	Fresh fruit	[93]
β -Fenchyl alcohol	Fresh fruit	[93]
Geranyl acetate	Fresh fruit	[93]
Isobornyl acetate	Fresh fruit	[93]
Isosilvestrene	Seed oil (essential oil)	[100]
Limonene	Dried seed kernel oil, fresh fruit and seed	[90, 91, 93]
Linalool	Dried seed kernel oil, fresh fruit and seed oil (essential oil)	[90, 93, 100]
<i>cis-para</i> -Menth-2-en-1-ol	Seed oil (essential oil)	[100]
Myrcene	Fresh fruit and seed oil (essential oil)	[93, 100]
<i>trans</i> - β -Ocimene	Fresh fruit	[93]
α -Phellandrene	Seed oil (essential oil)	[100]
β -Phellandrene	Aril oil and seed oil (essential oil)	[88, 100]
α -Pinene	Dried seed kernel oil, aril oil, fresh fruit and seed oil (essential oil)	[88, 90, 91, 93, 100]
Piperitenone oxide	Seed oil (essential oil)	[100]
Sabinene	Aril oil and seed oil (essential oil)	[88, 91, 100]
<i>cis</i> -Sabinene hydrate	Seed oil (essential oil)	[100]
<i>cis</i> -Sabinene hydrate acetate	Seed oil (essential oil)	[100]
<i>trans</i> -Sabinene hydrate	Seed oil (essential oil)	[100]
<i>trans</i> -Sabinene hydrate acetate	Seed oil (essential oil)	[100]
Saychellene	Fresh fruit	[93]
α -Terpinene	Dried seed kernel oil and aril oil	[88, 90, 93, 100]
γ -Terpinene	Dried seed kernel oil, aril oil, fresh fruit and seed oil	[88, 90, 93, 100]
Terpinen-4-ol	Dried seed kernel oil, aril oil and seed	[88, 90, 91, 93, 100]
α -Terpineol	Dried seed kernel oil and seed oil (essential oil)	[90, 100]

Table 9 Chemical constituents of *Myristica fragrans* (continued).

Compound	Part	Reference
Terpinolene	Aril oil, fresh fruit and seed oil (essential oil)	[88, 93, 100]
α -Terpinyl acetate	Seed oil (essential oil)	[100]
α -Thujene	Aril oil and seed oil (essential oil)	[88, 100]
Sesquiterpenes		
<i>trans</i> - α -Bergamotene	Fresh fruit and seed	[93, 100]
β -Bisabolene	Fresh fruit	[93]
δ -Cadinene naphthalene	Fresh fruit	[93]
<i>trans</i> - β -Caryophyllene	Fresh fruit	[93]
α -Copaene	Seed oil (essential oil)	[100]
β -Damascenone	Seed oil (essential oil)	[100]
<i>trans</i> - β -Farnesene	Fresh fruit	[93]
D-Germacrene	Fresh fruit	[93]
Guaiol	Fresh fruit	[93]
α -Humelene	Fresh fruit	[93]
<i>trans</i> -Methyl isoeugenol	Dried seed kernel oil and fresh fruit	[90, 93]
α -Muurolene	Fresh fruit	[93]
Phenylpropanoids		
D-Cymene	Seed oil (essential oil)	[100]
<i>p</i> -Cymene	Dried seed kernel oil	[90]
Eugenol	Dried seed kernel oil and fresh fruit	[90, 93]
Isocroweacin	Aril	[88]
<i>trans</i> -Isoeugenol	Aril	[88]
Methoxyeugenol	Aril acetone extract	[88]
Methyl eugenol	Dried seed kernel oil, fresh fruit and seed	[90, 93, 100]
Myristicin	Seed and aril, dried seed kernel oil, fresh fruit and seed	[84, 90, 91, 93, 100]
Safrole	Seed, aril and fresh fruit	[84, 88, 93, 100]
Neolignans		
Dehydrodiisoeugenol	Aril	[88]
Fatty acids		
Linoleic acid	Aril	[88]
Palmitic acid	Aril	[88]

Table 9 Chemical constituents of *Myristica fragrans* (continued).

Compound	Part	Reference
Hydrocarbons		
Elcosane	Fresh fruit	[93]
Heptacosane	Fresh fruit	[93]
Hexacosane	Fresh fruit	[93]
Octacosane	Fresh fruit	[93]
Octadecane	Fresh fruit	[93]

7 *Diospyros decandra* Lour.

**Figure 3** *Diospyros decandra* Lour.

7.1 Introduction

D. decandra is called as Siamese In-chan (Thai common name) [36]. In 35 years ago, its synonym is *Diospyros packmanni* Clarke [34], but nowadays, it is known as *Diospyros decandra* Lour.

7.2 Morphology

D. decandra is belonging to the family Ebenaceae. It is a mid-size tree with 10-20 m height, straight stem and brown-black bark. Leaves are simple, alternate, oblong or ovate shape. Margin is ovate with 2.5-3 cm width and 7-10 cm length. Apex is acute. Base is obtuse or acute. Surface is pubescent. Flower is dioecious. Staminate flowers are inflorescence. Floret is cream color. It has 5 petals

and 5 sepals with brown-red hair. Pistillate flower is solitary. It is creamy-white color. It has round ovary with hair. The character of pistillate flower similar to staminate flower but the size is bigger. Fruit is fleshy berry. It is round or flat shape and green color. Mature fruit is yellow, fragrant and edible. It has 3-4 round-ovate brown seeds [4, 34, 36-38].

7.3 Pharmacological activity

The pharmacological activities of *D. decandra* are listed in Table 10.

Table 10 Pharmacological activity of *Diospyros decandra*.

Activity	Part	Reference
Anti-fungus	Bark	[101]
Anti-HIV-1 integrase	Wood	[102]
Anti-malaria	Bark	[101]
Anti-mycobacteria	Bark	[101]
Anti-oxidation	Green and ripe fruit	[103]
Cytotoxicity	Bark	[101]

7.4 Chemical constituents

Chemical constituents of *D. decandra* are listed in Table 11.

Table 11 Chemical constituents of *Diospyros decandra*.

Compound	Part	Reference
Phenolic acids		
Caffeic acid	Green and ripe fruit	[103]
Chorogenic acid	Green and ripe fruit	[103]
<i>p</i> -Coumaric acid	Green and ripe fruit	[103]
Ferulic acid	Green and ripe fruit	[103]
Gallic acid	Green and ripe fruit	[103]
<i>p</i> -Hydroxy benzoic acid	Green and ripe fruit	[103]
Protocatechuic acid	Green and ripe fruit	[103]
Sinapinic acid	Green and ripe fruit	[103]
Syringic acid	Green and ripe fruit	[103]
Vanillic acid	Green and ripe fruit	[103]
Flavonoids		
Apigenin	Green and ripe fruit	[103]
Kaempferol	Green and ripe fruit	[103]
Luteolin	Green and ripe fruit	[103]
Myricetin	Green and ripe fruit	[103]
Quercetin	Green and ripe fruit	[103]
Rutin	Green and ripe fruit	[103]
Sugars		
D-(-)-Fructose	Raw fruit	[103]
D-(+)-Galactose	Raw fruit	[103]
D-(+)-Glucose	Raw fruit	[103]
D-(-)-Sorbitol	Raw fruit	[103]
D-(+)-Sucrose	Raw fruit	[103]
Triterpenes		
Betulinic acid	Bark	[101]
Diospyric acid A	Bark	[101]
Diospyric acid B	Bark	[101]
Diospyric acid C	Bark	[101]
Diospyric acid D	Bark	[101]
Diospyric acid E	Bark	[101]

8 *Tarennna hoensis* Pit.



Figure 4 *Tarennna hoensis* Pit.

8.1 Introduction

T. hoensis is found in sparse or dry evergreen or deciduous forests in many regions of Thailand. It is found in northeastern such as Nong Khai, Nakhon Ratchasima provinces, in southwestern such as Prachuap Khiri Khan province, in east such as Sa Kaeo, Prachin Buri, Chon Buri, Rayong, Chanthaburi and Trat provinces [104], and in south such as Surat Thani province [2, 104, 105]. Moreover it distributes in Cambodia and Vietnam [105]. However it is a rare plant species [106, 107].

8.2 Morphology

T. hoensis is belonging to the family Rubiaceae. It is a shrub or small tree, 5-10 m height and oval frutescent crown. Bark is light grey, entire or small fissure nook along stem length. Wood is white or pale yellow. Leaves are simple, obtuse shape or oblong margin, thick lamina, glabrous and shiny surface and flat petiole with stipule. Flowers are inflorescence. Floret is sympetalous. It is white with 4 sepals and 4 petals. Fresh fruit is ellipse with sepals and ripe fruit is black-purple [2, 4].

8.3 Pharmacological activity

The pharmacological activities of *T. hoensis* are listed in Table 12.

Table 12 Pharmacological activity of *Tarennna hoensis*.

Activity	Part	Reference
Anti-oxidation	Heartwood	[108]
Iron-chelating	Heartwood	[108]

8.4 Chemical constituents

Only one publication has been reported for the chemical constituents of *T. hoensis* as listed in Table 13.

Table 13 Chemical constituents of *Tarennna hoensis*.

Compound	Part	Reference
Flavonoids	Heartwood	[108]
Phenolics	Heartwood	[108]

9 *Mansonia gagei* J.R.Drumm. ex Prain



Figure 5 *Mansonia gagei* J.R.Drumm. ex Prain.

9.1 Introduction

Heartwood of *M. gagei* is used for cardiac-stimulant, anti-depressant [66], anti-emetic and refreshment [34, 109-111].

9.2 Morphology

M. gagei is belonging to the family Sterculiaceae. It is a deciduous tree in evergreen forest. Leaves are simple and alternate. Inflorescences are white. Fruit is spindle shape with triangle samara. Mature heartwood is pale-brown with black in wood and strong fragrant [4, 34, 112].

9.3 Pharmacological activity

The pharmacological activities of *M. gagei* are listed in Table 14.

Table 14 Pharmacological activity of *Mansonia gagei*.

Activity	Part	Reference
Acetylcholinesterase (AChE) and butyrylcholinesterase (BchE) inhibition	Heartwood	[113]
Acute toxicity	Not specified	[114]
Anti-estrogen	Heartwood	[43]
Anti-fungus	Heartwood	[112]
Anti-histamine	Not specified	[114]
Anti-oxidation	Heartwood	[112]
Atropine-like	Not specified	[114]
Cytotoxicity	Heartwood	[110]
Heart contraction stimulation	Not specified	[114]
Larvicide	Heartwood	[112]

9.4 Chemical constituents of *M. gagei*

Main chemical constituents of the heartwood of *M. gagei* are sesquiterpenes and coumarins, e.g. mansonones and mansorins, respectively. The chemical constituents are listed in Table 15.

Table 15 Chemical constituents of *Mansonia gagei*.

Compound	Part	Reference
Coumarins		
Mansorin A	Heartwood	[109, 110, 112, 115]
Mansorin B	Heartwood	[109, 110, 112]
Mansorin C	Heartwood	[109, 110, 112, 115]
Mansorin I	Heartwood	[109]
Mansorin II	Heartwood	[109]
Mansorin III	Heartwood	[109]
Sesquiterpenes		
Mansonone C	Heartwood	[109, 110, 112, 115]
Mansonone E	Heartwood	[112, 115]
Mansonone F	Heartwood	[109]
Mansonone G	Heartwood	[109, 110, 112, 115]
Mansonone H	Heartwood	[109, 110, 112, 115]
Mansonone N	Heartwood	[109, 111, 112]
Mansonone O	Heartwood	[109, 111, 112]
Mansonone P	Heartwood	[111, 112]
Mansonone Q	Heartwood	[111]
Mansonone R	Heartwood	[115]
Mansonone S	Heartwood	[109, 115]
Mansonone I	Heartwood	[109]
Dehydrooxoperezinone	Heartwood	[112]
Phenolics		
Acetovanillone	Heartwood	[109]
Mansoxetane	Heartwood	[115]

10 *Aglaia silvestris* (M. Roem.) Merr.



Figure 6 *Aglaia silvestris* (M. Roem.) Merr.

10.1 Introduction

In Thailand, *A. silvestris* is found in northern such as Chiang Mai, Chiang Rai and Tak provinces, in eastern such as Chaiyaphum province, in south-western such as Kanchanaburi and Phetchaburi provinces, in south-eastern such as Chanthaburi and Trat provinces, and in peninsular region such as Chumphon and Ranong provinces [116]. Apart from Thailand, it distributes in Laos, Cambodia, Vietnam, Malaysia, Indonesia, Philippines and New Guinea [116]. Wood has been used as fragrance. Aril is edible [116].

10.2 Morphology

A. silvestris is belonging to the family Meliaceae. It is found in evergreen forest. It is usually found nearby stream and sandstone or limestone bedrock [116]. Leaves are odd-pinnately compound and alternate. Lower surface is dark brown to golden brown scales. Margin is usually pale [116]. Fruit is round and green-yellow and fragrant [4].

10.3 Pharmacological activity

The pharmacological activities of *A. silvestris* are listed in Table 16.

Table 16 Pharmacological activity of *Aglaia silvestris*.

Activity	Part	Reference
Anti-cancer	Fruit and twig	[117]
Cytotoxicity	Fruit and twig	[117]

10.4 Chemical constituents

Chemical constituents of *A. silvestris* are listed in Table 17.

Table 17 Chemical constituents of *Aglaia silvestris*.

Compound	Part	Reference
Triterpenes		
Aglasilvinic acid	Dried leaves, stem and root bark	[118]
Cabraleone	Dried root bark	[119]
Eichlerianic acid	Dried root bark	[119]
Episilvestrol	Fruit and twig	[117]
17,24-Epoxy-25-hydroxybaccharan-3-one	Fruit and twig	[117]
17,24-Epoxy-25-hydroxy-3-oxobaccharan-21-oic Acid	Fruit and twig	[117]
Foveolin A	Dried root bark	[119]
Foveolin B	Dried root bark	[119]
Isoeichlerianic acid	Dried root bark	[119]
Isosilvaglin A	Dried leaves, stem and root bark	[118]
Methylfoveolate B	Dried leaves, stem and root bark	[118]
Methyl isoeichlerianate	Dried root bark	[119]
Methylisofoveolate B	Dried leaves, stem and root bark	[118]
Ocotillone	Dried root bark	[119]
Pregnacetal	Dried leaves, stem and root bark	[118]
Shoreic acid	Dried root bark	[119]
Silvaglenamin	Dried root bark	[120]
Silvaglins A	Dried leaves, stem and root bark	[118]
Silvestrol	Fruit and twig	[117]
Bisamides	Leaves	[121]
Lignans	Leaves	[121]

11 Chemical approach for identification and authentication of herbal medicines

One herbal medicine consists of many chemical constituents that are important for various biological activities. In traditional remedies, the efficacies of treatment are obtained from the combination of many chemical compounds in herbs. Different plant species provide different activities as well as different plant parts provide different properties. Then the misuse of plant species may cause of adverse effect of treatment. To ensure the herbal medicine utilization, herbal quality control is important.

The World Health Organization (WHO) suggests assessment herbal medicines for safety and effectiveness thus crude plant materials should be defined genus, species and authority to ensure correct plant [26]. The manners for herbal medicine identification are chromatographic and spectroscopic methods [122]. In this study, some techniques of chromatography and spectroscopy were concerned. The examples of chromatographic methods are thin layer chromatography (TLC) and gas chromatography (GC). TLC is an easy, flexible and inexpensive technique. GC is suitable for volatile and heat stable compounds. For more application, the GC and mass spectroscopic (MS) detector are connected to obtain the information of chemical constituents in samples, for example the analysis of chemical content in nutmeg oil [123]. The example of spectroscopic method is infrared spectroscopy (IR). It provides the overall information of chemical functional groups of compounds that are composed in samples. The chromatogram and spectrogram which display the character of herbal medicine are called fingerprint. Fingerprint analysis is the method that is suggested by WHO and U.S. pharmacopoeia convention to identify herbal medicines [26, 124].

11.1 Thin layer chromatography (TLC)

TLC is one of the chromatographic techniques that used to separate the mixtures [125]. The process of separation derives from two different phases. They are stationary phase (adsorbent layer) and mobile phase (solvent mixture). The compounds of sample are applied on stationary phase and eluted by mobile phase.

They move along the distance of examination, based on the principle of “like dissolve like”. Thereafter the TLC fingerprint is determined by R_f value and band color of compounds. TLC is applied to determine the compound content [126], detect the biological activity [127], monitor the progress of reaction and determine the purity of compounds [125], the adulteration and the plant identification [128, 129]. The active or chemical or general markers of many plants are used for identification and authentication of the species [130].

11.2 Gas chromatography/Mass spectroscopy (GC/MS)

GC is the chromatographic method that employs principle of separation similar to TLC in term of two phases of separation, but mobile phase of GC is gas. Thus the volatile substance is suitable for GC analysis. The GC fingerprint provides the aspect of analysts that can be used for their identification by comparing with related peaks or retention times of the references. Moreover hyphenated technique such as MS that is the detector connected with GC can enhance effectiveness of the analysis. The mass fragmentation pattern of compound is compared with those of compounds in database. Thus GC/MS is very useful for compound identification [131]. This technique can be applied for identification and authentication of herbal medicines. For example it was applied to authenticate and quality control of sandalwood oil from various sandalwood species [45].

11.3 Infrared spectroscopy (IR)

IR is one of the spectroscopic techniques. Its principle is molecular vibration influencing by dipole moment difference. Infrared absorption effects on dipole moment transformation of molecule. The frequency ranges of mid-infrared are $4000-400\text{ cm}^{-1}$ and wavelength are $2.5-1.5\text{ }\mu\text{m}$. The vibration of molecular infrared absorption is divided into stretching and bending vibrations. The character of molecular stretching vibration is similar to elongation and contraction of coiled spring. It is divided into symmetric and asymmetric stretchings. The molecular bending vibration can be divided into four types, i.e. scissoring, rocking, twisting and wagging. Commonly, the wavenumber of infrared spectra are divided into two major

regions, i.e. functional group region ($4000\text{-}1500\text{ cm}^{-1}$) and fingerprint region ($1500\text{-}400\text{ cm}^{-1}$), which can differentiate the aspect of molecule of individual compounds [132]. The important regions of IR spectrum are illustrated in Table 18.

Table 18 Interpretation of some important regions of infrared spectrum [133].

Wavenumber (cm^{-1})	Functional group	Characteristics of the peak
Functional group region ($4,000\text{-}1,500\text{ cm}^{-1}$)		
3,600-3,300	Alcohol O-H	Broad and strong
	Amine or amide N-H	Not broad and strong as OH
	Alkyne C-H	May be confirmed by weak stretching of $\text{C}\equiv\text{C}$ near $2,150\text{ cm}^{-1}$
3,000-2,500	Acid O-H	Very broad signal centered near $3,000\text{ cm}^{-1}$
3,200-3,000	Aromatic (sp^2) =C-H	Weak absorption
	Alkene (sp^2) =C-H	One or couple stronger than aromatic =C-H absorption
2,850 and 2,750	Aldehyde C-H	Two medium-intensity peaks on the right-hand shoulder of the alkyl C-H
2,260-2,210	Nitrile $\text{C}\equiv\text{N}$	Sharp of medium intensity peak
2,260-2,100	Alkyne $\text{C}\equiv\text{C}$	Vary intensity of peaks from medium to nothing
1,850-1,750	Anhydride C=O	Two absorption peaks, one near $1,830\text{-}1,800$ and another near $1,755\text{-}1,740$
1,750-1,700	Aldehyde C=O	-
	Ketone C=O	-
	Ester C=O	-
	Acid C=O	-
1,700-1,640	Amide C=O	Slightly lower response than normal C=O
	Conjugated C=O	Lower the absorption about $20\text{-}50\text{ cm}^{-1}$
1,680-1,620	Alkene C=C	Not intense as C=O
1,600-1,400	Aromatic C=C	Multiple sharp and medium peaks
1,465-1,450	Alkene C-H	-
1,450-1,375	Alkane C-H	-
Fingerprint region ($1,500\text{-}400\text{ cm}^{-1}$)		
1,300-1,000	C-O	Strong
1,500-400	Various functional groups	Unique pattern of absorptions, including single bond stretches and a wide variety of bending vibrations

IR has been used for herbal quality assessment and herbal quality control [134]. This technique has been applied for various herbal analyses such as identification of functional group for structure elucidation, identification of different plant species, identification of different plant part uses, identification morphological features. Moreover it has been applied for differentiation between genuine and adulterant, differentiation of different geographical regions, differentiation between wild and cultivated herbs and differentiation of different storage duration.

12 Preprocessing technique of chemical fingerprint

Before comparison complex data obtaining from chemical analysis such as fingerprint deriving from spectroscopic or chromatographic methods, preprocessing technique is important. It can enhance the appearance and improve the features of spectrum or chromatogram. For fingerprint analysis, the preprocessing data is better than the raw data. It is suitable for analysis in the next step. The preprocessing techniques used in this study are described below.

12.1 Smoothing

This transformation is relevant for variables. It can remove some noise of spectra or chromatogram to improve the data content. Savitzky-Golay algorithm is mostly applied for smoothing. It performs a best fit polynomial to successive data points. It determines the best fit center point for the polynomial fit as constrained by the data point segment [135-137]. This smoothing method is shown in Figure 7.

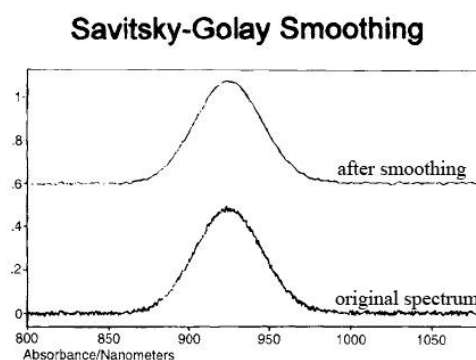


Figure 7 Savitsky-Golay smoothing [135].

12.2 Normalization

The purpose of this transformation is to scale the individual fingerprint obtaining from various samples to the same scale in order to compare or analyze the relationship of each other.

Unit vector normalization is one of transformation techniques. It normalizes sample-wise data X_i to unit vectors by using equation (1). It can be used for pattern normalization. [137].

$$newX_i = \frac{X_i}{\sqrt{\sum_j x_{ij}^2}} \quad (1)$$

Maximum normalization is an alternative to classical normalization which divides each row by its maximum absolute value. The maximum value becomes +1 when all values are positive. The minimum value becomes -1 when all values are negative [137].

12.3 Derivative

Derivative is used to remove baseline effects in spectra for the purpose of creating robust calibration models. This method also resolves the overlapping peaks and amplifies variations [136, 137]. First derivative is a simply method which very useful to removing baseline offset. This is because it measures the slope of the spectral curve at every point and the maximum data point will be changed to zero point. Second derivative is a measure of the change in the slope of curve and ignoring the offset. Therefore this method is useful for removing both offset and slope from a spectrum. The maximum data point will be changed to minimum data point [132, 137]. The Savitzky-Golay method is well known for smoothing and second derivative in spectroscopy such as NIR and MIR [138, 139]. The Savitzky-Golay method uses a convolution function, and thus the number of data points (segment) in the function must be specified. If the segment is too small, the result may be no better than using the simple difference method. If it is too large, the derivative will smooth out too much of the important information [137].

12.4 Alignment

Most chromatograms that obtained from various chromatographic analyses may appear the effect of retention time shift among samples. These are the problematic issues for chemometric analysis because the proper chromatographic data for comparison of the same compound in individual sample have to match to each others. For solving the retention time shift, the peak alignment method shall be untangled [140-142]. The example of alignment method is PAFFT correlation method (Peak alignment by Fast Fourier Transform). It works by dividing a spectrum into segments before the evaluation of best shift using Fast Fourier Transform which is an algorithm for transformation the function of time domain to frequency domain.

13 Chemometric methods for quality control of herbal medicines

13.1 Introduction of chemometrics

Since complex and various data from fingerprint analysis are difficult to integrate, the useful tool to contribute large and complex information is chemometrics. The definition of chemometrics mentioned in “Chemometrics: a text book” is the chemical discipline that uses mathematical, statistical, and other methods employing formal logic (a) to design or select optimal measurement procedures and experiments, and (b) to provide maximum relevant chemical information by analyzing chemical data [27]. In term of herbal medicines, fingerprint analysis is an analysis of entire compounds, which has effectiveness more than particular one chemical marker because activities of herbal medicines deriving from many chemical compounds of themselves [24].

13.2 Unsupervised pattern recognition

Unsupervised learning is one of the techniques of the pattern recognition which is not provided the prior knowledge to the method. The goal of unsupervised data analysis is to evaluate whether clustering exists in a data set without using class membership information in the calculation [29]. The famous three techniques of unsupervised exploratory analysis are similarity analysis (SA),

hierarchical cluster analysis (HCA) and principal component analysis (PCA) [29, 143].

13.2.1 Similarity analysis (SA)

The relationship between two variables is widely explained by correlation coefficient [27, 144]. In term of herbal fingerprint analysis, the data of variables can be obtained from various analysis methods, for instance, infrared spectroscopy, raman spectroscopy, nuclear magnetic resonance spectroscopy, thin layer chromatography, high performance liquid chromatography or gas chromatography, may also mass spectroscopy as detector [143]. Pearson correlation is mostly used to evaluate the fingerprint. To compare (dis)similarity of two fingerprints, the correlation coefficient (r) will be considered. The range of “r” will represent from -1 to 1, if “r” represents “0” that means dissimilarity of two variables or two fingerprints. Absolute relationship of two variables will appear when “r” equal 1, association in positive approach, or -1, association in negative approach. The equation of correlation coefficient is showed in Equation (2):

$$r(x_1, x_2) = \frac{\sum_{i=1}^n (x_{1i} - \bar{x}_1)(x_{2i} - \bar{x}_2)}{\sqrt{\sum_{i=1}^n (x_{1i} - \bar{x}_1)^2 \sum_{i=1}^n (x_{2i} - \bar{x}_2)^2}} \quad (2)$$

where x_{1i} and x_{2i} are the values measured at the i^{th} time point, and \bar{x}_{1i} and \bar{x}_{2i} are the means of two set of measurment.

13.2.2 Hierarchical cluster analysis (HCA)

Hierarchical cluster analysis (HCA) is used to group samples in row space by calculating the linkage and the distance between sample and other samples. Many linkage methods for example single linkage, complete linkage, average linkage, median (or centroid) linkage and Ward's method; and distance measurement, for example Euclidean distance, squared Euclidean distance, standardized Euclidean distance, Mahalanobis distance, Pearson correlation distance and Spearman's rank correlation distance can be used to this cluster analysis [143]. Only one clustering method and one calculated distance method that play a role on this study will be described.

Single linkage method is the measurement based on the distance of nearest neighbor to cluster the samples into the same group. The example of single linkage method is shown as grouping between A and B, D and E in Figure 8.

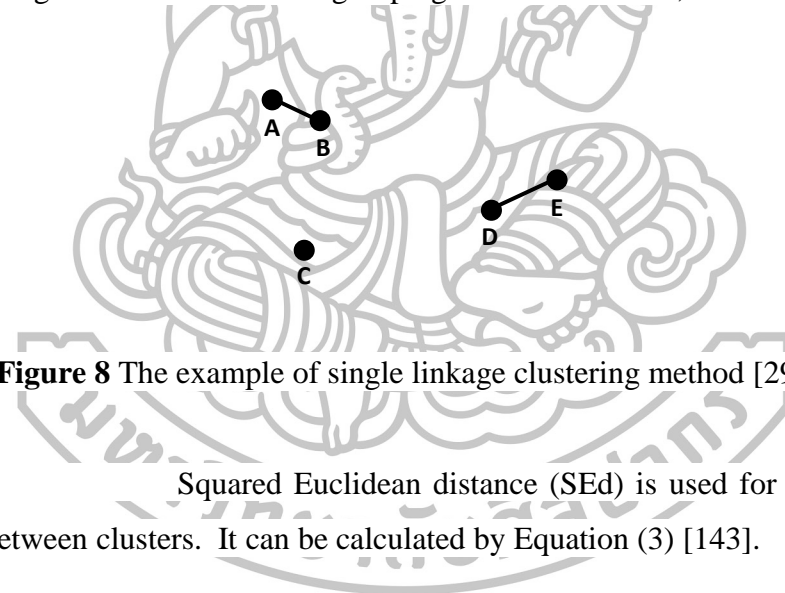


Figure 8 The example of single linkage clustering method [29].

Squared Euclidean distance (SEd) is used for measurement similarity between clusters. It can be calculated by Equation (3) [143].

$$SEd = \sum_{i=1}^n (x_i - y_i)^2 \quad (i = 1, 2, 3, \dots, n) \quad (3)$$

where x and y are values of two sets of measurement.

13.2.3 Principal component analysis (PCA) [29, 123]

PCA is one of the unsupervised pattern recognition techniques. This technique applied for reducing the number of numerous variables, for example wavenumber of IR analysis or retention time of GC/MS analysis. The new variable which is calculated from initial variables with linear combination is called “principle component (PC)”.

First principle component will combine the aspect of every initial variable (i.e. wavenumber or retention time) as much as possible. The next PC is independent from the first and other next components. The values that account on PC are eigenvalues. The directions of these new variables are called eigenvector. Latent PC is perpendicular with previous PC. The example is illustrated on Figure 9. PC1 is the first new variable which possesses the feature of each sample as much as possible. PC2 is perpendicular with PC1 and describes residue feature of the samples. All variables are described by PCs. For example, in term of the two new variables (two dimensions), if the feature of original variables is described by PC1 equal 98%, then the residues of feature of original variables are described by PC2 equal 2%.

The purpose of PCA is the distance explanation between a sample and others of the data set in less axes or dimensions. The maximum number of PCs is equal to variable or factor influencing on possible analysis. For example, ten variables of data set provide only ten PCs. Score and loading of PCA are important terms for the description of the information. Score is used for the explanation of sample features that correlate to latent variables (PCs). Loading is used for explanation of the original variables influencing on performing latent variables. Initial PCs such as PC1 and PC2 possess the feature of original variables more than the next PCs whereas the latter PCs possess more noise. The latter PCs may disturb PCA so it should be ignored.

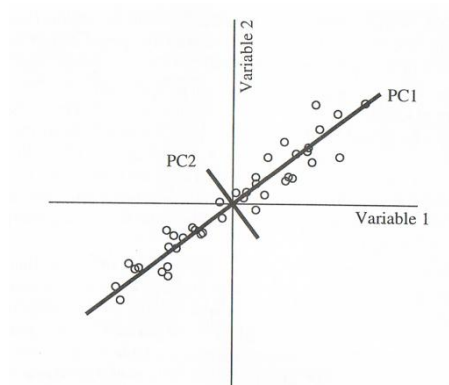


Figure 9 Establishment of new variable to principle component (PC) [29].

The equation of PCA is illustrated in Equation 4:

$$X = T.P + E \quad (4)$$

where X is matrix of data set, T is score, P is loading and E is noise of data set.

As well, Figure 10 explains matrix X. It is calculated from sum of multiply between score T and loading P. Score T is columns of t_1, t_2, \dots, t_i , of each component.

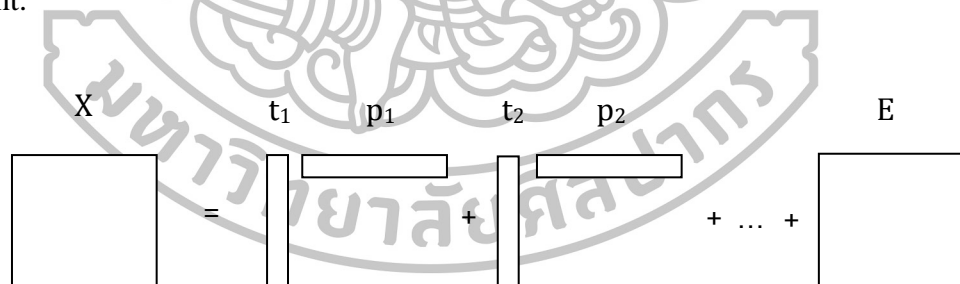


Figure 10 Relationship between data set, score, loading and noise for PCA.

13.3 Supervised pattern recognition

Supervised learning is the technique that applies to classify the new object or unknown sample on the basis of unsupervised learning. New object will be

classified to the proper class that is trained by using unsupervised pattern recognition such as PCA and PLS. This technique can contribute to know the characters of unknown object that fits to unsupervised technique. The steps of supervise pattern recognition are demonstrated as follows [145, 146].

- (1) Selection of training set: This consists of known objects of classification for which variables are measured.
- (2) Selection of variables: This step uses to accept or reject the variables influencing on classification. The variables without discriminating power are eliminated.
- (3) Performing of the model: A model is derived from training set that consists known objects and certain variables. The model may be called the calibration model.
- (4) Validation of the model: The calibration model is validated by independent test set or validation set for evaluation the reliability of the model.

Two supervised pattern recognitions that widely use for sample discrimination are SIMCA [147-151] and PLS-DA [32, 152-154].

13.3.1 Soft independent modeling of class analogy (SIMCA) [145, 146, 155-157]

SIMCA is a class-modeling method for which based on principle component (PCs) to explain the aspect of the model. On the basis of PCA, the matrix X ($n \times m$) which is sum of product of score (T), with n objects, and loading (P), with m variables, can be contributed to establish the prediction model of SIMCA. The description of matrix X can be described on Equation (5) where r is the optimum numbers of PCs that are evaluated by cross-validation method and E is the matrix of residues.

$$X = t_1p_1 + t_2p_2 + \dots + t_r p_r + E_{(n \times m)} \quad (5)$$

The PCA working for the training class of SIMCA is illustrated in Figure 11. Step 1 of one-dimension represents the distribution of objects (white dot) on PC1 (Figure 11a) axis. Then the model is performed like cylindrical shape (Figure 11c) and objects that distribute in the inner of this space will be class membership of this model describing using only PC1. When two-dimensions are considered, Figure 11b represents distribution of objects on both PC1 and PC2 axis as step 1. Then the boundary of the model performing from two-dimensions is shown in Figure 11d. Objects that distribute in the inner space of the model are classed into this model.

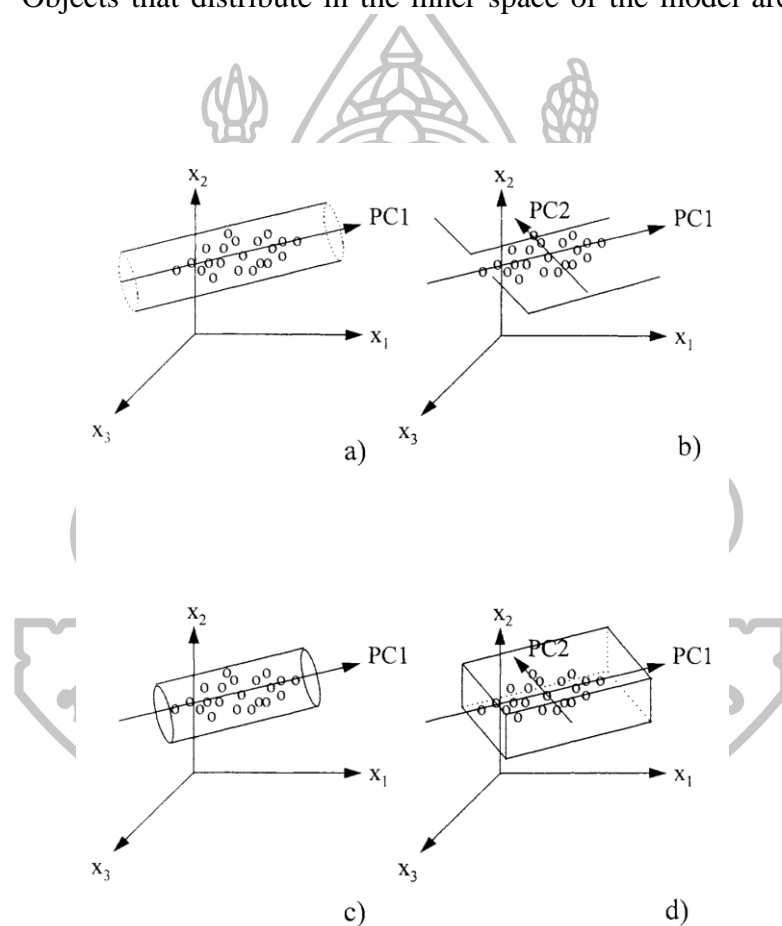


Figure 11 Illustration SIMCA steps using PCA: a) step 1 of one-dimension (1 PC) b) step 1 of two-dimensions (2 PCs) c) step 2 of one-dimension (1 PC) and d) step 2 of two-dimensions (2 PCs) [145].

The boundaries of model class are constructed on the basis of the distribution of the Euclidean distances between the training objects and the PCA model. This distribution relates with residue standard deviation (s_0) that are shown in Equation (6). A confidence limit of model is defined by the critical value of Euclidean distance showing in Equation (7). The residue standard deviation of unknown objects (s_p) are calculated by residues of unknown objects (eu) which related to the mean Euclidean distance between unknown object and PCA model, as shown in Equation (8).

$$s_0 = \sqrt{\frac{\sum_{i=1}^n \sum_{j=1}^m e_{ij}^2}{(n-r-1)(m-r)}} \quad (6)$$

$$s_{crit} = \sqrt{F_{crit} s_0^2} \quad (7)$$

$$s_p = \sqrt{\frac{\sum_{i=1}^m eu_{1j}^2}{(m-r)}} \quad (8)$$

where n is the number of object or sample, m is the number of variable, r is the selected PCs and e_{ij} is residue of i th object for j th (latent) variable

The unknown object will belong to the established model class when s_p is not larger than s_{crit} . s_{crit} is derived from F-test that calculates critical distance (F_{crit}) under significant confidence interval. If s_p is larger than s_{crit} , the unknown object is not membership of the model.

13.3.2 Partial least squares discrimination analysis (PLS-DA) [158-161]

PLS-DA is a classification method which explains relationship between measured value from analysis and character (cluster) of samples, based on modeling from partial least square (PLS). PLS is unsupervised analysis which is used to explain the relationship between matrix X (NxK) (the predictor), and matrix Y (NxJ) (the predicted or response). Where N is the number of samples, K is the number of measured variables (e.g. wavenumbers) and J is the number of predicted variables or categories (e.g. the determined class number) that relate to X. These are complex data; thus, in order to reduce the size of the data, latent variables (LV) or factors are employed:

$$X = TP + E \quad (9)$$

$$Y = UQ + F \quad (10)$$

where T, P and E are score matrices, loading terms and error terms of X, respectively; U, Q and F are score matrices, loading terms and error terms of Y, respectively.

In order to consider the relationship between X and Y, weight vector or loading weight (W) is important. It is applied to construct a linear combination from T score of original variables (Equation (11)).

$$T = XW \quad (11)$$

where T score is the score of latent variable.

For good prediction, Y uses same latent variable as X, thus U in Equation (10) were assumed as T:

$$Y = TQ + F \quad (12)$$

The combination of Equation (11) and (12) can be rewritten:

$$Y = XWQ + F \quad (13)$$

PLS-DA is a discrimination method. In the first step, calibration model is established from Equations (9) and (10). Y is the reference classes. It is coded as number "1" and "0" which refer to the interested group and other groups, respectively. For example, if there are three class groups, the reference number for establishment the model of the first group will be 1, 0 and 0. For the second group, the reference numbers are 0, 1 and 0. And they are 0, 0 and 1 for the last group. Thereafter the calibration model is validated by full cross validation. The predicted values are compared with the reference values. In the second step, the test samples are predicted with the calibration model. However the predicted values (Y) of test samples are not exact "1" or "0". Thus the criteria are calculated to determine the range of prediction. The test sample that is underlying within the criteria is considered as the member of the class.

13.4 Application of chemometrics on herbal identification

There were many publications about the application of chemometric methods on the identification of herbal medicines. Some of them were concluded in Table 19.

Table 19 Application of chemometrics on herbal identification.

Application	Chemical analysis	Chemometrics	Reference
Authentication of Cassia seed	HPLC	PCA	[162]
Authentication and quality assessment of Thyme	UV	HCA, PCA and SIMCA	[31]
Authentication of the plant material of three species of the genus <i>Bauhinia</i>	HPLC	HCA, PCA and SIMCA	[163]
Characterization of furocoumarins in the roots of <i>Angelica dahurica</i>	HPLC/DAD/ESI-MS ⁿ	SA	[164]
Classification of <i>Schizonepeta tenuifolia</i> Briq from different origin	GC/MS	HCA and PCA	[165]
Differentiation of geographical origin and maturity of the nutmeg.	GC/MS	PCA	[123]
Discrimination between <i>Valeriana officinalis</i> and other valerian species	HPLC/DAD	PCA, SIMCA and PLS-DA	[166]
Identification of Hawk-tea from different harvest time	HPLC	SA	[167]
Identification of Rhizoma gastrodiae (Tianma) from different producing areas	FT-IR	PCA and PLS-DA	[168]
Identification of forty-eight herbal Medicines	NIR	PCA and SIMCA	[169]
Identification of green tea	HPLC	SA	[144]
Identification of <i>Portulaca oleracea</i> L. from different sources	GC/MS and FT-IR	HCA and SA	[170]

SA = similarity analysis, HCA = hierarchical cluster analysis, PCA = principal component analysis, SIMCA = soft independent modeling of class analogy, PLS-DA = partial least squares discrimination analysis.

CHAPTER III

MATERIALS AND METHODS

1 Plant materials and authentic samples

Fifteen samples of Chan-thet (T1-T15), eighteen samples of Chan-khao (K1-K18), seventeen samples of Chan-chamot (M1-M17), ten samples of Chan-thana (TN1-TN10), and eleven samples of Chan-hom (H1-H11) were purchased from Thai traditional drugstores in various regions of Thailand during 2012 to 2013. The authentic samples of *Santalum album* L. (SA) and *Mansonia gagei* J.R.Drumm. ex Prain (MG) were collected from Prachuap-Khiri-Khan Silvicultural Research Station, Royal Forest Department. The authentic samples of *Myristica fragrans* Houtt. (MF), *Diospyros decandra* Lour. (DD), *Tarennia hoaensis* Pit. (TH), and *Aglaia silvestris* (M. Roem.) Merr. (AS) were collected from Chanthaburi Medicinal Plant Garden of Department of Medical Sciences of Ministry of Public Health. The authentic samples of *S. spicatum* (SS) and *S. lanceolatum* (SL) were the gifts obtained from Professor Dhanushka S. Hettiarachchi, a pharmacognosist of Wescrop group, Australia. All crude drug and authentic samples were chopped and ground by hammer mill (RetshGmbH SK1; Haan, Germany) to fine powder, and kept in the cold room at 4°C. The voucher specimens T1-T15, K1-K18, M1-M17, TN1-TN10, H1-H11, SA, MG, MF, DD, TH, AS, SS and SL were kept in the herbarium of Department of Pharmacognocny, Faculty of Pharmacy, Silpakorn University, Thailand.

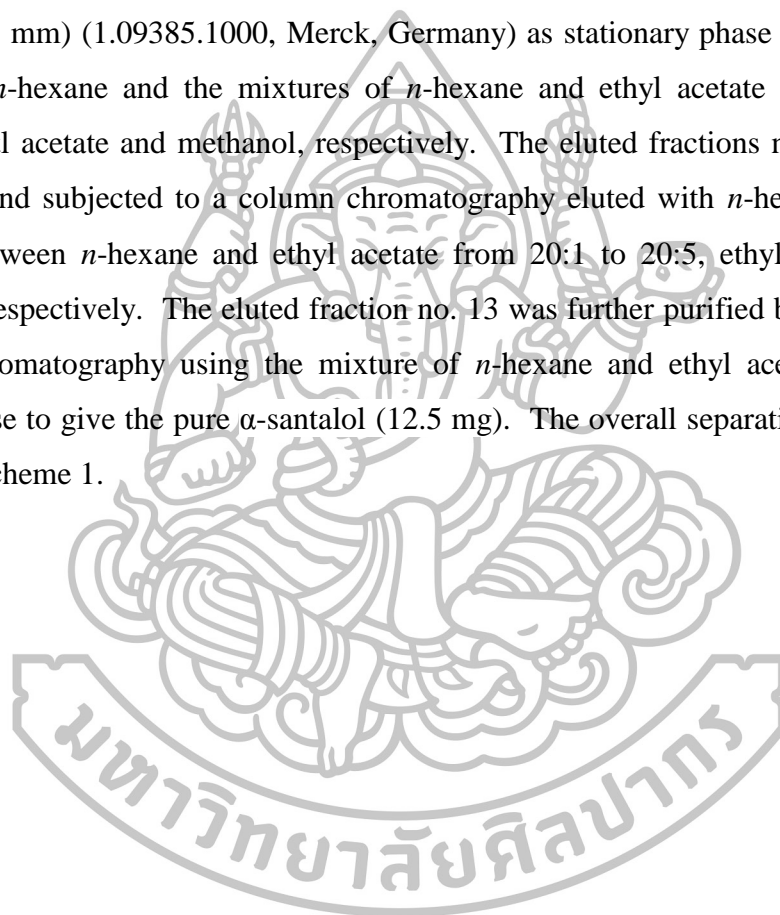
Authentic sandalwood oils were purchased from Eden Botanicals (USA). They were sandalwood oil obtained from *S. album* (sandalwood organic, steam distilled essential oil, originated from Sri Lanka), *S. album* (sandalwood-rare, steam distilled essential oil, originated from India), *S. spicatum* (sandalwood Australian-premium, steam distilled essential oil, originated from Australia/Wild), *S. austrocaledonicum* (sandalwood New Caledonia, steam distilled essential oil, New Caledonia), *S. austrocaledonicum* (sandalwood abs. New Caledonia, solvent extracted absolute, originated from New Caledonia/Wild) and *S. paniculatum* (sandalwood Royal Hawaiian, steam distilled essential oil, originated from Hawaii).

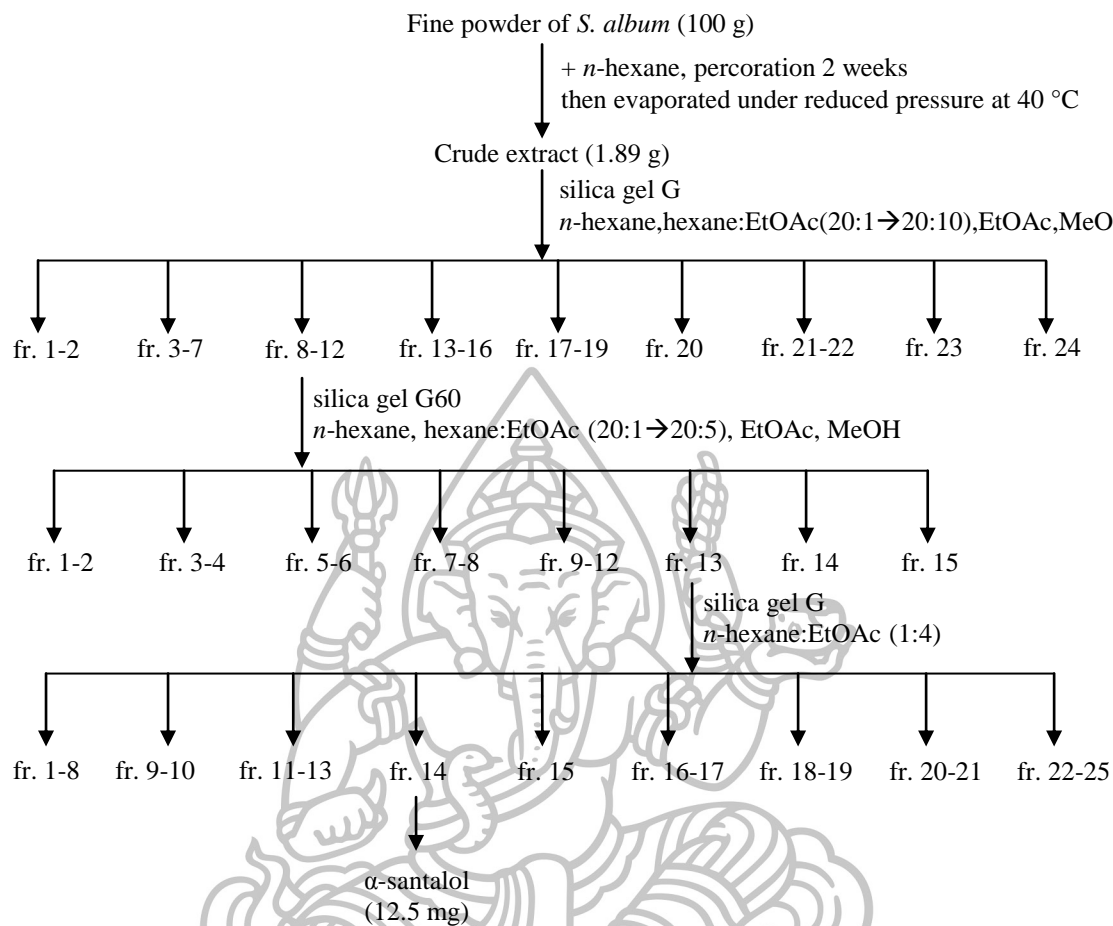
2 Chemical markers

2.1 Isolation of chemical markers

2.1.1 Isolation of α -santalol

The fine powder of the heartwood of *S. album* (100 g) was extracted by percolation with *n*-hexane. The extracted solution was evaporated under reduced pressure at 40 °C (Rotavapor; BÜCHI, Switzerland) to yield 1.89 g of the dry extract. Then it was separated by a column chromatography using silica gel G (size 0.040-0.063 mm) (1.09385.1000, Merck, Germany) as stationary phase with gradient elution of *n*-hexane and the mixtures of *n*-hexane and ethyl acetate from 20:1 to 20:10, ethyl acetate and methanol, respectively. The eluted fractions no. 8-12 were combined and subjected to a column chromatography eluted with *n*-hexane and the mixture between *n*-hexane and ethyl acetate from 20:1 to 20:5, ethyl acetate, and methanol, respectively. The eluted fraction no. 13 was further purified by a silica gel column chromatography using the mixture of *n*-hexane and ethyl acetate (1:4) as mobile phase to give the pure α -santalol (12.5 mg). The overall separation process is shown in Scheme 1.





Scheme 1 Isolation of α-santalol from the heartwood of *S. album*.

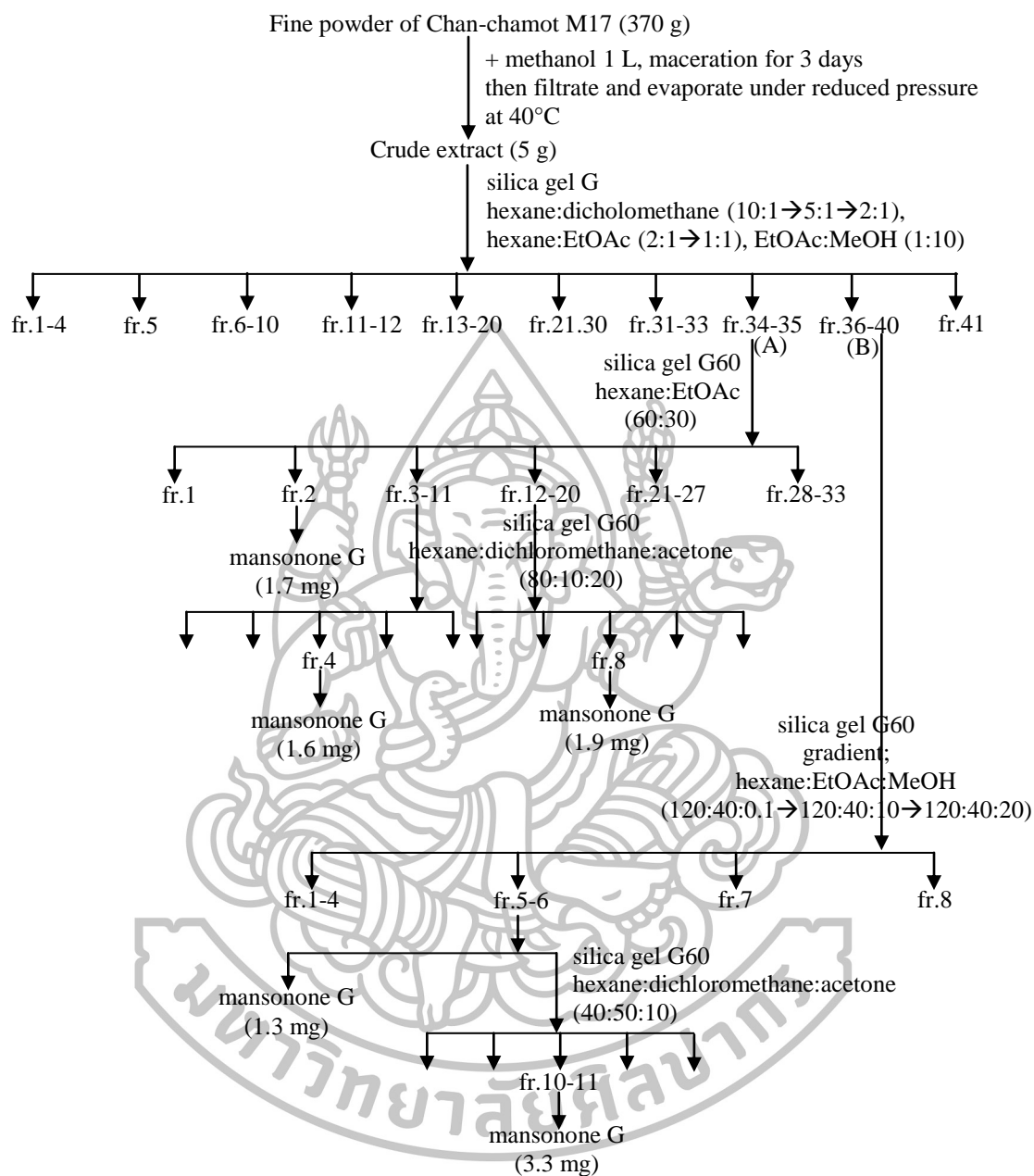
2.1.2 Isolation of mansonone G

The fine powder of the heartwood of a Chan-chamot sample (M17) (370 g) was extracted by maceration with methanol for three days. The extracted solution was filtrated through cotton wool and evaporated under reduced pressure at 40°C. The methanol extract (5.2 g) was eluted through silica gel G (size 0.040-0.063 mm) (1.09385.1000; Merck, Germany) column chromatography using gradient mobile phase of the mixture of *n*-hexane and dichloromethane (10:1 to 2:1), the mixture of *n*-hexane and ethyl acetate (2:1 to 1:1) and the mixture of ethyl acetate and methanol (1:10), respectively. Two portions from the combination of fractions no. 34-35 (A) and 36-40 (B) were further isolated.

Portion (A) was eluted through silica gel G column chromatography using the mixture of *n*-hexane and ethyl acetate (60:30). Fraction no. 2 was the pure mansonone G (1.7 mg). Fractions no. 3-11 were combined and subjected to a column chromatography eluted with the mixture of *n*-hexane, dichloromethane, and acetone (80:10:20). Mansonone G (1.6 mg) was crystallized from fraction no. 4. Fractions no. 12-20 were combined and subjected to a column chromatography eluted with the mixture of *n*-hexane, dichloromethane and acetone (80:10:20). The pure mansonone G (1.9 mg) was crystallized from fraction no. 8.

Portion (B) from the first column was subjected to a silica gel column chromatography eluted with the mixture of *n*-hexane, ethyl acetate and methanol (120:40:0.1, 120:40:10 and 120:40:20, respectively). Mansonone G (1.3 mg) was crystallized from fractions no. 5 and 6. Thereafter the mother liquor was evaporated to dryness and subjected to another silica column chromatography eluted with the mixture of *n*-hexane, dichloromethane and acetone (40:50:10). Mansonone G (3.3 mg) was crystallized from fractions no. 10-11.

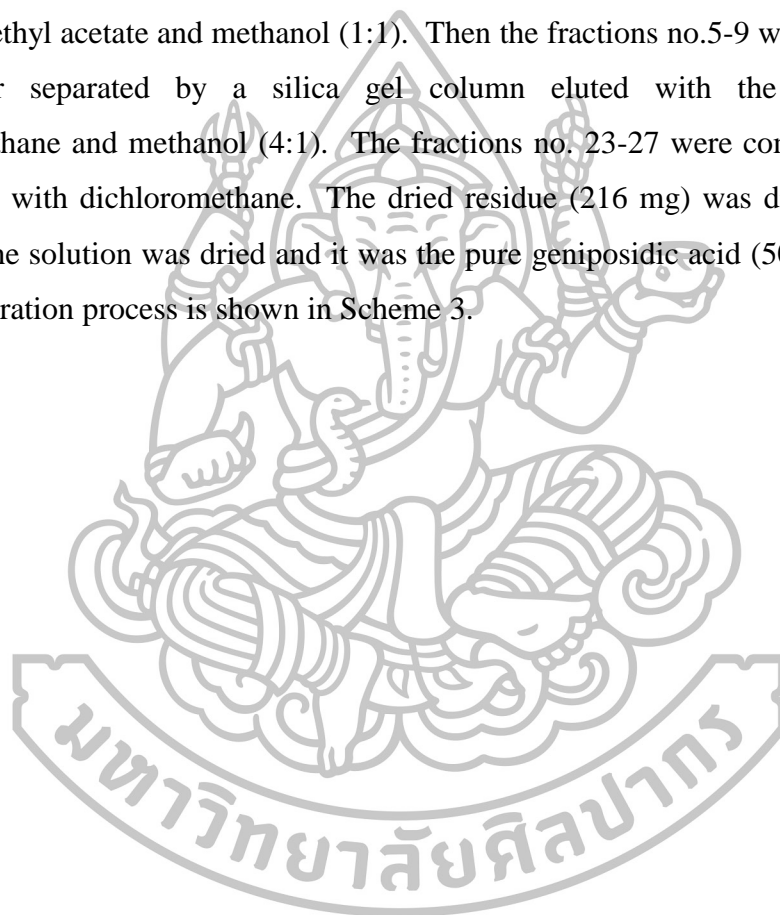
Total mansonone G obtained from these isolations was 9 mg. The separation process of mansonone G is shown in Scheme 2.

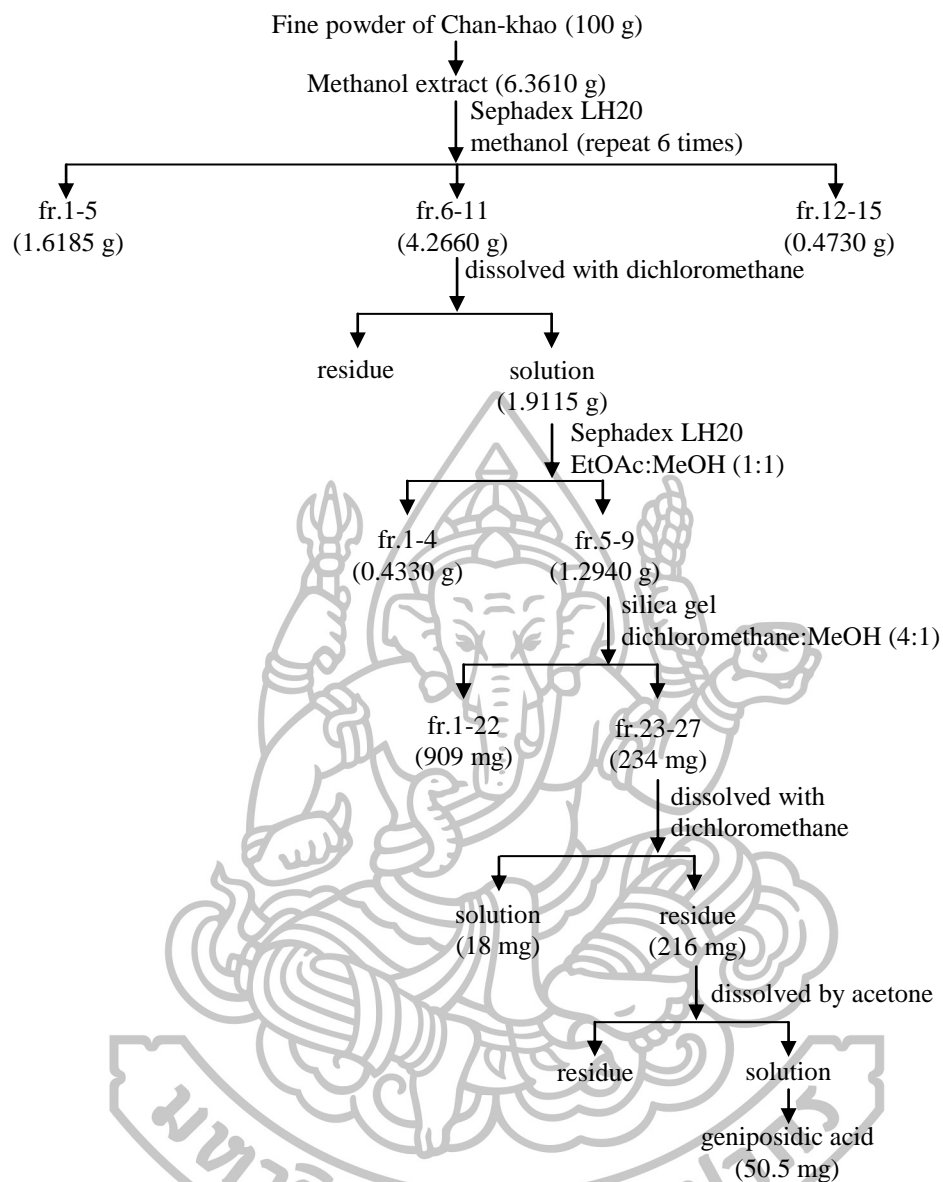


Scheme 2 Isolation of mansonone G from Chan-chamot sample (M17).

2.1.3 Isolation of geniposidic acid

The fine powder of the Chan-khao heartwood (100 g) was extracted by percolation with methanol. The methanol extract (6.3610 g) was subjected to a gel filtration column chromatography (SephadexTM LH-20, GE healthcare, Sweden) eluted with methanol. The fractions no. 6-11 (4.2660 g) were combined, dried and dissolved with dichloromethane by the aid of ultrasonication. The solution was separated by a gel filtration column chromatography eluted with the mixture of ethyl acetate and methanol (1:1). Then the fractions no.5-9 were combined and further separated by a silica gel column eluted with the mixture of dichloromethane and methanol (4:1). The fractions no. 23-27 were combined, dried and washed with dichloromethane. The dried residue (216 mg) was dissolved with acetone. The solution was dried and it was the pure geniposidic acid (50.5 mg). The overall separation process is shown in Scheme 3.





Scheme 3 Isolation of geniposidic acid from the heartwood of Chan-khao sample.

2.2 Structure elucidation of chemical markers

To interpret the structure of the isolated compounds, various spectroscopic techniques were applied. The infrared spectra were obtained on a Nicolet 4700 FT-IR, Thermo electron corporation, USA. The ^1H and ^{13}C of nuclear magnetic resonance spectra were obtained on a Bruker 300 Ultrashield, Karlsruhe, Germany. The EI-mass spectrum of α -santalol was determined by using Gas chromatography/Mass spectroscopy (6890N GC/5973MS, Agilent Technologies, Germany) operating at 70 eV. The (+)-ESI-mass spectra of mansonone G and geniposidic acid were determined by using Liquid Chromatography/Mass spectroscopy (1100 series LC/MSD Trap; Agilent Technologies, US).

3 Identification of Chan-thet, Chan-khao, Chan-chamot, Chan-thana and Chan-hom

3.1 Thin layer chromatography (TLC) fingerprint

3.1.1 Sample preparation

The fine powder of crude drug samples of Chan-thet, Chan-khao, Chan-chamot, Chan-thana and Chan-hom (500 mg) were extracted with 2 ml of methanol by sonication (Transonic; Elma[®], Germany) for 30 min. The supernatant solutions were used as test solutions.

The fine powder of authentic samples of *S. album*, *S. spicatum*, *S. lanceolatum*, *M. fragrans*, *D. decandra*, *T. hoaensis*, *M. gagei* and *A. silvestris* (500 mg) were extracted with 3 ml of methanol by sonication for 30 min. The supernatant solutions were used as authentic solutions.

α -Santalol, mansonone G and geniposidic acid were dissolved in methanol to the concentration of 1 mg/ml and used as standard solutions.

3.1.2 Chromatographic conditions

Stationary phase:	TLC aluminium sheet silica gel 60 GF ₂₅₄ (1.05554.0001; Merck, Germany)
Mobile phase:	1) <i>n</i> -Hexane:ethyl acetate: methanol (60:30:0.2 v/v/v), saturated for 1.5 hr, used for all crude drug samples 2) <i>n</i> -Hexane:ethyl acetate:methanol:glacial acetic acid (60:10:0.2:0.01 v/v/v/v), saturated for 1.5 hr, used for Chan-thet and Chan-hom samples 3) Dichloromethane:methanol:formic acid (60:10:1 v/v/v), saturated for 1.5 hr, used for Chan-khao and Chan-thana samples
Applied volume:	10 µl for test and authentic solutions 5 µl for standard solutions
Distance:	8 cm
Temperature:	25-30 °C
Drying:	Air dry
Detection:	a) under day light b) under ultraviolet light (254 and 366 nm) c) under day light after spraying with anisaldehyde-sulfuric acid TS, heat at 105 °C (TLC plate heater; CAMAG, Switzerland) until the color appear.

3.1.3 Data analysis

TLC chromatograms of samples, authentic samples and chemical markers were compared with each others. The chromatogram patterns were described by R_f value and color of appearing bands. The R_f value is the ratio of the

distance of the solute band moved on the adsorbent and the distance of the solvent moved on the adsorbent (solvent front) as Equation (14):

$$R_f = \frac{a}{b} \quad (14)$$

where a is the distance of solute band that moves on adsorbent, b is the distance of developing solvent that moves on adsorbent to the ending line.

3.2 Infrared spectroscopy (IR) fingerprint

3.2.1 Samples preparation

The fine powder of all crude drug samples and authentic samples were separately extracted with six solvents, i.e. *n*-hexane, dichloromethane, ethyl acetate, acetone, methanol and water, in the ratio of 1:20 w/v, by sonication for 30 min. Thereafter the extracted solutions were filtrated through cotton wool and evaporated to dryness under reduced pressure at 40-50 °C.

3.2.2 Examination procedure

The *n*-hexane, dichloromethane, ethyl acetate, acetone and methanol extracts were smeared as thin film on the potassium bromide (KBr) disc size 32x3 mm, drilled (Spectra-Tech Inc, USA), whereas the water extracts and the fine powder samples were blended with KBr powder (Fisher Scientific UK Ltd., UK) then they were pressed to thin plate. The Omnic 7.2a software (Thermo Electron Corporation, USA) was used for analysis. IR spectra were determined in the range of 4000-400 cm⁻¹, in the absorbance mode, with 16 scans and 4 cm⁻¹ of resolution.

3.2.3 Data preprocessing

The IR spectra were preprocessed with 11 smoothing points then they were saved by the Omnic 7.2a software as ACII files. Their data in the range of 1801-501 cm⁻¹ were arranged by Microsoft Office Excel 2007 software (Microsoft, WA, USA) to data metric of 675 x 79, where 675 are the number of variables (wavenumbers) and 79 are the number of samples (Chan-thet = 15, Chan-

khao = 18, Chan-chamot = 17, Chan-thana = 10, Chan-hom = 11 and authentic samples = 8). Thereafter the data was imported to the Unscrambler[®] X version 10.1 software (Camo Process AS, Norway). The data was transposed to 79 x 675 metric and preprocessed by unit vector normalization. Afterward the second derivative spectra were obtained by the Savitzky-Golay function with second derivative order, second polynomial order and fifteen smoothing points.

3.2.4 Data analysis

Three chemometric techniques, i.e. similarity analysis (SA), hierarchical cluster analysis (HCA) and principal component analysis (PCA) were used to analyse the data.

Similarity analysis (SA) was carried out by using Microsoft Excel 2007 software. The Pearson's correlation coefficient values (r) were used to describe the similarity among Chan(s) samples and authentic samples. The criterion of identification was $r \geq 0.90$ that meant very high correlation [171].

Hierarchical cluster analysis (HCA) was carried out by using the Unscrambler[®] X software. The clustering method was single-linkage clustering and the distance measurement from point to point of samples using square Euclidean distance.

Principal component analysis (PCA) was carried out by using the Unscrambler[®] X software. The algorithm was NIPALS. The optimum numbers of components were evaluated by using full cross validation method.

3.3 Gas chromatography (GC) fingerprint

3.3.1 Sample preparation

3.3.1.1 Essential oil preparation

The fine powder of three Chan-thet samples, the authentic *S. album*, *S. spicatum* and *S. lanceolatum* were distilled by steam distillation method that was applied from WHO and Thai Herbal Pharmacopoeia [122, 172]. The fine powder of a sample was contained into the round bottom flask then distilled water was added in approximate a half of the round bottom flask. The distilled

apparatus was set as Figure 12. Xylene (0.1 ml) was added to attach the essential oil of a sample. The mixture of a sample and liquid in the round bottom flask were heated. After boiling for 5 hr, they were stopped heating and cooled down at room temperature. Before GC/MS analysis, all essential oil were diluted by *n*-hexane at the concentration of 0.02 to 0.6 % v/v.

The authentic sandalwood oils of various *Santalum* species, i.e. *S. album*, *S. spicatum*, *S. austrocaledonicum* and *S. paniculatum* were diluted with *n*-hexane to the concentration of 0.1 % v/v.

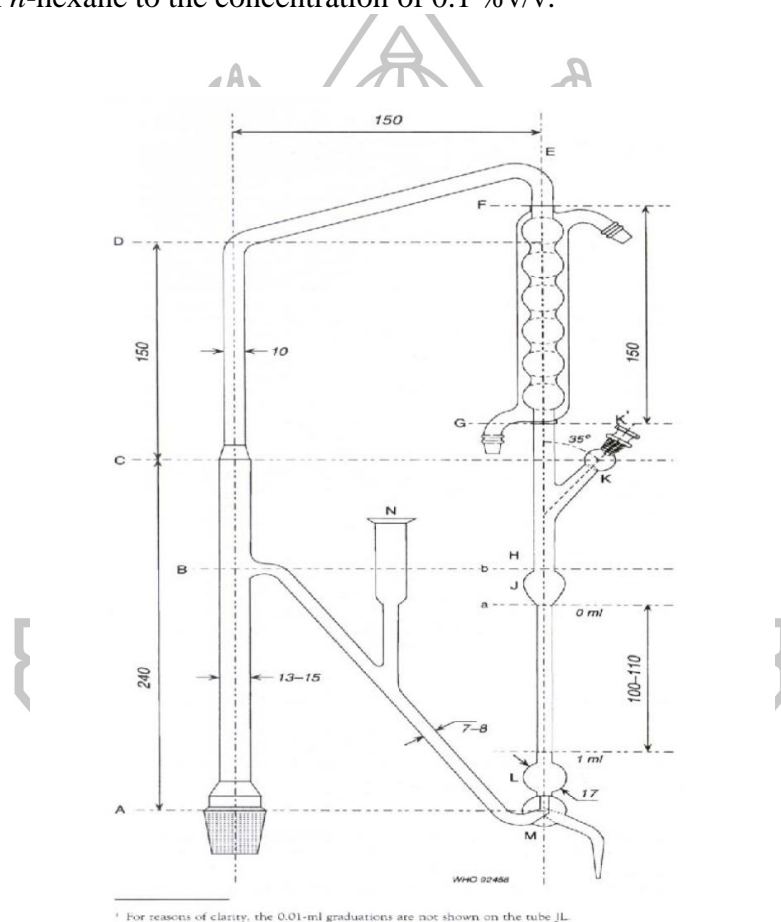


Figure 12 The illustration of the apparatus for essential oil distillation [122].

3.3.1.2 *n*-Hexane extracts preparation

The fine powders (200 mg) of all crude drug samples were extracted in *n*-hexane (2 ml) by sonication for 60 min. The supernatants were used for further analysis.

3.3.1.3 Chemical standard preparation

α -Santalol was dissolved with *n*-hexane to the concentrate of 0.1% v/v. It was a chemical marker of *Santalum* sp. Comparing with Kovats index (KI) value, the mixture of alkane standard was prepared for reference standard. The mixture of alkane standard was an alkane C₈-C₂₀ (Fluka, Switzerland) and an alkane C₂₁-C₄₀ (Fluka, Switzerland) standard that were mixed in the ratio 1:1.

3.3.2 Chromatographic condition

GC system:	6890N Network GC system 7683 series injector 7683 series autosampler, Agilent Technologies Chemstation data analysis software
Detector:	5973 Network Mass Selective Detector, Agilent Technologies
Column:	DB-5MS UI length 30 m, diameter narrowbore 0.250 mm, film 0.25 μ m, Agilent J&W, USA
Carrier gas:	Helium, flow rate 1.0 ml/min
Injection mode:	Splitless
Volume of injection:	1 μ l for hexane extract samples and 0.5 μ l for essential oil samples
Oven temperature program:	Initial, 50 $^{\circ}$ C 20 $^{\circ}$ C /min, 120 $^{\circ}$ C, 1 min 8 $^{\circ}$ C /min, 160 $^{\circ}$ C, 2 min 2 $^{\circ}$ C /min, 170 $^{\circ}$ C, 3 min 5 $^{\circ}$ C /min, 200 $^{\circ}$ C, 2 min 3 $^{\circ}$ C /min, 250 $^{\circ}$ C, 3 min 20 $^{\circ}$ C /min, 280 $^{\circ}$ C, 20 min
Ion source:	Electron Impact, 70 eV
Interface temperature:	280 $^{\circ}$ C

3.3.3 Data analysis

The chromatograms of *n*-hexane extracts and essential oils of crude drug and authentic samples were investigated. The retention time in the range of 15-23 min was chosen for the examination.

3.3.3.1 Data preprocessing

The chromatogram was preprocessed by using SpecAlign software version 2.4.1 (University of Oxford, UK). Firstly, a suitable chromatogram was chosen and imported to the software. Then it was averaged to generate an average chromatogram. Noise of the chromatogram was reduced by assignment the wavelet denoising at threshold 0.8, and the baseline was subtracted with window size 4. Other chromatograms were imported and aligned for peak shift by Peak alignment by Fast Fourier Transform (PAFFT) correlation method. Finally their noise was reduced by the same processing as mention above.

All aligned chromatograms (54 samples) were saved as ACII file then arranged the data by using Microsoft Excel 2007 to 1179 x 54 data metric, where 1179 are the number of the variables (retention times). The data were imported to the Unscrambler[®] X software and transposed to 54 x 1179 data metric. Then they were preprocessed by Savitzky-Golay smoothing at zero derivative order, zero polynomial and eleven smoothing points. Finally they were normalized by maximum normalization.

3.3.3.2 Data analysis

Three chemometric techniques, i.e. similarity analysis (SA), hierarchical cluster analysis (HCA) and principal component analysis (PCA) were used to analyse the data (see section 3.2.4).

3.3.3.3 Identification of chemical constituents in essential oils

Each peak of GC/MS chromatograms was identified by comparing its mass fragmentation pattern to those in the Wiley database (version

7th edition) and NIST database (version 2002). This identification was accepted when its matching was more than 90% of quality. Moreover the comparison of KI value was considered simultaneously. The KI value of each compound was obtained from the Equation (15). The KI value of the unknown compound was compared with the KI values of reference compounds published in the book of identification of essential oil components by gas chromatography/quadrupole mass spectroscopy [173] and/or the other reports. The KI value is calculated as follows:

$$KI = 100 \times \left[n + (N - n) \times \left(\frac{tr_{unknown} - tr_n}{tr_N - tr_n} \right) \right] \quad (15)$$

where n is the number of alkane carbons that has retention time close to the unknown peak in the early position, N is the number of alkane carbons that has retention time close to the unknown peak in the late position, $tr_{unknown}$ is retention time of the unknown peak, tr_n is retention time of alkane carbon that has retention time close to the unknown peak in the early position, tr_N is retention time of alkane carbon that has retention time close to unknown peak in the late position.

4 Development of authentication models

Two chemometric techniques were used to develop the models for the prediction of botanical species of Chan(s) crude drug samples. They were soft independent modeling of class analogy (SIMCA) and partial least squares-discriminant analysis (PLS-DA). The models were developed based on IR data.

4.1 Sample preparation

To establish the models, the suitable extracts and preprocessing method were chosen by using PCA. Initially, the six solvents, i.e. *n*-hexane, dichloromethane, ethyl acetate, acetone, methanol and water, and the fine powder

were investigated. All IR spectra were preprocessed by baseline correction and smoothing at 11 point by Omnic software and were saved as ASCII file. Thereafter they were imported to the Unscrambler[®] X software. IR spectra in the range of 1801-501 cm^{-1} were further preprocessed by unit vector normalized and second derivative using Savitzky-Golay methods as described in section 3.2.3. The 79×675 (samples×variables) matrix data of all crude drug and authentic samples was analyzed by PCA. The algorithm of analysis was NIPALS. The validation method was full cross validation. The extracts that could clearly classify the samples were chosen to establish the models.

After choosing the suitable solvent extract, the outlier was excluded from the examination by using hotelling T^2 with 1% of confidence. Thereafter the rest samples were separated into two groups by simple random sampling. The first group was the training set that was 60% of the sample group. This set was used to establish the calibration model. The second group was the test set that was 40% of the sample group. This set was used for external validation of the calibration models.

To establish the calibration models, the wavenumber in the range of 1801-501 cm^{-1} was preprocessed with two methods, i.e. normalization (unit vector) and second derivative (Savitzky-Golay) as described in section 3.2.3. And each spectrum was divided into three wavenumber ranges, i.e. 1801-501, 1801-1500 and 1498-501 cm^{-1} . The numbers of variables in these ranges were 675, 157 and 518, respectively. Then six models for each botanical species were established.

The other fifteen blind samples were used to test the models for application in common situation. These samples were selected and identified by Assoc. Prof. Dr. Uthai Sotanaphun.

4.2 Soft independent modeling of class analogy (SIMCA)

SIMCA is one of the sample prediction techniques for discrimination. The prediction model was based on PCA model (calibration model). The optimal PC number of PCA models was suggested by the software (Unscrambler[®] X). After development of the models, they were evaluated by test set and blind samples.

The efficiency of SIMCA methods was evaluated by sensitivity, specificity and accuracy [174]. Sensitivity referred to the effectiveness of model to define the samples that correctly accorded with the model (Equation (16)). Specificity referred to the effectiveness of model to reject the samples that not accorded with the model (Equation (17)). Accuracy referred to overall correction of the model (Equation (18)).

$$\text{Sensitivity} = \frac{TP}{TP + FN} \quad (16)$$

$$\text{Specificity} = \frac{TN}{TN + FP} \quad (17)$$

$$\text{Accuracy} = \frac{TP + TN}{TP + FP + TN + FN} \quad (18)$$

where TP is the true positive result or the true samples matching with the model; FN is the false negative result or the true samples not matching with the model; TN is the true negative result or the false samples not matching with the model; FP is the false positive result or the false samples matching with the model

The graphical predictions of samples were described by Cooman's plots which displayed the samples relating to establishment model of the two classes (models). The sample that located on left above or right below quadrants was clearly classified to each class (model). The sample that located on left below quadrant was

referred to the error of prediction models. The sample that located on right above quadrant was not a member of both models.

4.3 Partial least squares-discriminant analysis (PLS-DA)

To predict the sample using regression model, the PLS-DA was applied. PLS-DA is the prediction based on partial least square (PLS) regression model. As same as PCA, the PLS calibration was calculated by using NIPALS algorithm. The predictors (X) were used to predict the response (Y). X was the matrix of [samples \times wavenumbers]. Y was the matrix of [samples \times the reference number or the response or the predicted values]. They were determined as constant numbers 1 and 0, which were referred to the interesting class and other class, respectively. The optimum number of factors was evaluated by full cross validation method and suggested by the software (Unscrambler[®] X).

The performance of PLS model is evaluated by linearity and root mean squared error of cross validation (RMSECV) [157, 160, 175, 176].

$$RMSEC = \sqrt{\frac{\sum_{i=1}^N (y_{ref} - y_{cal})^2}{N - F - 1}} \quad (19)$$

$$RMSECV = \sqrt{\frac{\sum_{i=1}^N (y_{ref} - y_{pred,cv})^2}{N}} \quad (20)$$

where y_{ref} is the known value or reference value, y_{cal} and $y_{pred,cv}$ are the calculated value, N is the number of sample and F is the number of factors of the calibration model.

The efficiency of PLS-DA methods were validated with test set and explained by RMSEP.

$$RMSEP = \sqrt{\frac{\sum_{i=1}^M (y_{ref} - y_{pred})^2}{M}} \quad (21)$$

where y_{ref} is the determined value or reference value, y_{pred} is the calculated value of prediction, and M is the number of predicted samples.

To setup accepted criteria for the prediction, cutoff range was important. The samples that give a predicted response in the cutoff range were classified as the member of the group. The cutoff range was the range that covered the reference number (number 1) with cutoff value. It was “ $1 \pm$ cutoff value”. The cutoff value was the average of sum of the absolute of minimum (m), maximum (M) error (difference between predicted response and reference number) and RMSECV [178] (Equation (24)).

$$Cutoff\ value = \frac{(|m| + |M| + |RMSECV|)}{3} \quad (24)$$

As same as SIMCA, the efficiency of PLS-DA methods was evaluated by sensitivity, specificity and accuracy.

CHAPTER IV
RESULTS AND DISCUSSIONS

1 Plant materials

All crude drug samples used in this experiment were purchased from Thai traditional drugstores located at various locations of Thailand during 2012 to 2013. The details of crude drug samples and authentic samples are shown in Tables 20 and 21.

Table 20 Sources and characters of crude drug samples.

Voucher specimen	Name (Thai name)	Source	Character
T1		Bangkok	Tiny pieces of wood, characteristic fragrance
T2		Bangkok	Tiny pieces of wood, characteristic fragrance
T3		Nonthaburi	Tiny pieces of wood, characteristic fragrance
T4		Uttaradit	Tiny of wood attached with some bark, characteristic fragrance
T5		Nakhon Pathom	Pieces of wood attached with some bark, characteristic fragrance
T6		Nonthaburi	Tiny pieces of wood, characteristic fragrance
T7	Chan-thet	Nonthaburi	Pieces of wood, characteristic fragrance
T8	(จันทเทศ)	Nonthaburi	Tiny pieces of wood, characteristic fragrance
T9		Nonthaburi	Small pieces of wood, characteristic fragrance
T10		Saraburi	Tiny pieces of wood, characteristic fragrance
T11		Uttaradit	Tiny pieces of wood, characteristic fragrance
T12		Bangkok	Tiny pieces of wood, characteristic fragrance
T13		Phichit	Tiny pieces of wood, characteristic fragrance
T14		Roi Et	Fine powder, characteristic fragrance
T15		Songkhla	Pieces of wood attached with some bark, characteristic fragrance

Table 20 Sources and characters of crude drug samples (continued).

Voucher specimen	Name (Thai name)	Source	Character
K1		Bangkok	Pieces of wood attached with some bark
K2		Saraburi	Pieces of wood attached with some bark
K3		Roi Et	Pieces of wood attached with some bark
K4		Nakhon Pathom	Pieces of wood attached with some bark
K5		Nonthaburi	Pieces of wood attached with some bark
K6		Nonthaburi	Pieces of wood attached with some bark
K7		Nonthaburi	Pieces of wood attached with some bark
K8		Nonthaburi	Pieces of wood attached with some bark
K9	Chan-khao	Chiang Mai	Pieces of wood attached with some bark
K10	(จันทน์ขาว)	Phitsanulok	Pieces of wood attached with some bark
K11		Suphan Buri	Pieces of wood attached with some bark
K12		Phichit	Pieces of wood attached with some bark
K13		Nakhon Pathom	Pieces of wood attached with some bark
K14		Bangkok	Pieces of wood attached with some bark
K15		Bangkok	Pieces of wood attached with some bark
K16		Songkhla	Pieces of wood attached with some bark
K17		Nonthaburi	Pieces of wood attached with some bark
K18		Chiang Mai	Fine powder, characteristic fragrance



Table 20 Sources and characters of crude drug samples (continued).

Voucher specimen	Name (Thai name)	Source	Character
M1		Nonthaburi	Dark brown pieces of wood attached with some bark, characteristic fragrance
M2		Bangkok	Dark brown pieces of wood attached with some bark, characteristic fragrance
M3		Nonthaburi	Dark brown pieces of wood attached with some bark, characteristic fragrance
M4		Nonthaburi	Dark brown pieces of wood attached with some bark, characteristic fragrance
M5		Chiang Mai	Fine powder, characteristic fragrance
M6		Nonthaburi	Dark brown pieces of wood attached with some bark, characteristic fragrance
M7		Phitsanulok	Dark brown pieces of wood attached with some bark, characteristic fragrance
M8		Uttaradit	Dark brown pieces of wood attached with some bark, characteristic fragrance
M9	Chan-chamot (จินตนาชมนัด)	Roi Et	Dark brown pieces of wood attached with some bark, characteristic fragrance
M10		Nonthaburi	Dark brown pieces of wood attached with some bark, characteristic fragrance
M11		Songkhla	Dark brown pieces of wood attached with some bark, characteristic fragrance
M12		Saraburi	Dark brown pieces of wood attached with some bark, characteristic fragrance
M13		Uttaradit	Dark brown pieces of wood attached with some bark, characteristic fragrance
M14		Phichit	Dark brown pieces of wood attached with some bark, characteristic fragrance
M15		Bangkok	Dark brown pieces of wood attached with some bark, characteristic fragrance
M16		Bangkok	Dark brown pieces of wood attached with some bark, characteristic fragrance
M17		Nakhon Pathom	Dark brown pieces of wood attached with some bark, characteristic fragrance

Table 20 Sources and characters of crude drug samples (continued).

Voucher specimen	Name (Thai name)	Source	Character
TN1		Chiang Mai	Fine powder
TN2		Nakhon Pathom	Pieces of wood attached with some bark
TN3		Nonthaburi	Pieces of wood attached with some bark
TN4		Chiang Mai	Fine powder
TN5	Chan-thana	Nonthaburi	Pieces of wood attached with some bark
TN6	(จันทนา)	Bangkok	Pieces of wood attached with some bark
TN7		Bangkok	Pieces of wood attached with some bark
TN8		Nonthaburi	Pieces of wood attached with some bark
TN9		Bangkok	Pieces of wood attached with some bark
TN10		Nonthaburi	Pieces of wood attached with some bark
H1		Nakhon Pathom	Pieces of wood attached with some bark, characteristic fragrance
H2		Bangkok	Tiny pieces of wood, characteristic fragrance
H3		Chiang Mai	Tiny pieces of wood, characteristic fragrance
H4		Chiang Mai	Tiny pieces of wood, characteristic fragrance
H5		Phitsanulok	Tiny pieces of wood, characteristic fragrance
H6	Chan-hom	Bangkok	Tiny pieces of wood, characteristic fragrance
H7	(จันทน์หอม)	Nonthaburi	Tiny pieces of wood, characteristic fragrance
H8		Bangkok	Tiny pieces of wood, characteristic fragrance
H9		Nonthaburi	Tiny pieces of wood, specific fragrance
H10		Nonthaburi	Dark brown pieces of wood attached with some bark, characteristic fragrance
H11		Roi Et	Dark brown pieces of wood attached with some bark, characteristic fragrance

Table 21 Sources and characters of authentic samples.

Voucher specimen	Botanical name	Source	Chracter
SS	<i>Santalum spicatum</i>	Australia	Pieces of heartwood, charateristic fragrance
SL	<i>Santalum lanceolatum</i>	Australia	Pieces of heartwood, charateristic fragrance
SA	<i>Santalum album</i>	Prachuap Khiri Khan	Heartwood, charateristic fragrance
MG	<i>Mansonia gagei</i>	Prachuap Khiri Khan	Heartwood, charateristic fragrance
AS	<i>Aglaia silvestris</i>	Chanthaburi	Wood
TH	<i>Tarennia hoaensis</i>	Chanthaburi	Wood
DD	<i>Diospyros decandra</i>	Chanthaburi	Wood
MF	<i>Myristica fragrans</i>	Chanthaburi	Wood

The characters of crude drug samples and authentic samples are presented in Tables 20-21 and Figures 59-64. Most of Chan-thet samples (Figure 59) were tiny pieces of wood with characteristic fragrance. Chan-khao samples (Figure 60) were white pale wood, except that sample K18 was powder. All Chan-khao samples had no smell. The appearances of all Chan-chamot were dark brown wood except for sample M5 which was powder (Figure 61). Most of Chan-thana samples were white pale wood similar to Chan-khao, except that samples TN1 and TN4 were powder (Figure 62). Most of Chan-hom samples (Figure 63) were tiny pieces wood with characteristic fragrance similar to Chan-thet and some Chan-hom samples were dark brown wood similar to Chan-chamot.

2 Structure elucidation of chemical markers

The chemical standards used in this study were isolated in laboratory. They were α -santalol, mansonone G and geniposidic acid. Identification of their structures was described as follows.

2.1 α -Santalol

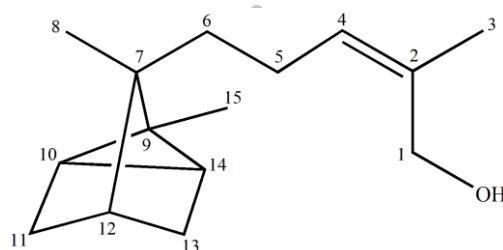


Figure 13 Structure of α -santalol.

α -Santalol (Figure 13) was colorless oil isolated from *S. album*. Based on EI-MS experiment, its molecular weight was 220 (Figure 65), corresponding with the molecular formula $C_{15}H_{24}O$. Its hydroxyl and olefinic functional groups were indicated by the IR bands at 3320 cm^{-1} and 1455 cm^{-1} , respectively (Figure 66). For more detail, NMR experiments were examined. The functional group $\text{CH}_3\text{-C}=\text{CH-}$ at positions 2 to 4 was proved based on the NMR data (Figures 67 and 68) which showed two olefinic carbon signals at δ_C 133.7 (C-2) and 129.5 (C4) ppm, one downfield proton signal at δ_H 5.31 ppm (*t*, $J = 7.4$, H-4) and downfield methyl signals at δ_H 1.79 ppm (H₃-3) and δ_C 21.2 ppm (C-3). The signals of the other two methyl groups at positions 8 and 15 were at δ_H 0.83 (*s*), δ_C 10.7 and δ_H 0.99 (*s*), δ_C 17.5 ppm, respectively. The methylene hydroxyl at position 1 was indicated by the downfield methylene signals at δ_H 4.14 (*s*) and δ_C 61.6 ppm. Moreover the overlapping two upfield signals at δ_H 0.83 ppm (*s*) were the characteristic methine protons at positions 10 and 14 of the rigid cyclopropane ring.

All of these spectral data confirmed the identification of this compound as α -santalol. Its ^1H and ^{13}C NMR data were compared with those previously reported [58]. It is shown in Table 22. α -Santalol is the major

sesquiterpene alcohol presented in volatile oil of various species of *Santalum*, including *S. album* [12, 45, 178-180].

Table 22 NMR assignment of α -santalol*.

Position	α -Santalol		Reference data [58]	
	δ_H	δ_C	δ_H	δ_C
1	4.14 (<i>s</i>)	61.6	4.14 (<i>s</i>)	61.6
2	-	133.7	-	133.7
3	1.79 (<i>s</i>)	21.3	1.79 (<i>s</i>)	21.3
4	5.31 (<i>t</i> , 7.4)	129.5	5.31 (<i>t</i> , 7.5)	129.5
5	1.98 (<i>m</i>)	22.9	1.97 (<i>m</i>)	23.0
6	1.19 (<i>m</i>)	35.0	1.14 (<i>m</i>)	35.0
	1.25 (<i>m</i>)		1.23 (<i>m</i>)	
7	-	27.4	-	27.4
8	0.83 (<i>s</i>)	10.7	0.83 (<i>s</i>)	10.7
9	-	45.9	-	45.9
10	0.83 (<i>s</i>)	19.5 ^a	0.83 (<i>d</i> , 3.0)	19.5 ^c
11	1.05 (<i>dd</i> , 7.5, 9.6)	31.0 ^b	1.05 (<i>t</i> , 10.5)	31.1 ^d
	1.60-1.70 (<i>m</i>)		1.57 (<i>t</i> , 10.5)	
12	1.56 (<i>m</i>)	38.2	1.50 (<i>m</i>)	38.2
13	1.05 (<i>dd</i> , 7.5, 9.6)	31.5 ^b	1.05 (<i>t</i> , 10.5)	31.5 ^d
	1.60-1.70 (<i>m</i>)		1.57 (<i>t</i> , 10.5)	
14	0.83 (<i>s</i>)	19.5 ^a	0.83 (<i>d</i> , 3.0)	19.6 ^c
15	0.99 (<i>s</i>)	17.5	0.99 (<i>s</i>)	17.5

* Chemical shift are reported as ppm (δ) from TMS in $CDCl_3$, signal multiplicity and coupling constant (Hz) are in parentheses.

^a The assignments may be interchanged.

^b The assignments may be interchanged.

^c The assignments may be interchanged.

^d The assignments may be interchanged.

2.2 Mansonone G

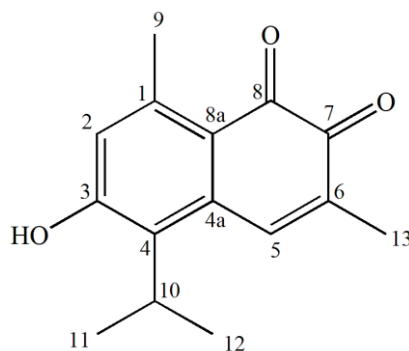


Figure 14 Structure of mansonone G.

Mansonone G (Figure 14) was yellow-orange amorphous powder isolated from one sample of Chan-chamot. Its ESI-MS (Figure 69) showed the $[M+H]^+$ ion peak at m/z 245, indicating the molecular formula as $C_{15}H_{16}O_3$. The IR bands (Figure 70) at 3309, 1655, 1644 and 1584 cm^{-1} indicated a hydroxyl, two conjugated carbonyl and a conjugated double bond, respectively; whereas the aromatic ring was suggested based on the IR bands at 1550 and 1458 cm^{-1} .

The ^{13}C -NMR spectrum (Figure 71) showed fifteen carbon signals. The ^1H -NMR spectrum (Figure 75) exhibited four methyl groups. Two symmetry doublet methyl signals at δ_{H} 1.42 ppm ($J = 7.2\text{ Hz}$) were assigned as CH_3 -11 and CH_3 -12 which geminal substituted on C-10 (δ_{C} 26.4 ppm). Then H-10 coupled with both CH_3 -11 and CH_3 -12 and presented as a septet signal (δ_{H} 3.58 ppm $J = 7.2\text{ Hz}$). The other two methyl groups were the singlet signals at δ 2.57 ppm (*s*, CH_3 -9) and δ 2.06 ppm (*s*, CH_3 -13). Their downfield signals were the anisotropic effect of aromatic ring and olefinic functional group, respectively. The present of olefinic group was confirmed by two downfield carbon signals at δ_{C} 138.4 (C-5) and δ_{C} 135.5 (C-6) ppm, and a downfield proton signal at δ_{H} 7.71 ppm (*s*, H-5). The present of aromatic ring was indicated by the downfield carbon signals at δ_{C} 146.3 (C-1), δ_{C} 120.3 (C-2), δ_{C} 132.5 (C-4), δ_{C} 135.2 (C-4a) and δ_{C} 125.1 ppm (C-8a) and an aromatic proton signal at δ_{H} 6.52 ppm (*s*, H-2). The aromatic carbon at δ_{C} 160.2 ppm (C-3) was on the downfield region due to inductive effect by electronegative of an oxygen atom. Finally, two carbonyl carbon signals at δ_{C} 182.5 and 180.4 ppm were assigned as C-7 and C-8, respectively.

All of these spectral data confirmed the identification of this compound as mansonone G. Its ^1H and ^{13}C NMR data were compared with those previously reported [181] and shown in Table 23. Mansonone G has been found in heartwood of *Mansonia gagei* [112] and aerial parts of *Thespesia populnea* [182].

Table 23 NMR assignment of mansonone G*.

Position	Mansonone G		Reference data [181]	
	δ_{H}	δ_{C}	δ_{H}	δ_{C}
1	-	146.3	-	146.6
2	6.52 (s)	120.3	6.56 (s)	119.9
3	-	160.2	-	162.2
4	-	132.5	-	133.2
4a	-	135.2	-	134.5
5	7.71 (s)	138.4	7.72 (s)	139.1
6	-	135.5	-	135.3
7	-	182.5	-	182.8
8	-	180.4	-	180.0
8a	-	125.1	-	122.7
9-CH ₃	2.57 (s)	23.1	2.58 (s)	23.3
10	3.58 (sept, 7.2)	26.4	3.58 (sept, 7.2)	26.8
11-CH ₃	1.42 (d, 7.2)	21.2	1.43 (d, 7.2)	21.2
12-CH ₃	1.42 (d, 7.2)	21.2	1.43 (d, 7.2)	21.2
13-CH ₃	2.06 (s)	16.1	2.07 (s)	15.9

* Chemical shift are reported as ppm (δ) from TMS in CDCl_3 , signal multiplicity and coupling constant (Hz) are in parentheses.

2.3 Geniposidic acid

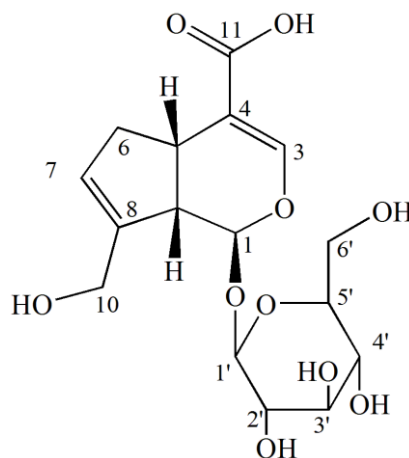


Figure 15 Structure of geniposidic acid.

Geniposidic acid (Figure 15) was isolated from one sample of Chan-khao. It was pale yellow semi-solid. Its ESI-MS spectrum (Figure 73) showed the molecular ion peak at m/z 374 $[M]^+$ corresponding with the molecular formula of $C_{16}H_{22}O_{10}$. Its hydroxyl, carboxyl and two olefinic functional groups were indicated by the IR bands at 3378, 1686 and 1631 cm^{-1} , respectively (Figure 74).

The ^{13}C -NMR (Figure 75) indicated sixteen carbon atoms. Based on DEPT-135° and DEPT-90° experiments, they were ten methine, three methylene and three quaternary carbons. In ^1H -NMR spectrum (Figure 76), two methine proton signals were showed at downfield region at δ_{H} 7.41 ppm (*s*, H-3) and δ_{H} 5.70 ppm (*brs*, H-7) because they were on the olefinic functional groups. Moreover the unusual more downfield of H-3 signal was the additional deshielding effect of the close oxygen atom at position 2. The present of two olefinic groups were indicated by the carbon signals at δ_{C} 153.4 (C-3), 113.0 (C-4) and 128.6 (C-7), 145.0 (C-8) ppm. A methylene hydroxyl functional group was indicated based on the downfield methylene signals at δ_{H} 4.09 ppm (*d*, $J = 14.4\text{ Hz}$) and 4.22 ppm (*d*, $J = 14.4\text{ Hz}$) of H₂-10. The downfield carbon signal at δ_{C} 171.2 ppm also indicated another carboxyl functional group. Substituted positions of these two functional groups were proved by HMBC experiment (Figure 77), which showed long-range correlations from H-10 to C-7 and C-8, and from H-3 to C-11. The ^1H NMR signals

in the range of 3-4 ppm and an anomeric signal at δ_H 4.62 ppm suggested a glucose moiety in the structure. The HMBC correlation between H-1 (δ_H 5.06 ppm) and C-1' (δ_C 100.5 ppm) (Figure 77) indicated that glucose attached to the aglycone at position 1. Stereochemistry of positions 1, 5 and 9 of the aglycone was proved by NOESY spectrum (Figure 78). The NOE correlation between H-5 and H-9 concluded the configuration of H-5 and H-9 to be in the same direction. But H-1 did not correlate with H-5 and H-9, therefore it was in the opposite direction.

All of these spectral data confirmed the identification of this compound as geniposidic acid. Its 1H and ^{13}C NMR data were compared with those previously reported [183] and shown in Table 24. Its HMBC correlations were shown in Figure 16 and Table 25. This compound has been reported in many plant species of family Rubiaceae, such as *Diodia teres*, *Galium tortumense*, *Genipa Americana*, *Canthium gilfillanii* and *Tarenna madagascariensis* [183-187].

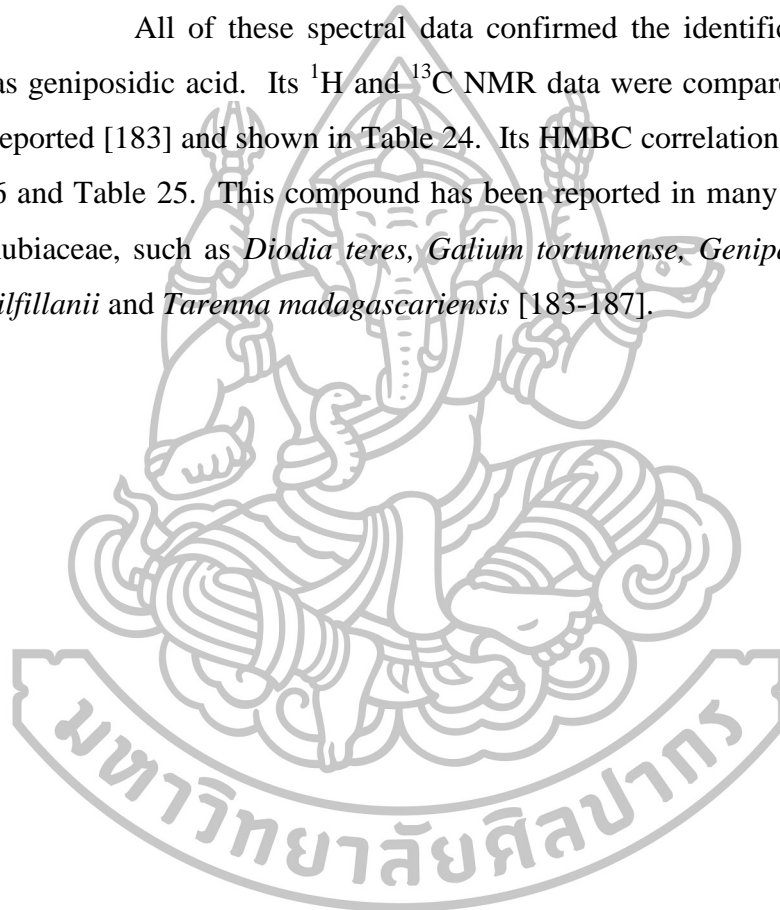


Table 24 NMR assignment of geniposidic acid*.

Position	Geniposidic acid		Reference data [182]	
	δ_{H}	δ_{C}	δ_{H}	δ_{C}
1	5.06 (<i>d</i> , 7.5)	98.4	5.00 (<i>d</i> , 7.2)	97.9
2				
3	7.41 (<i>s</i>)	153.4	7.25 (<i>s</i>)	154.5
4		113.0		116.4
5	3.08 (<i>m</i>)	36.84	3.13 (<i>m</i>)	37.3
6	2.01 (<i>dd</i> ; 16.3, 7.9)	39.9	2.00 (<i>dd</i> ; 16.0, 1.9)	39.9
	2.74 (<i>dd</i> ; 16.3, 7.9)		2.75 (<i>dd</i> ; 16.0, 8.4)	
7	5.70 (<i>brs</i>)	128.6	5.68 (<i>s</i>)	128.4
8		145.0		144.9
9	2.62 (<i>t</i> , 7.5)	47.2	2.58 (<i>m</i>)	47.2
10	4.09 (<i>d</i> , 14.4)	61.6	4.08 (<i>d</i> , 14.4)	61.6
	4.22 (<i>d</i> , 14.4)		4.21 (<i>d</i> , 14.4)	
11		171.2		174.5
1'	4.62 (<i>d</i> , 7.8)	100.5	4.63 (<i>d</i> , 8.0)	100.2
2'	3.14 (<i>d</i> , 8.1)	75.0	3.19-3.22 (<i>m</i>)	74.9
3'	3.28 (<i>d</i> , 9.0)	78.0	3.19-3.22 (<i>m</i>)	78.3
4'	3.17-3.20 (<i>m</i>)	71.7	3.19-3.22 (<i>m</i>)	71.5
5'	3.17-3.20 (<i>m</i>)	78.5	3.30 (<i>m</i>)	77.8
6'	3.54 (<i>dd</i> ; 7.6, 4.2)	62.8	3.74 (<i>m</i> , 2H)	62.6
	3.74 (<i>d</i> , 7.6)			

* Chemical shift are reported as ppm (δ) from TMS in CD₃OD, signal multiplicity and coupling constant (Hz) are in parentheses.

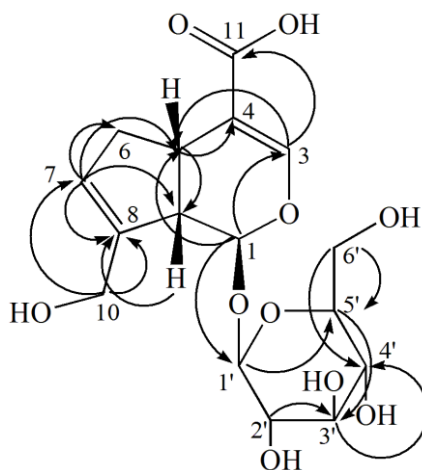


Figure 16 HMBC correlations of geniposidic acid.

Table 25 HMBC correlation of geniposidic acid.

Position	Carbon
1	C-5, C-1', C-8, C-3
3	C-5, C-1, C-4, C-11
5	C-6, C-9, C-1, C-4
6	C-7, C-8
7	C-5, C-6, C-9, C-10, C-8
9	C-5, C-6, C-1, C-7, C-8
10	C-9, C-7, C-8
Glucose	
1'	C-1, C3'
2'	C-1', C-3'
3'	C-4', C-2'
4'	C-3'
5'	C-3'
6'	C-4', C-5'

3 Identification of Chan-thet, Chan-khao, Chan-chamot, Chan-thana and Chan-hom

To identify the plant species of Chan(s), fifteen Chan-thet samples, eighteen Chan-khao samples, seventeen Chan-chamot samples, ten Chan-thana samples and eleven Chan-hom samples were used in this study. The authentic samples were *S. spicatum*, *S. album*, *S. lanceolatum*, *M. fragrans*, *T. hoaensis*, *D. decandra*, *M. gagei* and *A. silvestris*. The authentic volatile oils of various *Santalum* species were also used. α -Santalol, mansonone G and geniposidic acid, as described for their isolation and identification in previous section were used as chemical markers. Authentication was based on their TLC. IR and GC fingerprints coupled with chemometric analysis also applied for authentication. The details are described as follows.

3.1 TLC fingerprint

Two steps of TLC method were developed. Initially, all samples were preliminary screening by using the mixture of *n*-hexane, ethyl acetate and methanol (60:30:0.2) as developing solvent. Thereafter the results were confirmed by the other suitable solvent systems. The screening TLC chromatograms of Chan-thet, Chan-khao, Chan-chamot, Chan-thana and Chan-hom are shown in Figures 17, 19, 21, 22 and 24, respectively. And the confirmation results are shown in Figures 18, 20, 23, 25 for Chan-thet, Chan-khao, Chan-chamot, Chan-thana and Chan-hom, respectively.

3.1.1 Chan-thet

The screening TLC chromatograms of Chan-thet are shown in Figure 17. The chromatograms detected under UV (Figures 17(a) and 17(b)) were not clearly observed because most of the chemical constituents of Chan-thet might have not chromophore. The suitable detection was the observation under visible light after spray with anisaldehyde-sulfuric TS (Figure 17(c)). α -Santalol was the major compound of *Santalum* sp. [45], thus it was used as the chemical marker. Compared among authentic *Santalum* samples, α -santalol band of *S. album* was more intense than that found in *S. spicatum* and *S. lanceolatum*, respectively. It was corresponded

with previous studies which reported that α -santalol content in *S. album* was more than *S. spicatum* and *S. lanceolatum* [12, 83]. The obvious detection of α -santalol and a violet band at R_f 0.19 suggested that samples T4, T6 and T7 were *S. album*. The violet bands at R_f 0.90 and 0.70, the pale violet band at R_f 0.80 (α -santalol) and a purple band at R_f 0.79 suggested that samples T1-T3 and T8-T15 were *S. spicatum*. TLC chromatogram of *S. lanceolatum* was very similar to *S. spicatum*. The differences were the less intensity of the α -santalol band and the bands at R_f 0.70 and 0.90, whereas the band at R_f 0.79, the purple bands at R_f 0.20 and 0.40 were more intense. This suggested that sample T5 was *S. lanceolatum*.

The screening TLC results clearly indicated that all Chan-thet samples were *Santalum* species, not *M. fragrans*. However the identification among *Santalum* species was not clear cut because most of their different characteristic components were closely located on the upper part of the chromatograms. Then the other less polar solvent system was used to confirm the results. The solvent system of the mixture of *n*-hexane, ethyl acetate, methanol and acetic acid (60:10:0.2:0.01) was developed (Figures 18). Based on the detection with anisaldehyde-sulfuric acid TS (Figure 18(c)), the intense band of α -santalol at R_f 0.45 (α -santalol) was clearly detected in samples T4, T6 and T7. Then these samples were confirmed as *S. album*. The violet bands at R_f 0.30 and 0.60, a pale purple band at R_f 0.40 and a pale violet band at R_f 0.45 (α -santalol) confirmed samples T1-T3 and T8-T15 as *S. spicatum*. However sample T14 might be adulterated with other herbal samples. The ambiguity was suggested based on the fluorescence band at R_f 0.55 (Figure 18(b)). Sample T15 might be harvested from too young or too old tree since its compound contents were less than the others [12]. A purple band at R_f 0.40 and a very less intense pale violet band at R_f 0.45 (α -santalol) of sample T5 clearly indicated that it was *S. lanceolatum*.

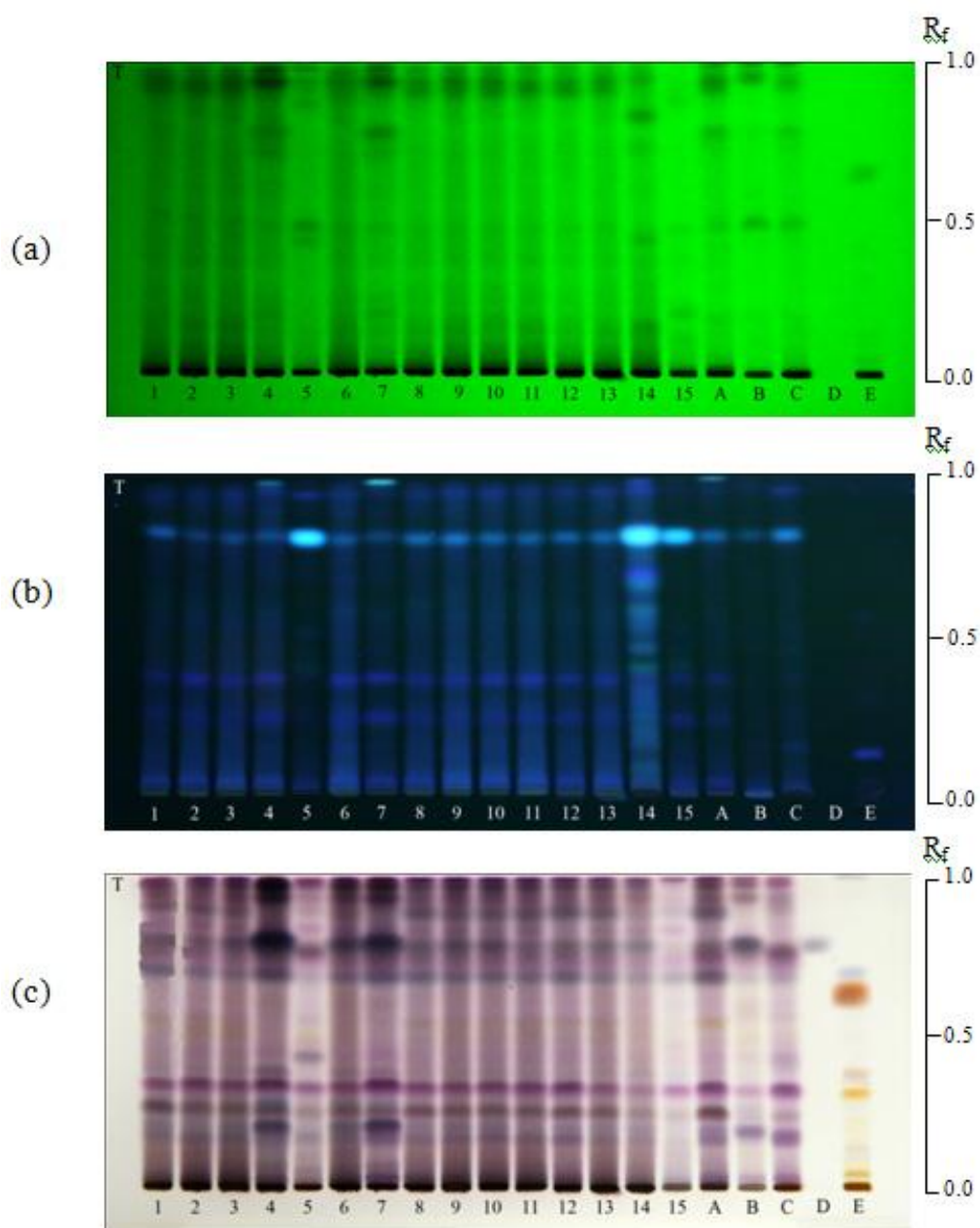


Figure 17 TLC chromatogram of Chan-thet methanol extracts using *n*-hexane : ethyl acetate : methanol (60:30:0.2) as mobile phase: (a) detection under UV 254 nm, (b) detection under UV 366 nm and (c) detection under visible light after spraying with anisaldehyde-sulfuric acid TS; 1-15 = samples T1-T15, A = *S. spicatum*, B = *S. album*, C = *S. lanceolatum*, D = α -santalol and E = *M. fragrans*.

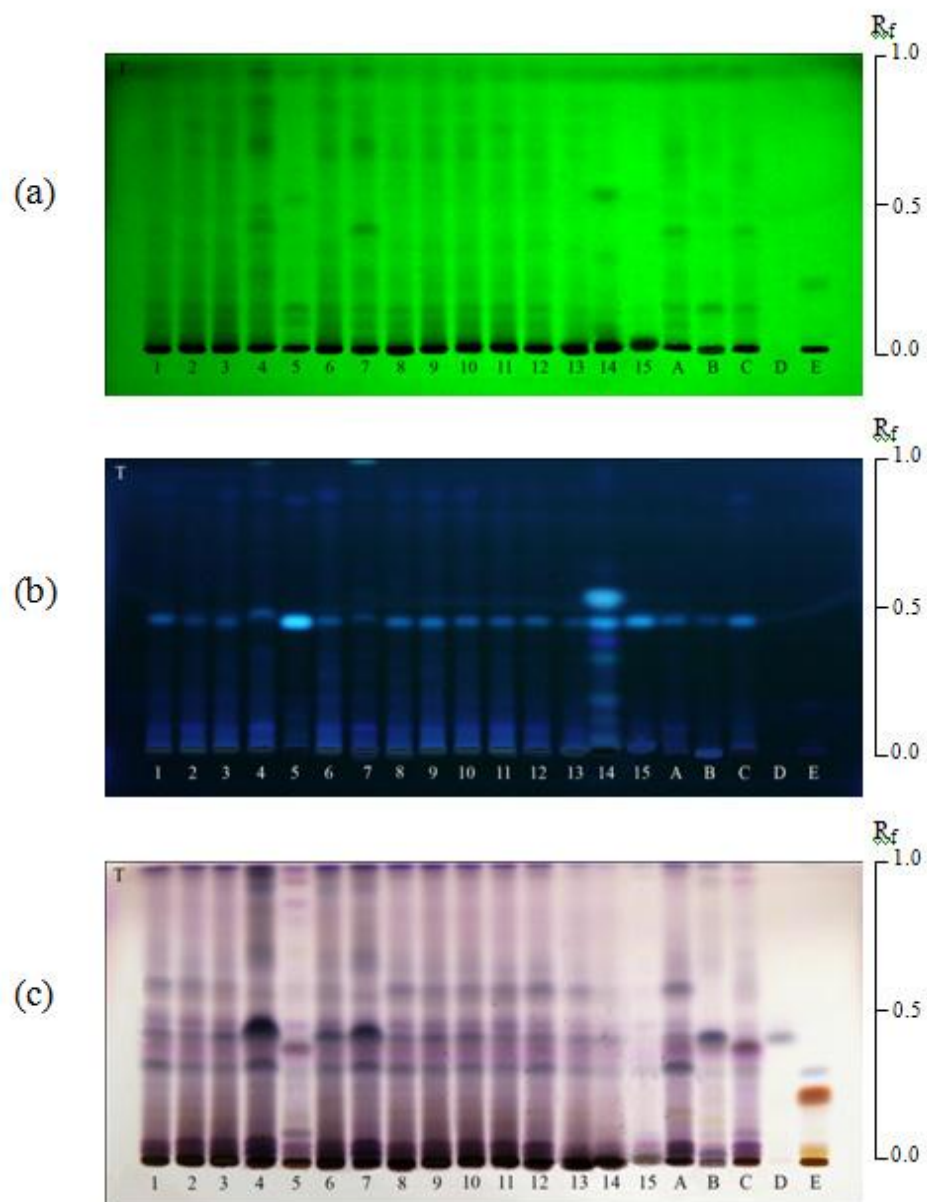


Figure 18 TLC chromatogram of Chan-thet methanol extracts using *n*-hexane : ethyl acetate : methanol : acetic acid (60:10:0.2:0.01) as mobile phase: (a) detection under UV 254 nm, (b) detection under UV 366 nm and (c) detection under visible light after spraying with anisaldehyde-sulfuric acid TS and heat at 105 °C for 5 min; 1-15 = T1-T15, A = *S. spicatum*, B = *S. album*, C = *S. lanceolatum*, D = α -santalol and E = *M. fragrans*.

3.1.2 Chan-khao

The screening TLC chromatograms of Chan-khao samples are shown in Figures 19. It was indicated that the chromatogram of sample K18 was different from the others. The detection under UV 254 nm (Figure 19(a)) and with anisaldehyde-sulfuric acid TS (Figure 19(a)) suggested that sample K18 was *S. spicatum*. However it might be adulterated with other herbal samples because the fluorescent bands under UV 366 nm (Figure 19(b)) were much intense than *S. spicatum*. This might be because of different quality of herb from planting sources, harvesting period or storage conditions. Chromatograms of the rest Chan-khao samples gave similar patterns, but they were not clearly identified to be the same as authentic samples. Because of the high polarity of most of their chemical compositions, another more polar solvent system was developed.

The mixture of dichloromethane, methanol and formic acid (60:10:1) was developed as a second mobile phase. Based on the results of this system (Figures 20), chromatograms of all Chan-khao samples were totally different from *D. decandra*. They could be divided into three groups. The first group was sample K18 which clearly differed from the others and was identified by the previous solvent system as *S. spicatum*. The second group consisted of samples K1-K6, K10-K13, K16 and K17. They gave the same TLC patterns as *T. hoensis*. The detection under UV 254 nm (Figure 20(a)) showed three quenching bands at R_f 0.35, 0.59 and 0.62; whereas the detection under UV 366 nm (Figure 20(b)) showed the fluorescent bands at R_f 0.20, 0.40, 0.59, 0.62 and 0.91. The detection under visible light after spraying with anisaldehyde-sulfuric acid TS (Figure 20(c)) showed a pale yellow band at R_f 0.32, a black band at R_f 0.35 and two violet bands at R_f 0.59 and 0.62. The band at R_f 0.35 was identified as geniposidic acid by comparing with the chemical marker. It was also detected in *T. hoensis*. Then samples in group 2 were identified as *T. hoensis*. The third group consisted of samples K7-K9, K14 and K15. They did not contain geniposidic acid and their chromatograms were different from all authentic samples. Therefore samples in this group could not be identified.

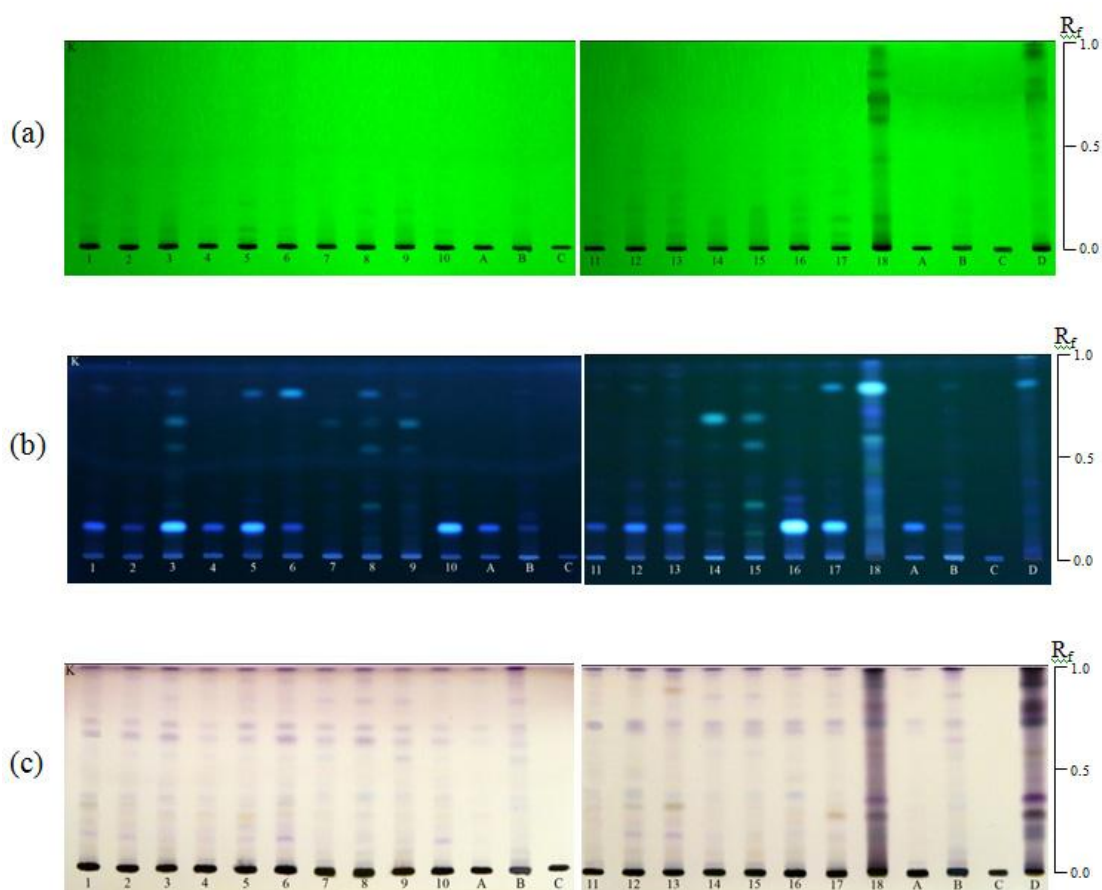


Figure 19 TLC chromatogram of Chan-khao methanol extracts using *n*-hexane : ethyl acetate : methanol (60:30:0.2) as mobile phase: (a) detection under UV 254 nm, (b) detection under UV 366 nm and (c) detection under visible light after spraying with anisaldehyde-sulfuric acid TS and heat at 105 °C for 5 min; 1-18 = K1-K18, A = *T. hoensis*, B = *D. decandra*, C = geniposidic acid and D = *S. spicatum*.

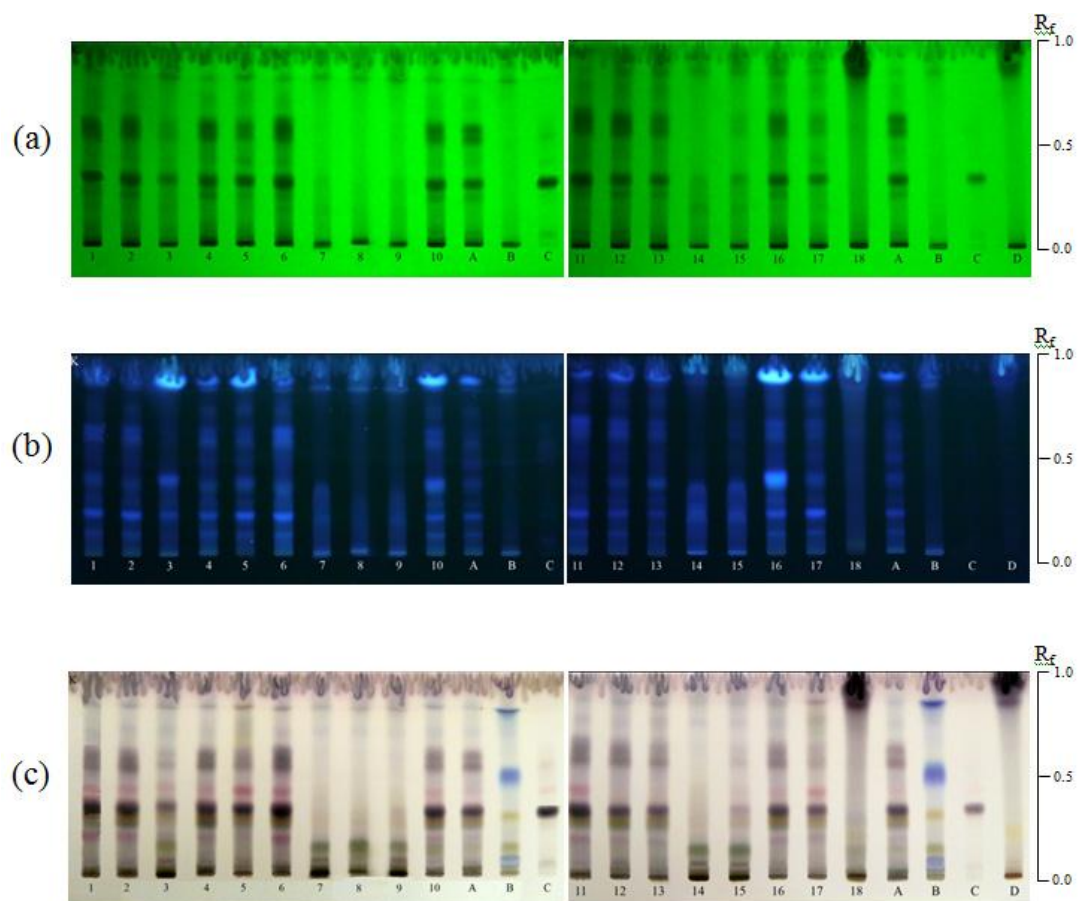
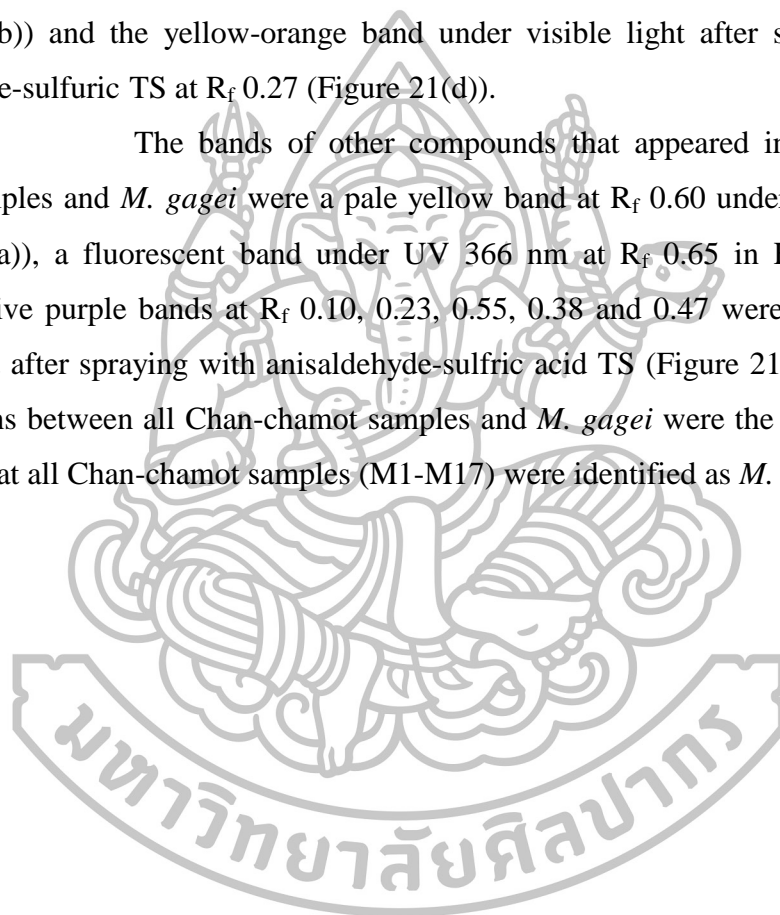


Figure 20 TLC chromatogram of Chan-khao methanol extracts using dichloromethane : methanol : formic acid (60:10:1) as mobile phase: (a) detection under UV 254 nm, (b) detection under UV 366 nm and (c) detection under visible light after spraying with anisaldehyde-sulfuric acid TS and heat at 105 °C for 5 min; 1-18 = K1-K18, A = *T. hoensis*, B = *D. Decandra*, C = geniposidic acid and D = *S. spicatum*.

3.1.3 Chan-chamot

TLC chromatograms of Chan-chamot and authentic samples are shown in Figures 21. All Chan-chamot samples differed from *A. silvestris*, *S. album*, *D. decandra* and *T. hoaensis*. All Chan-chamot samples and *M. gagei* found mansonone G that was an *ortho*-naphthoquinones compound. It was a yellow compound and could absorb UV light [188]. Then it was observed as the bright yellow band under visible light (Figure 21(a)), the quenching band under UV 254 nm (Figure 21(b)) and the yellow-orange band under visible light after spraying with anisaldehyde-sulfuric TS at R_f 0.27 (Figure 21(d)).

The bands of other compounds that appeared in both Chan-chamot samples and *M. gagei* were a pale yellow band at R_f 0.60 under visible light (Figure 21(a)), a fluorescent band under UV 366 nm at R_f 0.65 in Figure 21(C). Moreover five purple bands at R_f 0.10, 0.23, 0.55, 0.38 and 0.47 were found under visible light after spraying with anisaldehyde-sulfuric acid TS (Figure 21(d)). Overall TLC patterns between all Chan-chamot samples and *M. gagei* were the same. These indicated that all Chan-chamot samples (M1-M17) were identified as *M. gagei*.



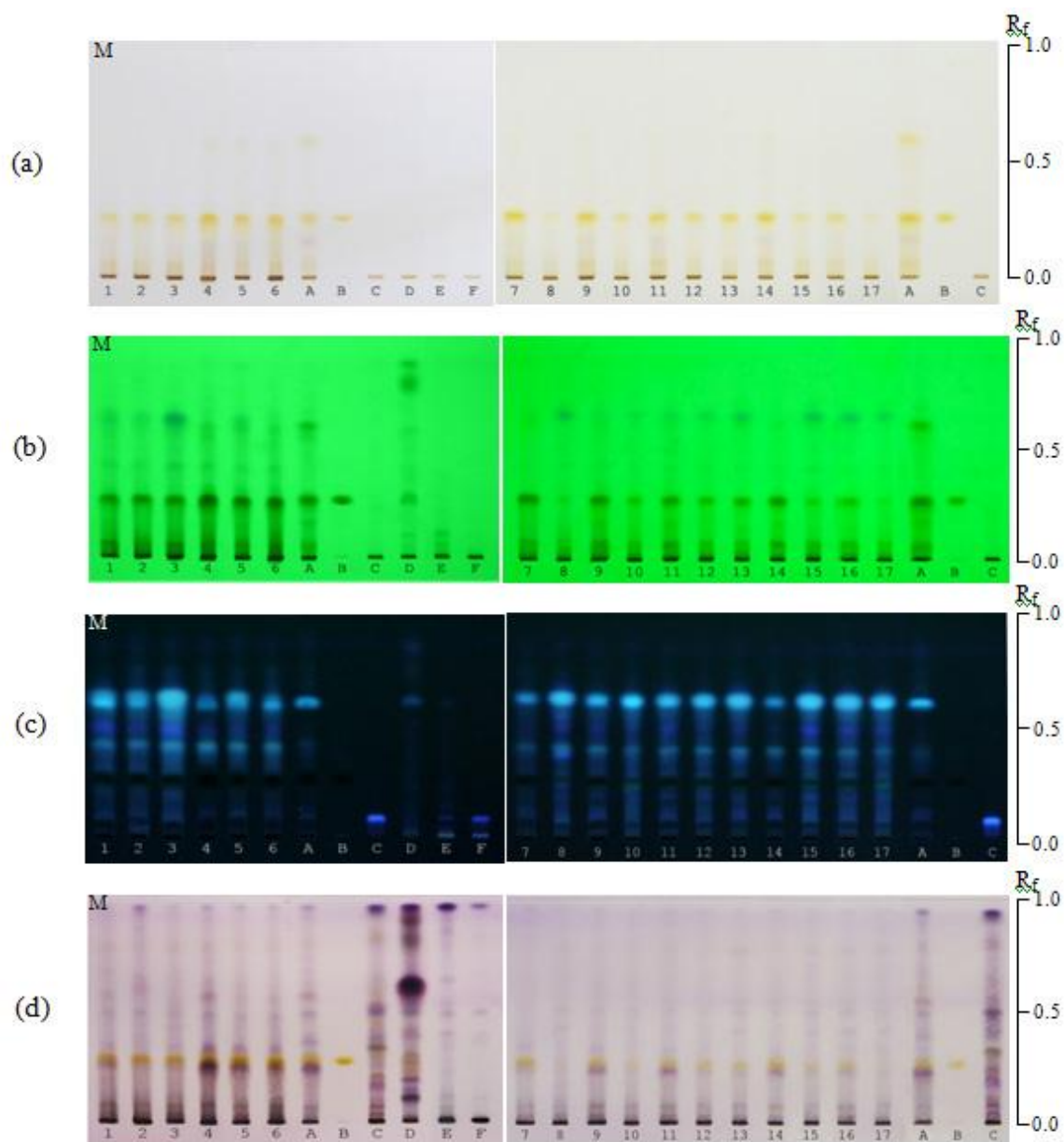
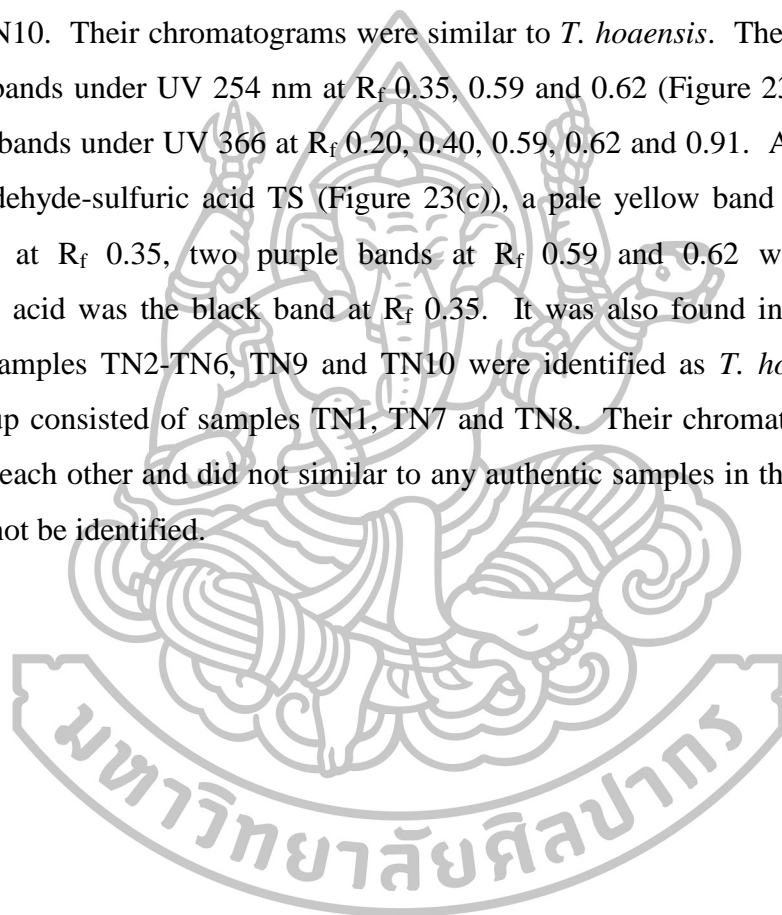


Figure 21 TLC chromatogram of Chan-chamot methanol extract using *n*-hexane : ethyl acetate : methanol (60:30:0.2) as mobile phase : (a) detection under visible light, (b) detection under UV 254 nm, (c) detection under UV 366 nm and (d) detection under visible light after spraying with anisaldehyde-sulfuric acid TS and heat at 105 °C for 5 min; 1-17 = M1-M17, A = *M. gagei*, B = Mansonone G, C = *A. silvestris*, D = *S. album*, E = *D. decandra* and F = *T. hoensis*.

3.1.4 Chan-thana

The screening TLC results of Chan-thana samples are shown in Figure 22. It was indicated that samples TN1, TN7 and TN8 differed from the others. Similar to Chan-khao samples, chemical compositions of Chan-thana were high polar. Therefore another more polar solvent was developed. It was the mixture of dichloromethane, methanol and formic acid (60:10:1). Chan-thana samples could be divided into two groups (Figures 23). The first group consisted of samples TN2-TN6, TN9 and TN10. Their chromatograms were similar to *T. hoensis*. They showed the quenching bands under UV 254 nm at R_f 0.35, 0.59 and 0.62 (Figure 23(a)); and the fluorescent bands under UV 366 at R_f 0.20, 0.40, 0.59, 0.62 and 0.91. After spraying with anisaldehyde-sulfuric acid TS (Figure 23(c)), a pale yellow band at R_f 0.32, a black band at R_f 0.35, two purple bands at R_f 0.59 and 0.62 were detected. Geniposidic acid was the black band at R_f 0.35. It was also found in *T. hoensis*. Therefore samples TN2-TN6, TN9 and TN10 were identified as *T. hoensis*. The second group consisted of samples TN1, TN7 and TN8. Their chromatograms were different to each other and did not similar to any authentic samples in this study, thus they could not be identified.



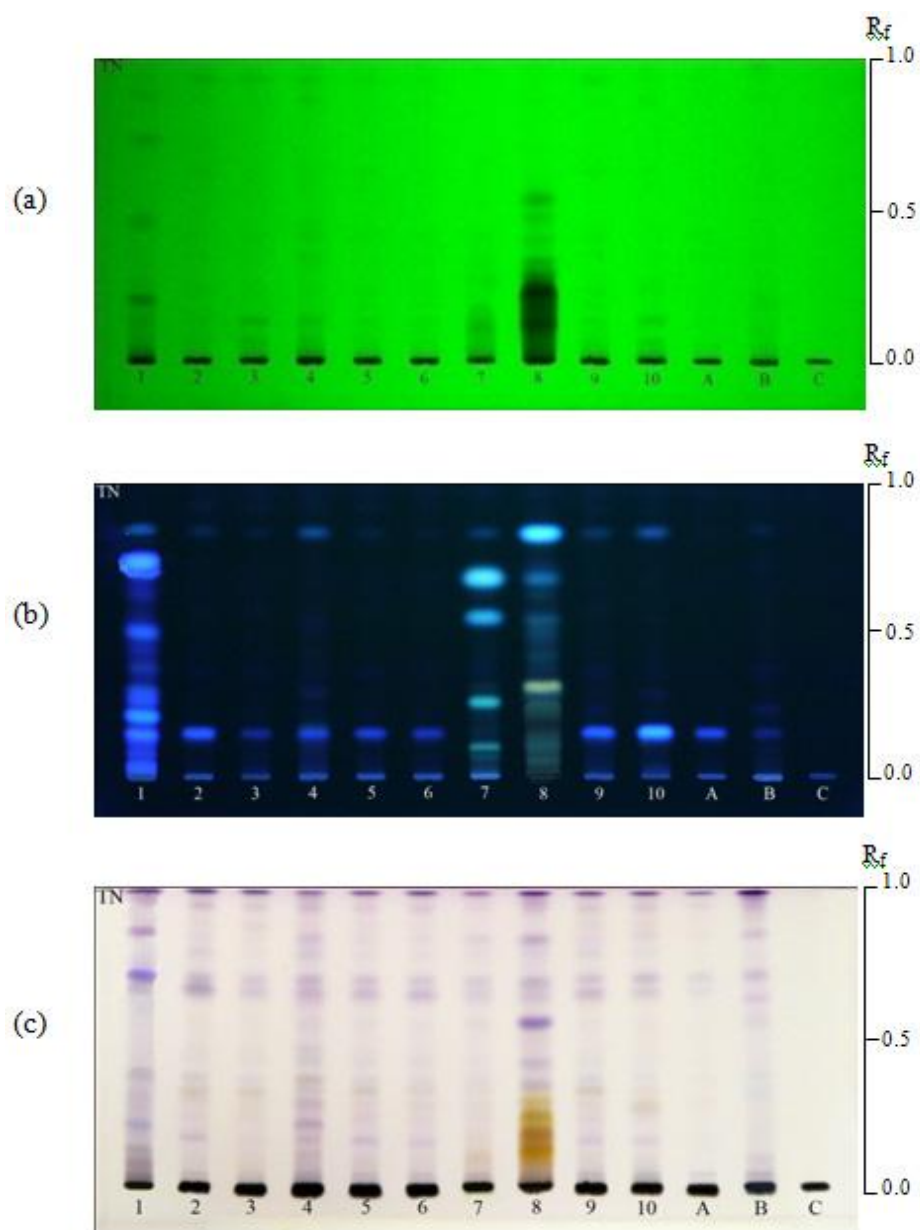


Figure 22 TLC Chromatogram of Chan-thana methanol extract using *n*-hexane : ethyl acetate : methanol (60:30:0.2) as mobile phase: (a) detection under UV 254 nm, (b) detection under UV 366 nm and (c) detection under visible light after spraying with anisaldehyde sulfuric acid TS and heat at 105 °C for 5 min; 1-10 = TN1-TN10, A = *T. hoensis*, B = *D. decandra* and C = geniposidic acid.

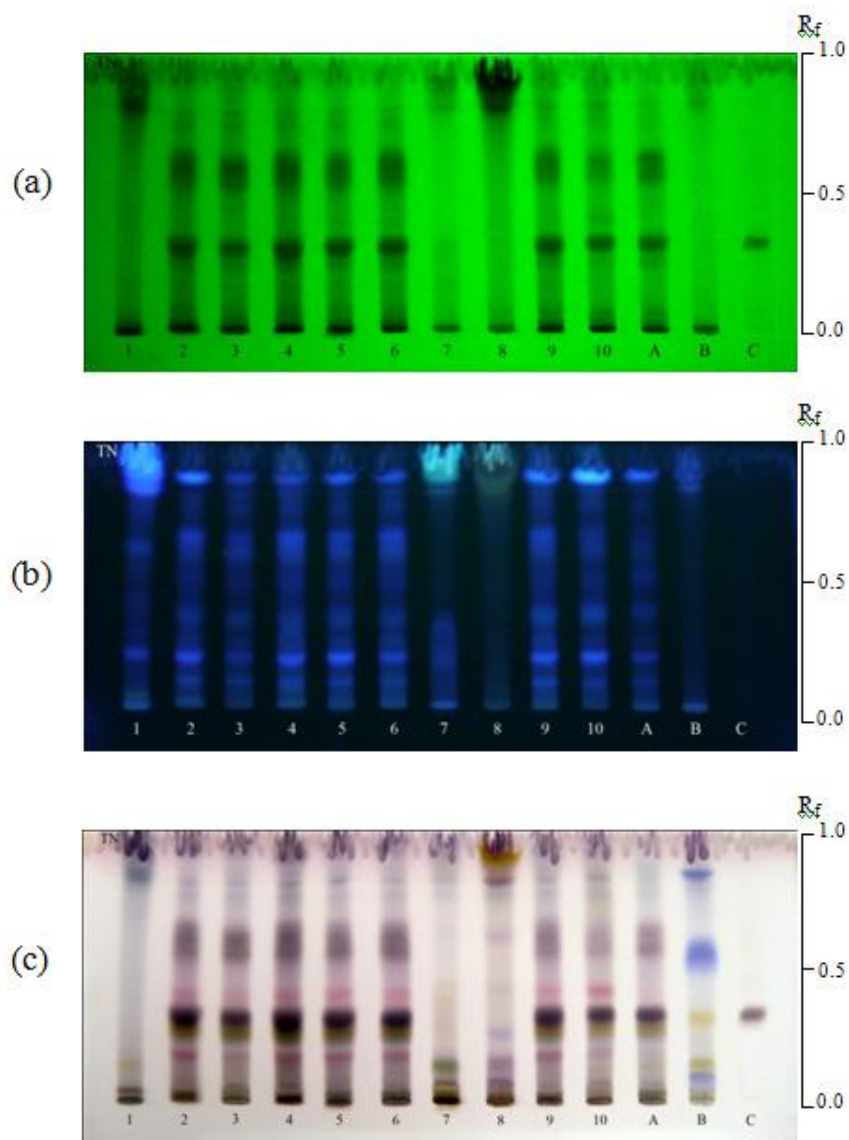


Figure 23 TLC Chromatogram of Chan-thana methanol extract using dichloromethane : methanol : formic acid (60:10:1) as mobile phase: (a) detection under UV 254 nm, (b) detection under UV 366 nm and (c) detection under visible light after spraying with anisaldehyde sulfuric acid TS and heat at 105 °C for 5 min; 1-10 = TN1-TN10, A = *T. hoensis*, B = *D. decandra* and C = geniposidic acid.

3.1.5 Chan-hom

The screening TLC results of Chan-hom samples are illustrated in Figure 24. Under visible light, samples H10 and H11 gave a bright yellow band at R_f 0.49, which also detected in *M. gagei*. This compound was mansonone G as described in previous section. Their chromatograms detected under UV and with anisaldehyde-sulfuric acid TS were also similar and confirmed them to be identified as *M. gagei*.

For samples H2-H9, as same as Chan-thet, the clear detection was shown with anisaldehyde-sulfuric acid TS (Figure 24(d)). They had two violet bands at R_f 0.90 and 0.70, a pale violet band at R_f 0.80 (α -santalol) and a purple band at R_f 0.79, as same as *S. spicatum*. To confirm the results, the other TLC system was developed using the mixture of *n*-hexane, ethyl acetate, methanol and acetic acid (60:10:0.2:0.01) as mobile phase (Figure 25). Above mentioned bands were more clearly separated and shown as two violet bands at R_f 0.30 and 0.60, a purple band at R_f 0.40 and a pale violet band at R_f 0.45 (α -santalol). Then samples H2-H9 were confirmed to be *S. spicatum*.

The rest sample H1 could not be identified by the preliminary TLC result (Figure 24) because its chromatogram was not clear. The other TLC system developed with the less polar solvent system (Figure 25) gave a better result. The violet band detected with anisaldehyde-sulfuric acid TS (Figure 25(c)) at R_f 0.45 (α -santalol) suggested that it was *Santalum* species. It had not two violet bands at R_f 0.30 and 0.60 which indicated that it was not *S. spicatum*. However its chromatogram was confusing between *S. album* and *S. lanceolatum*. Nevertheless it looked more similar to *S. lanceolatum* because of the less intense band of α -santalol and the more intense purple band at R_f 0.40.

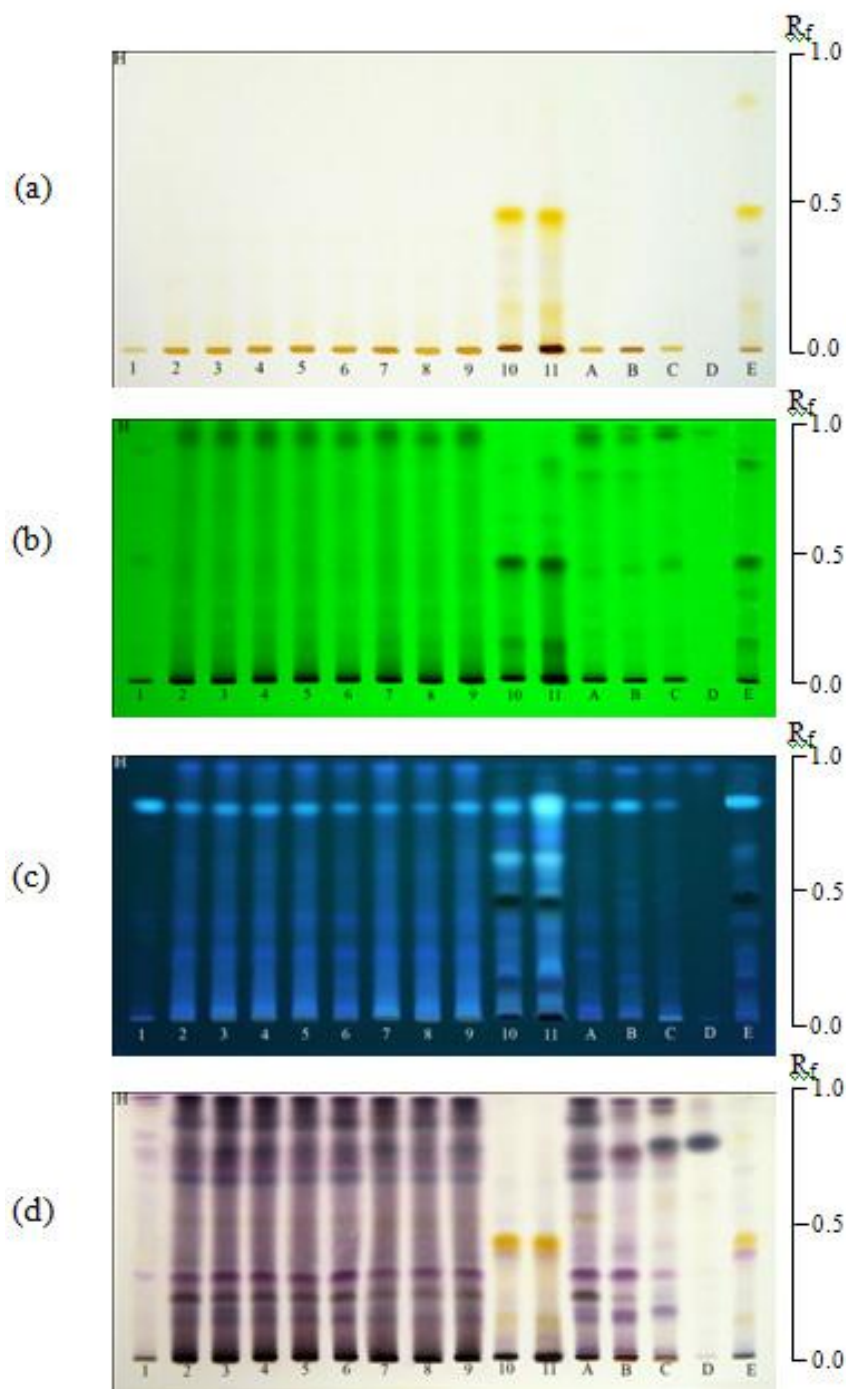


Figure 24 TLC Chromatogram of Chan-hom methanol extract using *n*-hexane : ethyl acetate : methanol (60:30:0.2) as mobile phase: (a) detection under visible light, (b) detection under UV 254 nm, (c) detection under UV 366 nm and (d) detection under visible light after spraying with anisaldehyde-sulfuric acid TS and heat at 105 °C for 5 min; 1-11 = H1-H11, A = *S. spicatum*, B = *S. lanceolatum*, C = *S. album*, D = α -santalol and E = *M. gagei*.

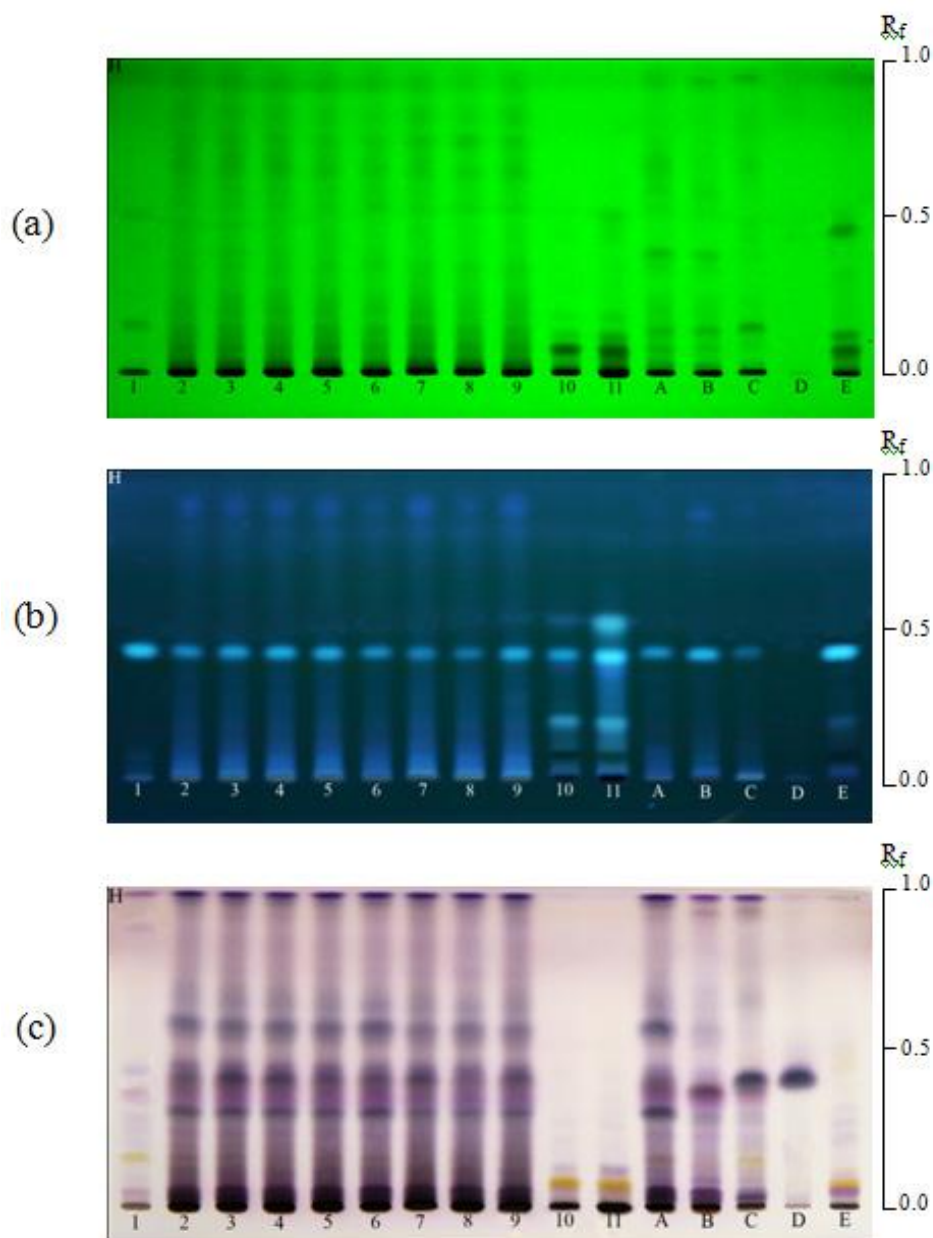


Figure 25 TLC Chromatogram of Chan-hom methanol extracts using *n*-hexane : ethyl acetate : methanol : acetic acid (60:10:0.2:0.01) as mobile phase: (a) detection under UV 254 nm, (b) detection under UV 366 nm and (c) detection under visible light after spraying with anisaldehyde-sulfuric acid TS and heat at 105 °C for 5 min; 1-11 = H1-H11, A = *S. spicatum*, B = *S. lanceolatum*, C = *S. album*, D = α -santalol and E = *M. gagei*.

3.2 IR fingerprint

IR fingerprint analysis was the other method used to identify Chan-thet, Chan-khao, Chan-chamot, Chan-thana and Chan-hom samples. IR spectra of all samples were obtained from sample extracted with various solvent, i.e. *n*-hexane, dichloromethane, ethyl acetate, acetone, methanol and water, and directly from the fine powders. Thereafter the spectra were preprocessed by normalization and second derivative methods. The normalized and the second derivative IR spectra of all samples are shown in Figures 79-85 and 86-92, respectively; whereas those of the authentic samples are shown in Figures 93-99 and 100-105, respectively. Only the IR region of 1801-501 cm^{-1} was selected for fingerprint analysis because the data from 4000-1801 cm^{-1} was OH and CH stretching which did not specify for discrimination and be easily disturbed by moisture during collection of the spectra.

Since IR spectra were very complex and difficult to interpret, they were analysed with the aid of chemometrics. Similarity analysis (SA), hierarchical cluster analysis (HCA) and principal component analysis (PCA) were the chemometric methods that were applied in this study.

3.2.1 Chan-thet

Correlation coefficients between IR spectra of all Chan-thet and authentic samples are shown in Tables 42-48. The results indicated that IR spectra of the water extract and the fine powders could not be used for the identification because correlation coefficients between Chan-thet samples and all authentic samples were not different. The IR spectra of the other extracts clearly indicated that all Chan-thet samples were not *M. fragrans*, *M. gagei* and *A. silvestris*. However differentiation between *Santalum* sp. and the other authentic samples was not clear. For example, the normalized IR spectra of the dichloromethane extract of many Chan-thet samples gave high correlation to both *Santalum* sp. and *T. hoensis* (Table 43), whereas those of the ethyl acetate, acetone and methanol extracts gave high correlation to both *Santalum* sp. and *D. decandra* (Tables 44-46). After second derivative preprocessing, even correlation coefficients of the IR spectra of these extracts of Chan-thet samples and *Santalum* sp. slightly decreased ($r = 0.58-0.96$), it is clearly different from the

other authentic samples. Therefore second derivative was the necessary preprocessing method. In conclusion all Chan-thet samples were *Santalum* sp. However correlation coefficient between Chan-thet samples and *S. album*, *S. spicatum* and *S. lanceolatum* were similar. Then it was impossible to identify their exact species by SA.

The IR spectra were further analysed by HCA. The HCA dendrograms of the water extract clustered all authentic samples together, then it was useless. The overall results of the other solvent extracts confirmed the result of SA that all Chan-thet samples were clustered into the same group as the three *Santalum* authentic samples. After preprocessing with second derivative method, most of the clustering was better. And the clearest ones were the HCA obtained from the *n*-hexane extract (group V in Figure 26), methanol extract (group VI, VII and VIII in Figure 27), and the fine powder (group VI in Figure 28). Moreover in the dendrograms of the methanol extract, samples T4 and T7 and *S. album* were separately clustered together (group VII in Figure 27). Then these two samples could be identified as *S. album*. Identification between *S. spicatum* and *S. lanceolatum* of the other samples was not possible because all HCA dendrograms were clustered into the same group. Therefore other Chan-thet samples could be only identified as either *S. spicatum* or *S. lanceolatum* by HCA



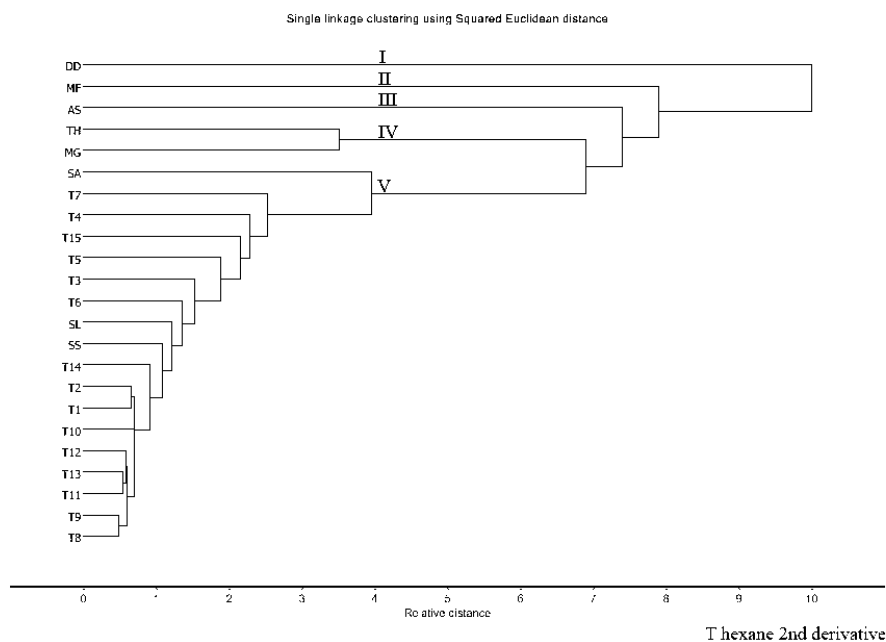


Figure 26 HCA dendrogram the second derivative IR spectra of the *n*-hexane extracts of Chan-thet samples (T1-T15), *S. album* (SA), *S. spicatum* (SS), *S. lanceolatum* (SL), *M. fragrans* (MF), *T. hoensis* (TH), *D. decandra* (DD), *M. gagei* (MG) and *A. silvestris* (AS).

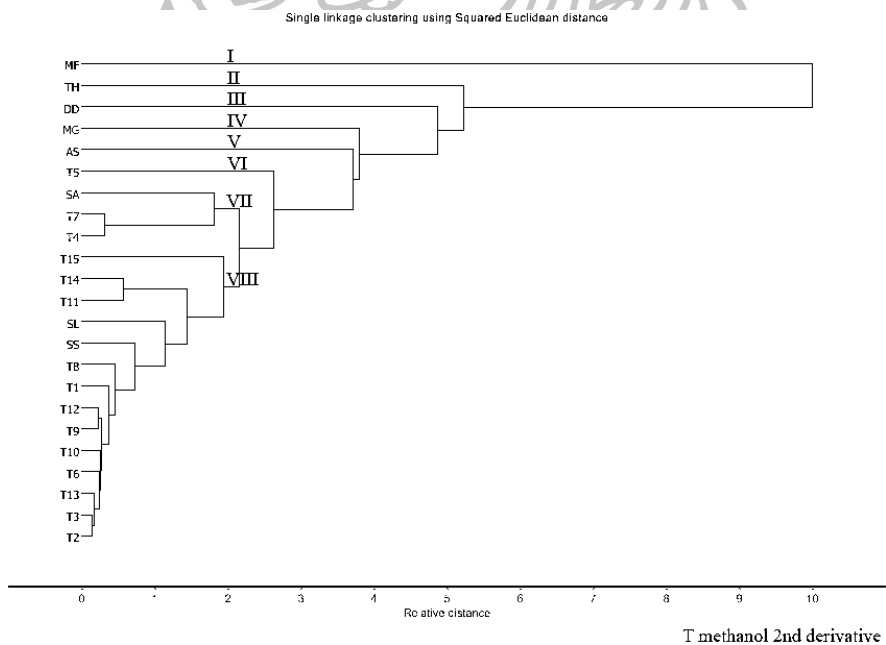


Figure 27 HCA dendrogram the second derivative IR spectra of the methanol extracts of Chan-thet samples (T1-T15), *S. album* (SA), *S. spicatum* (SS), *S. lanceolatum* (SL), *M. fragrans* (MF), *T. hoensis* (TH), *D. decandra* (DD), *M. gagei* (MG) and *A. silvestris* (AS).

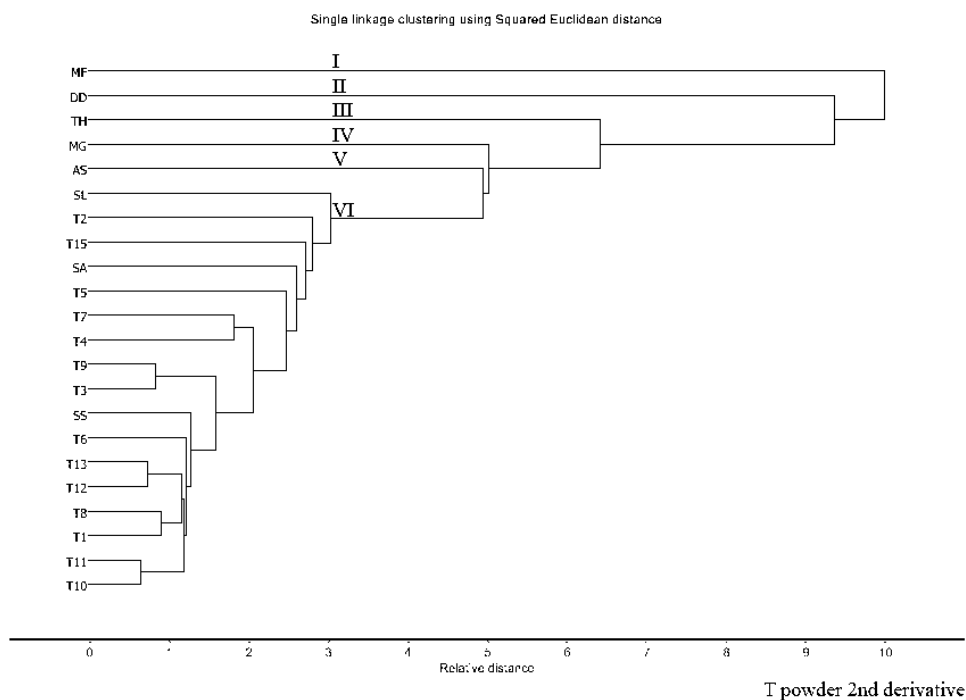


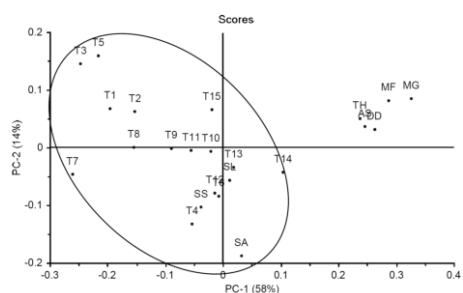
Figure 28 HCA dendrogram the second derivative IR spectra of the fine powders of Chan-thet samples (T1-T15), *S. album* (SA), *S. spicatum* (SS), *S. lanceolatum* (SL), *M. fragrans* (MF), *T. hoensis* (TH), *D. decandra* (DD), *M. gagei* (MG) and *A. silvestris* (AS).

PCA was the third method applied to IR spectra. The PC1 and PC2 score plots of the normalized IR spectra were slightly better than those of the second derivative IR spectra. Chan-thet samples and more than one authentic sample were clustered together in the score plots of the dichloromethane, ethyl acetate and water extracts and the fine powders, then they were useless for the identification. A clear result was PCA of the *n*-hexane extract that all Chan-thet samples were clustered with only the three *Santalum* authentic samples (Figure 29(a)). Therefore all samples were identified as *Santalum* sp. Their species identification could be further suggested by the score plots of the polar solvent extracts, i.e. acetone (Figure 29(b)) and methanol (Figure 29(c)) extracts, which divided the samples into two groups. As same as HCA, samples T4 and T7 were clustered with *S. album*, whereas the other samples were clustered with *S. spicatum* and *S. lanceolatum*. Identification between the later two species was impossible because they were clustered together in the score plots of all solvent extracts. These PCA results and also those of HCA suggested that

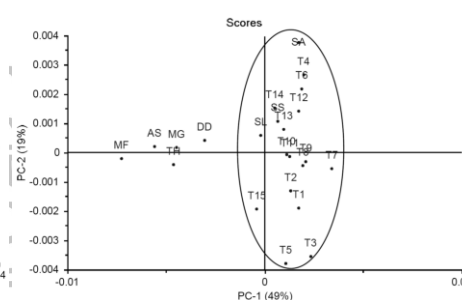
functional groups of non-polar constituents in three *Santalum* species were not much different. But in polar solvent extracts, those of *S. album* were different from the other two species.

(a) *n*-Hexane extract

: Normaliaed IR

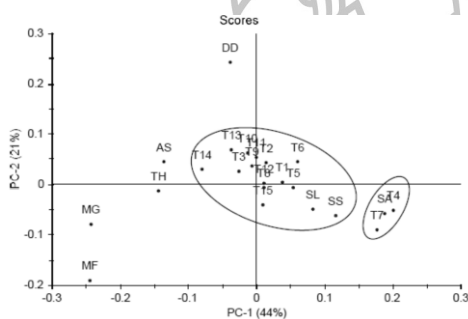


: Second derivative IR

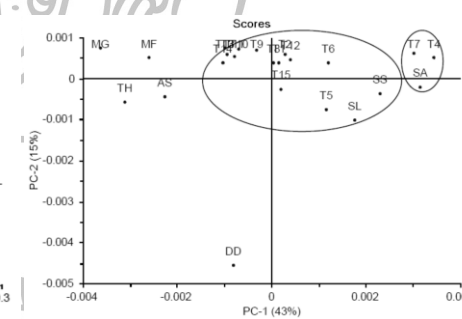


(b) Acetone extract

: Normaliaed IR

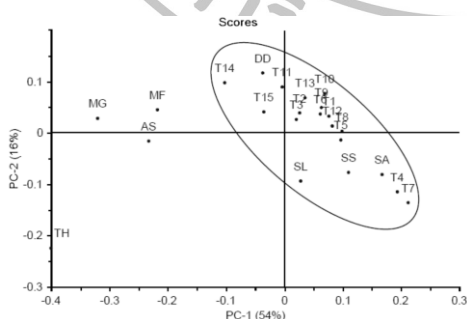


: Second derivative IR



(c) Methanol extract

: Normalized IR



: Second derivative IR

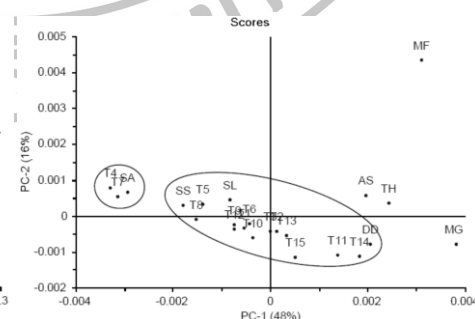


Figure 29 PC1 and PC2 score plots of the second derivative IR spectra of the (a) *n*-hexane, (b) acetone and (c) methanol extracts of Chan-thet samples (T1-T15), *S. album* (SA), *S. spicatum* (SS), *S. lanceolatum* (SL), *M. fragrans* (MF), *T. hoensis* (TH), *D. decandra* (DD), *M. gagei* (MG) and *A. silvestris* (AS).

In conclusion, SA could only assume that most of Chan-thet samples were *Santalum* species. HCA and PCA gave more information that most of them were identified as either *S. spicatum* or *S. lanceolatum*, and two samples (T4 and T7) were *S. album*. The *n*-hexane extract was the most suitable solvent for the identification of *Santalum* sp.

3.2.2 Chan-khao

Correlation coefficient between the IR spectra of all Chan-khao and authentic samples are shown in Tables 49-55. The fine powder could not be used for the identification because correlation coefficient between Chan-khao samples and all authentic samples were not much different (Table 55). The correlation coefficient between Chan-khao samples and authentic samples showed that the second derivative IR spectra of all samples were more significantly different. The clearest results were those obtained from the dichloromethane extract that 76% of Chan-thet samples were clearly identified as *T. hoaensis* (Table 50).

HCA of the IR spectra of various extracts and the fine powders of Chan-khao samples were further studied. Clustering of the second derivative spectra was slightly better. But HCA of the water extract clustered most of the authentic samples together. Those of the ethyl acetate extract could not differentiate between *T. hoaensis* and *M. gagei*. The functional groups of polar and semi-polar compounds found in these two authentic samples might be not much different. Then these solvents were useless for the identification. The overall results of the other solvents showed that most of Chan-khao samples were clustered into the same group as *T. hoaensis* (group VIII in Figure 30, group VII in Figures 31 and 32 and group VIII in Figure 33, respectively), confirming the results of SA. However sample K18 trended to be far from the other samples. In the dendrogram of the *n*-hexane extract, it was separately clustered with *S. spicatum* and *S. lanceolatum* (group VI in Figure 30). In agree with the TLC results, sample K18 was identified as *S. spicatum*. In the dendrogram of the fine powders, samples K7-K9, K14 and K15 were separated from the others (group VII in Figure 34), confirming the TLC result that identified them as unidentified species.

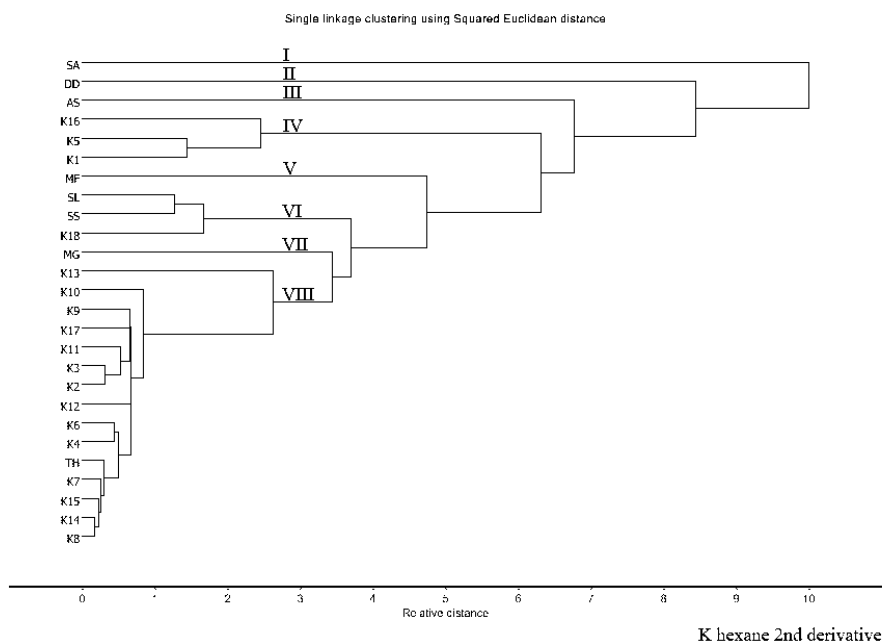


Figure 30 HCA dendrogram the second derivative IR spectra of the *n*-hexane extracts of Chan-khao samples (K1-K18), *S. album* (SA), *S. spicatum* (SS), *S. lanceolatum* (SL), *M. fragrans* (MF), *T. hoensis* (TH), *D. decandra* (DD), *M. gagei* (MG) and *A. silvestris* (AS).

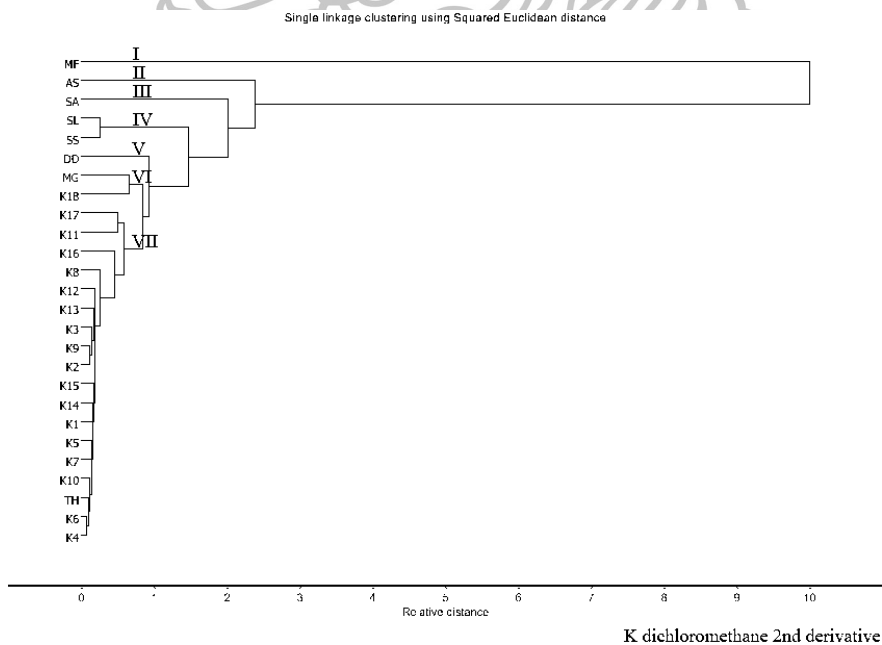


Figure 31 HCA dendrogram the second derivative IR spectra of the dichloromethane extracts of Chan-khao samples (K1-K18), *S. album* (SA), *S. spicatum* (SS), *S. lanceolatum* (SL), *M. fragrans* (MF), *T. hoensis* (TH), *D. decandra* (DD), *M. gagei* (MG) and *A. silvestris* (AS).

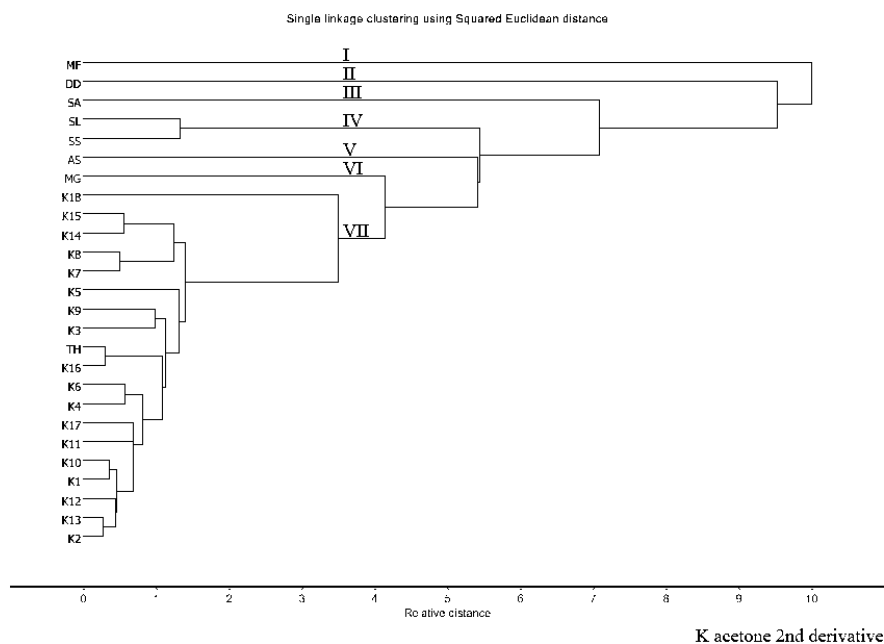


Figure 32 HCA dendrogram the second derivative IR spectra of the acetone extracts of Chan-khao samples (K1-K18), *S. album* (SA), *S. spicatum* (SS), *S. lanceolatum* (SL), *M. fragrans* (MF), *T. hoensis* (TH), *D. decandra* (DD), *M. gagei* (MG) and *A. silvestris* (AS).

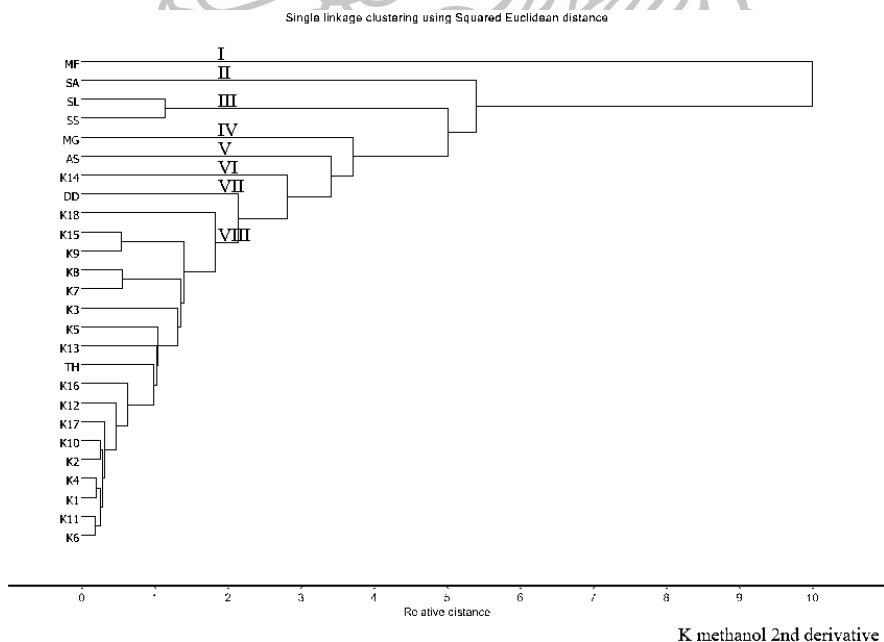


Figure 33 HCA dendrogram the second derivative IR spectra of the methanol extracts of Chan-khao samples (K1-K18), *S. album* (SA), *S. spicatum* (SS), *S. lanceolatum* (SL), *M. fragrans* (MF), *T. hoensis* (TH), *D. decandra* (DD), *M. gagei* (MG) and *A. silvestris* (AS).

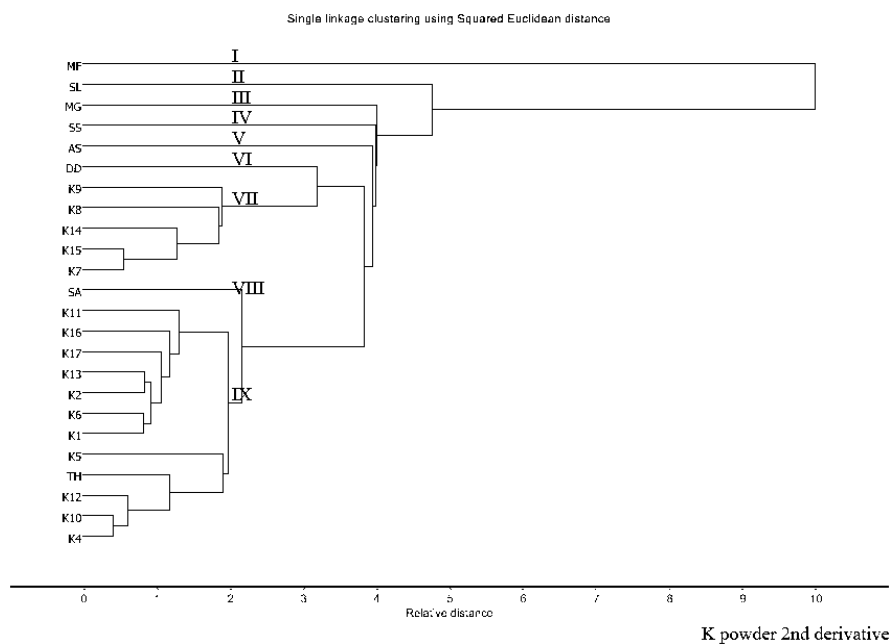


Figure 34 HCA dendrogram the second derivative IR spectra of the fine powders of Chan-khao samples (K1-K18), *S. album* (SA), *S. spicatum* (SS), *S. lanceolatum* (SL), *M. fragrans* (MF), *T. hoensis* (TH), *D. decandra* (DD), *M. gagei* (MG) and *A. silvestris* (AS).

In the PCA study, the PC1 and PC2 score plots of the second derivative IR spectra gave the slightly better results than the normalized IR spectra. However the normalized IR spectra and second derivative IR spectra of all solvent extracts and the fine powders could not identify Chan-khao samples because most of Chan-khao samples and more than one authentic sample were grouped together. Nevertheless, the second derivative IR spectra of the *n*-hexane extracts could cluster sample K18 into the same group as *S. lanceolatum* and *S. spicatum* (Figure 35). Therefore sample K18 were identified as either *S. lanceolatum* or *S. spicatum*. This result corresponded with the previous sections which suggested that the *n*-hexane extract was useful for the identification of *Santalum* samples. In overall, less than 60% variables were explained by PC1 and PC2 score plots of all solvent extracts. IR spectra of Chan-khao samples might have much variation and might similar to the spectra of many authentic samples. Thus only two PCs were not sufficient. First three PCs were considered for the explanation, and the best results were obtained

from the PCA of the acetone extracts. The three dimension score plots of PC1, PC2 and PC3 of the second derivative IR spectra of the acetone extract, accounting for 68% explanation, are shown in Figure 36. Chan-khao samples were clearly clustered with *T. hoensis* and sample K18 was separated from the others. This result corresponded with above results because sample K18 was not the same species as the others.

In conclusion, SA suggested that most of Chan-khao sample were *T. hoensis*. HCA and PCA confirmed the results and gain more information that one sample (K18) was *S. spicatum*. Moreover HCA gave other information that five samples (K7-K9, K14 and K15) were unidentified species.

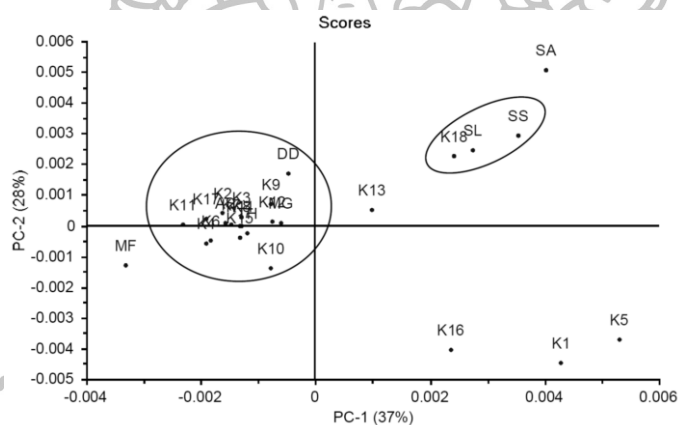


Figure 35 PC1 and PC2 score plots of the second derivative IR spectra of the *n*-hexane of Chan-khao samples (K1-K18), *S. album* (SA), *S. spicatum* (SS), *S. lanceolatum* (SL), *M. fragrans* (MF), *T. hoensis* (TH), *D. decandra* (DD), *M. gagei* (MG) and *A. silvestris* (AS).

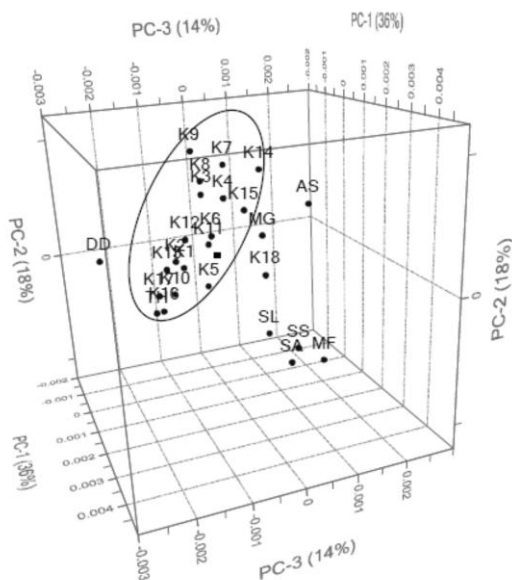


Figure 36 PC1, PC2 and PC3 three dimension score plots of the second derivative IR spectra of the acetone extract of Chan khao (K1-K18), *S. album* (SA), *S. spicatum* (SS), *S. lanceolatum* (SL), *M. fragrans* (MF), *T. hodensis* (TH), *D. decandra* (DD), *M. gagei* (MG) and *A. silvestris* (AS).

3.2.3 Chan-chamot

Correlation coefficients between the IR spectra of all Chan-chamot and authentic samples are shown in Tables 56-62. IR spectra of the *n*-hexane and water extracts, and the fine powders could not be used for the identification because all correlation coefficients were not clear (Tables 56, 61 and 62). The normalized IR spectra of the other solvents suggested that all Chan-chamot samples were possibly identified as *M. gagei*. After second derivative preprocessing, correlations between Chan-chamot samples and the other authentic samples were more clearly different. For example, the correlation coefficients of second derivative IR spectra between Chan-chamot samples and *M. gagei* of the acetone extract were 0.80-0.99 and the correlation coefficients between Chan-chamot samples and other authentic sample were 0.12-0.77 (Table 59). These suggested that second derivative preprocessing was important for identification. In conclusion, all Chan-chamot samples were identified as *M. gagei* by SA.

HCA were further studies and the results obtained from the second derivative IR spectra were slightly better than the normalized spectra. The overall results trended to cluster most of Chan-chamot samples with *M. gagei*. The clearest results were the HCA of the slightly polar to high polar solvents, i.e. ethyl acetate, acetone and methanol that clustered all Chan-chamot samples into the group of *M. gagei* (group VI in Figure 37, group VII in Figures 38 and 39, respectively). Then all Chan-chamot samples could be identified as *M. gagei*.

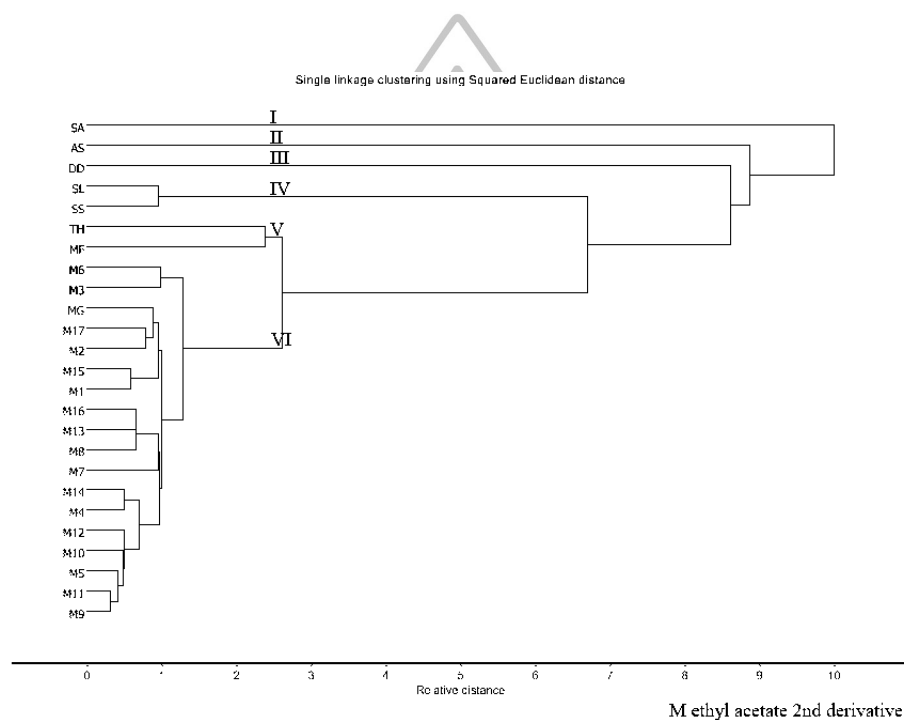


Figure 37 HCA dendrogram the second derivative IR spectra of the ethyl acetate extracts of Chan-chamot samples (M1-M17), *S. album* (SA), *S. spicatum* (SS), *S. lanceolatum* (SL), *M. fragrans* (MF), *T. hoensis* (TH), *D. decandra* (DD), *M. gagei* (MG) and *A. silvestris* (AS).

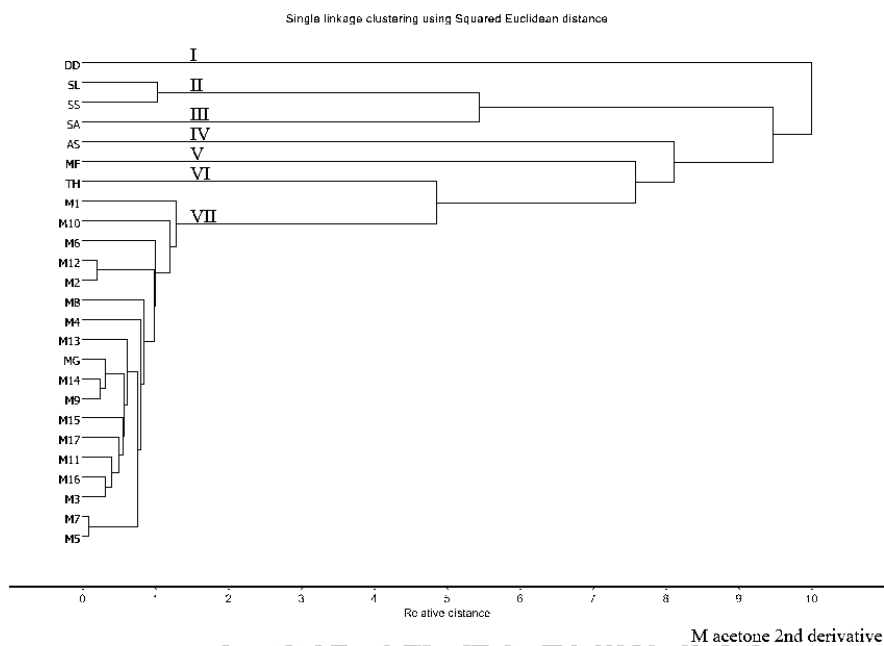


Figure 38 HCA dendrogram the second derivative IR spectra of the acetone extracts of Chan-chamot samples (M1-M17), *S. album* (SA), *S. spicatum* (SS), *S. lanceolatum* (SL), *M. fragrans* (MF), *T. hoagensis* (TH), *D. decandra* (DD), *M. gagei* (MG) and *A. silvestris* (AS).

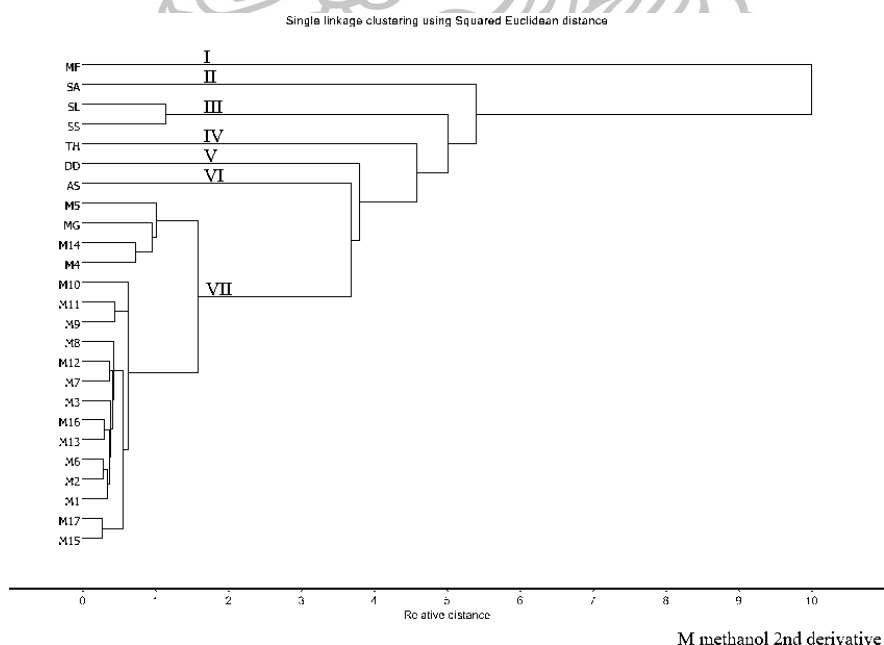


Figure 39 HCA dendrogram the second derivative IR spectra of the methanol extracts of Chan-chamot samples (M1-M17), *S. album* (SA), *S. spicatum* (SS), *S. lanceolatum* (SL), *M. fragrans* (MF), *T. hoagensis* (TH), *D. decandra* (DD), *M. gagei* (MG) and *A. silvestris* (AS).

For PCA study, the PC1 and PC2 score plots of the *n*-hexane, methanol and water extracts, and the fine powders clustered Chan-chamot samples with more than one authentic sample so these extracts could not be applied for the identification of Chan-chamot samples. The extracts prepared from slightly polar solvents, i.e. ethyl acetate and acetone extracts, gave better classification. The best result was the score plots between PC1 and PC2 of the ethyl acetate extract which showed that all Chan-chamot samples were *M. gagei* (Figure 40). However the acetone extract could not separate between *M. gagei* and *T. hoensis* because of the variation of IR spectra of Chan-chamot samples. This indicated that only two PCs were not sufficient to explain the variables. Thus PC3 were used together with PC1 and PC2 to classify the samples. The three dimension score plots of PC1, PC2 and PC3 of the acetone extracts are shown in Figure 41. All Chan-chamot samples were clustered into the same group as *M. gagei*. Then all Chan-chamot samples were identified as *M. gagei*.

In conclusion, all SA, HCA and PCA clearly identified all Chan-chamot samples as *M. gagei* and the suitable extracts for the identification were those prepared from the slightly polar solvents.

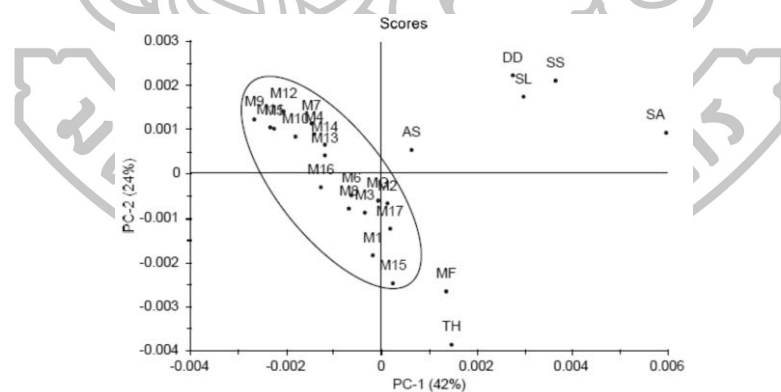


Figure 40 PC1 and PC2 score plots of the normalized and second derivative IR spectra of the ethyl acetate of Chan-chamot samples (M1-M17), *S. album* (SA), *S. spicatum* (SS), *S. lanceolatum* (SL), *M. fragrans* (MF), *T. hoensis* (TH), *D. decandra* (DD), *M. gagei* (MG) and *A. silvestris* (AS).

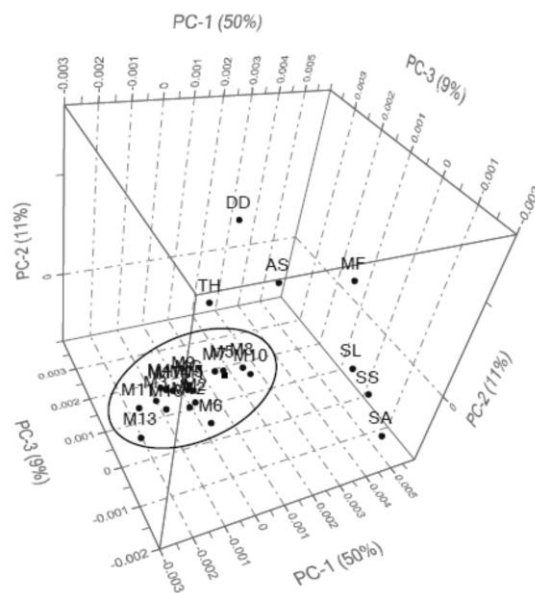


Figure 41 PC1, PC2 and PC3 three dimension score plots of the second derivative IR spectra of the acetone extracts of Chan-chamot (M1-M17), *S. album* (SA), *S. spicatum* (SS), *S. lanceolatum* (SL), *M. fragrans* (MF), *T. hoaensis* (TH), *D. decandra* (DD), *M. gagei* (MG) and *A. silvestris* (AS).

3.2.4 Chan-thana

Correlation coefficients between all Chan-thana and authentic samples are shown in Tables 63-69. The normalized IR spectra of all extracts and the fine powders could not be used for the identification because all correlation coefficients were not much different. However the second derivative IR spectra of most of Chan-thana samples gave slightly higher correlation coefficients to *T. hoaensis* than the other authentic samples. Thus most of Chan-thana samples were possibly identified as *T. hoaensis*.

HCA was further studied. Its overall results suggested that the second derivative preprocessing could cluster samples and authentic samples slightly better than the normalization preprocessing. However the dendrograms of the water extract and the fine powders could not cluster Chan-thana samples with any authentic samples. Moreover the ethyl acetate extract was useless because Chan-thana samples, *T. hoaensis*, *M. gagei* and *M. fragrans* were clustered into the same group. The HCA of the dichloromethane and acetone extracts clustered most of Chan-thana samples

with *T. hoagensis* (group IX in Figures 42 and 43, respectively), and samples TN1 and TN8 were separated from the others. This result corresponded with TLC that most of Chan-thana samples were *T. hoagensis* and samples TN1 and TN8 were unidentified species.

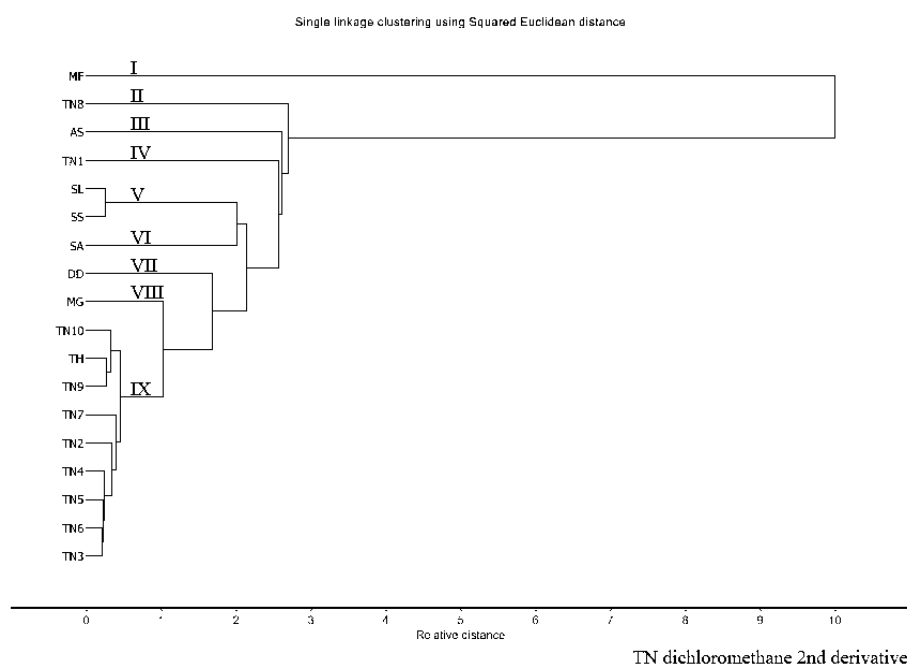


Figure 42 HCA dendrogram the second derivative IR spectra of the dichloromethane extracts of Chan-thana samples (TN1-TN10), *S. album* (SA), *S. spicatum* (SS), *S. lanceolatum* (SL), *M. fragrans* (MF), *T. hoagensis* (TH), *D. decandra* (DD), *M. gagei* (MG) and *A. silvestris* (AS).

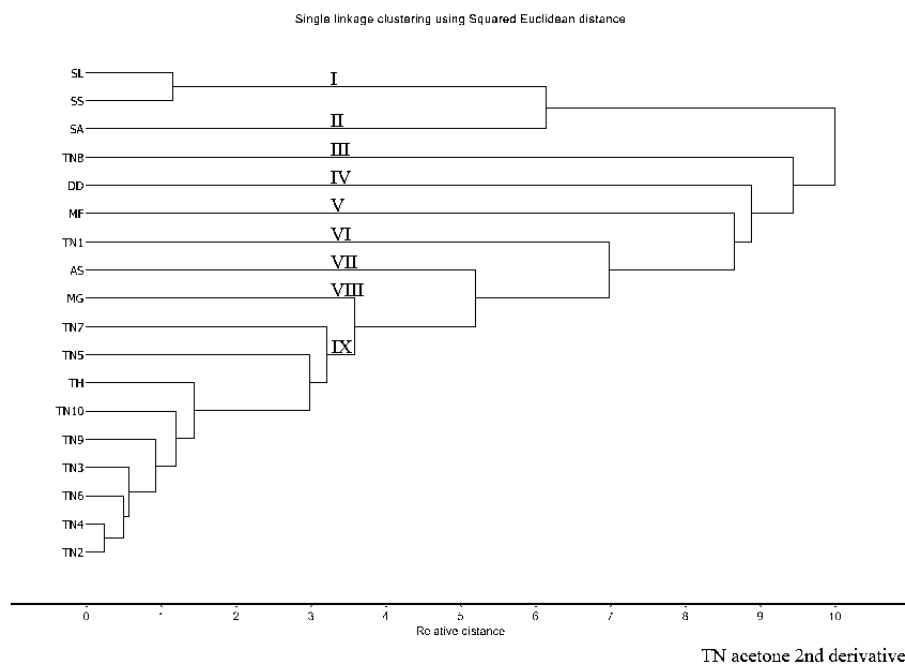


Figure 43 HCA dendrogram the second derivative IR spectra of the acetone extracts of Chan-thana samples (TN1-TN10), *S. album* (SA), *S. spicatum* (SS), *S. lanceolatum* (SL), *M. fragrans* (MF), *T. hoensis* (TH), *D. decandra* (DD), *M. gagei* (MG) and *A. silvestris* (AS).

PCA was studied and the PC1 and PC2 score plots indicated that both normalized and second derivative IR of all solvent extracts and the fine powders could not identify Chan-thana because most of Chan-thana samples were clustered with more than one authentic sample. Their spectra might have much variation and similar to many authentic samples. However some samples, i.e. TN1 and TN8 trended to separate from other Chan-thana samples. The species identification of these samples might be different from others. This result corresponded with the results of HCA that samples TN1 and TN8 were unidentified. PCA of the other Chan-thana samples needed more than two PCs for the explanation. The score plots of the first three PC of the acetone extract gave the best results (Figure 44). Its total variance explanation for normalized IR and second derivative IR spectra were 76% and 61%, respectively. Most of Chan-thana samples and *T. hoensis* were grouped into the same group. Samples TN1, TN7 and TN8 were separated from the

others and were not clustered with any authentic samples. These results corresponded with TLC. Therefore most of Chan-thana samples were *T. hoensis* and samples TN1, TN7 and TN8 were unidentified.

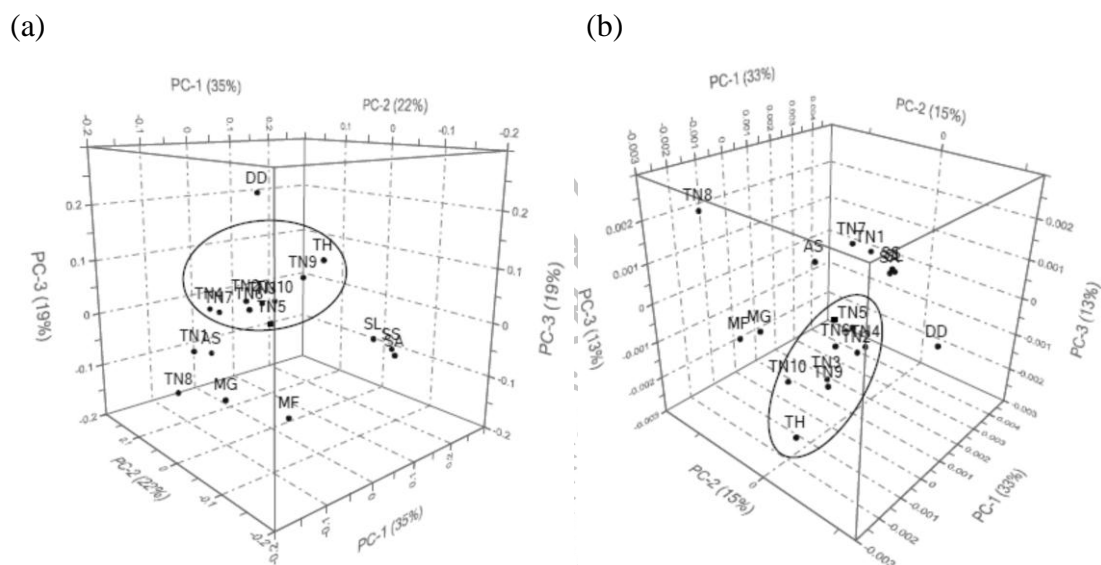


Figure 44 PC1, PC2 and PC3 three dimension score plots of (a) normalized IR spectra and (b) second derivative IR spectra of the acetone extract of Chan-thana (TN1-TN10), *S. album* (SA), *S. spicatum* (SS), *S. lanceolatum* (SL), *M. fragrans* (MF), *T. hoensis* (TH), *D. decandra* (DD), *M. gagei* (MG) and *A. silvestris* (AS).

In conclusion, SA gave only some idea that most of Chan-thana samples might be *T. hoensis*. HCA and PCA confirmed this suggestion. HCA gave more information that two samples (TN1 and TN8) were unidentified species, whereas PCA clearly indicated that not only these two samples but also TN7 were unidentified species.

3.2.5 Chan-hom

Correlation coefficients between all Chan-hom and authentic samples are shown in Tables 70-76. The IR spectra of the water extract and the fine powders could not be used for the identification because all of their correlation coefficients were not much different. All other extracts suggested that samples H10 and H11 were *M. gagei* based on their high correlation coefficient ($r > 0.90$). The

second derivative IR spectra of the ethyl acetate, acetone and methanol extracts showed that samples H2-H9 were either *S. spicatum* ($r = 0.64-0.95$) or *S. lanceolatum* ($r = 0.66-0.92$). Sample H1 were unidentified species because its correlations to all authentic samples were not certain.

The HCA dendrograms of Chan-hom showed that the clustering of the second derivative spectra was slightly better than the normalized spectra. The clear results were obtained from the ethyl acetate, acetone, methanol extracts which cluster samples H2-H9 with *S. spicatum* and *S. lanceolatum* (group VIII in Figures 45, 46 and 47, respectively), samples H10, H11 with *M. gagei* (group VII in Figures 45 and 46 and group II in Figure 47, respectively). Only sample H1 was separated from the others and was not clustered with any authentic samples, thus it was unidentified sample. These HCA results corresponded with that of SA.

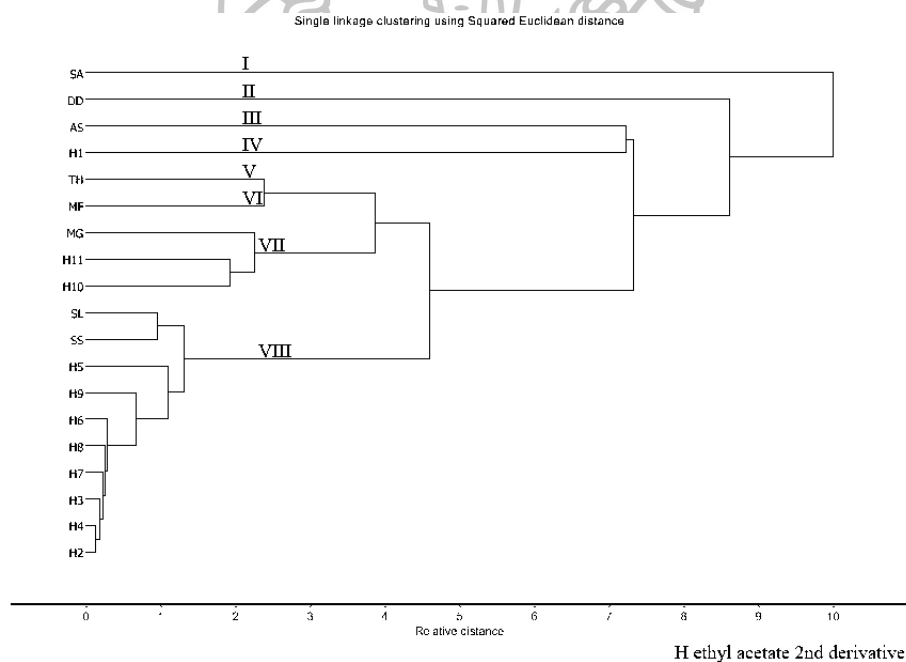


Figure 45 HCA dendrogram the second derivative IR spectra of the ethyl acetate extracts of Chan-hom samples (H1-H11), *S. album* (SA), *S. spicatum* (SS), *S. lanceolatum* (SL), *M. fragrans* (MF), *T. hoensis* (TH), *D. decandra* (DD), *M. gagei* (MG) and *A. silvestris* (AS).

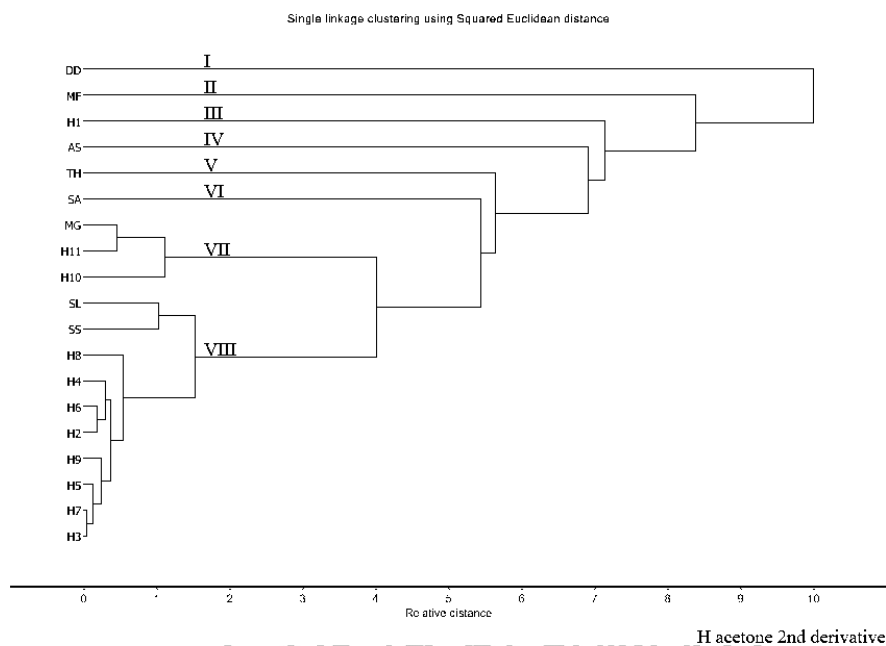


Figure 46 HCA dendrogram the second derivative IR spectra of the acetone extracts of Chan-hom samples (H1-H11), *S. album* (SA), *S. spicatum* (SS), *S. lanceolatum* (SL), *M. fragrans* (MF), *T. hoaensis* (TH), *D. decandra* (DD), *M. gagei* (MG) and *A. silvestris* (AS).

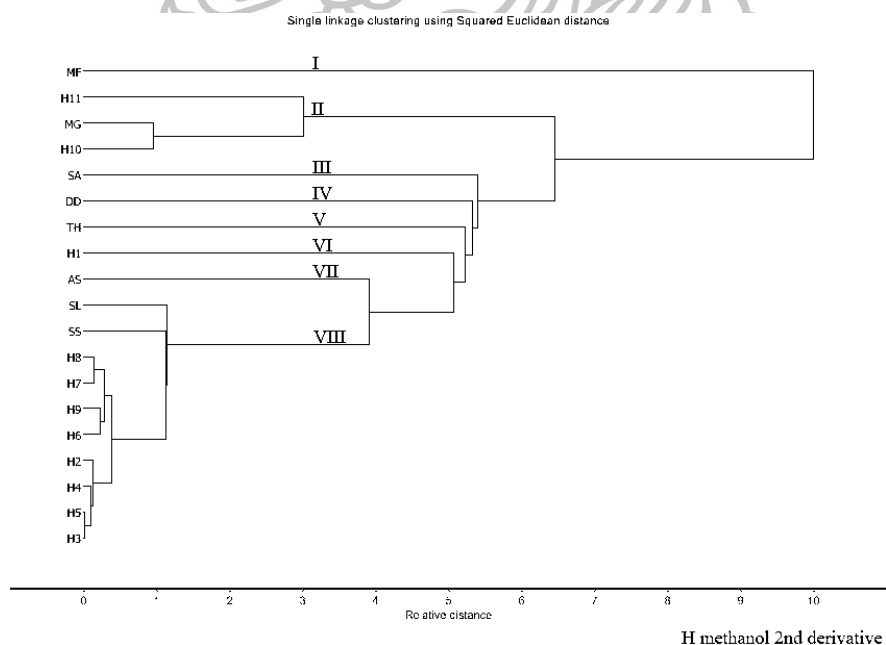


Figure 47 HCA dendrogram the second derivative IR spectra of the methanol extracts of Chan-hom samples (H1-H11), *S. album* (SA), *S. spicatum* (SS), *S. lanceolatum* (SL), *M. fragrans* (MF), *T. hoaensis* (TH), *D. decandra* (DD), *M. gagei* (MG) and *A. silvestris* (AS).

The results of SA and HCA were confirmed by PCA. The overall results of all solvent extracts, except the water extract and the fine powders, classified Chan-hom samples into three groups. The clearest result was that of methanol extract (Figure 48). The first group consisted of sample H10 and H11 and they were clustered with *M. gagei*. This result corresponded with all previous results which identified these samples as *M. gagei*. The second group was sample H1. It was separated from all authentic samples. Therefore its identification was impossible. The rest samples and the three authentic *Santalum* were clustered together as the third group. As mentioned in previous sections, *Santalum* species were difficult to differentiate therefore they could only be identified as either *S. album*, *S. spicatum* or *S. lanceolatum*.

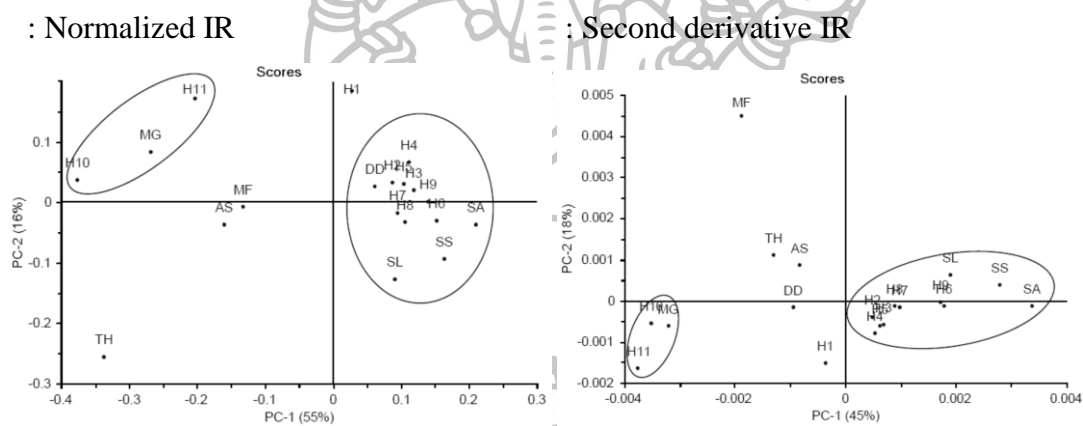


Figure 48 PC1 and PC2 score plots of the normalized and second derivative IR spectra of the methanol extracts of Chan-hom samples (H1-H11), *S. album* (SA), *S. spicatum* (SS), *S. lanceolatum* (SL), *M. fragrans* (MF), *T. hoensis* (TH), *D. decandra* (DD), *M. gagei* (MG) and *A. silvestris* (AS).

In conclusion, all SA, HCA and PCA indicated that two samples (H10 and H11) were *M. gagei* and one sample (H1) was unidentified species. The rest sample were *Santalum* species which could be further identified as either *S. spicatum* or *S. lanceolatum* by SA and HCA.

3.3 Gas chromatography (GC) fingerprint

GC fingerprints of the *n*-hexane extracts of crude drug and authentic samples (Figures 148-153) showed that only All Chan-khao samples except sample K18, all Chan-chamot samples, all Chan-thana samples and two samples of Chan-hom (H10 and H11) gave no interesting chromatograms. Among authentic samples, only three species of *Santalum* gave distinct chromatograms (Figure 148). Thus only samples and authentic samples of *Santalum* sp. were further intensively investigated. Moreover samples T1, T4 and T9 were selected for essential oil distillation. Essential oils of samples T1, T4 and T9 were selected to confirm the identification of *n*-hexane extracts. The analysis was carried out only on the retention time in the range of 15-23 min which gave the interesting characteristic.

3.3.1 Chemometric analysis

GC chromatograms obtained from the *n*-hexane extracts were analysed by using three chemometric methods, i.e. SA, HCA and PCA. The results of SA were shown in Table 26. The small similarity index calculated among GC chromatograms of three authentic species of *Santalum* ($r = 0.05-0.38$) indicated that their GC chromatograms were dissimilar and could be used for the identification. Similarity analysis of the GC chromatograms of Chan-thet (T1-T15), Chan-hom (H1-H9) and K18 (Table 26) indicated that these samples could be divided into three groups. The first group (samples T4, T6, T7 and T14) gave the highest correlation coefficient with *S. album* ($r = 0.88 \pm 0.13$). This suggested that samples in this group were *S. album*. The second group (samples T5 and H1) was most similar to *S. lanceolatum* because of the highest correlation coefficient ($r = 0.89 \pm 0.01$). However the third group (samples T1-T3, T8-T13, T15, H2-H4, H6-H9 and K18) could not be identified because their correlations with all three *Santalum* species were low ($r = 0.48-0.54$). All of these results suggested that only *S. album* and *S. lanceolatum* could be identified by SA.

The result of HCA is shown in Figure 49. All crude drug and authentic samples were clustered into two groups. Only samples T5 and H1 were clustered into the same group as *S. lanceolatum* (group I in Figure 49). This

confirmed the result of SA that these two samples were identified as *S. lanceolatum*. But all other crude drug samples were clustered into only one group (group II the Figure 49) which was the same group as the authentic *S. album* and *S. spicatum*. This suggested that HCA was not the suitable method for the classification between these two plant species.

Table 26 The similarity index of samples and authentic samples.

	Group 1 ^a	Group 2 ^b	Group 3 ^c	SA ^e	SS ^f	SL ^g
Group 1 ^a	0.84±0.13					
Group 2 ^b	0.17±0.03	0.95				
Group 3 ^c	0.65±0.13	0.36±0.03	0.92±0.05			
SA ^e	0.88±0.14	0.15±0.00	0.54±0.16	1.00		
SS ^f	0.35±0.14	0.30±0.01	0.54±0.08	0.16	1.00	
SL ^g	0.17±0.06	0.89±0.01	0.48±0.09	0.05	0.38	1.00

^aGroup 1 = T4, T6, T7 and T14

^bGroup 2 = T5 and H1

^cGroup 3 = T1-T3, T8-T13, T15, H2-H4, H6-H9 and K18

^eSA = *S. album*

^fSS = *S. spicatum*

^gSL = *S. lanceolatum*



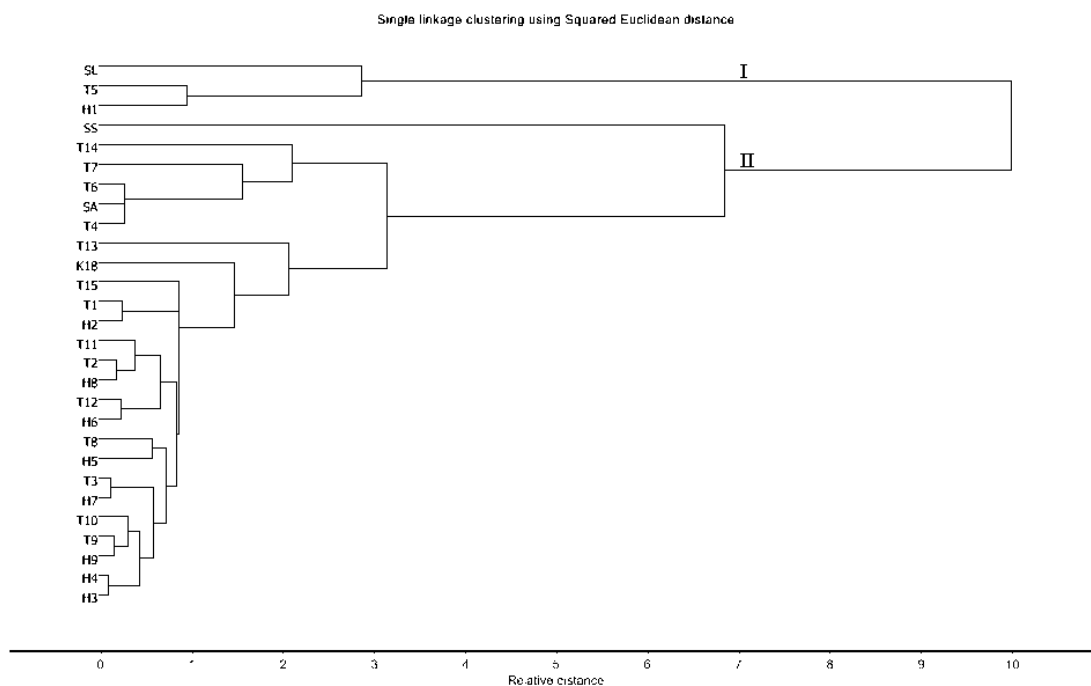
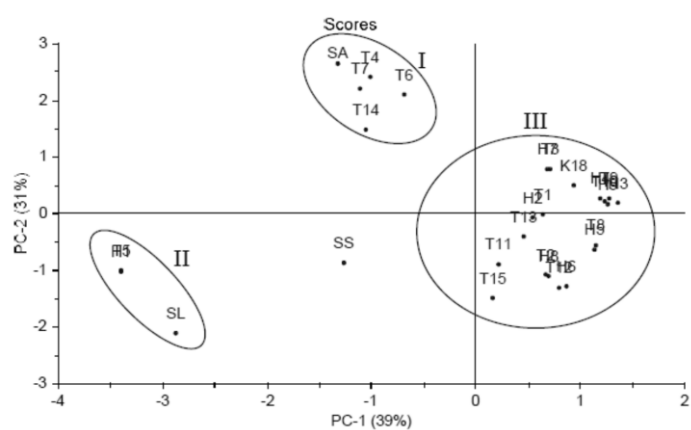


Figure 49 HCA dendrogram of GC chromatograms of the *n*-hexane extracts of Chan thet (T1-T15), Chan-khao (K18), Chan-hom (H2-H9), *S. album* (SA), *S. spicatum* (SS) and *S. lanceolatum* (SL) in the range of 15 to 23 min.

Identification of all samples could be clearly suggested by PCA. The PC1, PC2 and PC3 score plots (total explained variance 84%) are shown in Figure 50. All samples were classified into three groups (Figure 50). The variables that correlated to the classification of each group were explained by loading plot (Figure 51).

(a)



(b)

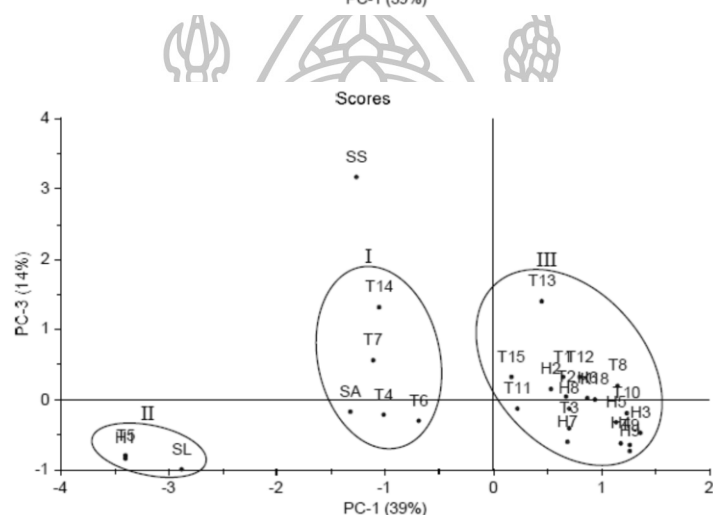
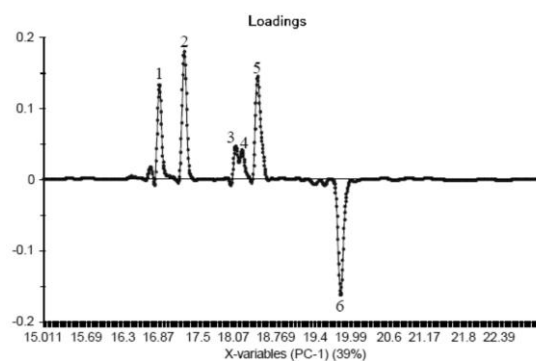


Figure 50 Score plots of (a) PC1 and PC2, and (b) PC1 and PC3 of the GC chromatograms of the *n*-hexane extracts of Chan-thet (T1-T15), Chan-hom (H1-H9), Chan-khao (K18), *S. spicatum* (SS), *S. album* (SA) and *S. lanceolatum* (SL).

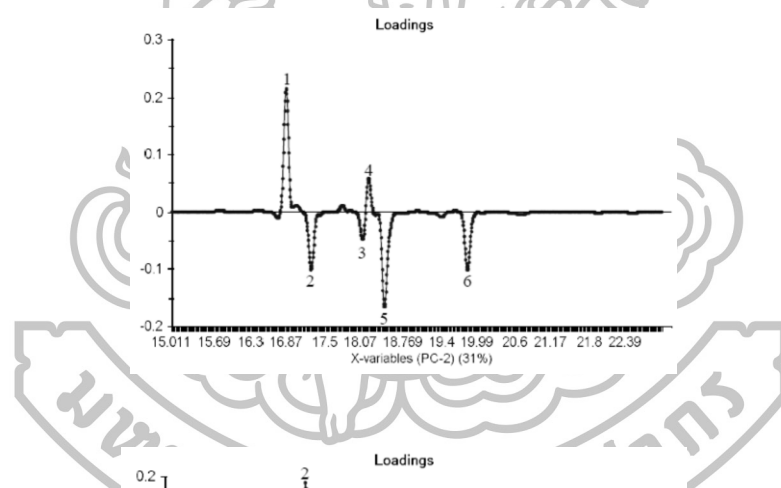
From score plots, the first group (samples T4, T6, T7 and T14) were clustered with *S. album*. This group was located on positive side of PC2 (Figure 50), thus the important explained variables were the peaks no.1 and no.4 (Figure 51(b)). The second group (samples T5 and H1) were clustered with *S. lanceolatum*. This group located on the negative side of PC1 thus this classification was explained by the peak no.6 (Figure 51(a)). The rest samples were grouped together but did not cluster with any authentic samples. This was group III in Figure 50. Group III located on the positive side of PC1 which was explained by the peaks no.1, 2, 3, 4 and no.5 (Figure 51(a)). Moreover it located on both positive and negative sides of PC2.

It suggested that intensity of peaks no. 1, 2, 3 and 5 was varied. Even this group could not be classified with any *Santalum* sp., it might be classified with *S. spicatum* because it closely located with *S. spicatum* in the score plot of Figure 50(a).

(a)



(b)



(c)

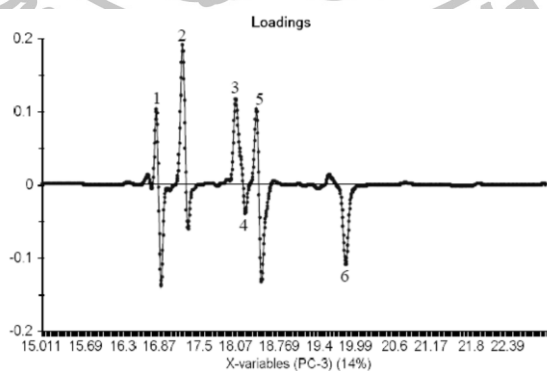


Figure 51 Loading plots of (a) PC1, (b) PC2 and (c) PC3 of the GC chromatograms of the *n*-hexane extracts of Chan-thet (T1-T15), Chan-hom (H1-H9), Chan-khao (K18), *S. spicatum* (SS), *S. album* (SA) and *S. lanceolatum* (SL).

The mean chromatograms (Figure 52) gave more obvious illustration of those three groups. The identification of chemical compositions in the *n*-hexane extract (section 3.3.2) gave information that peaks no. 1, 2, 3, 4, 5 and 6 were α -santalol, *Z*- α -*trans*-bergamotol, *trans*-farnesol, β -santalol, *trans*-nuciferol and *cis*-lanceol, respectively. Group I possessed peaks no. 1, 2, 4 and 5 that were similar to *S. album*. Group II possessed prominent peaks no. 5 and 6 that were similar to *S. lanceolatum*. It was clear that group I was *S. album* and group II was *S. lanceolatum*. Group III possessed peaks no. 1, 2, 3 and 5 that were similar to *S. spicatum*. However peak no. 4 in *S. spicatum* was less intensity whereas it was clearly observed in group III. Therefore other methods should be further applied to clear the identification of this group.

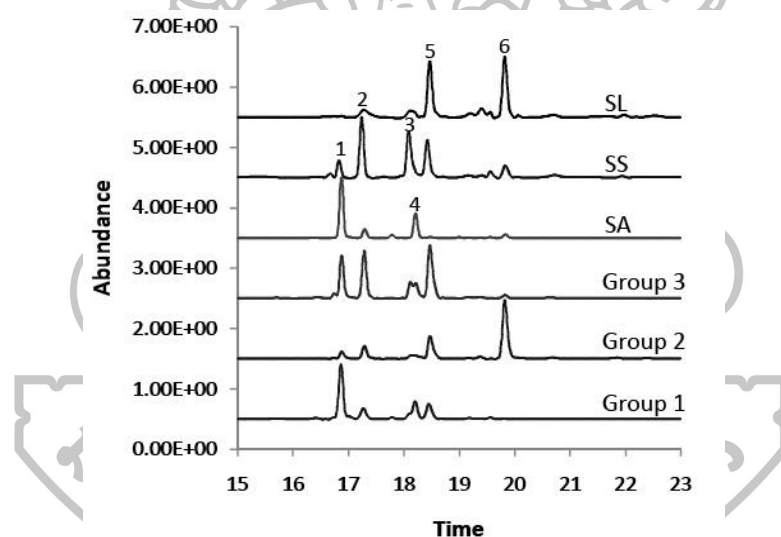


Figure 52 Mean GC chromatograms of the *n*-hexane extracts of samples group 1 (T4, T6, T7 and T14), group 2 (T5 and H1), and group 3 (T1-T3, T8-T13 and H2-H9); and GC chromatograms of the *n*-hexane extracts of *S. album* (SA), *S. spicatum* (SS) and *S. lanceolatum* (SL).

3.3.2 Identification of chemical compositions

To gain more information on the identification of all samples in previous sections, their chemical constituents were intensively investigated by GC/MS analysis and the calculation of Kovat index (KI) compared with data from NIST Standard Reference Database 69: NIST Chemistry *WebBook* (online database) and Adams's book [173]. The chemical compositions in the *n*-hexane extracts of the crude drug samples and the authentic *Santalum* samples are shown in Table 27. The interesting peaks of the chromatograms are illustrated in Figure 53. The labeled numbers on the chromatograms refer to compounds that are summarized in Table 27. The chemical constituents that were found in all crude drug samples and three *Santalum* species were α -santalol (peak no. 9), *trans*-nuciferol (peak no. 16) and *cis*-lanceol (peak no. 17). α -Santalol was the common compound of *Santalum* sp. It was a main constituent in *S. album* because it was the highest proportion (54.62%), corresponding with previous publication [12]. In this study, α -santalol was a major compound (the highest proportion) of samples T3-T4, T6-T7, T14, K18 and H7. However, only samples T4, T6 and T7 possessed the high content of this compound (42.25-45.93%). The characteristic chemical constituent of *S. album* was not only the highest content of α -santalol, but also the presence of *Z*- α -*trans*-bergamotol (peak no. 11). Retention time of this compound and α -bisabolol (peak no.10) was very close. *Z*- α -*trans*-bergamotol was found in only *S. album* but α -bisabolol was found in only *S. spicatum* and *S. lanceolatum*. Therefore samples T4, T6 and T7 were identified as *S. album* because they had *Z*- α -*trans*-bergamotol and the highest content of α -santalol. *S. lanceolatum* had less content of α -santalol but high content of *cis*-lanceol (peak no. 17). This difference could differentiate *S. lanceolatum* from other species. The GC chromatogram showed that samples T5 and H1 had the highest content of *cis*-lanceol. Therefore they were identified as *S. lanceolatum*. The rest samples had four major compounds which were α -santalol (peak no. 9), α -bisabolol (peak no 10), *trans*-farnesol (peak no. 13) and *trans*-nuciferol (peak no. 16). These compounds were also found in *S. spicatum*. Moreover the content of these compounds in the rest samples were similar to *S. spicatum* except the content of *trans*-farnesol. This point should further study. From three species of *Santalum*, only *S. spicatum* had high content of

both α -bisabolol and *trans*-nuciferol. These results indicated that the rest samples might be *S. spicatum*.

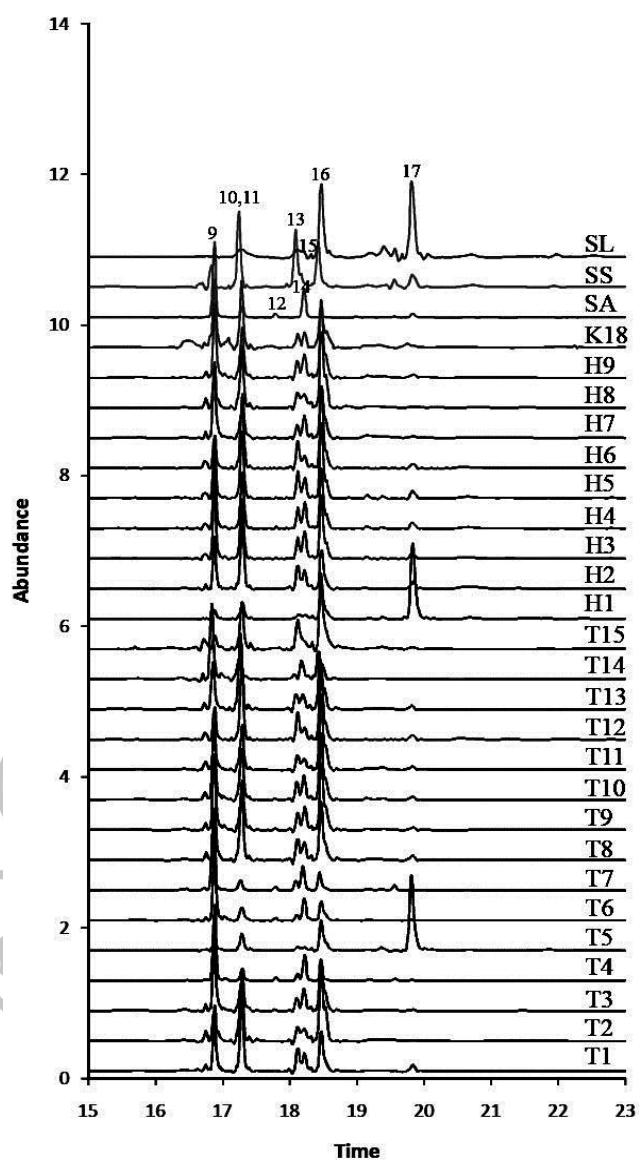


Figure 53 GC fingerprints of the *n*-hexane extracts of Chan-thet (T1-T15), Chan-hom (H1-H9), Chan-khao (K18), *S. album* (SA), *S. spicatum* (SS) and *S. lanceolatum* (SL).

Table 27 Composition of the *n*-hexane extracts of Chan-thet (T1-T15), Chan-hom (H1-H9), Chan-khao (K18) and authentic samples.

No.	RT*	RRT*	KI*	Compound	Composition (%)								
					T1	T2	T3	T4	T5	T6	T7	T8	T9
1	10.6	0.63	1427	α -Santalene	-	-	-	3.30	-	-	1.24	-	-
2	10.83	0.64	1434	α -Bergamotene	-	-	-	1.05	-	-	-	-	-
3	11.13	0.66	1455	<i>epi</i> - β -Santalene	-	-	-	1.66	-	-	0.76	-	-
4	11.35	0.67	1466	β -Santalene	-	-	-	0.00	-	0.97	1.05	-	-
5	11.75	0.70	1486	α -Curcumene	1.92	-	-	0.94	-	1.23	0.62	2.50	2.10
6	12.18	0.72	1506	α -Selinene	-	-	-	0.45	-	-	0.89	-	-
7	13.54	0.80	1562	Nerolidol	-	-	-	0.57	-	-	0.61	-	-
8	13.76	0.81	1571	Denderalasin	3.70	-	-	0.70	-	-	-	2.34	1.82
9	16.89	1.00	1679	α -Santalol	20.15	17.28	30.21	45.86	7.59	42.25	45.93	17.34	26.98
10	17.30	1.02	1690	α -Bisabolol	29.09	27.71	18.82	-	11.52	-	-	26.67	21.29
11	17.32	1.03	1691	<i>Z</i> - α - <i>trans</i> -Bergamotol	-	-	-	9.69	-	12.06	9.12	-	-
12	17.81	1.05	1705	<i>E</i> - <i>cis</i> - <i>epi</i> - β -Santalol	-	-	-	3.00	-	3.54	-	-	-
13	18.12	1.07	1741	<i>trans</i> -Farnesol	10.74	8.73	-	4.84	3.03	4.90	3.12	9.08	2.15
14	18.22	1.07	1717	β -Santalol	-	-	7.54	18.32	-	15.66	6.96	-	7.17
15	18.23	1.07	1717	β - <i>trans</i> -Santalol	7.72	5.79	10.15	-	3.27	-	16.12	9.22	-
16	18.48	1.09	1724	<i>trans</i> -Nuciferol	21.31	35.59	29.97	8.62	23.10	17.66	12.80	27.42	34.87
17	19.83	1.17	1759	<i>cis</i> -Lanceol	5.38	4.90	3.31	0.98	51.50	1.73	0.78	5.34	3.62

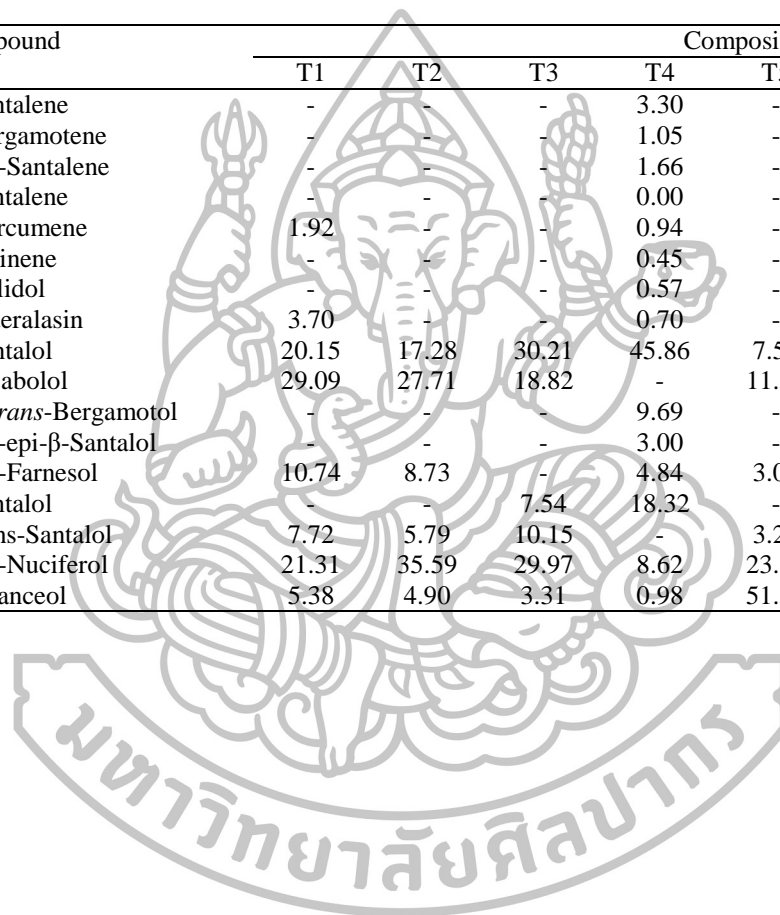


Table 27 Composition of the *n*-hexane extracts of Chan-thet (T1-T15), Chan-hom (H1-H9), Chan-khao (K18) and authentic samples (continued).

No.	RT*	RRT*	KI*	Compound	Composition (%)									
					T10	T11	T12	T13	T14	T15	K18	H1	H2	
1	10.6	0.63	1427	α -Santalene	1.06	-	-	-	-	-	-	-	-	-
2	10.83	0.64	1434	α -Bergamotene	-	-	-	-	-	-	-	-	-	-
3	11.13	0.66	1455	<i>epi</i> - β -Santalene	-	-	-	-	-	-	-	-	-	-
4	11.35	0.67	1466	β -Santalene	1.04	-	-	-	-	-	-	-	-	-
5	11.75	0.70	1486	α -Curcumene	2.69	3.20	2.25	3.40	-	-	-	-	-	1.92
6	12.18	0.72	1506	α -Selinene	-	-	-	-	-	-	-	-	-	-
7	13.54	0.80	1562	Nerolidol	1.33	2.44	-	-	-	-	-	-	-	-
8	13.76	0.81	1571	Denderalasin	2.17	2.68	3.03	3.46	-	-	-	-	-	3.70
9	16.89	1.00	1679	α -Santalol	23.82	14.51	14.37	17.59	35.37	10.31	19.85	7.59	20.15	
10	17.30	1.02	1690	α -Bisabolol	18.71	19.42	26.45	29.34	13.28	23.70	18.02	11.52	29.09	
11	17.32	1.03	1691	<i>Z</i> - α - <i>trans</i> -Bergamotol	-	-	-	-	-	-	-	-	-	-
12	17.81	1.05	1705	<i>E</i> - <i>cis</i> - <i>epi</i> - β -Santalol	-	-	-	-	-	-	-	-	-	-
13	18.12	1.07	1741	<i>trans</i> -Farnesol	1.50	7.05	9.97	8.18	3.95	19.94	4.94	3.03	10.74	
14	18.22	1.07	1717	β -Santalol	6.58	5.51	-	-	11.27	-	5.21	-	7.72	
15	18.23	1.07	1717	β - <i>trans</i> -Santalol	9.53	-	5.86	8.72	-	-	-	3.27	-	
16	18.48	1.09	1724	<i>trans</i> -Nuciferol	28.61	41.15	33.13	23.10	16.16	46.05	12.69	23.10	21.31	
17	19.83	1.17	1759	<i>cis</i> -Lanceol	2.95	4.04	4.94	6.22	19.98	-	4.13	51.50	5.38	

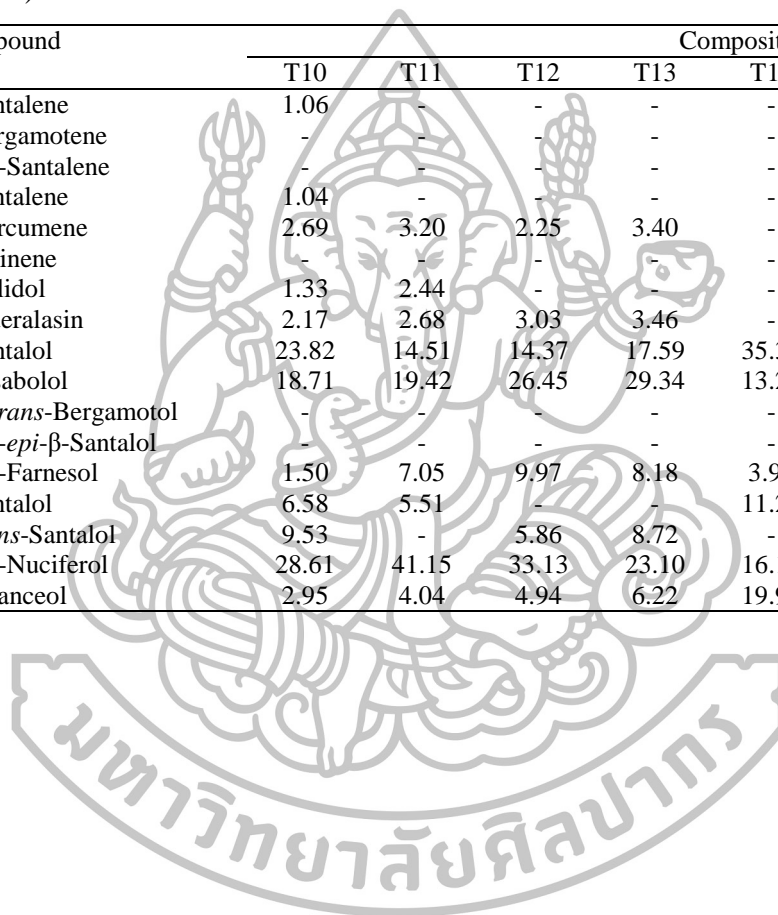
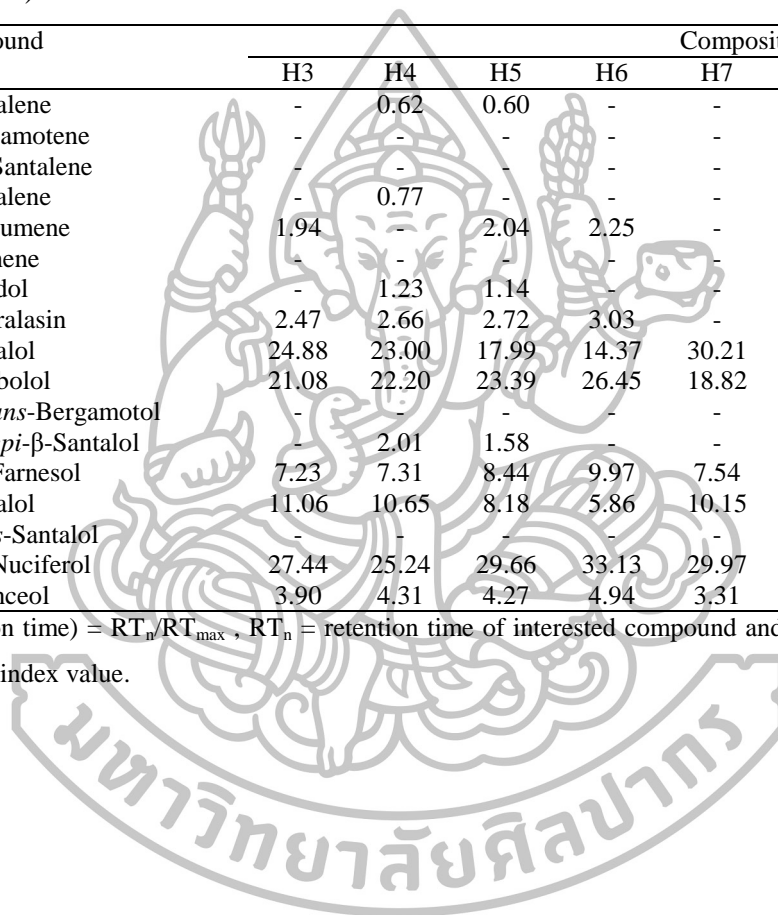


Table 27 Composition of the *n*-hexane extracts of Chan-thet (T1-T15), Chan-hom (H1-H9), Chan-khao (K18) and authentic samples (continued).

No.	RT*	RRT*	KI*	Compound	Composition (%)										
					H3	H4	H5	H6	H7	H8	H9	SS	SA	SL	
1	10.6	0.63	1427	α -Santalene	-	0.62	0.60	-	-	-	-	-	-	0.98	-
2	10.83	0.64	1434	α -Bergamotene	-	-	-	-	-	-	-	-	-	-	-
3	11.13	0.66	1455	epi- β -Santalene	-	-	-	-	-	-	-	-	-	1.01	-
4	11.35	0.67	1466	β -Santalene	-	0.77	-	-	-	-	-	-	-	1.73	-
5	11.75	0.70	1486	α -Curcumene	1.94	-	2.04	2.25	-	-	-	2.10	-	-	-
6	12.18	0.72	1506	α -Selinene	-	-	-	-	-	-	-	-	-	-	-
7	13.54	0.80	1562	Nerolidol	-	1.23	1.14	-	-	-	-	-	-	-	-
8	13.76	0.81	1571	Dendralasin	2.47	2.66	2.72	3.03	-	-	-	1.82	-	-	-
9	16.89	1.00	1679	α -Santalol	24.88	23.00	17.99	14.37	30.21	17.28	26.98	10.95	54.62	3.55	
10	17.30	1.02	1690	α -Bisabolol	21.08	22.20	23.39	26.45	18.82	27.71	21.29	30.53	-	9.49	
11	17.32	1.03	1691	<i>Z</i> - α - <i>trans</i> -Bergamotol	-	-	-	-	-	-	-	-	-	8.99	-
12	17.81	1.05	1705	<i>E</i> - <i>cis</i> - <i>epi</i> - β -Santalol	-	2.01	1.58	-	-	-	-	-	-	3.11	-
13	18.12	1.07	1741	<i>trans</i> -Farnesol	7.23	7.31	8.44	9.97	7.54	8.73	2.15	22.44	-	7.38	
14	18.22	1.07	1717	β -Santalol	11.06	10.65	8.18	5.86	10.15	5.79	7.17	5.60	23.77	-	
15	18.23	1.07	1717	β - <i>trans</i> -Santalol	-	-	-	-	-	-	-	-	-	-	
16	18.48	1.09	1724	<i>trans</i> -Nuciferol	27.44	25.24	29.66	33.13	29.97	35.59	34.87	20.87	1.87	36.89	
17	19.83	1.17	1759	<i>cis</i> -Lanceol	3.90	4.31	4.27	4.94	3.31	4.90	3.62	9.61	3.92	42.69	

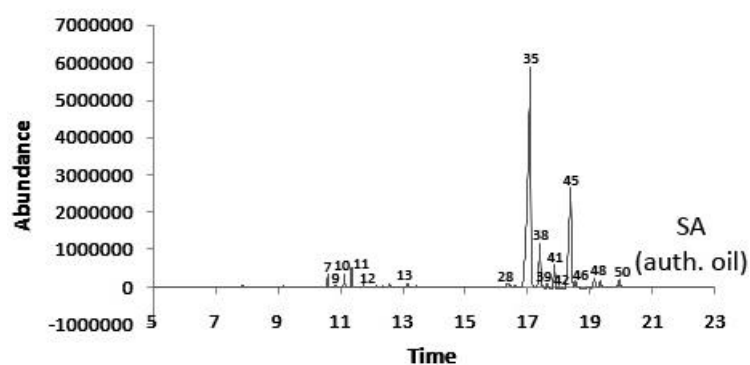
* RT = retention time, RRT (related retention time) = RT_n/RT_{max} , RT_n = retention time of interested compound and RT_{max} = retention time of compound that has maximum content in sample and KI = Kovat index value.



The essential oil analysis was used to confirm the results of the *n*-hexane extracts. Three crude drug samples were selected for the analysis. T4 was the representative sample of those identified as *S. album*, whereas samples T1 and T9 were used to clear the doubtful identification of *S. spicatum*. The analyses were the comparison of their chemical constituents with the essential oils distilled from three authentic *Santalum* species (*S. album*, *S. spicatum* and *S. lanceolatum*) and authentic essential oils of various *Santalum* species, i.e. *S. album*, *S. spicatum*, *S. austrocaledonicum* and *S. paniculatum*. The composition of essential oils and GC chromatograms of their essential oil are shown in Table 28 and Figure 54, respectively. α -Santalol (peak no. 35) and β -santalol (peak no. 45) were major compounds of *S. album*, *S. austrocaledonicum* and *S. paniculatum*, corresponding with previous publication [45]. Among all authentic samples, *S. album*, *S. austrocaledonicum* and *S. paniculatum* possessed high content of α -santalol more than 50%. Most of the compounds that were found in these three species were very similar. However some compounds could be used to discriminate them. It was α -curcumene (peak no. 49) that found only in *S. austrocaledonicum*. In addition, *cis*- α -santalol (peak no. 39) could be found in *S. album* and *S. austrocaledonicum* but could not be found in *S. paniculatum*. Sample T4 had high content of α -santalol (41.32%) and its chemical compositions were similar to *S. album*. Therefore its identification as *S. album* was confirmed. The chemical constituents of *S. spicatum* were obviously differed from *S. album*, *S. austrocaledonicum* and *S. paniculatum*. First, the content of α -santalol (peak no. 35) of *S. spicatum* was lower. Second, α -bisabolol (peak no.37) was found only in *S. spicatum* and *S. lanceolatum*. The difference between *S. spicatum* and *S. lanceolatum* were the highest content of *cis*-lanceol in *S. lanceolatum*. Moreover *S. lanceolatum* possessed the high content of nuciferol, whereas the content of α -santalol was very low. This result was similar to previous published data [83]. The samples T1 and T9 had chemical compositions similar to those of *S. spicatum*. Therefore samples T1 and T9 were clearly identified as *S. spicatum*. However the content of *trans*-farnesol in essential oil of authentic *S. spicatum* was higher than samples T1 and T9 because of the difference of planting location which had the different environment. Furthermore an older *S. spicatum* had

the less content of *trans*-farnesol [12], thus samples T1 and T9 might be derived from the older trees. Moreover the less rainfall season gave the high content of *trans*-farnesol in *S. spicatum* [12] thus the authentic *S. spicatum* might be derived from the summer season, whereas samples T1 and T9 might be derived from other season.

(a)



(b)

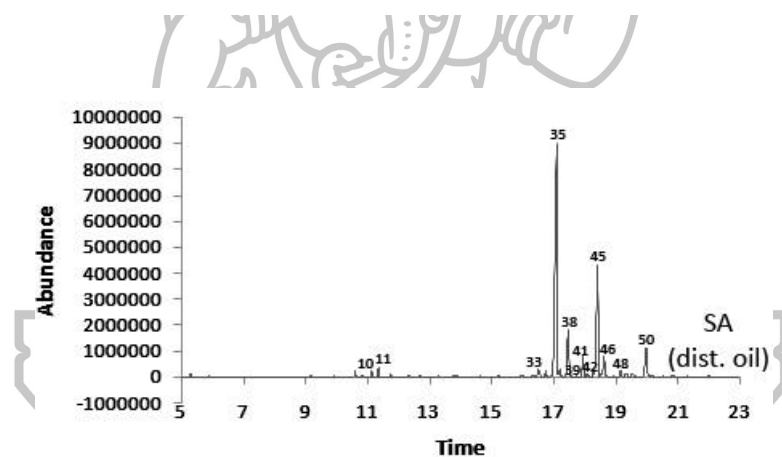
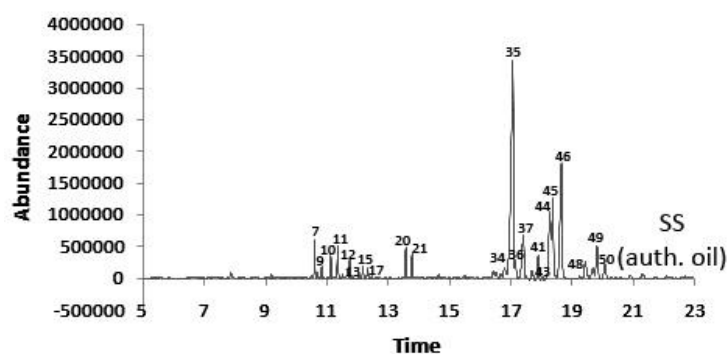
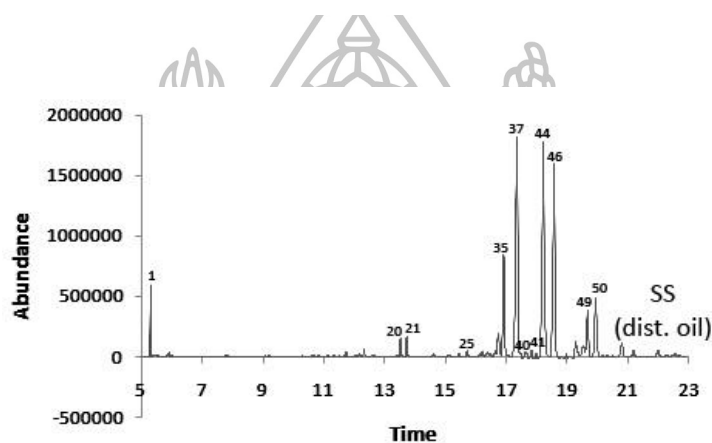


Figure 54 GC fingerprints of (a) authentic *S. album* (SA auth. oil), (b) distilled *S. album* (SA dist. oil), (c) authentic *S. spicatum* (SS auth. oil), (d) distilled *S. spicatum* (SS dist. oil), (e) distilled *S. lanceolatum* (SL dist. oil), (f) authentic *S. austrocaledonicum* (SAU auth. oil), (g) authentic *S. paniculatum* (SP auth. oil), (h) distilled sample T1 (T1 dist. oil), (i) distilled sample T4 (T4 dist. oil) and (j) distilled sample T9 (T9 dist. oil).

(c)



(d)



(e)

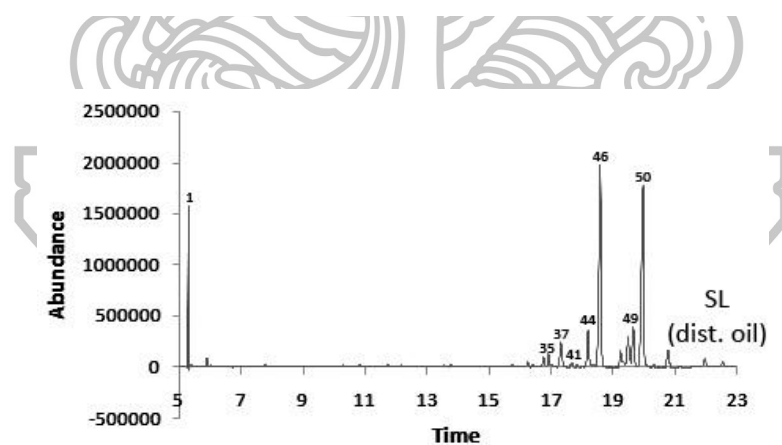
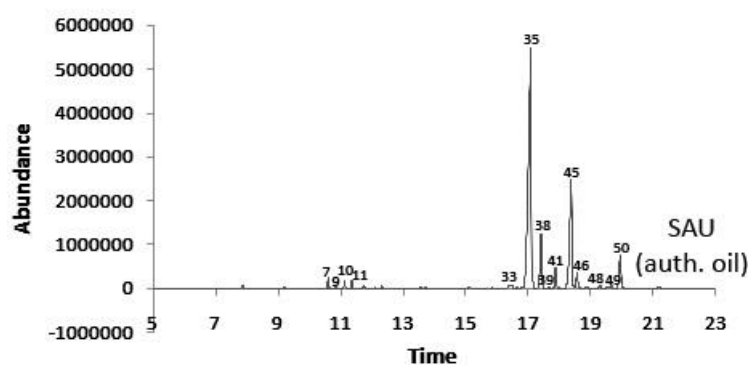
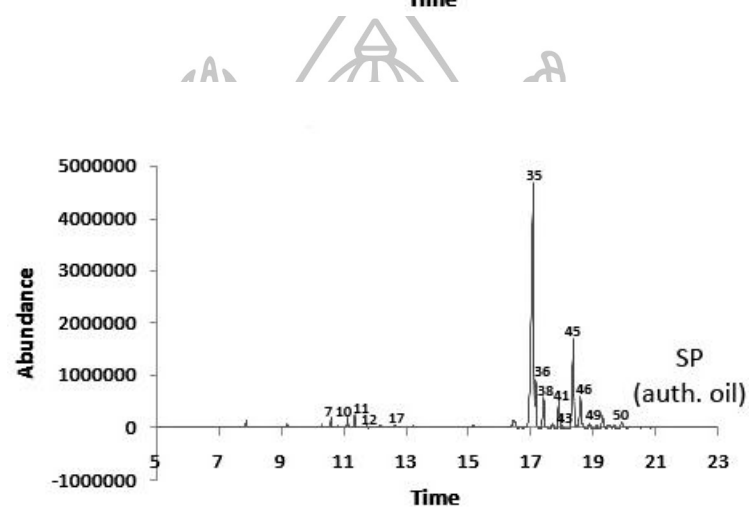


Figure 54 GC fingerprints of (a) authentic *S. album* (SA auth. oil), (b) distilled *S. album* (SA dist. oil), (c) authentic *S. spicatum* (SS auth. oil), (d) distilled *S. spicatum* (SS dist. oil), (e) distilled *S. lanceolatum* (SL dist. oil), (f) authentic *S. austrocaledonicum* (SAU auth. oil), (g) authentic *S. paniculatum* (SP auth. oil), (h) distilled sample T1 (T1 dist. oil), (i) distilled sample T4 (T4 dist. oil) and (j) distilled sample T9 (T9 dist. oil) (continued).

(f)



(g)



(h)

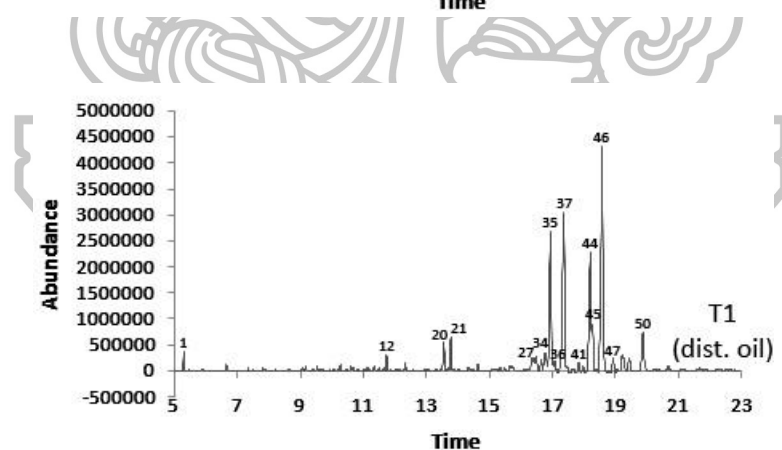
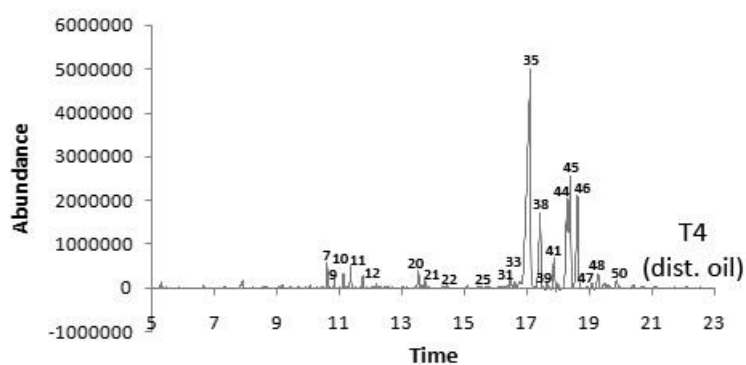


Figure 54 GC fingerprints of (a) authentic *S. album* (SA auth. oil), (b) distilled *S. album* (SA dist. oil), (c) authentic *S. spicatum* (SS auth. oil), (d) distilled *S. spicatum* (SS dist. oil), (e) distilled *S. lanceolatum* (SL dist. oil), (f) authentic *S. austrocaledonicum* (SAU auth. oil), (g) authentic *S. paniculatum* (SP auth. oil), (h) distilled sample T1 (T1 dist. oil), (i) distilled sample T4 (T4 dist. oil) and (j) distilled sample T9 (T9 dist. oil) (continued).

(i)



(j)

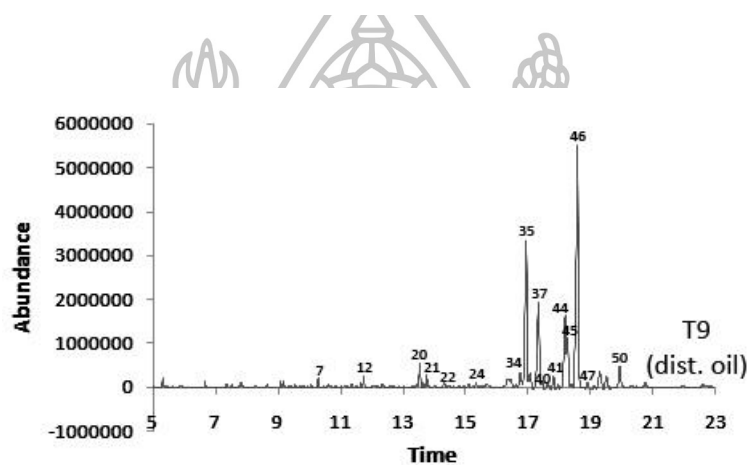


Figure 54 GC fingerprints of (a) authentic *S. album* (SA auth. oil), (b) distilled *S. album* (SA dist. oil), (c) authentic *S. spicatum* (SS auth. oil), (d) distilled *S. spicatum* (SS dist. oil), (e) distilled *S. lanceolatum* (SL dist. oil), (f) authentic *S. austrocaledonicum* (SAU auth. oil), (g) authentic *S. paniculatum* (SP auth. oil), (h) distilled sample T1 (T1 dist. oil), (i) distilled sample T4 (T4 dist. oil) and (j) distilled sample T9 (T9 dist. oil) (continued).

Table 28 Composition of the essential oils of Chan-thet samples (T1, T4 and T9) and various authentic *Santalum*.

No.	RT	RRT	KI	Compound	Composition (%)									
					SA dist.*	SA*	SL dist.*	SS dist.*	SS*	SAU*	SP*	T1*	T4*	T9*
1	5.27	0.31	1097	<i>o</i> -Tolualdehyde	0.25	-	10.04	2.79	-	-	-	0.82	0.19	0.55
2	5.90	0.34	1145	Benzyl alcohol	0.05	-	0.58	tr	-	-	-	-	-	-
3	6.62	0.39	1196	Acetophenone	-	-	-	-	-	-	-	0.09	0.45	-
4	7.52	0.44	1254	Propanal, 2-methyl-3-phenyl-	-	-	-	-	-	-	-	tr	tr	-
5	7.79	0.46	1270	<i>p</i> -Toluic acid	-	-	0.21	-	-	-	-	-	-	-
6	10.47	0.61	1420	α -Cedrene	-	-	-	tr	-	-	-	tr	0.05	-
7	10.60	0.62	1427	α -Santalene	0.55	0.88	-	-	2.08	0.74	0.82	-	1.15	0.17
8	10.68	0.62	1429	α -Cedrene	-	-	-	-	0.31	-	-	-	tr	-
9	10.84	0.63	1440	α -Bergamotene	0.13	0.16	-	-	0.64	0.12	-	-	0.37	0.19
10	11.13	0.65	1455	<i>epi</i> - β -Santalene	0.56	0.97	-	-	1.18	0.61	0.94	-	0.72	0.15
11	11.36	0.66	1466	β -Santalene	0.86	1.52	-	0.09	1.85	0.60	1.21	-	1.08	0.29
12	11.75	0.69	1486	α -Curcumene	0.31	0.31	-	-	1.15	0.24	0.33	0.94	0.71	0.82
13	12.04	0.70	1495	β -Selinene	-	-	-	-	0.34	-	-	-	tr	-
14	12.18	0.71	1506	α -Selinene	-	-	-	-	-	-	-	-	0.25	-
15	12.19	0.71	1506	γ -Selinene	-	-	-	-	0.89	-	-	-	-	-
16	12.31	0.72	1511	β -Bisabolene	0.11	-	-	-	-	0.27	-	-	-	0.06
17	12.33	0.72	1512	α -Cedrene	tr	tr	-	-	0.77	-	0.22	-	tr	-
18	12.71	0.74	1528	β -Sesquiphellandrene	-	-	-	tr	tr	-	-	-	-	-
19	13.06	0.76	1543	<i>cis</i> - α -Bisabolene	-	-	-	-	tr	-	-	-	-	-
20	13.53	0.79	1562	Nerolidol	-	tr	-	1.16	2.27	-	-	2.02	1.12	2.09
21	13.76	0.80	1571	Denderalasin	-	-	-	1.35	1.87	-	-	2.45	0.44	1.31
22	14.30	0.84	1591	γ -Cadinene	-	-	-	-	-	-	-	-	0.17	0.72
23	14.60	0.85	1602	Guaiol	-	-	-	tr	0.28	-	-	tr	-	0.17
24	15.64	0.91	1638	γ -Eudesmole	-	-	-	-	tr	-	-	tr	-	0.26
25	15.77	0.92	1642	α -Cedrene	tr	tr	0.32	0.48	0.51	tr	-	-	tr	-
26	16.27	0.95	1658	α -Longipinene	-	-	-	tr	-	-	-	-	-	-
27	16.37	0.96	1622	β -Eudesmol	-	-	-	-	-	-	-	1.99	-	-
28	16.41	0.96	1663	Diamantane	-	0.56	-	-	-	tr	tr	-	-	-

Table 28 Composition of the essential oils of Chan-thet samples (T1, T4 and T9) and various authentic *Santalum* (continued).

No.	RT	RRT	KI	Compound	Composition (%)									
					SA dist*	SA*	SL dist*	SS dist*	SS*	SAU*	SP*	T1*	T4*	T9*
29	16.43	0.96	1663	Longifolene	-	-	-	-	0.64	-	-	-	-	-
30	16.46	0.96	1664	Guaia-3,9-diene	-	-	-	-	-	-	-	1.79	-	-
31	16.48	0.96	1665	(+)-5-epi-Neointermedeol	-	-	-	-	-	-	-	-	0.86	-
32	16.53	0.97	1667	γ -Gurjunene	-	-	-	tr	0.64	-	-	-	-	-
33	16.66	0.97	1671	Santalol	0.95	-	-	-	-	0.23	tr	-	0.50	-
34	16.69	0.98	1672	Bulnesol	-	-	-	tr	0.53	-	-	1.19	-	0.60
35	17.11	1.00	1686	α -Santalol	48.48	55.55	1.59	9.22	31.19	53.39	52.32	14.10	41.32	18.57
36	17.15	1.00	1686	<i>cis</i> - α -Santalol	-	-	-	-	2.38	-	7.08	1.36	-	-
37	17.34	1.01	1692	α -Bisabolol	-	-	4.82	24.93	7.94	-	-	19.15	-	13.84
38	17.34	1.01	1692	<i>Z</i> - α - <i>trans</i> -Bergamotol	8.43	7.30	-	-	-	8.76	5.91	-	9.20	-
39	17.69	1.03	1702	<i>cis</i> - α -Santalol	0.50	1.18	-	-	-	0.71	-	-	1.34	-
40	17.70	1.03	1703	Cedren-13-ol, 8-	-	-	0.88	0.94	-	-	-	-	-	0.76
41	17.81	1.04	1705	<i>E</i> - <i>cis</i> - <i>epi</i> - β -Santalol	3.65	3.70	-	0.81	2.79	3.40	4.82	1.34	3.26	1.80
42	17.95	1.05	1709	α -Santalol	1.07	0.98	-	-	-	-	-	-	-	-
43	18.01	1.05	1711	<i>cis</i> - α -Santalol	-	-	-	-	0.41	tr	1.17	-	1.20	-
44	18.29	1.07	1720	<i>trans</i> -Farnesol	tr	-	5.90	25.95	8.09	-	-	14.72	9.88	10.92
45	18.36	1.07	1721	β -Santalol	21.33	22.09	-	-	9.01	21.07	16.22	4.18	12.75	4.65
46	18.49	1.08	1726	Nuciferol	5.21	1.50	33.94	20.42	15.24	3.01	6.49	26.94	10.61	36.91
47	18.90	1.11	1735	Farnesal	-	-	-	-	-	-	-	1.79	0.60	0.90
48	19.09	1.12	1741	β -Santalol	1.52	1.78	-	-	0.42	0.29	0.94	-	0.86	-
49	19.65	1.15	1755	α -Curcumene	-	-	7.04	5.04	4.18	0.65	-	-	-	-
50	19.85	1.16	1762	<i>cis</i> -Lanceol	6.02	1.53	34.69	6.83	2.40	5.88	1.53	5.23	1.34	3.79

*SA dist = *S. album* oil prepared by steam distillation in the laboratory, SA = authentic sandalwood oil of *S. album* originated from India, SL dist = *S. lanceolatum* oil prepared by steam distillation in the laboratory, SS dist = *S. spicatum* oil prepared by steam distillation in the laboratory, SS = authentic sandalwood oil of *S. spicatum* originated from Australia, SAU = authentic sandalwood oil of *S. austrocaledonicum* originated from New Caledonia, SP = authentic sandalwood oil of *S. paniculatum* originated from Hawaii, T1 = sample T1 oil, T4 = sample T4 oil and sample T9 oil.

3.4 Conclusion of the identification

The overall results of the identification of Chan-thet, Chan-khao, Chan-chamot, Chan-thana and Chan-hom samples using TLC, IR and GC analysis are shown in Table 29. TLC and GC indicated that all Chan-thet samples were *Santalum* species. Sample T5 was *S. lanceolatum*. Samples T4, T6 and T7 were *S. album*. The others were *S. spicatum*. But based on IR, only two samples (T4 and T7) were identified as *S. album*. IR could not differentiate the correct species between *S. spicatum* and *S. lanceolatum*, and the identification of samples T1-T3, T5-T6 and T8-T15 was different from TLC and GC.

Chan-khao samples were classified into three groups based on TLC. The first group (K1-K6, K10-K13, K16-K17, TN2-TN6, TN9 and TN10) was identified as *T. hoaensis*. The second group (K18) was identified as *S. spicatum*. The last group (K7-K9 and K14-K15) was unidentified. However this last group was identified as *T. hoaensis* by IR.

All Chan-chamot samples were identified as *M. gagei* by TLC and IR. Chan-thana samples were also undoubtedly identified by these two techniques. They could be divided into two groups. The first group (TN2-TN6 and TN9-TN10) was identified as *T. hoaensis*. The second group (TN1, TN7 and TN8) was unidentified.

Chan-hom samples were divided into three groups based on TLC. The first group (H1) was identified as *S. lanceolatum*. The second group (H2-H9) was identified as *S. spicatum*, whereas the last group (H10-H11) was *M. gagei*. The identification of the first two groups was confirmed by GC. However IR could not identify the first group. And in the same as the results of Chan-thet, IR could not identify the second group as either *S. spicatum* or *S. lanceolatum*.

Among three identification methods, TLC gave reliable results but only the TLC patterns of three *Santalum* species were difficult to discriminate. Therefore identification of some samples, such as sample H1, was slightly subjective. Advantage of GC was the clearest results comparing with the other two methods. But only the samples containing volatile compounds, e.g. *Santalum* sp. could be analyzed. IR was simple and used less chemical, but chemometric methods were needed for data analysis. Moreover its results were quite less accurate than the chromatographic techniques, then its results would be concerned latter after the after other methods.

Table 29 Identification results of Chan(s) using TLC, IR and GC.

	TLC	IR	GC
Chan-thet			
T1	<i>S. spicatum</i>	<i>S. spicatum</i> or <i>S. lanceolatum</i>	<i>S. spicatum</i>
T2	<i>S. spicatum</i>	<i>S. spicatum</i> or <i>S. lanceolatum</i>	<i>S. spicatum</i>
T3	<i>S. spicatum</i>	<i>S. spicatum</i> or <i>S. lanceolatum</i>	<i>S. spicatum</i>
T4	<i>S. album</i>	<i>S. album</i>	<i>S. album</i>
T5	<i>S. lanceolatum</i>	<i>S. spicatum</i> or <i>S. lanceolatum</i>	<i>S. lanceolatum</i>
T6	<i>S. album</i>	<i>S. spicatum</i> or <i>S. lanceolatum</i>	<i>S. album</i>
T7	<i>S. album</i>	<i>S. album</i>	<i>S. album</i>
T8	<i>S. spicatum</i>	<i>S. spicatum</i> or <i>S. lanceolatum</i>	<i>S. spicatum</i>
T9	<i>S. spicatum</i>	<i>S. spicatum</i> or <i>S. lanceolatum</i>	<i>S. spicatum</i>
T10	<i>S. spicatum</i>	<i>S. spicatum</i> or <i>S. lanceolatum</i>	<i>S. spicatum</i>
T11	<i>S. spicatum</i>	<i>S. spicatum</i> or <i>S. lanceolatum</i>	<i>S. spicatum</i>
T12	<i>S. spicatum</i>	<i>S. spicatum</i> or <i>S. lanceolatum</i>	<i>S. spicatum</i>
T13	<i>S. spicatum</i>	<i>S. spicatum</i> or <i>S. lanceolatum</i>	<i>S. spicatum</i>
T14	<i>S. spicatum</i>	<i>S. spicatum</i> or <i>S. lanceolatum</i>	<i>S. spicatum</i>
T15	<i>S. spicatum</i>	<i>S. spicatum</i> or <i>S. lanceolatum</i>	<i>S. spicatum</i>
Chan-khao			
K1	<i>T. hoaensis</i>	<i>T. hoaensis</i>	-
K2	<i>T. hoaensis</i>	<i>T. hoaensis</i>	-
K3	<i>T. hoaensis</i>	<i>T. hoaensis</i>	-
K4	<i>T. hoaensis</i>	<i>T. hoaensis</i>	-
K5	<i>T. hoaensis</i>	<i>T. hoaensis</i>	-
K6	<i>T. hoaensis</i>	<i>T. hoaensis</i>	-
K7	Unknown 1	<i>T. hoaensis</i>	-
K8	Unknown 1	<i>T. hoaensis</i>	-
K9	Unknown 1	<i>T. hoaensis</i>	-
K10	<i>T. hoaensis</i>	<i>T. hoaensis</i>	-
K11	<i>T. hoaensis</i>	<i>T. hoaensis</i>	-
K12	<i>T. hoaensis</i>	<i>T. hoaensis</i>	-
K13	<i>T. hoaensis</i>	<i>T. hoaensis</i>	-
K14	Unknown 1	<i>T. hoaensis</i>	-
K15	Unknown 1	<i>T. hoaensis</i>	-
K16	<i>T. hoaensis</i>	<i>T. hoaensis</i>	-
K17	<i>T. hoaensis</i>	<i>T. hoaensis</i>	-
K18	<i>S. spicatum</i>	<i>S. spicatum</i>	<i>S. spicatum</i>

Table 29 Identification results of Chan(s) using TLC, IR and GC (continued).

	TLC	IR	GC
Chan-chamot			
M1	<i>M. gagei</i>	<i>M. gagei</i>	-
M2	<i>M. gagei</i>	<i>M. gagei</i>	-
M3	<i>M. gagei</i>	<i>M. gagei</i>	-
M4	<i>M. gagei</i>	<i>M. gagei</i>	-
M5	<i>M. gagei</i>	<i>M. gagei</i>	-
M6	<i>M. gagei</i>	<i>M. gagei</i>	-
M7	<i>M. gagei</i>	<i>M. gagei</i>	-
M8	<i>M. gagei</i>	<i>M. gagei</i>	-
M9	<i>M. gagei</i>	<i>M. gagei</i>	-
M10	<i>M. gagei</i>	<i>M. gagei</i>	-
M11	<i>M. gagei</i>	<i>M. gagei</i>	-
M12	<i>M. gagei</i>	<i>M. gagei</i>	-
M13	<i>M. gagei</i>	<i>M. gagei</i>	-
M14	<i>M. gagei</i>	<i>M. gagei</i>	-
M15	<i>M. gagei</i>	<i>M. gagei</i>	-
M16	<i>M. gagei</i>	<i>M. gagei</i>	-
M17	<i>M. gagei</i>	<i>M. gagei</i>	-
Chan-thana			
TN1	Unknown 2	Unidentified	-
TN2	<i>T. hoaensis</i>	<i>T. hoaensis</i>	-
TN3	<i>T. hoaensis</i>	<i>T. hoaensis</i>	-
TN4	<i>T. hoaensis</i>	<i>T. hoaensis</i>	-
TN5	<i>T. hoaensis</i>	<i>T. hoaensis</i>	-
TN6	<i>T. hoaensis</i>	<i>T. hoaensis</i>	-
TN7	Unknown 1	Unidentified	-
TN8	Unknown 3	Unidentified	-
TN9	<i>T. hoaensis</i>	<i>T. hoaensis</i>	-
TN10	<i>T. hoaensis</i>	<i>T. hoaensis</i>	-

Table 29 Identification results of Chan(s) using TLC, IR and GC (continued).

	TLC	IR	GC
Chan-hom			
H1	<i>S. lanceolatum</i>	Unidentified	<i>S. lanceolatum</i>
H2	<i>S. spicatum</i>	<i>S. spicatum</i> or <i>S. lanceolatum</i>	<i>S. spicatum</i>
H3	<i>S. spicatum</i>	<i>S. spicatum</i> or <i>S. lanceolatum</i>	<i>S. spicatum</i>
H4	<i>S. spicatum</i>	<i>S. spicatum</i> or <i>S. lanceolatum</i>	<i>S. spicatum</i>
H5	<i>S. spicatum</i>	<i>S. spicatum</i> or <i>S. lanceolatum</i>	<i>S. spicatum</i>
H6	<i>S. spicatum</i>	<i>S. spicatum</i> or <i>S. lanceolatum</i>	<i>S. spicatum</i>
H7	<i>S. spicatum</i>	<i>S. spicatum</i> or <i>S. lanceolatum</i>	<i>S. spicatum</i>
H8	<i>S. spicatum</i>	<i>S. spicatum</i> or <i>S. lanceolatum</i>	<i>S. spicatum</i>
H9	<i>S. spicatum</i>	<i>S. spicatum</i> or <i>S. lanceolatum</i>	<i>S. spicatum</i>
H10	<i>M. gagei</i>	<i>M. gagei</i>	-
H11	<i>M. gagei</i>	<i>M. gagei</i>	-

In conclusion, five botanical species could be identified for Chan-thet, Chan-khao, Chan-chamot, Chan-thana and Chan-hom samples currently available in Thai traditional drugstores. They were *S. album*, *S. spicatum*, *S. lanceolatum*, *M. gagei* and *T. hoensis*. The conclusion is shown in Table 30



Table 30 Conclusion of species identification of Chan(s) in Thai traditional drugstores.

Chan(s)	Identification	Number (%)
Chan-thet	<i>S. album</i>	3 (20)
	<i>S. spicatum</i>	11 (73)
	<i>S. lanceolatum</i>	1 (7)
Chan-khao	<i>T. hoaensis</i>	12 (67)
	<i>S. spicatum</i>	1 (5)
	Unknown-1	5 (28)
Chan-chamot	<i>M. gagei</i>	17 (100)
Chan-thana	<i>T. hoaensis</i>	7 (70)
	Unknown-1	1 (10)
	Unknown-2	1 (10)
	Unknown-3	1 (10)
Chan-hom	<i>S. spicatum</i>	8 (73)
	<i>M. gagei</i>	2 (18)
	<i>S. lanceolatum</i>	1 (9)

Besides the identification of botanical species based on their chemical constituents, DNA fingerprint is widely used [190, 191]. This technique is used to produce a unique pattern for identification by simultaneous analysis of multiple loci in genome [190]. Even though this technique possesses the useful for identification, it requires the DNA of good quality, e.g. DNA integrity and the absence of PCR inhibitors. Moreover its process relies on a specific expertise. Thus the chemical fingerprint analysis as in this study which is less complex process than DNA fingerprint is more convenient for botanical identification.

4 Development of authentication models

The results of the previous section indicated that many plants species were substituted and used as Chan-thet, Chan-khao, Chan-chamot, Chan-thana and Chan-hom. Therefore reliable method for routine work is necessary to authenticate the samples in real application. IR coupled with chemometric methods was selected as the analysis method because it was simple, fast and used less chemical. The IR range of 1801-501 cm^{-1} was divided into two ranges. The first range was 1801-1500 cm^{-1} that was the information of functional groups of aldehyde, ketone, ester and acid, and olefinic functional groups of alkene and aromatic. The second range was 1498-501 cm^{-1} that was the characteristic region. The authentication models were established to identify the samples as either *Santalum*, *T. hoaensis* or *M. gagei*. SIMCA and PLS-DA were the applied chemometric methods. These techniques were supervised methods which were the continuous analysis methods after the unsupervised methods, i.e. PCA and PLS, respectively. The establishment process and the application of the models are described as follows.

4.1 Sample preparation

From the identification of Chan(s) in previous sections, all Chan(s) samples could be classified into four groups (Table 31). The first group consisted of all Chan-thet samples, some Chan-hom samples, and one Chan-khao sample that were identified as *Santalum*. Since three *Santalum* species (*S. album*, *S. spicatum* and *S. lanceolatum*) were commercially substituted in traditional drugstores and their discrimination using IR was quite difficult, then they were grouped into the same group. The second group consisted of most of Chan-khao and Chan-thana samples that were identified as *T. hoaensis*. The third group consisted of all Chan-chamot samples that were identified as *M. gagei*. The last group consisted of other samples that were unidentified.

Table 31 The group of different species of Chan(s).

Name	Sample in each groups*
<i>Santalum</i> group	T1-T15, H2-H9, K18, SS, SA and SL
MG group	M1-M17, H10, H11 and MG
TH group	K1-K17, TN2- TN6, TN9, TN10 and TH
Unidentified group	H1, TN1, TN7 and TN8

* T1-T15 = Chan-thet samples, K1-K18 = Chan-khao samples, M1-M17 = Chan-chamot samples, TN1-TN10 = Chan-thana samples, H1-H11 = Chan-hom samples, SS = *S. spicatum*, SA = *S. album*, SL = *S. lanceolatum*, MG = *M. gagei* and TH = *T. hoaensis*.

The suitable sample preparation was investigated. It must be able to discriminate the samples into their correct groups. PCA was used to choose the suitable solvent extract. IR spectra of all crude drugs and authentic samples were analyzed by PCA method. The result indicated that the acetone extract gave the clearest discrimination among all sample group (Figure 55). Therefore the acetone extract was selected for further examination.

The loading plot of PC1 and PC2 of the acetone extract (Figure 56) suggested that the wavenumbers at 1737 and 1708 cm^{-1} affected to the classification of *T. hoaensis* samples. The wavenumber which had the most effect on classification of *M. gagei* samples was 1598 cm^{-1} . For classification of *Santalum*, the wavenumber 1006 cm^{-1} had the most effect. Therefore the authentication models of each Chan(s) should cover these wavenumbers. The models were performed from the data of three IR ranges, i.e. 1801-501, 1801-1500 and 1498-501 cm^{-1} .

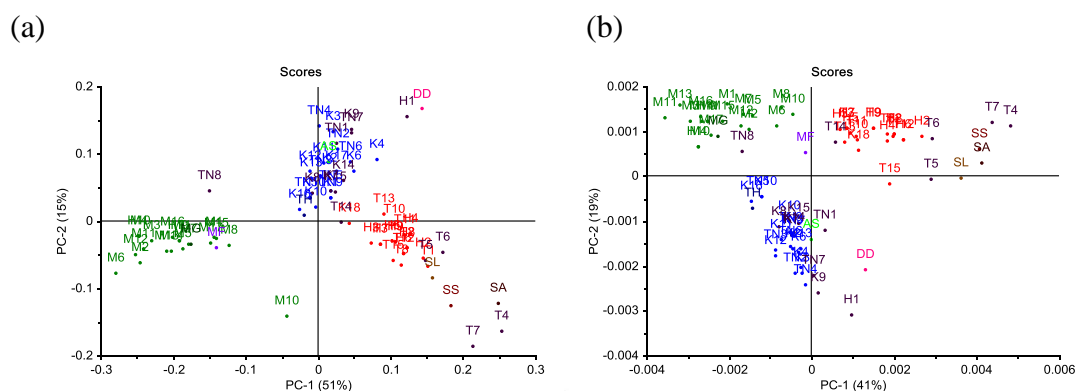


Figure 55 PC1 and PC2 score plots of the (a) normalized and (b) second derivative IR spectra of the acetone extract of Chan-thet samples (T1-T15), Chan-khao samples (K1-K18), Chan-chamot samples (M1-M17), Chan-thana samples (TN1-TN10), Chan-hom samples (H1-H11), *S. album* (SA), *S. spicatum* (SS), *S. lanceolatum* (SL), *M. fragrans* (MF), *T. hoensis* (TH), *D. decandra* (DD), *M. gagei* (MG) and *A. silvestris* (AS).

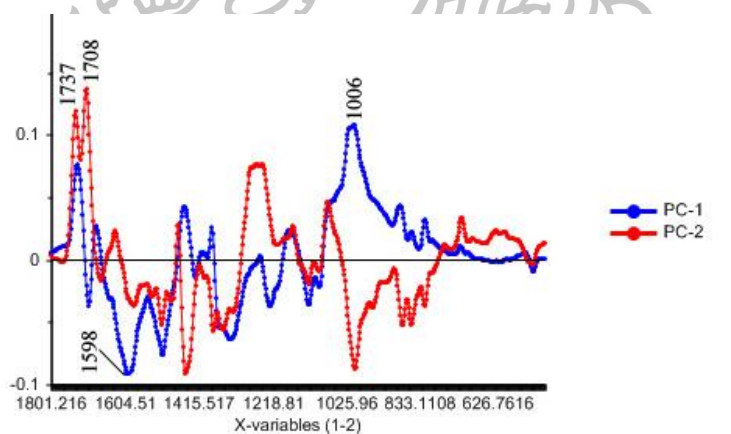


Figure 56 PC1 and PC2 loading plots of the normalized IR spectra of the acetone extracts of Chan-thet, Chan-khao, Chan-chamot, Chan-thana, and Chan-hom samples, *S. album*, *S. spicatum*, *S. lanceolatum*, *M. fragrans*, *T. hoensis*, *D. decandra*, *M. gagei* and *A. silvestris*.

To gain the harmonious group of each sample, outlier exclusion was important. The hotelling T^2 with 1% of confidence was used to consider for the outlier. Each sample group in Table 31 was analyzed by PCA. The hotelling T^2 limit of each group using both normalized IR and second derivative IR spectra are shown in Figure 57. The sample which was outside the circle of hotelling T^2 limit was considered as outlier and was not used to perform the models.

Outlier was not found in *Santalum* and TH groups. Normalized IR spectra of sample M10 was considered as outlier of MG group. Thus M10 was excluded from the normalized IR spectra data set of MG group. Afterward, the harmonious samples (sample size = 79) were randomly selected as training set (60%) and test set (40%). As previous recommendation in references [32, 153, 175, 177, 192, 193], sample size was 54-480, 60-83% of them should be used as training set. Thus the 60% for training set in this study was sufficient to examine. The training set and test set of the normalized IR and second derivative IR spectra are shown in Tables 32 and 33, respectively.

The models were also tested with the other fifteen blind samples. They were three *S. spicatum*, four *T. hoaensis*, three *M. gagei* and five other unidentified samples (Table 34). Their IR spectra were collected at different time period from those of the training set and the test set. Then applying of the establish models on these samples was considered as the used of models in common situation.

Table 32 Training set and test set of the normalized IR spectra of *Santalum* group, MG group and TH group.

No.	<i>Santalum</i> group		MG group		TH group	
	Training set	Test set	Training set	Test set	Training set	Test set
1	SS	T2	MG	M6	TH	K5
2	SA	T3	M1	M7	K1	K7
3	SL	T9	M2	M8	K2	K9
4	T1	T10	M4	M9	K3	K11
5	T4	T12	M3	M14	K4	K12
6	T5	T13	M5	M15	K6	TN2
7	T6	T14	M11	H10	K8	TN3
8	T7	H7	M12		K10	TN5
9	T8	T11	M13		K13	TN6
10	T15	H4	M16		K14	K17
11	H2		M17		K15	
12	H3		H11		K16	
13	H5				TN4	
14	H6				TN9	
15	H8				TN10	
16	H9					
17	K18					
Total	27		19		25	

* T = Chan-thet samples, K = Chan-khao samples, M = Chan-chamot samples, TN = Chan-thana samples, H = Chan-hom samples, SS = *S. spicatum*, SA = *S. album*, SL = *S. lanceolatum*, MG = *M. gagei* and TH = *T. hoaensis*.

Table 33 Training set and test set of the second derivative IR spectra of *Santalum* group, MG group and TH group.

No.	<i>Santalum</i> group		MG group		TH group	
	Training set	Test set	Training set	Test set	Training set	Test set
1	SS	T2	MG	M3	TH	K1
2	SA	T6	M1	M5	K2	K3
3	SL	T7	M2	M13	K4	K7
4	T1	T12	M7	M17	K5	K9
5	T3	T13	M8	H10	K8	K11
6	T5	H4	M9	H11	K10	K13
7	T8	H7	M10	M11	K12	K15
8	T9	H8	M12	M4	K14	TN2
9	T10	K18	M14		K17	TN5
10	T11	H9	M15		TN3	K16
11	T14		M16		TN4	
12	T15		M6		TN6	
13	H2				K6	
14	H3				TN9	
15	H5				TN10	
16	H6					
17	T4					
total	27		20		25	

* T = Chan-thet samples, K = Chan-khao samples, M = Chan-chamot samples, TN1 = Chan-thana samples, H1 = Chan-hom samples, SS = *S. spicatum*, SA = *S. album*, SL = *S. lanceolatum*, MG = *M. gagei* and TH = *T. hoaensis*.

Table 34 Identification of blind samples.

Blind sample	Identification
UN1	<i>S. spicatum</i>
UN2	Unidentified
UN3	<i>M. gagei</i>
UN4	Unidentified
UN5	<i>T. hoaensis</i>
UN6	Unidentified
UN7	<i>M. gagei</i>
UN8	<i>S. spicatum</i>
UN9	<i>T. hoaensis</i>
UN10	<i>T. hoaensis</i>
UN11	Unidentified
UN12	<i>M. gagei</i>
UN13	<i>S. spicatum</i>
UN14	<i>T. hoaensis</i>
UN15	Unidentified

4.2 Soft independent modeling of class analogy (SIMCA)

The training set was applied to establish the calibration models by using PCA. Eighteen PCA models were established based on two preprocessing methods and three IR ranges for three sample groups (*Santalum*, *M. gagei* and *T. hoaensis*) as shown in Table 35. The optimum principal components (PC) were automatically selected by the software. The explained variance percentages of all models were more than 80%. SIMCA classifications for the correct sample groups were performed on the basis of these PCA models. Eighteen PCA models were categorized to six SIMCA methods.

The models were challenged by the test set and the blind samples. The authentic samples of *M. fragrans*, *D. decandra* and *A. silvestris* were also included to test the models. The results of SIMCA classifications are shown in Table 36. It indicated that almost all of the samples were correctly matching with their correct groups.

Table 35 PCA models for the authentication of *Santalum*, TH and MG groups.

PCA model	Group type	Preprocessing technique	Range of wavenumber	Number of PC	Explained variance (%)		SIMCA method
					Calibration	Cross validation	
1	<i>Santalum</i>	Normalization	1801-501	12	99.71	91.23	1
2	MG	Normalization	1801-501	10	99.75	81.95	
3	TH	Normalization	1801-501	9	99.24	89.52	
4	<i>Santalum</i>	Normalization	1801-1500	7	98.85	94.08	2
5	MG	Normalization	1801-1500	7	99.57	95.34	
6	TH	Normalization	1801-1500	5	98.99	95.91	
7	<i>Santalum</i>	Normalization	1498-501	11	99.66	92.92	3
8	MG	Normalization	1498-501	7	98.30	81.89	
9	TH	Normalization	1498-501	9	99.35	89.85	
10	<i>Santalum</i>	Normalization + 2 nd derivative	1801-501	12	99.83	88.80	4
11	MG	Normalization + 2 nd derivative	1801-501	10	99.84	81.40	
12	TH	Normalization + 2 nd derivative	1801-501	12	99.88	85.01	
13	<i>Santalum</i>	Normalization + 2 nd derivative	1801-1500	10	99.83	95.64	5
14	MG	Normalization + 2 nd derivative	1801-1500	7	99.09	89.97	
15	TH	Normalization + 2 nd derivative	1801-1500	10	99.80	93.13	
16	<i>Santalum</i>	Normalization + 2 nd derivative	1498-501	8	98.79	86.86	6
17	MG	Normalization + 2 nd derivative	1498-501	10	99.87	81.36	
18	TH	Normalization + 2 nd derivative	1498-501	12	99.89	85.05	

Table 36 Classification of test samples and blind samples using SIMCA.

Test set	Group	SIMCA 1			SIMCA 2			SIMCA 3		
		Group			Group			Group		
		<i>Santalum</i>	MG	TH	<i>Santalum</i>	MG	TH	<i>Santalum</i>	MG	TH
T2	<i>Santalum</i>	/			/			/		
T3	<i>Santalum</i>	/			/			/		
T9	<i>Santalum</i>	/			/			/		
T10	<i>Santalum</i>	/			/			/		
T11	<i>Santalum</i>	/			/			/		
T12	<i>Santalum</i>	/			/			/		
T13	<i>Santalum</i>	/			/			/		
H4	<i>Santalum</i>	/			/			/		
H7	<i>Santalum</i>	/			/			/		
T14	<i>Santalum</i>	/			/			/		
M6	MG		/						/	
M7	MG		/						/	
M8	MG		/						/	
M9	MG		/						/	
M14	MG		/						/	
M15	MG		/						/	
H10	MG		/						/	
K5	TH			/			/			/
K11	TH			/			/			/
K12	TH			/			/			/
K17	TH			/			/			/
TN2	TH			/			/			/
TN3	TH			/			/			/
TN5	TH			/			/			/
TN6	TH			/			/			/
K7	TH			/			/			/
K9	TH			/			/			/
MF	<i>M. fragrans</i>									
AS	<i>A. silvestris</i>									
DD	<i>D. decandra</i>									
UN1	<i>Santalum</i>									
UN2	Unidentified									
UN3	MG		/						/	
UN4	Unidentified									
UN5	TH						/			/
UN6	Unidentified									
UN7	MG									
UN8	<i>Santalum</i>									
UN9	TH			/						/
UN10	TH			/			/			/
UN11	Unidentified									
UN12	MG		/			/			/	
UN13	<i>Santalum</i>				/			/		
UN14	TH						/			
UN15	Unidentified						/			

Table 36 Classification of test samples and blind samples using SIMCA (continued).

Test set	Group	SIMCA 4			SIMCA 5			SIMCA 6		
		Group			Group			Group		
		<i>Santalum</i>	MG	TH	<i>Santalum</i>	MG	TH	<i>Santalum</i>	MG	TH
T2	<i>Santalum</i>				/			/		
T12	<i>Santalum</i>	/			/			/		
T13	<i>Santalum</i>	/			/			/		
H4	<i>Santalum</i>	/			/			/		
H7	<i>Santalum</i>	/			/			/		
H8	<i>Santalum</i>				/			/		
H9	<i>Santalum</i>	/			/			/		
K18	<i>Santalum</i>	/			/			/		
T6	<i>Santalum</i>	/			/			/		
T7	<i>Santalum</i>							/		
M3	MG		/			/			/	
M4	MG		/			/				
M5	MG		/			/				
M11	MG		/			/			/	
M13	MG		/			/			/	
M17	MG		/			/			/	
H10	MG		/			/			/	
H11	MG		/			/			/	
K1	TH			/			/			/
K3	TH			/			/			/
K11	TH			/			/			/
K13	TH			/			/			/
K16	TH			/			/			/
TN2	TH			/			/			/
TN5	TH			/			/			/
K7	TH			/			/			/
K9	TH			/			/			/
K15	TH			/			/			/
MF	<i>M. fragrans</i>									
AS	<i>A. silvestris</i>									
DD	<i>D. decandra</i>									
UN1	<i>Santalum</i>	/			/	/			/	
UN2	Unidentified	/							/	
UN3	MG		/			/			/	
UN4	Unidentified	/							/	
UN5	TH									/
UN6	Unidentified		/		/	/			/	
UN7	MG		/			/			/	
UN8	<i>Santalum</i>									
UN9	TH			/						/
UN10	TH			/			/			/
UN11	Unidentified						/			
UN12	MG		/			/			/	
UN13	<i>Santalum</i>	/			/					
UN14	TH									
UN15	Unidentified				/				/	

Efficiency of each SIMCA was evaluated and the results were presented as accuracy, sensitivity and specificity (Table 37). Evaluation using the test set showed that all SIMCA methods gave more than 80% accuracy, more than 80% sensitivity and 100% specificity. The model using normalized IR data in the range of 1801-501 cm^{-1} (SIMCA 1) gave the best accuracy (100%), better than the models using separated ranges of functional groups (1801-1500 cm^{-1} , SIMCA 2) and fingerprint (1498-501 cm^{-1} , SIMCA 3). However the model using second derivative IR data gave no significantly different efficiency between the IR range of 1801-501 cm^{-1} (SIMCA 4) and the models using separated ranges (SIMCA 5 and SIMCA 6). Therefore importance of the IR data ranges of the functional groups and fingerprint could not be concluded.

Table 37 Percentage of accuracy, sensitivity and specificity of test set and blind samples classification using SIMCA.

Method	Test set			Blind samples		
	Accuracy (%)	Sensitivity (%)	Specificity (%)	Accuracy (%)	Sensitivity (%)	Specificity (%)
SIMCA 1	100	100	100	60	40	100
SIMCA 2	93	93	100	60	60	60
SIMCA 3	97	96	100	80	70	100
SIMCA 4	84	82	100	53	60	40
SIMCA 5	90	89	100	33	50	0
SIMCA 6	94	93	100	47	60	20

Comparing with the test set, evaluation of all SIMCA methods with blind samples gave lower efficiency (Table 36). It might be because of the variation of IR spectra collected from different time period. Moreover more noise in the spectra might be enlarged by the second derivative and caused the significant lower efficiency of SIMCA 4-6. SIMCA 3 had the highest efficiency. It used the PCA models of normalized IR spectra in the range of 1498-501 cm^{-1} . This result suggested that the fingerprint region was the most significant for the authentication.

SIMCA 3 gave 80% accuracy for the prediction of the blind samples, thus it was interesting to study in more detail. Cooman's plot was the graphical plot of sample distances between two models. Figure 58 are shown the classification of the blind samples distances between the models of *Santalum* and MG groups, *Santalum* and TH groups, and MG and TH groups. The classification between *Santalum* and MG groups gave 60% accuracy. Two-thirds of the blind *M. gagei* samples (UN3 and 7) and *Santalum* samples (UN1 and 13) were correctly predicted. One blind *M. gagei* sample (UN12) and one blind *Santalum* sample (UN8) were located at the left-below and right-upper quadrants of Figure 58(a), respectively. Therefore the models misclassified UN12 as either *Santalum* or MG groups, and UN8 as neither *Santalum* nor MG groups. Among the blind unidentified samples, only UN11 was correctly predicted. Three blind unidentified samples, i.e. UN2, 6 and 15, were classified as *Santalum* and the other one (UN4) was classified as MG group. In the left-upper quadrant, five samples were predicted into *Santalum* group but only two samples (UN1 and 13) were correct. Thus the error of this classification (40%) was influenced by the prediction of *Santalum* and unidentified groups.

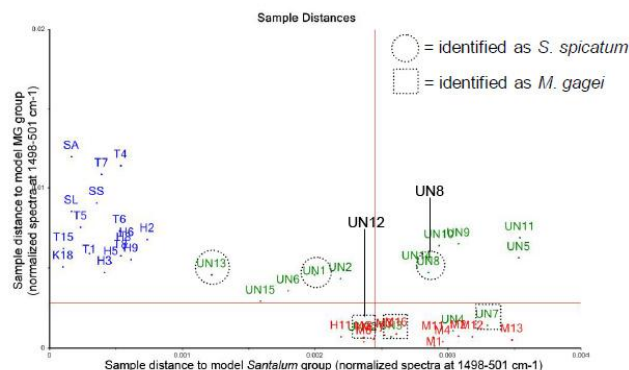
In Figure 58(b), the classification between *Santalum* and TH groups gave 67% accuracy. All blind *T. hoagensis* samples (UN5, 9, 10 and 14) were correctly predicted. In contrast, six blind samples were predicted as *Santalum* group but in reality, only two samples (UN1 and 13) were correct. Therefore the major misclassification was the prediction of the other blind samples (UN 2, 6, 12 and 15) as *Santalum* group.

For discrimination between MG and TH groups (Figure 58(c)), all blind *M. gagei* samples (UN3, 7 and 12) and blind *T. hoagensis* samples (UN5, 9, 10 and 14) were correctly predicted. Only one unidentified sample (UN4) was misclassified. Therefore the classification of the blind samples using graphical plot of sample distance between *M. gagei* and *T. hoagensis* was 93% correct.

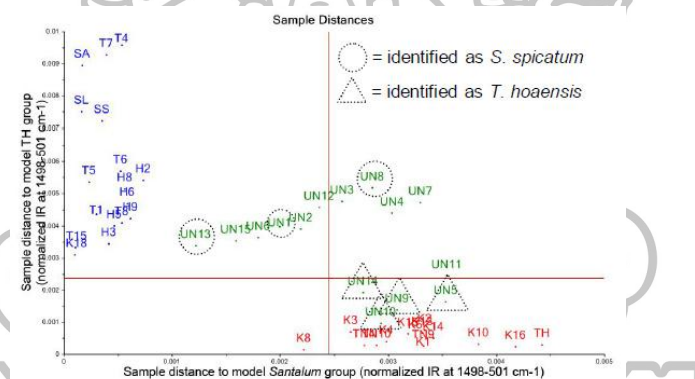
In overall, some blind unidentified samples, i.e. UN2, 4, 6 and 15 were classified into *Santalum* or *M. gagei* groups. It suggested that their IR spectra might be not much different from *Santalum* and *M. gagei*. Moreover the main error was influenced by the *Santalum* model. Since it was constructed from three species of

Santalum, then it had high variation. More samples should be used to construct a more reliable model in future.

(a) *Santalum* group vs MG group



(b) *Santalum* group vs TH group



(c) MG group vs TH group

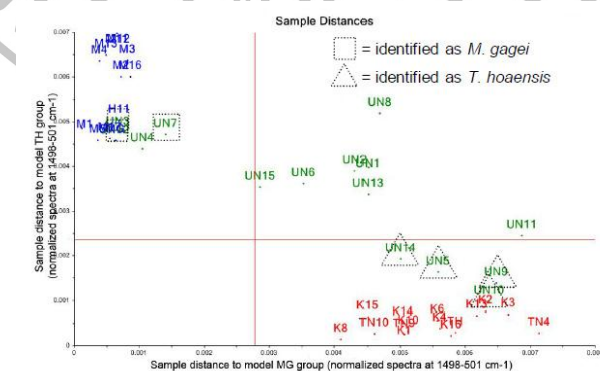


Figure 58 Authentication of the blind samples (green mark) using SIMCA 3; (a) sample distance between *Santalum* group (blue mark) and MG group (red mark), (b) sample distance between *Santalum* group (blue mark) and TH group (red mark), and (c) sample distance between MG group and (blue mark) and TH group (red mark).

4.3 Partial least squares-discriminant analysis (PLS-DA)

The other method for the authentication of Chan(s) was PLS-DA. This method was originated by construction the models based on PLS (unsupervised method). As same as SIMCA, the training set (Tables 32 and 33) was used to construct the calibration models. Then prediction efficiency of these models was evaluated by the test set and the blind samples (Tables 32-34). This method was used to predict the samples by discrimination the samples into one class or another. The predictors were compared with the reference to classify them. The reference numbers were determined as 0 and 1 which were referred to the members of two classes. In this study, three groups, i.e. *Santalum* group, MG group and TH group were investigated. The interesting group was assigned as number 1, then another group as number 0.

Six PLS classification models are shown in Table 38 and shown as the plots between the regression coefficient and wavenumber in Figure 154-159. The optimum number of the factors of PLS models 1-6 were 4, 6, 5, 3, 4 and 3, respectively. They were automatically selected by the software. The explained were 84-95%. The linearities of all models were presented as R^2 and they were 0.77-0.95. It suggested that the correct prediction results were obtained by using these models. All models possessed low RMSECV (0.1-0.2). It meant that these models possessed good prediction ability.

Table 38 Linearity (R^2), root mean square error of cross validation (RMSECV) and optimum factors of PLS model 1-6.

PLS model	Group type*	Preprocessing technique	Range of wavenumber	Number of factor	R^2	RMSECV	Explained variance (%)
1	<i>Santalum</i>	Normalization	1801-501	4	0.9412	0.1208	94.68
	MG	Normalization	1801-501	4	0.9500	0.1019	94.68
	TH	Normalization	1801-501	4	0.9499	0.1086	94.68
2	<i>Santalum</i>	Normalization	1801-1500	6	0.8691	0.1802	85.62
	MG	Normalization	1801-1500	6	0.9371	0.1143	85.62
	TH	Normalization	1801-1500	6	0.7710	0.2321	85.62
3	<i>Santalum</i>	Normalization	1498-501	5	0.9392	0.1228	94.45
	MG	Normalization	1498-501	5	0.9535	0.0983	94.45
	TH	Normalization	1498-501	5	0.9421	0.1167	94.45
4	<i>Santalum</i>	Normalization + 2 nd derivative	1801-501	3	0.8969	0.1600	91.62
	MG	Normalization + 2 nd derivative	1801-501	3	0.9198	0.1290	91.62
	TH	Normalization + 2 nd derivative	1801-501	3	0.9334	0.1252	91.62
5	<i>Santalum</i>	Normalization + 2 nd derivative	1801-1500	4	0.8239	0.2091	84.00
	MG	Normalization + 2 nd derivative	1801-1500	4	0.9107	0.1362	84.00
	TH	Normalization + 2 nd derivative	1801-1500	4	0.7947	0.2198	84.00
6	<i>Santalum</i>	Normalization + 2 nd derivative	1498-501	3	0.8875	0.1671	90.91
	MG	Normalization + 2 nd derivative	1498-501	3	0.9038	0.1414	90.91
	TH	Normalization + 2 nd derivative	1498-501	3	0.9365	0.1222	90.91

*MG = *M. gagei* and TH = *T. hoensis*

Before evaluate the efficiency of the constructed PLS-DA models with tested samples, the prediction range should be determined by the application of cutoff value. The cutoff value was calculated from the leave-one out cross validation of each model and calculated for the RMSECV, the minimum difference and maximum difference of predicted values from the reference values. Then sum of their absolute values were average. The cutoff range was the differences from the number 1 (reference value). The prediction value within the cutoff range was considered as the member of that model [166]. The cutoff values and cutoff ranges of each model are shown in Table 39.

All PLS-DA models were tested with the test set and the blind samples. The results of test set (Figure 160-165) showed the correct trend of the prediction because the prediction of each sample showed the correct members of each

group. For example, PLS-DA method 4 (Figure 163(a)) showed that the response of samples T2, T6, T7, T12, T13, H4, H7, H8, H9 and K18 (members of *Santalum* group, see Table 33) were close to “1”, whereas the response of the other samples were close to “0”. It meant that these samples might be identified as *Santalum* group and the other samples were not the members of this group. However the absolutely correct prediction was determined by comparing the prediction values with the cutoff range of each model. The overall classification results of both test set and blind samples were concluded in Table 40

Table 39 Cutoff values and cutoff ranges of PLS-DA methods 1-6 of *Santalum* group, MG group and TH group.

PLS model	Reference group	Cutoff values	Cutoff range
1	<i>Santalum</i> group	0.2341	0.7659-1.2341
	MG group	0.1698	0.8302-1.1698
	TH group	0.1547	0.8453-1.1547
2	<i>Santalum</i> group	0.2773	0.7227-1.2773
	MG group	0.2023	0.7977-1.2023
	TH group	0.3154	0.6846-1.3154
3	<i>Santalum</i> group	0.2086	0.7914-1.2086
	MG group	0.1546	0.8454-1.1546
	TH group	0.1652	0.8348-1.1652
4	<i>Santalum</i> group	0.3227	0.6773-1.3227
	MG group	0.1713	0.8287-1.1713
	TH group	0.2118	0.7882-1.2118
5	<i>Santalum</i> group	0.33774	0.6623-1.3377
	MG group	0.1592	0.8408-1.1592
	TH group	0.3576	0.6424-1.3576
6	<i>Santalum</i> group	0.3592	0.6408-1.3592
	MG group	0.2158	0.7842-1.2158
	TH group	0.1851	0.8149-1.1851

Prediction efficiency of the models was evaluated by accuracy, sensitivity and specificity (Table 41). The overall results using the test set showed that efficiency of all models did not much differ from each other. But the evaluation with the blind samples indicated that model PLS-DA 4 had the best efficiency in all accuracy, sensitivity and sensitivity. Therefore both function and fingerprint IR regions ($1801\text{-}501\text{ cm}^{-1}$) were important for PLS-DA prediction. The second derivative preprocessing might improve the quality of IR spectra, thus the efficiency of prediction was higher than the normalization preprocessing.

Table 41 Percentage of accuracy, sensitivity and specificity of test set and blind samples classification using PLS-DA.

	Test set			Blind samples		
	Accuracy (%)	Sensitivity (%)	Specificity (%)	Accuracy (%)	Sensitivity (%)	Specificity (%)
PLS-DA 1	80	78	100	73	80	60
PLS-DA 2	90	93	67	53	50	60
PLS-DA 3	77	78	67	73	70	80
PLS-DA 4	87	89	67	87	80	100
PLS-DA 5	77	82	33	33	60	40
PLS-DA 6	81	82	67	53	60	40

Focusing on PLS-DA 4, it gave the best prediction for MG group because its RMSEP (0.0823) was the lowest. The RMSEP of *Santalum* and TH group were 0.1345 and 0.1227, respectively. The evaluation results using the test set and the blind samples were not much different. In contrast with the SIMCA, they were greatly different. Therefore PLS-DA was more precise and was a better prediction method than SIMCA in common situation.

PLS-DA provided better the overall results than SIMCA, which corresponded with published reports [154, 194-196]. The best SIMCA method was obtained from the normalized IR spectra in the range of $1498\text{-}501\text{ cm}^{-1}$. It suggested that SIMCA might not require second derivative preprocessing for a good prediction.

PCA that was used as the model of SIMCA focused on accounting of spectral information and variation of the member within the class [154,196]. This might be the reason that SIMCA method did not need the second derivative preprocessing and the fingerprint region was significant. The best PLS-DA method was obtained from the second derivative IR spectra in the range of 1801-501 cm^{-1} . It suggested that the second derivative preprocessing might be important technique for a good prediction using PLS-DA. The IR spectra of each member of the classes had the variation. The second derivative technique could reduce the noise, offset and slope of the spectra. Therefore this technique could remove variation of IR spectra and highlight the true spectral difference [196]. This confirmed that the second derivative preprocessing was important for PLS-DA.

PLS-DA might be a suitable method for IR data because the performance of PLS-DA depended on characteristic of samples [194]. Moreover the wavenumbers related to the classification group were firstly abstracted and constructed as a regression equation. Thereafter importance of each wavenumber was considered and assigned for regression coefficient. The high regression coefficient value will be assigned for the important variable. In general, noise was excluded in the first step or assigned as a non-important variable in the second step. Then variation of non-important wavenumbers during IR collection of the test set and the blind samples in different time period and noise were not much affect the efficiency of the PLS-DA method. In this study, classification using PLS-DA gave better reproducibility than SIMCA because the character of IR data was consecutive.

CHAPTER V

CONCLUSIONS

Five crude drugs whose names possess the word “Chan” as prefix, i.e. Chan-thet, Chan-khao, Chan-chamot, Chan-thana and Chan-hom, are popularly used in Thai traditional medicine. They are heartwood and their characters are quite similar. Moreover their vernacular names are very complex. Therefore confusion and substitution of these crude drugs might be easily happen. The objective of this study was to identify the botanical species of these crude drug samples currently available in Thai traditional drugstores. Moreover the authentication models for future routine work were also established.

Several samples were collected from various regions of Thailand. According to the marker approach, identification of each crude drug was accomplished by TLC and GC. Three pure compounds isolated in laboratory, i.e. α -santalol, mansonone G and geniposidic acid, were used as the chemical markers. Based on the pattern approach, their chromatographic patterns and also IR spectra were compared with those of the authentic samples. Chemometric methods, i.e. similarity analysis (SA), hierarchical cluster analysis (HCA) and principal component analysis (PCA), were applied for data analysis. Chemical constituents of some crude drugs were also confirmed and compared with authentic samples by using GC/MS technique.

The identification results concluded that all crude drugs could be classified into three groups:

1. Chan-thet and Chan-hom: Most of Chan-thet and Chan-hom samples were *S. spicatum*. Some Chan-thet samples were *S. album* and *S. lanceolatum*. *S. album* is the highest quality sandalwood among *Santalum* species. Nowadays most of sandalwood used in Thailand is imported from Australia. Then it was undoubt that crude drugs found in Thai traditional drugstore were *S. spicatum*. Besides *S. spicatum*, some samples of Chan-hom were *M. gagei*.

2. Chan-khao and Chan-thana: Most of Chan-khao and Chan-thana samples were *Tarenna hoensis*. One sample of Chan-khao was *S. spicatum*. However rather high numbers of Chan-khao and Chan-thana samples were unidentified and they were more than one unidentified species. This finding indicated that quality of these two crude drugs should be much concerned.

3. Chan-chamot: All Chan-chamot samples were *M. gagei*.

Considering on the identification technique, each technique has its own advantage and disadvantage. TLC is a basic experiment method but it needs expertise to succeed and long processing time. In this study, TLC gave satisfy results, but only the identification of *Santalum* species was obscure. It was because the chemical constituents among *Santalum* species were not much different. The main difference was their contents. IR is rapid, low applied solvent volume and inexpensive. Based on IR coupled with chemometric methods (SA, HCA and PCA), the second derivative could improve the analysis results.

SA was quite not a good method for the identification of this study, since IR spectrum was the data of functional groups founded in the samples. One sample consisted of many compounds that might have same functional groups and also found in other samples or authentic samples. Therefore IR bands of similar compounds in each sample might appear and effect to analysis using Pearson's correlation coefficient. Moreover noise could easily cause the dissimilarity and it was enlarged by the secondary derivation preprocessing. Generally, SA often applied for chromatographic data [143, 189].

Solvent selection for the preparation of the extracts was important for data analysis using HCA and PCA. The extracts prepared from semi-polar solvents might be not good for the identification because they could not differentiate among various authentic samples. The slightly high polar solvents gave the good results for the identification of *T. hoensis* and *M. gagei*, whereas the non-polar solvent was suitable for the identification of *Santalum* sp. The water extracts gave no specific results for the identification of any samples because their major constituents might be saccharides commonly found in all samples.

PCA gave clearer identification than HCA because it could abstract only the important data and presented as the first two or three PCs. Comparing between three chemometric methods based on IR data, PCA was the clearest identification, and HCA was clearer than SA.

GC gave two kinds of data. The first data was chemical constituents that obtained from mass spectrophotometer (MS) detector. The second data was fingerprint that could be further analyzed by chemometric methods. However the drawback of GC/MS was specific application on only the volatile samples. Therefore in this study, only the *Santalum* samples could be analysed by this technique. GC fingerprint coupled with PCA was the technique that could obviously discriminate among the different species of *Santalum*, whereas SA and HCA were still ambiguous.

Models for discrimination among *M. gagei*, *T. hoaensis* and *Santalum* samples in routine work based on the IR data were established. Two techniques used in this study were soft independent modeling of class analogy (SIMCA) and partial least squares-discriminant analysis (PLS-DA). The satisfy prediction model for SIMCA was the model obtained from the normalized IR spectra in the range of 1498-501 cm^{-1} . It possessed 97% accuracy for the validation prediction and 80% accuracy for the prediction in common situation. The clearest discrimination was the prediction between *M. gagei* and *T. hoaensis*. The satisfy prediction model of PLS-DA was the model obtained from the second derivative IR spectra in the range of 1801-501 cm^{-1} . Accuracy of both prediction of validation and prediction in common situation were 87%. This indicated that PLS-DA was more precise than SIMCA.

This study found that there were three species of *Santalum* available in Thai traditional drugstores. However the sample size of each species was limit. Then all three *Santalum* were combined and only one model was established. The models of each species of *Santalum* were interesting to develop in the future.

REFERENCES

1. คณะกรรมการพัฒนาระบบยาแห่งชาติ. บัญชียาหลักแห่งชาติ พ.ศ. 2555. นนทบุรี: ม.ป.ท.; 2555.
2. ชยันต์ พิเชียรสุนทร, แม้นมาส ชวลิต และ วิเชียร จีรวงส์. คำอธิบายตำราพระโอสถพระนารายณ์ ฉบับเฉลิมพระเกียรติ 72 พรรษามหाराชา 5 ธันวาคม พุทธศักราช 2542. กรุงเทพฯ: อมรินทร์และมูลนิธิภูมิปัญญา; 2544.
3. วุฒิ วุฒิธรรมเวช. เครื่องยาไทย 1. ม.ป.ท.: ศิลป์สยามบรรจุกัญจน์และการพิมพ์; 2552.
4. สวณพฤษศาสตร์ภาคตะวันออก (เขานินซอน) งานสวณพฤษศาสตร์ศูนย์การศึกษาการพัฒนา เขานินซอนอันเนื่องมาจากพระราชดำริ. พิษสมุนไพรรักษาปัสมุนไพรรักษาเขานินซอน ฉบับสมบูรณ์. ฉะเชิงเทรา: ม.ป.ท.; 2550.
5. นพมาศ สุนทรเจริญนนท์, นงลักษณ์ เรื่องวิเศษ. คุณภาพเครื่องยาไทยจากงานวิจัยสู่การพัฒนา อย่างยั่งยืน. กรุงเทพฯ: สำนักงานคณะกรรมการวิจัยแห่งชาติ; 2551.
6. ชยันต์ พิเชียรสุนทร, วิเชียร จีรวงส์. คู่มือเภสัชกรรมแผนไทย เล่ม 2 เครื่องยาพฤษวัตถุ. กรุงเทพฯ: อมรินทร์; 2545.
7. พรศักดิ์ มีแก้ว. การทดลองปลูกไม้หอมแก่นจันทน์ (*Santalum album* Linn.). ใน งานสัมมนา ทางวนวัฒนวิทยา ครั้งที่ 8 “เทคโนโลยีวนวัฒนเพื่อขจัดความยากจน”. มหาวิทยาลัยเกษตรศาสตร์. กรุงเทพฯ; 2545. หน้า 172-9.
8. สำนักงานหอพรรณไม้ สำนักวิจัยการอนุรักษ์ป่าไม้และพันธุ์พืช กรมอุทยานแห่งชาติสัตว์ป่าและพันธุ์พืช กระทรวงทรัพยากรธรรมชาติและสิ่งแวดล้อม. ชื่อพรรณไม้แห่งประเทศไทย เต็ม สมิตินันท์ ฉบับแก้ไขเพิ่มเติม พ.ศ. 2557. กรุงเทพฯ: สำนักงานพระพุทธศาสนาแห่งชาติ; 2557.
9. วิชาญ เอียดทอง. มารูจักไม้จันทน์กับธรรมเนียมพระบรมศพและพระศพเจ้านาย. วารสารการ จัดการป่าไม้ 2551;2(4):29-45.
10. สุภาพร ผลจันทร์. ข้อกำหนดมาตรฐานเครื่องยาสมุนไพรรักษาโรค จันทน์แดง จันทน์ขาว และจันทน์ผา [วิทยานิพนธ์ปริญญาโท สาขาเภสัชเคมีและผลิตภัณฑ์ธรรมชาติ]. ขอนแก่น: มหาวิทยาลัยขอนแก่น; 2552.

11. คณะกรรมการคุ้มครองและส่งเสริมภูมิปัญญาการแพทย์แผนไทย. ตำราอ้างอิงยาสมุนไพรไทย เล่ม 1 เฉลิมพระเกียรติพระบาทสมเด็จพระเจ้าอยู่หัว เนื่องในมหามงคลสมัยที่ทรงครองสิริราชสมบัติครบ 60 ปี. กรุงเทพฯ: อมรินทร์พริ้นติ้งแอนด์พับลิชชิ่ง; 2551.
12. Brand JE, Fox JED, Pronk G, Cornwell C. Comparison of oil concentration and oil quality from *Santalum spicatum* and *S. album* plantation, 8-25 years old, with those from mature *S. spicatum* natural stands. Aust For 2007;70(4):235-41.
13. Tat TH. Forthcoming roving sandalwood workshop. Sandalwood Research Newsletter 1996;5:3.
14. Burgess P. Germplasm conservation of sandalwood. Sandalwood Research Newsletter, 1994;2:5.
15. IFS US. Sandalwood - scope for commercial propagation on community lands in India. Sandalwood Research Newsletter 1995;4:1-2.
16. Bristow M, Taylor D, Robson K. Queens sandalwood (*Santalum lanceolatum*) : regeneration following harvesting. Sandalwood Research Newsletter 2000;11:4-7.
17. Jones P. Sandalwood re-visited in Western Australia. Sandalwood Research Newsletter 2001;12:2-4.
18. Vernes T, Robson K. Indian sandalwood industry in Australia. Sandalwood Research Newsletter. 2002;16:1-3.
19. Clake M. Australia's sandalwood industry - An overview and analysis of research needs. Kingston: Rural Industries Research and Development Corporation 2006. Available from:<https://rirdc.infoservices.com.au/downloads/06-131.pdf>.
20. Kamboj A. Analytical evaluation of herbal drugs. in Vallisuta O, editor. Drug Discovery research in pharmacognosy. InTech. Available from:<http://www.intechopen.com/books/drug-discovery-research-in-pharmacognosy/analytical-evaluation-of-herbaldrugs>.
21. Kunle OF, Egharevba HO, Ahmadu PO. Standardization of herbal medicines - A review. Int J of Biodivers and Conserv 2012.;4(3):101-12.

22. Xie P, Chen S, Liang Y-z, Wang X, Tian R, Upton R. Chromatographic fingerprint analysis-a rational approach for quality assessment of traditional Chinese herbal medicine. *J Chromatogr A* 2006;1112:171-80.
23. Abdullah F, Ling SK, Man S, Tan AL, Tan HP, Abdullah Z. Characterization and identification of *Labisia pumila* by multi-steps infrared spectroscopy. *Vib Spectrosc* 2012;62:200-6.
24. Razmovski-Naumovski V, Tongkao-on W, Kimble B, Qiao VL, Beilun L, Li KM, et al. Multiple chromatographic and chemometric methods for quality standardisation of Chinese herbal medicines. *Tradit Chin Med Mater Med* 2010;12(1):99-106.
25. Tistaert C, Dejaegher B, Heyden YV. Chromatographic separation techniques and data handling methods for herbal fingerprints: A review. *Analytica Chimica Acta* 2011;690:148-61.
26. World Health Organization. Guidelines for the assesment of herbal medicines. Geneva; 1991.
27. Massart DL, Vandeginste BGM, Deming SN, Michotte Y, Kaufman L, editors. *Chemometrics : a text book*. New York: Elsevier science; 1988.
28. Brereton RG. *Chemometrics*. West Sussex: John Wiley & Sons; 2003.
29. Beebe KR, Pell RJ, Seasholtz MB, editors. *Chemometrics : a practical guide*. New York: John Wiley & Sons; 1998.
30. Gad H.A, El-Ahmady SH, Abou-Shoer M, Al-Azizi MM. Application of chemometrics in authentication of herbal medicines: A Review. *Phytochem Anal* 2013;24(1):1-24.
31. Gad HA, El-Ahmady SH, Abou-Shoer M, Al-Azizi MM. A modern approach to the authentication and quality assessment of thyme using uv spectroscopy and chemometric analysis. *Phytochem Anal* 2013;24:520-6.
32. Wong KH, Razmovski-Naumovski V, Li KM, Li GQ, Chan K. Differentiation of *Pueraria lobata* and *Pueraria thomsonii* using partial least square discriminant analysis (PLS-DA). *J Pharm Biomed Anal* 2013;84:5-13.
33. วุฒิ วุฒิธรรมเวช. คัมภีร์เภสัชรัตนโกสินทร์. กรุงเทพฯ: ศิลป์สยามบรรณกิจภัณฑ์และการพิมพ์; 2547.

34. เสี่ยม พงษ์บุญรอด. ไม้เทศเมืองไทย สรรพคุณของยาเทศและยาไทย. กรุงเทพฯ: โรงพิมพ์กรุงธน; 2522.
35. นิจศิริ เรืองรังษี, ธวัชชัย มังคละคุปต์. สมุนไพรไทย เล่ม 1. กรุงเทพฯ: บีเฮลท์ดี; 2547.
36. เอี่ยมพร วิสมหมาย, ปณิธาน แก้วดวงเทียน. ไม้ป่ายืนต้นของไทย 1. กรุงเทพฯ: เอชเอ็นกรุ๊ป; 2547.
37. ลีนา ผู้พัฒน์พงศ์. สมุนไพรไทย ตอนที่ 5. กรุงเทพฯ: ฝ่ายพฤกษศาสตร์ป่าไม้ กองบำรุง กรมป่าไม้; 2530.
38. ภาควิชาเภสัชพฤกษศาสตร์ คณะเภสัชศาสตร์ มหาวิทยาลัยมหิดล. สยามโกสัชยพฤกษ: ภูมิปัญญาของชาติ. กรุงเทพฯ: คณะเภสัชศาสตร์ มหาวิทยาลัยมหิดล; 2538.
39. ไชยศ ทีปกร จันทรพิทักษ์. ตำรับยาไทย. สงขลา: สิ้นไชยเภสัช; 2525.
40. ชมพร ไชยล้อม. ประมวลตำรับยาไทย. นนทบุรี: โสภณการพิมพ์; 2554.
41. Brand JE. Genotypic variation in *Santalum album*. Sandalwood Research Newsletter 1994;2:2-4.
42. Mckinnell FH. Status of management and silviculture research on sandalwood in western Australia and Indonesia. USDA Forest Service Gen. Tech. Rep 1990; PSW-122.
43. Fallick K. Relevance of the chemical constituency of East Indian Sandalwood essential oil to therapeutic and traditional uses [online] [cited 2014 Dec 8] Available from: http://www.australiannaturaltherapistsassociation.com.au/downloads/bursary/2009/ANTA-Bursary_Kate_Fallick.pdf.
44. Kim TH, Ito H, Hayashi K, Hasegawa T, Machiguchi T, Yoshida T. Aromatic constituents from the heartwood of *Santalum album* L. Chem Pharm Bull 2005;53(6):641-4.
45. Howes MR, Simmonds MSJ, Kite GC. Evaluation of the quality of sandalwood essential oils by gas chromatography-mass spectrometry. J Chromatogr A 2004;1028:307-12.
46. Matsuo Y, Mimaki Y. α -Santalol derivatives from *Santalum album* and their cytotoxic activities. Phytochemistry 2012;77:304-11.

47. Nautiyal OH, Analytical and Fourier transform infrared spectroscopy evaluation of sandalwood oil extracted with various process techniques. *J Nat Prod* 2011;4:150-7.
48. Sciarrone D, Costa R, Ragonese C, Tranchida PQ, Tedone L, Santi L, et al. Application of a multidimensional gas chromatography system with simultaneous mass spectrometric and flameionization detection to the analysis of sandalwood oil. *J Chromatogr A* 2011;1218:137-42.
49. Radomiljac AM, McComb JA, Shea SR. Field establishment of *Santalum album* L. the effect of the time of introduction of a pot host (*Alternanthera nana* R. Br.). *For Ecol Manage* 1998;111:107-18.
50. Misra BB, Dey S. Comparative phytochemical analysis and antibacterial efficacy of *in vitro* and *in vivo* extracts from East Indian sandalwood tree (*Santalum album* L.). *Appl Microbiol* 2012;55:476-86.
51. Grag SC. Essential oils as therapeutics. *Nat Prod Radiance* 2005;4(1):18-26.
52. Singh R, Singh S, Jeyabalan G, Ali A. An overview on traditional medicinal plants as aphrodisiac agent. *J Pharmacogn Phytochem* 2012;1(4):43-56.
53. Parek J, Jadeja D, Chanda S. Efficacy of aqueous and methanol extracts of some medicinal plants for potential antibacterial activity. *Turk J Biol* 2005;29:203-10.
54. Parekh, J. Chanda SV, In vitro antimicrobial activity and phytochemical analysis of some Indian medicinal plants. *Turk J Biol* 2007;31:53-8.
55. Chibnall AC, Piper SH, Mangouri HAE. The wax from the leaves of sandal (*Santalum album* Linn.). *Biochem J* 1937;31(11):1981-6.
56. Dev S. Prime ayurvedic plants drugs. New Delhi: Anamaya Publishers; 2006.
57. Oyen LPA, Dung NX, editors. Plant resources of south-east Asia. Bogor: Prosea foundation; 1999.
58. Okugawa H, Ueda R, Matsumoto K, Kawanishi K, Kato A. Effect of α -santalol and β -santalol from sandalwood on the central nervous system in mice. *Phytomedicine* 1995;2(2):119-126.
59. Pallavi KJ, Singh R, Singh S, Singh K, Farswan M, Singh V. Aphrodisiac agents from Medicinal Plants: A Review. *J Chem Pharm Res* 2011;3(2):911-21.

60. Tu X, Ling F, Huang A, Zhang Q, Wang G. Anthelmintic efficacy of *Santalum album* (santalaceae) against monogenean infections in goldfish. *Parasitol Res* 2013;112:2839-45.
61. Hire KK, Dhale DA. Antimicrobial effect and insilico admet prediction of *Santalum album* L. *Int J Pharm Bio Sci* 2012;3(4):727-34.
62. Dozmorov MG, Yang Q, Wu W, Wren J, Suhail MM, Woolley CL, et al. Differential effects of selective frankincense (Ru Xiang) essential oil versus non-selective sandalwood (Tan Xiang) essential oil on cultured bladder cancer cells: a microarray and bioinformatics study. *Chin Med* 2014;9(18):1-12.
63. Kulkarni CR, Joglekar MM, Patil SB, Arvindekar AU. Antihyperglycemic and antihyperlipidemic effect of *Santalum album* in streptozotocin induced diabetic rats. *Pharm Biol* 2012;50(3):360-5.
64. Misra BB, Dey S. Evaluation of *in vivo* anti-hyperglycemic and antioxidant potentials of α -santalol and sandalwood oil. *Phytomedicine* 2013;20:409-16.
65. Sindhu KR, Upma, Kumar A, Arora S. *Santalum album* Linn: A review on morphology, phytochemistry and pharmacological aspects. *Int J Pharm Res* 2010;2(1):914-19.
66. Harsha, SPSC, Khan MI, Prabhakar P, Giridhar P. Cyanidin-3-glucoside, nutritionally important constituents and *in vitro* antioxidant activities of *Santalum album* L. berries. *Food Res Int* 2013;50:275-81.
67. Ahmed N, Khan MSA, Jais AMM, Mohtarrudin N, Ranjbar M, Amjad MS, et al. Anti-ulcer activity of sandalwood (*Santalum album* L.) stem hydro-alcoholic extract in three gastric-ulceration models of Wistar rats. *Boletín Latinoamericano y del Caribe de Plantas Medicinales y Aromáticas* 2013;12(1):81-91.
68. Benencia F, Courreges MC. Antiviral activity of sandalwood oil against Herpes simplex viruses-1 and -2. *Phytomedicine* 1999;6(6):119-23.
69. Chilampalli C, Zhang X, Kaushik RS, Young A, Zeman D, Hildreth MB, et al. Chemopreventive effects of combination of honokiol and magnolol with α -santalol on skin cancer developments. *Drug Discov Ther* 2013;7(3):109-115.
70. Dickinson SE, Olson ER, Levenson C, Janda J, Rusche JJ, Alberts DS, et al. A novel chemopreventive mechanism for a traditional medicine: East Indian

sandalwood oil induces autophagy and cell death in proliferating keratinocytes. Arch Biochem Biophys 2014;558:143-52.

71. Amer A, Mehlhorn H. Larvicidal effects of various essential oils against *Aedes*, *Anopheles*, and *Culex* larvae (Diptera, Culicidae). Parasitol Res 2006;99:466-72.
72. Liu YD, Longmore RB, Boddy MR, Fox JED. Separation and identification of Triximenynin from *Santalum spicatum* R. Br. J Am Oil Chem Soc 1997;74(10):1269-72.
73. Byrne M, Macdonald B, Brand J. Phylogeography and divergence in the chloroplast genome of Western Australian Sandalwood (*Santalum spicatum*). Heredity 2003;91:389-95.
74. Forest Product Commission. The good oil Western Australian sandalwood. Harvey; 2011.
75. Byrne M, MacDonald B, Broadhurst L, Brand J. Regional genetic differentiation in Western Australian sandalwood (*Santalum spicatum*) as revealed by nuclear RFLP analysis. Theor Appl Genet 2003;107:1208-14.
76. Palombo EA, Semple SJ. Antibacterial activity of traditional Australian medicinal plants. J Ethnopharmacol 2001;77:151-7.
77. Payne SE, Kotze AC, Durmic Z, Vercoe PE. Australian plants show anthelmintic activity toward equine cyathostomins *in vitro*. Vet Parasitol 2013;196:153-60.
78. Gulati V, Harding IH, Palombo EA. Enzyme inhibitory and antioxidant activities of traditional medicinal plants: Potential application in the management of hyperglycemia. BMC Complement Altern Med 2012;12(77):1-9.
79. Semple SJ, Reynolds GD, O'Leary MC, Flower RLP. Screening of Australian medicinal plants for antiviral activity. J Ethnopharmacol 1998;60:163-72.
80. Spafford H, Jardine A, Carver S, Tarala K, Wees Mv, Weinstein P. Laboratory determination of efficacy of *Santalum spicatum* extract for mosquito control. J Am Mosq Control Assoc 2007;23(3):304-11.
81. Warburton CL, James EA, Fripp YJ, Trueman SJ, Wallace HM. Clonality and sexual reproductive failure in remnant populations of *Santalum lanceolatum* (Santalaceae). Biol Conserv 2000;96:45-54.

82. Harden GJ, editor. Flora of New Southwales volume 3. Sydney: NSW University Press; 1992.
83. Page T. Sandalwood oil. Queensland: J.C.U. Agroforestry and Novel Crops Unit, Cairns; 2002.
84. Chaichit C, editor. Thai herbs and herbal products. Bangkok: National Identity office Office of the Prime Minister; 2004.
85. Ozaki Y, Soedigdo S, Wattimena YR, Suganda AG. Antiinflammatory effect of mace, aril of *Myristica fragrans* Houtt., and its active principles. Japan J Pharmacol 1989;49:155-63.
86. Olajide OA, Ajayi FF, Ekhelar AI, Awe SO, Makinde JM, Alada ARA. Biological effects of *Myristica fragrans* (nutmeg) extract. Phytother Res 1999;13:344-5.
87. Dorman HJD, Deans SG. Antimicrobial agents from plants: antibacterial activity of plant volatile oils. J Appl Microbiol 2000;88:308-16.
88. Singh G, Marimuthu P, Heluani CSD, Catalan C. Antimicrobial and antioxidant potentials of essential oil and acetone extract of *Myristica fragrans* Houtt. (aril part). J Food Sci 2005;70(2):141-8.
89. Yanti, Rukayadi Y, Kim KH, Hwang JK. *In vitro* anti-biofilm activity of aacelignan isolated from *Myristica fragrans* Houtt. against aral primary colonizer bacteria. Phytother Res, 2008;22:308-12.
90. Wahab A, Haq RU, Ahmed A, Khan RA, Raza M. Anticonvulsant activities of nutmeg oil of *Myristica fragrans*. Phytother Res 2009;23:153-8.
91. Valente VMM, Jham GN, Dhingra OD, Ghiviriga I. Composition and antifungal activity of the Brazilian *Myristica fragrans* Houtt essential oil. J Food Saf 2011;31:197-202.
92. Rani P, Khullar N. Antimicrobial evaluation of some medicinal plants for their anti-enteric potential against multi-drug resistant *Salmonella typhi*. Phytother Res 2004;18:670-3.
93. Piaru SP, Mahmud R, Majid AMSA, Ismail S, Man CN. Chemical composition, antioxidant and cytotoxicity activities of the essential oils of *Myristica fragrans* and *Morinda citrifolia*. J Sci Food Agric 2012;92:593-7.

94. Dorman HJD, Figueiredo AC, Barroso JG, Deans SG. *In vitro* evaluation of antioxidant activity of essential oils and their components. *Flavour Fragr J* 2000;15:12-6.
95. Kang JW, Min BS, Lee JH. Anti-platelet activity of erythro-(7*S*,8*R*)-7-acetoxy-3,4,3',5'-tetramethoxy-8-O-4'-neolignan from *Myristica fragrans*. *Phytother Res* 2013;27:1694-9.
96. Gonçalves JLS, Lopes RC, Oliveira, Costa SS, Miranda MMFS, Romanos MTV, Santos NSO, Wigg MD, et al. *In vitro* anti-rotavirus activity of some medicinal plants used in Brazil against diarrhea. *J Ethnopharmacol* 2005;99:403-7.
97. Yang S, Na M, Jang JP, Kim KA, Kim BY, Sung NJ, et al. Inhibition of Protein Tyrosine Phosphatase 1B by Lignans from *Myristica fragrans*. *Phytother Res* 2006;20:680-2.
98. Sonavane GS, Sarveiya VP, Kasture VS, Kasture SB. Anxiogenic activity of *Myristica fragrans* seeds. *Pharmacol Biochem Behav* 2002;71:239-44.
99. Mahady GB, Pendland SL, Stoia A, Hamill FA, Fabricant D, Dietz BM, et al. *In vitro* susceptibility of *Helicobacter pylori* to botanical extracts used traditionally for the treatment of gastrointestinal disorders. *Phytother Res* 2005;19:988-91.
100. Piras A, Rosa A, Marongiu B, Atzeri A Dessì MA, Falconieri D, et al. Extraction and separation of volatile and fixed oils from seeds of *Myristica fragrans* by supercritical CO₂: chemical composition and cytotoxic activity on caco-2 cancer cells. *J Food Sci* 2012;77(4):448-53.
101. Nareeboon P, Kraus W, Beifuss U, Conrad J, Klaiber I, Sutthivaiyakit S. Novel 24-nor-, 24-nor-2,3-seco-, and 3,24-dinor-2,4-seco-ursane triterpenes from *Diospyros decandra*: evidences for ring A biosynthetic transformations. *Tetrahedron* 2006;62:5519-26.
102. Bunluepuech K, Tewtrakul S. Anti - HIV-1 integrase activity of Thai medicinal plants. *Songklanakarin J Sci Technol* 2009;31(3):289-92.
103. Kubola J, Siriamornpun S, Meeso N. Phytochemicals, vitamin C and sugar content of Thai wild fruits. *Food Chem* 2011;126:972-81.

104. Chamchumroon V, Puff C, The Rubiaceae of Ko Chang, south-eastern Thailand. Thai For Bull (BOT.) 2003;31:13-26.
105. Kesonbua W, Chantaranothai P. A checklist of the genus *Tarenna Gaertn.* (Rubiaceae) in Thailand. Thai For Bull (BOT.) 2008;36:18-45.
106. Worapratheep K. Taxonomy of vascular plants in Koh Tao Mo, Koh Phra and Koh Phra Noi, Chon Buri province. Department of Botany, Faculty of Science, Chulalongkorn: Bangkok; 2002.
107. สุวิทย์ วรรณศรี. ความหลากหลายทางชีวภาพและการใช้ประโยชน์จากสมุนไพรบริเวณพื้นที่ภูแพงม้า อำเภอห้วยเม็ก จังหวัดเพชรบูรณ์. สำนักบริหารโครงการส่งเสริมการวิจัย ในอุดมศึกษาและพัฒนามหาวิทยาลัยวิจัยแห่งชาติ สำนักงานคณะกรรมการการอุดมศึกษา: เพชรบูรณ์; 2556.
108. รัชชัย นาใจคง.ฤทธิ์ต้านอนุมูลอิสระและการเกิดสารประกอบเชิงซ้อนกับเหล็กของสมุนไพรไทยบางชนิด. วารสารวิทยาศาสตร์ มข. 2557;42(1):149-58.
109. EIL-Halawany AM, Chung MH, Ma CM, Komatsu K, Nishihara T, Hattori M. Anti-estrogenic activity of mansorins and mansonones from the heartwood of *Mansonia gagei* DRUMM. Chem Pharm Bull 2007;55(9):1332-7.
110. Tiew P, Puntumchai A, Kokpol U, Chavasiri W. Coumarins from the heartwoods of *Mansonia gagei* Drum. Phytochemistry 2002;60:773-6.
111. Tiew P, Loset JR, Kokpol U, Schenk K, Jaiboon N, Chaichit N, et al. Four new sesquiterpenoid derivatives from the heartwood of *Mansonia gagei*. J Nat Prod 2002;65:1332-5.
112. Tiew P, Loser JR, Kokpol U, Chavasiri W, Hostettmann K. Antifungal, antioxidant and larvicidal activities of compounds isolated from the heartwood of *Mansonia gagei*. Phytother Res 2003;17:190-3
113. Changwong N, Sabphon C, Ingkaninan K, Sawasdee P. Acetyl- and butyrylcholinesterase inhibitory activities of mansorins and mansonones. Phytother Res 2012;26:392-6.
114. มงคล โมกขะสมิต, กมล สวัสดิ์มงคล, วันทนางามวัฒน์. การศึกษาเภสัชวิทยาของจันทน์ชะมด. วารสารของกรมวิทยาศาสตร์การแพทย์ 2514;13(1):27-35.

115. Tiew P, Takayam H, Kitajim M, Aimi N, Kokpola U, Chavasiri W. A novel neolignan, mansoxetane, and two new sesquiterpenes, mansonones R and S, from *Mansonia gagei*. *Tetrahedron Lett* 2003;44:6759-61.
116. Wongprasert T, Phengklai C, Boonthavikoon T. A synoptic account of the Meliaceae of Thailand. *Thai For Bull (BOT.)*. 2011;39:210-66.
117. Hwang BY, Su BN, Chai H, Mi Q, Kardono LBS, Afriastini JJ. Silvestrol and episilvestrol, potential anticancer rocaglate derivatives from *Aglaia silvestris*. *J Org Chem* 2004;69(10):3351-8.
118. Pointinger S, Promdang S, Vajrodaya, Pannell CM, Hofer O, Mereiter K, et al. Silvaglins and related 2,3-secodammarane derivatives-unusual types of triterpenes from *Aglaia silvestris*. *Phytochemistry* 2008;69:2696-703.
119. Seger C, Pointinger S, Greger H, Hofer O. Isoeichlerianic acid from *Aglaia silvestris* and revision of the stereochemistry of foveolin B. *Tetrahedron Lett* 2008;49:4313-5.
120. Hofer O, Pointinger S, Brecker L, Peter K, Greger H. Silvaglenamin-a novel dimeric triterpene alkaloid from *Aglaia silvestris*. *Tetrahedron Lett* 2009;50:467-8.
121. Brader G, Vajrodaya, Greger H, Bacher M, Halchhauser, Hofer O. Bisamides, lignans, triterpenes, and insecticidal cyclopenta[b]benzofurans from *Aglaia* Species *J Nat Prod* 1998;61(12):1482-91.
122. World Health Organization Geneva, editor. Quality control methods for medicinal plant materials. England; 1998.
123. Dupuy N, Molinet J, Mehl F, Nanlohy F, Dréau YL, Kister J. Chemometric analysis of mid infrared and gas chromatography data of Indonesian nutmeg essential oils. *Ind Crops Prod* 2013;43:596-601.
124. Convention U.S.P. Monographs in the Herbal Medicines Compendium Guidelines Document Version 1.0: May 20, 2013 [online] 2013 [cited 2015 12 May]; Available from: https://hmc.usp.org/sites/default/files/documents/HMC/GN_Resource/HMC%20Monograph%20Guidelines%20v.%201.0_GC%20link%20updated.pdf.
125. Bele AA, Khale A. An overview on thin layer chromatography. *Int J Pharm Sci Res* 2011;2(2):256-67.

126. Marchand E, Atemnkeng MA, Vanermen S, Plaizier-Vercammen J. Development and validation of a simple thin layer chromatographic method for the analysis of artemisinin in *Artemisia annua* L. plant extracts. *Biomed Chromatogr* 2008;22:454-9.
127. Marston A. Thin-layer chromatography with biological detection in phytochemistry. *J Chromatogr A* 2011;1218:2676-83.
128. Mohammad A, Bhawani SA, Sharma S. Analysis of herbal products by thin-layer chromatography: a review. *Int J Pharma Bio Sci* 2010;1(2):1-50.
129. Wang P, ZhiguoY. Species authentication and geographical origin discrimination of herbal medicines by near infrared spectroscopy : A review. *J Pharma Analysis*, 2015;5(5):277-84.
130. Rasheed A, Satyanarayana KV, Gulabi PS, Sindhura M, Shama SN, Reddy AK. Standardization: Accessing key for herbal drug safety assurance. *J Pharm Res* 2011;4(5):1322-5.
131. Liang YZ, Xie P, Chan K. Quality control of herbal medicines. *J Chromatogr B* 2004;812:53-70.
132. Stuart B. *Modern Infrared spectroscopy*. Greenwich: John Wiley & Son; 1996.
133. Joshi DD. *Herbal drugs and fingerprints*. India: Springer; 2012.
134. Sun S, Chen J, Zhou Q, Lu G, Chan K. Application of mid-Infrared spectroscopy in the quality control of Traditional Chinese Medicines. *Planta Med* 2010;76:1987-96.
135. Workman J, Springteen AW, editors. Appendix B: Practices of data preprocessing for optical spectrophotometry In: *Applied spectroscopy*. San Diego: Academic Press; 1998.
136. Davis R, Mauer LJ. Fourier transform infrared (FT-IR) spectroscopy: A rapid tool for detection and analysis of foodborne pathogenic bacteria. *Current Research, Technology and Education Topics in Applied Microbiology and Microbial Biotechnology* 2010;1:1582-94.
137. CAMO. The Unscrambler X [computer program].Version 10.1. Oslo; 2009-2010.

138. Gaydou V, Kister J, Dupuy N. Evaluation of multiblock NIR/MIR PLS predictive models to detect adulteration of diesel biodiesel blends by vegetal oil. *Chemometr Intell Lab Syst* 2011;106:190-7.
139. Rinnan As, Berg Fvd, Engelsen SB. Review of the most common pre-processing techniques for near-infrared spectra. *Trends Analyt Chem* 2009;28(10):1201-22.
140. Niu W, Knight E, Xia Q, McGarvey BD. Comparative evaluation of eight software programs for alignment of gas chromatography-mass spectrometry chromatograms in metabolomics experiments. *J Chromatogr A* 2014;1374:199-206.
141. Sandasi M, Kamatou GPP, Combrinck S, Viljoen AM. A chemotaxonomic assessment of four indigenous South African Lippia species using GC-MS and vibrational spectroscopy of the essential oils. *Biochem Syst Ecol* 2013;51:142-52.
142. Hovell AMC, Pereira EJ, Arruda NP, Rezende CM. Evaluation of alignment methods and data pretreatments on the determination of the most important peaks for the discrimination of coffee varieties Arabica and Robusta using gas chromatography-mass spectroscopy. *Anal Chim Acta* 2010;678:160-8.
143. Goodarzi M, Russell PJ, Heyden YV. Similarity analyses of chromatographic herbal fingerprints: A review. *Anal Chim Acta* 2013;804:16-28.
144. Alaerts G, Erps JV, Pieters S, Dumarey M, Nederkassel AMv, Goodazi M. Similarity analyses of chromatographic fingerprints as tools for identification and quality control of green tea. *J Chromatogr B* 2012;910:61-70.
145. Vandeginste BGM, Massart DL, Buydens LMC, Jong DS, Lewi PJ, Smers-Verbeke J. Chapter 33 - Supervised Pattern Recognition. In: *Data Handling in Science and Technology* volume 20 part 2. Elsevier; 1998. p.207-41.
146. Berrueta LA, Alonso-Salces RM, Héberger Ka. Supervised pattern recognition in food analysis. *J Chromatogr A* 2007;1158:196-214.
147. Casale M, Zunin P, Cosulich ME, Pistarino E, Perego P, Lanteri S. Characterisation of table olive cultivar by NIR spectroscopy. *Food Chem* 2010;122:1261-5.

148. Teixeira LSG, Oliveira FS, Santos HC, Cordeiro PWL, Almeida SQ. Multivariate calibration in Fourier transform infrared spectrometry as a tool to detect adulterations in Brazilian gasoline. *Fuel* 2008;87:346-52.
149. Al-Holy MA, Lin M, Cavinato AG, Rasco BA. The use of Fourier transform infrared spectroscopy to differentiate *Escherichia coli* O157:H7 from other bacteria inoculated into apple juice. *Food Microbiol* 2006;23:162-8.
150. Quiñones-Islas N, Meza-Márquez OG, Osorio-Revilla G, Gallardo-Velazquez T. Detection of adulterants in avocado oil by Mid-FTIR spectroscopy and multivariate analysis. *Food Res Int* 2013;51:148-54.
151. Osorio MT, Downey G, Moloney AP, Röhrle FT, Luciano G, Schmidt O. Beef authentication using dietary markers: Chemometric selection and modelling of significant beef biomarkers using concatenated data from multiple analytical methods. *Food Chem* 2013;141:2795-801.
152. Almeida RM, Fidelis CV, Barata LS, Poppi R. Classification of Amazonian rosewood essential oil by Raman spectroscopy and PLS-DA with reliability estimation. *Talanta* 2013;117:305-11.
153. Bassbasi M, Luca MD, Ioele G, Oussama A, Ragno G. Prediction of the geographical origin of butters by partial least square discriminant analysis (PLS-DA) applied to infrared spectroscopy (FTIR) data. *J Food Compost Anal* 2014;33:210-5.
154. Tang G, Tain K, Song X, Xiong Y, Min S. Comparison of several supervised pattern recognition techniques for detecting additive methamidophos in rotenone preparation by near-infrared spectroscopy. *Spectrochim Acta A: Mol Biomol Spectrosc* 2014;121:678-84.
155. Oliveira FSd, Teixeira LSG, Araujo MCU, Kornd M. Screening analysis to detect adulterations in Brazilian gasoline samples using distillation curves. *Fuel* 2004;83:917-23.
156. Candolfi A, Maesschalck RD, Massart DL, Hailey PA, Harrington ACE. Identification of pharmaceutical excipients using NIR spectroscopy and SIMCA. *J Pharm Biomed Anal* 1999;19:923-35.
157. Meza-Marquez OG, Gallardo-Velazquez T, Osorio-Revilla G. Application of mid-infrared spectroscopy with multivariate analysis and self independent

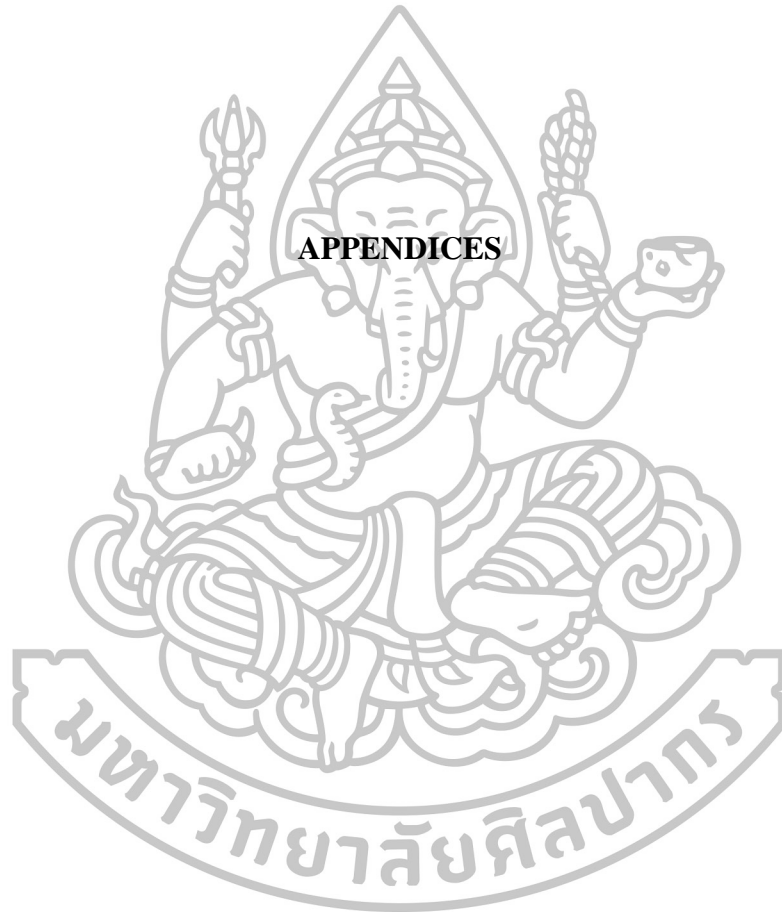
- modeling of class analogies (SIMCA) for the detection of adulterants in minced beef. *Meat Sci* 2010;86:511-9.
158. Anzanello MJ, Ortiz RS, Limberger R, Mariotti K. PLS-DA wavenumber selection for the categorization of medicine samples based on multiple criteria. *Forensic Sci Int* 2014;242:111-6.
159. Felipe-Sotelo M, Tauler R, Vives I, Grimalt JO. Assessment of the environmental and physiological processes determining the accumulation of organochlorine compounds in European mountain lake fish through multivariate analysis (PCA and PLS). *Sci Total Environ* 2008;404:148-61.
160. Almeida MRd, Correa DN, Rocha WFC, Scafi FJO, Poppi RJ. Discrimination between authentic and counterfeit banknotes using Raman spectroscopy and PLS-DA with uncertainly estimation. *Microchem J* 2013;109:170-7.
161. Oliveri P, Lopez MI, Casolino MC, Ruisanchez I. Partial least squares density modeling (PLS-DM) - A new class-modeling strategy applied to the authentication of olives in brine by near-infrared spectroscopy. *Anal Chim Acta* 2014;851:30-36.
162. Lai YH, Ni YN, Kokot S. Authentication of Cassia seeds on the basis of two-wavelength HPLC fingerprinting with the use of chemometrics. *Chin Chem Lett* 2010;21:213-6.
163. Soares PK, Scarminio IS. Multivariate chromatographic fingerprint preparation and authentication of plant material from the genus *Bauhinia*. *Phytochem Anal*, 2008;19:78-85.
164. Kan J, Zhou L, Sun J, Han J, Guo DA. Chromatographic fingerprint analysis and characterization of furocoumarins in the roots of *Angelica dahurica* by HPLC/DAD/ESI-MSⁿ technique. *J Pharm Biomed Anal* 2008;47:778-85.
165. Chun MH, Kim EK, Yua SM, Oh MS, Jung JH. GC/MS combined with chemometrics methods for quality control of *Schizonepeta tenuifolia* Briq: Determination of essential oils. *Microchem J*, 2011;97:274-81.
166. Lucio-Gutiérrez JR, Coello J, MasPOCH S. Enhanced chromatographic fingerprinting of herb materials by multi-wavelength selection and chemometrics. *Anal Chim Acta* 2012;710:40-9.

167. Ma T, Huang C, Meng X, Zhang Q, Zhang L, Lv X. Fingerprint analysis of Hawk-tea by high-performance liquid chromatography. *Food Chem* 2011;129:551-6.
168. Fan Q, Chen C, Lin Y, Zhang C, Liu B, Zhao S. Fourier Transform Infrared (FT-IR) Spectroscopy for discrimination of *Rhizoma gastrodiae* (Tianma) from different producing areas. *J Mol Struct* 2013;1051:66-71.
169. Yang IC, Tsai CY, Hsieh KW, Yang CW, Ouyang F. Integration of SIMCA and near-infrared spectroscopy for rapid and precise identification of herbal medicines. *J Food Drug Anal* 2013;21:268-78.
170. Zhu H, Wang Y, Liang H, Chen Q, Zhao P, Tao J. Identification of *Portulaca oleracea* L. from different sources using GC-MS and FT-IR spectroscopy. *Talanta* 2010;81:129-35.
171. Mukaka MM, Statistics Corner: A guide to appropriate use of Correlation coefficient in medical research. *Malawi Med J* 2012;24(3):69-71.
172. Department of Medical Sciences, M.o.P.H. Thai Herbal Pharmacopoeia volume III. Nonthaburi; 2009.
173. Adams RP. Identification of essential oil components by gas chromatography/quadrupole mass spectroscopy. Illinois: Allured; 2001.
174. Sotaphun U, Phaechamud T, Dechwisissakul P. Rapid Screening Method for Curcuminoid Content in Turmeric (*Curcuma longa* Linn.). *Thai Pharm Health Sci J* 2007;2(2):125-30.
175. Silva VAGd, Talhavini M, Pexoto ICF, Zacca JJ, Maldaner AO, Braga JWB. Non-destructive identification of different types and brands of blue pen inks in cursive handwriting by visible spectroscopy and PLS-DA for forensic analysis. *Microchem J*, 2014;116:235-43.
176. Xie L, Ye X, Liu D, Ying Y. Quantification of glucose, fructose and sucrose in bayberry juice by NIR and PLS. *Food Chem* 2009;114:1135-40.
177. Lucio-Gutiérrez JR, Coello J, Maspoch S. Application of near infrared spectral fingerprinting and pattern recognition techniques for fast identification of *Eleutherococcus senticosus*. *Food Res Int* 2011;44:557-65.
178. Doran J, Thomson L, Brophy J, Goldsack B, Bulai P, Faka'osi T. Variation in heartwood oil composition of young sandalwood trees in the South Pacific

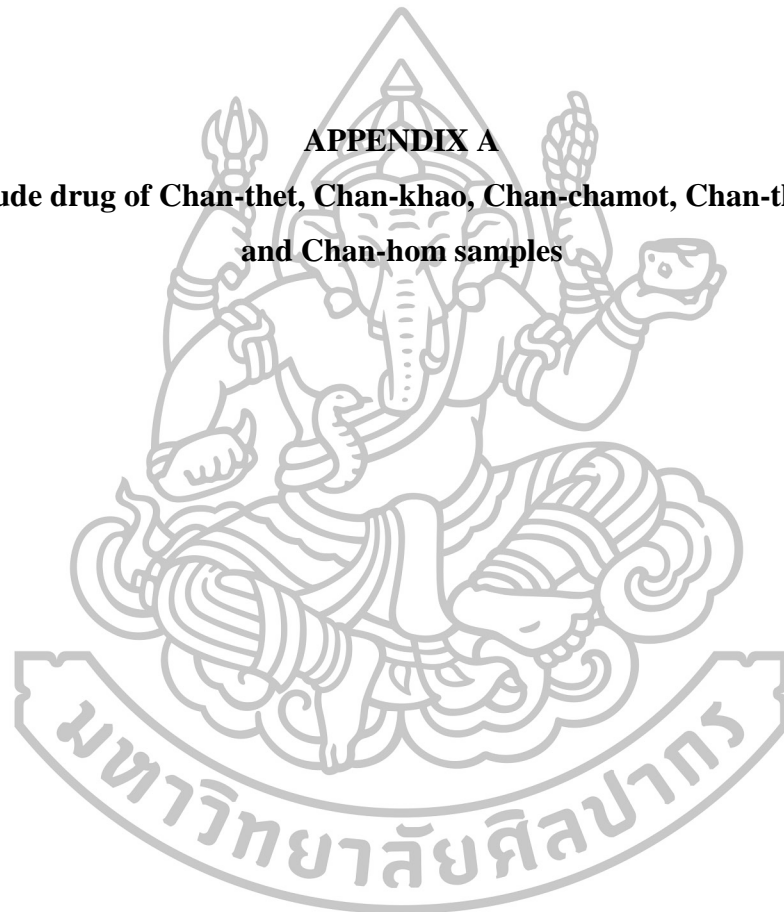
- (*Santalum yasi*, *S. album* and F1 hybrids in Fiji, and *S. yasi* in Tonga and Niue). Sandalwood Research Newsletter 2005;20:3-7.
179. Burdock GA, Carabin IG. Safety assessment of sandalwood oil (*Santalum album* L.). Food Chem Toxicol 2008;46:421-32.
180. Subasinghe U, Gamage M, Hettiarachchi DS. Essential oil content and composition of Indian sandalwood (*Santalum album*) in Sri Lanka. J For Res 2013;24(1):127-30.
181. Boonsri S. Chemical constituents from the roots of *Cratoxylum formosum* and *Artocarpus integer* and the stem of *Thespesia populnea* [Doctor of philosophy in Organic chemistry dissertation]. Songkla: Prince of Songkla University; 2010.
182. Sengab AEB, Elgindi MR, Mansour MA. Sesquiterpenes quinones from *Thespesia populnea* and their biological studies. J pharmacogn phytochem 2013;2(3):136-9.
183. Lee JH, Ku CH, Baek NI, Park HW, Kim DK. Phytochemical constituents from *Diodia teres*. Arch Pharm Res 2004;27(1):40-3.
184. Güvenalp Z, Kiliç N, Kazaz C, Kaya Y, Demirezer LÖ. Chemical constituents of *Galium tortumense*. Turk J Chem 2006;30:515-23.
185. Guarnaccia R, Madyastha KM, Tegtmeier E, Coscia CJ. Geniposidic acid, an iridoid glucoside from *Genipa americana*. Tetrahedron Lett. 1972;50:5125-7.
186. Nahratedt A, Rockenbach J, Wray V. Phenylpropanoid glycosides, a furanone glucoside and geniposidic acid from members of the Rubiaceae. Phytochemistry 1995;39(2):375-8.
187. Djoudi R, Bertrand C, Fiasson JL, Comte G, Fenet B. Polyphenolics and iridoid glycosides from *Tarenna madagascariensis*. Biochem Syst Ecol 2007;35:314-6.
188. National Center for Biotechnology Information. 1,2-naphthoquinone-Compound Summary. [online] [cited 2014 Oct 5] Available from: <http://pubchem.ncbi.nlm.nih.gov/summary/summary.cgi?cid=10667>.
189. Lu GH, Chan K, Liang YZ, Leung K, Chan CL, Jiang Z, et al. Development of high-performance liquid chromatographic fingerprints for distinguishing

- Chinese *Angelica* from related umbelliferae herbs. *J Chromatogr A* 2005;1073:383-92.
190. Yip PY, Chau CF, Mak CY, Kwan HS. DNA methods for identification of Chinese medicinal materials. *Chin Med* 2007;2(9):1-19.
191. Kondo K, Shiba M, Yamaji H, Morota T, Zhengmin C, Huixia P, et al. Species identification of licorice using nrDNA and cpDNA genetic markers. *Biol Pharm Bull* 2007;30(8):1497-502.
192. Kwon YK, Ahn MS, Park JS, Liu JR, In DS, Min BW, et al. Discrimination of cultivation ages and cultivars of ginseng leaves using Fourier transform infrared spectroscopy combined with multivariate analysis. *J Ginseng Res* 2014;38:52-8.
193. Borràs E, Mestres M, Aceña L, Busto O, Ferré J, Boqué R, et al. Identification of olive oil sensory defects by multivariate analysis of mid infrared spectra. *Food Chem* 2015;187:197-203.
194. Pholpho T, Pathaveerat S, Sirisomboon P. Classification of longan fruit bruising using visible spectroscopy. *J Food Eng* 2011;104:169-72.
195. Vitale R, Bevilacqua M, Bucci R, Magrì AD, Magrì AL, Marini F. A rapid and non-invasive method for authenticating the origin of pistachio samples by NIR spectroscopy and chemometrics. *Chemometr Intell Lab Syst* 2013;121:90-9.
196. Yip WL, Soosainather TC, Dyrstad K, Sande SA. Classification of structurally related commercial contrast media by near infrared spectroscopy. *J Pharm Biomed Anal* 2014;90:148-60.

APPENDICES



APPENDIX A
Crude drug of Chan-thet, Chan-khao, Chan-chamot, Chan-thana
and Chan-hom samples



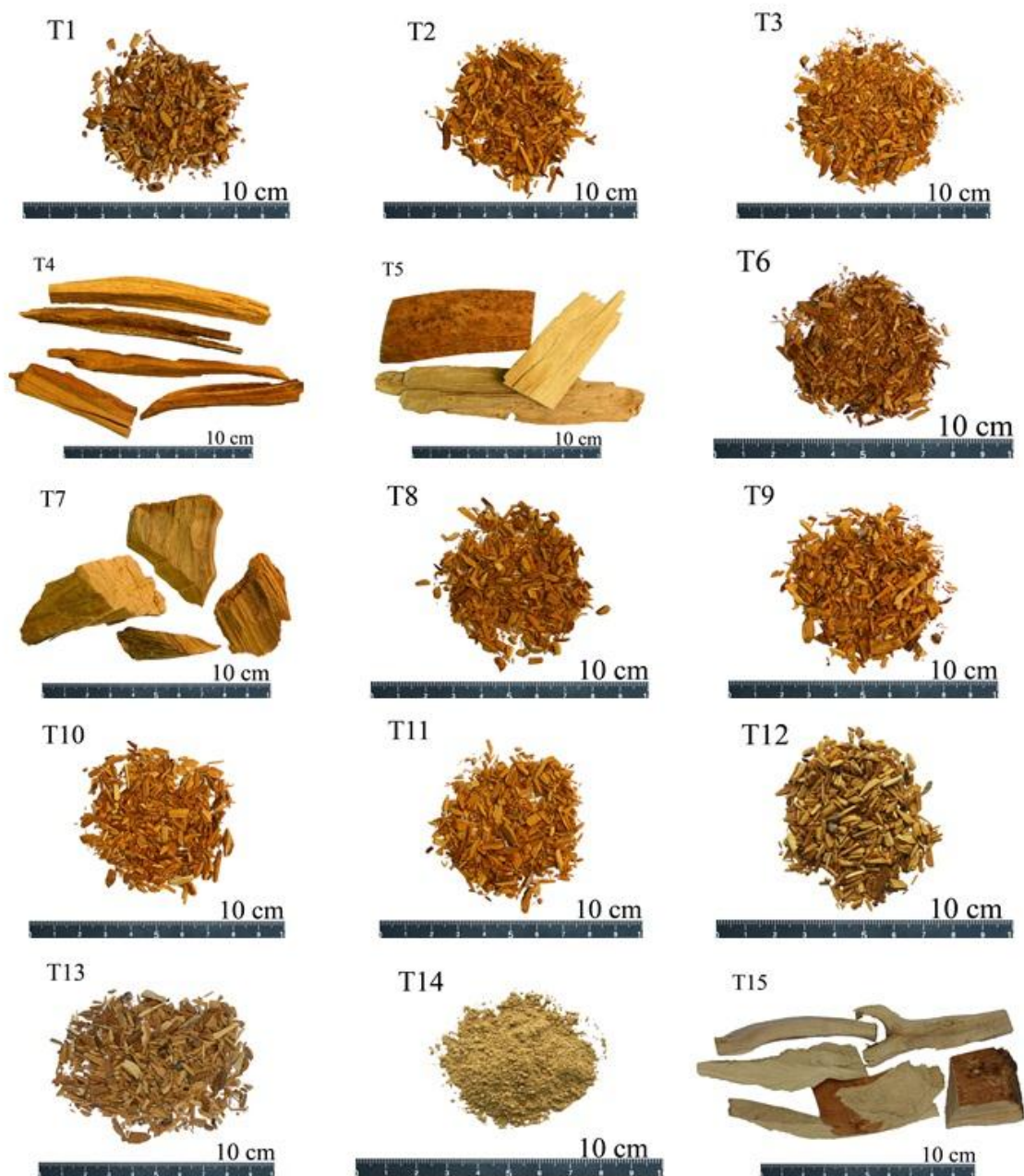


Figure 59 Characters of fifteen Chan-thet crude drug samples (T1-T15).



Figure 60 Characters of eighteen Chan-khao crude drug samples (K1-K18).



Figure 61 Characters of seventeen Chan-chamot crude drug samples (M1-M17).



Figure 62 Characters of ten Chan-thana crude drug samples (TN1-TN10).

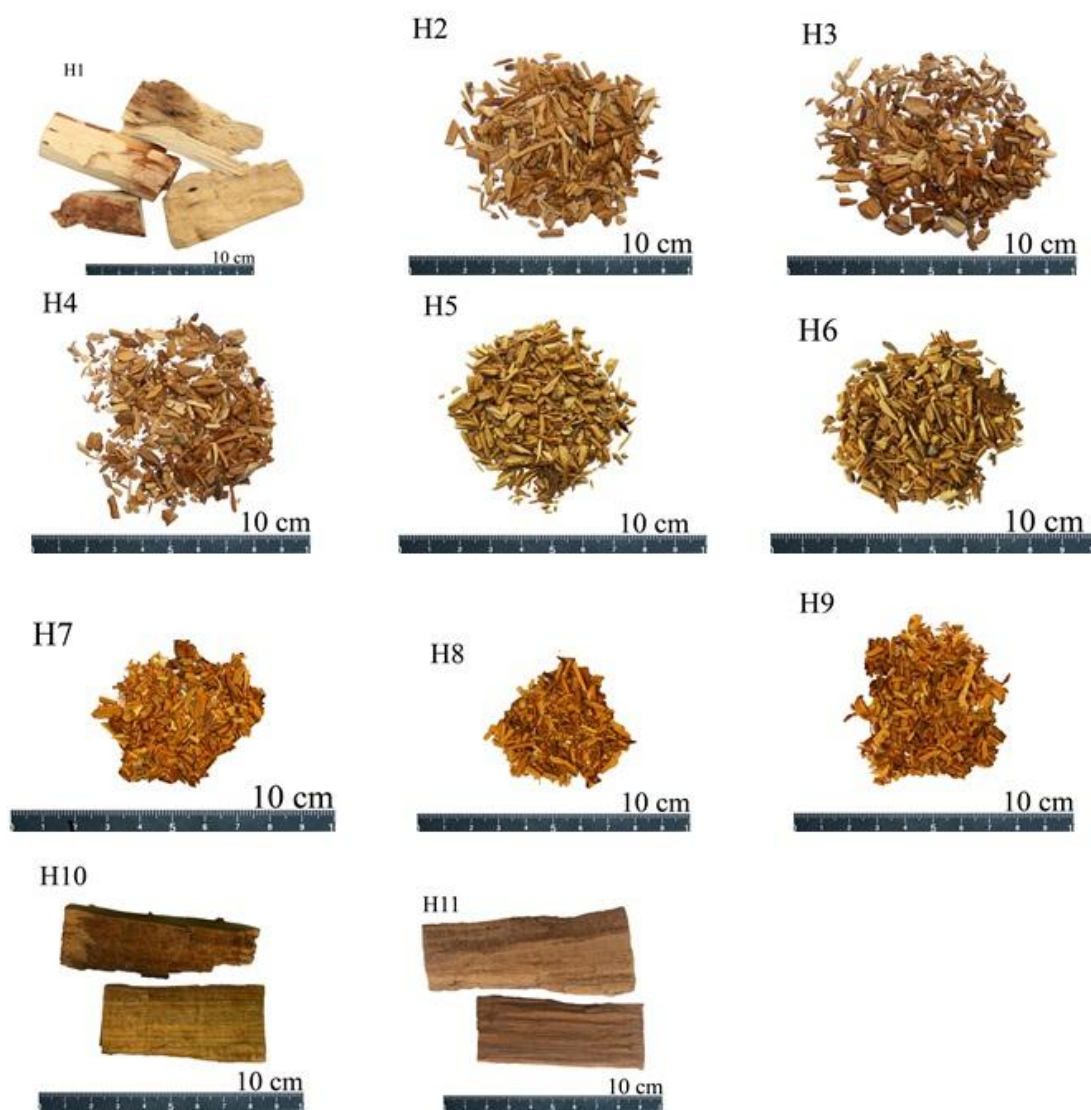
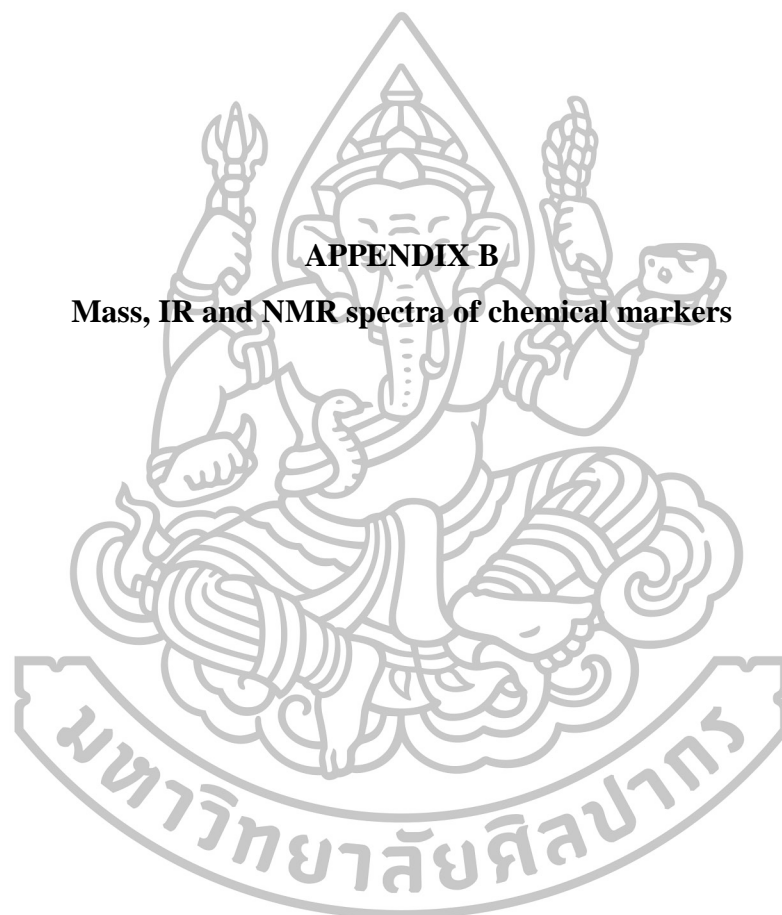


Figure 63 Characters of eleven Chan-hom crude drug samples (H1-H11).



Figure 64 Characters of authentic samples: *S. spicatum*, *S. album*, *S. lanceolatum*, *M. fragrans*, *T. hoensis*, *D. decandra*, *M. gagei* and *A. silvestris*.



APPENDIX B

Mass, IR and NMR spectra of chemical markers

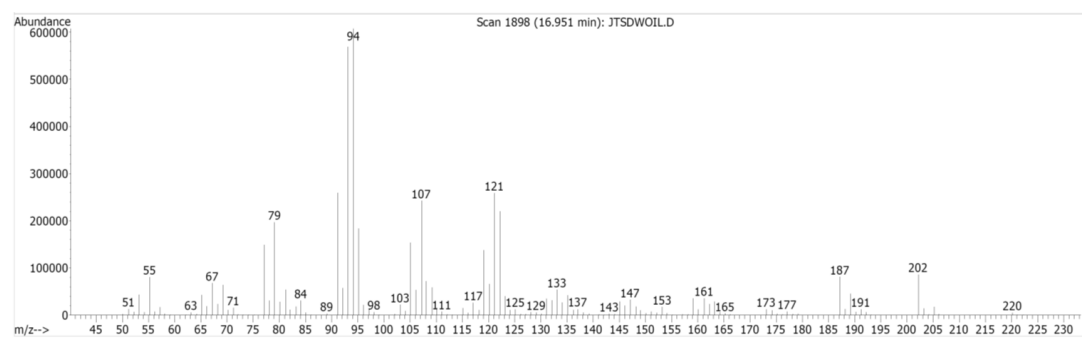


Figure 65 EI-MS mass spectrum of α -santalol.

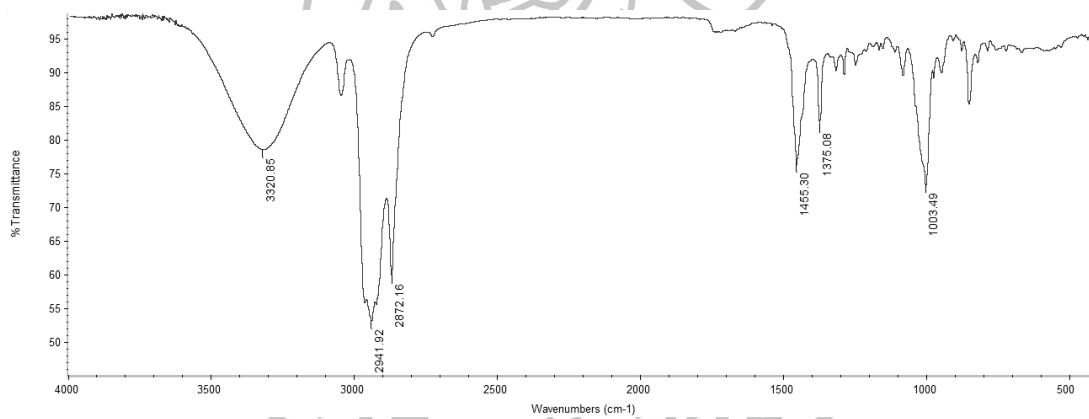


Figure 66 IR spectrum of α -santalol (dry film).

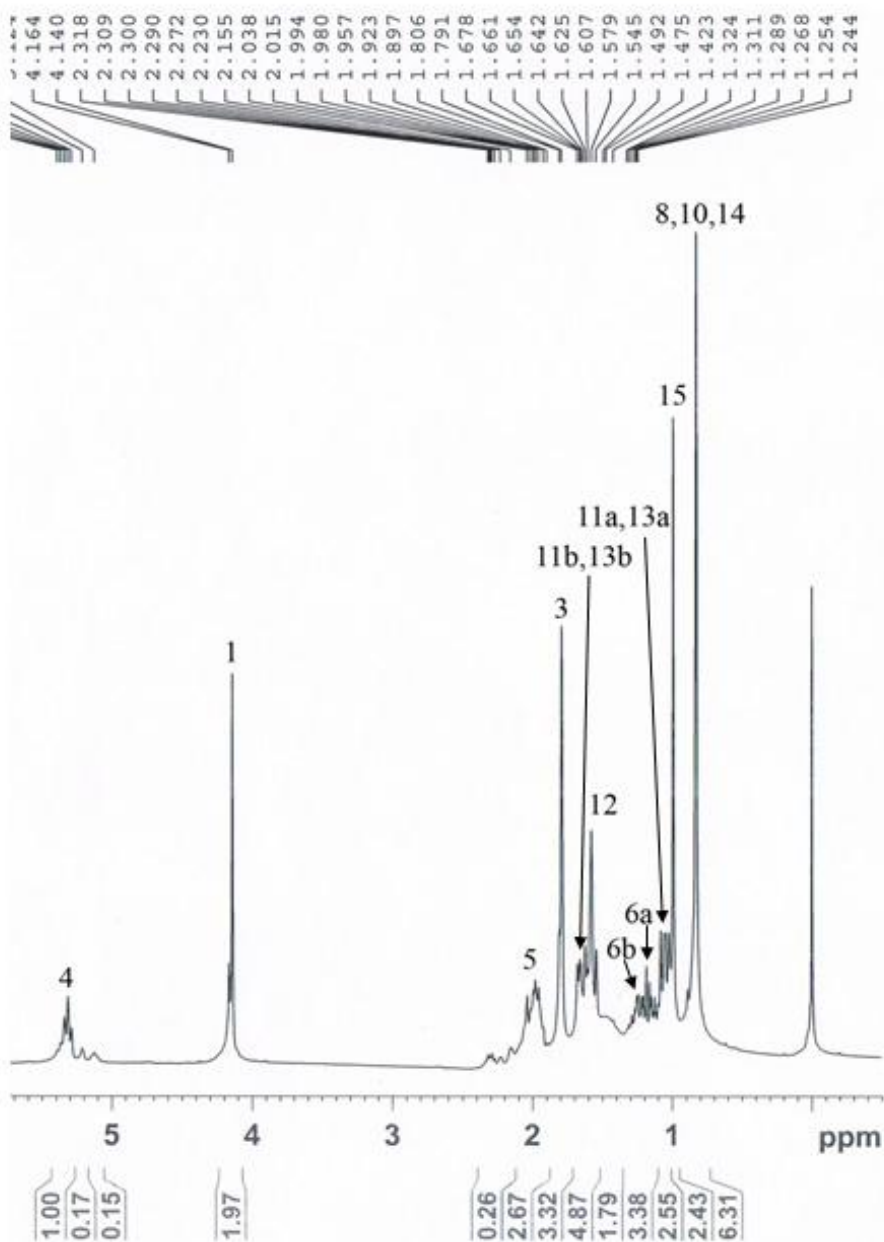


Figure 67 $^1\text{H-NMR}$ spectrum (300 MHz) of α -santalol (in CDCl_3).

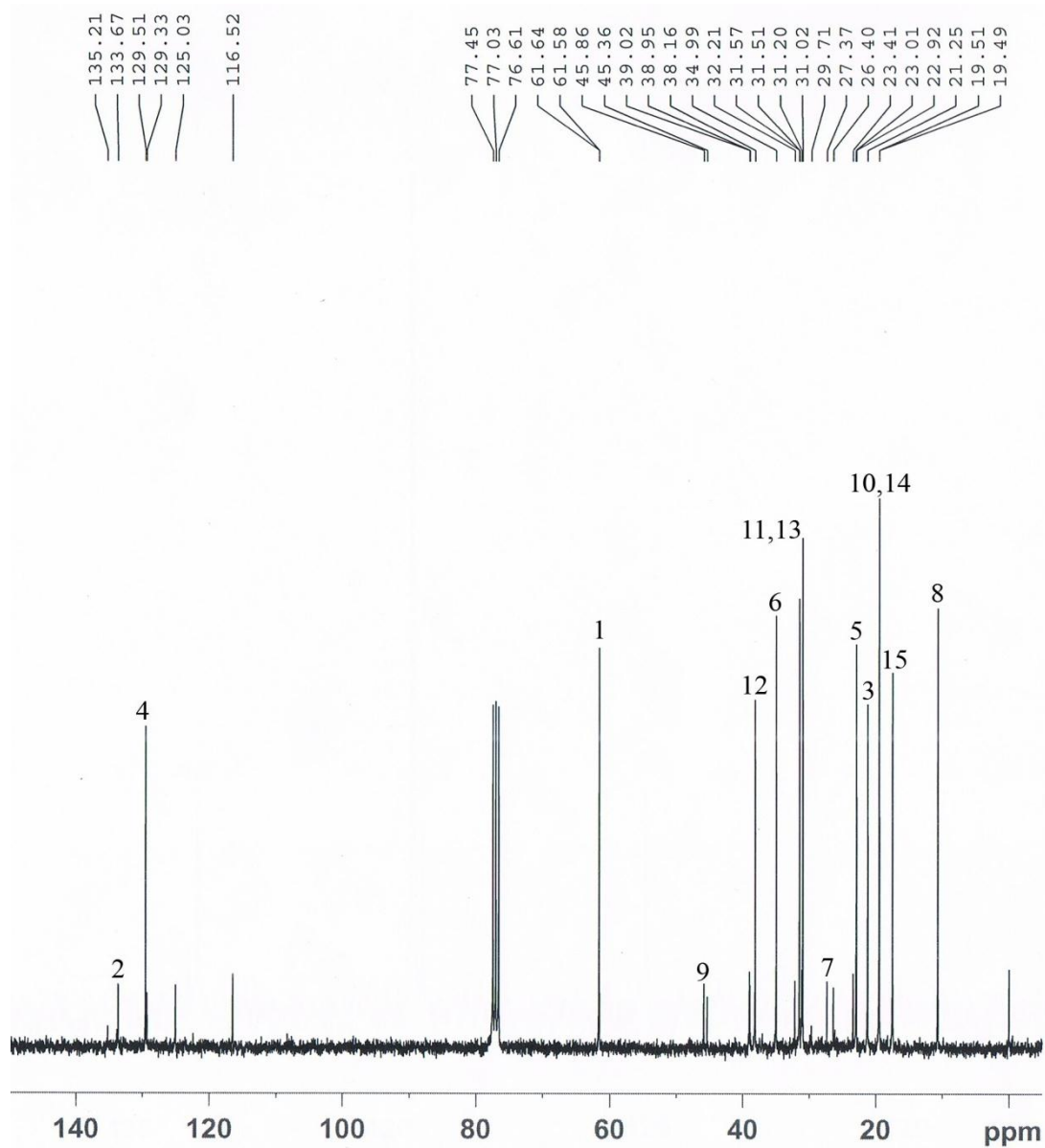


Figure 68 ^{13}C -NMR spectrum (75 MHz) of α -santalol (in CDCl_3).

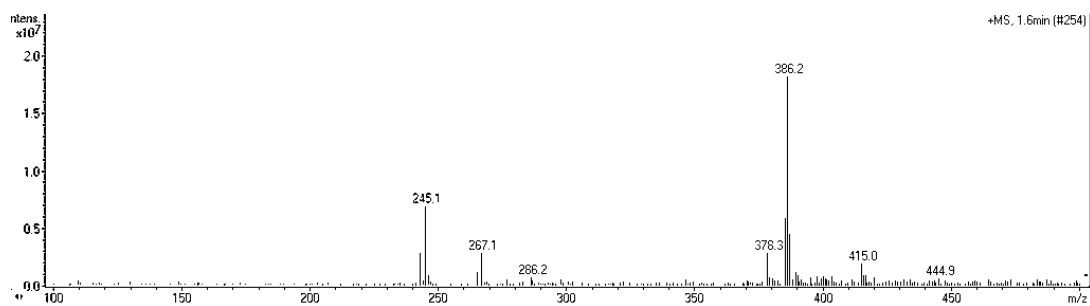


Figure 69 (+)-ESI-MS mass spectrum of mansonone G.

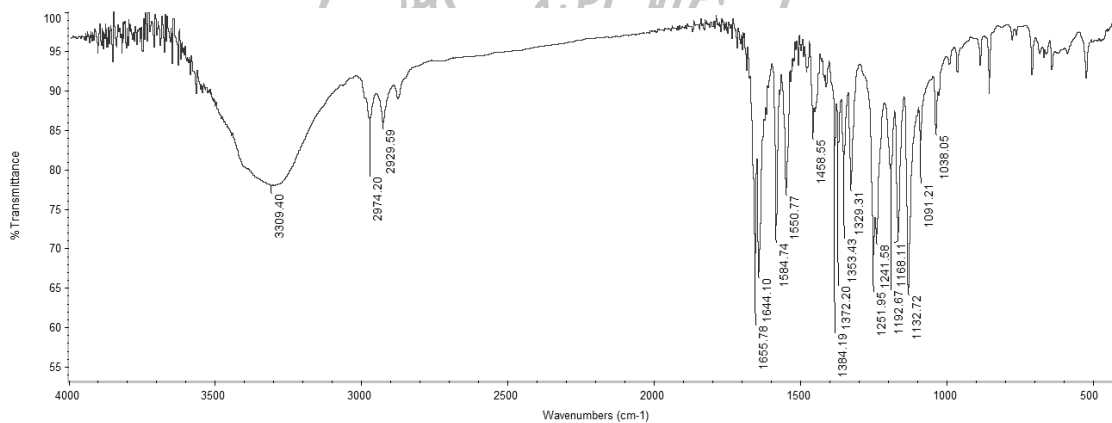


Figure 70 IR spectrum of mansonone G (KBr).

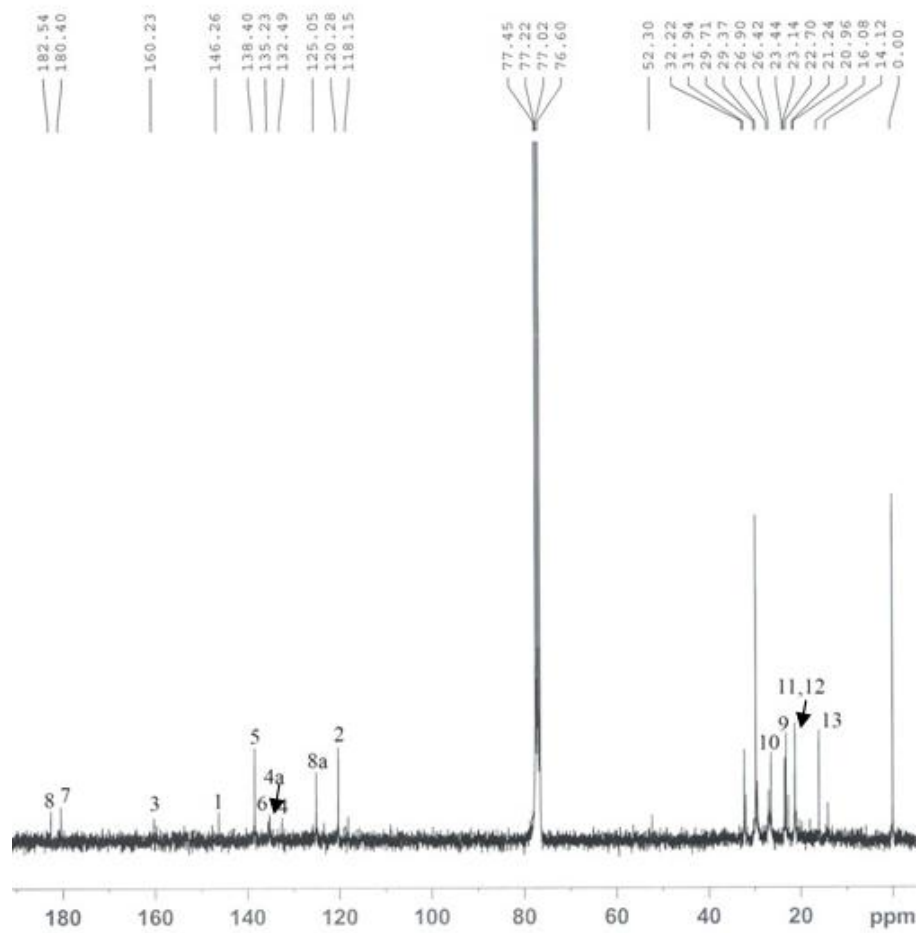


Figure 71 ^{13}C -NMR spectrum (75 MHz) of mansonone G (in CDCl_3).

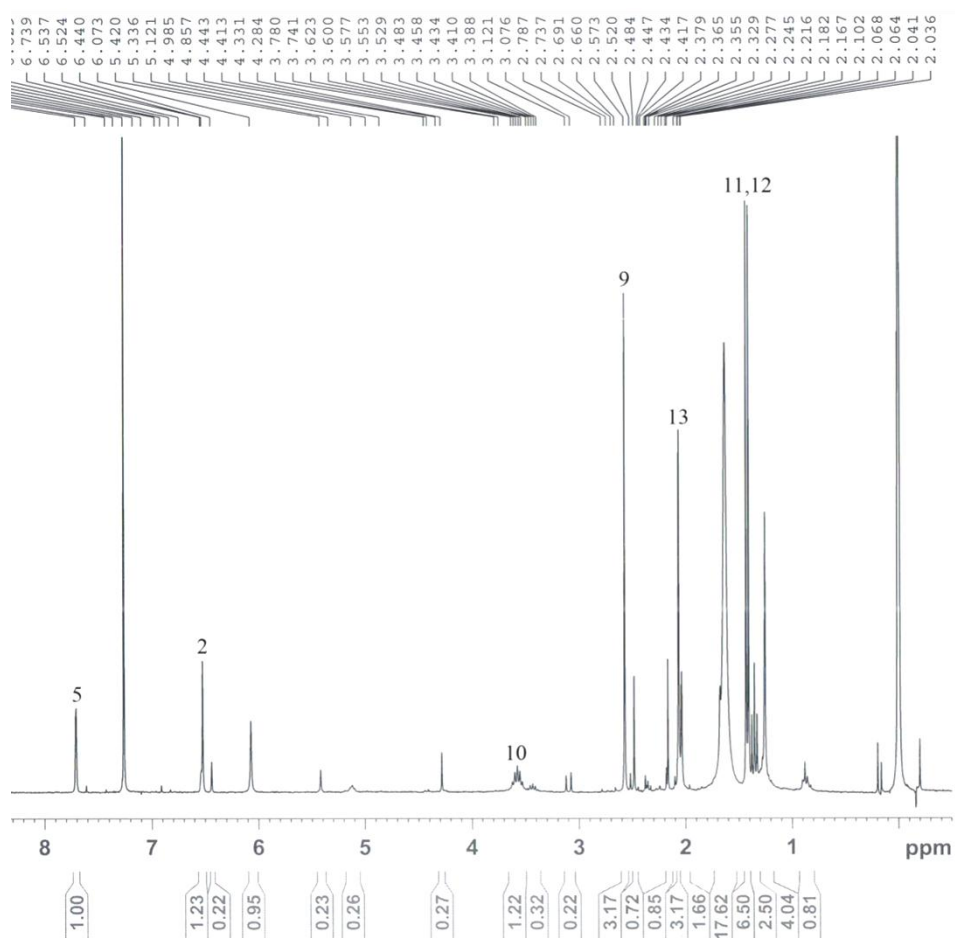


Figure 72 $^1\text{H-NMR}$ spectrum (300 MHz) of mansonone G (in CDCl_3).

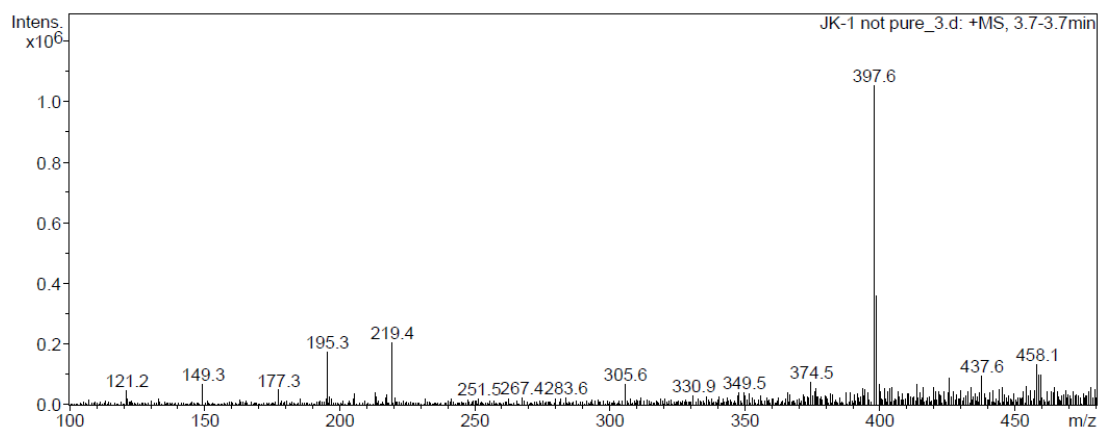


Figure 73 (+)-ESI-MS mass spectrum of geniposidic acid.

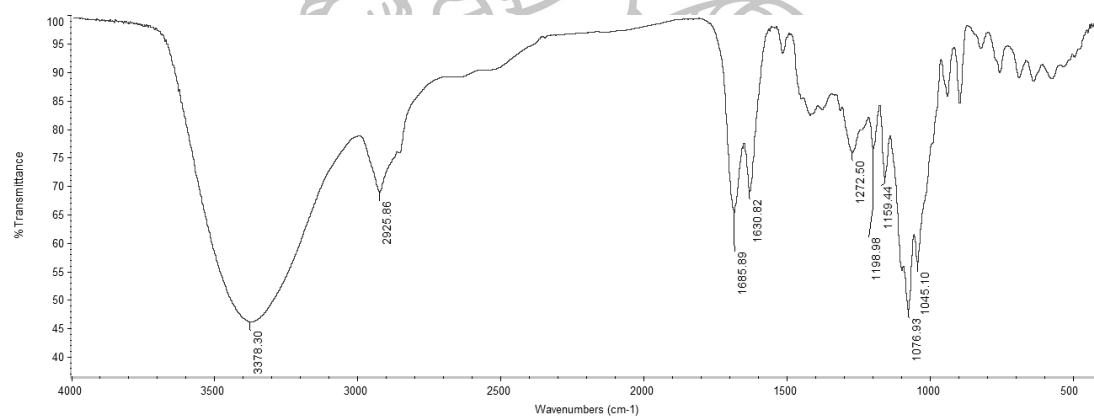


Figure 74 IR spectrum of geniposidic acid (dry film).

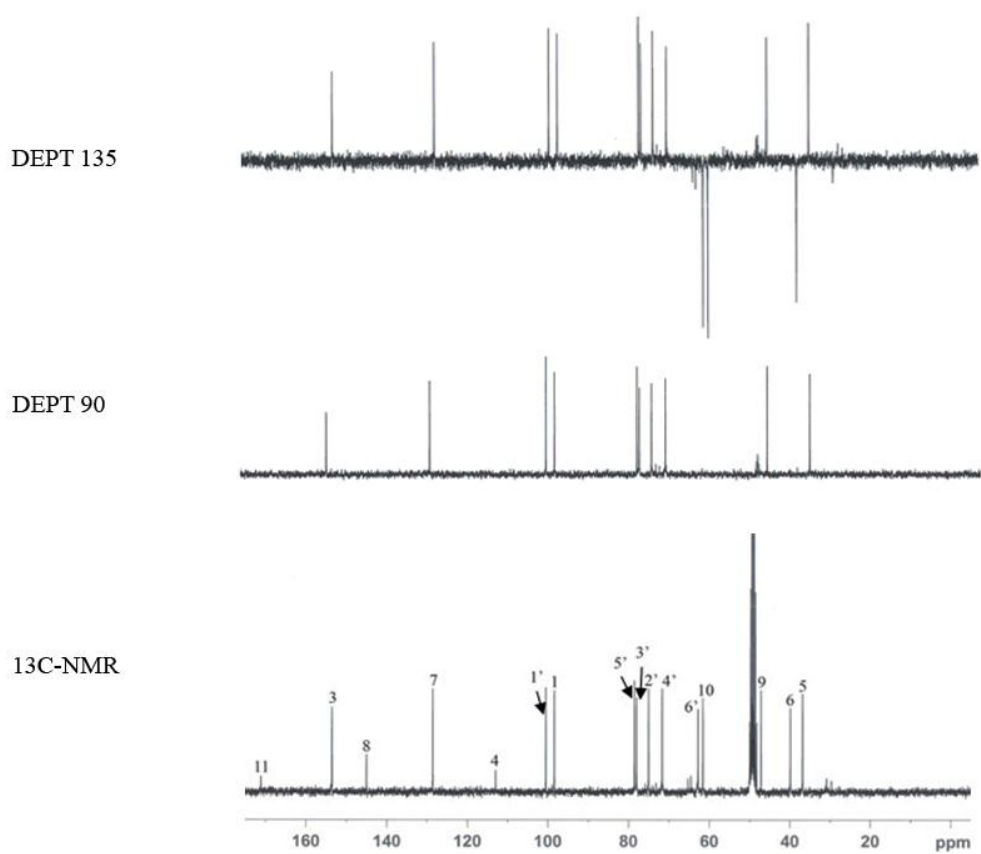


Figure 75 ¹³C-NMR, DEPT 90° and DEPT 135° spectrum (75 MHz) of geniposidic acid (in CD₃OD).

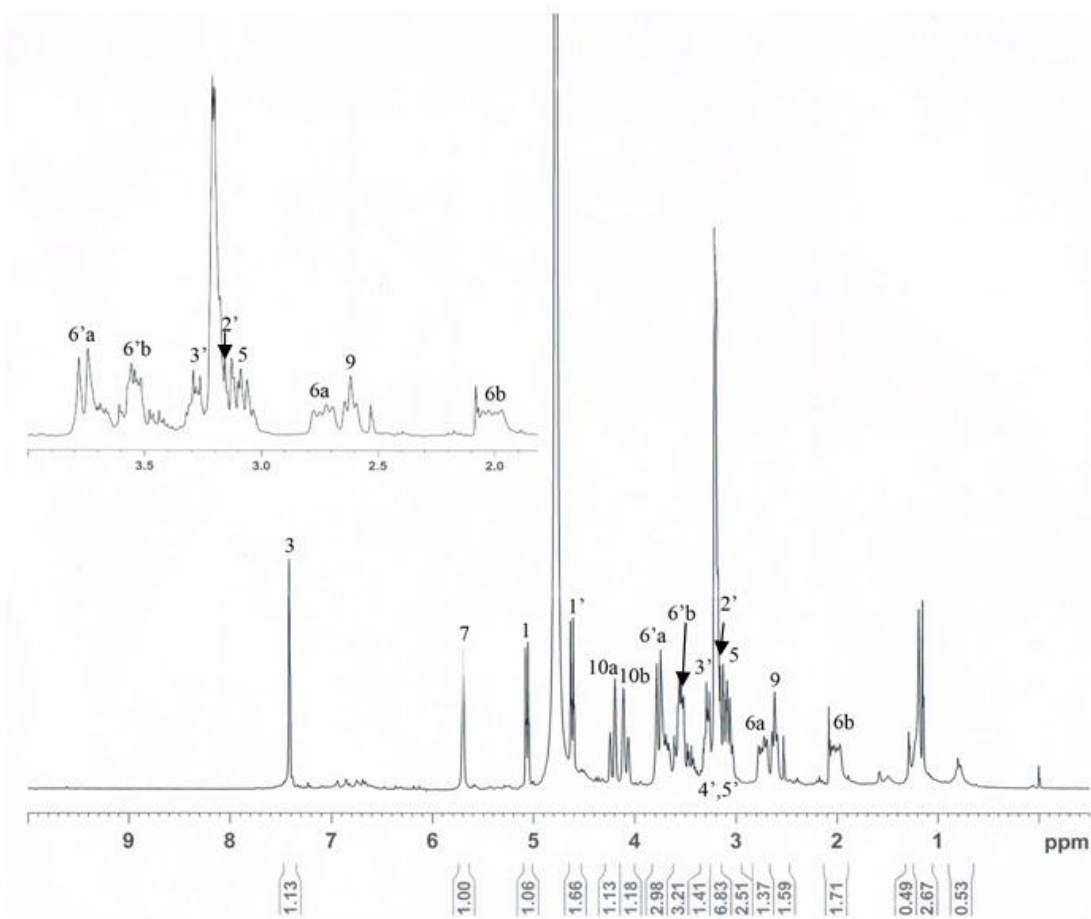


Figure 76 $^1\text{H-NMR}$ spectrum (300 MHz) of geniposidic acid (in CD_3OD).

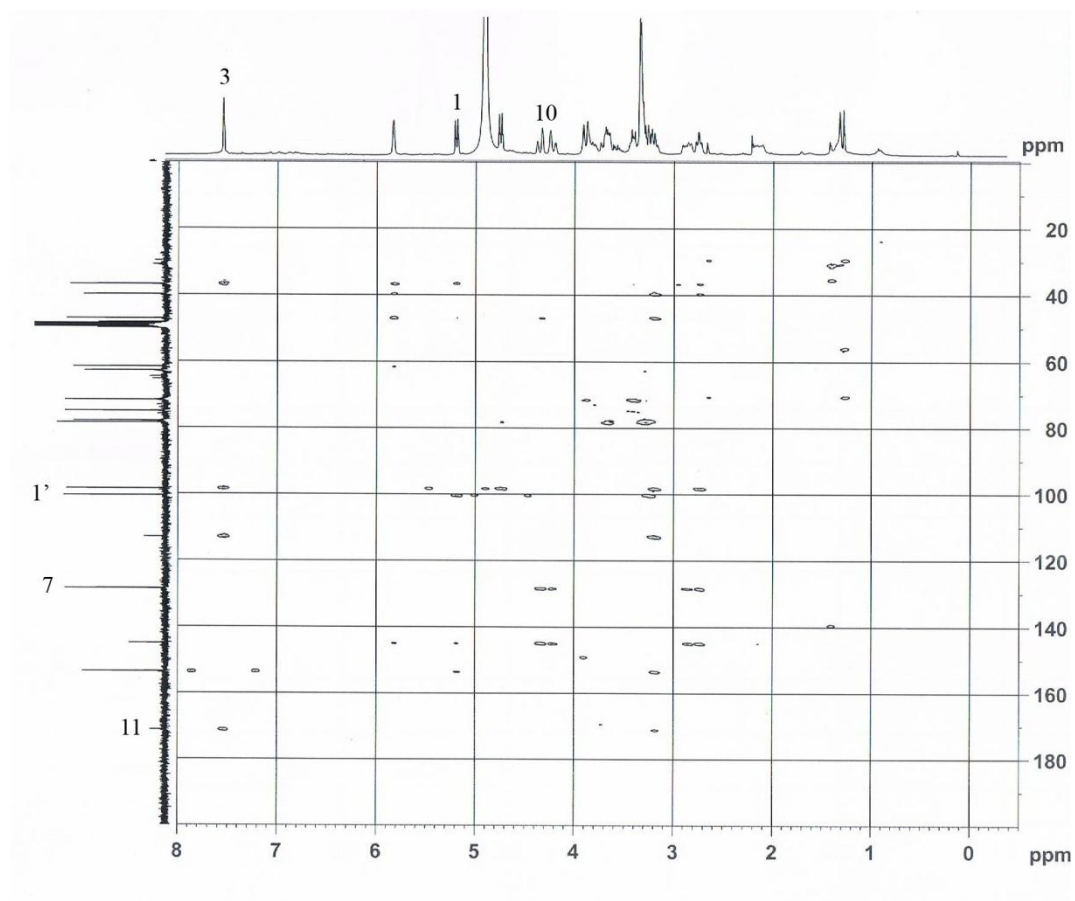


Figure 77 HMBC spectrum of geniposidic acid (in CD₃OD).

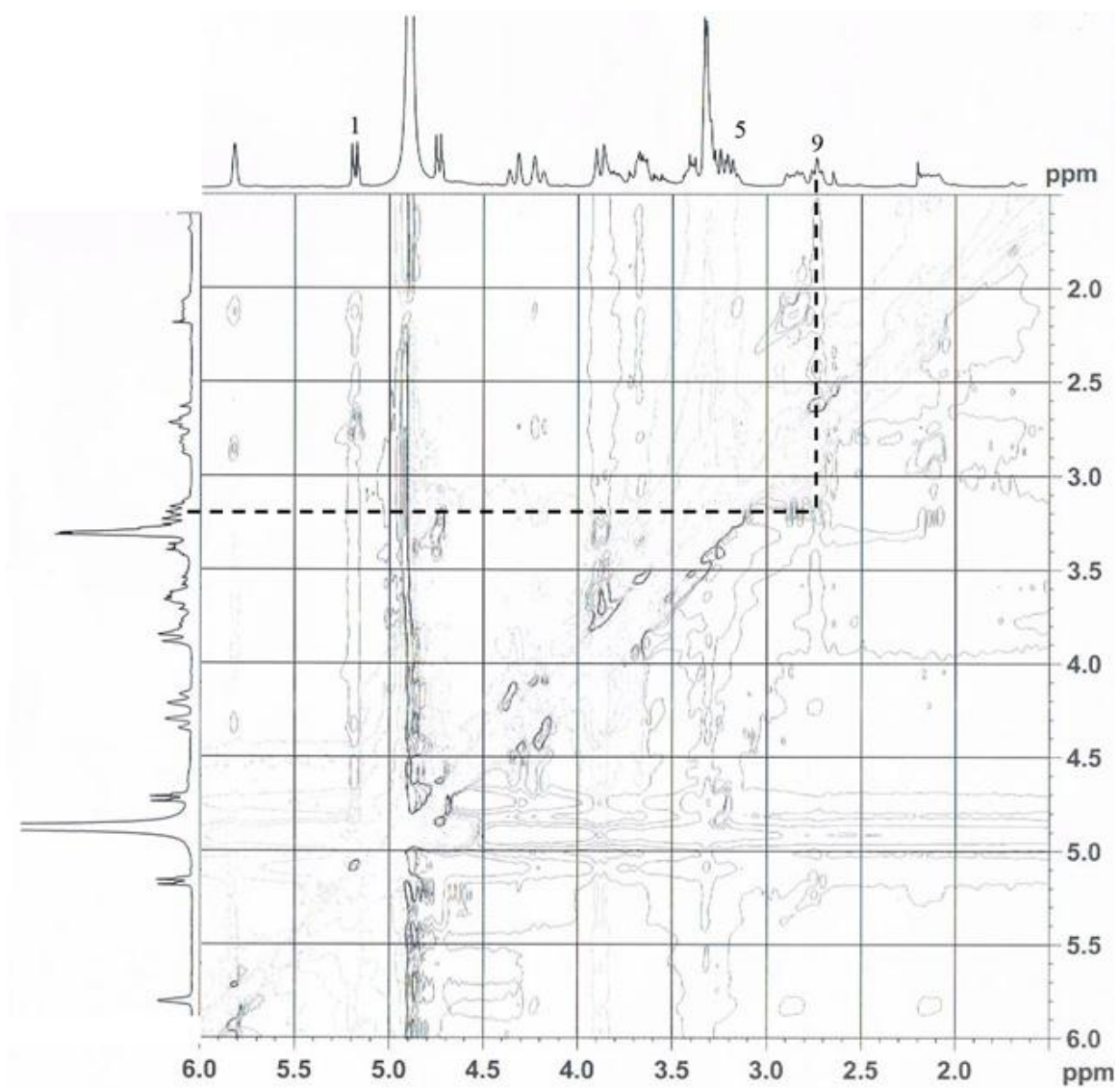


Figure 78 NOSEY spectrum of geniposidic acid (in CD₃OD).

APPENDIX C
IR spectra of Chan-thet, Chan-khao, Chan-chamot, Chan-thana,
Chan-hom and authentic samples



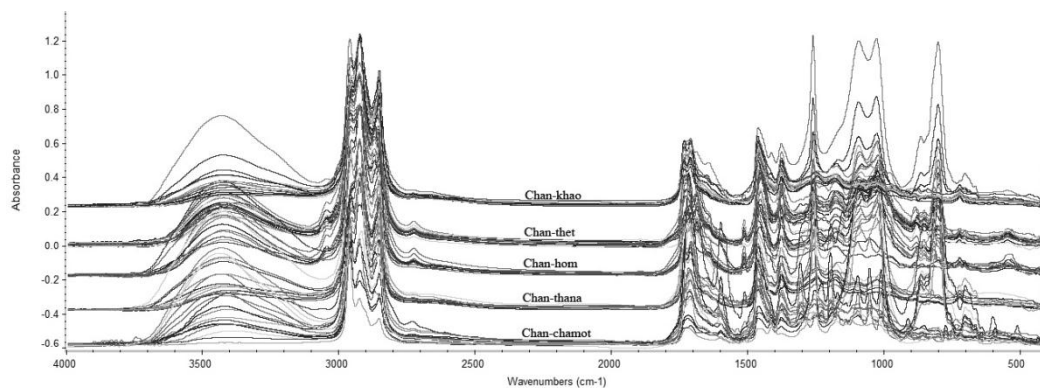


Figure 79 IR spectra of the *n*-hexane extracts of Chan-thet, Chan-khao, Chan-chamot, Chan-thana and Chan-hom samples after normalization preprocessing.

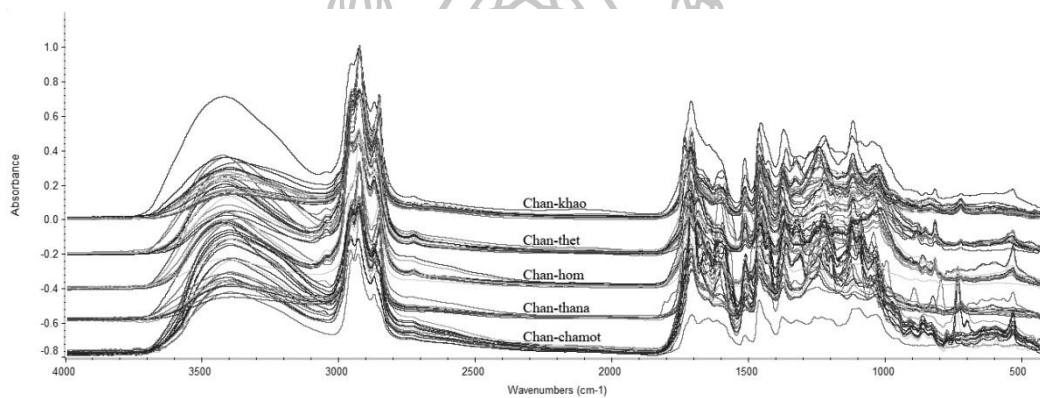


Figure 80 IR spectra of the dichloromethane extracts of Chan-thet, Chan-khao, Chan-chamot, Chan-thana and Chan-hom samples after normalization preprocessing.

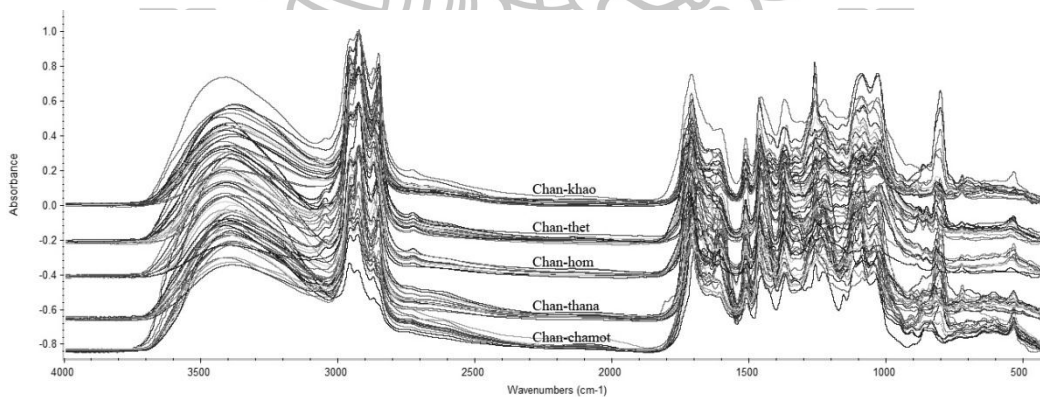


Figure 81 IR spectra of the ethyl acetate extracts of Chan-thet, Chan-khao, Chan-chamot, Chan-thana and Chan-hom samples after normalization preprocessing.

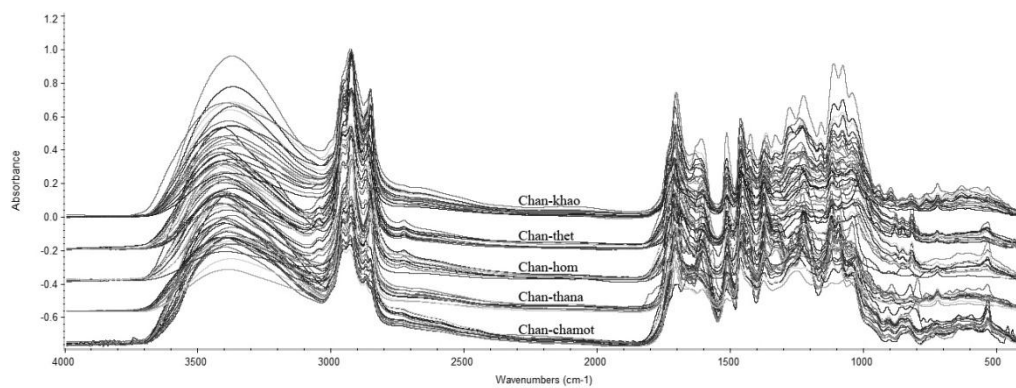


Figure 82 IR spectra of the acetone extracts of Chan-thet, Chan-khao, Chan-chamot, Chan-thana and Chan-hom samples after normalization preprocessing.

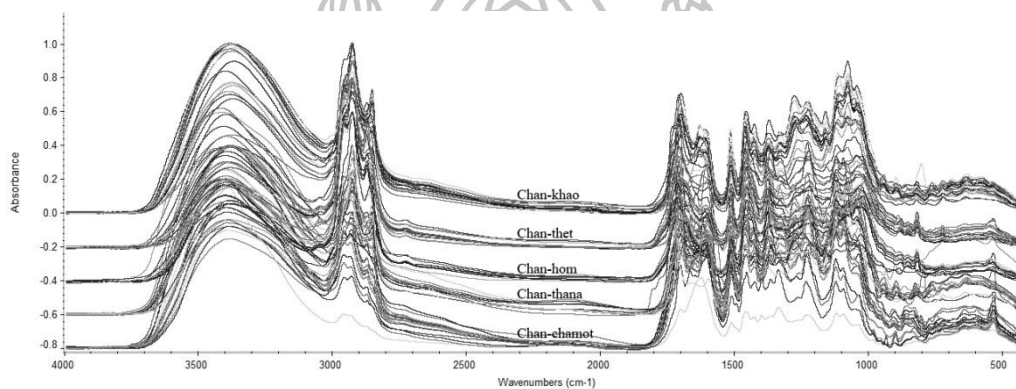


Figure 83 IR spectra of the methanol extracts of Chan-thet, Chan-khao, Chan-chamot, Chan-thana and Chan-hom samples after normalization preprocessing.

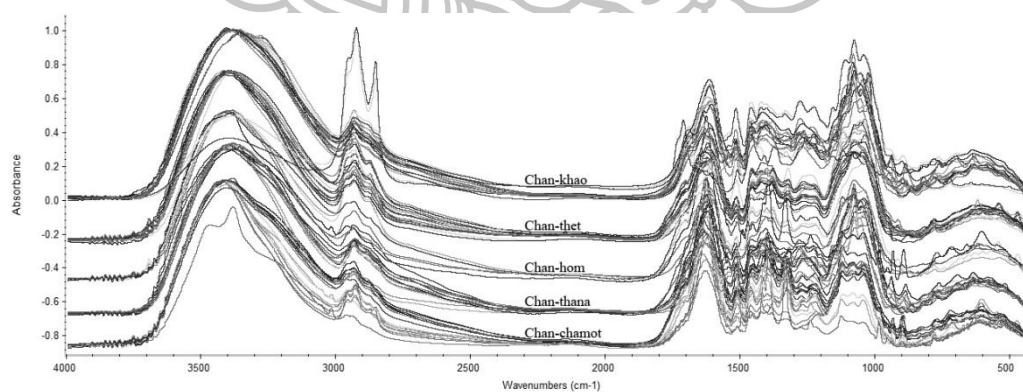


Figure 84 IR spectra of the water extracts of Chan-thet, Chan-khao, Chan-chamot, Chan-thana and Chan-hom after samples normalization preprocessing.

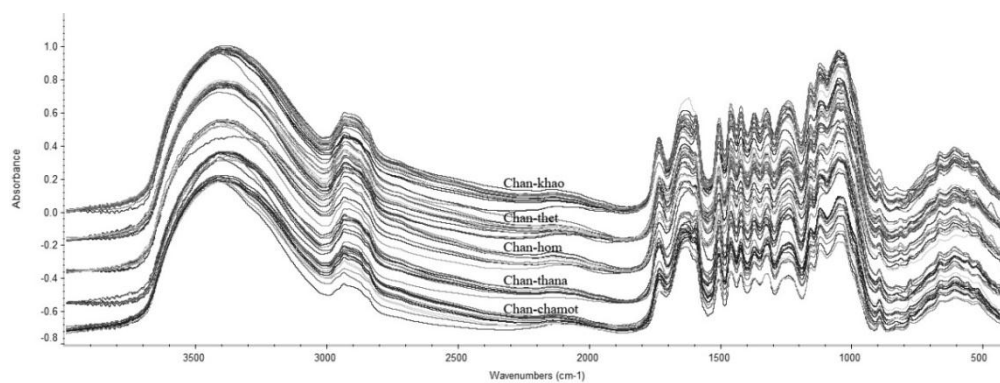


Figure 85 IR spectra of the fine powders of Chan-thet, Chan-khao, Chan-chamot, Chan-thana and Chan-hom samples after normalization preprocessing.

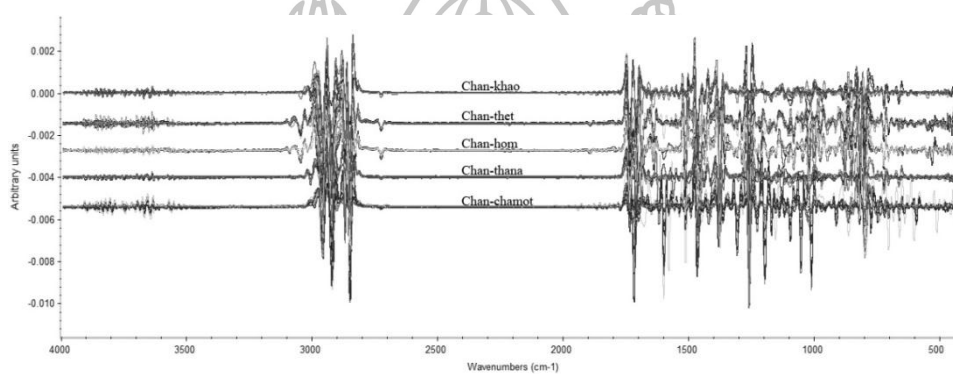


Figure 86 IR spectra of the *n*-hexane extracts of Chan-thet, Chan-khao, Chan-chamot, Chan-thana and Chan-hom samples after normalization and second derivative preprocessing.

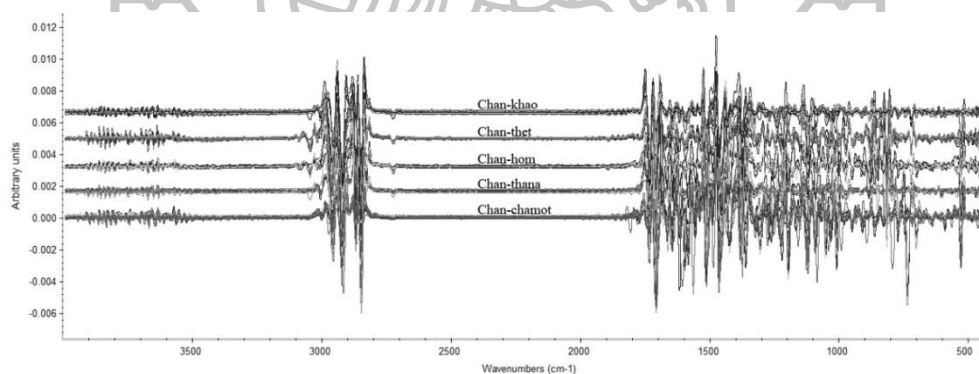


Figure 87 IR spectra of the dichloromethane extracts of Chan-thet, Chan-khao, Chan-chamot, Chan-thana and Chan-hom samples after normalization and second derivative preprocessing.

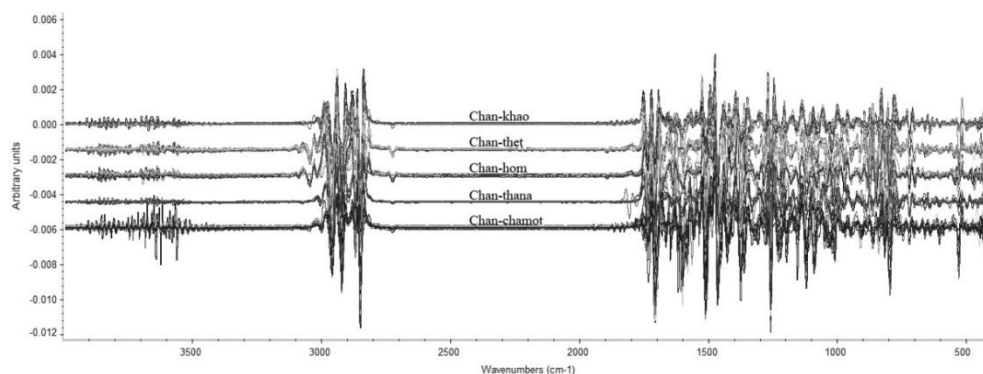


Figure 88 IR spectra of the ethyl acetate extracts of Chan-thet, Chan-khao, Chan-chamot, Chan-thana and Chan-hom samples after normalization and second derivative preprocessing.

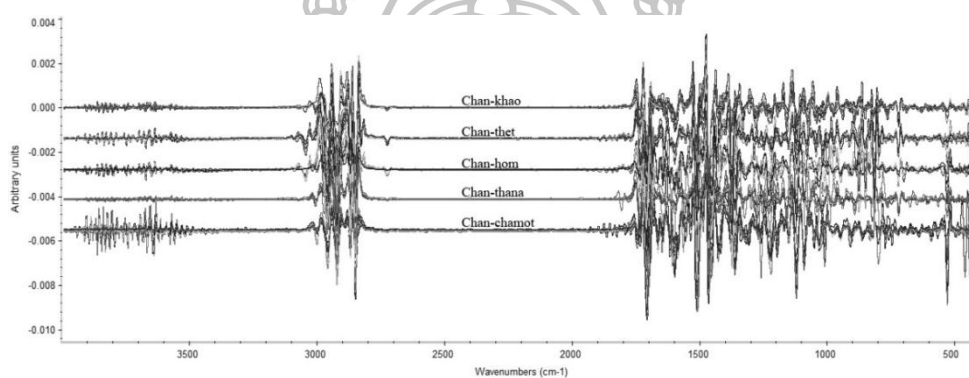


Figure 89 IR spectra of the acetone extracts of Chan-thet, Chan-khao, Chan-chamot, Chan-thana and Chan-hom samples after normalization and second derivative preprocessing.

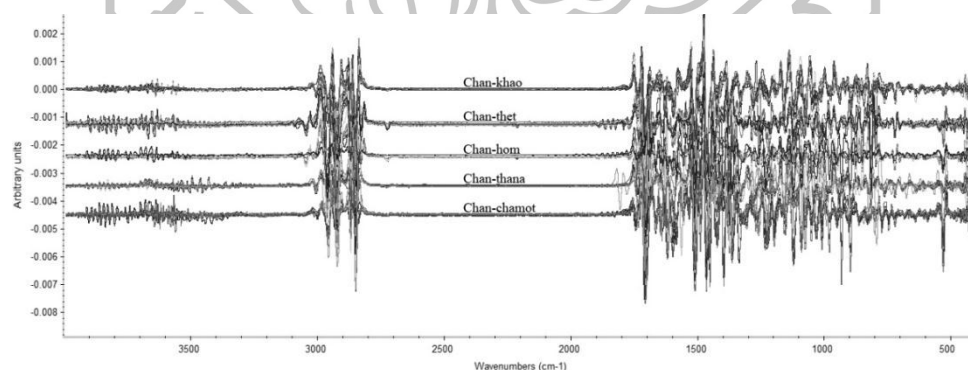


Figure 90 IR spectra of the methanol extracts of Chan-thet, Chan-khao, Chan-chamot, Chan-thana and Chan-hom samples after normalization and second derivative preprocessing.

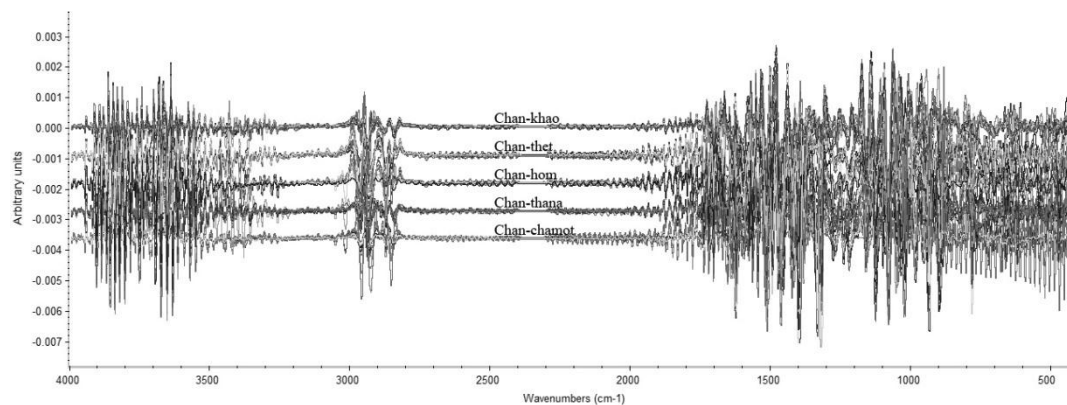


Figure 91 IR spectra of the water extracts of Chan-thet, Chan-khao, Chan-chamot, Chan-thana and Chan-hom samples after normalization and second derivative preprocessing.

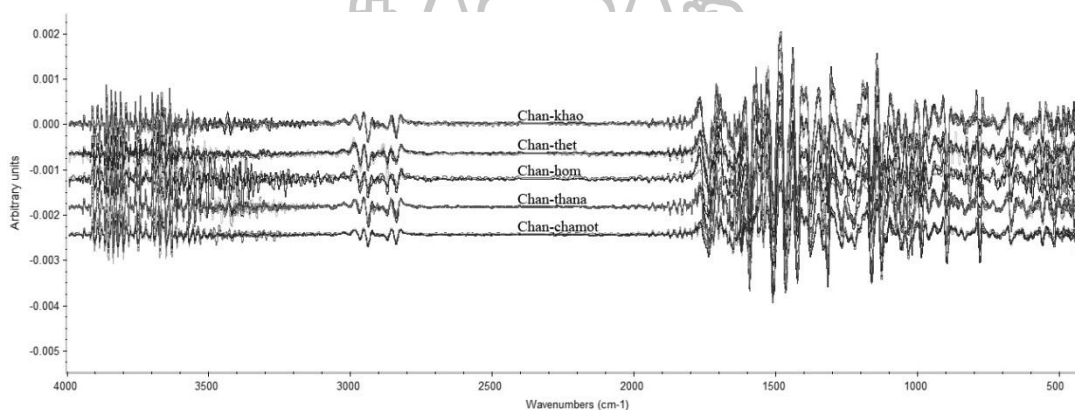


Figure 92 IR spectra of the fine powders of Chan-thet, Chan-khao, Chan-chamot, Chan-thana and Chan-hom samples after normalization and second derivative preprocessing.

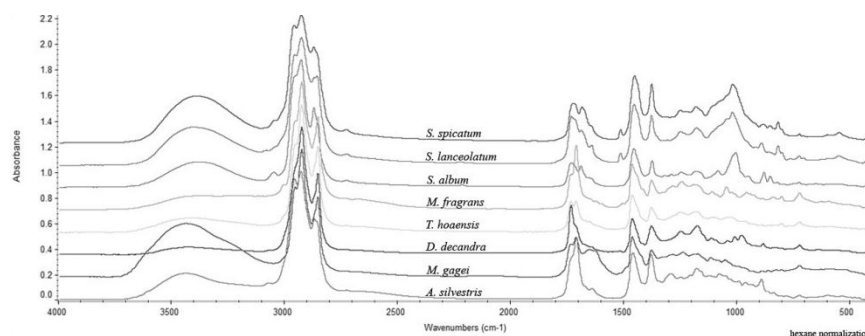


Figure 93 IR spectra of the *n*-hexane extracts of *S. album*, *S. spicatum*, *S. lanceolatum*, *M. fragrans*, *T. hoensis*, *D. decandra*, *M. gagei* and *A. silvestris* after normalization preprocessing.

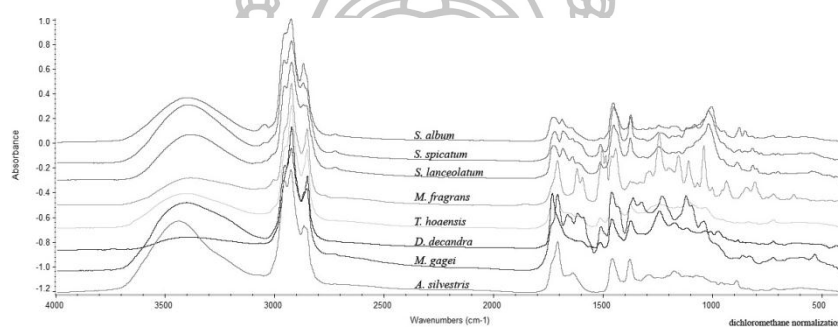


Figure 94 IR spectra of the dichloromethane extracts of *S. album*, *S. spicatum*, *S. lanceolatum*, *M. fragrans*, *T. hoensis*, *D. decandra*, *M. gagei* and *A. silvestris* after normalization preprocessing.

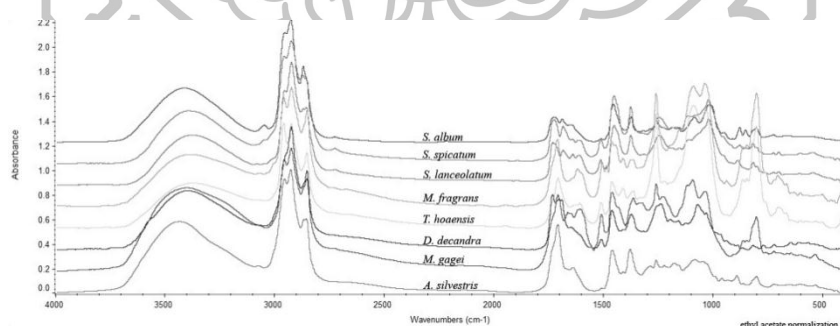


Figure 95 IR spectra of the ethyl acetate extracts of *S. album*, *S. spicatum*, *S. lanceolatum*, *M. fragrans*, *T. hoensis*, *D. decandra*, *M. gagei* and *A. silvestris* after normalization preprocessing.

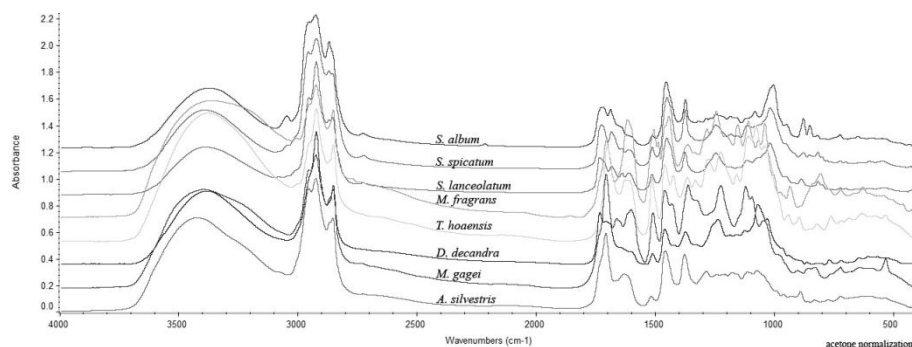


Figure 96 IR spectra of the acetone extracts of *S. album*, *S. spicatum*, *S. lanceolatum*, *M. fragrans*, *T. hoensis*, *D. decandra*, *M. gagei* and *A. silvestris* after normalization preprocessing.

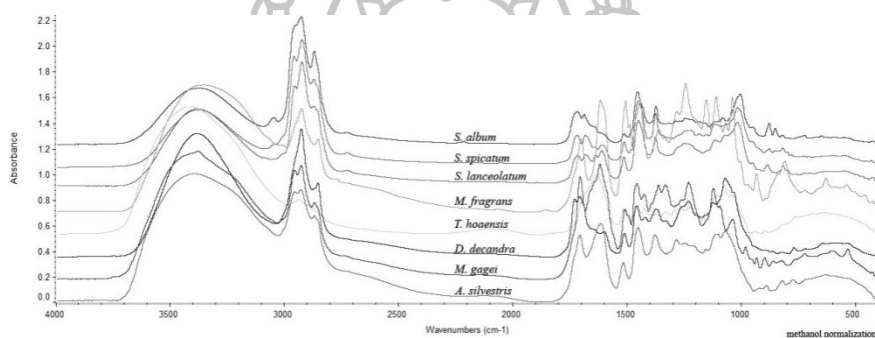


Figure 97 IR spectra of the methanol extracts of *S. album*, *S. spicatum*, *S. lanceolatum*, *M. fragrans*, *T. hoensis*, *D. decandra*, *M. gagei* and *A. silvestris* after normalization preprocessing.

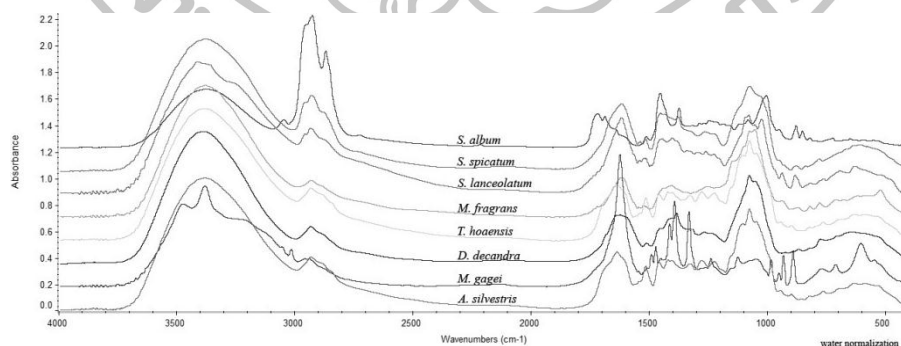


Figure 98 IR spectra of the water extracts of *S. album*, *S. spicatum*, *S. lanceolatum*, *M. fragrans*, *T. hoensis*, *D. decandra*, *M. gagei* and *A. silvestris* after normalization preprocessing.

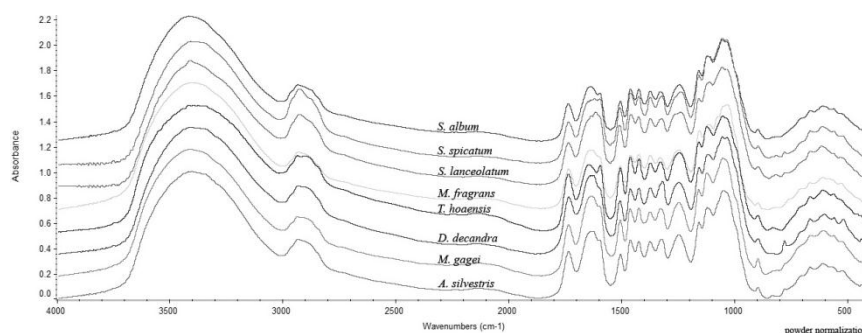


Figure 99 IR spectra of the fine powders of *S. album*, *S. spicatum*, *S. lanceolatum*, *M. fragrans*, *T. hoensis*, *D. decandra*, *M. gagei* and *A. silvestris* after normalization preprocessing.

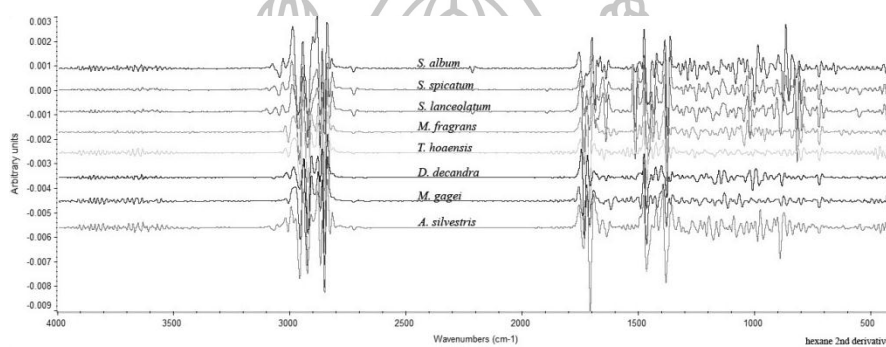


Figure 100 IR spectra of the *n*-hexane extracts of *S. album*, *S. spicatum*, *S. lanceolatum*, *M. fragrans*, *T. hoensis*, *D. decandra*, *M. gagei* and *A. silvestris* after normalization and second derivative preprocessing.

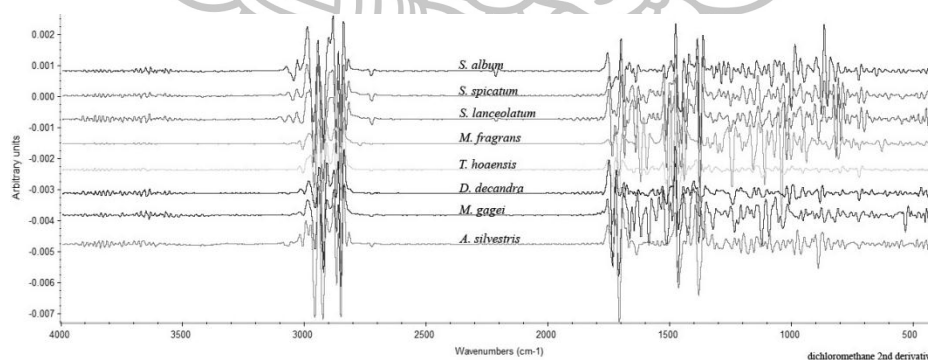


Figure 101 IR spectra of the dichloromethane extracts of *S. album*, *S. spicatum*, *S. lanceolatum*, *M. fragrans*, *T. hoensis*, *D. decandra*, *M. gagei* and *A. silvestris* after normalization and second derivative preprocessing.

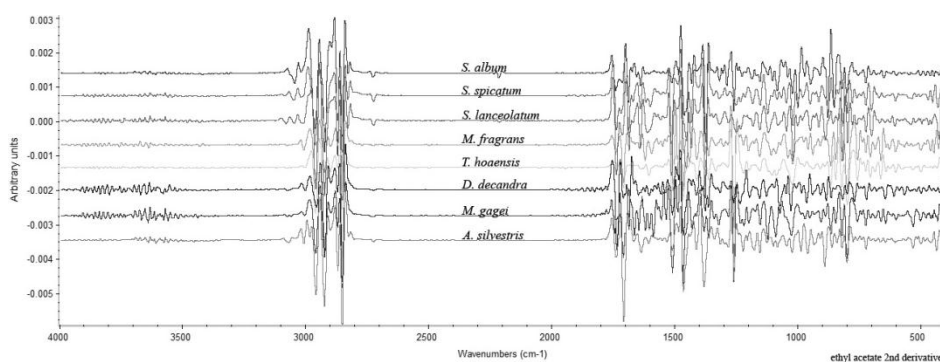


Figure 102 IR spectra of the ethyl acetate extracts of *S. album*, *S. spicatum*, *S. lanceolatum*, *M. fragrans*, *T. hoensis*, *D. decandra*, *M. gagei* and *A. silvestris* after normalization and second derivative preprocessing.

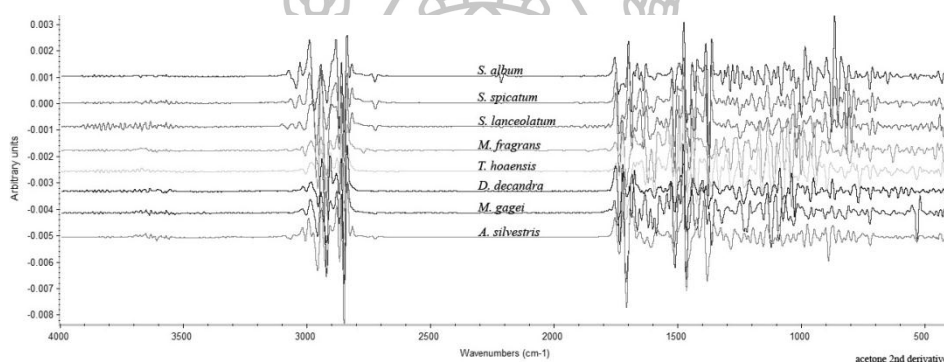


Figure 103 IR spectra of the acetone extracts of *S. album*, *S. spicatum*, *S. lanceolatum*, *M. fragrans*, *T. hoensis*, *D. decandra*, *M. gagei* and *A. silvestris* after normalization and second derivative preprocessing.

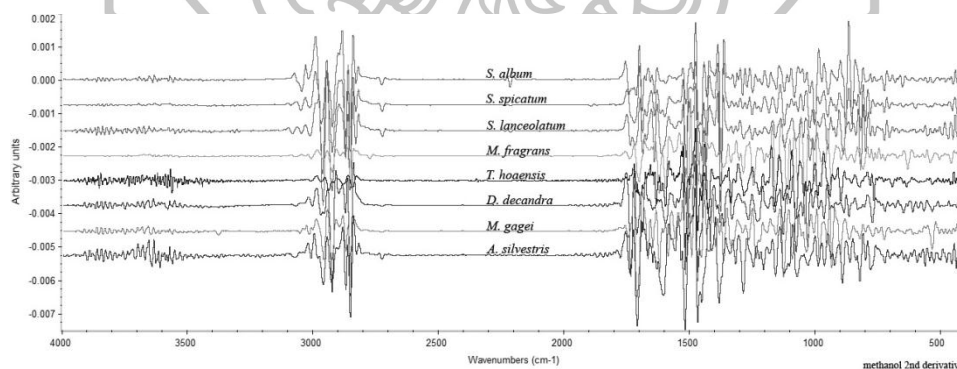


Figure 104 IR spectra of the methanol extracts of *S. album*, *S. spicatum*, *S. lanceolatum*, *M. fragrans*, *T. hoensis*, *D. decandra*, *M. gagei* and *A. silvestris* after normalization and second derivative preprocessing.

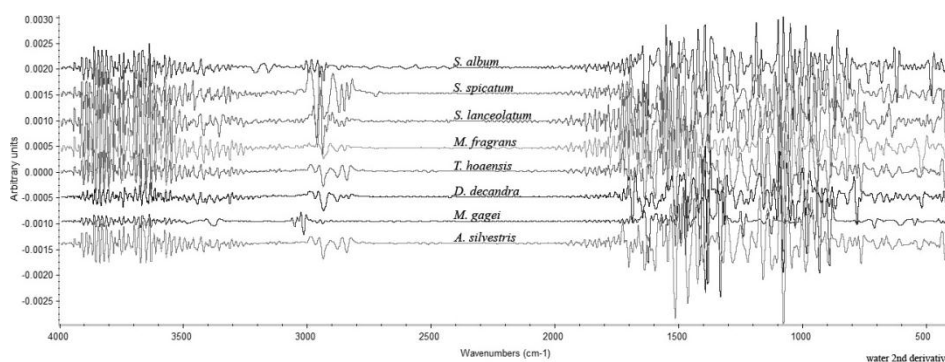


Figure 105 IR spectra of the water extracts of *S. album*, *S. spicatum*, *S. lanceolatum*, *M. fragrans*, *T. hoensis*, *D. decandra*, *M. gagei* and *A. silvestris* after normalization and second derivative preprocessing.

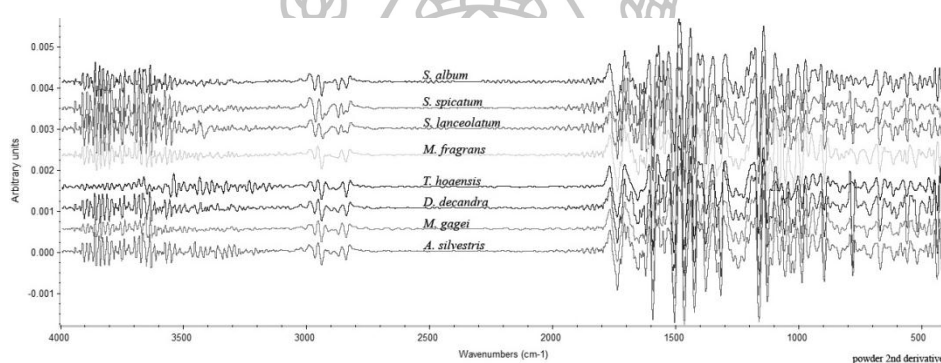
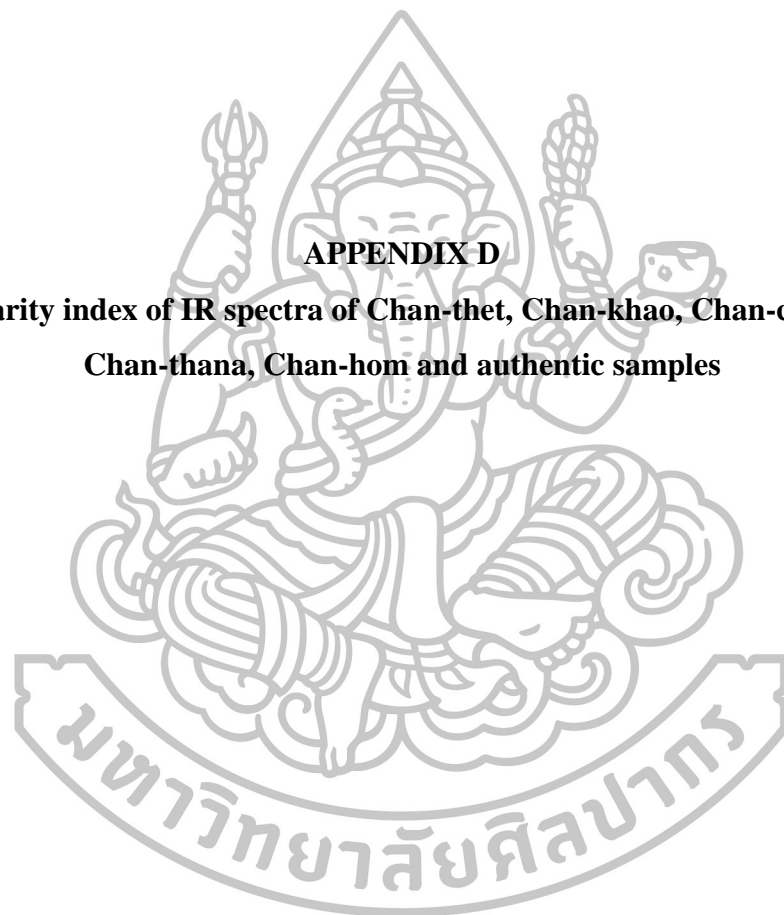


Figure 106 IR spectra of the fine powders of *S. album*, *S. spicatum*, *S. lanceolatum*, *M. fragrans*, *T. hoensis*, *D. decandra*, *M. gagei* and *A. silvestris* after normalization and second derivative preprocessing.



APPENDIX D

**Similarity index of IR spectra of Chan-thet, Chan-khao, Chan-chamot,
Chan-thana, Chan-hom and authentic samples**

Table 42 Similarity index between the IR spectra of the *n*-hexane extracts of Chan-thet and authentic samples.

H	Preprocessing method															
	Normalization								Normalization and second derivative							
	SA	SS	SL	MF	MG	AS	TH	DD	SA	SS	SL	MF	MG	AS	TH	DD
T1	0.81	0.91	0.90	0.61	0.49	0.70	0.70	0.66	0.64	0.80	0.78	0.26	0.36	0.31	0.51	0.50
T2	0.83	0.93	0.93	0.65	0.55	0.75	0.74	0.71	0.65	0.87	0.86	0.31	0.41	0.38	0.55	0.53
T3	0.75	0.85	0.85	0.57	0.48	0.64	0.65	0.59	0.51	0.65	0.63	0.19	0.26	0.22	0.41	0.39
T4	0.95	0.96	0.93	0.63	0.53	0.72	0.72	0.67	0.94	0.83	0.72	0.18	0.28	0.24	0.33	0.38
T5	0.76	0.85	0.86	0.60	0.49	0.67	0.68	0.63	0.48	0.61	0.68	0.29	0.37	0.33	0.52	0.48
T6	0.94	0.97	0.99	0.77	0.71	0.87	0.86	0.82	0.87	0.92	0.87	0.27	0.41	0.36	0.51	0.57
T7	0.85	0.91	0.88	0.53	0.42	0.61	0.62	0.56	0.79	0.79	0.71	0.14	0.24	0.20	0.34	0.34
T8	0.86	0.94	0.93	0.63	0.50	0.71	0.71	0.67	0.73	0.91	0.87	0.24	0.34	0.32	0.48	0.51
T9	0.90	0.96	0.97	0.73	0.64	0.81	0.81	0.77	0.76	0.91	0.88	0.26	0.38	0.33	0.51	0.54
T10	0.91	0.96	0.98	0.78	0.70	0.87	0.85	0.82	0.75	0.92	0.91	0.34	0.44	0.40	0.56	0.56
T11	0.91	0.97	0.98	0.76	0.67	0.85	0.84	0.81	0.71	0.93	0.93	0.35	0.46	0.43	0.60	0.61
T12	0.94	0.99	0.99	0.77	0.68	0.86	0.85	0.82	0.76	0.97	0.93	0.27	0.39	0.38	0.50	0.55
T13	0.92	0.97	0.99	0.80	0.72	0.89	0.88	0.85	0.77	0.95	0.95	0.36	0.48	0.45	0.60	0.64
T14	0.93	0.93	0.97	0.85	0.81	0.93	0.92	0.89	0.82	0.90	0.90	0.39	0.53	0.46	0.64	0.68
T15	0.88	0.94	0.97	0.79	0.72	0.86	0.88	0.84	0.59	0.78	0.84	0.49	0.62	0.54	0.78	0.73

H = *n*-Hexane extract, SA = *S. album*, SS = *S. spicatum*, SL = *S. lanceolatum*, MF = *M. fragrans*, AS = *A. silvestris*, TH = *T. hoaensis*, DD = *D. decandra* and T1-T15 = Chan-thet samples.

Table 43 Similarity index between the IR spectra of the dichloromethane extracts of Chan-thet and authentic samples.

D	Preprocessing method															
	Normalization								Normalization and second derivative							
	SA	SS	SL	MF	MG	AS	TH	DD	SA	SS	SL	MF	MG	AS	TH	DD
T1	0.88	0.95	0.96	0.61	0.74	0.78	0.88	0.78	0.76	0.93	0.90	0.18	0.42	0.54	0.69	0.62
T2	0.87	0.94	0.95	0.63	0.76	0.79	0.89	0.81	0.68	0.89	0.85	0.22	0.51	0.55	0.68	0.56
T3	0.88	0.93	0.94	0.62	0.77	0.83	0.90	0.82	0.73	0.88	0.84	0.22	0.51	0.59	0.69	0.55
T4	0.91	0.93	0.93	0.47	0.51	0.61	0.69	0.62	0.93	0.88	0.81	0.16	0.16	0.31	0.41	0.44
T5	0.93	0.94	0.96	0.63	0.77	0.85	0.90	0.83	0.78	0.90	0.96	0.15	0.33	0.50	0.63	0.68
T6	0.90	0.92	0.92	0.60	0.79	0.88	0.91	0.82	0.80	0.88	0.83	0.22	0.47	0.57	0.67	0.55
T7	0.93	0.98	0.98	0.56	0.64	0.67	0.78	0.67	0.91	0.94	0.89	0.12	0.21	0.34	0.48	0.48
T8	0.90	0.95	0.96	0.64	0.77	0.81	0.89	0.81	0.76	0.95	0.90	0.20	0.41	0.49	0.63	0.56
T9	0.87	0.93	0.94	0.63	0.78	0.83	0.90	0.82	0.63	0.78	0.75	0.22	0.60	0.62	0.72	0.48
T10	0.85	0.88	0.90	0.62	0.79	0.86	0.91	0.86	0.53	0.67	0.64	0.22	0.63	0.62	0.69	0.41
T11	0.86	0.90	0.92	0.65	0.80	0.85	0.91	0.85	0.55	0.72	0.71	0.21	0.64	0.60	0.72	0.49
T12	0.87	0.92	0.93	0.63	0.78	0.83	0.90	0.84	0.63	0.83	0.81	0.21	0.56	0.59	0.69	0.50
T13	0.84	0.88	0.90	0.63	0.79	0.87	0.91	0.86	0.50	0.65	0.63	0.24	0.65	0.65	0.70	0.40
T14	0.80	0.87	0.87	0.68	0.91	0.86	0.93	0.81	0.54	0.65	0.61	0.27	0.80	0.64	0.81	0.48
T15	0.86	0.93	0.94	0.73	0.85	0.80	0.95	0.83	0.67	0.82	0.80	0.22	0.64	0.55	0.84	0.69

D = Dichloromethane extract, SA = *S. album*, SS = *S. spicatum*, SL = *S. lanceolatum*, MF = *M. fragrans*, AS = *A. silvestris*, TH = *T. hoaensis*, DD = *D. decandra* and T1-T15 = Chan-thet samples.

Table 44 Similarity index between the IR spectra of the ethyl acetate extracts of Chan-thet and authentic samples.

E	Preprocessing method															
	Normalization								Normalization and second derivative							
	SA	SS	SL	MF	MG	AS	TH	DD	SA	SS	SL	MF	MG	AS	TH	DD
T1	0.86	0.90	0.89	0.59	0.84	0.93	0.56	0.93	0.62	0.78	0.78	0.42	0.64	0.69	0.37	0.51
T2	0.85	0.95	0.94	0.69	0.83	0.87	0.66	0.90	0.63	0.88	0.86	0.31	0.53	0.54	0.27	0.52
T3	0.85	0.95	0.94	0.67	0.82	0.89	0.64	0.91	0.68	0.87	0.84	0.31	0.48	0.55	0.26	0.50
T4	0.93	0.96	0.94	0.65	0.70	0.73	0.62	0.74	0.87	0.85	0.78	0.16	0.19	0.25	0.12	0.40
T5	0.92	0.95	0.94	0.80	0.83	0.85	0.78	0.86	0.77	0.81	0.84	0.56	0.58	0.57	0.56	0.58
T6	0.86	0.93	0.92	0.64	0.81	0.91	0.61	0.91	0.69	0.80	0.79	0.34	0.50	0.59	0.28	0.50
T7	0.91	0.86	0.87	0.86	0.77	0.67	0.86	0.68	0.87	0.74	0.69	0.63	0.50	0.38	0.67	0.36
T8	0.88	0.96	0.95	0.74	0.87	0.88	0.71	0.89	0.72	0.85	0.83	0.56	0.69	0.58	0.56	0.52
T9	0.88	0.95	0.95	0.74	0.84	0.87	0.72	0.90	0.76	0.89	0.86	0.47	0.57	0.57	0.45	0.50
T10	0.85	0.93	0.93	0.68	0.83	0.89	0.66	0.92	0.69	0.86	0.86	0.39	0.57	0.58	0.36	0.56
T11	0.85	0.92	0.92	0.69	0.87	0.91	0.67	0.93	0.62	0.74	0.76	0.59	0.77	0.67	0.59	0.55
T12	0.88	0.98	0.97	0.71	0.86	0.83	0.69	0.88	0.69	0.93	0.91	0.30	0.50	0.49	0.26	0.54
T13	0.85	0.93	0.92	0.66	0.86	0.91	0.63	0.93	0.65	0.81	0.82	0.48	0.70	0.62	0.46	0.58
T14	0.82	0.91	0.92	0.81	0.93	0.85	0.79	0.89	0.66	0.68	0.69	0.71	0.87	0.67	0.72	0.52
T15	0.89	0.95	0.95	0.85	0.89	0.83	0.82	0.85	0.72	0.79	0.78	0.65	0.76	0.61	0.67	0.61

E = Ethyl acetate extract, SA = *S. album*, SS = *S. spicatum*, SL = *S. lanceolatum*, MF = *M. fragrans*, AS = *A. silvestris*, TH = *T. hoaensis*, DD = *D. decandra* and T1-T15 = Chan-thet samples.

Table 45 Similarity index between the IR spectra of the acetone extracts of Chan-thet and authentic samples.

A	Preprocessing method															
	Normalization								Normalization and second derivative							
	SA	SS	SL	MF	MG	AS	TH	DD	SA	SS	SL	MF	MG	AS	TH	DD
T1	0.90	0.96	0.95	0.72	0.77	0.82	0.87	0.90	0.73	0.89	0.85	0.32	0.50	0.60	0.52	0.52
T2	0.89	0.95	0.95	0.75	0.83	0.86	0.88	0.92	0.67	0.84	0.81	0.33	0.55	0.58	0.56	0.50
T3	0.88	0.93	0.93	0.76	0.86	0.89	0.87	0.91	0.60	0.71	0.71	0.38	0.70	0.64	0.66	0.50
T4	0.98	0.98	0.95	0.61	0.66	0.74	0.75	0.79	0.93	0.88	0.80	0.21	0.13	0.36	0.26	0.39
T5	0.94	0.98	0.98	0.74	0.80	0.86	0.84	0.88	0.77	0.91	0.94	0.28	0.36	0.58	0.44	0.60
T6	0.92	0.96	0.95	0.70	0.77	0.84	0.85	0.91	0.82	0.90	0.84	0.31	0.36	0.52	0.45	0.51
T7	0.96	0.98	0.96	0.67	0.69	0.72	0.79	0.79	0.91	0.91	0.84	0.22	0.20	0.40	0.34	0.40
T8	0.91	0.97	0.96	0.76	0.83	0.86	0.87	0.90	0.70	0.87	0.85	0.35	0.54	0.60	0.56	0.54
T9	0.89	0.94	0.94	0.75	0.84	0.89	0.87	0.92	0.68	0.81	0.79	0.35	0.60	0.64	0.58	0.48
T10	0.88	0.93	0.93	0.74	0.85	0.90	0.85	0.92	0.62	0.73	0.74	0.37	0.67	0.69	0.60	0.48
T11	0.88	0.93	0.93	0.72	0.82	0.88	0.84	0.91	0.59	0.73	0.74	0.35	0.66	0.64	0.61	0.51
T12	0.91	0.97	0.97	0.75	0.83	0.83	0.88	0.91	0.72	0.90	0.88	0.33	0.50	0.62	0.52	0.51
T13	0.86	0.91	0.92	0.74	0.85	0.91	0.87	0.93	0.58	0.70	0.71	0.38	0.72	0.72	0.64	0.48
T14	0.83	0.90	0.91	0.80	0.91	0.90	0.89	0.91	0.62	0.70	0.70	0.40	0.77	0.68	0.70	0.55
T15	0.91	0.91	0.97	0.79	0.84	0.87	0.86	0.88	0.70	0.83	0.82	0.36	0.57	0.64	0.59	0.62

A = Acetone extract, SA = *S. album*, SS = *S. spicatum*, SL = *S. lanceolatum*, MF = *M. fragrans*, AS = *A. silvestris*, TH = *T. hoaensis*, DD = *D. decandra* and T1-T15 = Chan-thet samples.

Table 46 Similarity index between the IR spectra of the methanol extracts of Chan-thet and authentic samples.

M	Preprocessing method															
	Normalization								Normalization and second derivative							
	SA	SS	SL	MF	MG	AS	TH	DD	SA	SS	SL	MF	MG	AS	TH	DD
T1	0.89	0.95	0.95	0.72	0.63	0.79	0.48	0.92	0.79	0.92	0.88	0.30	0.36	0.62	0.46	0.58
T2	0.88	0.94	0.94	0.75	0.66	0.82	0.51	0.95	0.73	0.88	0.87	0.31	0.43	0.64	0.50	0.61
T3	0.91	0.94	0.94	0.73	0.69	0.83	0.51	0.93	0.76	0.88	0.87	0.32	0.44	0.66	0.53	0.60
T4	0.97	0.98	0.94	0.58	0.47	0.64	0.34	0.78	0.94	0.90	0.84	0.19	0.03	0.41	0.29	0.36
T5	0.95	0.91	0.87	0.57	0.54	0.69	0.35	0.82	0.79	0.84	0.88	0.25	0.17	0.52	0.32	0.48
T6	0.92	0.95	0.94	0.72	0.65	0.80	0.47	0.92	0.84	0.90	0.88	0.30	0.36	0.62	0.50	0.60
T7	0.96	0.98	0.94	0.57	0.44	0.62	0.33	0.76	0.93	0.93	0.88	0.17	0.05	0.43	0.31	0.37
T8	0.94	0.97	0.95	0.69	0.61	0.78	0.46	0.90	0.81	0.96	0.92	0.24	0.19	0.55	0.37	0.48
T9	0.91	0.94	0.94	0.73	0.67	0.81	0.49	0.93	0.80	0.93	0.90	0.29	0.33	0.62	0.47	0.54
T10	0.91	0.93	0.92	0.71	0.66	0.80	0.45	0.93	0.76	0.89	0.88	0.30	0.42	0.66	0.47	0.59
T11	0.88	0.88	0.88	0.73	0.74	0.83	0.47	0.93	0.53	0.64	0.67	0.31	0.65	0.67	0.49	0.61
T12	0.93	0.97	0.96	0.72	0.62	0.77	0.43	0.90	0.78	0.95	0.92	0.27	0.31	0.60	0.44	0.53
T13	0.88	0.92	0.91	0.72	0.64	0.79	0.45	0.94	0.72	0.85	0.84	0.31	0.47	0.67	0.50	0.65
T14	0.80	0.80	0.83	0.77	0.84	0.90	0.59	0.92	0.52	0.56	0.59	0.34	0.75	0.69	0.53	0.68
T15	0.85	0.92	0.94	0.85	0.78	0.87	0.53	0.91	0.65	0.76	0.77	0.32	0.56	0.64	0.64	0.72

M = Methanol extract, SA = *S. album*, SS = *S. spicatum*, SL = *S. lanceolatum*, MF = *M. fragrans*, AS = *A. silvestris*, TH = *T. hoaensis*, DD = *D. decandra* and T1-T15 = Chan-thet samples.

Table 47 Similarity index between the IR spectra of the water extracts of Chan-thet and authentic samples.

W	Preprocessing method															
	Normalization								Normalization and second derivative							
	SA	SS	SL	MF	MG	AS	TH	DD	SA	SS	SL	MF	MG	AS	TH	DD
T1	0.59	0.94	0.90	0.92	0.43	0.94	0.94	0.92	0.28	0.62	0.32	0.30	-0.02	0.60	0.60	0.61
T2	0.69	0.97	0.95	0.84	0.53	0.92	0.91	0.89	0.23	0.74	0.26	0.20	-0.11	0.54	0.54	0.49
T3	0.70	0.95	0.94	0.75	0.52	0.88	0.87	0.79	0.16	0.76	0.39	0.29	-0.05	0.68	0.68	0.52
T4	0.73	0.99	0.97	0.85	0.51	0.92	0.92	0.93	0.20	0.86	0.39	0.27	-0.14	0.54	0.54	0.60
T5	0.72	0.96	0.96	0.82	0.56	0.93	0.92	0.85	0.11	0.60	0.38	0.39	0.10	0.64	0.64	0.54
T6	0.73	0.97	0.96	0.78	0.55	0.90	0.89	0.83	0.19	0.82	0.39	0.28	-0.07	0.62	0.62	0.54
T7	0.71	0.98	0.95	0.86	0.56	0.92	0.92	0.94	0.18	0.89	0.43	0.32	-0.09	0.56	0.56	0.55
T8	0.73	0.99	0.97	0.85	0.53	0.92	0.92	0.92	0.22	0.84	0.38	0.33	-0.06	0.55	0.55	0.60
T9	0.65	0.97	0.94	0.83	0.47	0.93	0.92	0.86	0.17	0.75	0.29	0.20	-0.13	0.53	0.53	0.45
T10	0.78	0.99	0.97	0.81	0.58	0.90	0.90	0.91	0.24	0.82	0.36	0.28	-0.11	0.58	0.58	0.61
T11	0.78	0.97	0.95	0.81	0.61	0.88	0.88	0.92	0.25	0.82	0.33	0.30	-0.09	0.54	0.54	0.58
T12	0.73	0.99	0.97	0.85	0.55	0.92	0.92	0.92	0.22	0.85	0.40	0.36	-0.06	0.55	0.55	0.59
T13	0.76	0.95	0.93	0.77	0.62	0.86	0.85	0.85	0.27	0.81	0.36	0.31	-0.04	0.60	0.60	0.61
T14	0.78	0.98	0.97	0.83	0.59	0.91	0.90	0.90	0.13	0.71	0.40	0.57	0.10	0.72	0.72	0.73
T15	0.67	0.97	0.95	0.91	0.50	0.95	0.95	0.93	0.13	0.57	0.33	0.47	0.14	0.72	0.72	0.70

W = Water extract, SA = *S. album*, SS = *S. spicatum*, SL = *S. lanceolatum*, MF = *M. fragrans*, AS = *A. silvestris*, TH = *T. hoaensis*, DD = *D. decandra* and T1-T15 = Chan-thet samples.

Table 48 Similarity index between the IR spectra of the fine powders of Chan-thet and authentic samples.

P	Preprocessing method															
	Normalization								Normalization and second derivative							
	SA	SS	SL	MF	MG	AS	TH	DD	SA	SS	SL	MF	MG	AS	TH	DD
T1	0.99	0.99	0.99	0.99	0.99	1.00	0.99	1.00	0.98	0.99	0.98	0.94	0.98	0.97	0.97	0.96
T2	0.99	0.99	0.99	0.99	0.98	0.99	0.98	0.99	0.96	0.97	0.6	0.92	0.94	0.94	0.95	0.93
T3	0.99	0.99	0.99	0.99	0.99	0.99	0.99	0.99	0.97	0.99	0.98	0.93	0.96	0.95	0.97	0.95
T4	0.99	0.99	0.99	0.99	0.99	0.99	0.98	0.99	0.98	0.99	0.98	0.93	0.96	0.96	0.96	0.95
T5	1.00	0.99	0.99	1.00	0.99	0.99	0.99	0.99	0.99	0.99	0.97	0.95	0.98	0.98	0.98	0.96
T6	0.99	1.00	0.99	0.99	0.98	0.98	0.98	0.98	0.98	0.99	0.97	0.94	0.97	0.97	0.97	0.95
T7	0.99	1.00	0.99	0.99	0.99	0.99	0.99	0.99	0.98	0.99	0.98	0.94	0.97	0.97	0.97	0.96
T8	0.99	1.00	1.00	0.99	0.99	0.99	0.99	0.99	0.99	0.99	0.98	0.94	0.98	0.98	0.98	0.96
T9	0.96	0.97	0.98	0.98	0.98	0.98	0.98	0.99	0.97	0.99	0.98	0.93	0.96	0.95	0.96	0.95
T10	0.99	1.00	0.99	0.99	0.99	0.99	0.99	0.99	0.98	0.99	0.98	0.94	0.97	0.97	0.98	0.96
T11	0.99	0.99	1.00	0.99	0.99	0.99	0.99	0.99	0.98	1.00	0.98	0.94	0.97	0.97	0.97	0.97
T12	0.99	1.00	1.00	0.99	0.99	0.99	0.99	0.99	0.99	0.99	0.98	0.94	0.98	0.97	0.98	0.96
T13	0.99	1.00	1.00	0.99	0.98	0.99	0.99	0.99	0.98	0.99	0.98	0.94	0.97	0.97	0.98	0.96
T14	nd	nd	nd	nd	nd	nd	nd	nd	nd	nd	nd	nd	nd	nd	nd	nd
T15	1.00	0.99	0.99	1.00	0.99	0.99	0.99	0.99	0.99	0.98	0.96	0.96	0.98	0.98	0.98	0.96

P = Fine powder, SA = *S. album*, SS = *S. spicatum*, SL = *S. lanceolatum*, MF = *M. fragrans*, AS = *A. silvestris*, TH = *T. hoaensis*, DD = *D. decandra*, T1-T15 = Chan-thet samples and nd = not determined.

Table 49 Similarity index between the IR spectra of the *n*-hexane extracts of Chan-khao and authentic samples.

H	Preprocessing methods															
	Normalization								Normalization and second derivative							
	SA	SS	SL	MF	MG	AS	TH	DD	SA	SS	SL	MF	MG	AS	TH	DD
K1	0.59	0.69	0.71	0.51	0.45	0.55	0.58	0.50	0.21	0.32	0.39	0.42	0.43	0.37	0.56	0.39
K2	0.82	0.79	0.86	0.95	0.90	0.94	0.99	0.95	0.49	0.58	0.71	0.83	0.87	0.79	0.98	0.82
K3	0.85	0.81	0.87	0.95	0.85	0.93	0.99	0.94	0.47	0.57	0.69	0.85	0.86	0.78	0.98	0.81
K4	0.80	0.78	0.85	0.95	0.89	0.96	0.98	0.93	0.42	0.52	0.64	0.91	0.91	0.83	0.98	0.72
K5	0.51	0.64	0.63	0.39	0.30	0.45	0.46	0.41	0.17	0.27	0.31	0.26	0.27	0.23	0.40	0.29
K6	0.80	0.78	0.85	0.97	0.88	0.96	0.98	0.93	0.41	0.48	0.61	0.92	0.90	0.83	0.97	0.71
K7	0.80	0.77	0.84	0.93	0.90	0.94	0.98	0.94	0.45	0.56	0.69	0.80	0.86	0.79	0.98	0.84
K8	0.83	0.82	0.88	0.94	0.88	0.95	0.99	0.95	0.47	0.59	0.71	0.83	0.89	0.80	0.99	0.82
K9	0.86	0.85	0.90	0.93	0.89	0.94	0.99	0.94	0.52	0.63	0.74	0.80	0.86	0.77	0.97	0.83
K10	0.82	0.82	0.88	0.93	0.91	0.93	0.98	0.91	0.44	0.55	0.67	0.83	0.87	0.77	0.98	0.75
K11	0.81	0.78	0.86	0.95	0.87	0.94	0.97	0.95	0.46	0.55	0.68	0.86	0.88	0.81	0.98	0.78
K12	0.84	0.84	0.90	0.93	0.88	0.94	0.98	0.94	0.52	0.63	0.74	0.79	0.87	0.76	0.98	0.81
K13	0.85	0.84	0.86	0.85	0.87	0.85	0.93	0.82	0.55	0.62	0.69	0.74	0.85	0.68	0.92	0.75
K14	0.83	0.83	0.89	0.93	0.86	0.95	0.99	0.94	0.46	0.57	0.69	0.84	0.89	0.80	0.99	0.81
K15	0.85	0.85	0.90	0.93	0.85	0.95	0.99	0.94	0.46	0.57	0.69	0.86	0.90	0.80	0.99	0.77
K16	0.73	0.80	0.84	0.71	0.63	0.74	0.79	0.71	0.32	0.43	0.53	0.58	0.61	0.53	0.77	0.59
K17	0.82	0.80	0.87	0.95	0.88	0.94	0.99	0.95	0.47	0.56	0.68	0.81	0.85	0.74	0.98	0.84
K18	0.85	0.84	0.89	0.83	0.90	0.88	0.89	0.83	0.73	0.89	0.92	0.52	0.63	0.57	0.75	0.74

H = *n*-Hexane extract, SA = *S. album*, SS = *S. spicatum*, SL = *S. lanceolatum*, MF = *M. fragrans*, AS = *A. silvestris*, TH = *T. hoaensis*, DD = *D. decandra* and K1-K18 = Chan-khao samples.

Table 50 Similarity index between the IR spectra of the dichloromethane extracts of Chan-khao and authentic samples.

D	Preprocessing methods															
	Normalization								Normalization and second derivative							
	SA	SS	SL	MF	MG	AS	TH	DD	SA	SS	SL	MF	MG	AS	TH	DD
K1	0.76	0.78	0.80	0.75	0.91	0.88	0.98	0.90	0.48	0.51	0.53	0.28	0.81	0.67	0.96	0.67
K2	0.74	0.77	0.79	0.73	0.89	0.87	0.98	0.92	0.51	0.53	0.57	0.29	0.79	0.70	0.97	0.72
K3	0.75	0.77	0.80	0.71	0.86	0.88	0.96	0.94	0.51	0.54	0.59	0.30	0.76	0.72	0.94	0.76
K4	0.79	0.80	0.82	0.72	0.87	0.90	0.98	0.91	0.49	0.48	0.51	0.30	0.80	0.78	0.99	0.65
K5	0.78	0.76	0.77	0.67	0.89	0.93	0.94	0.85	0.54	0.51	0.54	0.28	0.74	0.78	0.95	0.71
K6	0.79	0.77	0.79	0.70	0.86	0.93	0.97	0.92	0.50	0.47	0.50	0.31	0.78	0.80	0.97	0.69
K7	0.77	0.81	0.81	0.76	0.92	0.88	0.99	0.88	0.47	0.52	0.53	0.27	0.82	0.72	0.98	0.67
K8	0.73	0.77	0.78	0.78	0.92	0.84	0.97	0.87	0.45	0.51	0.51	0.27	0.82	0.67	0.95	0.63
K9	0.73	0.79	0.80	0.74	0.88	0.83	0.96	0.92	0.52	0.58	0.62	0.27	0.76	0.63	0.93	0.77
K10	0.79	0.79	0.81	0.71	0.86	0.91	0.98	0.91	0.53	0.54	0.57	0.27	0.76	0.76	0.98	0.71
K11	0.72	0.69	0.73	0.68	0.79	0.85	0.92	0.96	0.49	0.49	0.57	0.28	0.66	0.66	0.87	0.81
K12	0.70	0.74	0.76	0.74	0.89	0.82	0.96	0.91	0.49	0.55	0.58	0.25	0.76	0.59	0.92	0.73
K13	0.73	0.76	0.78	0.72	0.88	0.83	0.95	0.93	0.55	0.58	0.63	0.24	0.70	0.58	0.89	0.81
K14	0.82	0.84	0.85	0.73	0.87	0.90	0.98	0.90	0.55	0.58	0.58	0.32	0.76	0.80	0.96	0.71
K15	0.77	0.82	0.83	0.75	0.91	0.88	0.98	0.87	0.45	0.48	0.49	0.31	0.80	0.74	0.95	0.61
K16	0.67	0.77	0.76	0.78	0.94	0.76	0.94	0.80	0.37	0.46	0.45	0.23	0.77	0.49	0.86	0.52
K17	0.73	0.68	0.72	0.68	0.78	0.83	0.89	0.97	0.51	0.51	0.60	0.21	0.55	0.55	0.80	0.92
K18	0.81	0.85	0.85	0.66	0.91	0.90	0.94	0.82	0.52	0.65	0.63	0.23	0.80	0.66	0.82	0.52

D = Dichloromethane extract, SA = *S. album*, SS = *S. spicatum*, SL = *S. lanceolatum*, MF = *M. fragrans*, AS = *A. silvestris*, TH = *T. hoensis*, DD = *D. decandra* and K1-K18 = Chan-khao samples.

Table 51 Similarity index between the IR spectra of the ethyl acetate extracts of Chan-khao and authentic samples.

E	Preprocessing methods															
	Normalization								Normalization and second derivative							
	SA	SS	SL	MF	MG	AS	TH	DD	SA	SS	SL	MF	MG	AS	TH	DD
K1	0.80	0.87	0.88	0.92	0.92	0.78	0.90	0.81	0.52	0.43	0.48	0.81	0.89	0.67	0.87	0.53
K2	0.78	0.88	0.88	0.74	0.93	0.87	0.71	0.94	0.48	0.49	0.56	0.59	0.83	0.72	0.60	0.67
K3	0.77	0.85	0.85	0.72	0.89	0.91	0.68	0.95	0.50	0.49	0.56	0.65	0.83	0.79	0.61	0.66
K4	0.77	0.88	0.88	0.70	0.87	0.88	0.68	0.92	0.41	0.50	0.56	0.33	0.65	0.68	0.32	0.66
K5	0.79	0.89	0.89	0.67	0.91	0.89	0.64	0.93	0.44	0.51	0.56	0.36	0.67	0.69	0.36	0.68
K6	0.76	0.88	0.87	0.67	0.89	0.90	0.64	0.93	0.41	0.46	0.52	0.41	0.71	0.70	0.39	0.61
K7	0.75	0.84	0.82	0.58	0.85	0.92	0.53	0.93	0.41	0.46	0.50	0.45	0.73	0.75	0.40	0.58
K8	0.74	0.87	0.85	0.59	0.87	0.89	0.53	0.91	0.47	0.60	0.63	0.34	0.68	0.67	0.29	0.67
K9	0.74	0.81	0.81	0.65	0.89	0.89	0.61	0.95	0.50	0.51	0.58	0.59	0.83	0.72	0.58	0.67
K10	0.74	0.87	0.87	0.76	0.92	0.79	0.75	0.87	0.38	0.41	0.46	0.46	0.74	0.61	0.52	0.55
K11	0.74	0.84	0.84	0.64	0.88	0.88	0.61	0.96	0.43	0.53	0.62	0.37	0.65	0.66	0.33	0.73
K12	0.73	0.85	0.85	0.66	0.91	0.87	0.63	0.94	0.44	0.51	0.58	0.43	0.74	0.67	0.43	0.67
K13	0.79	0.82	0.84	0.86	0.91	0.80	0.86	0.86	0.56	0.47	0.53	0.80	0.87	0.65	0.84	0.60
K14	0.78	0.87	0.85	0.66	0.87	0.93	0.62	0.93	0.43	0.41	0.46	0.56	0.75	0.78	0.51	0.54
K15	0.81	0.89	0.89	0.77	0.94	0.90	0.74	0.92	0.49	0.46	0.52	0.68	0.85	0.76	0.68	0.59
K16	0.71	0.86	0.86	0.67	0.93	0.82	0.65	0.89	0.34	0.45	0.49	0.34	0.68	0.55	0.37	0.55
K17	0.75	0.77	0.79	0.95	0.82	0.69	0.95	0.74	0.52	0.37	0.42	0.89	0.83	0.58	0.94	0.47
K18	0.78	0.89	0.89	0.65	0.93	0.89	0.62	0.93	0.54	0.66	0.68	0.53	0.85	0.63	0.55	0.57

E = Ethyl acetate extract, SA = *S. album*, SS = *S. spicatum*, SL = *S. lanceolatum*, MF = *M. fragrans*, AS = *A. silvestris*, TH = *T. hoensis*, DD = *D. decandra* and K1-K18 = Chan-khao samples.

Table 52 Similarity index between the IR spectra of the acetone extracts of Chan-khao and authentic samples.

A	Preprocessing methods															
	Normalization								Normalization and second derivative							
	SA	SS	SL	MF	MG	AS	TH	DD	SA	SS	SL	MF	MG	AS	TH	DD
K1	0.78	0.86	0.88	0.85	0.87	0.85	0.98	0.92	0.45	0.46	0.53	0.48	0.73	0.70	0.93	0.61
K2	0.77	0.85	0.88	0.84	0.87	0.86	0.97	0.93	0.47	0.47	0.55	0.45	0.72	0.71	0.91	0.64
K3	0.76	0.82	0.86	0.80	0.87	0.91	0.88	0.94	0.48	0.52	0.61	0.42	0.73	0.77	0.75	0.69
K4	0.83	0.88	0.89	0.77	0.85	0.93	0.88	0.94	0.49	0.49	0.56	0.43	0.73	0.82	0.75	0.61
K5	0.77	0.85	0.87	0.85	0.91	0.89	0.97	0.91	0.34	0.32	0.39	0.52	0.81	0.70	0.95	0.51
K6	0.81	0.87	0.89	0.81	0.87	0.91	0.93	0.94	0.48	0.48	0.55	0.48	0.73	0.80	0.84	0.62
K7	0.80	0.87	0.90	0.85	0.90	0.90	0.89	0.90	0.47	0.51	0.54	0.38	0.79	0.72	0.72	0.60
K8	0.79	0.87	0.90	0.87	0.92	0.88	0.90	0.90	0.44	0.48	0.53	0.39	0.81	0.68	0.78	0.62
K9	0.77	0.84	0.88	0.78	0.85	0.89	0.84	0.94	0.51	0.57	0.65	0.36	0.69	0.72	0.66	0.73
K10	0.75	0.84	0.87	0.85	0.87	0.82	0.99	0.90	0.42	0.43	0.50	0.47	0.69	0.64	0.96	0.58
K11	0.78	0.84	0.87	0.82	0.89	0.92	0.92	0.91	0.43	0.42	0.49	0.45	0.78	0.79	0.86	0.58
K12	0.77	0.84	0.88	0.86	0.91	0.90	0.94	0.91	0.43	0.44	0.51	0.47	0.77	0.75	0.90	0.59
K13	0.75	0.83	0.87	0.85	0.89	0.86	0.96	0.92	0.48	0.50	0.58	0.44	0.70	0.67	0.90	0.68
K14	0.80	0.88	0.90	0.83	0.89	0.92	0.90	0.93	0.44	0.47	0.51	0.42	0.76	0.77	0.66	0.54
K15	0.80	0.88	0.90	0.85	0.89	0.90	0.94	0.93	0.46	0.49	0.54	0.45	0.76	0.78	0.75	0.57
K16	0.70	0.80	0.83	0.85	0.86	0.78	0.99	0.88	0.29	0.29	0.36	0.50	0.72	0.54	0.99	0.47
K17	0.74	0.83	0.87	0.82	0.84	0.82	0.97	0.94	0.44	0.46	0.54	0.48	0.67	0.63	0.94	0.68
K18	0.84	0.91	0.92	0.80	0.90	0.92	0.89	0.91	0.66	0.79	0.77	0.38	0.67	0.68	0.64	0.58

A = Acetone extract, SA = *S. album*, SS = *S. spicatum*, SL = *S. lanceolatum*, MF = *M. fragrans*, AS = *A. silvestris*, TH = *T. hoensis*, DD = *D. decandra* and K1-K18 = Chan-khao samples.

Table 53 Similarity index between the IR spectra of the methanol extracts of Chan-khao and authentic samples.

M	Preprocessing methods															
	Normalization								Normalization and second derivative							
	SA	SS	SL	MF	MG	AS	TH	DD	SA	SS	SL	MF	MG	AS	TH	DD
K1	0.71	0.80	0.87	0.84	0.76	0.91	0.73	0.93	0.42	0.45	0.55	0.43	0.61	0.62	0.92	0.74
K2	0.74	0.80	0.86	0.80	0.75	0.90	0.70	0.95	0.46	0.45	0.54	0.41	0.63	0.67	0.88	0.77
K3	0.78	0.82	0.86	0.79	0.72	0.86	0.56	0.97	0.52	0.51	0.56	0.31	0.64	0.68	0.64	0.86
K4	0.70	0.80	0.88	0.85	0.76	0.90	0.75	0.90	0.39	0.43	0.54	0.42	0.60	0.62	0.94	0.70
K5	0.79	0.83	0.87	0.81	0.77	0.91	0.63	0.96	0.53	0.49	0.56	0.40	0.61	0.73	0.72	0.77
K6	0.72	0.81	0.88	0.84	0.75	0.90	0.70	0.93	0.38	0.40	0.51	0.45	0.61	0.64	0.90	0.69
K7	0.74	0.85	0.89	0.80	0.62	0.83	0.57	0.94	0.46	0.48	0.51	0.29	0.66	0.59	0.63	0.80
K8	0.78	0.86	0.90	0.78	0.64	0.84	0.55	0.97	0.50	0.51	0.54	0.30	0.62	0.62	0.58	0.82
K9	0.66	0.77	0.86	0.76	0.66	0.86	0.74	0.92	0.45	0.47	0.53	0.30	0.59	0.56	0.68	0.83
K10	0.73	0.82	0.88	0.80	0.70	0.89	0.70	0.95	0.46	0.47	0.57	0.43	0.59	0.68	0.88	0.75
K11	0.73	0.80	0.87	0.82	0.74	0.90	0.71	0.94	0.41	0.44	0.54	0.42	0.60	0.65	0.90	0.72
K12	0.75	0.81	0.87	0.84	0.79	0.91	0.65	0.95	0.46	0.45	0.55	0.41	0.68	0.69	0.83	0.78
K13	0.77	0.81	0.86	0.82	0.78	0.89	0.64	0.95	0.53	0.51	0.57	0.35	0.61	0.63	0.76	0.82
K14	0.71	0.81	0.86	0.76	0.57	0.80	0.60	0.92	0.38	0.39	0.43	0.27	0.52	0.53	0.48	0.68
K15	0.71	0.83	0.90	0.82	0.68	0.87	0.67	0.93	0.43	0.48	0.55	0.35	0.61	0.63	0.73	0.81
K16	0.72	0.80	0.87	0.86	0.77	0.90	0.68	0.93	0.41	0.45	0.55	0.44	0.64	0.65	0.90	0.73
K17	0.74	0.81	0.87	0.80	0.71	0.87	0.65	0.96	0.44	0.42	0.52	0.44	0.62	0.65	0.87	0.79
K18	0.79	0.83	0.86	0.82	0.83	0.91	0.60	0.93	0.54	0.63	0.66	0.37	0.74	0.71	0.63	0.72

M = Methanol extract, SA = *S. album*, SS = *S. spicatum*, SL = *S. lanceolatum*, MF = *M. fragrans*, AS = *A. silvestris*, TH = *T. hoensis*, DD = *D. decandra* and K1-K18 = Chan-khao samples.

Table 54 Similarity index between the IR spectra of the water extracts of Chan-khao and authentic samples.

W	Preprocessing methods															
	Normalization								Normalization and second derivative							
	SA	SS	SL	MF	MG	AS	TH	DD	SA	SS	SL	MF	MG	AS	TH	DD
K1	0.64	0.96	0.96	0.85	0.45	0.97	0.96	0.90	0.06	0.50	0.56	0.35	0.07	0.76	0.76	0.58
K2	0.49	0.90	0.90	0.89	0.29	0.96	0.96	0.90	0.07	0.45	0.80	0.27	0.11	0.55	0.55	0.47
K3	0.77	0.97	0.97	0.85	0.58	0.93	0.92	0.91	0.08	0.60	0.37	0.62	0.10	0.80	0.80	0.65
K4	0.58	0.95	0.94	0.89	0.39	0.98	0.98	0.92	0.05	0.51	0.58	0.32	0.14	0.79	0.79	0.55
K5	0.68	0.97	0.97	0.86	0.50	0.97	0.96	0.89	0.08	0.47	0.35	0.38	0.15	0.93	0.93	0.61
K6	0.65	0.96	0.95	0.87	0.45	0.98	0.97	0.92	0.01	0.41	0.26	0.34	0.07	0.93	0.93	0.59
K7	0.77	0.98	0.97	0.83	0.60	0.91	0.91	0.91	0.04	0.57	0.30	0.64	0.07	0.66	0.66	0.62
K8	0.81	0.97	0.97	0.79	0.63	0.88	0.88	0.90	0.10	0.57	0.37	0.67	0.06	0.64	0.64	0.67
K9	0.77	0.98	0.97	0.85	0.58	0.92	0.91	0.92	0.07	0.61	0.36	0.63	0.06	0.67	0.67	0.61
K10	0.60	0.96	0.95	0.87	0.40	0.98	0.98	0.91	0.05	0.52	0.52	0.37	0.13	0.86	0.86	0.59
K11	0.52	0.91	0.91	0.88	0.32	0.96	0.96	0.91	0.03	0.43	0.71	0.30	0.05	0.59	0.59	0.51
K12	0.52	0.92	0.91	0.87	0.31	0.98	0.98	0.86	-0.02	0.45	0.26	0.31	0.07	0.96	0.96	0.54
K13	0.54	0.93	0.92	0.87	0.33	0.98	0.98	0.87	0.02	0.49	0.36	0.27	0.11	0.94	0.94	0.55
K14	0.79	0.96	0.96	0.82	0.63	0.89	0.89	0.91	0.05	0.53	0.32	0.65	0.07	0.65	0.65	0.54
K15	0.78	0.97	0.97	0.81	0.61	0.91	0.90	0.88	0.04	0.53	0.34	0.63	0.08	0.67	0.67	0.55
K16	0.62	0.95	0.95	0.85	0.42	0.97	0.96	0.86	0.02	0.45	0.30	0.33	0.10	0.95	0.95	0.56
K17	0.66	0.96	0.96	0.89	0.47	0.97	0.97	0.91	0.07	0.51	0.35	0.35	0.14	0.92	0.92	0.61
K18	0.75	0.99	0.98	0.82	0.57	0.91	0.91	0.92	0.15	0.57	0.70	0.44	0.18	0.43	0.43	0.56

W = Water extract, SA = *S. album*, SS = *S. spicatum*, SL = *S. lanceolatum*, MF = *M. fragrans*, AS = *A. silvestris*, TH = *T. hoensis*, DD = *D. decandra* and K1-K18 = Chan-khao samples.

Table 55 Similarity index between the IR spectra of the fine powders of Chan-khao and authentic samples.

P	Preprocessing methods															
	Normalization								Normalization and second derivative							
	SA	SS	SL	MF	MG	AS	TH	DD	SA	SS	SL	MF	MG	AS	TH	DD
K1	0.99	1.00	1.00	0.99	0.98	0.99	0.99	0.99	0.98	0.98	0.97	0.95	0.97	0.97	0.99	0.95
K2	0.98	0.99	0.99	0.98	0.98	0.98	1.00	0.99	0.98	0.97	0.96	0.94	0.97	0.96	0.99	0.94
K3	nd	nd	nd	nd	nd	nd	nd	nd	nd	nd	nd	nd	nd	nd	nd	nd
K4	0.99	0.99	0.99	0.99	0.98	0.98	0.99	0.98	0.98	0.97	0.95	0.94	0.97	0.97	1.00	0.94
K5	0.99	0.99	0.99	1.00	0.99	1.00	0.99	0.99	0.99	0.98	0.96	0.95	0.98	0.98	0.99	0.95
K6	0.99	1.00	1.00	0.99	0.98	0.99	0.99	0.99	0.98	0.98	0.97	0.95	0.97	0.97	0.99	0.95
K7	0.99	0.99	0.99	0.99	0.99	0.99	0.99	0.99	0.96	0.98	0.97	0.94	0.97	0.96	0.97	0.97
K8	0.98	0.96	0.97	0.98	0.99	0.99	0.97	0.98	0.96	0.97	0.96	0.93	0.97	0.96	0.96	0.98
K9	0.96	0.96	0.97	0.98	0.99	0.98	0.97	0.99	0.94	0.97	0.96	0.91	0.95	0.96	0.94	0.99
K10	0.99	0.99	0.99	0.99	0.98	0.98	0.99	0.98	0.98	0.97	0.96	0.95	0.97	0.97	0.99	0.94
K11	0.99	0.99	1.00	0.99	0.99	0.99	1.00	0.99	0.98	0.98	0.96	0.95	0.97	0.97	0.99	0.95
K12	0.99	0.99	0.99	0.99	0.98	0.99	1.00	0.99	0.98	0.97	0.95	0.95	0.97	0.97	1.00	0.94
K13	0.98	0.99	0.99	0.98	0.97	0.98	0.99	0.97	0.97	0.97	0.96	0.93	0.96	0.95	1.00	0.93
K14	0.99	0.98	0.98	0.99	1.00	1.00	0.98	0.99	0.97	0.98	0.97	0.93	0.97	0.97	0.96	0.98
K15	0.99	0.99	0.99	0.99	0.99	0.99	0.99	0.99	0.97	0.98	0.97	0.95	0.97	0.97	0.97	0.98
K16	0.99	0.99	0.99	0.99	0.98	0.99	1.00	0.99	0.98	0.97	0.96	0.94	0.97	0.97	0.99	0.94
K17	0.99	0.99	0.99	0.99	0.98	0.99	1.00	0.98	0.98	0.97	0.96	0.94	0.97	0.97	1.00	0.94
K18	nd	nd	nd	nd	nd	nd	nd	nd	nd	nd	nd	nd	nd	nd	nd	nd

P = Fine powder extract, SA = *S. album*, SS = *S. spicatum*, SL = *S. lanceolatum*, MF = *M. fragrans*, AS = *A. silvestris*, TH = *T. hoensis*, DD = *D. decandra*, K1-K18 = Chan-khao samples and nd = not determined.

Table 56 Similarity index between the IR spectra of the *n*-hexane extracts of Chan-chamot and authentic samples.

H	Preprocessing methods															
	Normalization								Normalization and second derivative							
	SA	SS	SL	MF	MG	AS	TH	DD	SA	SS	SL	MF	MG	AS	TH	DD
M1	0.28	0.43	0.41	0.13	0.04	0.18	0.19	0.13	0.02	0.10	0.11	0.05	0.04	0.01	0.14	0.06
M2	0.58	0.70	0.70	0.46	0.40	0.51	0.54	0.45	0.22	0.34	0.38	0.29	0.33	0.25	0.45	0.32
M3	0.57	0.66	0.68	0.52	0.51	0.56	0.57	0.50	0.24	0.35	0.35	0.12	0.13	0.12	0.28	0.26
M4	0.71	0.71	0.76	0.79	0.97	0.80	0.86	0.74	0.43	0.53	0.63	0.76	0.92	0.74	0.91	0.70
M5	0.81	0.82	0.87	0.90	0.91	0.91	0.93	0.84	0.43	0.54	0.58	0.65	0.72	0.58	0.73	0.53
M6	0.85	0.88	0.92	0.88	0.87	0.92	0.95	0.89	0.50	0.59	0.68	0.73	0.89	0.72	0.91	0.68
M7	0.78	0.79	0.85	0.85	0.94	0.90	0.91	0.82	0.39	0.52	0.60	0.67	0.78	0.65	0.81	0.63
M8	0.58	0.53	0.61	0.78	0.78	0.76	0.72	0.65	0.09	0.18	0.16	0.31	0.21	0.20	0.20	0.06
M9	0.71	0.68	0.75	0.83	0.95	0.83	0.85	0.75	0.34	0.44	0.48	0.52	0.60	0.47	0.60	0.45
M10	0.80	0.77	0.84	0.93	0.90	0.94	0.98	0.94	0.45	0.56	0.69	0.80	0.86	0.79	0.98	0.84
M11	0.72	0.72	0.78	0.82	0.93	0.85	0.85	0.75	0.25	0.34	0.37	0.43	0.48	0.36	0.49	0.36
M12	0.27	0.42	0.40	0.11	0.02	0.17	0.17	0.11	-0.01	0.08	-0.09	0.00	0.00	-0.03	0.10	0.03
M13	0.70	0.68	0.75	0.84	0.84	0.85	0.82	0.75	0.15	0.24	0.23	0.34	0.30	0.24	0.30	0.16
M14	0.72	0.74	0.79	0.76	0.94	0.79	0.84	0.72	0.41	0.53	0.62	0.67	0.81	0.64	0.85	0.65
M15	0.32	0.46	0.44	0.15	0.05	0.21	0.22	0.16	0.02	0.10	0.11	0.04	0.03	0.00	0.14	0.07
M16	0.41	0.53	0.52	0.27	0.17	0.30	0.32	0.25	0.09	0.18	0.18	0.12	0.11	0.07	0.22	0.12
M17	0.33	0.48	0.46	0.18	0.10	0.24	0.25	0.19	0.04	0.13	0.15	0.07	0.08	0.03	0.18	0.10

H = *n*-Hexane extract, SA = *S. album*, SS = *S. spicatum*, SL = *S. lanceolatum*, MF = *M. fragrans*, AS = *A. silvestris*, TH = *T. hoensis*, DD = *D. decandra* and M1-M17 = Chan-chamot samples.

Table 57 Similarity index between the IR spectra of the dichloromethane extracts of Chan-chamot and authentic samples.

D	Preprocessing methods															
	Normalization								Normalization and second derivative							
	SA	SS	SL	MF	MG	AS	TH	DD	SA	SS	SL	MF	MG	AS	TH	DD
M1	0.74	0.87	0.84	0.70	0.94	0.77	0.91	0.71	0.49	0.55	0.55	0.21	0.82	0.65	0.91	0.58
M2	0.62	0.75	0.73	0.70	0.96	0.67	0.83	0.65	0.29	0.43	0.40	0.12	0.63	0.37	0.60	0.39
M3	0.63	0.73	0.71	0.68	0.96	0.74	0.84	0.66	0.28	0.38	0.37	0.11	0.67	0.37	0.57	0.26
M4	0.59	0.70	0.69	0.73	0.99	0.74	0.85	0.68	0.09	0.11	0.09	0.27	0.94	0.55	0.66	0.21
M5	0.59	0.70	0.69	0.71	0.99	0.74	0.86	0.69	0.13	0.16	0.14	0.25	0.94	0.59	0.69	0.27
M6	0.56	0.74	0.71	0.72	0.95	0.61	0.81	0.62	0.31	0.42	0.40	0.19	0.75	0.38	0.65	0.38
M7	0.61	0.72	0.71	0.71	0.99	0.74	0.86	0.69	0.12	0.19	0.16	0.22	0.93	0.50	0.66	0.23
M8	0.67	0.73	0.73	0.69	0.96	0.83	0.89	0.75	0.13	0.18	0.15	0.13	0.75	0.44	0.56	0.14
M9	0.60	0.70	0.69	0.70	0.99	0.75	0.84	0.68	0.10	0.15	0.14	0.22	0.92	0.52	0.65	0.21
M10	0.67	0.78	0.77	0.71	0.98	0.80	0.90	0.73	0.20	0.28	0.25	0.22	0.93	0.59	0.75	0.29
M11	0.57	0.67	0.66	0.70	0.98	0.74	0.83	0.66	0.05	0.08	0.06	0.22	0.89	0.52	0.59	0.11
M12	0.63	0.71	0.70	0.69	0.98	0.79	0.87	0.71	0.14	0.21	0.19	0.17	0.89	0.49	0.66	0.24
M13	0.58	0.68	0.66	0.70	0.96	0.75	0.85	0.67	0.10	0.18	0.13	0.23	0.85	0.49	0.61	0.14
M14	0.58	0.69	0.67	0.72	0.99	0.73	0.84	0.66	0.08	0.12	0.10	0.26	0.94	0.57	0.66	0.19
M15	0.71	0.82	0.81	0.72	0.95	0.80	0.91	0.74	0.26	0.33	0.30	0.17	0.78	0.50	0.68	0.26
M16	0.63	0.75	0.73	0.71	0.96	0.72	0.86	0.67	0.27	0.38	0.34	0.16	0.70	0.38	0.61	0.29
M17	0.70	0.80	0.79	0.72	0.97	0.81	0.92	0.75	0.22	0.29	0.27	0.19	0.88	0.57	0.75	0.29

D = Dichloromethane extract, SA = *S. album*, SS = *S. spicatum*, SL = *S. lanceolatum*, MF = *M. fragrans*, AS = *A. silvestris*, TH = *T. hoensis*, DD = *D. decandra* and M1-M17 = Chan-chamot samples.

Table 58 Similarity index between the IR spectra of the ethyl acetate extracts of Chan-chamot and authentic samples.

E	Preprocessing methods															
	Normalization								Normalization and second derivative							
	SA	SS	SL	MF	MG	AS	TH	DD	SA	SS	SL	MF	MG	AS	TH	DD
M1	0.72	0.83	0.84	0.84	0.98	0.73	0.82	0.77	0.39	0.29	0.32	0.80	0.94	0.61	0.84	0.34
M2	0.64	0.72	0.73	0.67	0.96	0.70	0.65	0.75	0.40	0.39	0.41	0.71	0.92	0.56	0.75	0.43
M3	0.63	0.77	0.78	0.69	0.97	0.69	0.68	0.76	0.36	0.36	0.37	0.62	0.85	0.49	0.68	0.34
M4	0.58	0.77	0.76	0.55	0.95	0.75	0.51	0.81	0.29	0.36	0.37	0.45	0.87	0.60	0.44	0.37
M5	0.56	0.75	0.74	0.53	0.94	0.73	0.50	0.78	0.19	0.24	0.27	0.41	0.83	0.60	0.39	0.34
M6	0.51	0.57	0.58	0.48	0.86	0.62	0.47	0.67	0.33	0.31	0.35	0.61	0.90	0.56	0.65	0.39
M7	0.55	0.73	0.72	0.46	0.92	0.76	0.42	0.81	0.16	0.24	0.28	0.32	0.78	0.55	0.30	0.35
M8	0.70	0.82	0.81	0.68	0.97	0.84	0.65	0.87	0.32	0.28	0.30	0.65	0.89	0.56	0.69	0.34
M9	0.52	0.70	0.69	0.44	0.90	0.74	0.39	0.78	0.11	0.15	0.20	0.34	0.75	0.60	0.31	0.28
M10	0.64	0.81	0.80	0.59	0.96	0.79	0.56	0.83	0.22	0.29	0.32	0.44	0.85	0.63	0.42	0.35
M11	0.51	0.70	0.69	0.43	0.90	0.71	0.39	0.75	0.13	0.17	0.20	0.34	0.77	0.57	0.32	0.28
M12	0.54	0.72	0.71	0.46	0.91	0.74	0.42	0.79	0.17	0.27	0.29	0.32	0.79	0.54	0.29	0.33
M13	0.60	0.76	0.76	0.55	0.95	0.75	0.51	0.80	0.21	0.31	0.32	0.44	0.84	0.50	0.43	0.30
M14	0.59	0.76	0.75	0.54	0.94	0.78	0.49	0.83	0.26	0.35	0.34	0.45	0.86	0.56	0.43	0.30
M15	0.73	0.80	0.81	0.85	0.96	0.73	0.84	0.76	0.39	0.25	0.27	0.84	0.87	0.51	0.90	0.28
M16	0.65	0.81	0.80	0.65	0.98	0.78	0.62	0.82	0.25	0.27	0.30	0.59	0.91	0.59	0.60	0.33
M17	0.74	0.85	0.85	0.77	0.98	0.79	0.74	0.82	0.39	0.33	0.36	0.77	0.93	0.56	0.82	0.38

E = Ethyl acetate extract, SA = *S. album*, SS = *S. spicatum*, SL = *S. lanceolatum*, MF = *M. fragrans*, AS = *A. silvestris*, TH = *T. hoaensis*, DD = *D. decandra* and M1-M17 = Chan-chamot samples.

Table 59 Similarity index between the IR spectra of the acetone extracts of Chan-chamot and authentic samples.

A	Preprocessing methods															
	Normalization								Normalization and second derivative							
	SA	SS	SL	MF	MG	AS	TH	DD	SA	SS	SL	MF	MG	AS	TH	DD
M1	0.67	0.77	0.80	0.87	0.98	0.85	0.85	0.80	0.18	0.20	0.23	0.33	0.91	0.50	0.68	0.30
M2	0.56	0.69	0.73	0.89	0.97	0.76	0.85	0.71	0.35	0.38	0.41	0.39	0.90	0.54	0.76	0.45
M3	0.59	0.70	0.73	0.87	0.99	0.82	0.84	0.73	0.18	0.17	0.23	0.39	0.95	0.57	0.74	0.32
M4	0.58	0.69	0.72	0.88	0.99	0.82	0.83	0.71	0.25	0.23	0.28	0.43	0.97	0.62	0.75	0.40
M5	0.60	0.71	0.74	0.87	0.99	0.83	0.81	0.73	0.21	0.23	0.27	0.43	0.96	0.55	0.73	0.35
M6	0.52	0.65	0.70	0.88	0.95	0.71	0.82	0.67	0.40	0.47	0.48	0.37	0.80	0.46	0.68	0.44
M7	0.62	0.72	0.76	0.88	0.99	0.83	0.83	0.75	0.19	0.19	0.24	0.42	0.96	0.55	0.74	0.33
M8	0.68	0.77	0.80	0.86	0.98	0.86	0.83	0.79	0.26	0.31	0.32	0.32	0.82	0.42	0.67	0.39
M9	0.61	0.72	0.75	0.88	0.99	0.84	0.84	0.74	0.15	0.13	0.19	0.41	0.97	0.60	0.70	0.28
M10	0.69	0.81	0.82	0.84	0.86	0.68	0.88	0.74	0.33	0.37	0.39	0.38	0.86	0.46	0.71	0.41
M11	0.59	0.69	0.72	0.87	0.99	0.81	0.83	0.71	0.14	0.12	0.18	0.41	0.96	0.58	0.71	0.27
M12	0.55	0.67	0.71	0.88	0.98	0.79	0.83	0.70	0.33	0.36	0.38	0.39	0.92	0.55	0.73	0.43
M13	0.61	0.72	0.75	0.87	0.99	0.81	0.86	0.74	0.19	0.20	0.23	0.38	0.95	0.53	0.70	0.28
M14	0.61	0.72	0.75	0.88	1.00	0.82	0.84	0.73	0.17	0.17	0.22	0.43	0.99	0.59	0.73	0.31
M15	0.68	0.77	0.80	0.86	0.99	0.87	0.86	0.79	0.21	0.22	0.26	0.38	0.95	0.58	0.73	0.33
M16	0.62	0.73	0.76	0.87	0.99	0.84	0.86	0.76	0.20	0.20	0.24	0.40	0.96	0.57	0.71	0.31
M17	0.68	0.78	0.81	0.89	0.99	0.84	0.89	0.81	0.24	0.25	0.30	0.38	0.96	0.59	0.77	0.41

A = Acetone extract, SA = *S. album*, SS = *S. spicatum*, SL = *S. lanceolatum*, MF = *M. fragrans*, AS = *A. silvestris*, TH = *T. hoaensis*, DD = *D. decandra* and M1-M17 = Chan-chamot samples.

Table 60 Similarity index between the IR spectra of the methanol extracts of Chan-chamot and authentic samples.

M	Preprocessing methods															
	Normalization								Normalization and second derivative							
	SA	SS	SL	MF	MG	AS	TH	DD	SA	SS	SL	MF	MG	AS	TH	DD
M1	0.62	0.67	0.73	0.84	0.96	0.94	0.71	0.82	0.29	0.31	0.36	0.34	0.87	0.58	0.56	0.64
M2	0.67	0.71	0.74	0.83	0.93	0.89	0.57	0.85	0.26	0.29	0.34	0.32	0.86	0.56	0.53	0.61
M3	0.64	0.68	0.72	0.83	0.95	0.89	0.58	0.80	0.21	0.25	0.30	0.28	0.83	0.51	0.47	0.52
M4	0.37	0.38	0.46	0.65	0.94	0.83	0.79	0.55	0.11	0.08	0.16	0.35	0.94	0.47	0.53	0.50
M5	0.30	0.32	0.43	0.58	0.88	0.81	0.87	0.49	0.23	0.23	0.30	0.33	0.83	0.49	0.60	0.50
M6	0.63	0.68	0.73	0.84	0.95	0.90	0.59	0.81	0.19	0.22	0.28	0.34	0.89	0.54	0.50	0.54
M7	0.64	0.69	0.73	0.85	0.93	0.90	0.58	0.83	0.22	0.23	0.29	0.35	0.89	0.57	0.51	0.58
M8	0.53	0.53	0.58	0.71	0.96	0.88	0.69	0.72	0.22	0.21	0.28	0.33	0.85	0.55	0.55	0.61
M9	0.59	0.65	0.70	0.84	0.96	0.89	0.61	0.78	0.17	0.17	0.23	0.33	0.88	0.54	0.45	0.50
M10	0.66	0.71	0.74	0.82	0.92	0.89	0.57	0.84	0.21	0.24	0.28	0.30	0.86	0.55	0.46	0.54
M11	0.65	0.69	0.73	0.84	0.93	0.88	0.56	0.81	0.18	0.18	0.23	0.33	0.88	0.54	0.43	0.49
M12	0.64	0.68	0.72	0.82	0.94	0.89	0.58	0.83	0.23	0.26	0.31	0.34	0.86	0.57	0.50	0.60
M13	0.65	0.72	0.76	0.86	0.92	0.89	0.61	0.83	0.23	0.30	0.32	0.30	0.81	0.49	0.45	0.50
M14	0.37	0.40	0.49	0.65	0.94	0.84	0.81	0.54	0.08	0.07	0.14	0.33	0.90	0.44	0.53	0.46
M15	0.72	0.77	0.81	0.84	0.89	0.93	0.64	0.90	0.33	0.38	0.40	0.30	0.77	0.57	0.51	0.64
M16	0.66	0.71	0.75	0.84	0.93	0.90	0.60	0.84	0.25	0.31	0.34	0.32	0.81	0.53	0.51	0.58
M17	0.74	0.80	0.84	0.85	0.89	0.93	0.63	0.91	0.39	0.44	0.46	0.30	0.73	0.61	0.55	0.71

M = Methanol extract, SA = *S. album*, SS = *S. spicatum*, SL = *S. lanceolatum*, MF = *M. fragrans*, AS = *A. silvestris*, TH = *T. hoaensis*, DD = *D. decandra* and M1-M17 = Chan-chamot samples.

Table 61 Similarity index between the IR spectra of the water extracts of Chan-chamot and authentic samples.

W	Preprocessing methods															
	Normalization								Normalization and second derivative							
	SA	SS	SL	MF	MG	AS	TH	DD	SA	SS	SL	MF	MG	AS	TH	DD
M1	0.75	0.92	0.93	0.77	0.62	0.88	0.87	0.81	0.16	0.56	0.30	0.23	0.08	0.59	0.59	0.50
M2	0.83	0.86	0.88	0.62	0.73	0.77	0.76	0.71	0.19	0.54	0.30	0.19	0.09	0.60	0.60	0.50
M3	0.90	0.79	0.82	0.47	0.85	0.62	0.61	0.62	0.21	0.19	0.27	0.27	0.46	0.48	0.48	0.30
M4	0.88	0.62	0.67	0.30	0.96	0.45	0.44	0.48	0.16	-0.01	0.17	0.16	0.91	0.25	0.25	0.13
M5	0.89	0.85	0.88	0.59	0.80	0.72	0.72	0.71	0.20	0.45	0.29	0.31	0.24	0.50	0.50	0.48
M6	0.91	0.82	0.86	0.49	0.79	0.66	0.65	0.64	0.25	0.34	0.29	0.27	0.42	0.54	0.54	0.40
M7	0.90	0.85	0.88	0.54	0.77	0.71	0.70	0.67	0.26	0.45	0.32	0.22	0.35	0.59	0.59	0.47
M8	0.86	0.87	0.90	0.58	0.71	0.75	0.74	0.69	0.16	0.55	0.32	0.21	0.20	0.68	0.68	0.51
M9	0.90	0.86	0.89	0.54	0.74	0.71	0.70	0.68	0.26	0.56	0.40	0.28	0.18	0.56	0.56	0.52
M10	0.76	0.93	0.92	0.80	0.63	0.87	0.87	0.85	0.28	0.50	0.37	0.29	0.20	0.64	0.64	0.53
M11	nd	nd	nd	nd	nd	nd	nd	nd	nd	nd	nd	nd	nd	nd	nd	nd
M12	0.84	0.91	0.92	0.63	0.69	0.79	0.78	0.74	0.17	0.61	0.39	0.28	0.15	0.69	0.69	0.58
M13	0.84	0.50	0.56	0.21	0.99	0.32	0.31	0.38	0.19	-0.05	0.13	0.10	0.98	0.12	0.12	0.06
M14	0.93	0.77	0.81	0.42	0.85	0.59	0.58	0.59	0.23	0.21	0.23	0.23	0.51	0.45	0.45	0.35
M15	0.65	0.92	0.89	0.89	0.52	0.90	0.90	0.90	0.34	0.50	0.34	0.37	0.14	0.57	0.57	0.62
M16	0.91	0.78	0.83	0.45	0.87	0.62	0.61	0.60	0.18	0.11	0.23	0.21	0.83	0.34	0.34	0.22
M17	0.80	0.92	0.93	0.72	0.67	0.84	0.83	0.79	0.21	0.55	0.35	0.26	0.21	0.66	0.66	0.55

W = Water extract, SA = *S. album*, SS = *S. spicatum*, SL = *S. lanceolatum*, MF = *M. fragrans*, AS = *A. silvestris*, TH = *T. hoaensis*, DD = *D. decandra*, M1-M17 = Chan-chamot samples and nd = not determined.

Table 62 Similarity index between the IR spectra of the fine powders of Chan-chamot and authentic samples

P	Preprocessing methods															
	Normalization								Normalization and second derivative							
	SA	SS	SL	MF	MG	AS	TH	DD	SA	SS	SL	MF	MG	AS	TH	DD
M1	0.96	0.97	0.98	0.98	0.99	0.98	0.97	0.99	0.97	0.98	0.97	0.93	0.98	0.97	0.96	0.97
M2	0.91	0.91	0.92	0.93	0.96	0.95	0.92	0.95	0.97	0.97	0.96	0.92	0.97	0.96	0.95	0.95
M3	0.95	0.96	0.97	0.96	0.98	0.97	0.96	0.98	0.95	0.97	0.96	0.90	0.95	0.95	0.94	0.97
M4	0.98	0.98	0.99	0.98	0.99	0.99	0.98	0.99	0.97	0.98	0.96	0.93	0.98	0.97	0.97	0.96
M5	nd	nd	nd	nd	nd	nd	nd	nd	nd	nd	nd	nd	nd	nd	nd	nd
M6	0.96	0.97	0.98	0.98	0.99	0.98	0.98	0.99	0.96	0.98	0.97	0.93	0.97	0.96	0.96	0.96
M7	0.88	0.90	0.92	0.91	0.94	0.93	0.92	0.94	0.94	0.97	0.96	0.91	0.95	0.94	0.95	0.95
M8	0.97	0.98	0.99	0.98	0.98	0.98	0.98	0.98	0.97	0.98	0.97	0.92	0.97	0.96	0.97	0.95
M9	nd	nd	nd	nd	nd	nd	nd	nd	nd	nd	nd	nd	nd	nd	nd	nd
M10	0.89	0.88	0.90	0.91	0.94	0.93	0.90	0.93	0.95	0.96	0.94	0.90	0.95	0.94	0.94	0.93
M11	0.94	0.95	0.96	0.96	0.97	0.97	0.96	0.97	0.96	0.97	0.96	0.92	0.96	0.95	0.96	0.94
M12	0.94	0.95	0.96	0.96	0.97	0.96	0.96	0.97	0.95	0.97	0.96	0.91	0.95	0.94	0.95	0.94
M13	0.92	0.93	0.95	0.94	0.96	0.95	0.94	0.96	0.95	0.97	0.95	0.91	0.95	0.95	0.95	0.94
M14	0.97	0.98	0.99	0.98	0.99	0.99	0.98	0.99	0.98	0.98	0.97	0.93	0.98	0.97	0.97	0.96
M15	0.91	0.92	0.94	0.93	0.95	0.95	0.94	0.96	0.94	0.97	0.96	0.90	0.96	0.95	0.95	0.97
M16	0.94	0.92	0.92	0.95	0.97	0.96	0.93	0.95	0.98	0.98	0.95	0.93	0.98	0.97	0.96	0.95
M17	0.97	0.98	0.99	0.98	0.99	0.98	0.98	0.99	0.96	0.98	0.96	0.93	0.97	0.96	0.97	0.96

P = Fine powder, SA = *S. album*, SS = *S. spicatum*, SL = *S. lanceolatum*, MF = *M. fragrans*, AS = *A. silvestris*, TH = *T. hoensis*, DD = *D. decandra*, M1-M17 = Chan-chamot samples and nd = not determined.

Table 63 Similarity index between the IR spectra of the *n*-hexane extracts of Chan-thana and authentic samples.

H	Preprocessing methods															
	Normalization								Normalization and second derivative							
	SA	SS	SL	MF	MG	AS	TH	DD	SA	SS	SL	MF	MG	AS	TH	DD
TN1	0.74	0.69	0.78	0.88	0.88	0.91	0.90	0.89	0.37	0.46	0.56	0.66	0.77	0.68	0.80	0.64
TN2	0.80	0.79	0.86	0.96	0.87	0.95	0.97	0.94	0.42	0.49	0.63	0.85	0.85	0.78	0.96	0.79
TN3	0.83	0.81	0.87	0.95	0.91	0.94	0.99	0.93	0.50	0.59	0.70	0.85	0.90	0.79	0.99	0.77
TN4	0.80	0.77	0.84	0.93	0.94	0.93	0.95	0.90	0.46	0.55	0.67	0.84	0.87	0.81	0.96	0.80
TN5	0.80	0.77	0.85	0.95	0.88	0.95	0.97	0.95	0.44	0.52	0.67	0.83	0.87	0.78	0.98	0.82
TN6	0.77	0.72	0.81	0.96	0.90	0.93	0.96	0.93	0.41	0.50	0.64	0.89	0.87	0.81	0.97	0.77
TN7	0.74	0.69	0.77	0.87	0.96	0.87	0.91	0.86	0.45	0.56	0.68	0.81	0.87	0.79	0.97	0.82
TN8	0.84	0.83	0.90	0.93	0.88	0.96	0.97	0.96	0.47	0.53	0.68	0.71	0.82	0.74	0.94	0.88
TN9	0.59	0.69	0.71	0.51	0.45	0.55	0.58	0.50	0.21	0.32	0.39	0.42	0.43	0.37	0.56	0.39
TN10	0.51	0.64	0.63	0.39	0.30	0.45	0.46	0.41	0.17	0.27	0.31	0.26	0.27	0.23	0.40	0.29

H = *n*-Hexane extract, SA = *S. album*, SS = *S. spicatum*, SL = *S. lanceolatum*, MF = *M. fragrans*, AS = *A. silvestris*, TH = *T. hoensis*, DD = *D. decandra* and TN1-TN10 = Chan-thana samples.

Table 64 Similarity index between the IR spectra of the dichloromethane extracts of Chan-thana and authentic samples.

D	Preprocessing methods															
	Normalization									Normalization and second derivative						
	SA	SS	SL	MF	MG	AS	TH	DD	SA	SS	SL	MF	MG	AS	TH	DD
TN1	0.66	0.60	0.62	0.56	0.75	0.87	0.82	0.85	0.30	0.35	0.38	0.13	0.53	0.54	0.58	0.57
TN2	0.75	0.70	0.73	0.69	0.81	0.90	0.92	0.93	0.44	0.41	0.48	0.31	0.76	0.76	0.92	0.72
TN3	0.77	0.75	0.78	0.70	0.84	0.88	0.95	0.95	0.53	0.53	0.59	0.28	0.72	0.71	0.93	0.77
TN4	0.74	0.73	0.76	0.72	0.85	0.87	0.93	0.95	0.50	0.51	0.58	0.28	0.68	0.68	0.89	0.85
TN5	0.76	0.72	0.76	0.66	0.77	0.86	0.90	0.98	0.51	0.47	0.57	0.20	0.59	0.63	0.82	0.86
TN6	0.72	0.68	0.72	0.67	0.79	0.86	0.92	0.97	0.47	0.46	0.55	0.24	0.65	0.66	0.87	0.83
TN7	0.77	0.81	0.83	0.71	0.85	0.85	0.92	0.91	0.45	0.49	0.55	0.28	0.67	0.68	0.86	0.80
TN8	0.59	0.65	0.65	0.68	0.94	0.78	0.83	0.73	0.09	0.02	0.07	0.14	0.46	0.41	0.38	0.13
TN9	0.76	0.78	0.80	0.75	0.91	0.88	0.98	0.90	0.48	0.51	0.53	0.28	0.81	0.67	0.96	0.67
TN10	0.78	0.76	0.77	0.67	0.89	0.93	0.94	0.85	0.54	0.51	0.54	0.28	0.74	0.78	0.95	0.71

D = Dichloromethane extract, SA = *S. album*, SS = *S. spicatum*, SL = *S. lanceolatum*, MF = *M. fragrans*, AS = *A. silvestris*, TH = *T. hoaensis*, DD = *D. decandra* and TN1-TN10 = Chan-thana samples.

Table 65 Similarity index between the IR spectra of the ethyl acetate extracts of Chan-thana and authentic samples.

E	Preprocessing methods															
	Normalization									Normalization and second derivative						
	SA	SS	SL	MF	MG	AS	TH	DD	SA	SS	SL	MF	MG	AS	TH	DD
TN1	0.69	0.73	0.73	0.49	0.78	0.90	0.44	0.92	0.32	0.47	0.51	0.27	0.48	0.52	0.18	0.58
TN2	0.77	0.86	0.86	0.70	0.90	0.88	0.67	0.95	0.48	0.53	0.61	0.51	0.75	0.70	0.49	0.72
TN3	0.78	0.86	0.87	0.85	0.91	0.82	0.84	0.89	0.52	0.45	0.52	0.75	0.86	0.70	0.78	0.61
TN4	0.74	0.86	0.87	0.67	0.93	0.86	0.64	0.94	0.40	0.49	0.57	0.40	0.73	0.63	0.41	0.68
TN5	0.80	0.87	0.87	0.76	0.89	0.89	0.74	0.94	0.53	0.49	0.57	0.68	0.83	0.77	0.66	0.68
TN6	0.75	0.79	0.80	0.95	0.83	0.71	0.96	0.75	0.50	0.33	0.37	0.90	0.82	0.64	0.95	0.44
TN7	0.73	0.77	0.78	0.58	0.85	0.91	0.54	0.95	0.44	0.45	0.53	0.55	0.71	0.74	0.49	0.59
TN8	0.57	0.69	0.70	0.45	0.86	0.80	0.41	0.84	0.14	0.11	0.19	0.30	0.44	0.53	0.25	0.23
TN9	0.80	0.87	0.88	0.92	0.92	0.78	0.90	0.81	0.52	0.43	0.48	0.81	0.89	0.67	0.87	0.53
TN10	0.74	0.87	0.87	0.76	0.92	0.79	0.75	0.87	0.38	0.41	0.46	0.46	0.74	0.61	0.52	0.55

E = Ethyl acetate extract, SA = *S. album*, SS = *S. spicatum*, SL = *S. lanceolatum*, MF = *M. fragrans*, AS = *A. silvestris*, TH = *T. hoaensis*, DD = *D. decandra* and TN1-TN10 = Chan-thana samples.

Table 66 Similarity index between the IR spectra of the acetone extracts of Chan-thana and authentic samples.

A	Preprocessing methods															
	Normalization									Normalization and second derivative						
	SA	SS	SL	MF	MG	AS	TH	DD	SA	SS	SL	MF	MG	AS	TH	DD
TN1	0.73	0.77	0.81	0.72	0.83	0.91	0.72	0.85	0.37	0.45	0.52	0.28	0.56	0.65	0.44	0.61
TN2	0.79	0.85	0.89	0.82	0.88	0.92	0.91	0.93	0.49	0.50	0.58	0.43	0.73	0.78	0.81	0.66
TN3	0.78	0.85	0.88	0.84	0.90	0.90	0.95	0.92	0.41	0.42	0.51	0.47	0.77	0.75	0.90	0.60
TN4	0.75	0.79	0.83	0.79	0.87	0.93	0.87	0.91	0.50	0.52	0.60	0.44	0.70	0.79	0.78	0.68
TN5	0.80	0.87	0.90	0.85	0.90	0.90	0.89	0.90	0.47	0.51	0.54	0.38	0.79	0.72	0.72	0.60
TN6	0.82	0.87	0.89	0.79	0.88	0.93	0.89	0.94	0.45	0.46	0.54	0.43	0.77	0.79	0.81	0.62
TN7	0.79	0.84	0.88	0.77	0.85	0.92	0.81	0.92	0.44	0.49	0.56	0.36	0.66	0.77	0.53	0.57
TN8	0.62	0.70	0.75	0.83	0.93	0.86	0.79	0.76	0.12	0.05	0.15	0.27	0.58	0.52	0.42	0.17
TN9	0.78	0.86	0.88	0.85	0.87	0.85	0.98	0.92	0.45	0.46	0.53	0.48	0.73	0.70	0.93	0.61
TN10	0.77	0.85	0.87	0.85	0.91	0.89	0.97	0.91	0.34	0.32	0.39	0.52	0.81	0.70	0.95	0.51

A = Acetone extract, SA = *S. album*, SS = *S. spicatum*, SL = *S. lanceolatum*, MF = *M. fragrans*, AS = *A. silvestris*, TH = *T. hoaensis*, DD = *D. decandra* and TN1-TN10 = Chan-thana samples.

Table 67 Similarity index between the IR spectra of the methanol extracts of Chan-thana and authentic samples.

M	Preprocessing methods															
	Normalization								Normalization and second derivative							
	SA	SS	SL	MF	MG	AS	TH	DD	SA	SS	SL	MF	MG	AS	TH	DD
TN1	0.74	0.73	0.75	0.76	0.82	0.85	0.52	0.88	0.23	0.25	0.30	0.25	0.73	0.55	0.40	0.62
TN2	0.58	0.69	0.80	0.73	0.69	0.86	0.88	0.81	0.34	0.34	0.47	0.37	0.44	0.51	0.95	0.58
TN3	0.72	0.80	0.87	0.83	0.78	0.92	0.74	0.93	0.42	0.42	0.53	0.40	0.63	0.65	0.90	0.72
TN4	0.71	0.78	0.86	0.79	0.73	0.91	0.77	0.93	0.45	0.44	0.54	0.41	0.55	0.63	0.91	0.74
TN5	0.62	0.71	0.82	0.79	0.78	0.91	0.87	0.83	0.34	0.36	0.49	0.40	0.53	0.56	0.95	0.62
TN6	0.78	0.83	0.89	0.81	0.78	0.92	0.69	0.96	0.43	0.43	0.53	0.42	0.64	0.69	0.84	0.76
TN7	0.72	0.81	0.89	0.79	0.69	0.88	0.71	0.94	0.45	0.47	0.54	0.31	0.58	0.63	0.66	0.84
TN8	0.61	0.63	0.69	0.79	0.94	0.90	0.62	0.79	0.08	0.00	0.11	0.17	0.51	0.35	0.24	0.26
TN9	0.71	0.80	0.87	0.84	0.76	0.91	0.73	0.93	0.42	0.45	0.55	0.43	0.61	0.62	0.92	0.74
TN10	0.79	0.83	0.87	0.81	0.77	0.91	0.63	0.96	0.53	0.49	0.56	0.40	0.61	0.73	0.72	0.77

M = Methanol extract, SA = *S. album*, SS = *S. spicatum*, SL = *S. lanceolatum*, MF = *M. fragrans*, AS = *A. silvestris*, TH = *T. hoaensis*, DD = *D. decandra* and TN1-TN10 = Chan-thana samples.

Table 68 Similarity index between the IR spectra of the water extracts of Chan-thana and authentic samples.

W	Preprocessing methods															
	Normalization								Normalization and second derivative							
	SA	SS	SL	MF	MG	AS	TH	DD	SA	SS	SL	MF	MG	AS	TH	DD
TN1	0.80	0.94	0.94	0.70	0.65	0.84	0.83	0.80	0.13	0.51	0.29	0.44	0.13	0.56	0.56	0.66
TN2	0.65	0.95	0.95	0.80	0.47	0.95	0.94	0.83	0.00	0.45	0.58	0.32	0.10	0.82	0.82	0.48
TN3	0.60	0.96	0.95	0.87	0.41	0.98	0.98	0.89	0.07	0.47	0.54	0.34	0.17	0.83	0.83	0.55
TN4	0.62	0.96	0.96	0.87	0.43	0.98	0.98	0.91	0.05	0.48	0.76	0.33	0.12	0.70	0.70	0.53
TN5	0.61	0.94	0.92	0.90	0.45	0.97	0.97	0.95	0.03	0.42	0.29	0.41	0.08	0.91	0.91	0.62
TN6	0.59	0.95	0.94	0.88	0.40	0.98	0.98	0.91	0.05	0.48	0.50	0.36	0.08	0.80	0.80	0.59
TN7	0.71	0.94	0.91	0.89	0.56	0.89	0.89	0.96	0.02	0.53	0.29	0.74	0.06	0.63	0.63	0.59
TN8	0.90	0.87	0.88	0.56	0.73	0.70	0.69	0.72	0.15	0.57	0.22	0.44	0.05	0.55	0.55	0.59
TN9	0.64	0.96	0.96	0.85	0.45	0.97	0.96	0.90	0.06	0.50	0.56	0.35	0.07	0.76	0.76	0.58
TN10	0.68	0.97	0.97	0.86	0.50	0.97	0.96	0.89	0.08	0.47	0.35	0.38	0.15	0.93	0.93	0.61

W = Water extract, SA = *S. album*, SS = *S. spicatum*, SL = *S. lanceolatum*, MF = *M. fragrans*, AS = *A. silvestris*, TH = *T. hoaensis*, DD = *D. decandra* and TN1-TN10 = Chan-thana samples.

Table 69 Similarity index between the IR spectra of the fine powders of Chan-thana and authentic samples.

P	Preprocessing methods															
	Normalization								Normalization and second derivative							
	SA	SS	SL	MF	MG	AS	TH	DD	SA	SS	SL	MF	MG	AS	TH	DD
TN1	0.99	0.99	0.99	0.99	0.98	0.99	0.97	0.98	0.94	0.95	0.94	0.94	0.94	0.96	0.91	0.97
TN2	0.99	1.00	1.00	0.99	0.98	0.99	0.99	0.99	0.97	0.98	0.97	0.94	0.97	0.97	0.98	0.97
TN3	0.98	0.99	0.99	0.99	0.98	0.98	1.00	0.98	0.98	0.97	0.95	0.94	0.97	0.96	0.99	0.94
TN4	0.98	1.00	0.99	0.98	0.97	0.98	0.99	0.98	0.97	0.98	0.97	0.95	0.97	0.97	0.98	0.95
TN5	0.97	0.99	0.99	0.98	0.97	0.98	0.99	0.98	0.96	0.97	0.96	0.93	0.96	0.95	0.99	0.94
TN6	0.98	0.99	0.99	0.98	0.97	0.98	0.99	0.98	0.97	0.97	0.96	0.95	0.96	0.97	0.99	0.95
TN7	0.99	0.99	0.99	0.99	0.99	1.00	0.99	1.00	0.96	0.98	0.97	0.94	0.97	0.97	0.96	0.98
TN8	0.92	0.94	0.96	0.95	0.96	0.96	0.95	0.97	0.93	0.96	0.95	0.88	0.93	0.93	0.93	0.96
TN9	0.99	1.00	1.00	0.99	0.98	0.99	0.99	0.99	0.98	0.98	0.97	0.95	0.97	0.97	0.99	0.95
TN10	0.99	0.99	0.99	1.00	0.99	1.00	0.99	0.99	0.99	0.98	0.96	0.95	0.98	0.98	0.99	0.95

P = Fine powder, SA = *S. album*, SS = *S. spicatum*, SL = *S. lanceolatum*, MF = *M. fragrans*, AS = *A. silvestris*, TH = *T. hoaensis*, DD = *D. decandra* and TN1-TN10 = Chan-thana samples.

Table 70 Similarity index between the IR spectra of the *n*-hexane extracts of Chan-hom and authentic samples.

H	Preprocessing methods															
	Normalization									Normalization and second derivative						
	SA	SS	SL	MF	MG	AS	TH	DD	SA	SS	SL	MF	MG	AS	TH	DD
H1	0.83	0.78	0.85	0.94	0.91	0.94	0.97	0.92	0.49	0.61	0.74	0.85	0.88	0.84	0.97	0.80
H2	0.94	0.98	0.99	0.77	0.70	0.87	0.86	0.83	0.79	0.96	0.92	0.29	0.41	0.39	0.53	0.58
H3	0.93	0.98	0.99	0.78	0.72	0.87	0.86	0.82	0.82	0.96	0.93	0.32	0.44	0.41	0.54	0.58
H4	0.93	0.97	0.99	0.80	0.73	0.89	0.88	0.84	0.78	0.93	0.92	0.38	0.47	0.44	0.58	0.58
H5	0.91	0.97	0.99	0.79	0.72	0.89	0.87	0.83	0.74	0.93	0.93	0.39	0.48	0.45	0.59	0.59
H6	0.94	0.99	0.99	0.77	0.68	0.86	0.85	0.82	0.76	0.97	0.93	0.27	0.39	0.38	0.50	0.55
H7	0.75	0.85	0.85	0.57	0.48	0.64	0.65	0.59	0.51	0.65	0.63	0.19	0.26	0.22	0.41	0.39
H8	0.83	0.93	0.93	0.65	0.55	0.75	0.74	0.71	0.65	0.87	0.86	0.31	0.41	0.38	0.55	0.53
H9	0.90	0.96	0.97	0.73	0.64	0.81	0.81	0.77	0.76	0.91	0.88	0.26	0.38	0.33	0.51	0.54
H10	0.71	0.71	0.76	0.79	0.97	0.80	0.86	0.74	0.43	0.53	0.63	0.76	0.92	0.74	0.91	0.70
H11	0.71	0.68	0.75	0.83	0.95	0.83	0.85	0.75	0.34	0.44	0.48	0.52	0.60	0.47	0.60	0.45

H = *n*-Hexane extract, SA = *S. album*, SS = *S. spicatum*, SL = *S. lanceolatum*, MF = *M. fragrans*, AS = *A. silvestris*, TH = *T. hoensis*, DD = *D. decandra* and H1-H11 = Chan-hom samples.

Table 71 Similarity index between the IR spectra of the dichloromethane extracts of Chan-hom and authentic samples.

D	Preprocessing methods															
	Normalization									Normalization and second derivative						
	SA	SS	SL	MF	MG	AS	TH	DD	SA	SS	SL	MF	MG	AS	TH	DD
H1	0.82	0.77	0.80	0.65	0.79	0.91	0.93	0.95	0.60	0.61	0.67	0.28	0.62	0.75	0.85	0.80
H2	0.88	0.93	0.94	0.65	0.82	0.86	0.93	0.83	0.67	0.85	0.81	0.23	0.59	0.62	0.72	0.52
H3	0.88	0.92	0.93	0.65	0.81	0.86	0.92	0.84	0.62	0.76	0.73	0.24	0.62	0.63	0.72	0.47
H4	0.86	0.91	0.92	0.64	0.80	0.86	0.92	0.84	0.57	0.70	0.68	0.24	0.63	0.63	0.71	0.44
H5	0.86	0.89	0.91	0.63	0.80	0.87	0.91	0.85	0.50	0.64	0.61	0.22	0.65	0.64	0.69	0.37
H6	0.87	0.92	0.93	0.63	0.78	0.83	0.90	0.84	0.63	0.83	0.81	0.21	0.56	0.59	0.69	0.50
H7	0.88	0.93	0.94	0.62	0.77	0.83	0.90	0.82	0.73	0.88	0.84	0.22	0.51	0.59	0.69	0.55
H8	0.87	0.94	0.95	0.63	0.76	0.79	0.89	0.81	0.68	0.89	0.85	0.22	0.51	0.55	0.68	0.56
H9	0.87	0.93	0.94	0.63	0.78	0.83	0.90	0.82	0.63	0.78	0.75	0.22	0.60	0.62	0.72	0.48
H10	0.59	0.70	0.69	0.73	0.99	0.74	0.85	0.68	0.09	0.11	0.09	0.27	0.94	0.55	0.66	0.21
H11	0.60	0.70	0.69	0.70	0.99	0.75	0.84	0.68	0.10	0.15	0.14	0.22	0.92	0.52	0.65	0.21

D = Dichloromethane extract, SA = *S. album*, SS = *S. spicatum*, SL = *S. lanceolatum*, MF = *M. fragrans*, AS = *A. silvestris*, TH = *T. hoensis*, DD = *D. decandra* and H1-H11 = Chan-hom samples.

Table 72 Similarity index between the IR spectra of the ethyl acetate extracts of Chan-hom and authentic samples.

E	Preprocessing methods															
	Normalization									Normalization and second derivative						
	SA	SS	SL	MF	MG	AS	TH	DD	SA	SS	SL	MF	MG	AS	TH	DD
H1	0.73	0.78	0.76	0.48	0.73	0.92	0.41	0.92	0.48	0.55	0.63	0.42	0.63	0.77	0.32	0.69
H2	0.86	0.94	0.93	0.64	0.85	0.90	0.61	0.92	0.63	0.84	0.83	0.39	0.61	0.61	0.35	0.53
H3	0.88	0.95	0.95	0.67	0.85	0.89	0.64	0.92	0.68	0.86	0.85	0.37	0.57	0.59	0.32	0.55
H4	0.88	0.93	0.93	0.63	0.85	0.91	0.60	0.93	0.69	0.85	0.85	0.41	0.61	0.59	0.38	0.56
H5	0.83	0.91	0.90	0.62	0.83	0.92	0.59	0.93	0.48	0.64	0.66	0.39	0.60	0.66	0.34	0.41
H6	0.88	0.98	0.97	0.71	0.86	0.83	0.69	0.88	0.69	0.93	0.91	0.30	0.50	0.49	0.26	0.54
H7	0.85	0.95	0.94	0.67	0.82	0.89	0.64	0.91	0.68	0.87	0.84	0.31	0.48	0.55	0.26	0.50
H8	0.85	0.95	0.94	0.69	0.83	0.87	0.66	0.90	0.63	0.88	0.86	0.31	0.53	0.54	0.27	0.52
H9	0.88	0.95	0.95	0.74	0.84	0.87	0.72	0.90	0.76	0.89	0.86	0.47	0.57	0.57	0.45	0.50
H10	0.58	0.77	0.76	0.55	0.95	0.75	0.51	0.81	0.29	0.36	0.37	0.45	0.87	0.60	0.44	0.37
H11	0.52	0.70	0.69	0.44	0.90	0.74	0.39	0.78	0.11	0.15	0.20	0.34	0.75	0.60	0.31	0.28

E = Ethyl acetate extract, SA = *S. album*, SS = *S. spicatum*, SL = *S. lanceolatum*, MF = *M. fragrans*, AS = *A. silvestris*, TH = *T. hoensis*, DD = *D. decandra* and H1-H11 = Chan-hom samples.

Table 73 Similarity index between the IR spectra of the acetone extracts of Chan-hom and authentic samples.

A	Preprocessing methods															
	Normalization								Normalization and second derivative							
	SA	SS	SL	MF	MG	AS	TH	DD	SA	SS	SL	MF	MG	AS	TH	DD
H1	0.81	0.83	0.85	0.65	0.77	0.91	0.70	0.87	0.54	0.61	0.69	0.33	0.59	0.78	0.49	0.68
H2	0.92	0.97	0.97	0.73	0.81	0.86	0.86	0.91	0.75	0.93	0.88	0.31	0.43	0.58	0.46	0.49
H3	0.87	0.93	0.93	0.77	0.88	0.89	0.87	0.91	0.59	0.69	0.70	0.39	0.74	0.64	0.67	0.51
H4	0.90	0.95	0.95	0.73	0.83	0.89	0.87	0.92	0.70	0.83	0.81	0.35	0.58	0.66	0.56	0.49
H5	0.89	0.94	0.94	0.74	0.85	0.89	0.87	0.91	0.60	0.72	0.73	0.37	0.70	0.66	0.64	0.48
H6	0.91	0.97	0.97	0.75	0.83	0.88	0.88	0.91	0.72	0.90	0.88	0.33	0.50	0.62	0.52	0.51
H7	0.88	0.93	0.93	0.76	0.86	0.89	0.87	0.91	0.60	0.71	0.71	0.38	0.70	0.64	0.66	0.50
H8	0.89	0.95	0.95	0.75	0.83	0.86	0.88	0.92	0.67	0.84	0.81	0.33	0.55	0.58	0.56	0.50
H9	0.89	0.94	0.94	0.75	0.84	0.89	0.87	0.92	0.68	0.81	0.79	0.35	0.60	0.64	0.58	0.48
H10	0.58	0.69	0.72	0.88	0.99	0.82	0.83	0.71	0.25	0.23	0.28	0.43	0.97	0.62	0.75	0.40
H11	0.61	0.72	0.75	0.88	0.99	0.84	0.84	0.74	0.15	0.13	0.19	0.41	0.97	0.60	0.70	0.28

A = Acetone extract, SA = *S. album*, SS = *S. spicatum*, SL = *S. lanceolatum*, MF = *M. fragrans*, AS = *A. silvestris*, TH = *T. hoaensis*, DD = *D. decandra* and H1-H11 = Chan-hom samples.

Table 74 Similarity index between the IR spectra of the methanol extracts of Chan-hom and authentic samples.

M	Preprocessing methods															
	Normalization								Normalization and second derivative							
	SA	SS	SL	MF	MG	AS	TH	DD	SA	SS	SL	MF	MG	AS	TH	DD
H1	0.80	0.72	0.72	0.62	0.72	0.79	0.44	0.86	0.59	0.56	0.60	0.28	0.58	0.70	0.42	0.70
H2	0.90	0.93	0.92	0.75	0.73	0.83	0.48	0.92	0.68	0.83	0.83	0.33	0.53	0.67	0.51	0.60
H3	0.91	0.94	0.93	0.74	0.68	0.81	0.45	0.93	0.72	0.84	0.83	0.31	0.52	0.67	0.49	0.59
H4	0.90	0.92	0.91	0.73	0.72	0.82	0.47	0.92	0.68	0.79	0.80	0.32	0.55	0.68	0.49	0.59
H5	0.90	0.93	0.92	0.74	0.71	0.83	0.48	0.93	0.69	0.83	0.82	0.31	0.53	0.68	0.50	0.60
H6	0.93	0.97	0.96	0.72	0.62	0.77	0.43	0.90	0.78	0.95	0.92	0.27	0.31	0.60	0.44	0.53
H7	0.91	0.94	0.94	0.73	0.69	0.83	0.51	0.93	0.76	0.88	0.87	0.32	0.44	0.66	0.53	0.60
H8	0.88	0.94	0.94	0.75	0.66	0.82	0.51	0.95	0.73	0.88	0.87	0.31	0.43	0.64	0.50	0.61
H9	0.91	0.94	0.94	0.73	0.67	0.81	0.49	0.93	0.80	0.93	0.90	0.29	0.33	0.62	0.47	0.54
H10	0.37	0.38	0.46	0.65	0.94	0.83	0.79	0.55	0.11	0.08	0.16	0.35	0.94	0.47	0.53	0.50
H11	0.59	0.65	0.70	0.84	0.96	0.89	0.61	0.78	0.17	0.17	0.23	0.33	0.88	0.54	0.45	0.50

M = Methanol extract, SA = *S. album*, SS = *S. spicatum*, SL = *S. lanceolatum*, MF = *M. fragrans*, AS = *A. silvestris*, TH = *T. hoaensis*, DD = *D. decandra* and H1-H11 = Chan-hom samples.

Table 75 Similarity index between the IR spectra of the water extracts of Chan-hom and authentic samples.

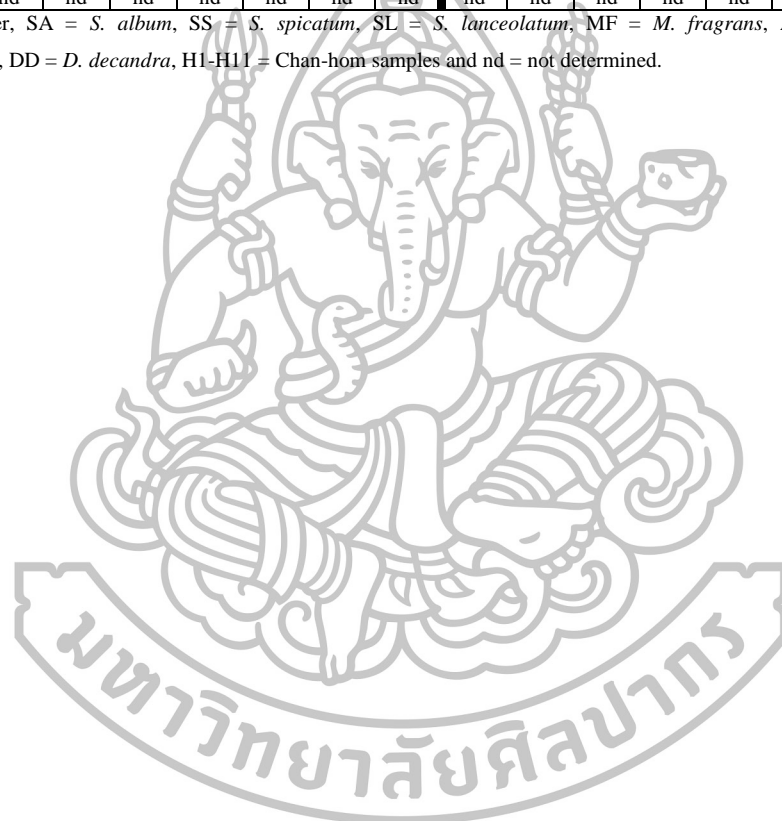
W	Preprocessing methods															
	Normalization								Normalization and second derivative							
	SA	SS	SL	MF	MG	AS	TH	DD	SA	SS	SL	MF	MG	AS	TH	DD
H1	0.82	0.94	0.94	0.80	0.66	0.85	0.85	0.90	0.24	0.48	0.37	0.50	0.18	0.60	0.60	0.74
H2	0.78	0.90	0.87	0.70	0.70	0.79	0.78	0.82	0.25	0.77	0.37	0.27	-0.02	0.65	0.65	0.56
H3	0.77	0.98	0.97	0.83	0.57	0.90	0.90	0.91	0.25	0.81	0.41	0.36	-0.04	0.56	0.56	0.64
H4	0.76	0.98	0.96	0.81	0.59	0.90	0.90	0.89	0.24	0.82	0.36	0.29	-0.06	0.62	0.62	0.61
H5	0.73	0.98	0.96	0.85	0.54	0.92	0.91	0.91	0.24	0.83	0.37	0.34	-0.06	0.53	0.53	0.59
H6	0.73	0.99	0.97	0.85	0.55	0.92	0.92	0.92	0.22	0.85	0.40	0.36	-0.06	0.55	0.55	0.59
H7	0.70	0.95	0.94	0.75	0.52	0.88	0.87	0.79	0.16	0.76	0.39	0.29	-0.05	0.68	0.68	0.52
H8	0.69	0.97	0.95	0.84	0.52	0.92	0.91	0.89	0.23	0.74	0.26	0.20	-0.11	0.54	0.54	0.49
H9	0.65	0.97	0.94	0.83	0.47	0.93	0.92	0.86	0.17	0.75	0.29	0.20	-0.13	0.53	0.53	0.45
H10	0.88	0.62	0.67	0.30	0.96	0.45	0.44	0.48	0.16	-0.01	0.17	0.16	0.91	0.25	0.25	0.13
H11	0.90	0.86	0.89	0.54	0.74	0.71	0.70	0.68	0.26	0.56	0.40	0.28	0.18	0.56	0.56	0.52

W = Water extract, SA = *S. album*, SS = *S. spicatum*, SL = *S. lanceolatum*, MF = *M. fragrans*, AS = *A. silvestris*, TH = *T. hoaensis*, DD = *D. decandra* and H1-H11 = Chan-hom samples.

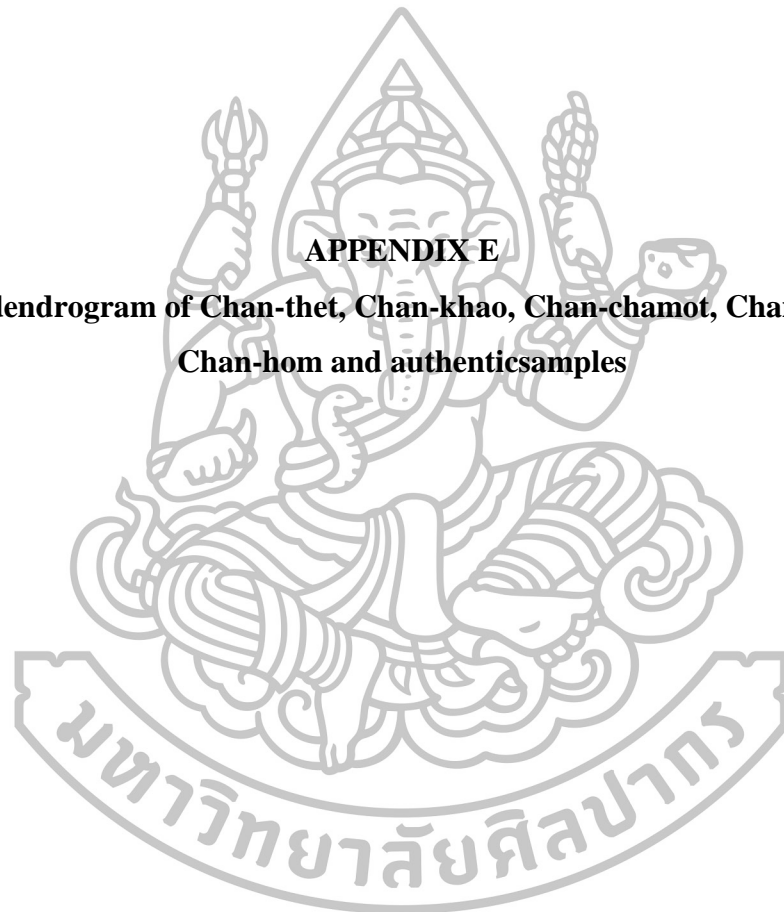
Table 76 Similarity index between the IR spectra of the fine powders of Chan-hom and authentic samples.

P	Preprocessing methods															
	Normalization								Normalization and second derivative							
	SA	SS	SL	MF	MG	AS	TH	DD	SA	SS	SL	MF	MG	AS	TH	DD
H1	0.96	0.98	0.99	0.97	0.97	0.97	0.99	0.98	0.94	0.96	0.96	0.92	0.94	0.93	0.98	0.93
H2	0.98	0.99	0.99	0.99	0.98	0.99	0.99	0.99	0.98	0.99	0.98	0.94	0.97	0.96	0.98	0.95
H3	0.96	0.98	0.99	0.97	0.97	0.98	0.99	0.98	0.95	0.97	0.98	0.91	0.95	0.93	0.98	0.93
H4	0.94	0.96	0.98	0.96	0.96	0.96	0.98	0.98	0.94	0.97	0.97	0.91	0.94	0.93	0.96	0.93
H5	0.95	0.97	0.98	0.97	0.97	0.97	0.98	0.98	0.95	0.97	0.98	0.91	0.94	0.93	0.97	0.93
H6	0.99	1.00	1.00	0.99	0.99	0.99	0.99	0.99	0.99	0.99	0.98	0.94	0.98	0.97	0.98	0.96
H7	0.99	0.99	0.99	0.99	0.99	0.99	0.99	0.99	0.97	0.99	0.98	0.93	0.96	0.95	0.97	0.95
H8	0.99	0.99	0.99	0.99	0.98	0.99	0.98	0.99	0.96	0.97	0.96	0.92	0.94	0.94	0.95	0.93
H9	0.96	0.97	0.98	0.98	0.98	0.98	0.98	0.99	0.97	0.99	0.98	0.93	0.96	0.95	0.96	0.95
H10	0.98	0.98	0.99	0.98	0.99	0.99	0.98	0.99	0.97	0.98	0.96	0.93	0.98	0.97	0.97	0.96
H11	nd	nd	nd	nd	nd	nd	nd	nd	nd	nd	nd	nd	nd	nd	nd	nd

P = Fine powder, SA = *S. album*, SS = *S. spicatum*, SL = *S. lanceolatum*, MF = *M. fragrans*, AS = *A. silvestris*, TH = *T. hoensis*, DD = *D. decandra*, H1-H11 = Chan-hom samples and nd = not determined.



APPENDIX E
HCA dendrogram of Chan-thet, Chan-khao, Chan-chamot, Chan-thana,
Chan-hom and authentic samples



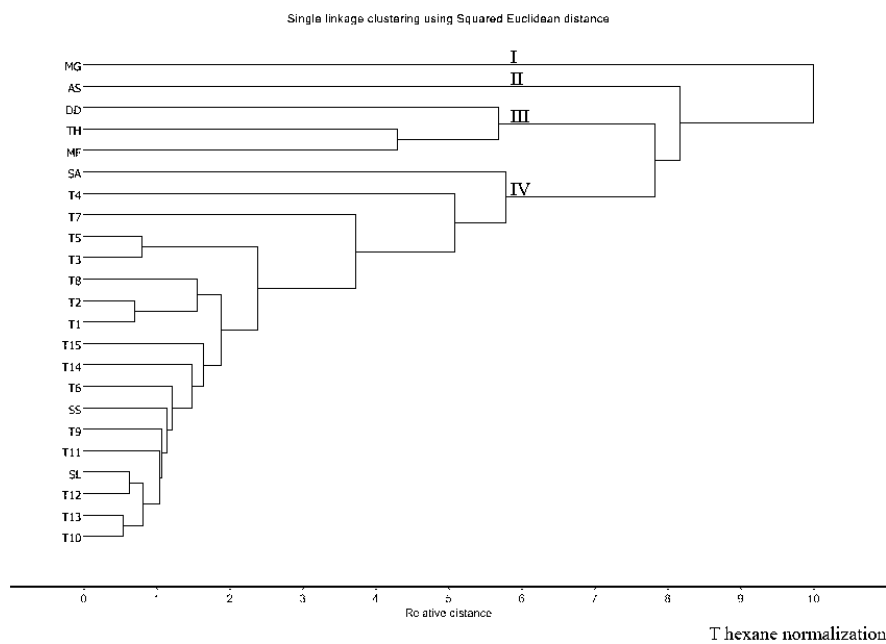


Figure 107 HCA dendrogram the IR spectra of the *n*-hexane extracts of Chan-thet samples (T1-T15), *S. album* (SA), *S. spicatum* (SS), *S. lanceolatum* (SL), *M. fragrans* (MF), *T. hoagensis* (TH), *D. decandra* (DD), *M. gagei* (MG) and *A. silvestris* (AS) after normalization preprocessing.

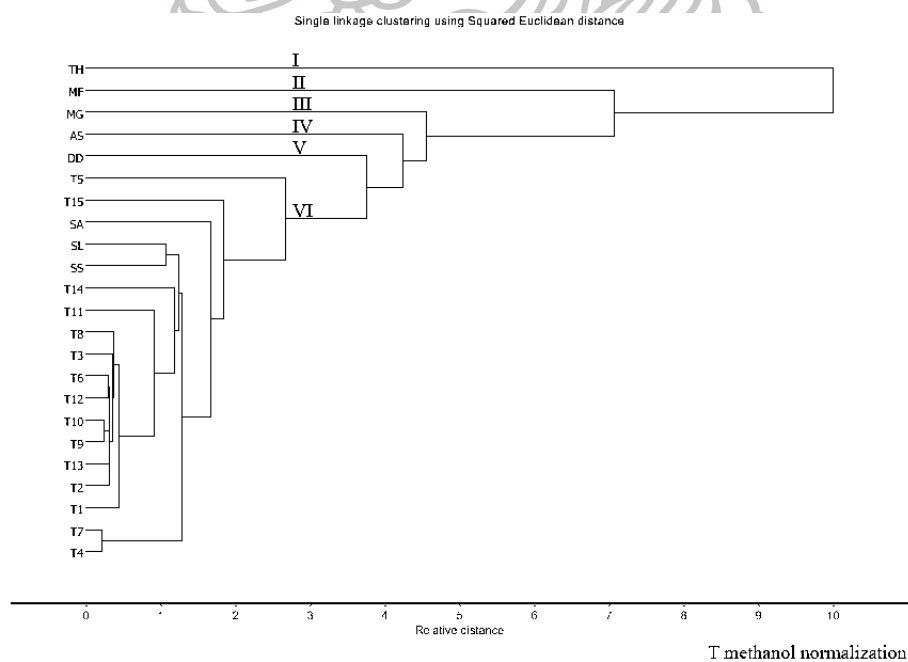
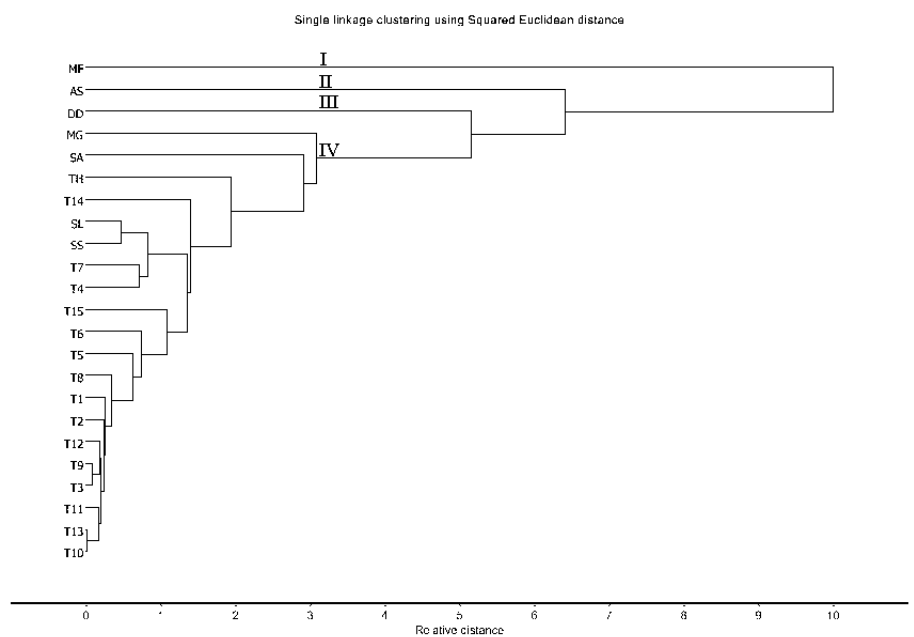


Figure 108 HCA dendrogram the IR spectra of the methanol extracts of Chan-thet samples (T1-T15), *S. album* (SA), *S. spicatum* (SS), *S. lanceolatum* (SL), *M. fragrans* (MF), *T. hoagensis* (TH), *D. decandra* (DD), *M. gagei* (MG) and *A. silvestris* (AS) after normalization preprocessing.

(a)



(b)

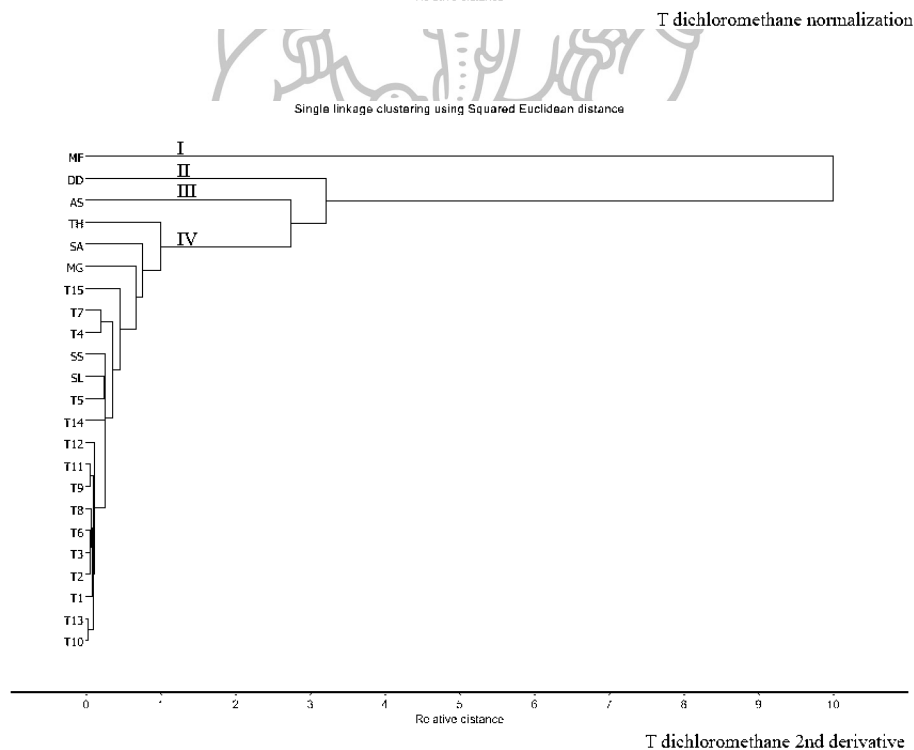
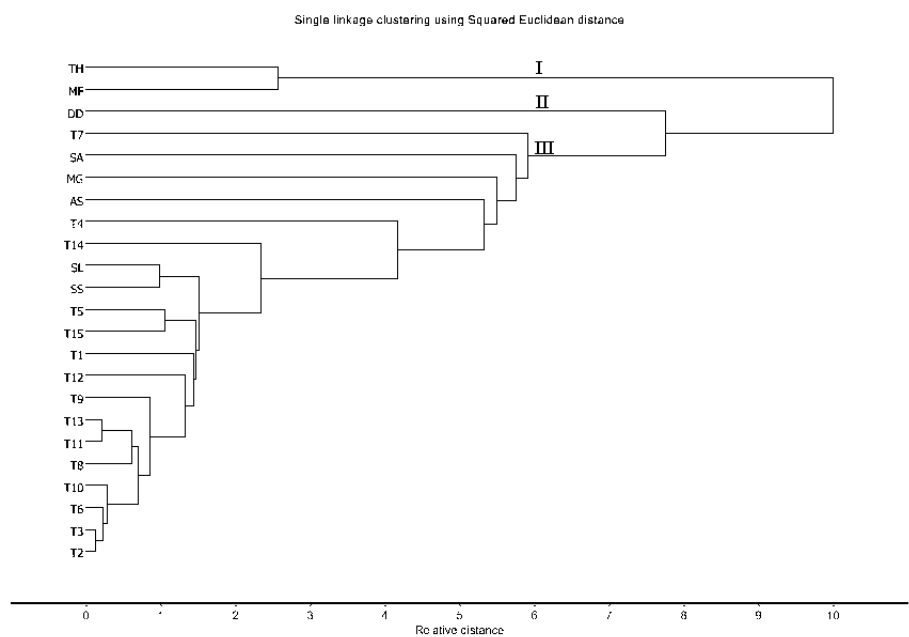


Figure 109 HCA dendrogram the IR spectra of the dichloromethane extracts of Chan-thet samples (T1-T15), *S. album* (SA), *S. spicatum* (SS), *S. lanceolatum* (SL), *M. fragrans* (MF), *T. hoensis* (TH), *D. decandra* (DD), *M. gagei* (MG) and *A. silvestris* (AS) after (a) normalization and (b) second derivative preprocessing.

(a)



(b)

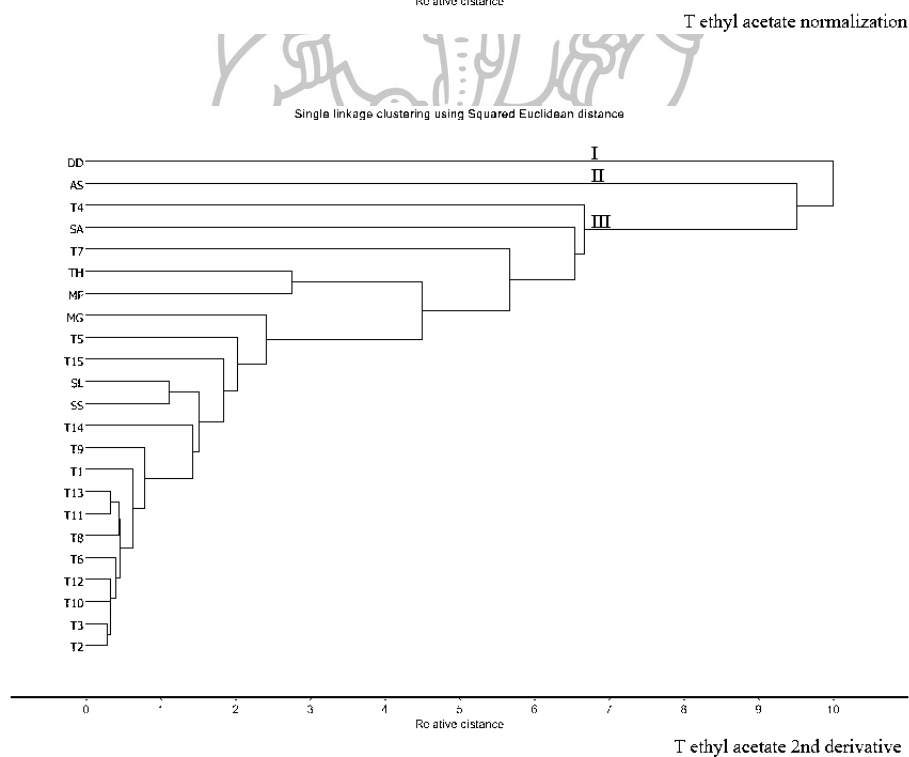
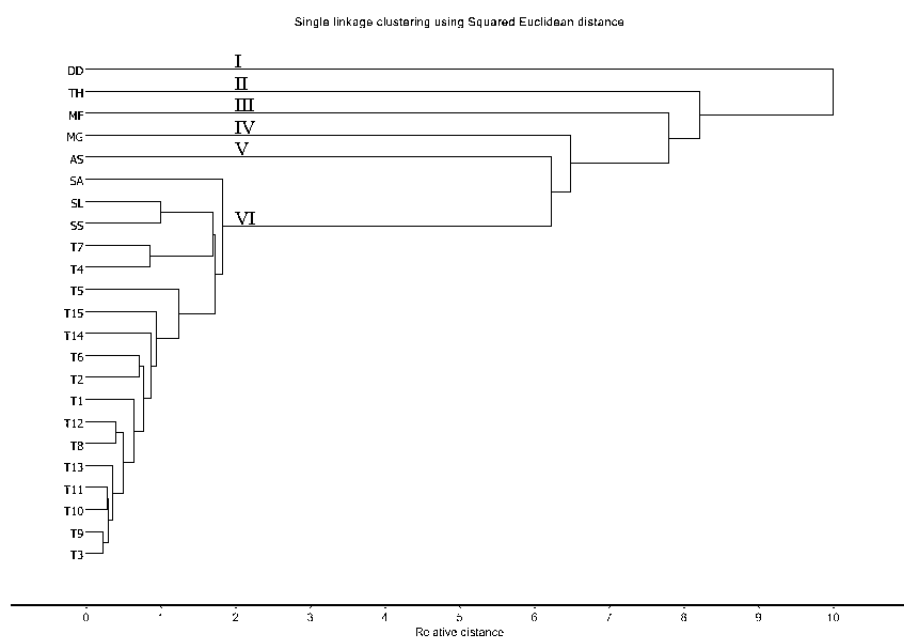


Figure 110 HCA dendrogram the IR spectra of the ethyl acetate extracts of Chan-thet samples (T1-T15), *S. album* (SA), *S. spicatum* (SS), *S. lanceolatum* (SL), *M. fragrans* (MF), *T. hoensis* (TH), *D. decandra* (DD), *M. gagei* (MG) and *A. silvestris* (AS) after (a) normalization and (b) second derivative preprocessing.

(a)



(b)

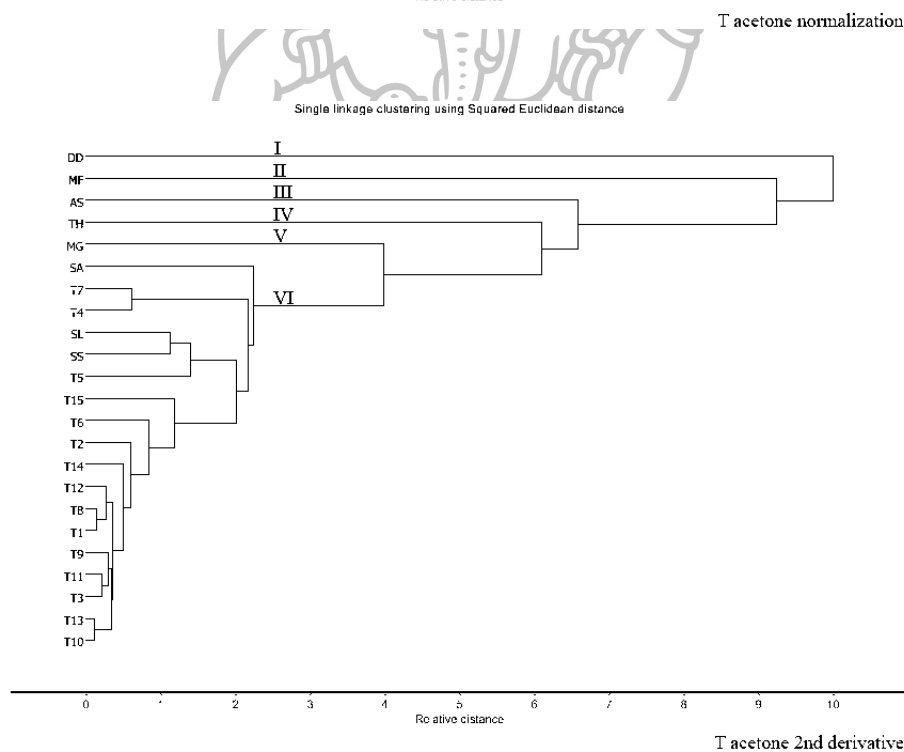
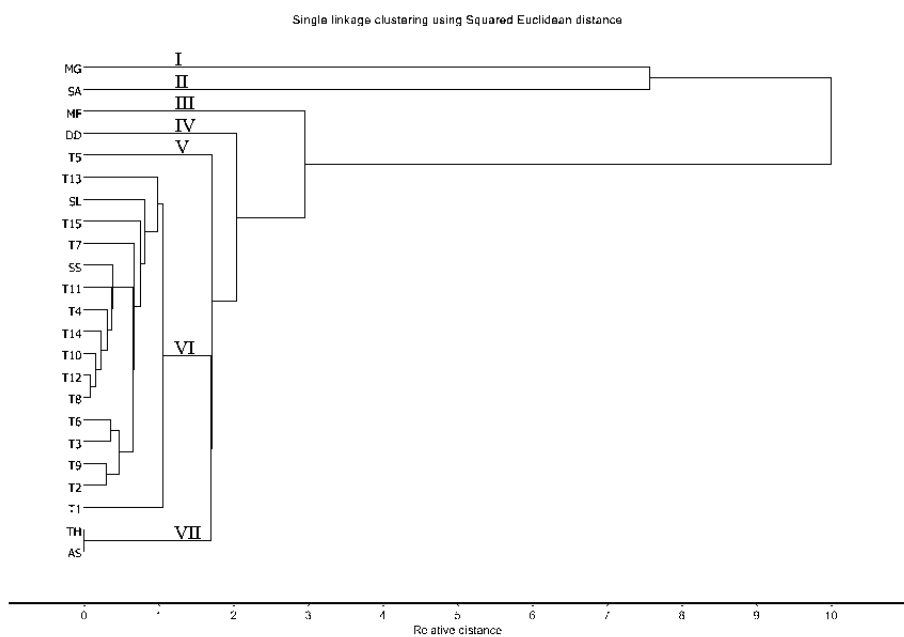


Figure 111 HCA dendrogram the IR spectra of the acetone extracts of Chan-thet samples (T1-T15), *S. album* (SA), *S. spicatum* (SS), *S. lanceolatum* (SL), *M. fragrans* (MF), *T. hoensis* (TH), *D. decandra* (DD), *M. gagei* (MG) and *A. silvestris* (AS) after (a) normalization and (b) second derivative preprocessing.

(a)



(b)

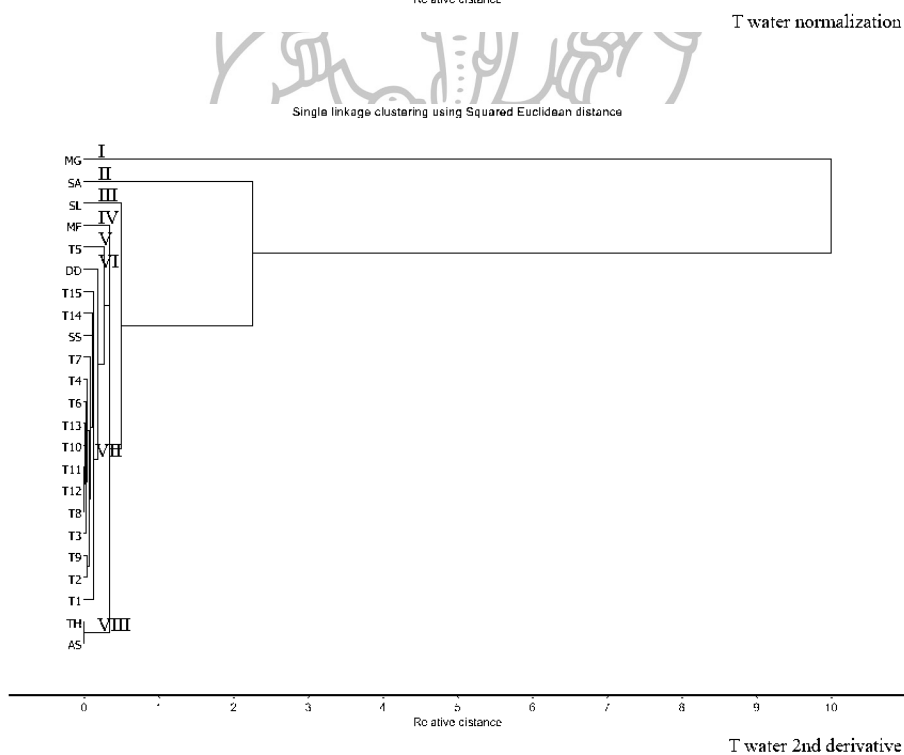


Figure 112 HCA dendrogram the IR spectra of the water extracts of Chan-thet samples (T1-T15), *S. album* (SA), *S. spicatum* (SS), *S. lanceolatum* (SL), *M. fragrans* (MF), *T. hoensis* (TH), *D. decandra* (DD), *M. gagei* (MG) and *A. silvestris* (AS) after (a) normalization and (b) second derivative preprocessing.

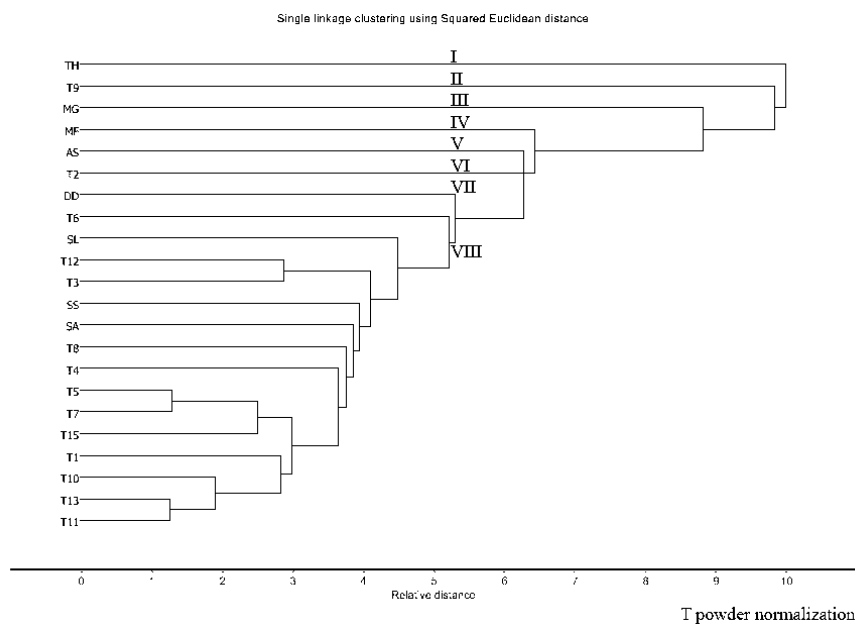


Figure 113 HCA dendrogram the IR spectra of the fine powders of Chan-thet samples (T1-T15), *S. album* (SA), *S. spicatum* (SS), *S. lanceolatum* (SL), *M. fragrans* (MF), *T. hoensis* (TH), *D. decandra* (DD), *M. gagei* (MG) and *A. silvestris* (AS) after normalization preprocessing.

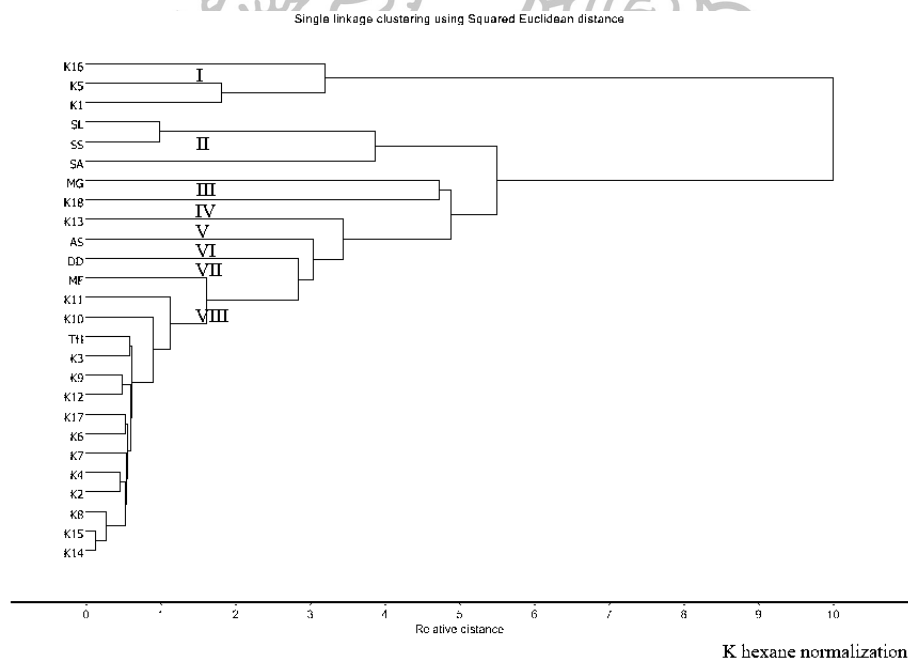
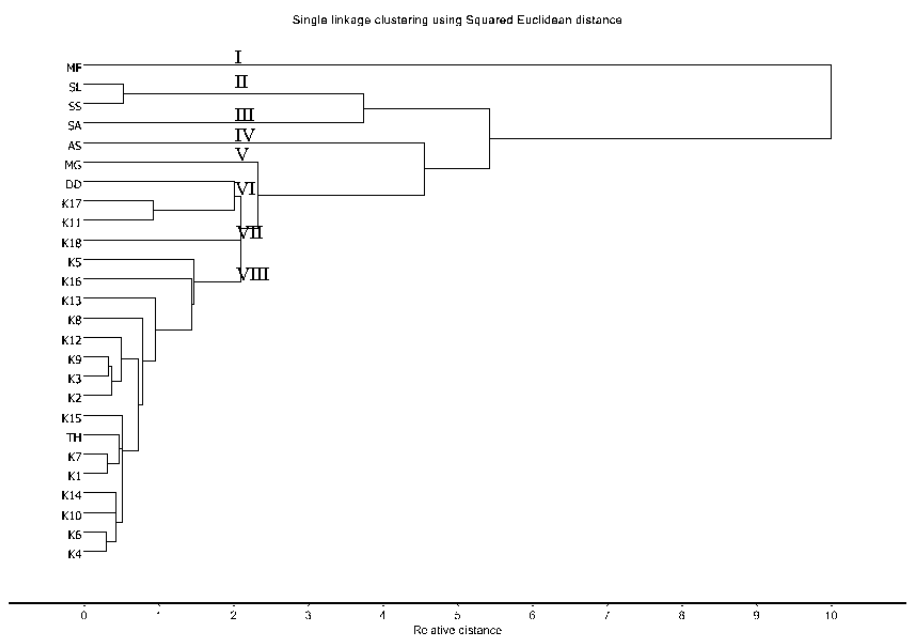


Figure 114 HCA dendrogram the IR spectra of the *n*-hexane extracts of Chan-khao samples (K1-K18), *S. album* (SA), *S. spicatum* (SS), *S. lanceolatum* (SL), *M. fragrans* (MF), *T. hoensis* (TH), *D. decandra* (DD), *M. gagei* (MG) and *A. silvestris* (AS) after normalization and preprocessing.

(a)



(b)

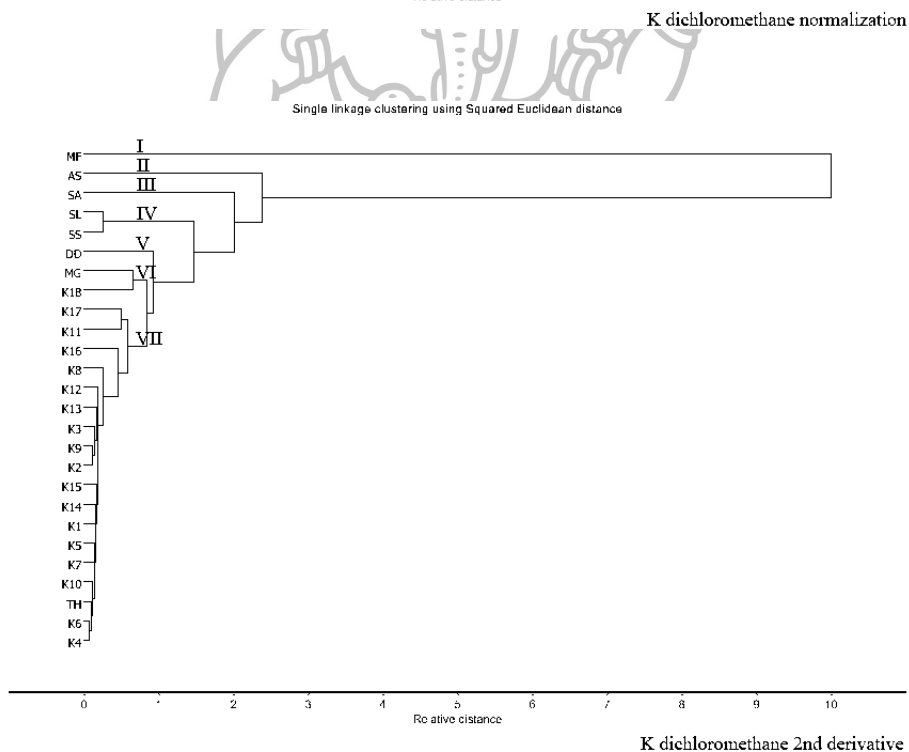
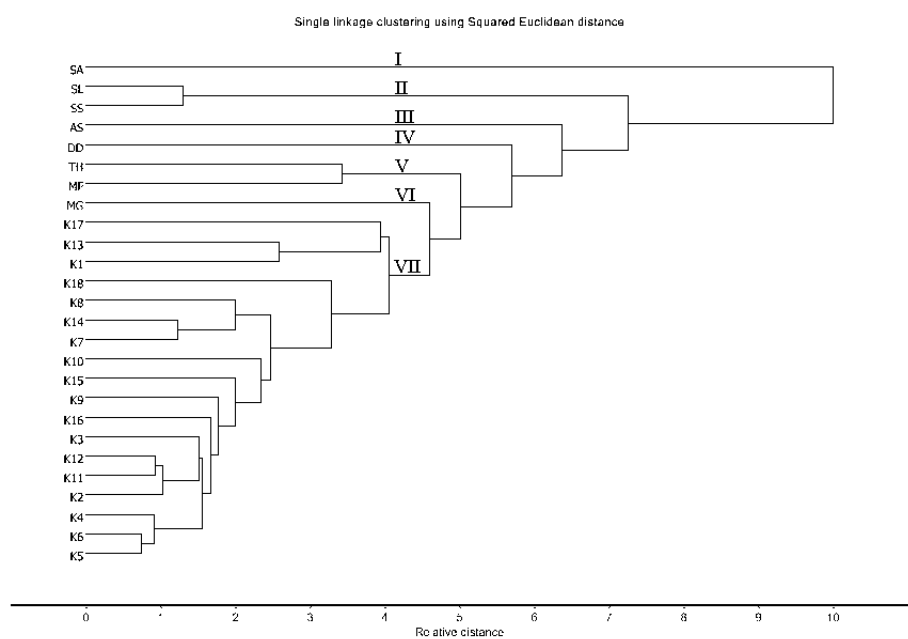


Figure 115 HCA dendrogram the IR spectra of the dichloromethane extracts of Chan-khao samples (K1-K18), *S. album* (SA), *S. spicatum* (SS), *S. lanceolatum* (SL), *M. fragrans* (MF), *T. hoensis* (TH), *D. decandra* (DD), *M. gagei* (MG) and *A. silvestris* (AS) after (a) normalization and (b) second derivative preprocessing.

(a)



(b)

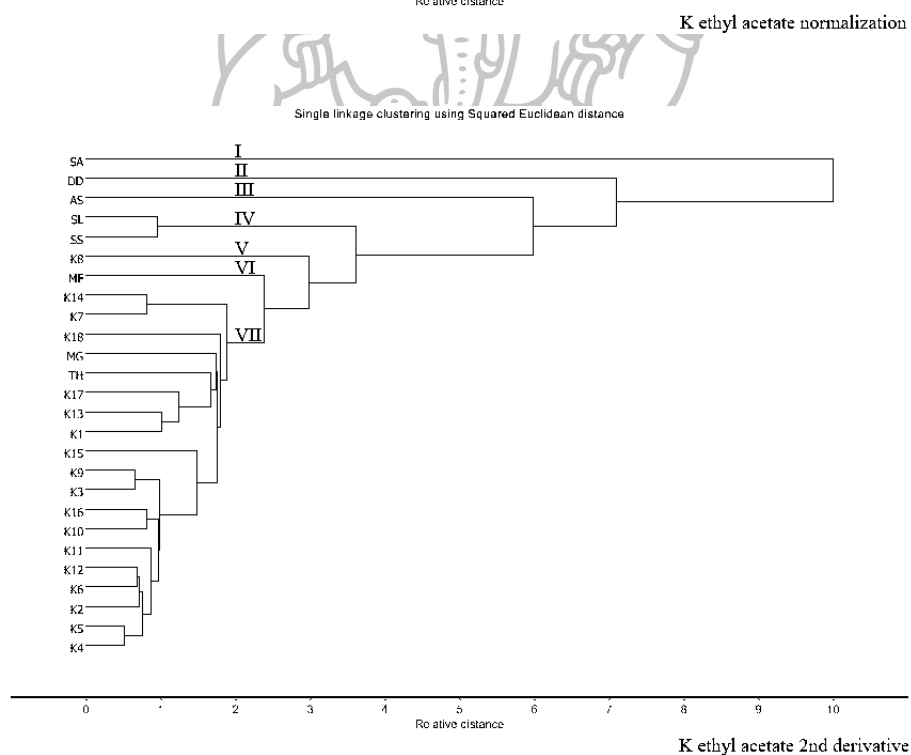
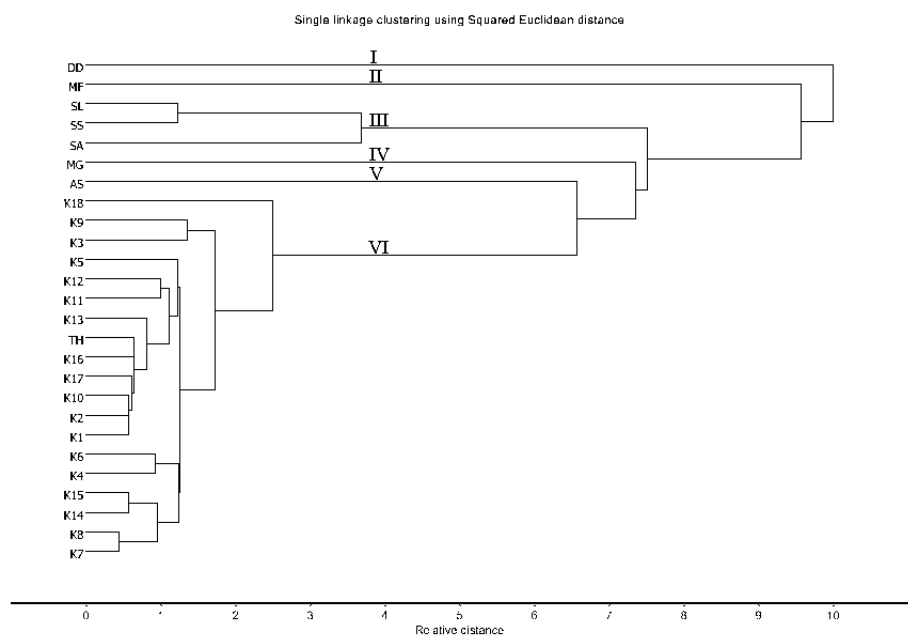


Figure 116 HCA dendrogram the IR spectra of the ethyl acetate extracts of Chan-khao samples (K1-K18), *S. album* (SA), *S. spicatum* (SS), *S. lanceolatum* (SL), *M. fragrans* (MF), *T. hoensis* (TH), *D. decandra* (DD), *M. gagei* (MG) and *A. silvestris* (AS) after (a) normalization and (b) second derivative preprocessing.

(a)



(b)

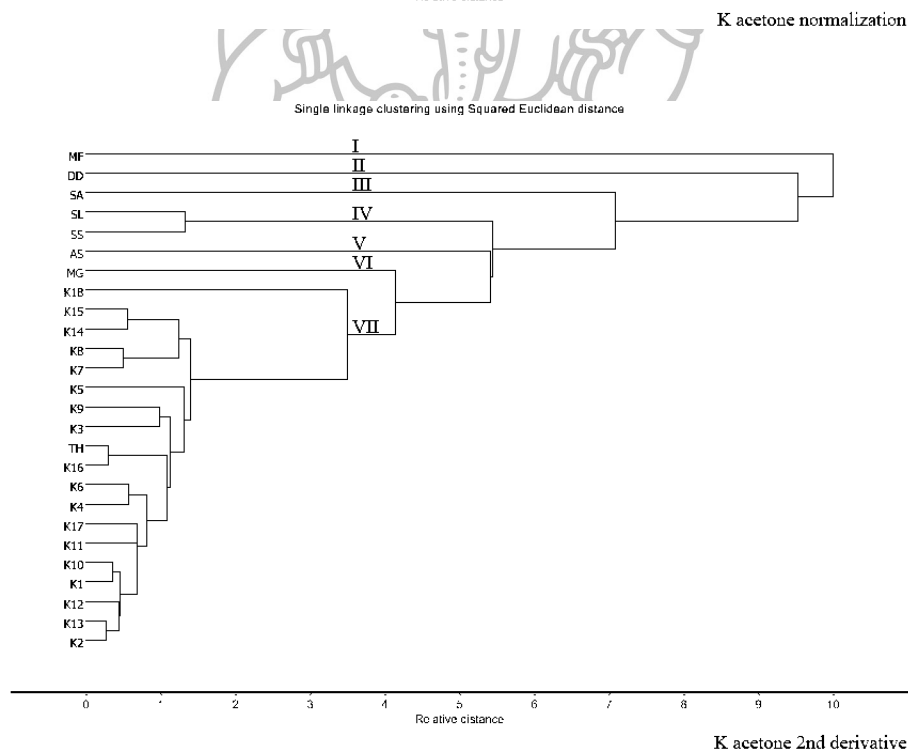
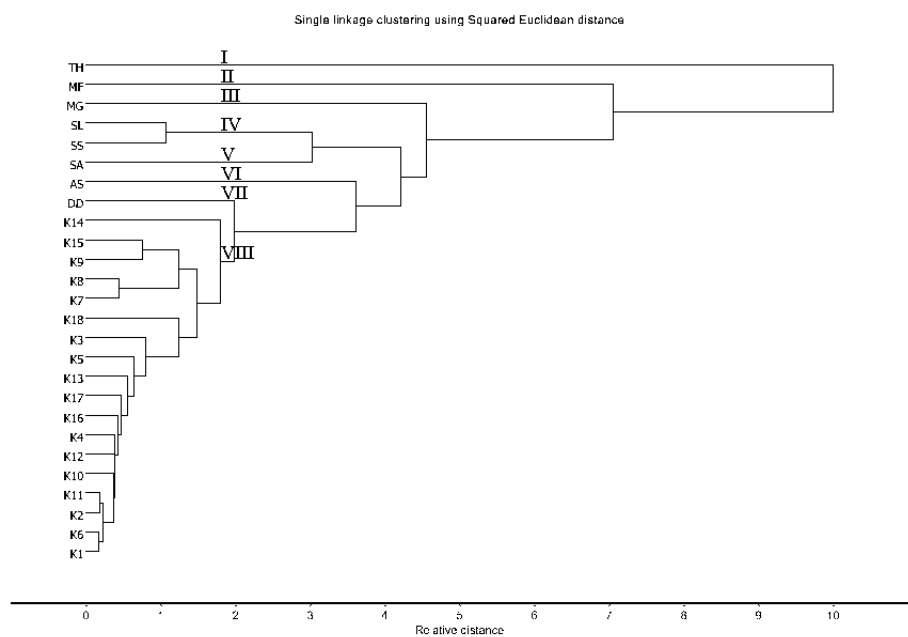


Figure 117 HCA dendrogram the IR spectra of the acetone extracts of Chan-khao samples (K1-K18), *S. album* (SA), *S. spicatum* (SS), *S. lanceolatum* (SL), *M. fragrans* (MF), *T. hoensis* (TH), *D. decandra* (DD), *M. gagei* (MG) and *A. silvestris* (AS) after (a) normalization and (b) second derivative preprocessing.

(a)



(b)

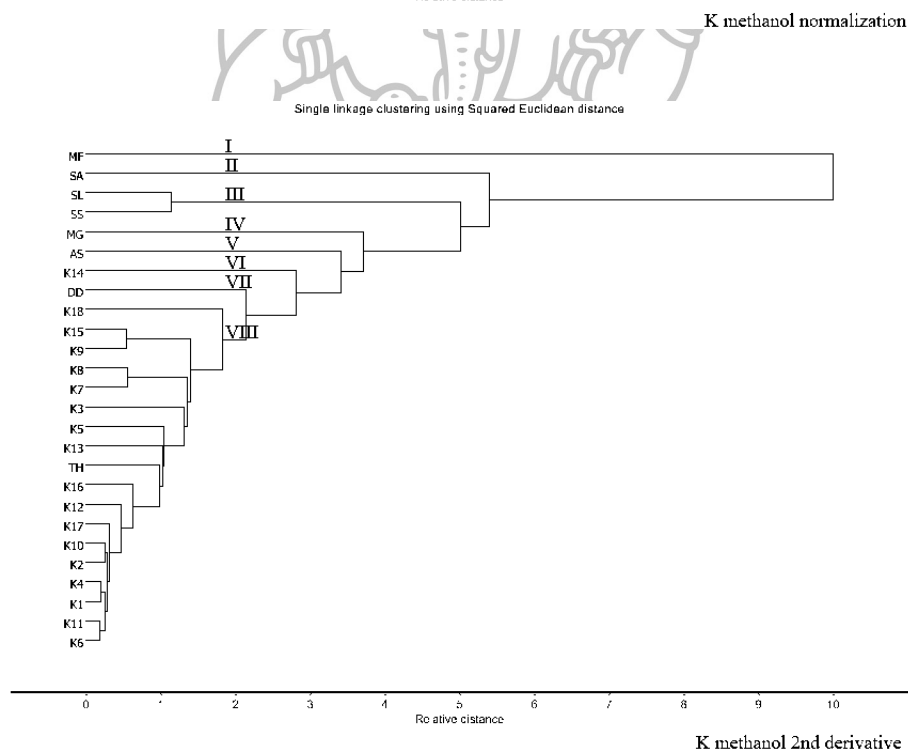
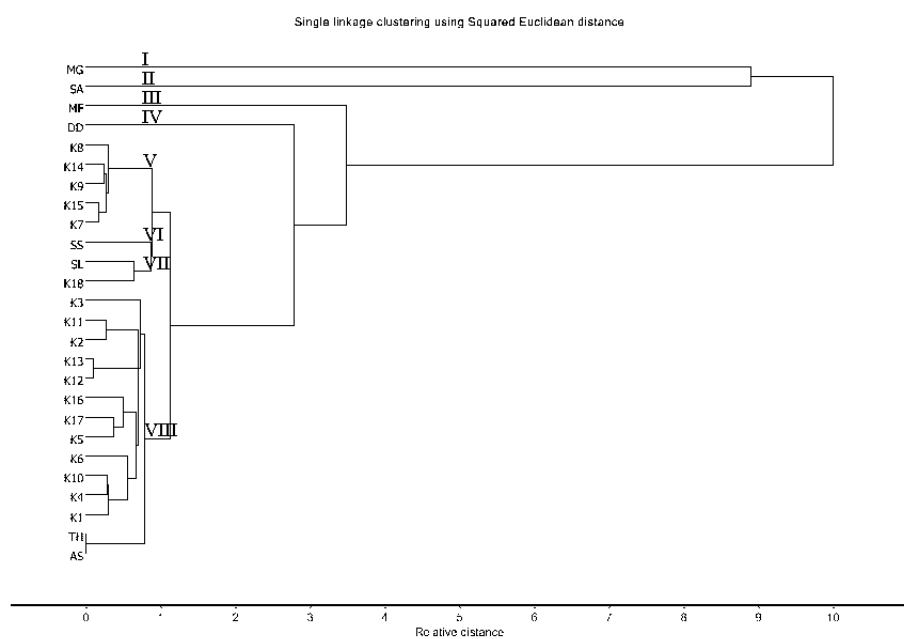


Figure 118 HCA dendrogram the IR spectra of the methanol extracts of Chan-khao samples (K1-K18), *S. album* (SA), *S. spicatum* (SS), *S. lanceolatum* (SL), *M. fragrans* (MF), *T. hoensis* (TH), *D. decandra* (DD), *M. gagei* (MG) and *A. silvestris* (AS) after (a) normalization and (b) second derivative preprocessing.

(a)



(b)

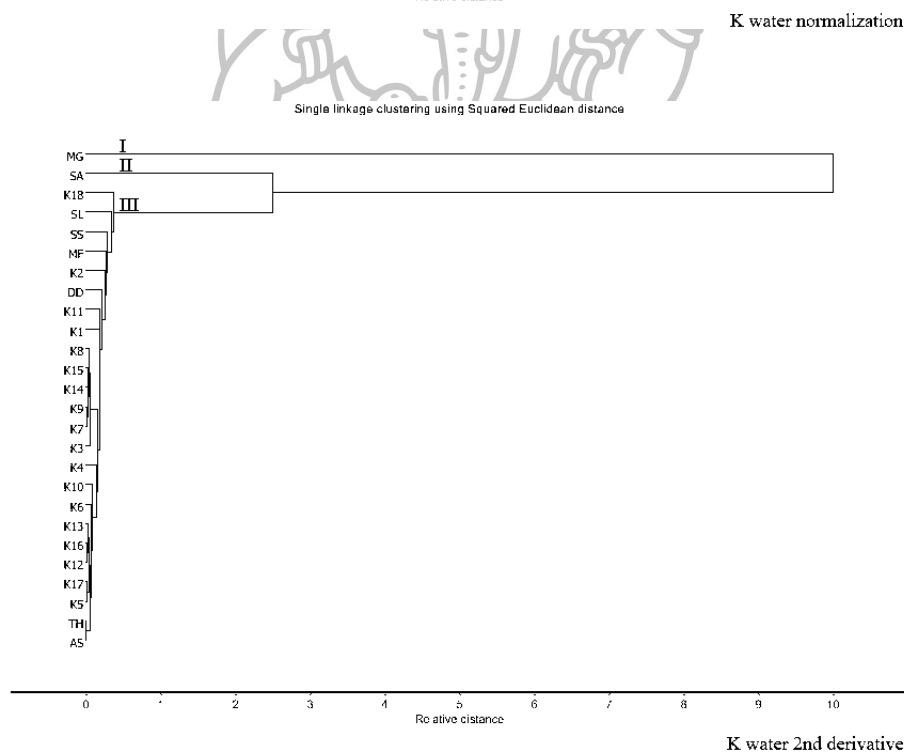


Figure 119 HCA dendrogram the IR spectra of the water extracts of Chan-khao samples (K1-K18), *S. album* (SA), *S. spicatum* (SS), *S. lanceolatum* (SL), *M. fragrans* (MF), *T. hoensis* (TH), *D. decandra* (DD), *M. gagei* (MG) and *A. silvestris* (AS) after (a) normalization and (b) second derivative preprocessing.

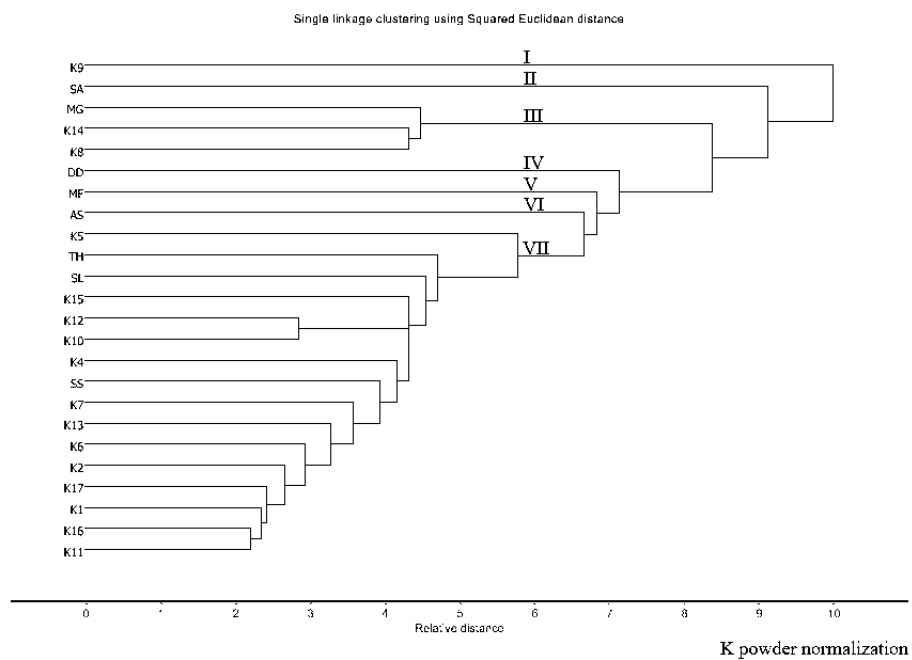
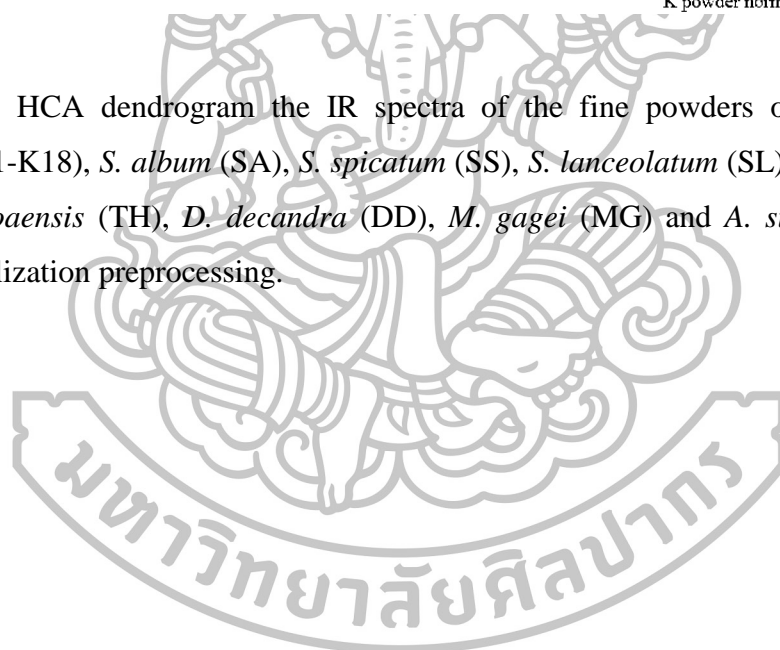
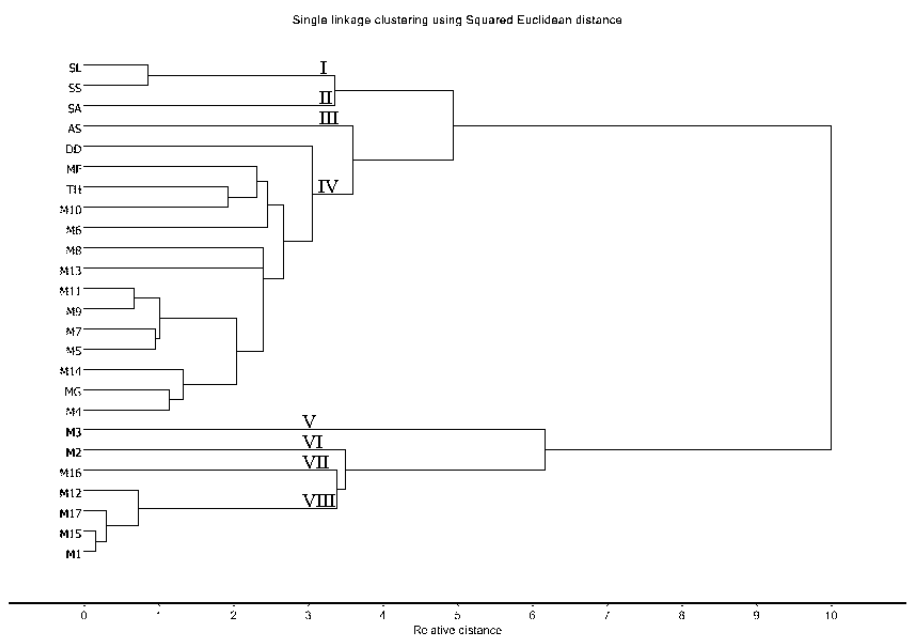


Figure 120 HCA dendrogram the IR spectra of the fine powders of Chan-khao samples (K1-K18), *S. album* (SA), *S. spicatum* (SS), *S. lanceolatum* (SL), *M. fragrans* (MF), *T. hoensis* (TH), *D. decandra* (DD), *M. gagei* (MG) and *A. silvestris* (AS) after normalization preprocessing.



(a)



(b)

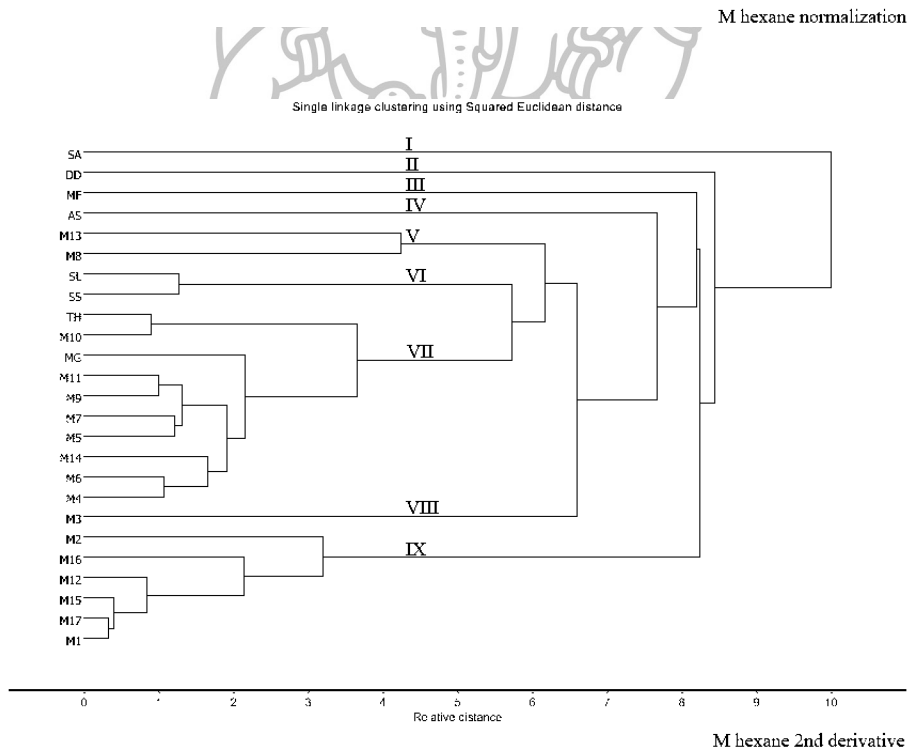
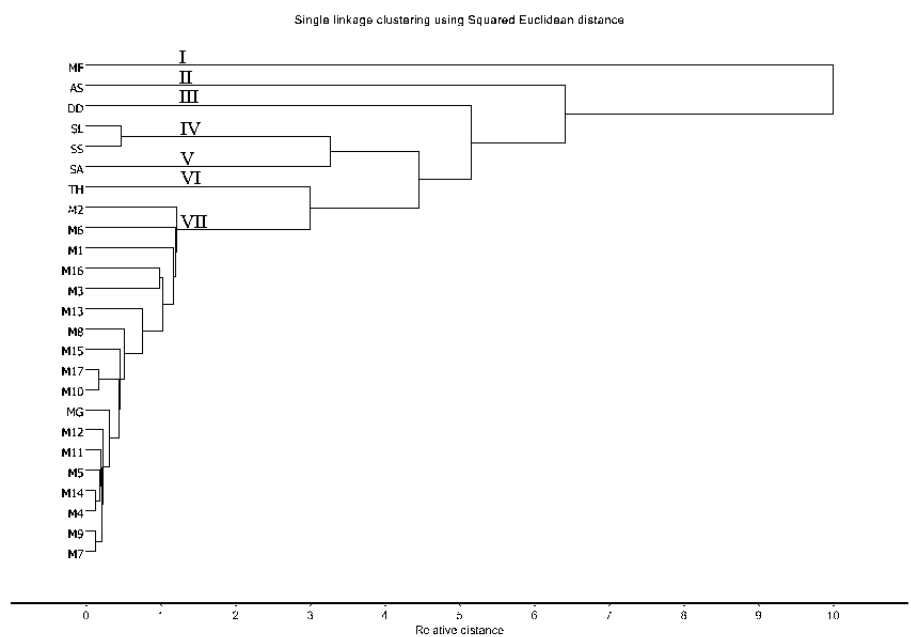


Figure 121 HCA dendrogram the IR spectra of the *n*-hexane extracts of Chan-chamot samples (M1-M17), *S. album* (SA), *S. spicatum* (SS), *S. lanceolatum* (SL), *M. fragrans* (MF), *T. hoaensis* (TH), *D. decandra* (DD), *M. gagei* (MG) and *A. silvestris* (AS) after (a) normalization and (b) second derivative preprocessing.

(a)



(b)

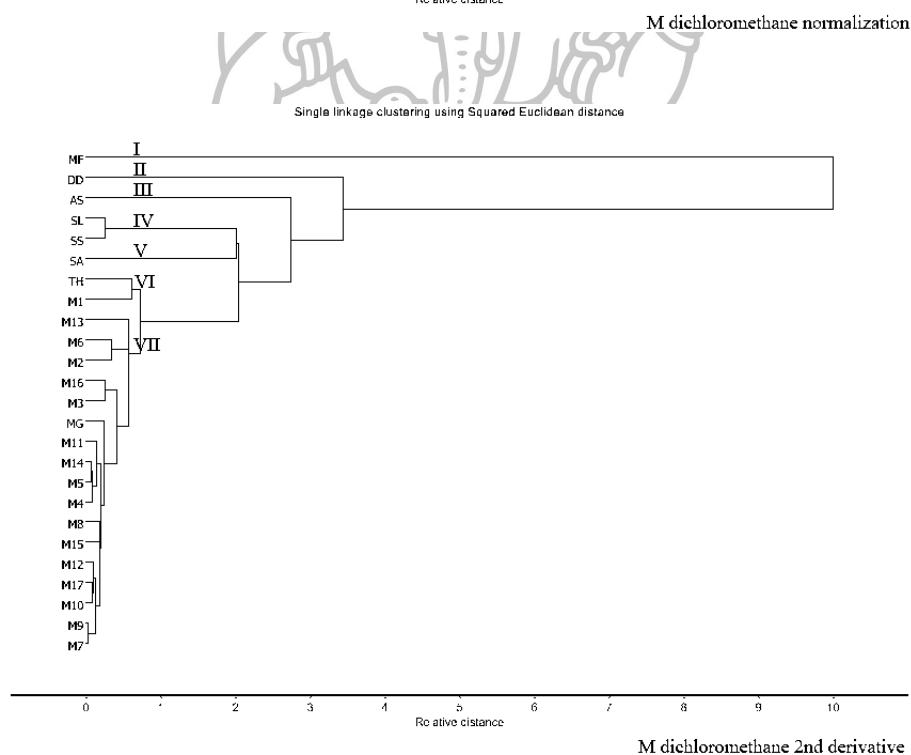
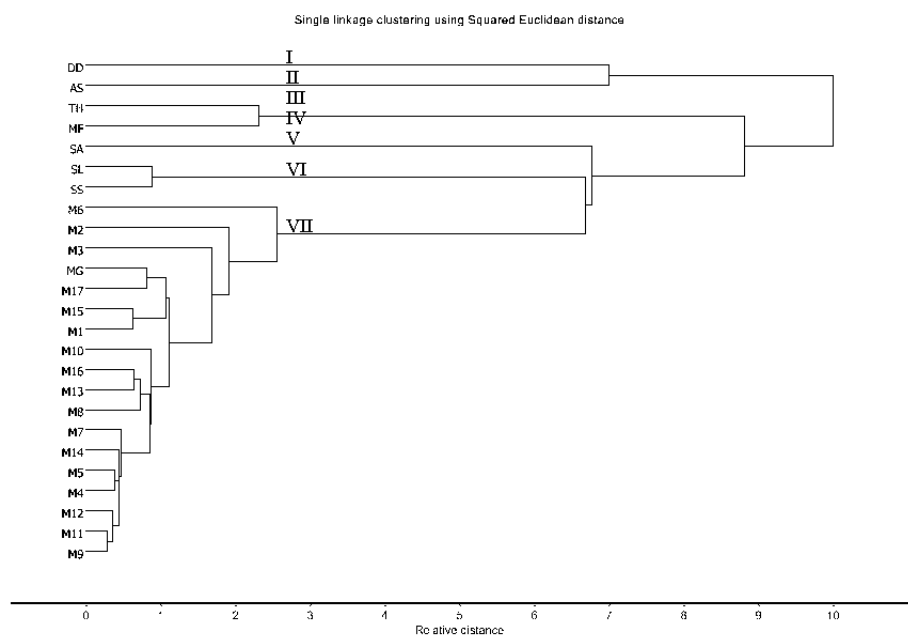


Figure 122 HCA dendrogram the IR spectra of the dichloromethane extracts of Chan-chamot samples (M1-M17), *S. album* (SA), *S. spicatum* (SS), *S. lanceolatum* (SL), *M. fragrans* (MF), *T. hoaensis* (TH), *D. decandra* (DD), *M. gagei* (MG) and *A. silvestris* (AS) after (a) normalization and (b) second derivative preprocessing.

(a)



(b)

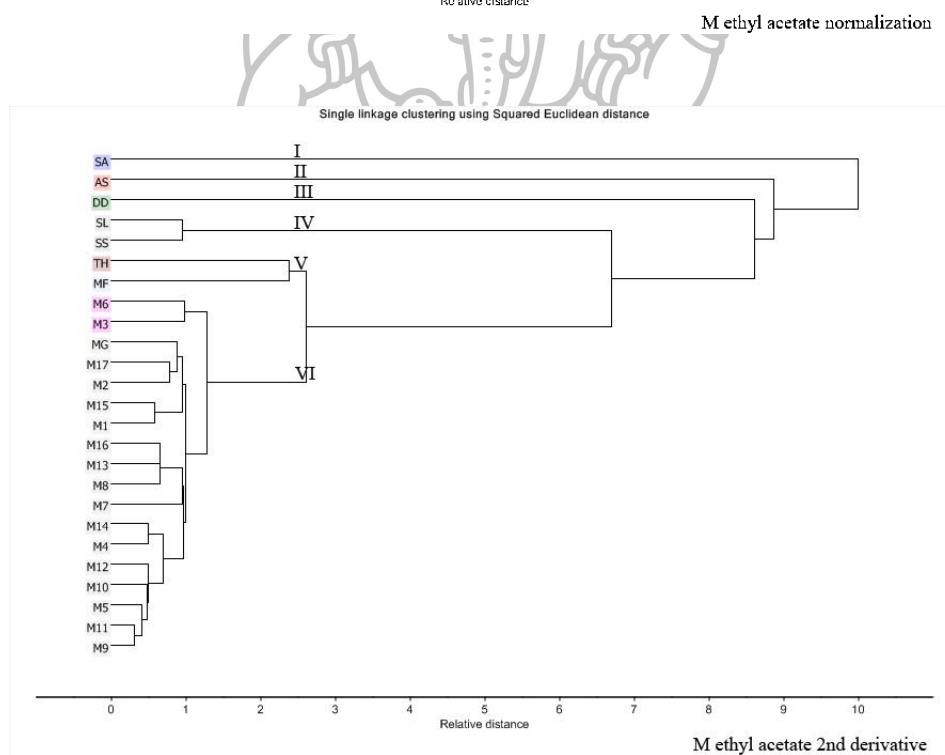
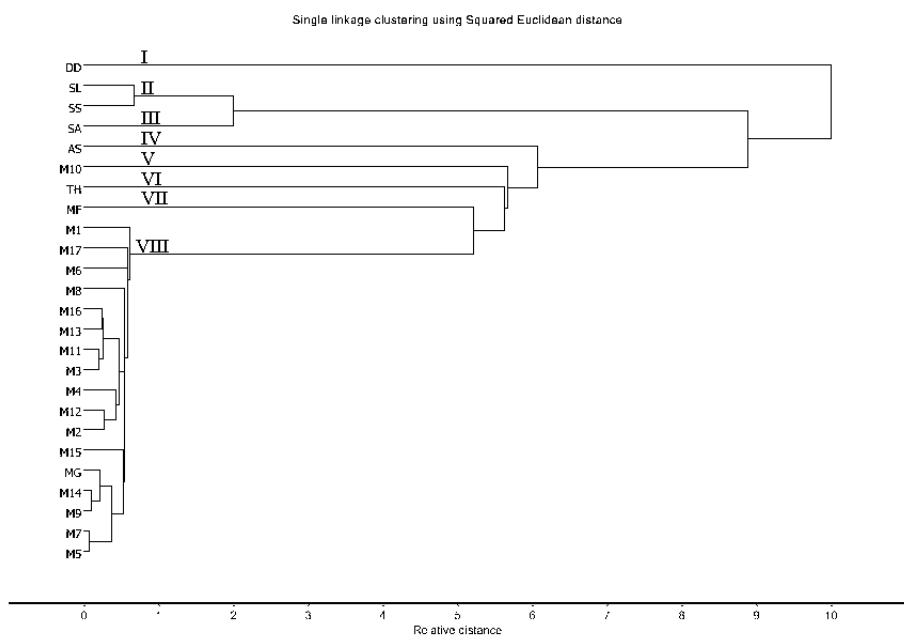


Figure 123 HCA dendrogram the IR spectra of the ethyl acetate extracts of Chan-chamot samples (M1-M17), *S. album* (SA), *S. spicatum* (SS), *S. lanceolatum* (SL), *M. fragrans* (MF), *T. hoensis* (TH), *D. decandra* (DD), *M. gagei* (MG) and *A. silvestris* (AS) after (a) normalization and (b) second derivative preprocessing.

(a)



(b)

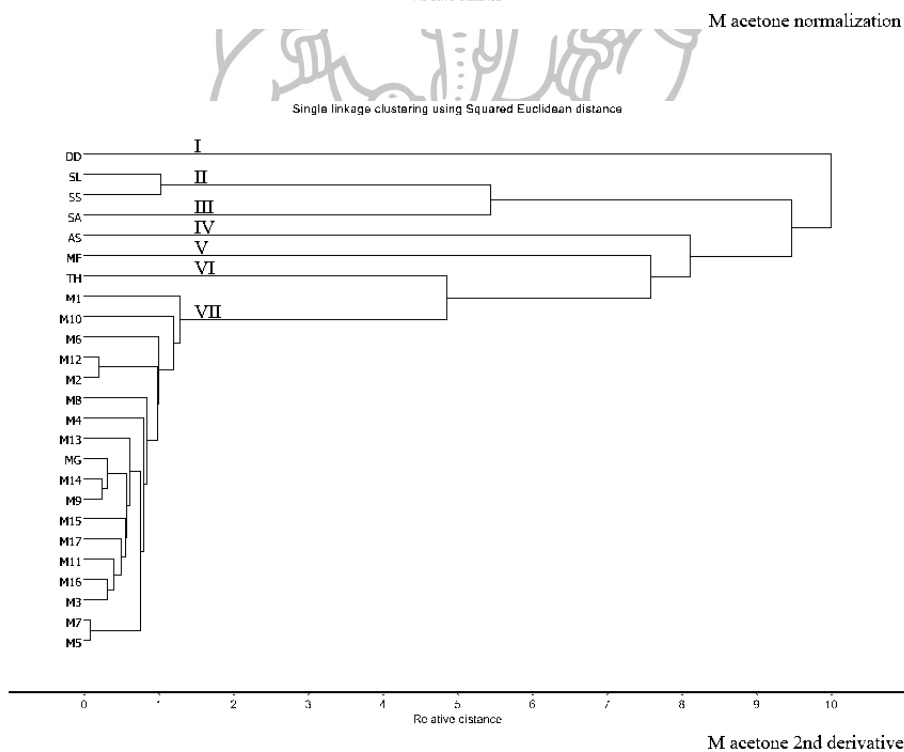
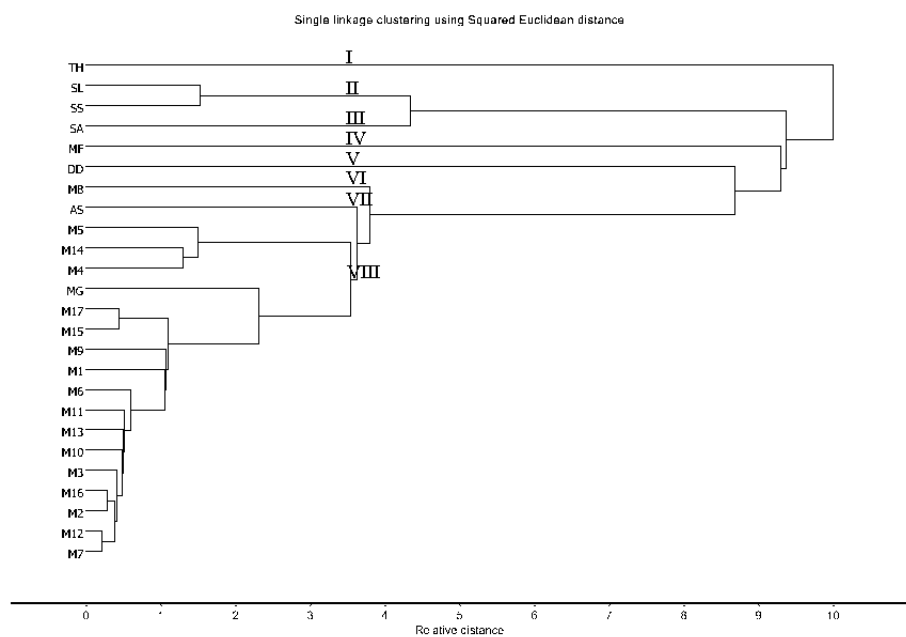


Figure 124 HCA dendrogram the IR spectra of the acetone extracts of Chan-chamot samples (M1-M17), *S. album* (SA), *S. spicatum* (SS), *S. lanceolatum* (SL), *M. fragrans* (MF), *T. hoaensis* (TH), *D. decandra* (DD), *M. gagei* (MG) and *A. silvestris* (AS) after (a) normalization and (b) second derivative preprocessing.

(a)



(b)

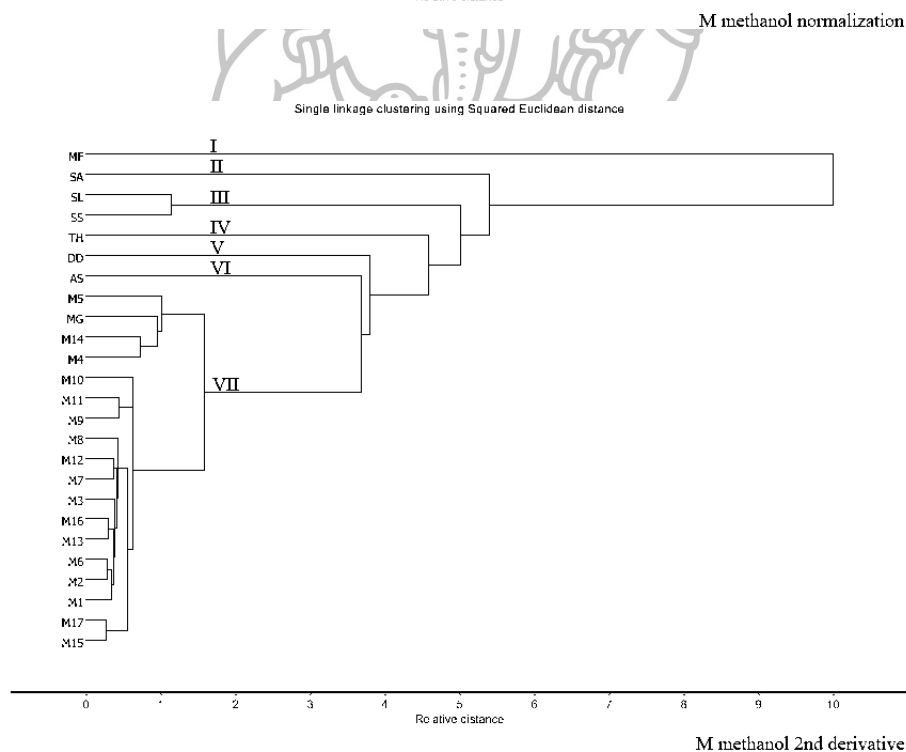
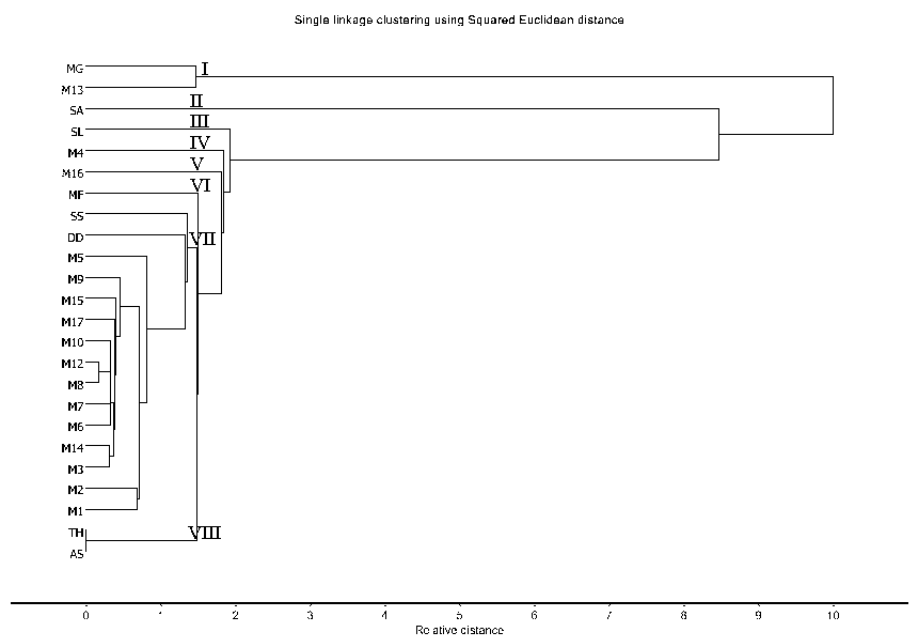


Figure 125 HCA dendrogram the IR spectra of the methanol extracts of Chan-chamot samples (M1-M17), *S. album* (SA), *S. spicatum* (SS), *S. lanceolatum* (SL), *M. fragrans* (MF), *T. hoaensis* (TH), *D. decandra* (DD), *M. gagei* (MG) and *A. silvestris* (AS) after (a) normalization and (b) second derivative preprocessing.

(a)



(b)

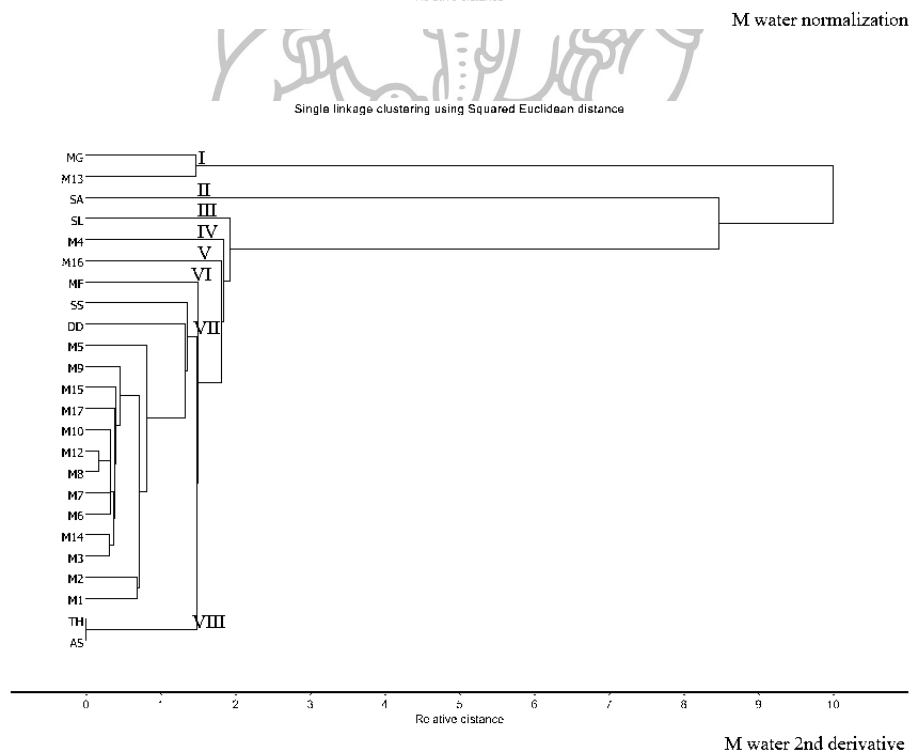
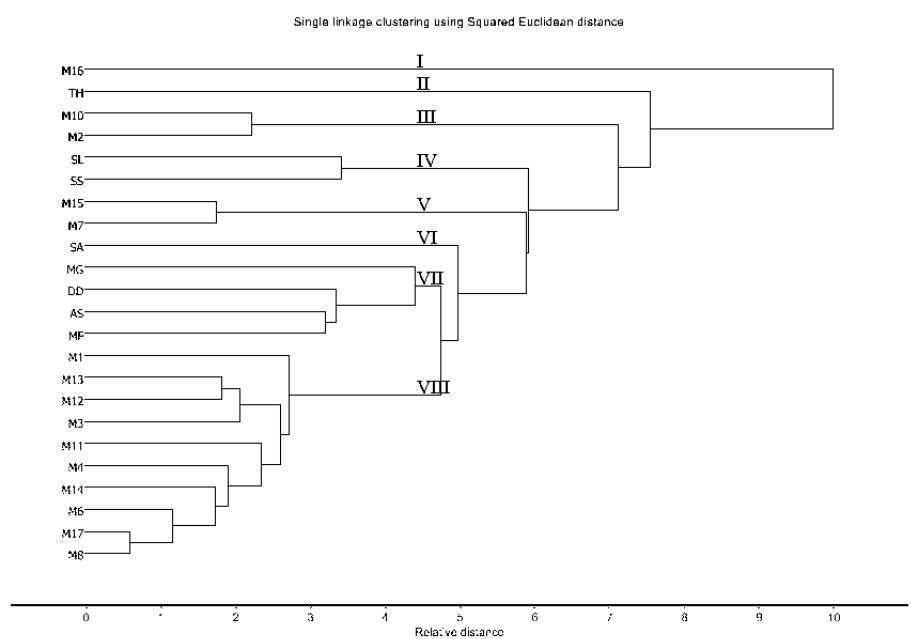


Figure 126 HCA dendrogram the IR spectra of the water extracts of Chan-chamot samples (M1-M17), *S. album* (SA), *S. spicatum* (SS), *S. lanceolatum* (SL), *M. fragrans* (MF), *T. hoensis* (TH), *D. decandra* (DD), *M. gagei* (MG) and *A. silvestris* (AS) after (a) normalization and (b) second derivative preprocessing.

(a)



(b)

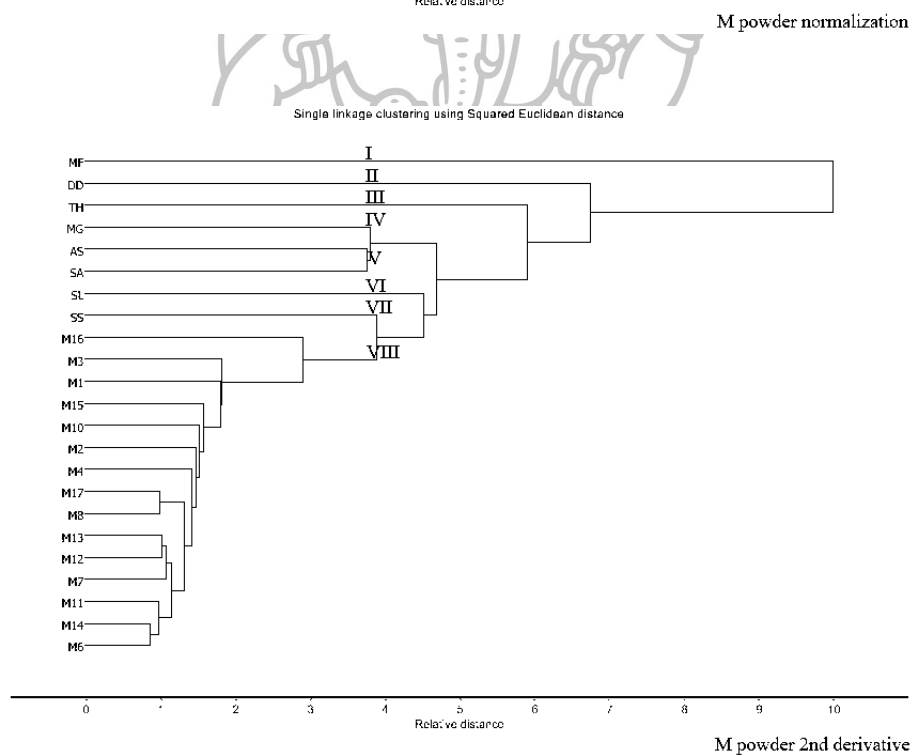
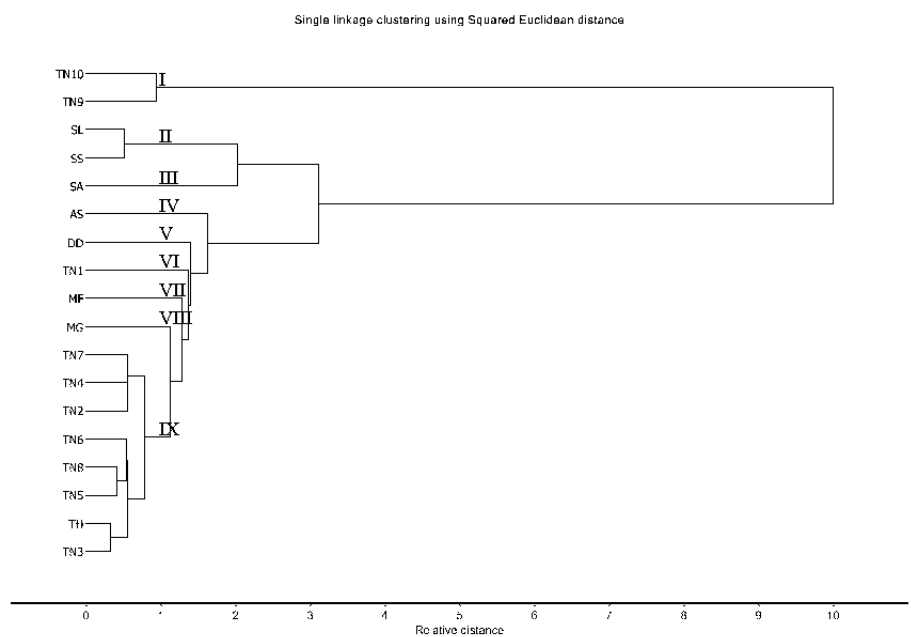


Figure 127 HCA dendrogram the IR spectra of the fine powders of Chan-chamot samples (M1-M17), *S. album* (SA), *S. spicatum* (SS), *S. lanceolatum* (SL), *M. fragrans* (MF), *T. hoensis* (TH), *D. decandra* (DD), *M. gagei* (MG) and *A. silvestris* (AS) after (a) normalization and (b) second derivative preprocessing.

(a)



(b)

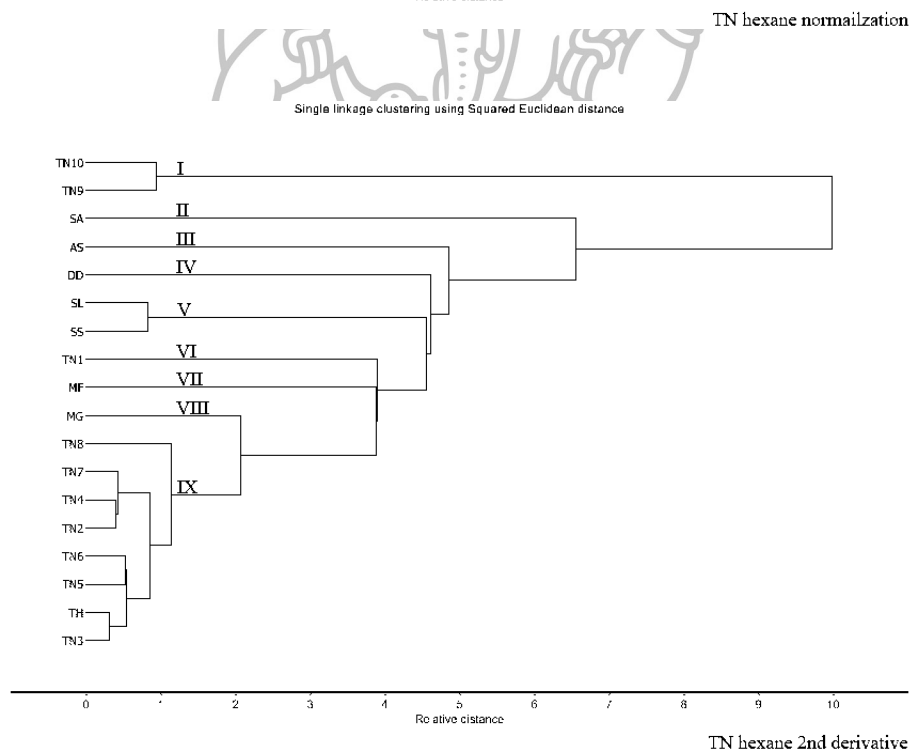
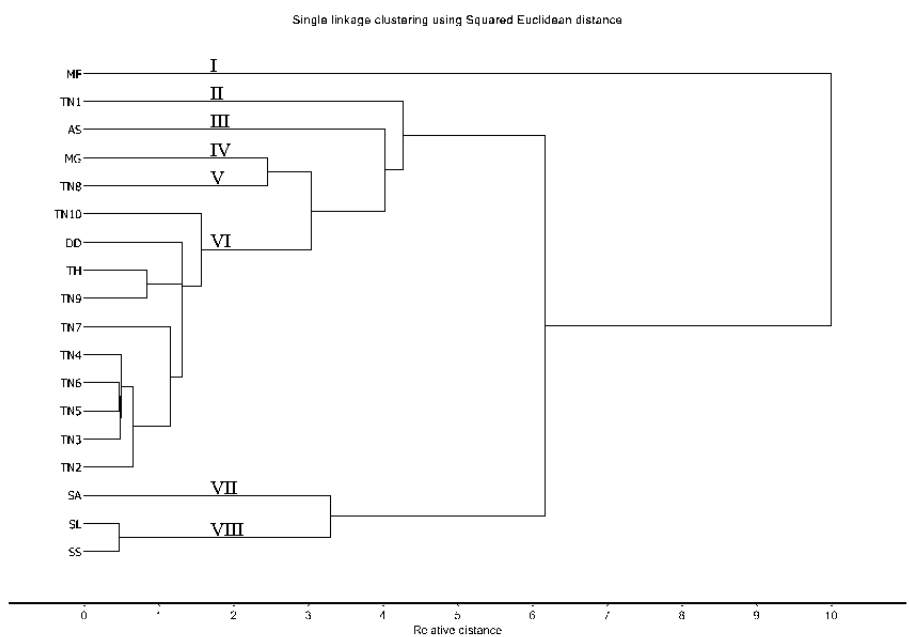


Figure 128 HCA dendrogram the IR spectra of the *n*-hexane extracts of Chan-thana samples (TN1-TN10), *S. album* (SA), *S. spicatum* (SS), *S. lanceolatum* (SL), *M. fragrans* (MF), *T. hoensis* (TH), *D. decandra* (DD), *M. gagei* (MG) and *A. silvestris* (AS) after (a) normalization and (b) second derivative preprocessing.

(a)



(b)

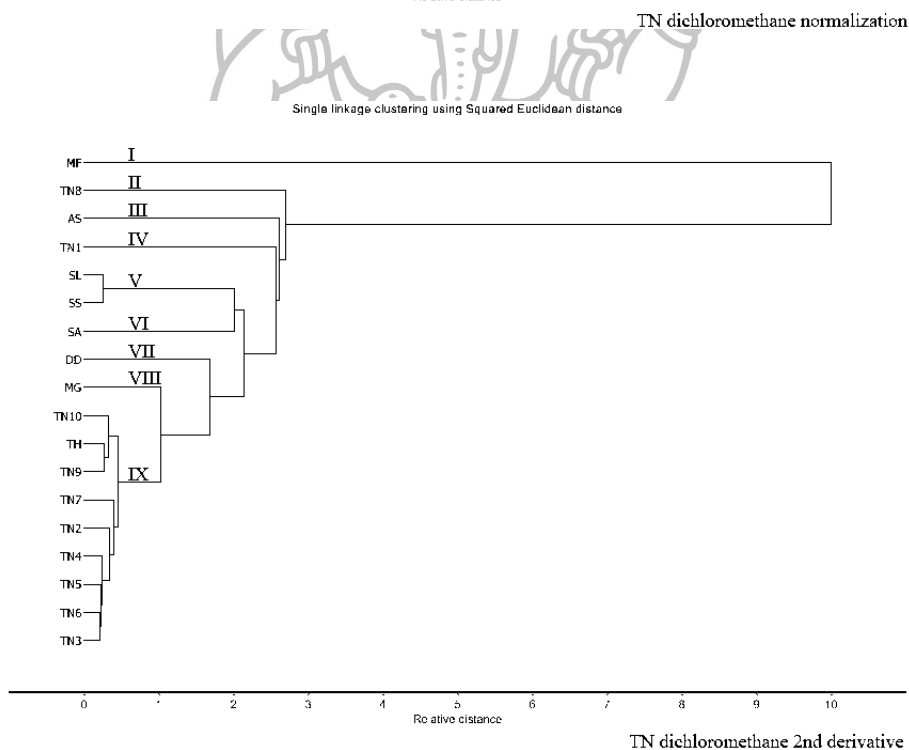
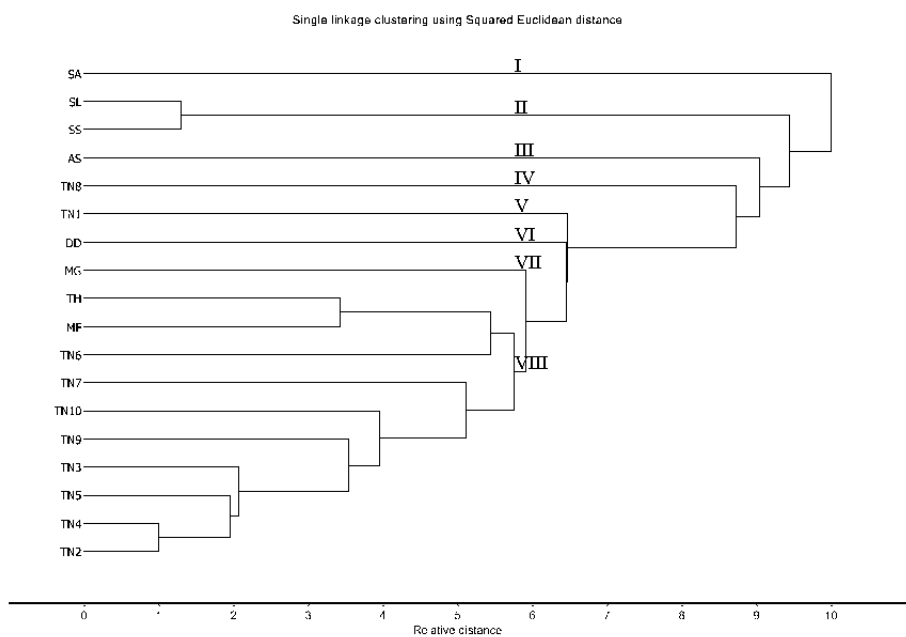


Figure 129 HCA dendrogram the IR spectra of the dichloromethane extracts of Chan-thana samples (TN1-TN10), *S. album* (SA), *S. spicatum* (SS), *S. lanceolatum* (SL), *M. fragrans* (MF), *T. hoensis* (TH), *D. decandra* (DD), *M. gagei* (MG) and *A. silvestris* (AS) after (a) normalization and (b) second derivative preprocessing.

(a)



(b)

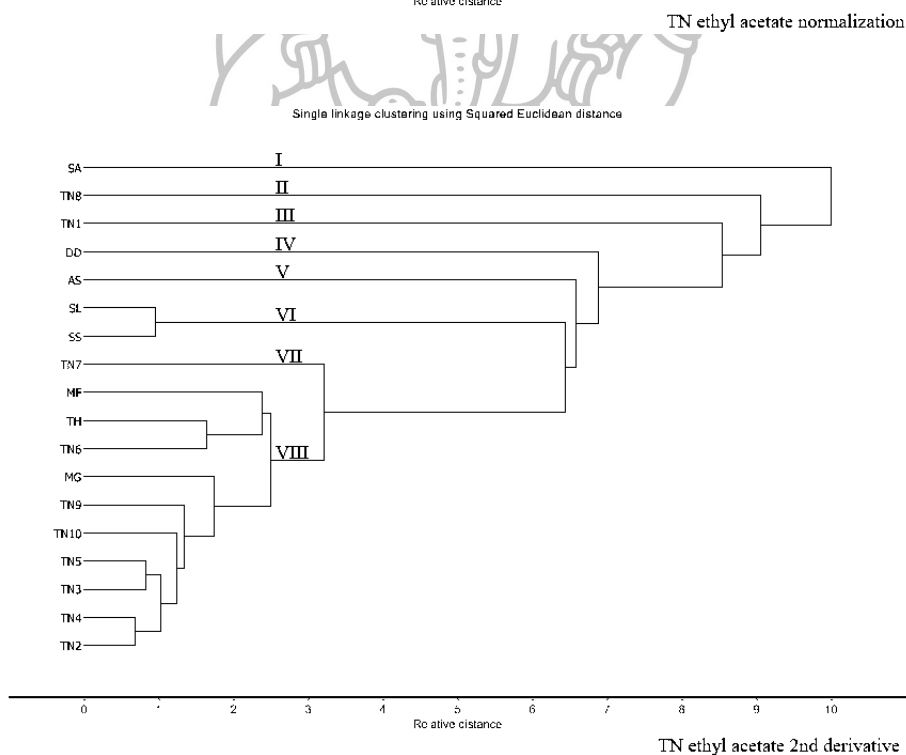
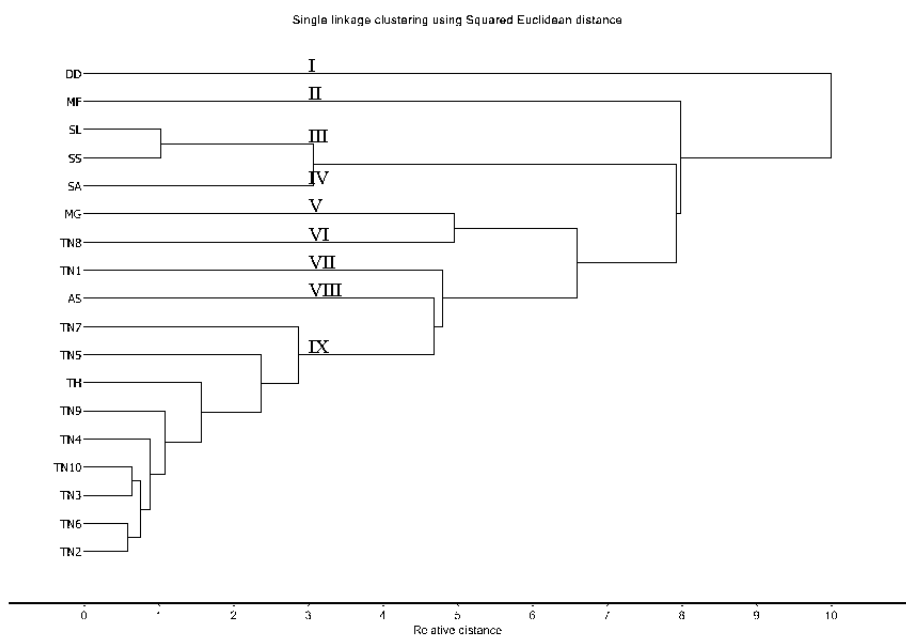


Figure 130 HCA dendrogram the IR spectra of the ethyl acetate extracts of Chan-thana samples (TN1-TN10), *S. album* (SA), *S. spicatum* (SS), *S. lanceolatum* (SL), *M. fragrans* (MF), *T. hoaensis* (TH), *D. decandra* (DD), *M. gagei* (MG) and *A. silvestris* (AS) after (a) normalization and (b) second derivative preprocessing.

(a)



(b)

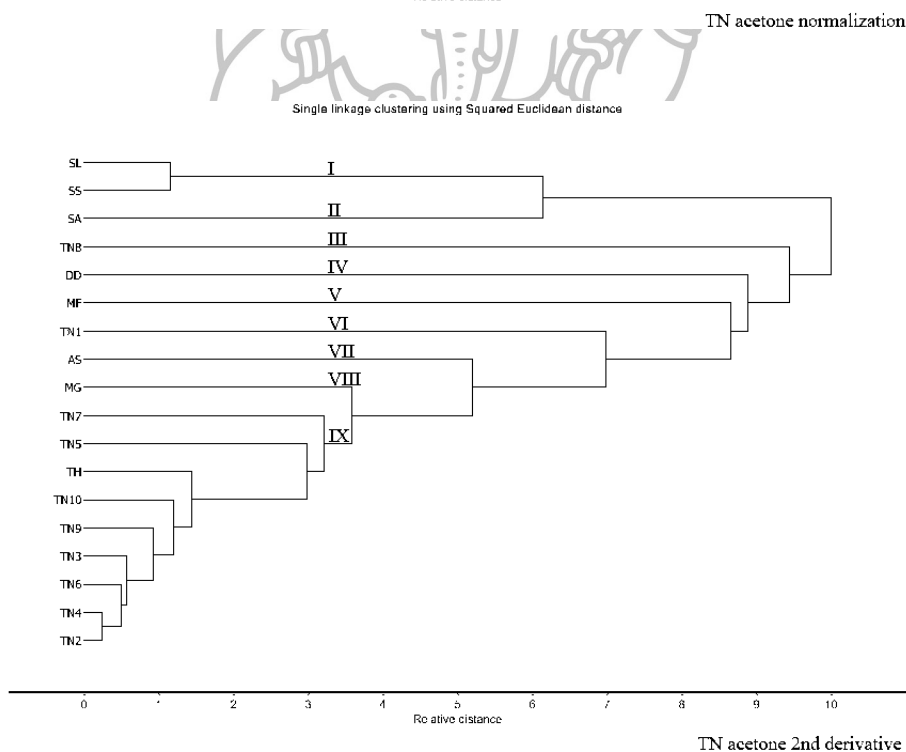
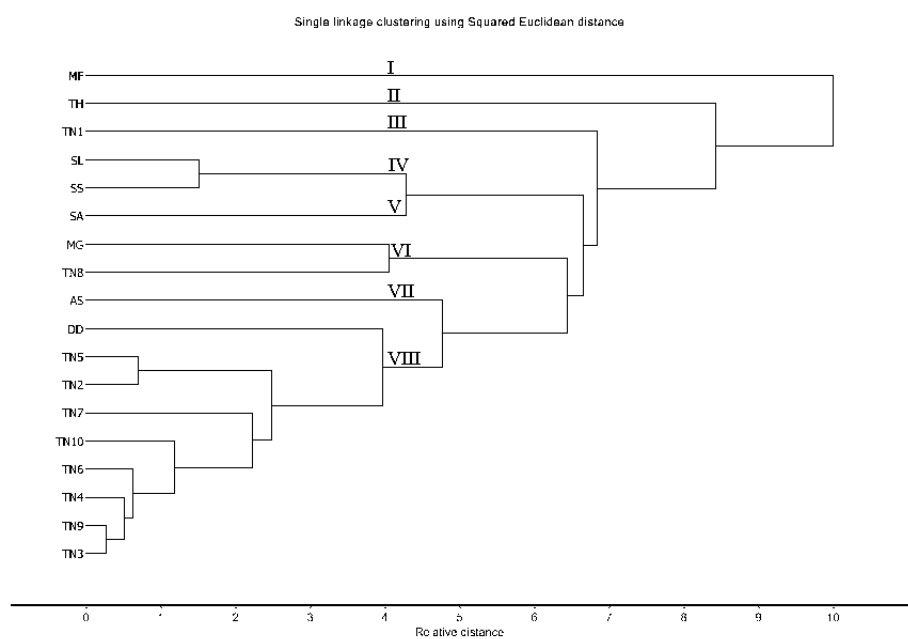


Figure 131 HCA dendrogram the IR spectra of the acetone extracts of Chan-thana samples (TN1-TN10), *S. album* (SA), *S. spicatum* (SS), *S. lanceolatum* (SL), *M. fragrans* (MF), *T. hoensis* (TH), *D. decandra* (DD), *M. gagei* (MG) and *A. silvestris* (AS) after (a) normalization and (b) second derivative preprocessing.

(a)



(b)

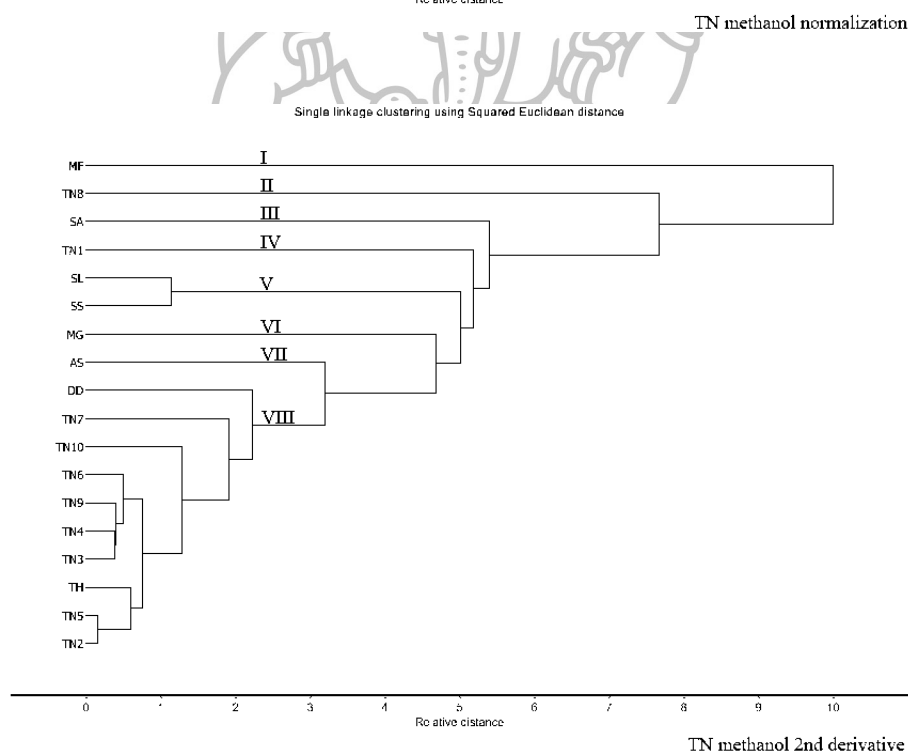
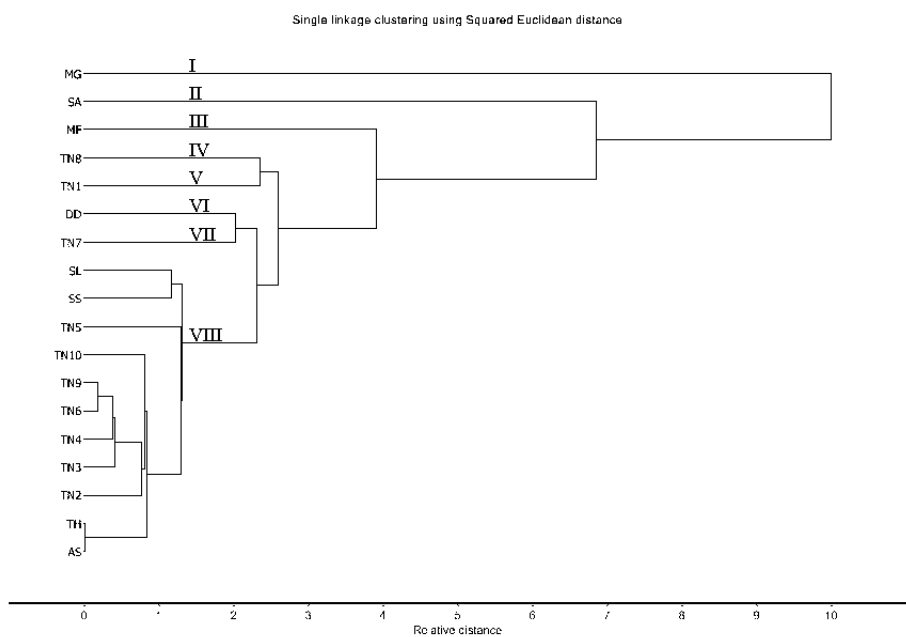


Figure 132 HCA dendrogram the IR spectra of the methanol extracts of Chan-thana samples (TN1-TN10), *S. album* (SA), *S. spicatum* (SS), *S. lanceolatum* (SL), *M. fragrans* (MF), *T. hoensis* (TH), *D. decandra* (DD), *M. gagei* (MG) and *A. silvestris* (AS) after (a) normalization and (b) second derivative preprocessing.

(a)



(b)

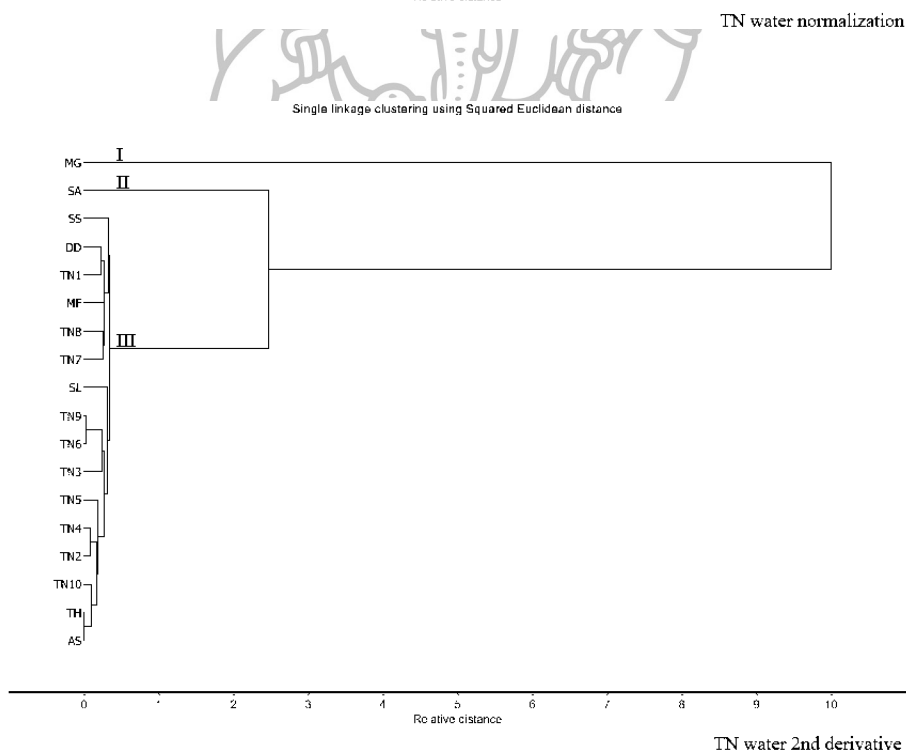
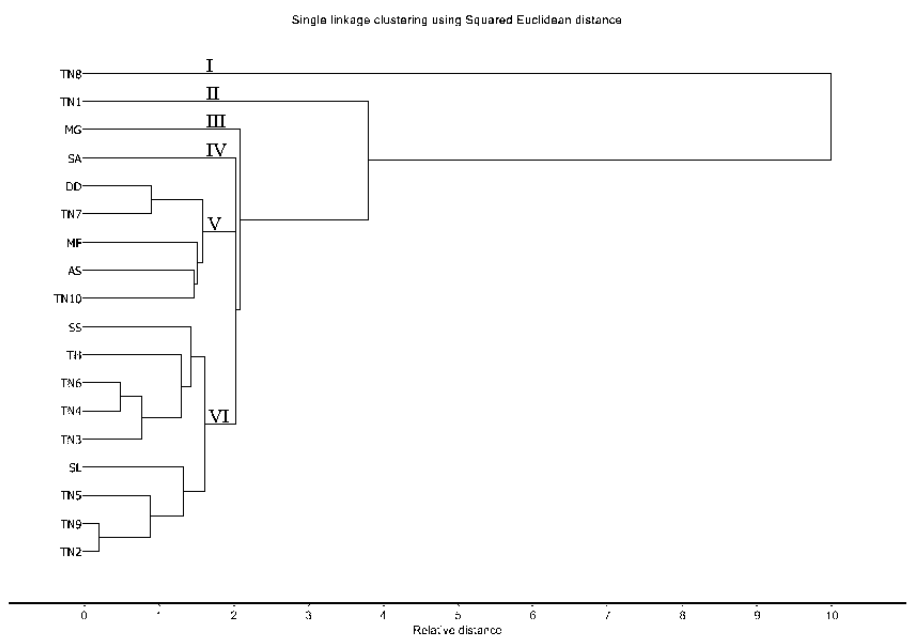


Figure 133 HCA dendrogram the IR spectra of the water extracts of Chan-thana samples (TN1-TN10), *S. album* (SA), *S. spicatum* (SS), *S. lanceolatum* (SL), *M. fragrans* (MF), *T. hoensis* (TH), *D. decandra* (DD), *M. gagei* (MG) and *A. silvestris* (AS) after (a) normalization and (b) second derivative preprocessing.

(a)



(b)

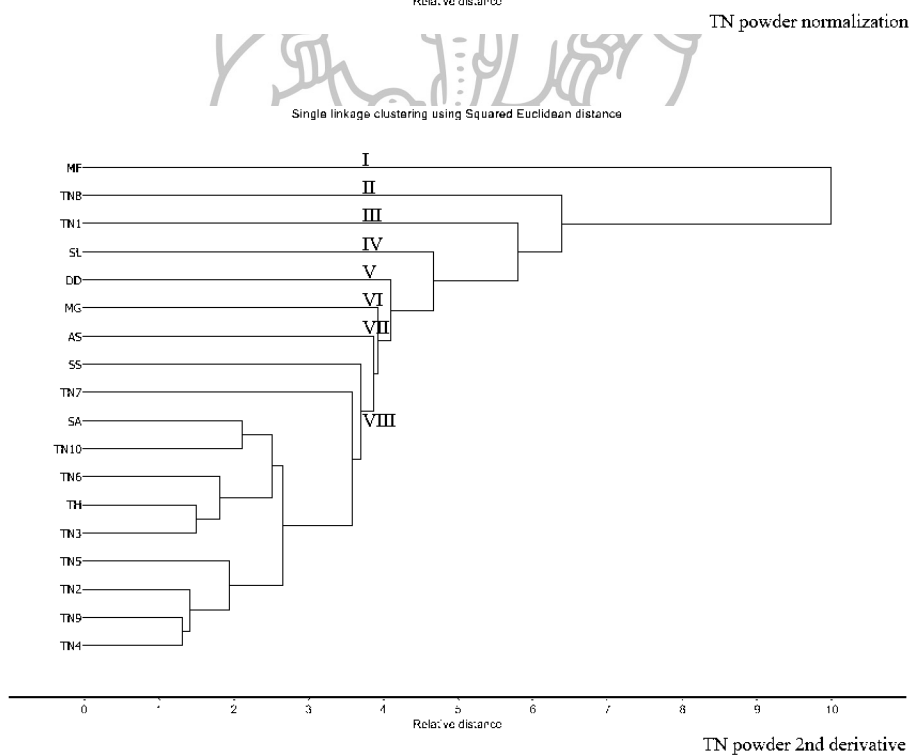
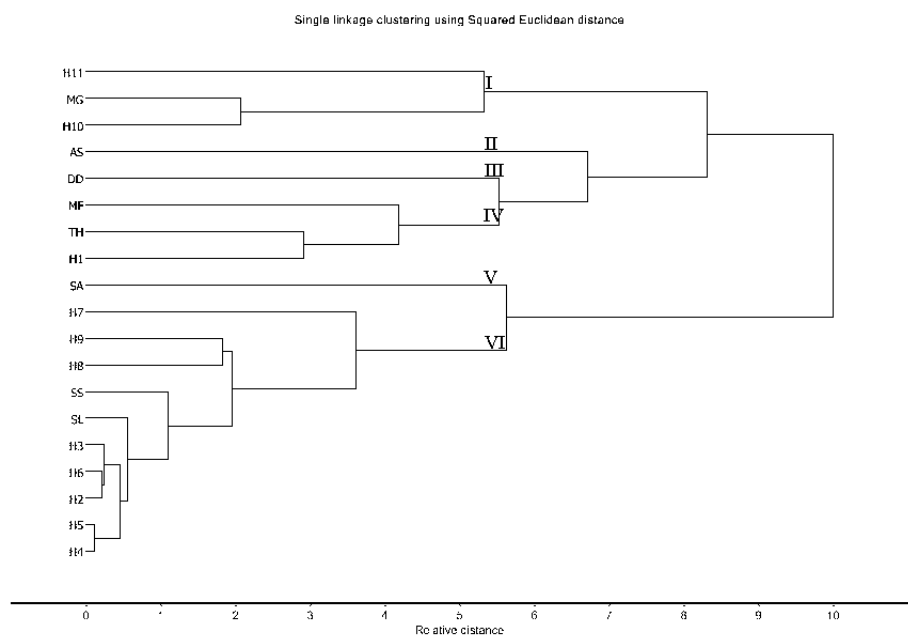


Figure 134 HCA dendrogram the IR spectra of the fine powders of Chan-thana samples (TN1-TN10), *S. album* (SA), *S. spicatum* (SS), *S. lanceolatum* (SL), *M. fragrans* (MF), *T. hoensis* (TH), *D. decandra* (DD), *M. gagei* (MG) and *A. silvestris* (AS) after (a) normalization and (b) second derivative preprocessing.

(a)



(b)

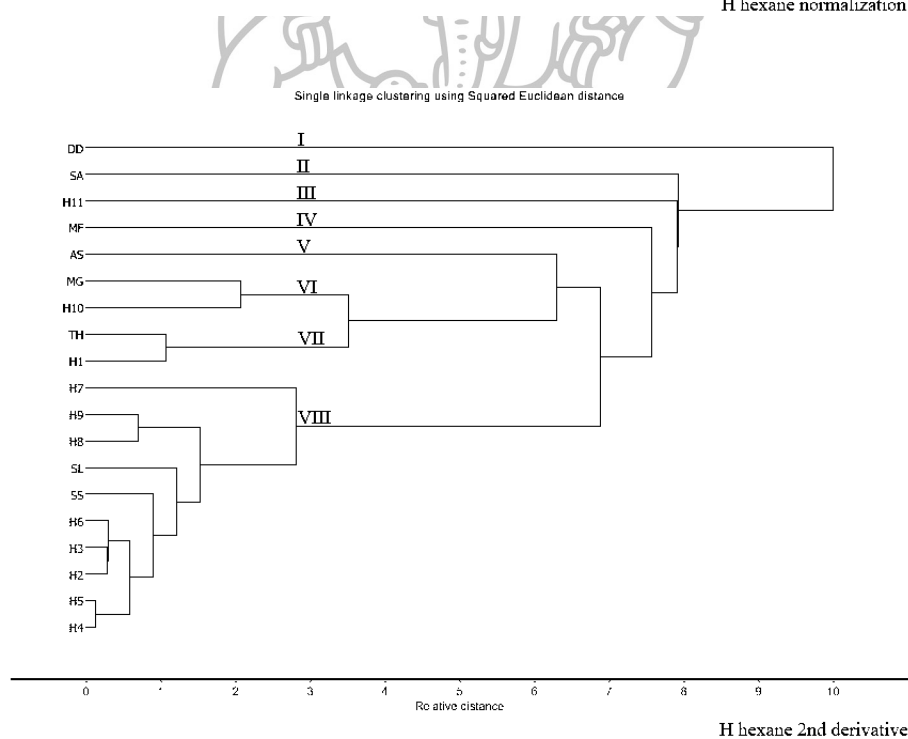
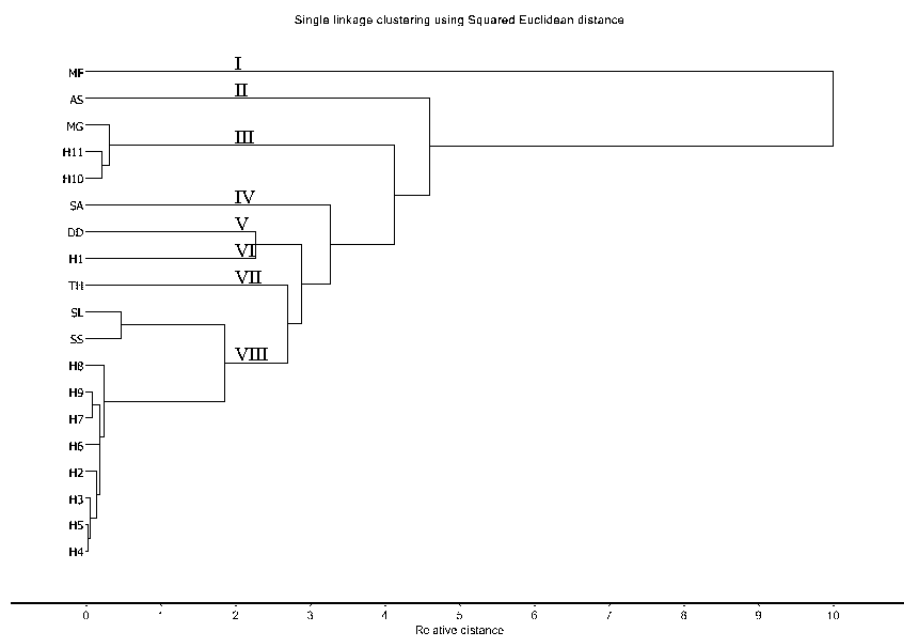


Figure 135 HCA dendrogram the IR spectra of the *n*-hexane extracts of Chan-hom samples (H1-H11), *S. album* (SA), *S. spicatum* (SS), *S. lanceolatum* (SL), *M. fragrans* (MF), *T. hoensis* (TH), *D. decandra* (DD), *M. gagei* (MG) and *A. silvestris* (AS) after (a) normalization and (b) second derivative preprocessing.

(a)



(b)

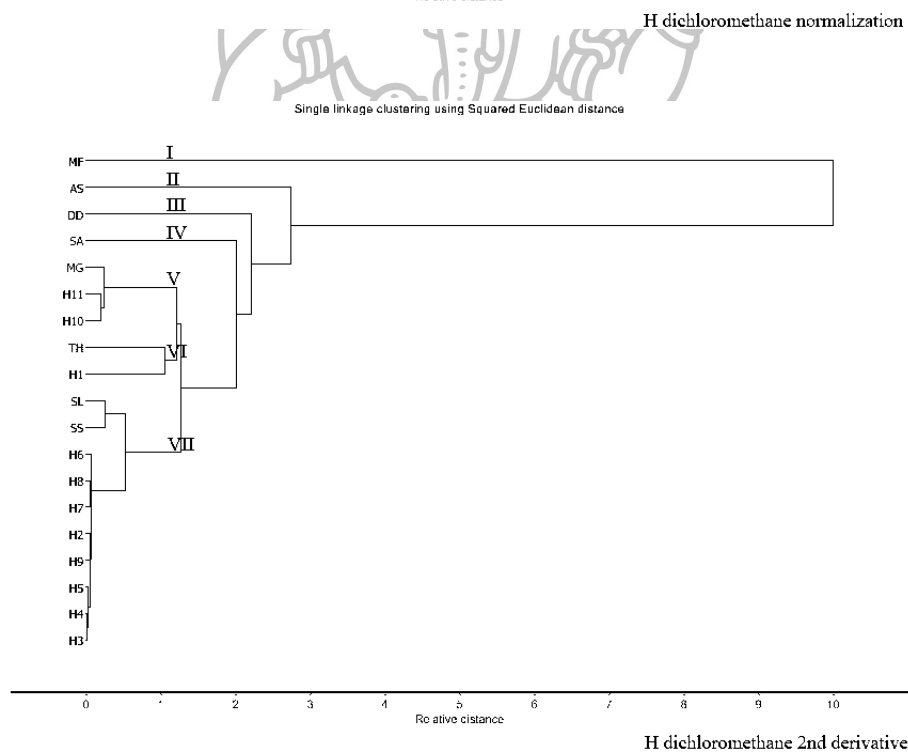
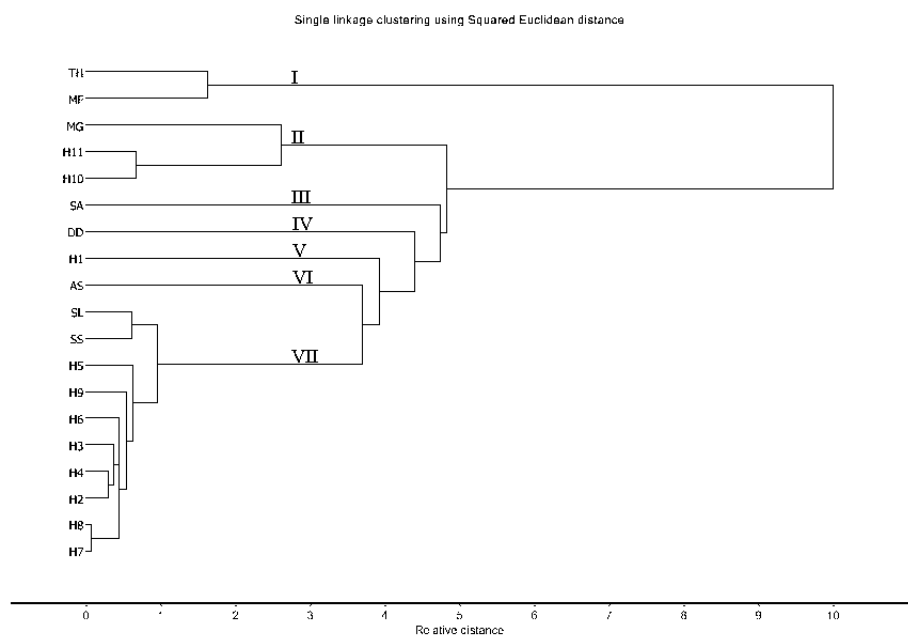


Figure 136 HCA dendrogram the IR spectra of the dichloromethane extracts of Chan-hom samples (H1-H11), *S. album* (SA), *S. spicatum* (SS), *S. lanceolatum* (SL), *M. fragrans* (MF), *T. hoensis* (TH), *D. decandra* (DD), *M. gagei* (MG) and *A. silvestris* (AS) after (a) normalization and (b) second derivative preprocessing.

(a)



(b)

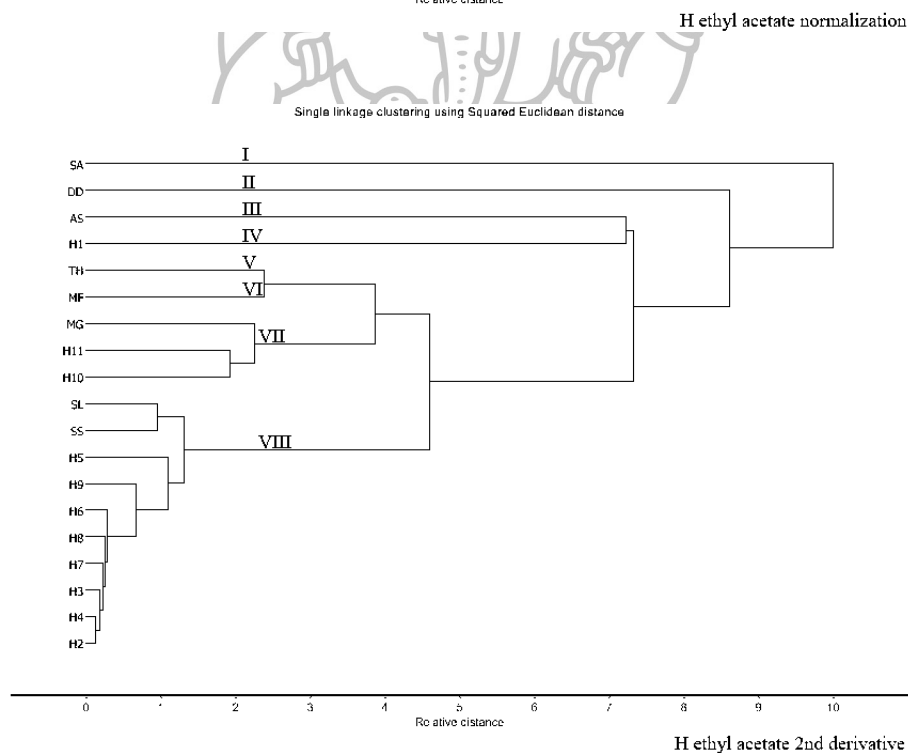
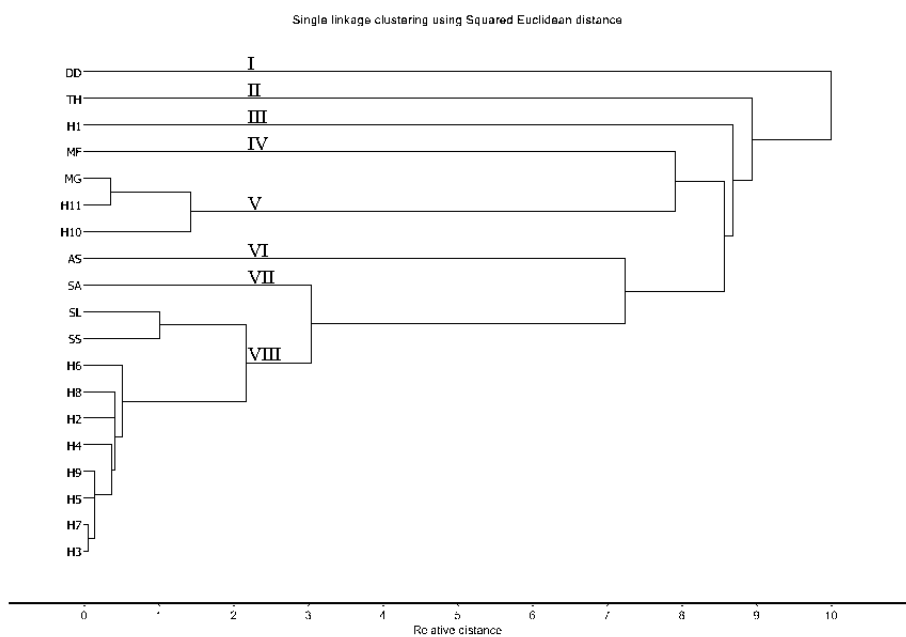


Figure 137 HCA dendrogram the IR spectra of the ethyl acetate extracts of Chan-hom samples (H1-H11), *S. album* (SA), *S. spicatum* (SS), *S. lanceolatum* (SL), *M. fragrans* (MF), *T. hoensis* (TH), *D. decandra* (DD), *M. gagei* (MG) and *A. silvestris* (AS) after (a) normalization and (b) second derivative preprocessing.

(a)



(b)

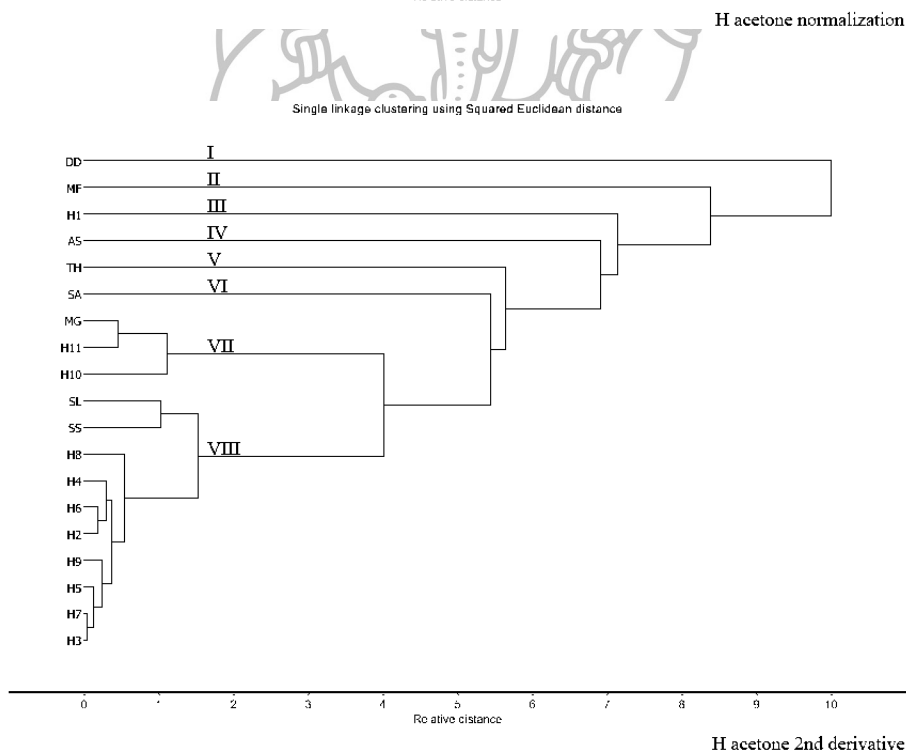
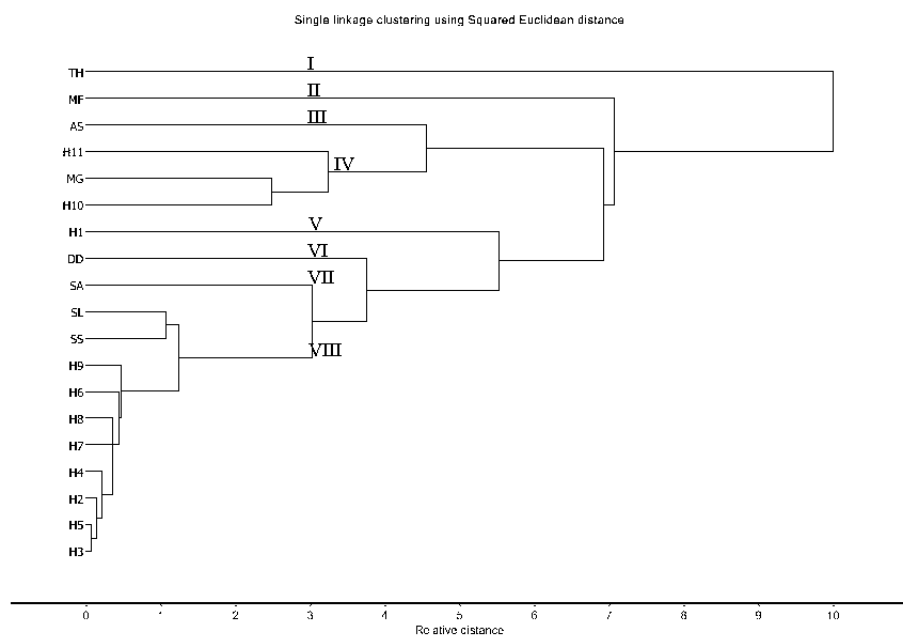


Figure 138 HCA dendrogram the IR spectra of the acetone extracts of Chan-hom samples (H1-H11), *S. album* (SA), *S. spicatum* (SS), *S. lanceolatum* (SL), *M. fragrans* (MF), *T. hoensis* (TH), *D. decandra* (DD), *M. gagei* (MG) and *A. silvestris* (AS) after (a) normalization and (b) second derivative preprocessing.

(a)



(b)

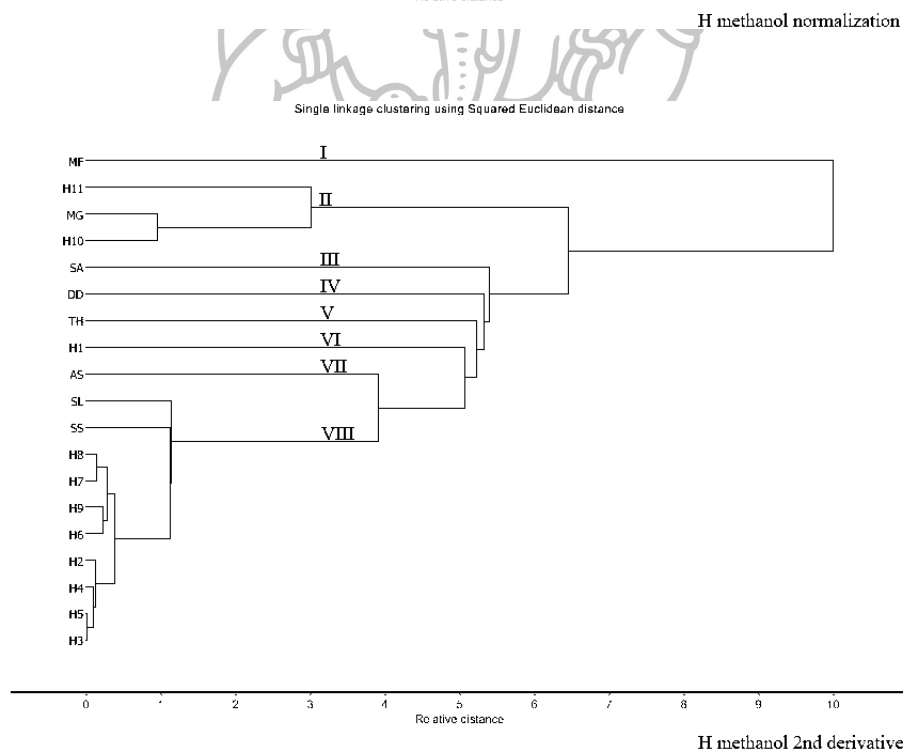
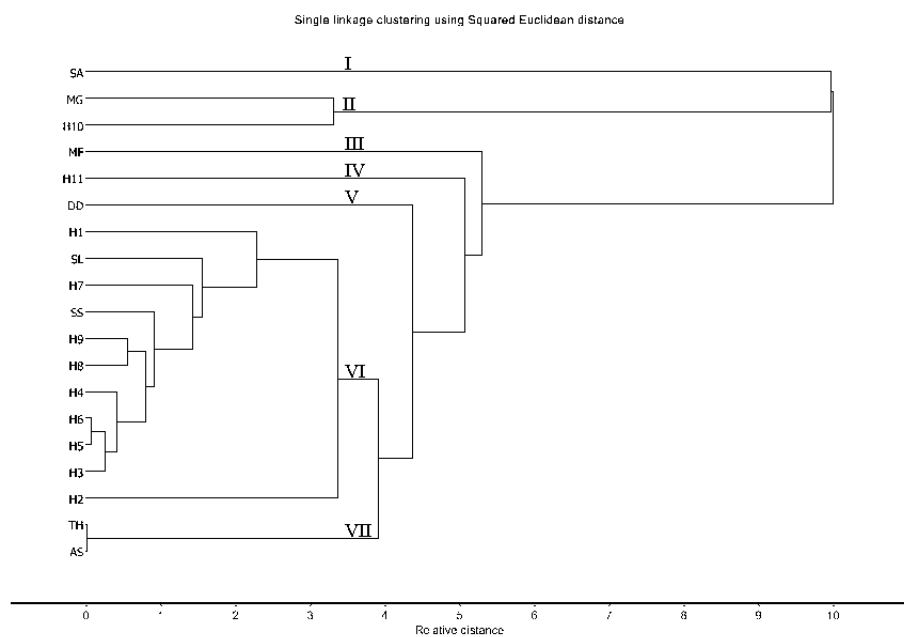


Figure 139 HCA dendrogram the IR spectra of the methanol extracts of Chan-hom samples (H1-H11), *S. album* (SA), *S. spicatum* (SS), *S. lanceolatum* (SL), *M. fragrans* (MF), *T. hoaensis* (TH), *D. decandra* (DD), *M. gagei* (MG) and *A. silvestris* (AS) after (a) normalization and (b) second derivative preprocessing.

(a)



(b)

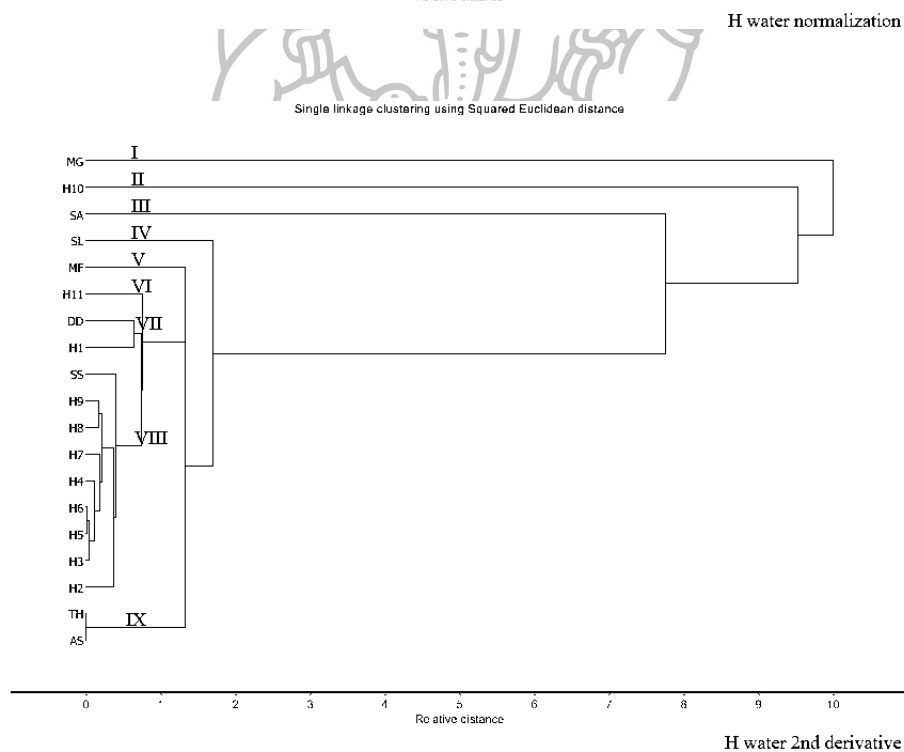
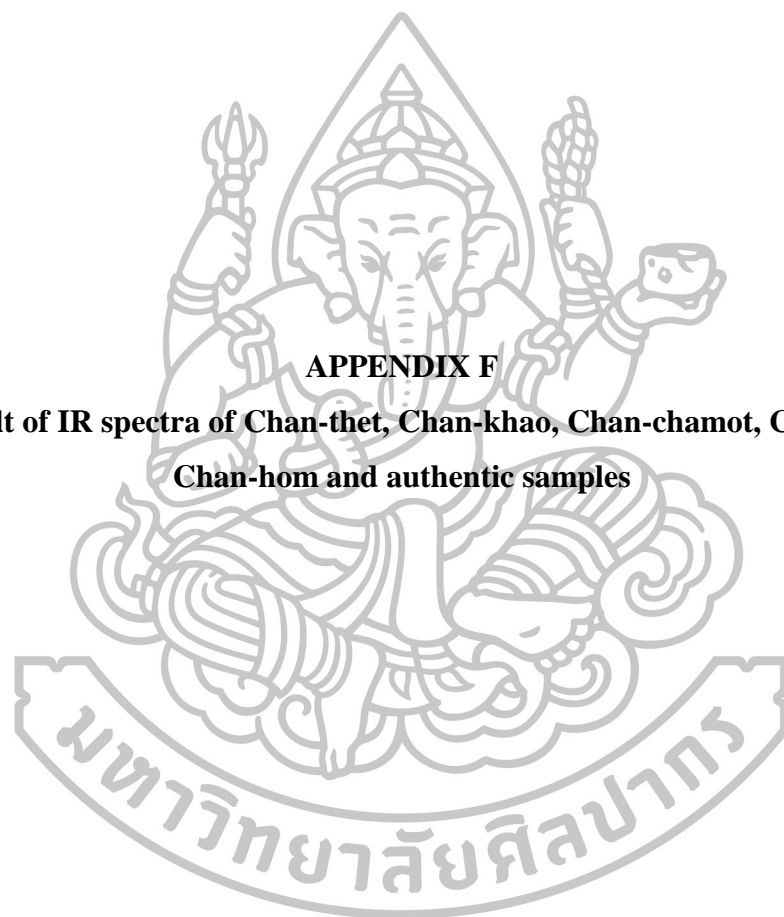


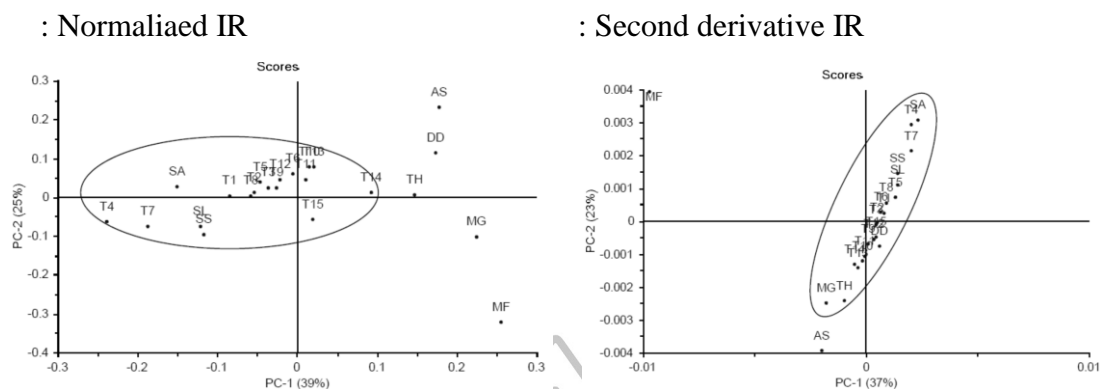
Figure 140 HCA dendrogram the IR spectra of the water extracts of Chan-hom samples (H1-H11), *S. album* (SA), *S. spicatum* (SS), *S. lanceolatum* (SL), *M. fragrans* (MF), *T. hoensis* (TH), *D. decandra* (DD), *M. gagei* (MG) and *A. silvestris* (AS) after (a) normalization and (b) second derivative preprocessing.



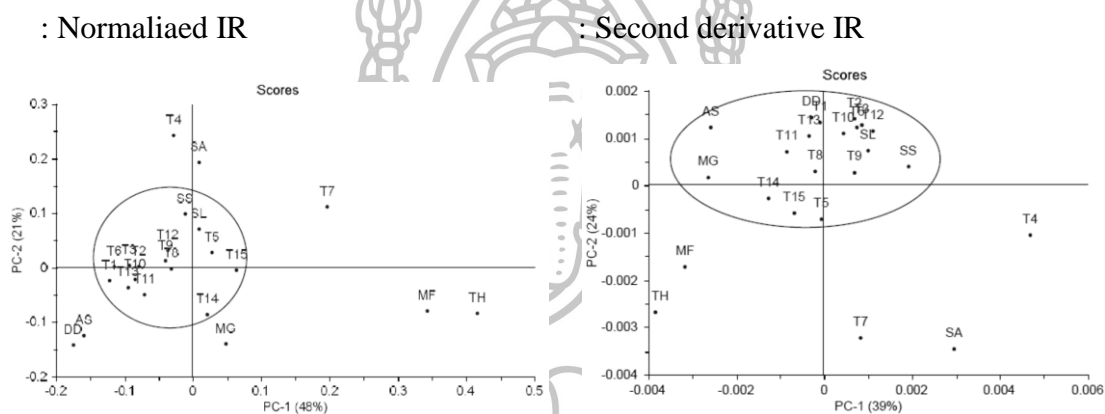
APPENDIX F

**PCA result of IR spectra of Chan-thet, Chan-khao, Chan-chamot, Chan-thana,
Chan-hom and authentic samples**

(a) Dichloromethane extract



(b) Ethyl acetate extract



(c) Water extract

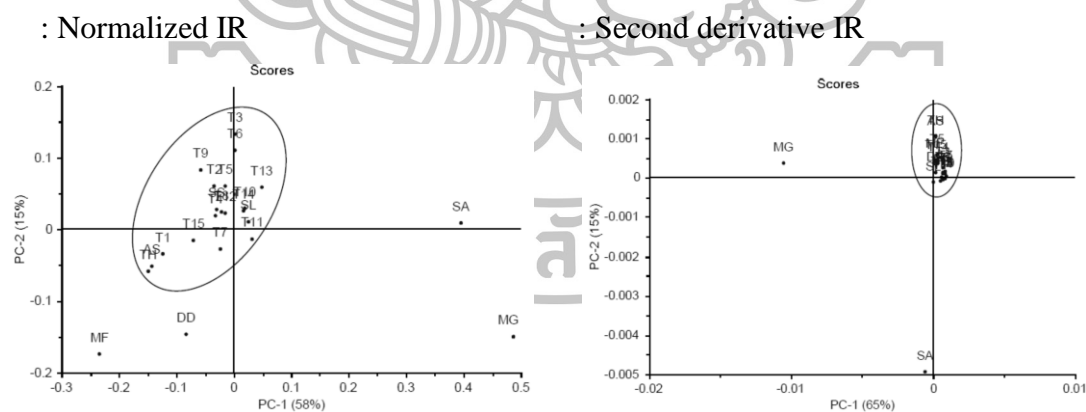


Figure 142 PC1 and PC2 score plots of the normalized and second derivative IR spectra of the (a) dichloromethane, (b) ethyl acetate, and (c) water extracts, and (d) the fine powders of Chan-thet samples (T1-T15), *S. album* (SA), *S. spicatum* (SS), *S. lanceolatum* (SL), *M. fragrans* (MF), *T. hoensis* (TH), *D. decandra* (DD), *M. gagei* (MG) and *A. silvestris* (AS).

(d) Fine powders

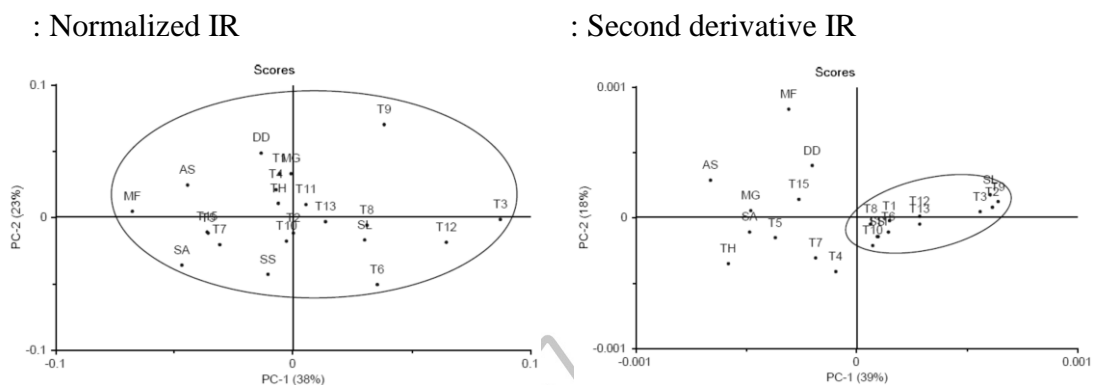
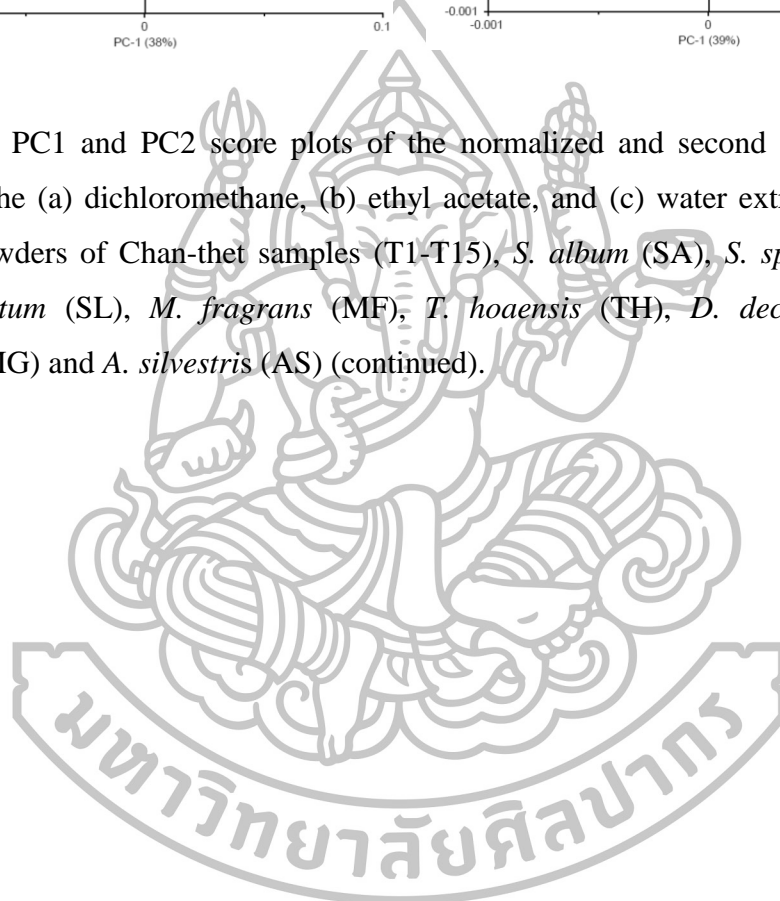
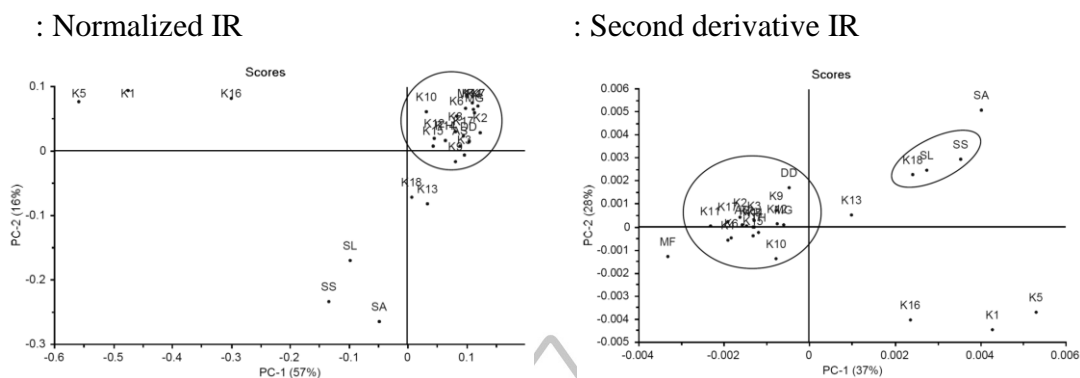
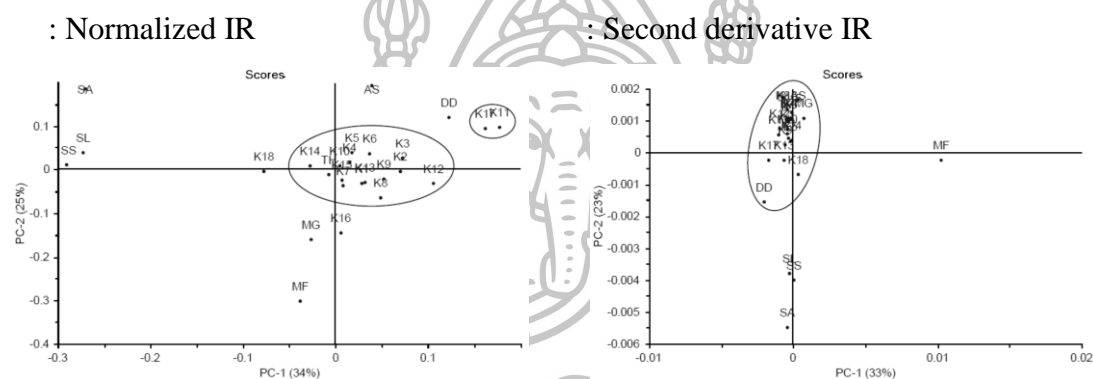


Figure 142 PC1 and PC2 score plots of the normalized and second derivative IR spectra of the (a) dichloromethane, (b) ethyl acetate, and (c) water extracts, and (d) the fine powders of Chan-thet samples (T1-T15), *S. album* (SA), *S. spicatum* (SS), *S. lanceolatum* (SL), *M. fragrans* (MF), *T. hoensis* (TH), *D. decandra* (DD), *M. gagei* (MG) and *A. silvestris* (AS) (continued).



(a) *n*-Hexane extract

(b) Dichloromethane extract



(c) Ethyl acetate extract

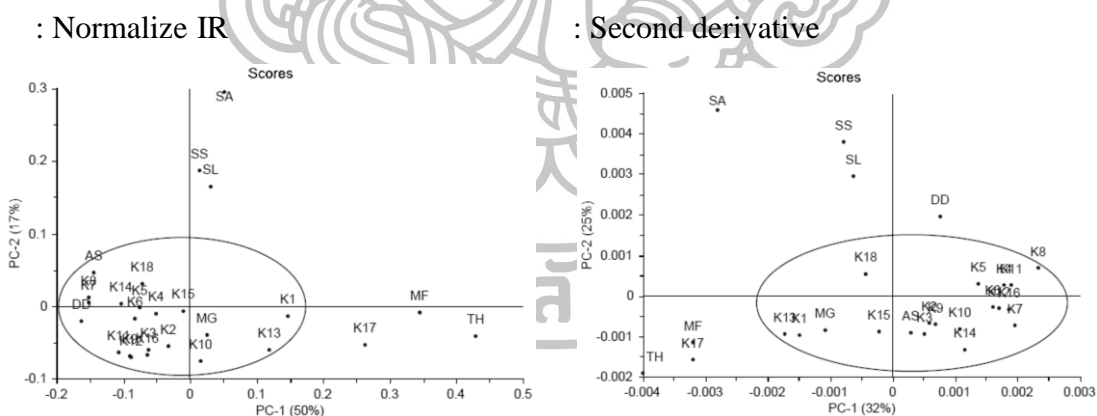
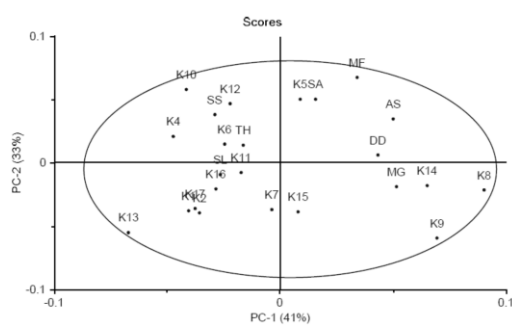


Figure 143 PC1 and PC2 score plots of the normalized and second derivative IR spectra of the (a) *n*-hexane, (b) dichloromethane, (c) ethyl acetate, (d) acetone, (e) methanol and (f) water extracts; and (g) the fine powders of Chan-khao samples (K1-K18), *S. album* (SA), *S. spicatum* (SS), *S. lanceolatum* (SL), *M. fragrans* (MF), *T. hoensis* (TH), *D. decandra* (DD), *M. gagei* (MG) and *A. silvestris* (AS).

(g) Fine powders

: Normalized IR



: Second derivative

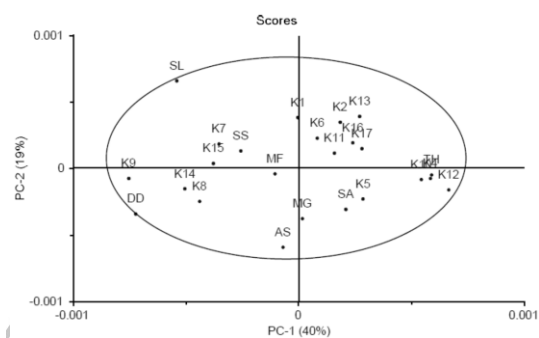
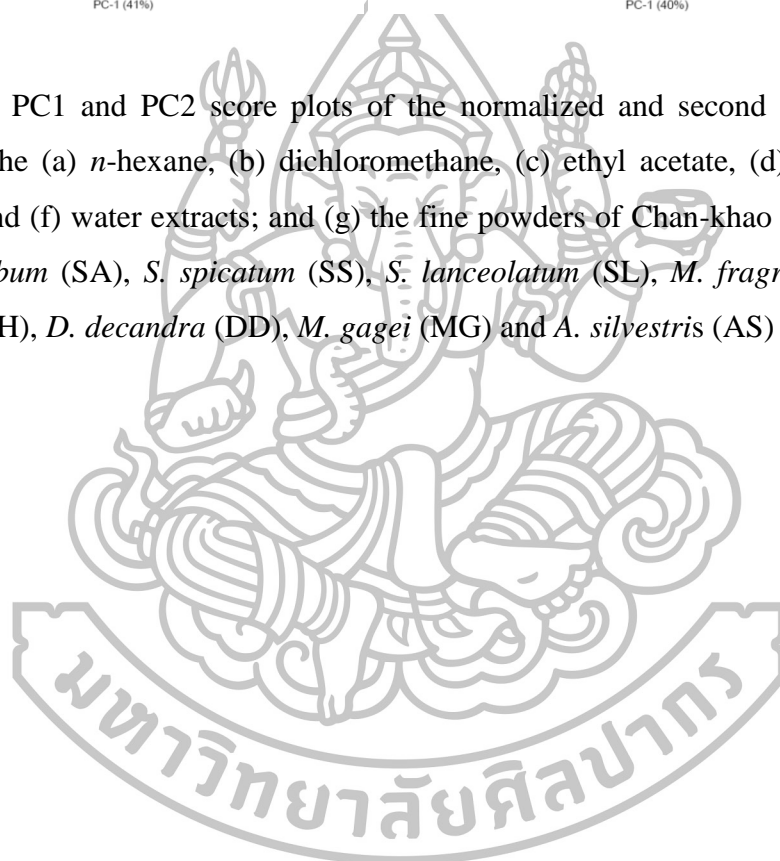
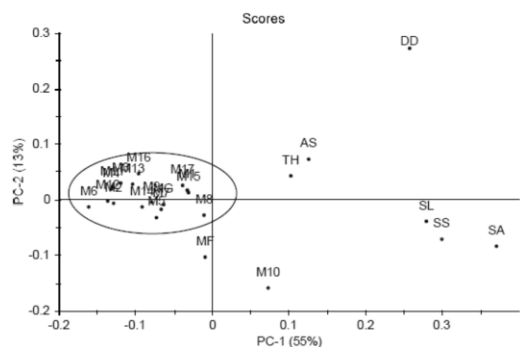


Figure 143 PC1 and PC2 score plots of the normalized and second derivative IR spectra of the (a) *n*-hexane, (b) dichloromethane, (c) ethyl acetate, (d) acetone, (e) methanol and (f) water extracts; and (g) the fine powders of Chan-khao samples (K1-K18), *S. album* (SA), *S. spicatum* (SS), *S. lanceolatum* (SL), *M. fragrans* (MF), *T. hoensis* (TH), *D. decandra* (DD), *M. gagei* (MG) and *A. silvestris* (AS) (continued).

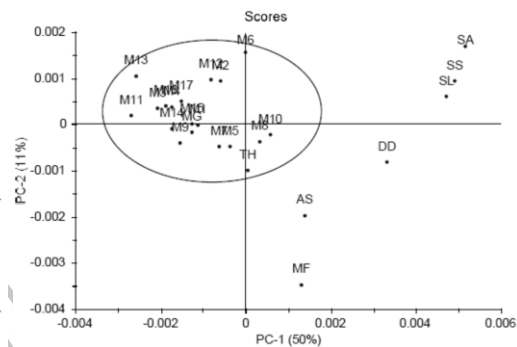


(d) Acetone extract

: Normalized IR

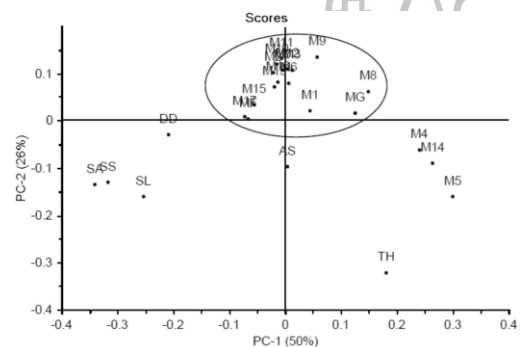


: Second derivative

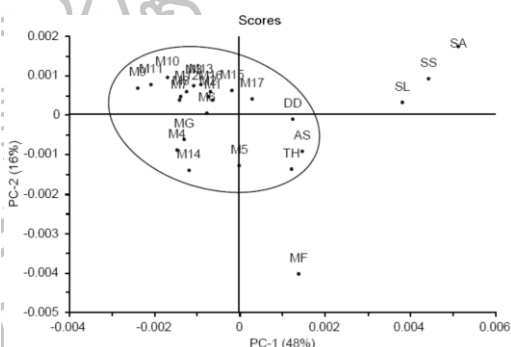


(e) Methanol extract

: Normalized IR

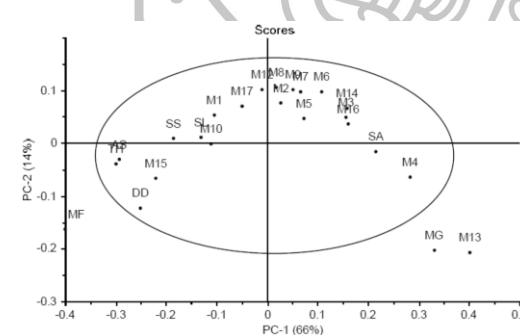


: Second derivative IR



(f) Water extract

: Normalized IR



: Second derivative IR

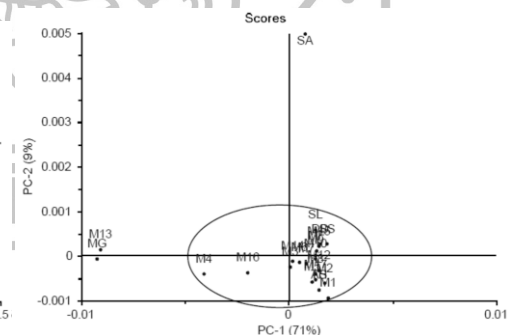


Figure 144 PC1 and PC2 score plots of the normalized and second derivative IR spectra of the (a) *n*-hexane, (b) dichloromethane, (c) ethyl acetate, (d) acetone, (e) methanol and (f) water extracts; and (g) the fine powders of Chan-chamot samples (M1-M17), *S. album* (SA), *S. spicatum* (SS), *S. lanceolatum* (SL), *M. fragrans* (MF), *T. hoensis* (TH), *D. decandra* (DD), *M. gagei* (MG) and *A. silvestris* (AS) (continued).

(g) Fine powders

: Normalized IR

: Second derivative IR

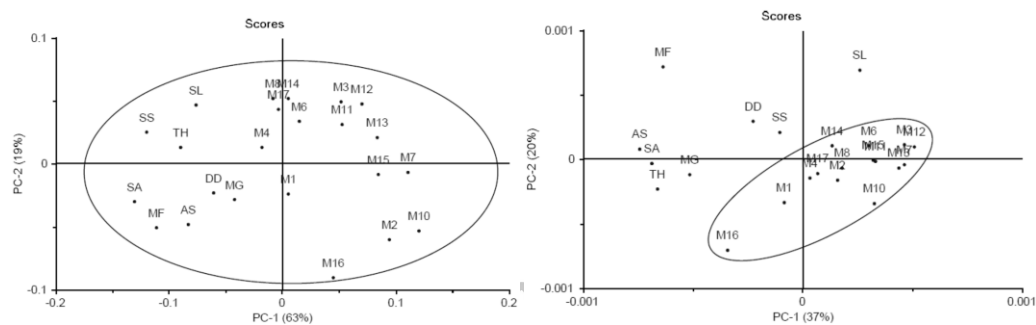
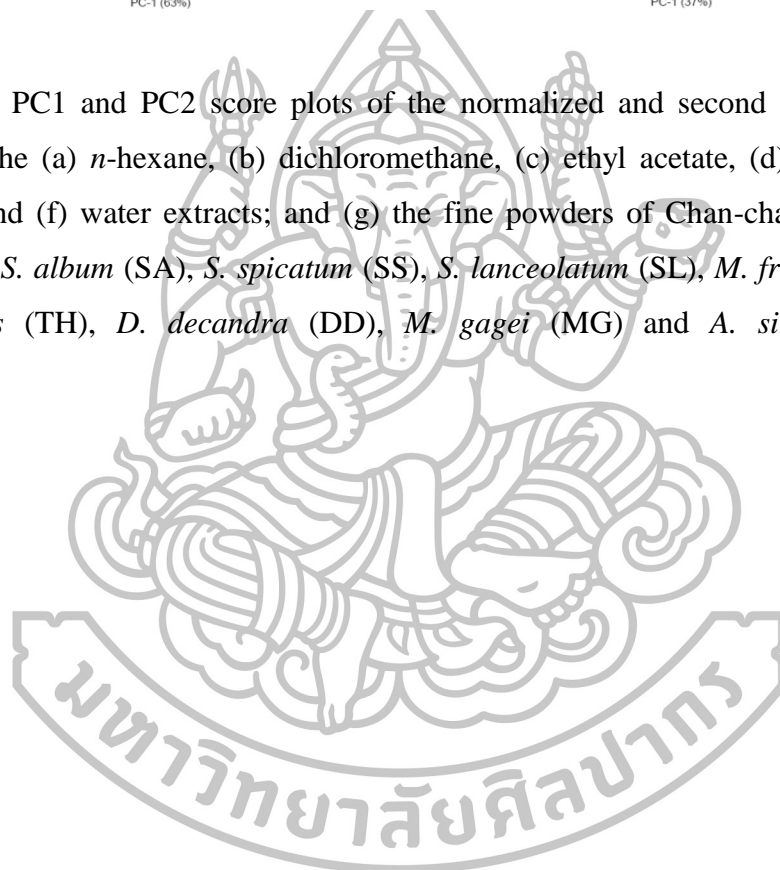
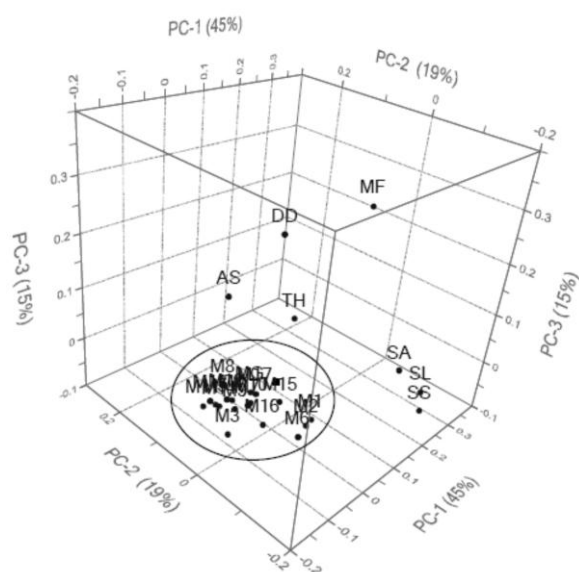


Figure 144 PC1 and PC2 score plots of the normalized and second derivative IR spectra of the (a) *n*-hexane, (b) dichloromethane, (c) ethyl acetate, (d) acetone, (e) methanol and (f) water extracts; and (g) the fine powders of Chan-chamot samples (M1-M17), *S. album* (SA), *S. spicatum* (SS), *S. lanceolatum* (SL), *M. fragrans* (MF), *T. hoensis* (TH), *D. decandra* (DD), *M. gagei* (MG) and *A. silvestris* (AS) (continued).



(a)



(b)

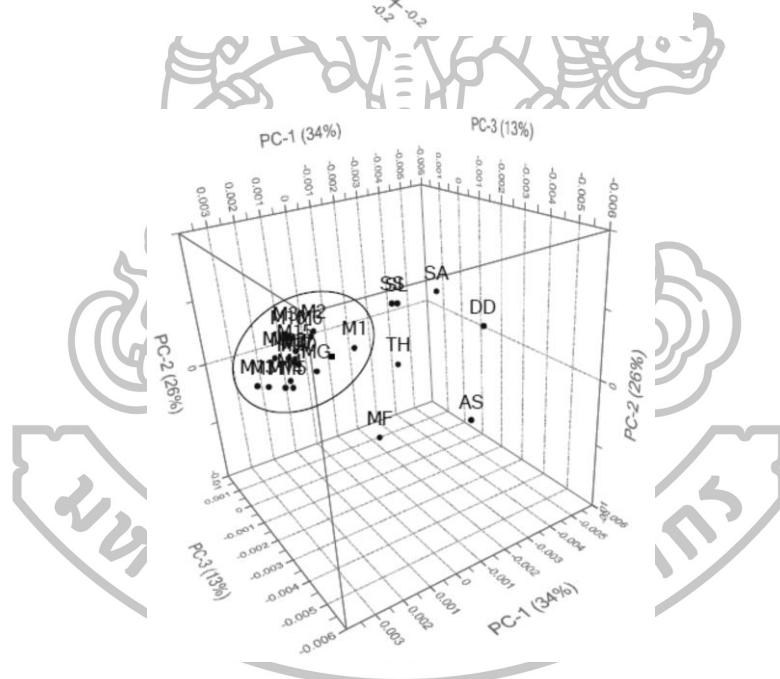
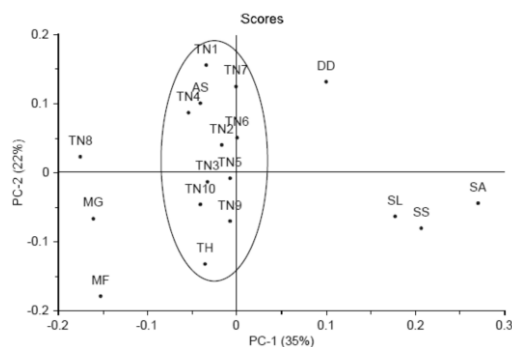


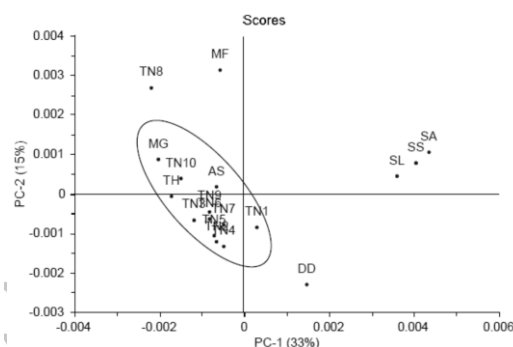
Figure 145 PC1, PC2 and PC3 three dimension score plots of (a) normalized IR spectra and (b) second derivative IR spectra of the dichloromethane extracts of Chamchamot (M1-M17), *S. album* (SA), *S. spicatum* (SS), *S. lanceolatum* (SL), *M. fragrans* (MF), *T. hoensis* (TH), *D. decandra* (DD), *M. gagei* (MG) and *A. silvestris* (AS).

(d) Acetone extract

: Normalized IR

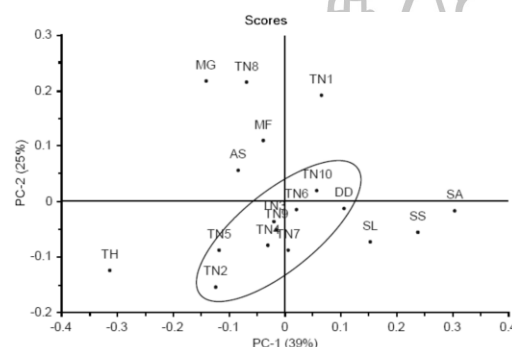


: Second derivative IR

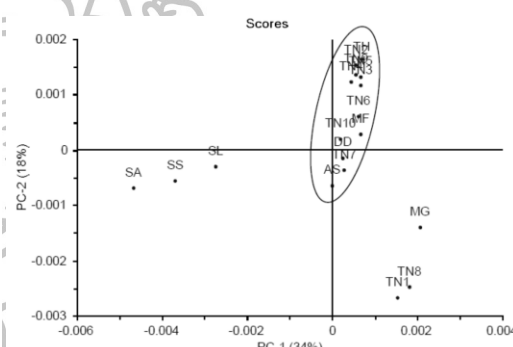


(e) Methanol extract

Normalized IR

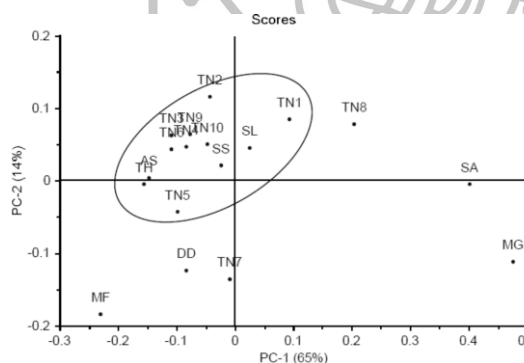


: Second derivative IR



(f) Water extract

: Normalized IR



: Second derivative IR

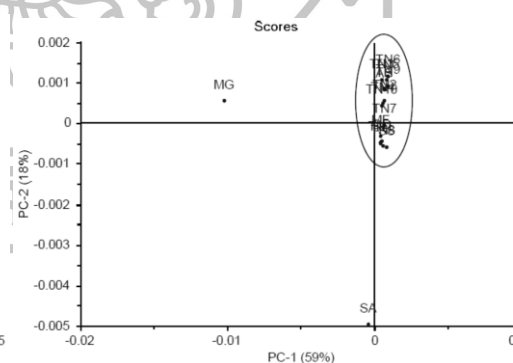
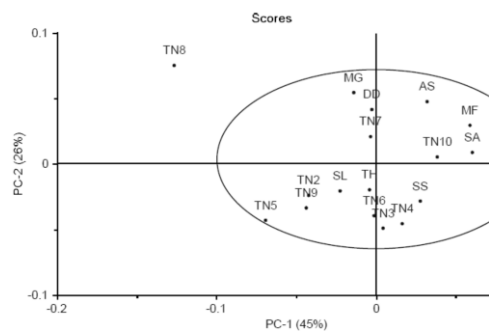


Figure 146 PC1 and PC2 score plots of the normalized and second derivative IR spectra of the (a) *n*-hexane, (b) dichloromethane, (c) ethyl acetate, (d) acetone, (e) methanol and (f) water extracts; and (g) the fine powders of Chan-thana samples (TN1-TN10), *S. album* (SA), *S. spicatum* (SS), *S. lanceolatum* (SL), *M. fragrans* (MF), *T. hoensis* (TH), *D. decandra* (DD), *M. gagei* (MG) and *A. silvestris* (AS) (continued).

(g) Fine powders

: Normalized IR



: Second derivative IR

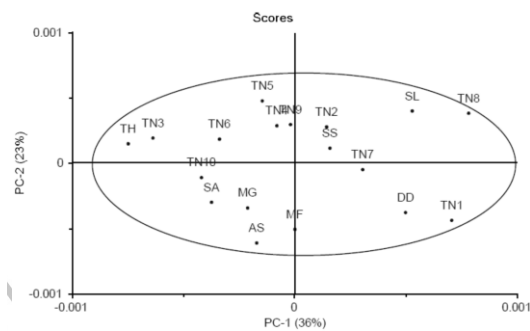
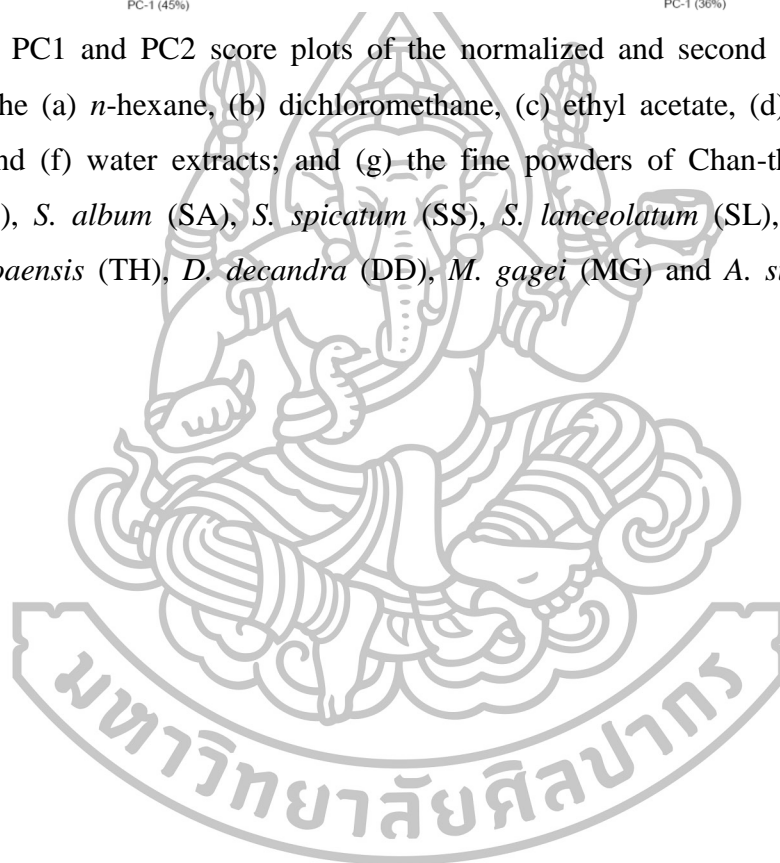
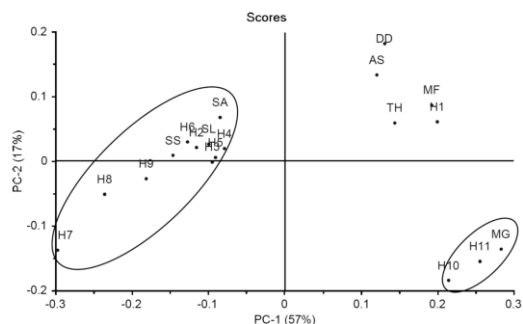


Figure 146 PC1 and PC2 score plots of the normalized and second derivative IR spectra of the (a) *n*-hexane, (b) dichloromethane, (c) ethyl acetate, (d) acetone, (e) methanol and (f) water extracts; and (g) the fine powders of Chan-thana samples (TN1-TN10), *S. album* (SA), *S. spicatum* (SS), *S. lanceolatum* (SL), *M. fragrans* (MF), *T. hoensis* (TH), *D. decandra* (DD), *M. gagei* (MG) and *A. silvestris* (AS) (continued).

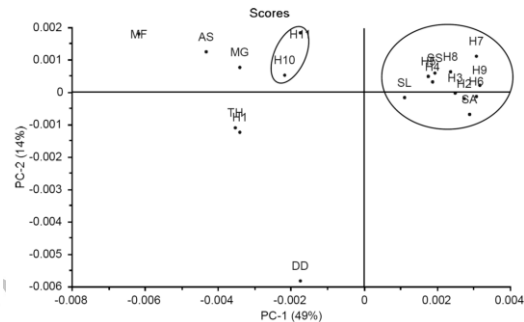


(a) *n*-Hexane extract

: Normalized IR

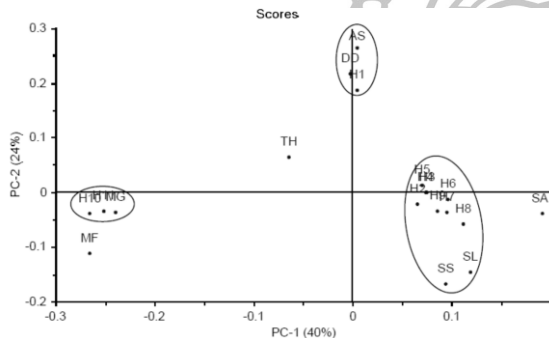


: Second derivative IR

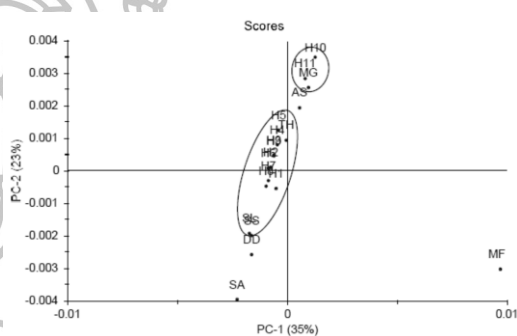


(b) Dichloromethane extract

: Normalized IR

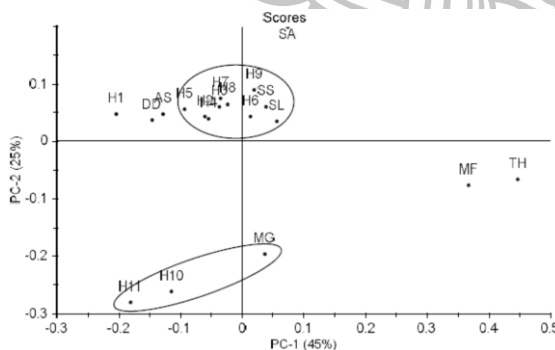


: Second derivative IR



(c) Ethyl acetate extract

: Normalized IR



: Second derivative IR

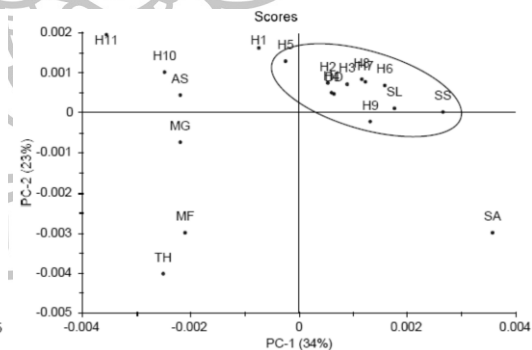


Figure 147 PC1 and PC2 score plots of the normalized and second derivative IR spectra of the (a) *n*-hexane, (b) dichloromethane, (c) ethyl acetate, (d) acetone, (e) methanol and (f) water extracts; and (g) the fine powders of Chan-hom samples (H1-H11), *S. album* (SA), *S. spicatum* (SS), *S. lanceolatum* (SL), *M. fragrans* (MF), *T. hoensis* (TH), *D. decandra* (DD), *M. gagei* (MG) and *A. silvestris* (AS).

(g) Fine powders

: Normalized IR

: Second derivative IR

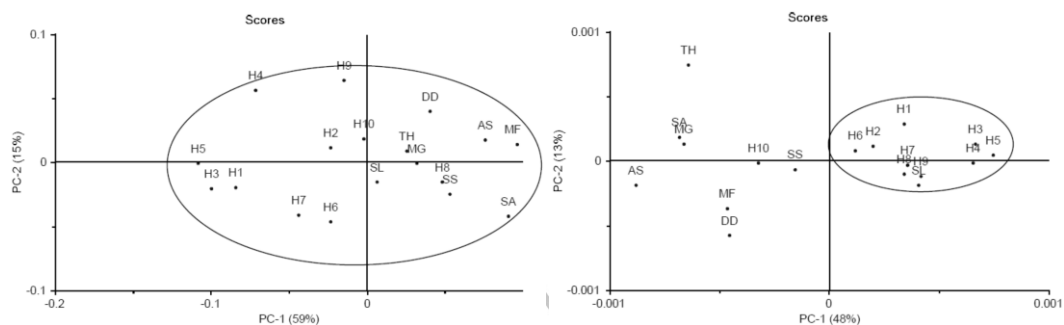
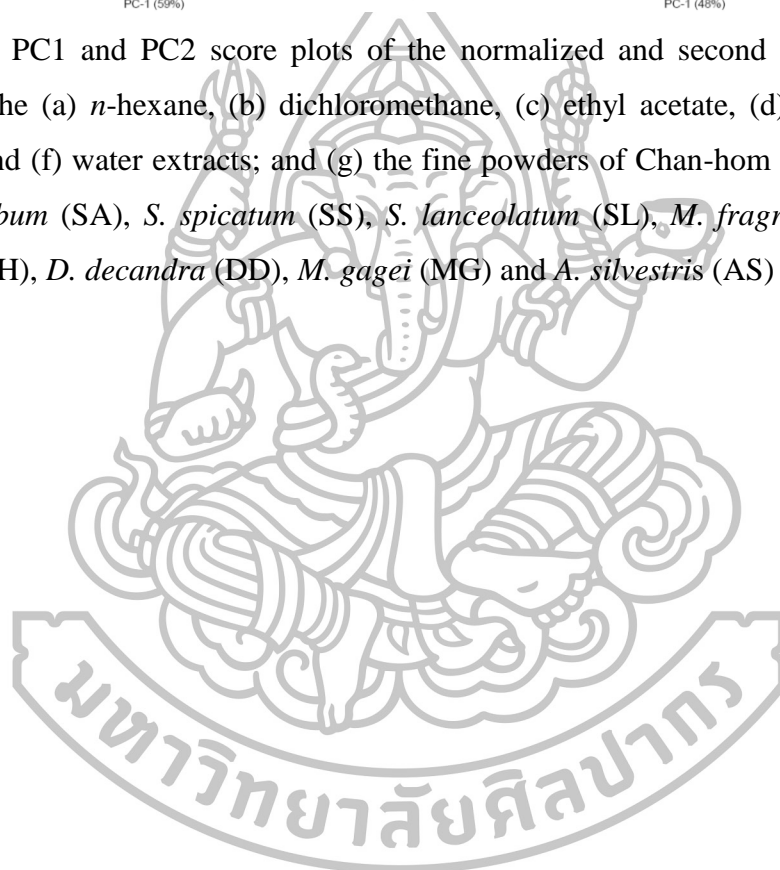
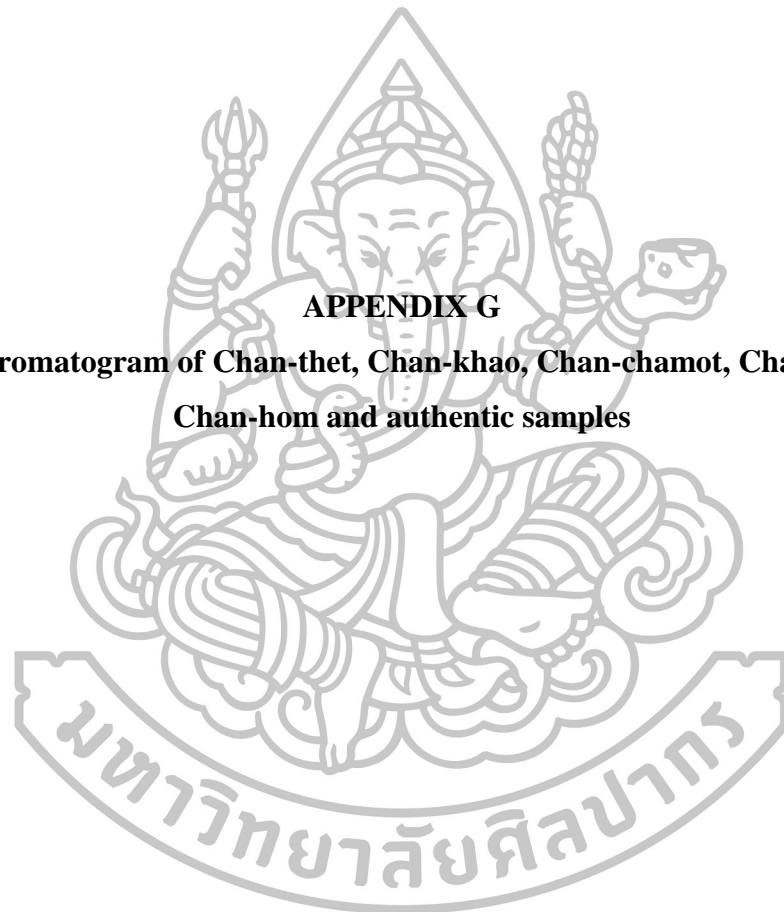


Figure 147 PC1 and PC2 score plots of the normalized and second derivative IR spectra of the (a) *n*-hexane, (b) dichloromethane, (c) ethyl acetate, (d) acetone, (e) methanol and (f) water extracts; and (g) the fine powders of Chan-hom samples (H1-H11), *S. album* (SA), *S. spicatum* (SS), *S. lanceolatum* (SL), *M. fragrans* (MF), *T. hoensis* (TH), *D. decandra* (DD), *M. gagei* (MG) and *A. silvestris* (AS) (continued).



APPENDIX G
GC chromatogram of Chan-thet, Chan-khao, Chan-chamot, Chan-than,
Chan-hom and authentic samples



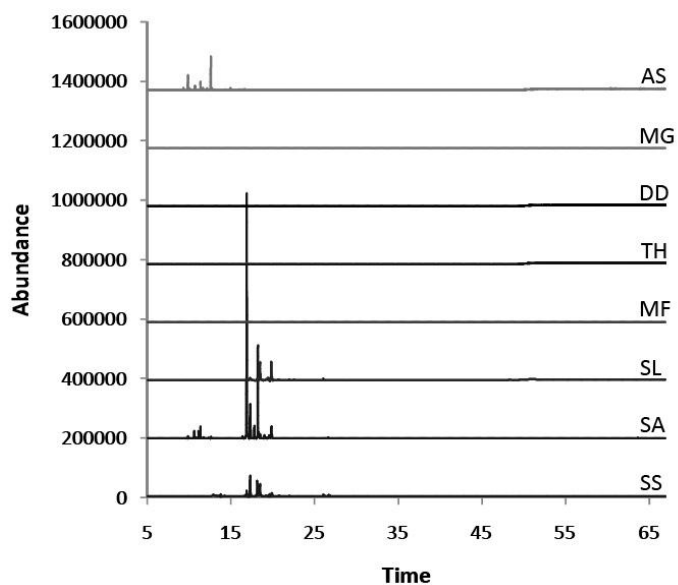


Figure 148 GC fingerprints of the *n*-hexane extracts of *S. spicatum* (SS), *S. album* (SA), *S. lanceolatum* (SL), *M. fragrans* (MF), *T. hoaensis* (TH), *D. decandra* (DD) and *M. gagei* (MG).

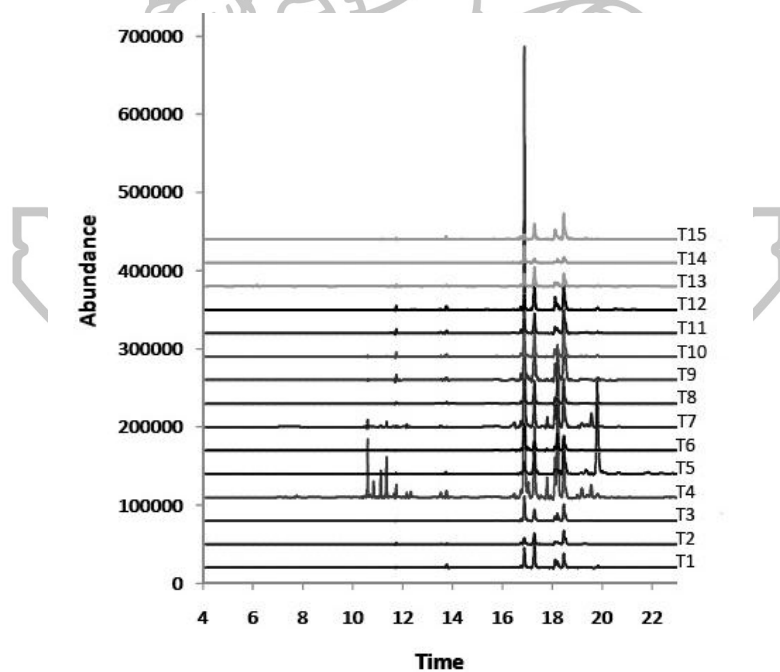


Figure 149 GC fingerprints of the *n*-hexane extracts of Chan-thet samples (T1-15).

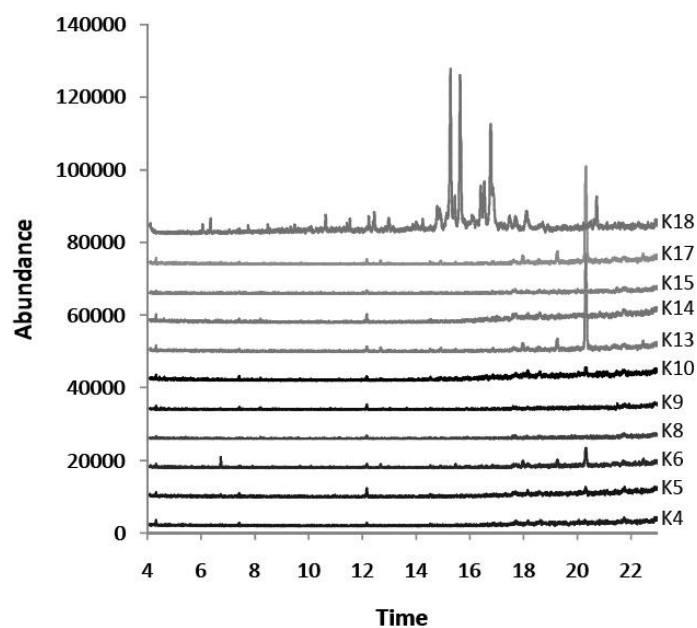


Figure 150 GC fingerprints of the *n*-hexane extracts of Chan-khao samples (K4-6, K8-K10, K13-15 and K17-K18).

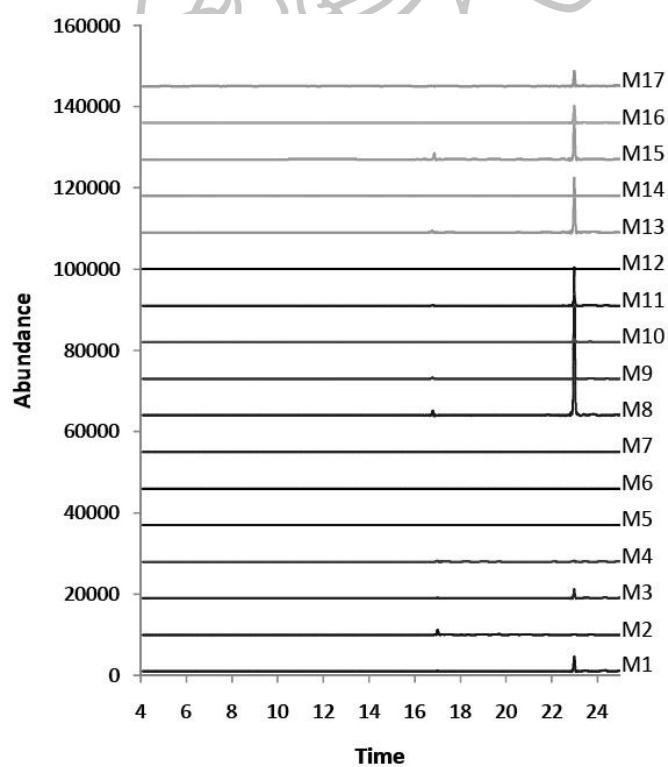


Figure 151 GC fingerprints of the *n*-hexane extracts of Chan-chamot samples (M1-M17).

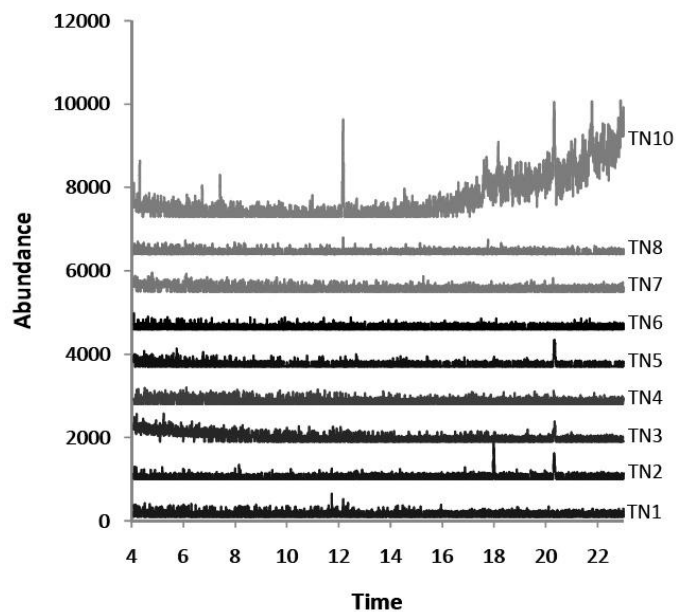


Figure 152 GC fingerprints of the *n*-hexane extracts of Chan-thana samples (TN1-TN8 and TN10).

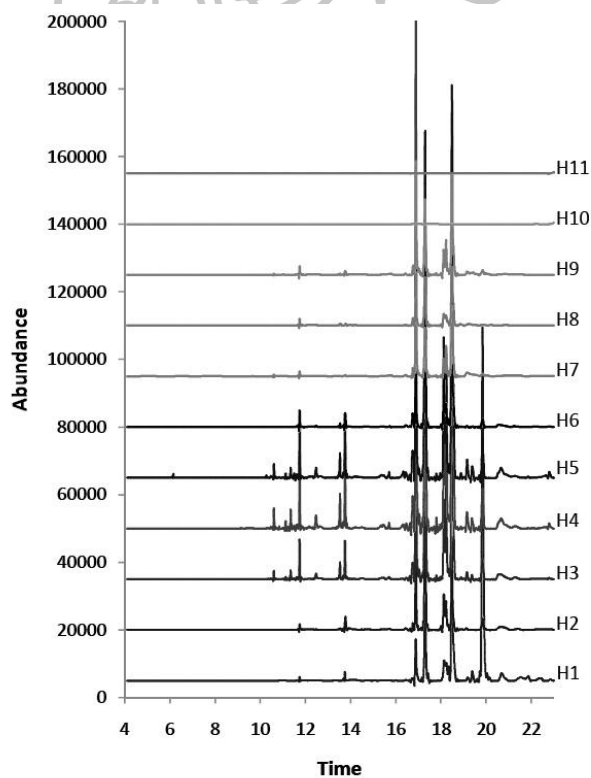
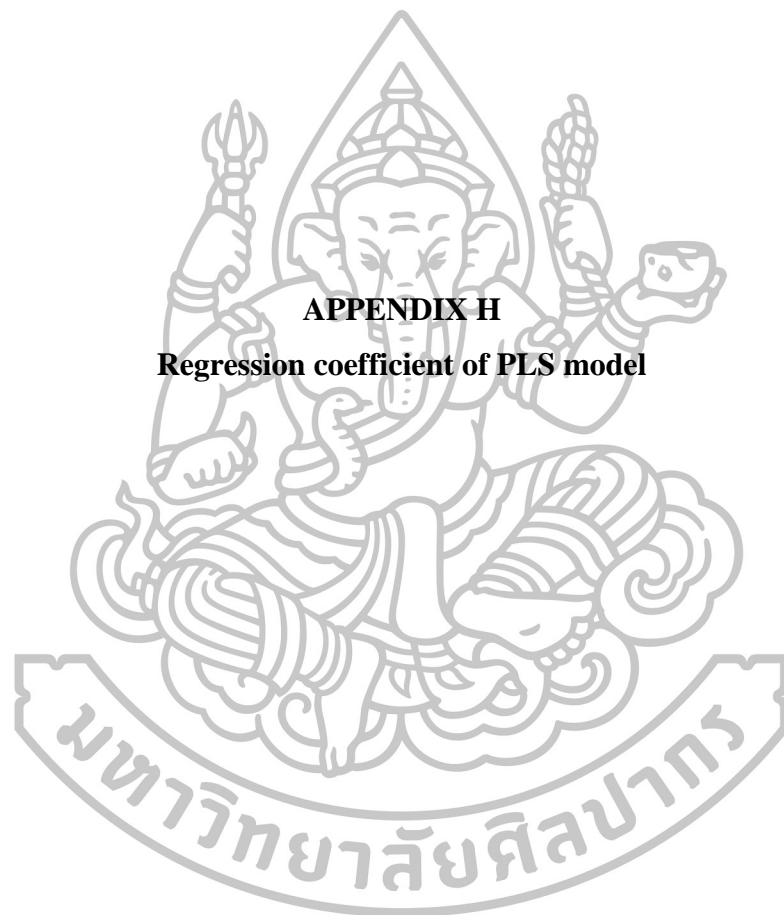
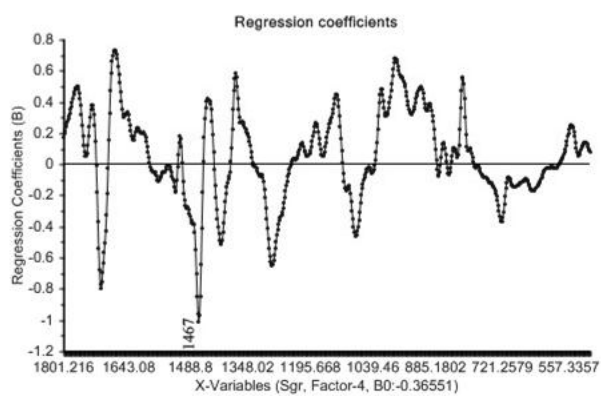


Figure 153 GC fingerprints of the *n*-hexane extract of Chan-hom samples (H1-H11).

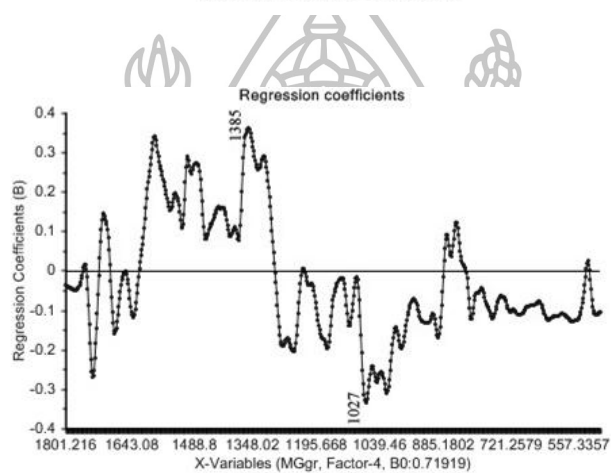


APPENDIX H
Regression coefficient of PLS model

(a)



(b)



(c)

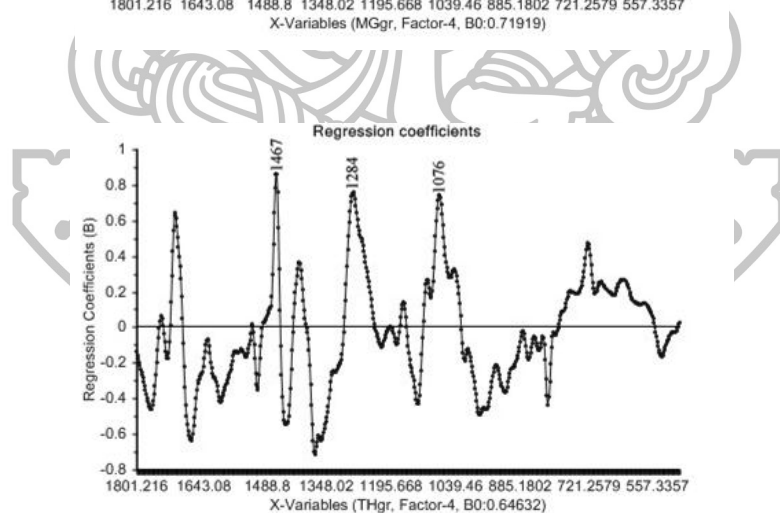
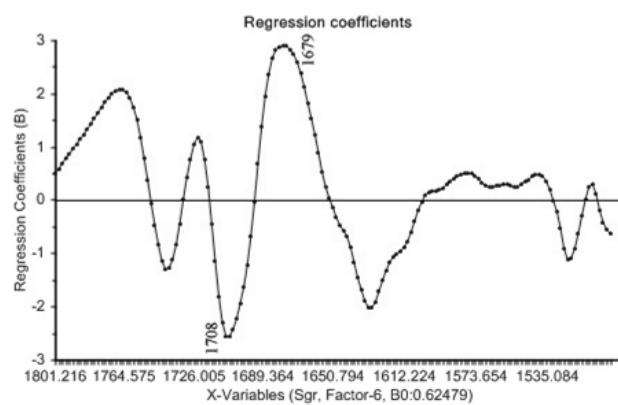
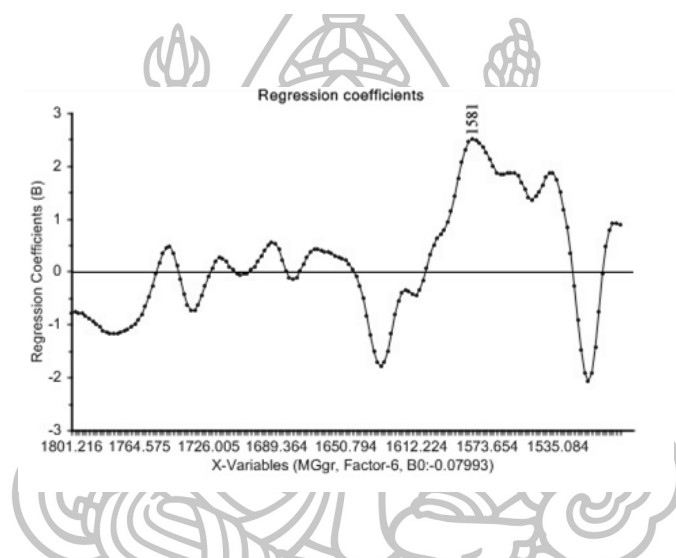


Figure 154 Regression coefficients of PLS models 1 (normalized IR spectra at 1801-501 cm^{-1}) of (a) *Santalum* group, (b) MG group and (c) TH group.

(a)



(b)



(c)

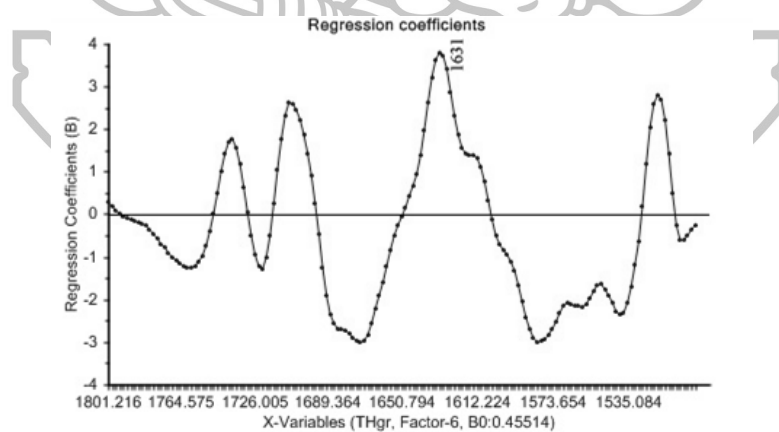
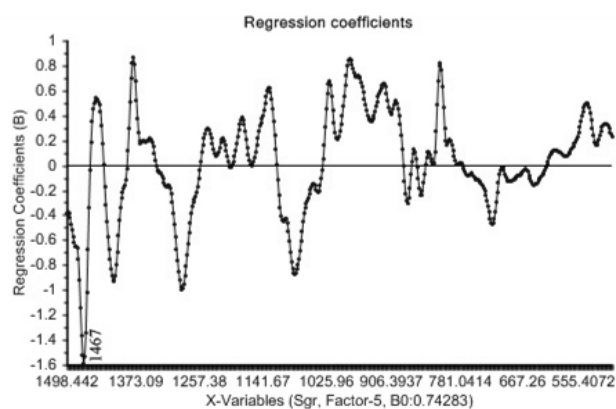
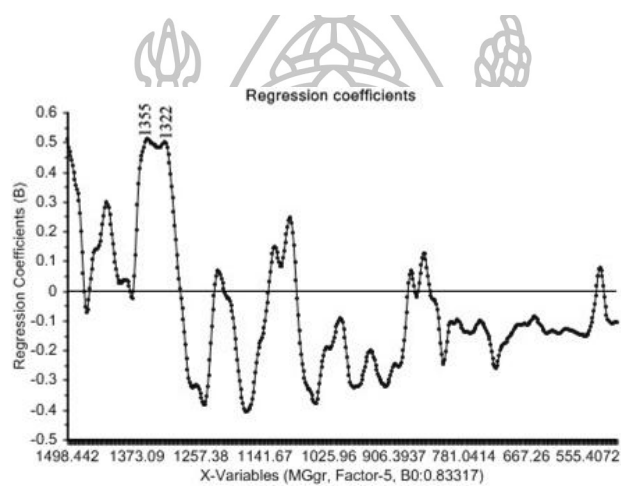


Figure 155 Regression coefficient of PLS model 2 (normalized IR spectra at 1801-1500 cm^{-1}) of (a) *Santalum* group, (b) MG group and (c) TH group.

(a)



(b)



(c)

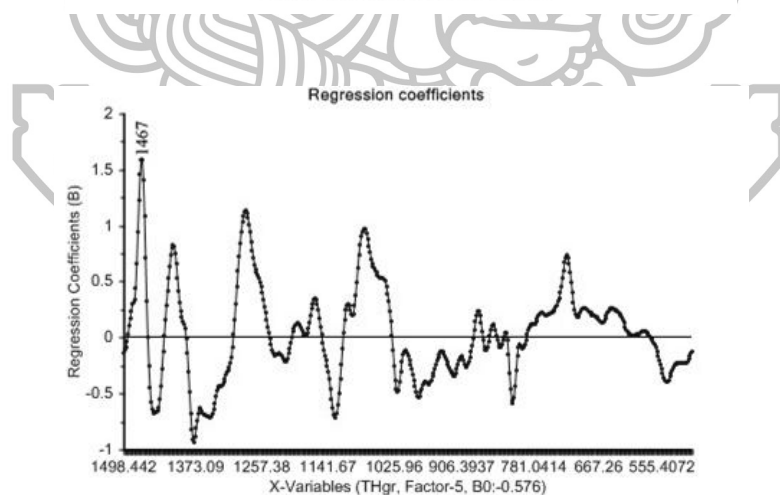
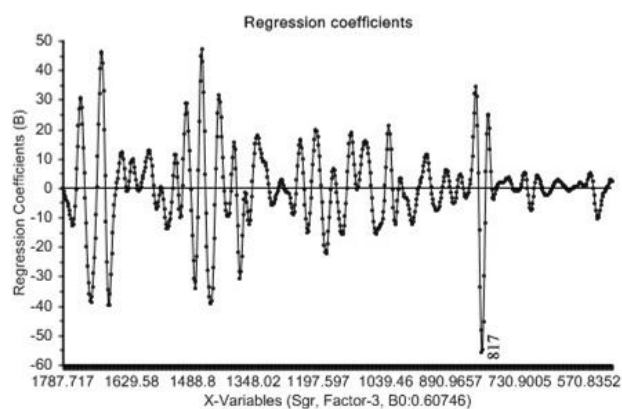
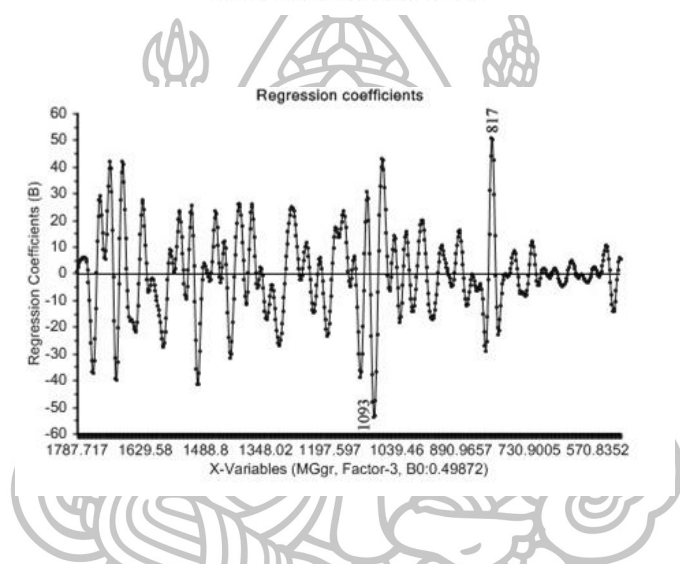


Figure 156 Regression coefficient of PLS model 3 (normalized IR spectra at 1498-501 cm^{-1}) of (a) *Santalum* group, (b) MG group and (c) TH group.

(a)



(b)



(c)

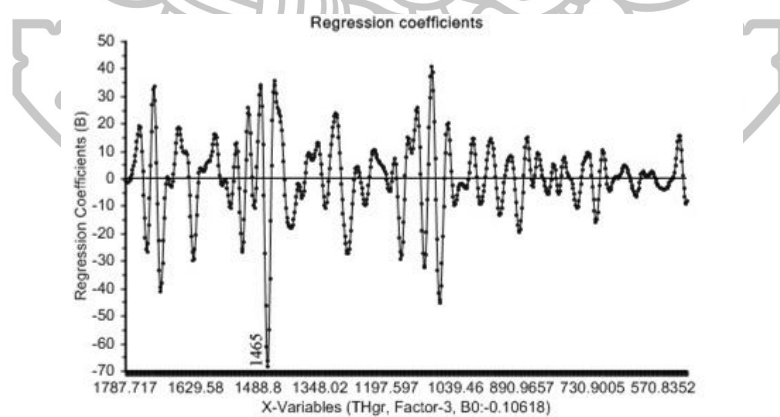
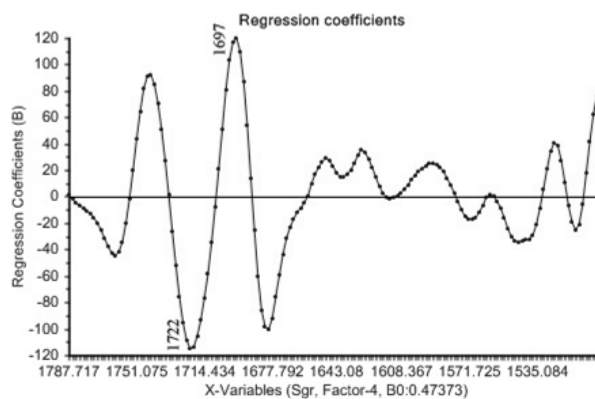
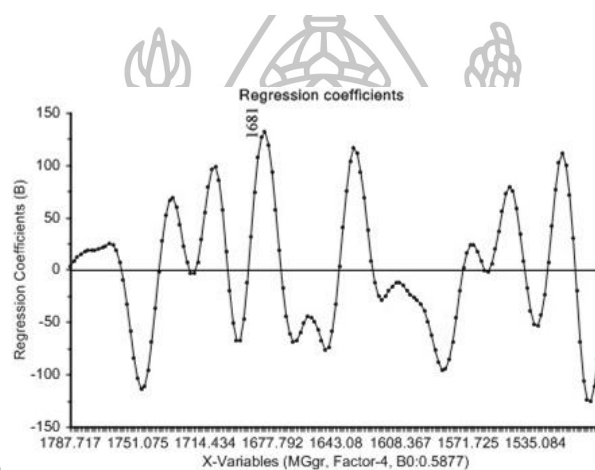


Figure 157 Regression coefficient of PLS model 4 (normalized and second derivative IR spectra at $1801\text{--}501\text{ cm}^{-1}$) of (a) *Santalum* group, (b) MG group and (c) TH group.

(a)



(b)



(c)

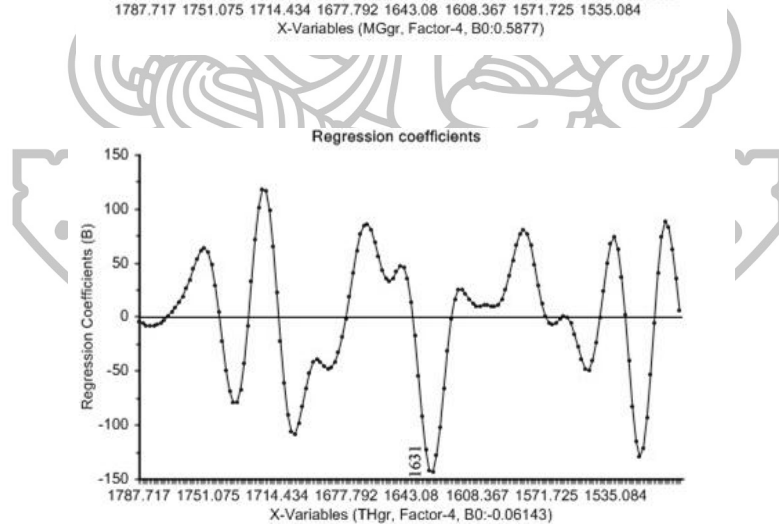
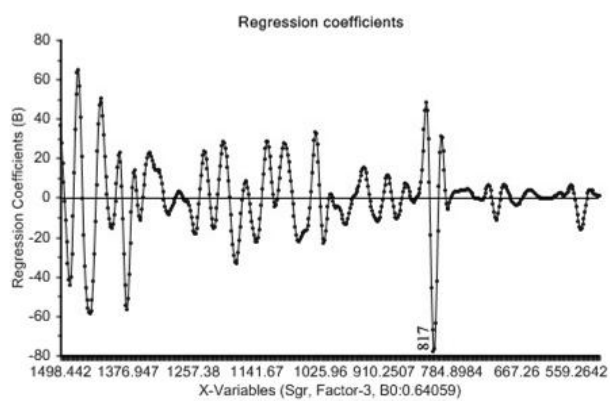
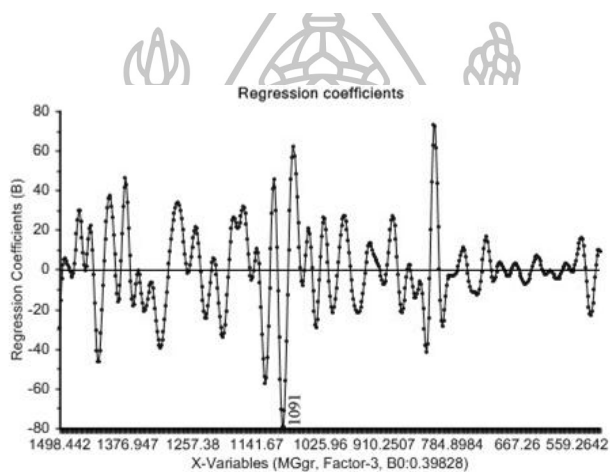


Figure 158 Regression coefficient of PLS model 5 (normalized and second derivative IR spectra at $1801\text{--}1500\text{ cm}^{-1}$) of (a) *Santalum* group, (b) MG group and (c) TH group.

(a)



(b)



(c)

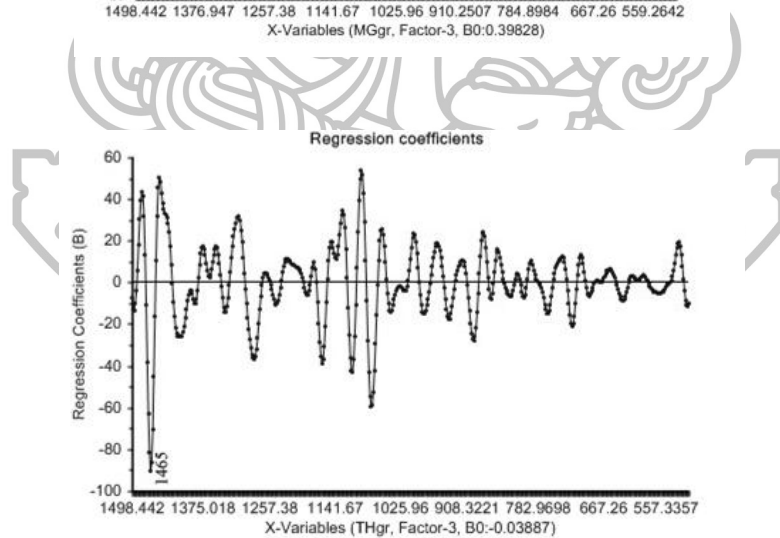
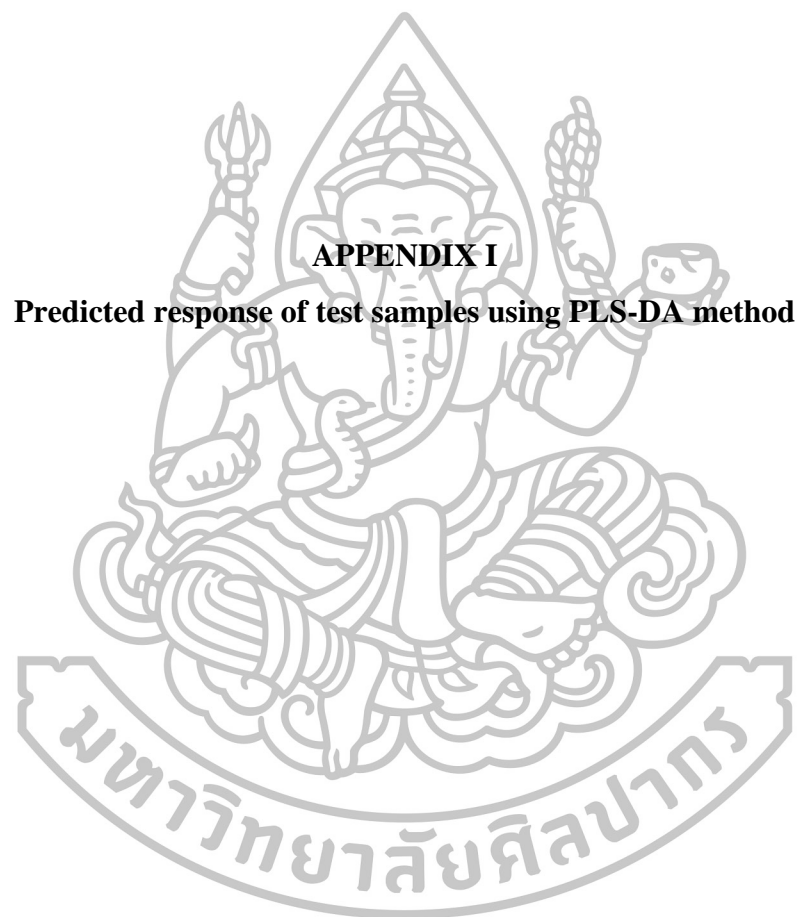
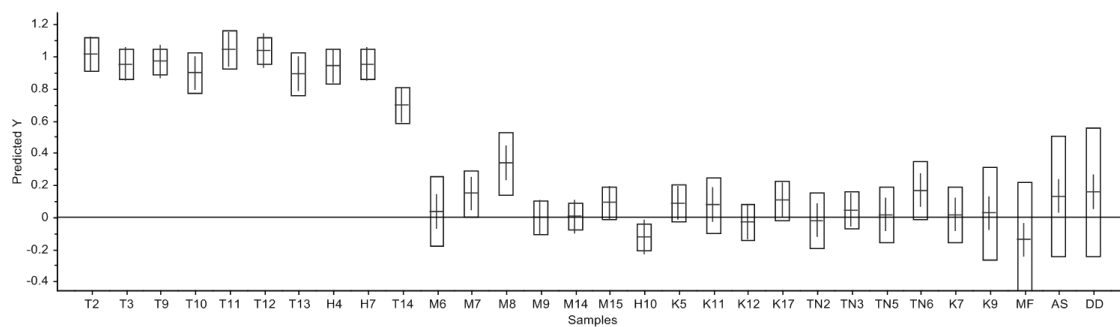


Figure 159 Regression coefficient of PLS model 6 (normalized and second derivative IR spectra at 1498-501 cm⁻¹) of (a) *Santalum* group, (b) MG group and (c) TH group.

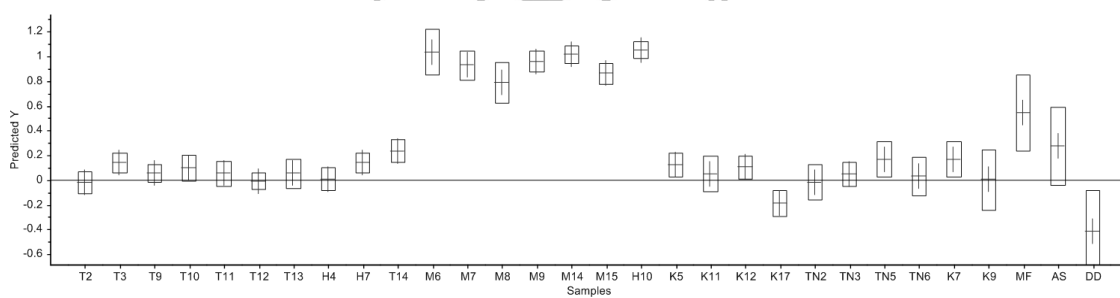


APPENDIX I

Predicted response of test samples using PLS-DA method

(a) *Santalum* group

(b) MG group



(c) TH group

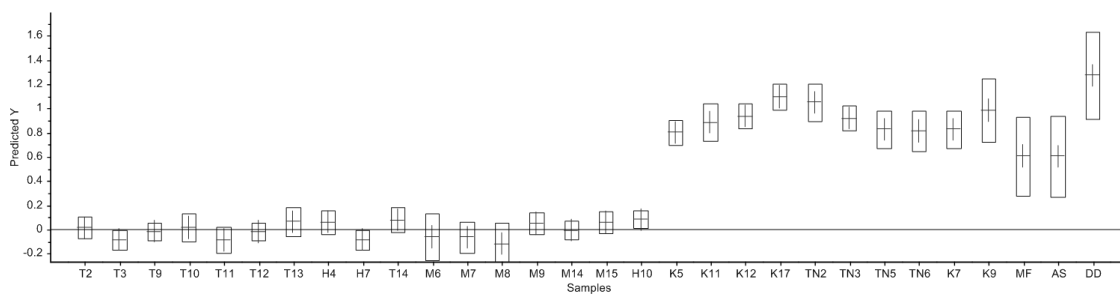
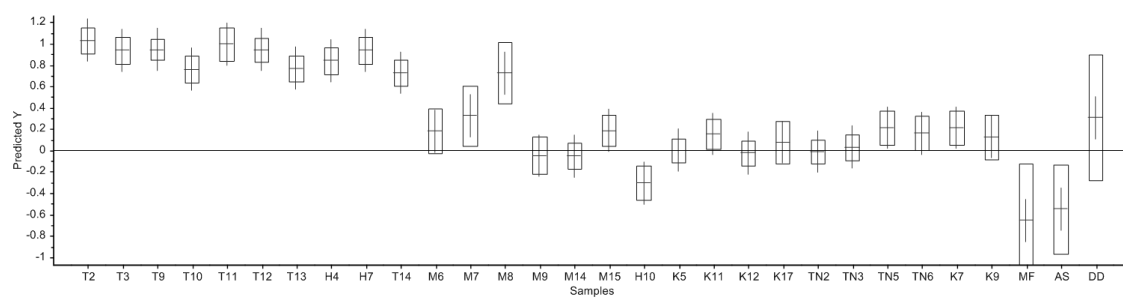
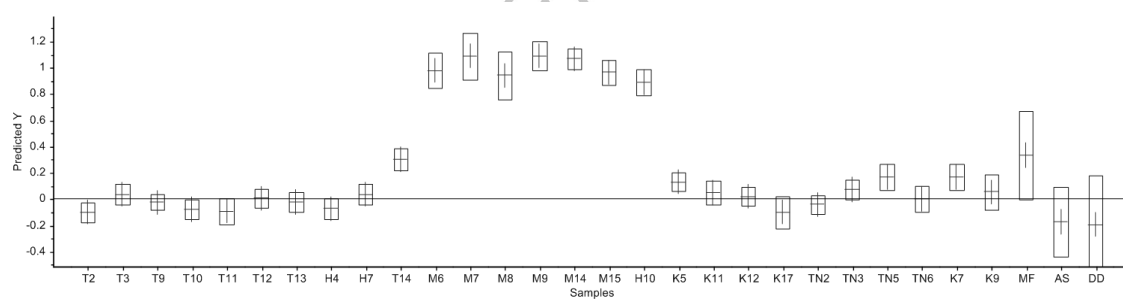


Figure 160 Prediction of test set samples using PLS-DA method 1 of (a) *Santalum* group, (b) MG group and (c) TH group.

(a) *Santalum* group

(b) MG group



(c) TH group

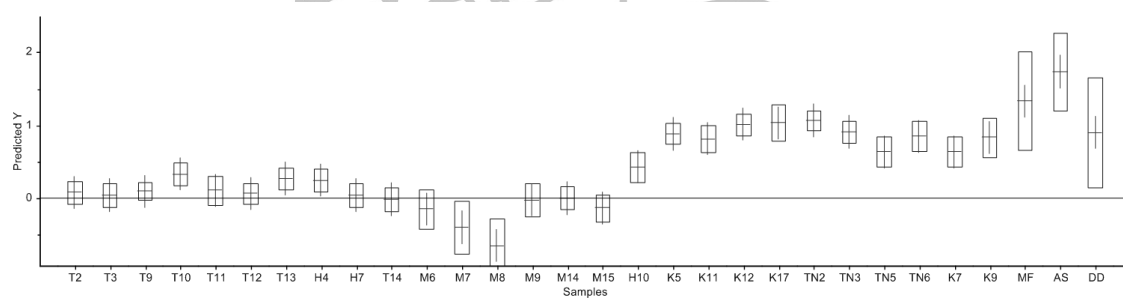
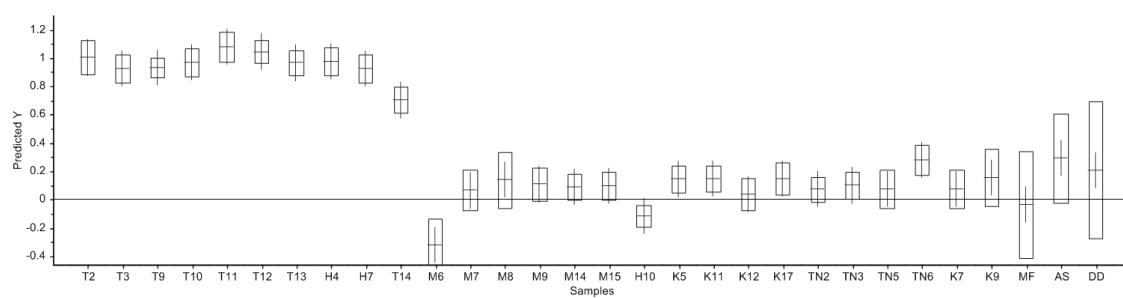
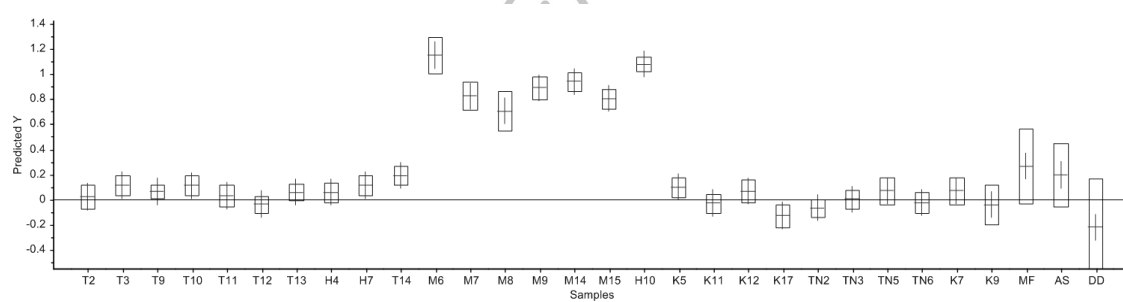


Figure 161 Prediction of test set samples using PLS-DA method 2 of (a) *Santalum* group, (b) MG group and (c) TH group.

(a) *Santalum* group

(b) MG group



(c) TH group

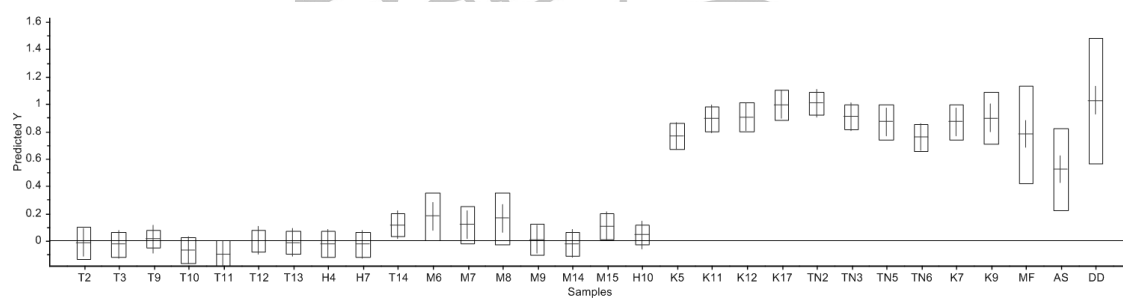
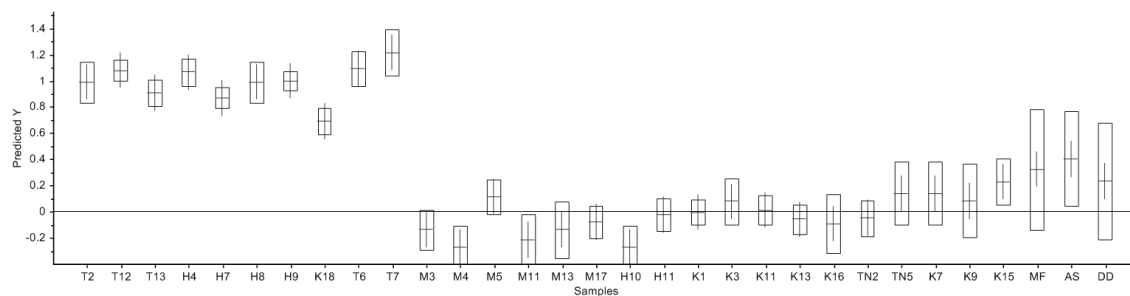
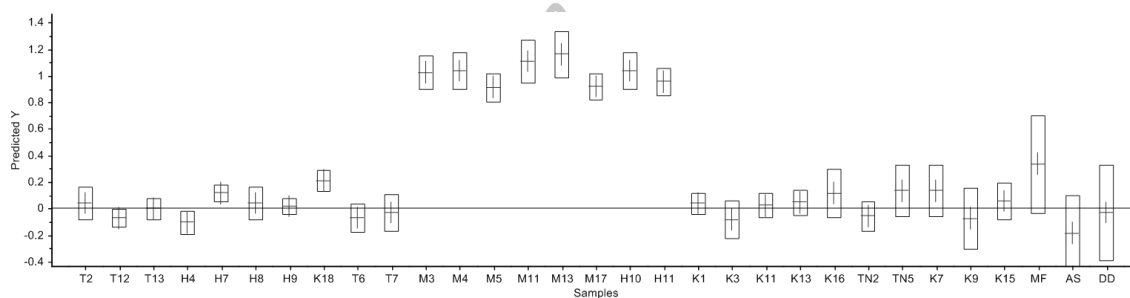


Figure 162 Prediction of test set samples using PLS-DA method 3 of (a) *Santalum* group, (b) MG group and (c) TH group.

(a) *Santalum* group

(b) MG group



(c) TH group

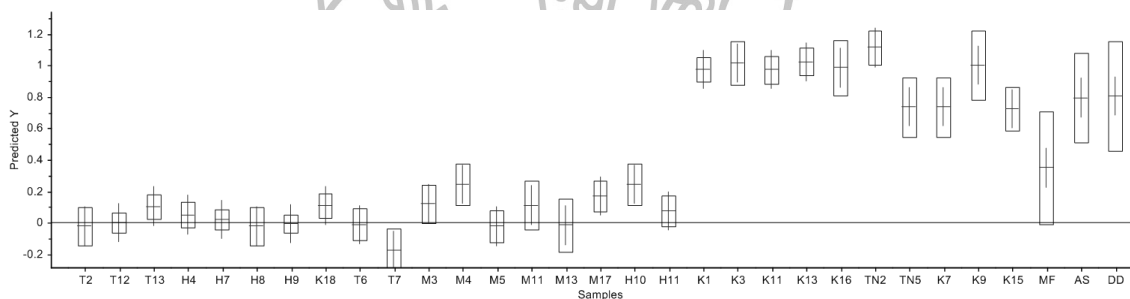
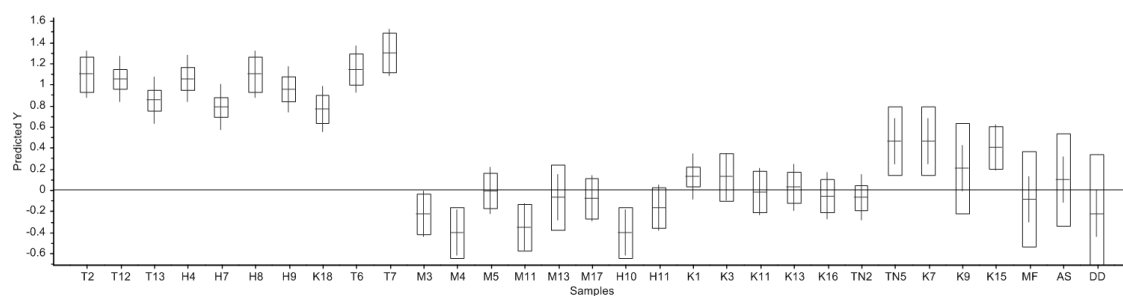
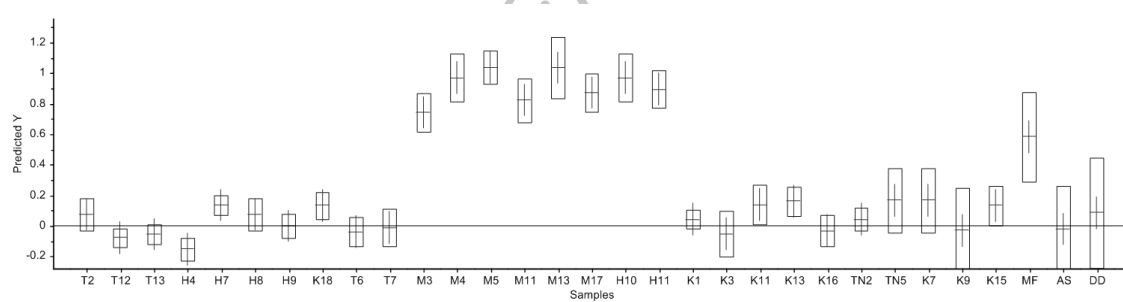


Figure 163 Prediction of test set samples of using PLS-DA method 4 (a) *Santalum* group, (b) MG group and (c) TH group.

(a) *Santalum* group

(b) MG group



(c) TH group

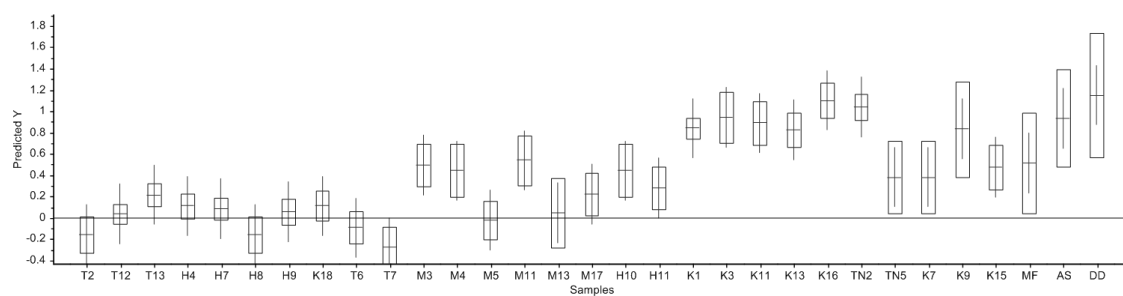
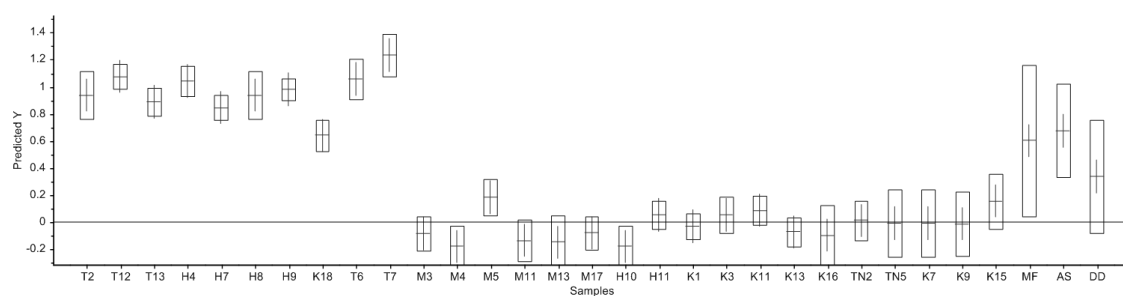
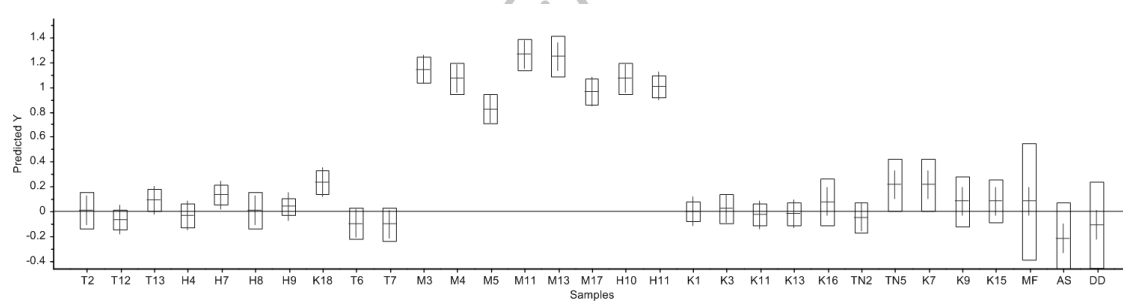


Figure 164 Prediction of test set samples using PLS-DA method 5 of (a) *Santalum* group, (b) MG group and (c) TH group.

(a) *Santalum* group

(b) MG group



(c) TH group

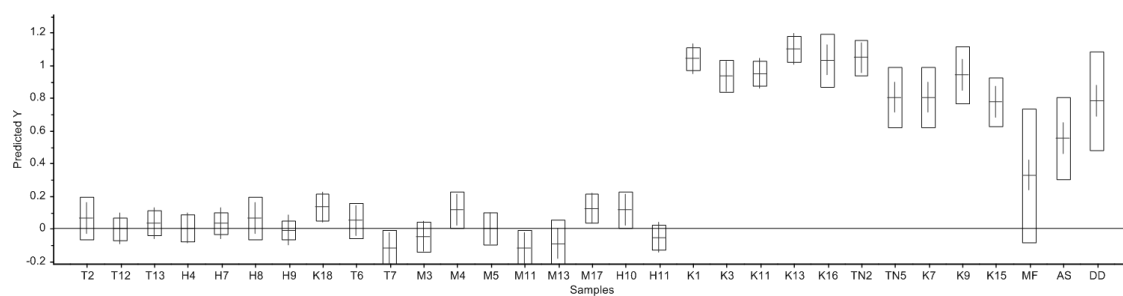


Figure 165 Prediction of test set samples using PLS-DA method 6 of (a) *Santalum* group, (b) MG group and (c) TH group.

Biography

Name : Miss Sununta Srisopon

Date of Birth : 20 January 1984

Home Address : 80/6 Tiwanon Rd, Tambon Talardkwan,
Amphore Meaung, Nonthaburi 11000 Thailand

Education :

2005 Bachelor of Pharmacy, Silpakorn University

2009 Master of Pharmacy, Naresuan University

Work :

2010 Pharmacist, Practitioner Level, Medicinal Plant Research
Institute, Department of Medicinal Sciences, Ministry of public
Health

Publication :

- 1 Srisopon S, Burana-osot J, Sotanaphun U. Botanical identification of Chan-khao and Chan-thana by thin-layer chromatography. *TPHSJ* 2015;10(1):19-24.
- 2 Srisopon S, Burana-osot J, Sotanaphun U. Identification of Chan-chamot by thin-layer chromatography. *TBPS* 2016;11(1):in press.
- 3 Srisopon S, Phattanawasin P, Burana-osot J, Sotanaphun U. Quality control of crude drugs of “Phikud Navakot” based on antioxidative and total phenolic contents. The Fourth International Conference on Natural Products for Health and Beauty (NATPRO4). 28-30 November 2012. Chiangmai, Thailand, p. 352.
4. Sotanaphun U, Phattanawasin P, Burana-osot J, Srisopon S. Botanical identification of Kot-chula-lampha in current use by thin-layer chromatography. *TPHSJ* 2013;8(1):1-6.
5. Burana-osot J, Phattanawasin P, Srisopon S, Ashok PK, Huang B, Sotanaphun U. Authentication of a Thai crude drug “Kot-chula-lumpa” using Gas Chromatography-Mass Spectrometry and Multivariate Data Analysis. *TJPS* 2014;38(2):74-81.